

# **RAGE-Based Strategies For The Control of Gene Expression**

Elizabeth A. Lovejoy

Submitted for the degree of PhD

University of Edinburgh, 1999



## **Declaration**

All of the work described in this thesis has been carried out by myself. Assistance from others and any collaborations are acknowledged at the relevant places within the text.

Elizabeth A. Lovejoy, March 1999.



# Contents

<b>Title page</b>	<b>1</b>
<b>Declaration</b>	<b>2</b>
<b>Contents</b>	<b>3</b>
<b>Acknowledgements</b>	<b>10</b>
<b>Abbreviations</b>	<b>11</b>
<b>Abstract</b>	<b>12</b>
<b>Chapter 1 – Introduction</b>	<b>14</b>
1.1. Introduction	15
1.2. Background: Animal Models of Human Disease	15
1.2.1. Transgenic Mice	16
1.2.2. Introduction of Specific Alterations Into the Mammalian Genome	17
1.2.2.1. Mouse Embryo-Derived Cell Types	18
1.2.2.1.a. Embryonal Carcinoma Cells	18
1.2.2.1.b. Embryonal Stem Cells	19
1.2.2.1.c. ES Cell Differentiation	19
1.2.2.1.d. ES Cell Mediated Transgenesis	21
1.2.2.2. Homologous Recombination	22
1.2.2.3. Gene Targeting	27
1.2.2.4. Gene Targeting Strategies	30
1.2.2.4.a. Insertion Type Targeting Strategies	30
1.2.2.4.b. Replacement Type Targeting Strategies	30
1.2.2.5. Factors Affecting Homologous Recombination	37
1.2.2.6. Introducing Exogenous DNA into ES Cells and Identifying Recombinants	40
1.2.2.6.a. Positive Selection	41
1.2.2.6.b. Positive/Negative Selection	41
1.2.2.6.c. Double Replacement/Tag and Exchange Targeting Strategies	42
1.2.2.6.d. Crippled Selectable Marker Genes	44
1.3. Inducible Gene Targeting	45
1.3.1. The Flp/FRT System: Background	46
1.3.2. The Cre/loxP System: Background	48
1.3.3. Applications of the Cre/loxP System: Inducible Gene Targeting	51
1.3.3.1. Regulating the Activity of Cre Recombinase	52
1.3.3.1.a. Tissue-specific Promoters	52
1.3.3.1.b. Cre Fusion Proteins	54
1.3.3.1.c. Inducible Promoters	54
1.3.3.1.d. Global Promoters	55
1.3.3.1.e. Viral Delivery	55
1.3.3.1.f. Other Cre Delivery Systems	58

1.3.3.2. Inducible Control of Gene Expression Using the Cre/loxP System	58
1.3.3.2.a. Site-specific Insertion	59
1.3.3.2.b. Site-specific Excisional Recombination of Exogenous DNA Sequences	60
1.3.3.2.c. Site-specific Excisional Recombination of Endogenous DNA Sequences	60
1.3.3.2.d. Chromosomal Manipulations Using Cre Recombinase	63
1.3.4. Historical Perspective	64
1.4. p53	64
1.4.1. Genomic Organisation and Transcriptional Regulation of p53	65
1.4.2. p53: Functional Domains and Structure	67
1.4.2.1. p53: The Amino Terminus	69
1.4.2.2. p53: The Proline Rich Linker	70
1.4.2.3. p53: The Core Domain	71
1.4.2.4. The Carboxy Terminus of p53	72
1.4.3. Mechanisms of p53 Activity Regulation	72
1.4.3.1. p53 in the Normal Cell	73
1.4.3.1.a. Latent p53	73
1.4.3.1.b. Cellular Compartmentalisation	75
1.4.3.2. Negative Autoregulation by Mdm2	76
1.4.3.3. Covalent Modification	78
1.4.3.3.a. Phosphorylation	79
1.4.3.3.b. Other Posttranslational Modifications of p53	83
1.4.3.4. Redox Regulation	84
1.4.4. Induction of p53	84
1.4.5. Biological Activities of p53	86
1.4.5.1. Transcriptional Activation by p53	86
1.4.5.2. Transcriptional Repression by p53	89
1.4.5.3. p53 and Translation Control	90
1.4.5.4. p53: Direct Interaction With Other Proteins	90
1.4.5.4.a. Cellular Proteins	90
1.4.5.4.b. Viral Proteins	92
1.4.5.5. p53-Dependent Apoptosis	93
1.4.5.6. Cell Cycle Control/Checkpoints and p53	95
1.4.5.6.a. p53-Dependent G1 Arrest	95
1.4.5.6.b. p53 and the G2/M Transition	96
1.4.5.6.c. p53 and Other Cell Cycle Checkpoints	96
1.4.5.6.d. Growth Arrest or Apoptosis	97
1.4.6. p53 in Development	101
1.4.7. p53 and Tumourigenesis	101
1.4.7.1. Attenuated Apoptosis	102
1.4.7.2. Increased Genomic Instability	103
1.4.7.3. Increased Proliferative Capacity	103
1.4.7.4. Increased Invasiveness and Metastasis	103
1.4.7.5. IncreasedAngiogenesis	104

1.4.8. p53 Related Proteins	104
1.4.9. Conclusions	105
1.5. Replicative Cellular Senescence	106
1.5.1. Introduction	106
1.5.2. Senescence <i>in vivo</i>	107
1.5.3. Genetic Regulation of Senescence	108
1.5.3.1. Chromosomal Localisation of Pro-senescence Genes	108
1.5.3.2. Individual Pro-senescence Genes	109
1.5.3.2.a. RB	110
1.5.3.2.b. p53	112
1.5.3.2.c. p21	114
1.5.3.2.d. p16 <sup>INK4a</sup>	114
1.5.3.2.e. p33 <sup>ING1</sup>	115
1.5.3.3. Anti-senescence Genes	115
1.5.4. Cellular Immortalisation-Bypassing M2	116
1.5.5. Senescence Activation	117
1.5.6. Summary	118
<b>Chapter 2 - Recombination Activated Gene Expression</b>	<b>120</b>
2.1. Introduction	121
2.2. Conditional Gene Expression – The Floxed STOP Approach	123
2.3. Aims	125
2.4. Construction of pFloxSTOP	125
2.4.1. The pGT1.8IRES $\beta$ geo Plasmid	126
2.4.1.1. Removal of the IRES From pGT1.8IRES $\beta$ geo	128
2.4.2. The pTA $\beta$ geo Plasmid	131
2.4.2.1. Introducing the loxP Sites	133
2.4.2.2. Modifying pFloxTA $\beta$ geo Polylinker	137
2.4.3. Inserting the STOP into pFloxTA $\beta$ geo	137
2.5. Is pFloxSTOP a Functional Substrate For Cre Recombinase ?	140
2.5.1. Excisive Recombination in BNN132 Cells	140
2.6. Summary	143
2.7. Inducible Control of Gene Expression <i>in vitro</i>	143
2.7.1. The Enhanced Green Fluorescent Protein Gene	145
2.7.2. Construction of pFloxEGFP	145
2.7.3. Introducing pFloxEGFP into ES Cells	146
2.7.3.1. Analysis of G418 <sup>R</sup> Clones	150
2.7.3.1.a. $\beta$ galactosidase Expression	150
2.7.3.1.b. EGFP Marker Gene Status	150
2.8. Clone FE13 – Introducing Cre Recombinase	152
2.8.1. Characterisation of an ES Cell Differentiation State-Specific Promoter Sequence	152
2.8.1.1. Background	152
2.8.1.2. Results	153
2.8.2. Replication-defective Recombinant Adenoviridae	155
2.8.2.1. Determination of the Optimal Adenovirus Titre For ES Cell Infection	156

2.8.2.2. AdCre Infection of Differentiated FE13 ES Cells	159
2.8.2.2.a. Episomal AdCre Detection	159
2.8.2.2.b. pFloxEGFP Recombination Status	159
2.8.2.2.b.i. PCR Strategy	163
2.8.2.2.b.ii. Southern Blot Strategy	163
2.8.2.2.c. EGFP Expression Data	166
2.8.2.2.c.i. FACS and UV Microscopy Data	166
2.8.2.2.c.ii. Quantitative RT-PCR Detection of EGFP mRNA	168
2.8.2.2.c.iii. Confirmation of the Absence of EGFP Protein	170
2.8.2.2.d. $\beta$ galactosidase Expression Data	173
2.8.2.2.d.i. $\beta$ gal Activity	173
2.8.2.2.d.ii. Histochemical $\beta$ gal Detection and Scoring	175
2.9. Discussion	179
<b>Chapter 3 – RAGE-Based Strategies to Achieve Conditional Upregulation of the Murine p53 Gene <i>in vivo</i></b>	<b>192</b>
3.1. Introduction	193
3.2. Aims	195
3.3. Do Primary Mouse Embryonic Fibroblasts Express SA $\beta$ -gal?	195
3.3.1. Human SA $\beta$ -gal	195
3.3.2. Murine $\beta$ -galactosidases	196
3.3.3. Does the Expression of SA $\beta$ -gal Correlate With Passage Number?	199
3.3.3.1. Continuous Passaging of MEFs	199
3.3.3.2. SA $\beta$ -gal Timecourse Results	199
3.3.4. Murine SA $\beta$ -gal <i>in vivo</i>	202
3.3.5. Summary	207
3.4. Design of a Conditional p53 Expression Vector	207
3.4.1. Basic Strategy	207
3.5. Construction of pICDP(for)	209
3.5.1. The p53 cDNA	209
3.5.2. Inserting the PGK Promoter into p53pTAg	209
3.5.3. Inserting the Floxed STOP Cassette into pPGKp53	212
3.5.4. Testing pICDNA(rev) in BNN 132 Cells	212
3.5.5. Substitution of the Floxed STOP Cassette Within pICDNA(rev)	217
3.5.5.1. Construction of pFloxSTOP(for)	217
3.5.5.2. Inserting the Floxed STOP Cassette from pFloxSTOP(for) into pPGKp53	220
3.5.6. Inserting the <i>pac</i> Gene into pICDNA(for)	220
3.5.7. Summary	222
3.6. Introducing pICDP(for) Into p53 Null MEFs by Calcium Phosphate Precipitation	225
3.6.1. Determination of Puromycin Sensitivity of p53 Null MEFs	225
3.6.2. Stable Transfection of p53 Null MEFs	225

3.6.3. Introducing Cre Recombinase into MEF/pICDP(for) Clones	227
3.6.3.1. Determination of Optimal Titre for EF Infection	227
3.6.3.2. Infection of MEF/pICDP(for) Clones With AdCre	227
3.6.4. PCR-Based Analysis of MEF Clones	229
3.6.4.1. PCR Detection of Episomal Adenovirus Molecules	229
3.6.4.2. Recombination Specific PCR Strategy	229
3.6.5. Immunohistochemical Detection of p53 Status	233
3.6.6. SA $\beta$ -gal Detection	236
3.7. Discussion	236
<b>Chapter 4 – Inducible Gene Targeting of the Mouse p53 Gene</b>	<b>248</b>
4.1. Introduction – Inducible Gene Targeting	249
4.2. Inducible Gene Targeting of the Murine p53 Gene	254
4.2.1. Structure of the p53 Locus	254
4.2.2. Targeting Strategy	254
4.3. Aims	257
4.4. Inducible Gene Targeting Vector Construction	257
4.4.1. Obtaining a Genomic Clone Homologous to Target Locus	257
4.4.1.1. <i>In vivo</i> Cloning	260
4.4.2. Inserting the Floxed STOP Cassette Into pIVC	264
4.4.3. Testing pIGTV in BNN132 Cells	264
4.5. Summary	269
4.6. Inducible Gene Targeting	269
4.6.1. Introducing pIGTV Into ES Cells	269
4.6.2. The Screening Strategy	269
4.6.2.1. Southern Blot Analysis	270
4.6.2.2. Targeting Frequency	270
4.6.3. Cre-mediated Excisive Recombination	273
4.7. Discussion	273
<b>Chapter 5 – Discussion</b>	<b>278</b>
<b>Chapter 6 – Materials and Methods</b>	<b>286</b>
6.1. Manipulation of DNA	287
6.1.1. Transformation of Bacteria with Plasmid DNA	287
6.1.2. Calcium Chloride Preparation of Competent BNN 132 Cells	287
6.1.3. Preparation of Bacterial Glycerol Stocks	288
6.1.4. Small Scale Preparation of Plasmid DNA	288
6.1.5. Large Scale Preparation of Plasmid DNA	289
6.1.6. Restriction Digest Analysis of Plasmid DNA	290
6.1.7. Agarose Gel Electrophoresis of DNA	290
6.1.8. Extraction of DNA Fragments From Agarose Gels	291
6.1.9. DNA Ligation	292
6.1.10. Dephosphorylation of Vectors	293
6.1.11. Blunting 3' and 5' Overhangs of Linear DNA	293
6.1.11.a. Klenow Reaction	293
6.1.11.b. T4 DNA Polymerase	294

6.1.12. DNA Sequence Analysis	294
6.1.12.1. DNA Template Preparation	294
6.1.12.2. Dideoxy Sequencing	295
6.1.13. Southern Blotting	297
6.1.13.1. Preparation of DNA	297
6.1.12.3. DNA Transfer	297
6.1.12.4. Prehybridisation	298
6.1.12.5. Generation of Radiolabelled Probes	298
6.1.12.6. Hybridisation	298
6.1.14. Polymerase Chain Reaction	299
6.1.14.1. p53-Based PCR Strategies	299
6.1.14.1.a. FX PCR	299
6.1.14.1.b. F3K PCR	300
6.1.14.1.c. SR PCR	301
6.1.14.1.d. PCR To Genotype the p53 Status of Efs	301
6.1.14.1.e. p53 cDNA PCR	302
6.1.14.1.f. neo/In PCR	303
6.1.14.1.g. Southern Probe PCR	304
6.1.14.2. Other PCR Strategies	305
6.1.14.2.a. neo-EGFP PCR	305
6.1.14.2.b. CMV-EGFP PCR	306
6.1.14.2.c. Episomal Adenovirus Detection PCR	307
6.1.14.3. RT-PCR Strategies	308
6.1.14.3.a. Mouse $\beta$ -actin RT-PCR	308
6.1.14.3.b. EGFP RT-PCR	308
6.2. Embryonic Stem Cell Culture	309
6.2.1. Media Preparation	309
6.2.2. Culture Conditions	310
6.2.3. Passaging ES Cells	310
6.2.4. Freezing ES Cells	311
6.2.5. Defrosting ES Cells	311
6.2.6. ES Cell Electroporation	312
6.2.7. Picking and Maintaining Clones	312
6.2.8. Extraction of Genomic DNA from ES Cells	313
6.2.9. Karyotyping of ES Cells	313
6.2.10. Infection of ES and EF Cells With Recombinant Adenovirus	314
6.3. Detection of Marker Gene Expression	314
6.3.1. $\beta$ -galactosidase Histochemical Detection	314
6.3.1.1. Histochemical Detection of Bacterial $\beta$ -gal (pH 7.0)	314
6.3.1.2. Histochemical detection of Lysozomal $\beta$ -gal (pH 4.0)	315
6.3.1.3. Histochemical Detection of Mammalian SA $\beta$ -gal (pH 6.0)	316
6.3.2. $\beta$ -galactosidase Activity Quantification	317
6.3.2.1. Protein Extract Preparation	317
6.3.2.2. Protein Concentration Assay	317
6.3.2.3. $\beta$ -gal Enzyme Assay	318
6.3.3. Detection of EGFP Expression	318
6.3.3.1. Flow Cytometric Analysis of EGFP Expression in	

ES Cells	318
6.4. Embryonic Fibroblast Culture	319
6.4.1. Isolation of Primary Embryonic Fibroblasts	320
6.4.2. Preparation of Genomic DNA from Embryonic Fibroblasts	320
6.4.3. Calcium Phosphate Transfection of Embryonic Fibroblasts	320
6.4.4. Immunohistochemical Detection of p53 Protein in Embryonic Fibroblasts	321
6.5. Manipulation of RNA	323
6.5.1. RNA Extraction	323
6.5.2. Reverse Transcription	324
<b>References</b>	<b>325</b>
<b>Appendix 1 – Publications</b>	<b>371</b>

## **Acknowledgements**

I would like to begin by thanking my supervisors Dr Alan Clarke and Professor David Harrison for their support, advice and sense of humour. I am also grateful to the National Pathological Society of Great Britain and Ireland for the prize fellowship that paid the mortgage during my time in the lab. There are many people without whose help this work would never have been completed and to whom special thanks are owed. Sarah Howie for her flow cytometry expertise. Dominic Rannie for providing adenovirus on tap. Eleanor Duff for her “special” Christmas present. Bob Morris for ordering things when it wasn’t order day and I didn’t even have a grant. Sandrine Prost for proofreading above and beyond the call of duty and finally, Scott Lyons for too many things to name. A big thanks to everybody else for making the lab the place it is, funny, entertaining, rude and frequently downright offensive (you know who you are!). Finally a big thank you to David for convincing me to finish the damned project, putting up with me while I did so and picking up the pieces afterwards.



## Abbreviations

APRT	Adenine Phosphoribosyl Transferase
ATM	Ataxia Telangiecstasia Mutated
DT-A	Diphtheria Toxin-A
EC Cell	Embryonic Carcinoma
(E)GFP	(Enhanced) Green Fluorescent Protein
ENU	EthylNitrosourea
ES Cell	Embryonic Stem Cell
FS	Forward Scatter
HAT	Hypoxanthine, Aminopterin, Thymidine Medium
HATs	Histone Acetyltransferases
HDFs	Human Diploid Fibroblasts
HPRT	Hypoxanthine Phosphoribosyl Transferase
HR	Homologous Recombination
HSV-tk	Herpes Simplex Virus-thymidine kinase
IGT	Inducible Gene Targeting
IR	Ionising Radiation
LCR	Locus Control Region
LIF	Leukaemia Inhibitory Factor
MEFs	Mouse Embryonic Fibroblasts
m.o.i	Multiplicity of Infection
PCR	Polymerase Chain Reaction
RA	Retinoic Acid
RAGE	Recombinase Activated Gene Expression
ROS	Reactive Oxygen Species
rPPT	Rat preprotachykinin gene
RT-PCR	Reverse Transcription-Polymerase Chain Reaction
SS	Side Scatter
SV40 TAG	Simian Virus 40, T Antigen
6-tG	6-Thioguanine
UTR	Untranslated Region

## Abstract

The Cre/loxP site-specific recombinase system evolved within bacteriophage P1 as a mechanism to maintain correct unit copy segregation of the prophage within host cells. This thesis reports the application of this system to regulate gene expression in murine cells. To achieve the regulation of gene expression a novel floxed STOP cassette was designed, constructed and tested in murine embryonic fibroblasts (EF) and embryonic stem (ES) cells. It was shown that the floxed STOP cassette could be used successfully to regulate the transcription of the Enhanced Green Fluorescent Protein (EGFP) marker gene in ES cells. However, no expression of the EGFP gene could be detected at the protein level and several reasons for this observation are discussed.

The floxed STOP cassette was also utilised in strategies to achieve conditional expression of the tumour suppressor gene p53. A complex array of biological functions have been assigned to p53. For example, p53 is known to be involved in the regulation of apoptosis, multiple cell cycle checkpoints and the onset of replicative cellular senescence. The development of novel approaches to achieve conditional p53 expression should be a valuable tool and permit further investigation into the pleiotropic nature of p53 function. Therefore, the floxed STOP cassette was used to regulate the expression of a p53 cDNA in p53 null primary EF cells *in vitro*. The upregulation of p53 expression after Cre administration was detected, but at a low frequency, by immunohistochemistry. The response of EF cells to the expression of p53 in terms of replicative cellular senescence was also characterised, including the first description of senescence-associated  $\beta$ -galactosidase expression in any murine cell. The floxed STOP technology was also used in an attempt to regulate the expression of the endogenous murine p53 gene *in vivo*. The successful integration of the floxed STOP cassette, via an inducible gene targeting strategy, into the murine p53 locus of ES cells is reported.

Two methods were explored to achieve regulated expression of Cre recombinase *in vitro*, the novel technology of recombinant adenoviridae and the identification of embryonal stem cell differentiation state-specific promoter regulatory sequences.

In conclusion, this thesis has explored the feasibility of using Cre/loxP-based technologies to regulate gene expression. Several test plasmids were constructed and characterised and all demonstrated that the application of floxed STOP-based approaches is not as straightforward as suggested by the relatively small body of literature in this field.

# **Chapter 1**

## **Introduction**

# Chapter 1

## Introduction

### 1.1. Introduction

The relevance of animal models of human disease is particularly well illustrated with the example of cancer. The pathogenesis of cancer is a multi-step process characterised by the accumulation of critical genetic lesions within the cell. To date, many studies have described a bewildering variety of molecular genetic abnormalities, the significance of which to pathogenesis is often obscure. Indeed, it is probable that many of these abnormalities are epiphenomenal rather than of crucial importance. Furthermore, despite the value of such genetic and epidemiological approaches, they are limited and essentially descriptive. Thus considerable effort and resources have been directed towards creating accurate animal models of human diseases, such as cancer. Although animal models may never provide exact representations of a human disease, they do permit dissection of specific molecular and biochemical pathways that may be involved. Furthermore, they allow a variety of genetic manipulations that would be technically and ethically impracticable with human tissues.

### 1.2. Background - Animal Models of Human Disease

The mouse has become one of the most commonly used disease model systems. The reasons for this are manifold, their small size, relative resistance to infection, large litter size and a short generation time. Perhaps the most significant advantage in early studies was the observed variation in coat colour, the study of which allowed some of the earliest insights into mouse genetics. For example, the inheritance patterns of the coat colour marker albino was used for the first breeding experiment to demonstrate Mendelian inheritance in the mouse (Castle & Allen, 1903).

As the field of mammalian genetics expanded, researchers moved on to study and identify the genetic traits associated with non-coat colour related variations in mice. These studies resulted in the characterisation of over 1000 spontaneously arising

mutations (Doolittle, 1996). In depth analysis of such mutations revealed that many showed phenotypic similarities to human diseases. Hence, the potential of the mouse as a model system for human disease became apparent. However, it was obvious that a more efficient system for generating and characterising mutations was needed rather than relying on the spontaneous generation of interesting mutations. For example, several thousand genetic diseases are known in humans (McKusick, 1978) the vast majority of which have no direct parallel in experimental animals. One way of circumventing this problem was the use of random mutagenesis protocols, such as the treatment of male mice with ethylnitrosourea (ENU) or chlorambucil (Russell *et al*, 1989) and subsequently to screen offspring for dominant or recessive mutations. A notable success with this technique was the generation of *Min* mice (multiple intestinal neoplasia) that have a mutation in the mouse homologue of the human APC (adenomatous polyposis coli) gene (Moser *et al*, 1990). The introduced mutation results in the expression of a truncated *Apc* protein and these animals have provided a valuable model system for the related human disease, Familial Adenomatous Polyposis Coli (FAP) (Grodin *et al*, 1991). However, it should be noted that while human FAP patients and the *Min* mouse have mutations in homologous genes, the phenotypes are not identical (see Lovejoy *et al*, 1996).

Since the production of the first animal models of human disease, such as the *Min* mouse, technological advances and refinements of the concept being examined have led to increasingly accurate and informative models. For example, as individual genes important in disease processes were characterised, the newer technologies of transgenic mouse production and gene targeting allowed a more direct analysis of the molecular function of such genes. This work is discussed below.

### **1.2.1. Transgenic Mice**

The first reported transgenic mice were produced by injecting purified SV40 genomic DNA into the blastocoel cavity of mouse blastocysts. Viral DNA sequences could be detected in the tissues of resulting animals indicating the successful integration of viral genomes into host chromosomes (Jaenisch *et al*, 1974). Today transgenic mice

are most commonly produced by microinjection of DNA directly into the pronuclei of fertilised mouse eggs (Gordon *et al*, 1980).

Since their development, transgenic strains of mice have proved to be valuable tools in the study of the genetics and pathogenesis of many human diseases. Phenotypic alterations which occur as a direct consequence of transgene expression can provide evidence to implicate specific genes in a given disease process. Where transgene expression can be shown to model human disease, such mice could be used as test systems to determine the efficacy of treatment regimes and crossing onto different backgrounds may reveal extragenic modifiers of the phenotype.

However, the transgenic approach has limitations. For example, both the copy number and position of transgene integration cannot be predicted, yet both of these parameters can exert significant influence over phenotype (reviewed by Palmiter & Brinster, 1986). Also, because of the random nature of integration there is a significant risk of insertional mutagenesis. If the transgene integrates within a coding sequence and abolishes expression, the transgenic phenotype will be complicated by additional effects due to loss of expression of the endogenous gene. Perhaps the most significant drawback to transgenic models generated through pronuclear injection is the difficulty in creating null alleles as exogenous genetic material can only be added to the genome.

A major advance in our ability to create mouse models of human disease was the development of gene targeting technology that facilitates the introduction of specific mutations into the mouse germline.

### **1.2.2. Introduction of Specific Alterations into the Mammalian Genome**

Gene targeting is the term used to describe the introduction of defined genetic alterations into the genome of the mouse, an approach that takes advantage of two technological developments. Firstly, isolation and characterisation of pluripotent ES cell lines (see Section 1.2.2.1) and secondly, the harnessing of the cellular

homologous recombination machinery to permit site-specific mutagenesis (see Section 1.2.2.2). Together these provided a powerful tool for introducing specifically engineered mutations into ES cells, allowing the generation of precisely defined mutant mouse strains.

### **1.2.2.1. Mouse Embryo-Derived Cell Types**

#### **1.2.2.1.a. Embryonal Carcinoma Cells**

Two morphologically distinct cell populations can be distinguished within a 3.5 d.p.c. mouse embryo. Firstly, cells from the inner cell mass (ICM) and secondly those which form the trophectoderm. The second differentiation process that occurs in the blastocyst prior to implantation is the division of the ICM into primitive endoderm and epiblast (discussed in greater depth in Hogan *et al*, 1986). Several lines of evidence exist which demonstrate that the ICM and epiblast are the pluripotential tissues of the early embryo that constitute the germ-line and give rise to all somatic tissues of the embryo proper, in addition to some of the extraembryonic components (reviewed in Smith, 1992).

The ectopic grafting of early mouse embryos results in the high frequency generation of teratocarcinomas (Solter *et al*, 1970). Grafts from 8.5 d.p.c. embryos generate only fully differentiated, benign teratomas, whereas approximately 50% of grafts from 6.5-7.5 d.p.c. embryos give rise to malignant teratocarcinomas (Damjanov *et al*, 1971). Both teratocarcinomas and teratomas arise by differentiation from a pluripotential malignant cell population, the embryonal carcinoma (EC) cells. If all the EC cells in a tumour differentiate, the result is a teratoma. However, any residual undifferentiated EC cells give rise to a malignant teratocarcinoma. The epiblast origin of such tumours has been established by dissection of the embryos prior to ectopic grafting (Diwan & Stevens, 1976).

EC cells share a high level of morphological, ultrastructural and biochemical identity with ICM/epiblast cells. Indeed there is evidence that EC cells do not differ intrinsically in any irreversible way from normal epiblast cells, but are malignant due



to an abnormal microenvironment. For example, some EC cell lines are able to contribute to the host ICM when reintroduced into a blastocyst (Mintz & Illmensee, 1975) or aggregated with morulae (Stewart, 1982). Although pluripotency of a specific EC cell line has been reported (Stewart & Mintz, 1981), the vast majority of such cell lines are aneuploid. This has imposed significant limitations on the application of the EC cell system for the transgenic modification of the mouse germ-line or as a model system for the study of mouse embryogenesis.

#### **1.2.2.1.b. Embryonal Stem Cells**

These limitations were circumvented in 1981 with publications from two laboratories which reported the derivation of non-transformed, pluripotential early embryonic stem cells, ES cells (Evans & Kaufman, 1981; Martin, 1981). ES cells were derived from the ICM of 3.5 d.p.c. blastocysts and were initially maintained *in vitro* by co-culture with feeder layers. Extensive ES cell differentiation was observed when the cells were cultured in the absence of feeder cells, implying that the maintenance of the undifferentiated stem cell phenotype is an active process (Smith & Hooper, 1987). The need for co-culture with feeder layers was bypassed with the discovery that undifferentiated ES cells could be maintained in medium conditioned by the Buffalo rat liver cell line BRL (Smith & Hooper, 1987). The macromolecule subsequently identified as a potent inhibitor of ES cell differentiation was Differentiation Inhibiting Activity (DIA) (Williams *et al*, 1988), identical to the previously described D-Factor (Tomida *et al*, 1984) or Leukaemia Inhibitory Factor (LIF) (Gearing *et al*, 1987). The culturing of ES cells in the presence of DIA/LIF and medium additionally supplemented with  $\beta$ -mercaptoethanol and serum is sufficient to maintain an undifferentiated pluripotential population (Nichols *et al*, 1990). However, even with these culture conditions a background of spontaneous differentiation is observed (reviewed in Smith, 1992).

#### **1.2.2.1.c. ES Cell Differentiation**

As already mentioned, if ES cells are cultured at low density in the absence of LIF, differentiation occurs, generating cells which are morphologically distinct from the

starting population (Smith & Hooper, 1987). The population of differentiated cells is thought to contain a mixture of endoderm and ill-defined mesoderm-like cells (Mummery *et al*, 1990).

ES cells cultured at higher density in the absence of LIF proliferate, forming groups of cells. Cell clumps can either be dislodged manually or cultured on bacterial grade plasticware in which case they never adhere. The end result of either approach is the same; the production of suspension aggregates containing differentiated ES cells. These aggregates are called embryoid bodies due to their superficial resemblance to the egg cylinder of a day 6 mouse embryo. The level of differentiation of the cells which constitute an embryoid body can be further increased by allowing them to adhere to a tissue culture dish and form outgrowths (discussed in greater depth in Hooper, 1992).

ES cell differentiation can also be induced by retinoic acid (RA) exposure. Interestingly, the exposure of ES cells to RA can give rise to distinct differentiation products depending on the presence or absence of LIF (Mummery *et al*, 1990). Furthermore, concentration dependent effects have also been observed when embryoid bodies are exposed to RA (Fisher *et al*, 1989). Exposure to specific growth factors can also influence the differentiation products generated from embryoid bodies, for example, nerve growth factor exposure increases the yield of neuron-like cells (Wobus *et al*, 1988).

Despite characterisation of the morphological endpoints of ES cell differentiation, the underlying molecular changes are unclear. However, recent research has identified some of very early events after the induction of differentiation. For example, Stat5 is not expressed in undifferentiated ES cells yet transcripts were detectable as early as 12 hours after treatment with RA and 36 hours after withdrawal of LIF (Nemetz & Hocke, 1998). In addition, ES cells cultured in the presence of LIF express low or undetectable levels of cyclin E/CDK2, p21, p27 and Cyclin D/CDK4. Withdrawal of LIF stimulates the upregulation of expression of all of the above and activates the

expression of *Brachury* and *Goosecoid*, two early markers of mesoderm differentiation (Savatier, 1995).

#### 1.2.2.1.d. ES Cell-Mediated Transgenesis

As with EC cells, ES cells can also be re-introduced into blastocysts to generate chimaeric progeny (Bradley *et al*, 1984). However, while the abnormal karyotype characteristic of the majority of EC cell lines makes germ-line colonisation infrequent, the normal chromosome complement of ES cells allows reproducible germ-line colonisation. The pluripotential nature of ES cells made them an ideal system with which to attempt transgenic manipulation of the mouse genome but to achieve this goal, the twin technologies of genetic manipulation *in vitro* and ES cell germ-line transmission needed to be combined. Despite initial problems (Stewart *et al*, 1985; Evans *et al*, 1985), in 1986 the first paper was published which reported the successful generation of transgenic mice via the ES cell route (Gossler *et al*, 1986). This early work focussed on the addition of genetic material to ES cells either by transfection or retroviral infection but the logical next step was the manipulation of specific endogenous genes. This was achieved by two independent research groups working on the same gene, *hypoxanthine guanine phosphoribosyl transferase (Hprt)* (Hooper *et al*, 1987; Kuehn *et al*, 1987). The *Hprt* gene was an ideally suited to this approach for several reasons. In both humans and mice the gene is X-linked thus male cells are hemizygous, *Hprt* null cells can be separated from their wild type counterparts on the basis of altered drug sensitivity and the generation of *Hprt* null mice offered the tantalising possibility of a mouse model of the human disease, Lesch-Nyhan syndrome which is caused by *Hprt* deficiency (Nyhan, 1973). Although both groups were successful in introducing mutations into the *Hprt* gene and subsequent generation of mutant mice no phenotypic alterations were observed in these animals. Further work suggested that differences in purine metabolism between mice and humans were to blame for the absence of a phenotype in the *Hprt* null animals (Redhead *et al*, 1996). Nevertheless, this work was a crucial breakthrough that simultaneously demonstrated both the potential of this technology and the limitations of mouse models of human disease.

The generation of *Hprt* null mice was not achieved by gene targeting and instead relied on random mutagenesis, either chemical or insertional. While these approaches demonstrated the feasibility of ES cell genetic manipulation *in vitro* and subsequent return to host blastocysts they were unsuitable for the specific modification of non-selectable genes. It was with this aim in mind that gene targeting was developed (see Section 1.2.2.3.)

#### **1.2.2.2. Homologous Recombination**

Homologous recombination (HR) describes the process of DNA strand breakage and reunion which occurs between chromosomes within regions of sequence homology. This process occurs in prokaryotic organisms and in eukaryotic organisms during meiosis, mitosis and DNA repair (reviewed in Bollag *et al*, 1989).

HR in mammalian cells can occur between introduced exogenous DNA molecules (Extra-Chromosomal Recombination, ECR), between homologous sequences within a chromosome (Intra-Chromosomal Recombination, ICR), between homologous sequences on sister chromatids (Inter-Chromosomal Recombination) and finally between an introduced piece of DNA and a chromosomal sequence (gene targeting). All of these types of recombination are thought to proceed by similar, but poorly defined, molecular mechanisms within cells.

Two major models have been proposed to explain homologous recombination. Both postulate that HR is initiated by the generation of a single strand of DNA (ssDNA). The free end of the ssDNA molecule subsequently invades a homologous double stranded DNA duplex producing a heteroduplex structure. As the donor ssDNA molecule pairs with the recipient dsDNA sequence a loop of uncut recipient DNA (D-loop) is displaced from the heteroduplex. The two models differ in the mechanism by which this structure is resolved. In the Meselson-Radding model of

**Figure 1.1** - *The Meselson-Radding Model of Homologous Recombination*

The Meselson-Radding Model of Homologous Recombination.

- A) Recombination is initiated by the formation of a single strand nick in one DNA molecule.
- B) At the 3' end of the nick site repair synthesis begins leading to the displacement of the single strand of DNA which then invades the other DNA duplex. This invasion displaces a D-loop in the other homologue.
- C) The D-loop is degraded and an asymmetric heteroduplex is created.
- D) Ligation produces a Holliday junction that is able to migrate along the DNA molecules.
- E) The Holliday junction can be resolved in two ways firstly, by simply cutting the crossed strands giving the recombination products shown. Such products are the result of gene conversion without crossover.
- F) In the second alternative, the Holliday junction undergoes isomerisation and then strand cleavage generating crossover products, also with segments that have undergone gene conversion.

**Figure 1.1** – *The Meselson Radding Model of Homologous Recombination*

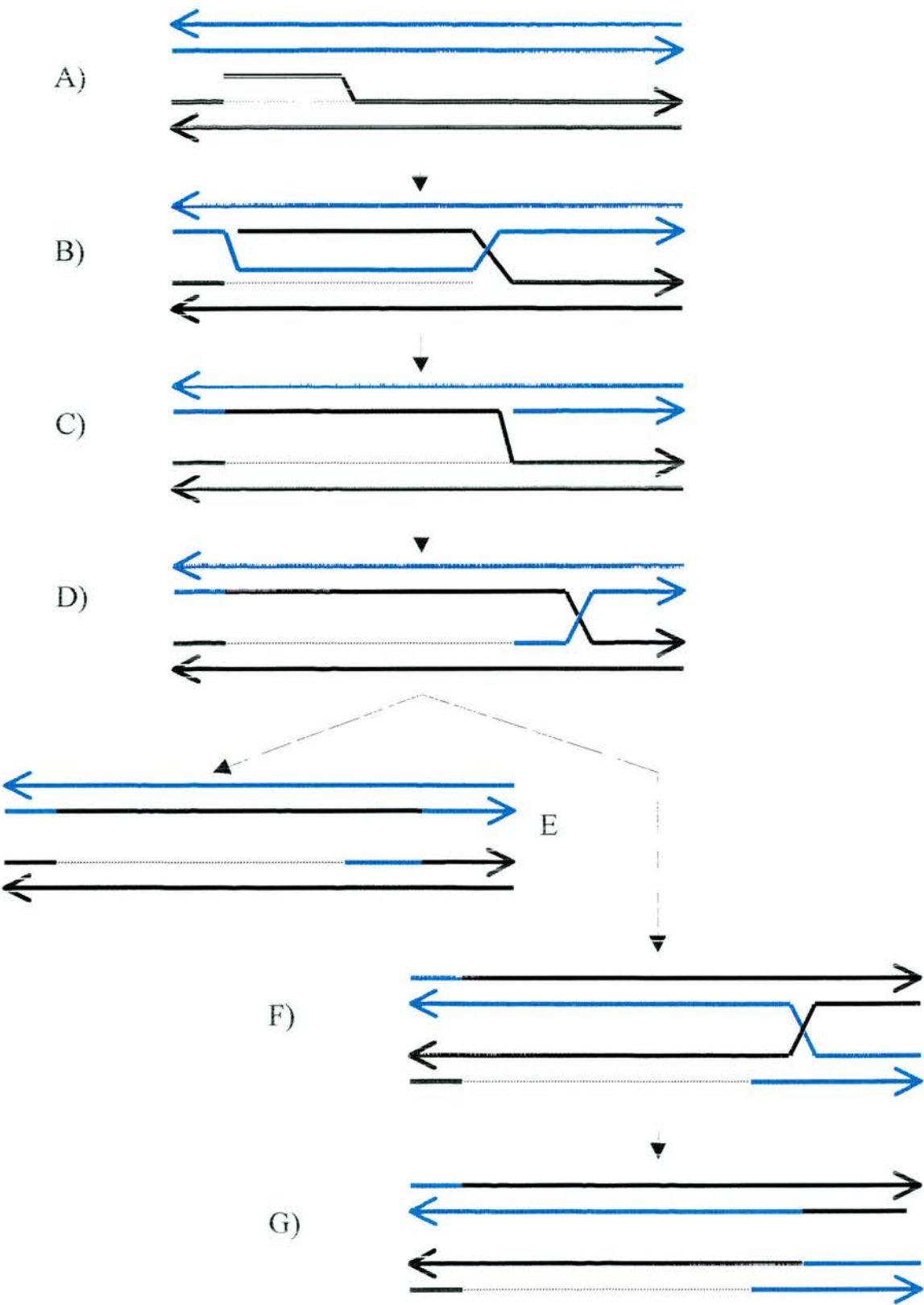


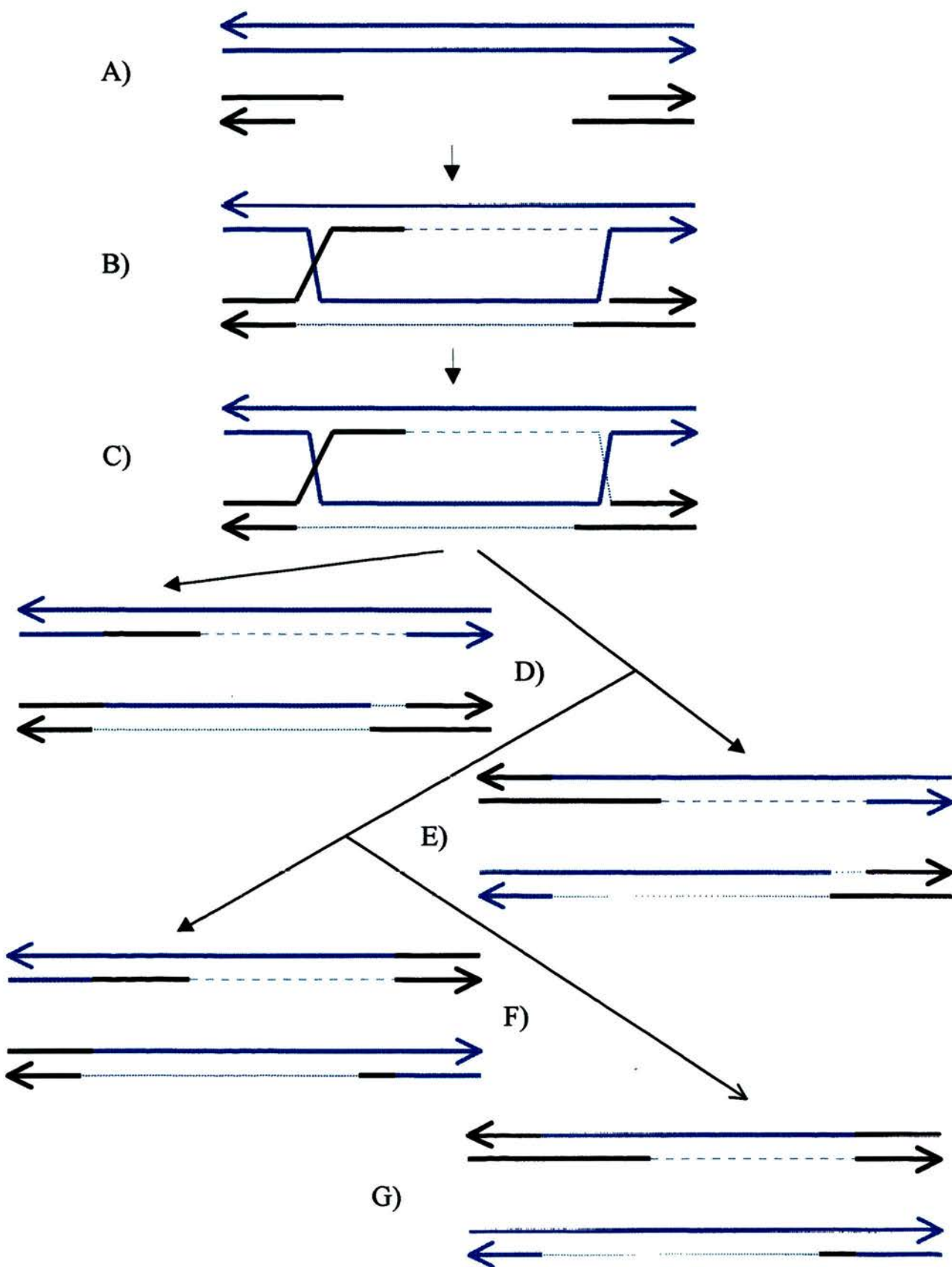
**Figure 1.2 –*The Double Strand Break Model of Homologous Recombination***

The Double Strand Break Model of Homologous Recombination.

- A) Recombination is initiated by the formation of a double strand break in one DNA molecule.
- B) One single strand DNA molecule from the double strand break site then invades the duplex of the other homologue leading to the displacement of a D-loop which is enlarged by repair synthesis. To complete the repair of the double strand break, repair synthesis is initiated from the second 3' end at the original double strand break site.
- C) Ligation then generates two Holliday junctions, both of which can move via branch migration. The two Holliday junctions can be resolved in four different ways.
- D) Neither junction undergoes isomerisation and the crossed strands within the junctions are cut.
- E) If the left hand Holliday junction undergoes isomerisation the recombination products shown in E) are the outcome.
- F) If the right hand Holliday junction undergoes isomerisation the recombination products shown in F) are the outcome.
- G) If both the left and right hand Holliday junctions undergo isomerisation the recombination products shown in G) are the outcome.



**Figure 1.2 – The Double Strand Break Model of Homologous Recombination**





HR the D-loop is degraded creating a free end of ssDNA in the recipient molecule (Meselson & Radding, 1975). The free ssDNA end in the recipient is then able to ligate to the remaining free end in the donor molecule forming an exchange structure called a Holliday Junction (Holliday, 1964) (Figure 1.1). The Double-Strand Break-Repair Model of homologous recombination also envisages the generation of a D-loop but rather than this sequence being degraded it acts as a template for repair synthesis of the donor strand (Orr-Weaver *et al*, 1981). After repair synthesis is complete ligation of free ssDNA ends results in the formation of two Holliday Junctions (Figure 1.2). In both of these models the junction(s) between the two homologues are able to migrate along the DNA by continued strand transfer within the crossover(s). Depending on how the Holliday Junctions are resolved several outcomes are possible, the reciprocal exchange of genetic material (crossover), a non-reciprocal exchange (gene conversion), or a gene conversion with an associated crossover (Figure 1.3).

#### **1.2.2.3. Gene Targeting**

The term gene targeting is used to describe the introduction of defined modifications into specific chromosomal loci via HR with exogenous DNA sequences (termed targeting vectors). The first endogenous gene to be modified by HR with a targeting vector was the human  $\beta$ -globin gene (Smithies *et al*, 1985) and the targeted modification of different loci within other non-ES cell lines has since been reported by other groups (for example, Adair *et al*, 1989).

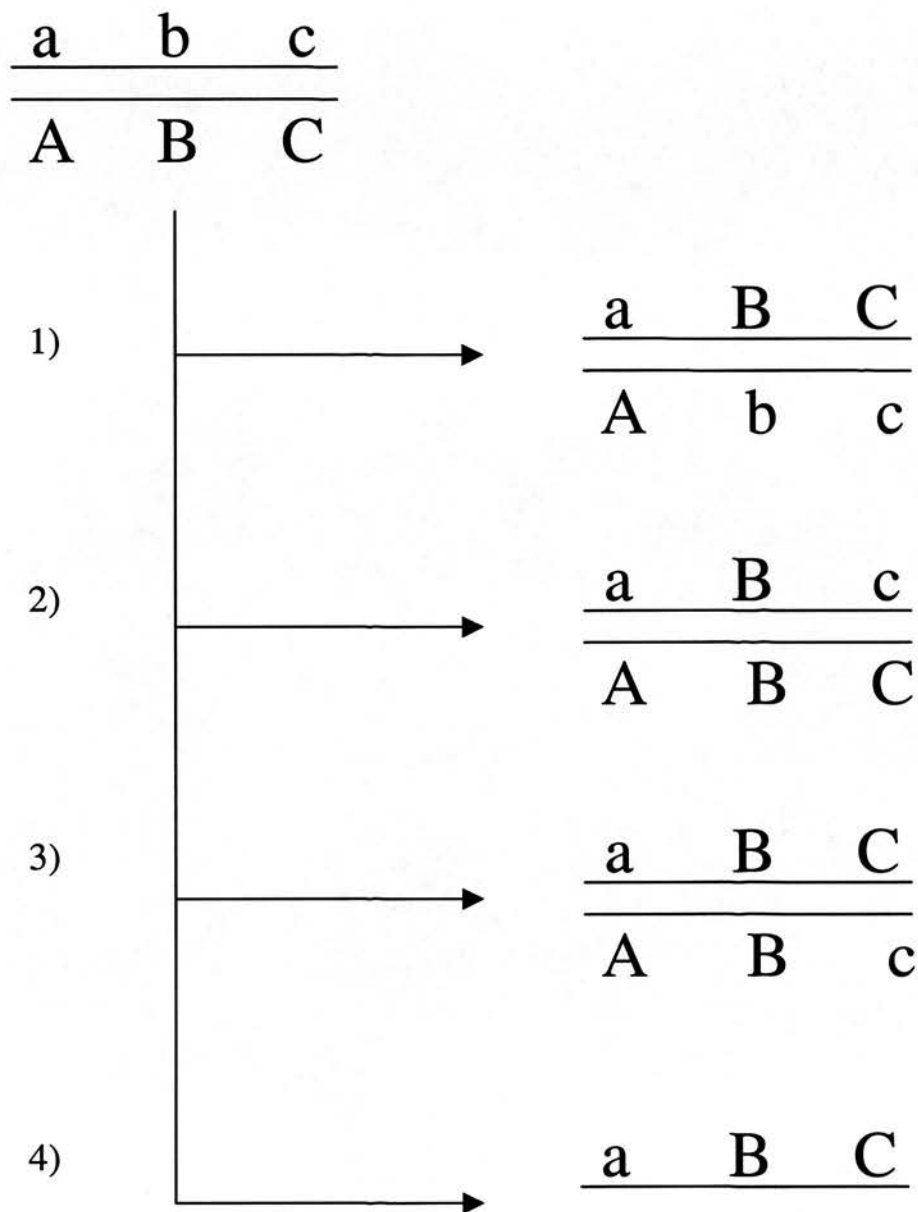
For the same reasons that the endogenous *Hprt* gene was the target of early mutagenesis strategies (Section 1.2.2.1), it was also used for the development and optimisation of gene targeting protocols in ES cells. Subsequently, two groups reported the disruption of the gene via HR in ES cells (Doetschman *et al*, 1988; Thomas & Capecchi, 1987). The application of gene targeting to non-selectable genes required the development of novel targeting strategies and this work is summarised in the following sections.

### **Figure 1.3 – *Types of Recombination Event***

If the two DNA duplexes shown at the top of this figure undergo recombination there are four types of outcome (one thick black line represents a double stranded DNA duplex).

- A) Reciprocal exchange when there is a straightforward exchange of genetic material between the DNA duplexes.
- B) Gene conversion occurs after a non-reciprocal exchange of genetic material whereby the genetic information is copied from one duplex to another.
- C) Gene conversion with an associated crossover.
- D) Non-conservative recombination. As the name implies, when DNA duplexes undergo this type of recombination event, DNA is lost from opposite ends of the molecules and the remaining DNA is sufficient only to reconstitute one duplex.

**Figure 1.3** –Types of Recombination Event



#### **1.2.2.4. Gene Targeting Strategies**

##### **1.2.2.4.a. Insertion Type (O-Type) Targeting Strategies**

Insertion type targeting strategies have been developed to allow the introduction of subtle mutations into target genes by a two step approach termed either 'Hit and Run' (Hasty *et al*, 1991) or 'In-Out' (Valancius & Smithies, 1991) (Figure 1.4). In the first stage of this process O-type targeting vectors, linearised within the region of homology, integrate into the genome via a single crossover event within the region of homology. This insertion event creates a duplication of the region of homology within the targeted genomic locus but importantly specific mutations can be introduced into the targeting vector. In the second stage of this process, reversion, the duplication of homology is resolved via intra-chromosomal HR. Two outcomes are possible, the first is that all integrated vector derived sequences are lost and the locus is restored to wild type. The second is that vector derived homologous sequences, including any engineered mutations, are retained and a region of chromosomal sequence is lost.

Interestingly, significantly different targeting and reversion frequencies have been reported by groups using identical strategies on different loci. For example, when 'Hit and Run' targeting was used to create duplications of homology at both the *Hprt* and *Hox-2.6* loci, the frequency of reversion was 1000 times greater at the *Hox-2.6* locus (Hasty *et al*, 1991). Hence, while this work demonstrated the feasibility of insertion type targeting strategies it also highlighted the locus-dependent nature of both targeting and reversion frequencies.

##### **1.2.2.4.b. Replacement Type ( $\Omega$ -Type) Targeting Strategies**

A typical replacement targeting vector consists of two regions of DNA homologous to the target locus that are interrupted by a positive selection marker e.g. *neomycin phosphotransferase (neo)* or *puromycin N-acetyltransferase (pac)* (see Section 1.2.2.6). This type of vector is linearised outwith the regions of homology as the aim is to insert only the selectable marker, not the whole vector, into the chromosome. The selectable marker can either replace part of the genomic sequence and so

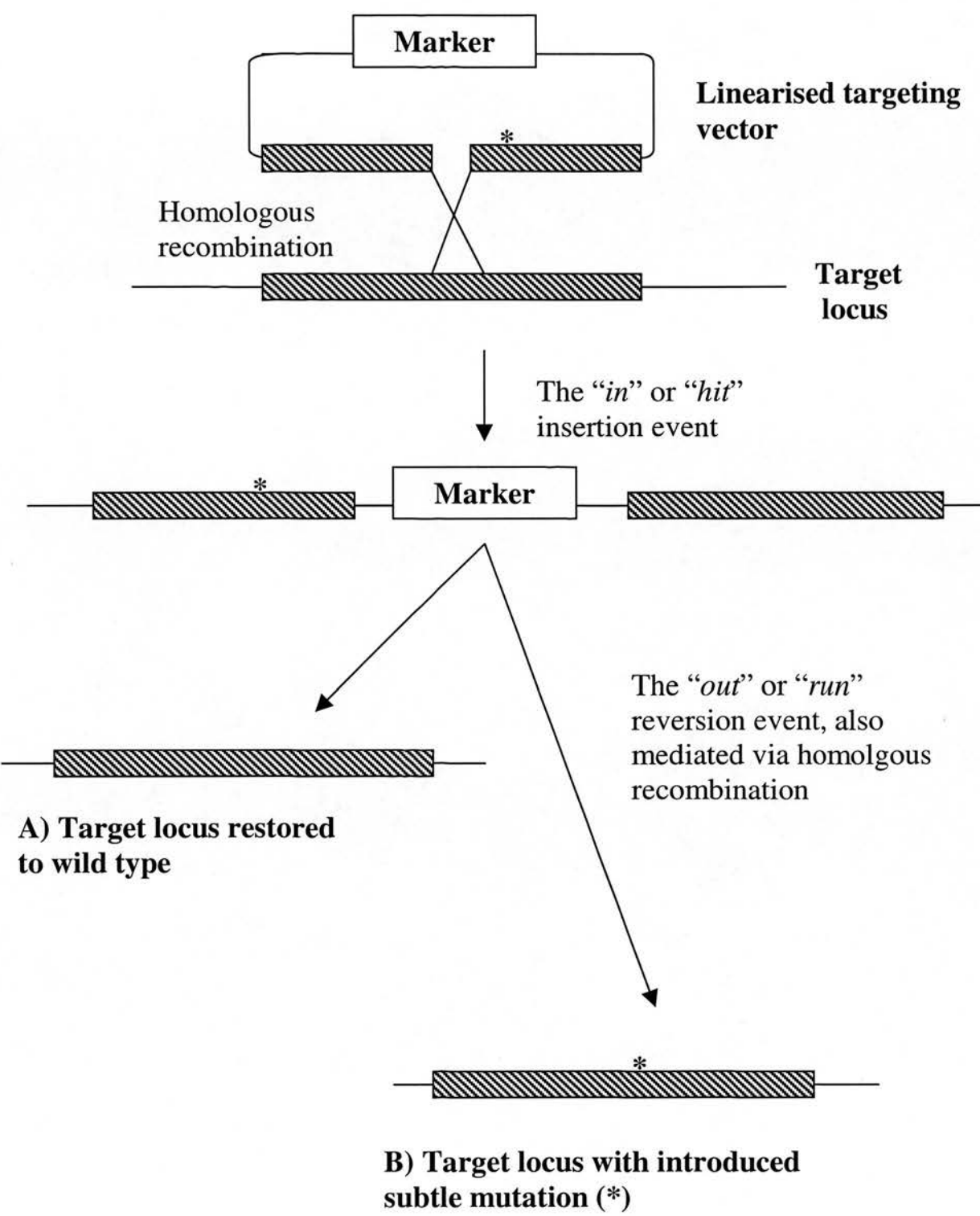
### **Figure 1.4 – An Insertion or “In and Out” Gene Targeting Strategy**

Insertion type targeting vectors are linearised within the region of homology (hatched boxes). When such vectors are introduced into cells, a single crossover event mediated by homologous recombination between the chromosomal target sequence and the region of the homology, results in the integration of the complete vector into the target locus. This is referred to as the “in” or “hit” event and generates a duplication of homology within the target locus. The duplication of homology can be resolved in two ways.

- A) Homologous recombination results in the loss of all targeting vector derived sequences from the target locus, which is consequently restored to wild type.
- B) Homologous recombination results in the excision of some targeting vector derived sequences but also some chromosomally derived sequences from the target locus. Crucially, the original region of homology present within the targeting vector is retained within the target locus and if this had been previously engineered to contain subtle mutations (\*), these will be introduced in the target locus.

Both ways of resolving the duplication of homology are referred to as either the “out” or “run” event. The types of selectable markers that can be incorporated into insertion type targeting vectors are discussed in Section 1.2.2.6.

**Figure 1.4 – An Insertion or “In and Out” Gene Targeting Strategy**

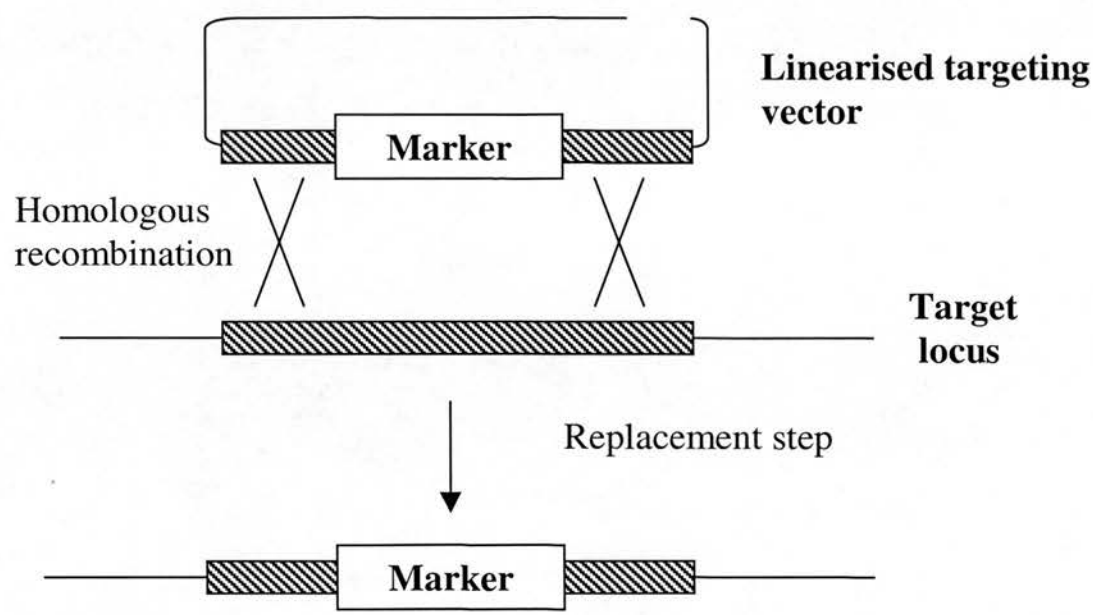


introduce a deletion, or insert into the genomic sequence thereby disrupting the target gene. Both outcomes are therefore designed to disrupt expression of the endogenous gene (Figure 1.5). This simple replacement strategy can be used successfully to create null alleles but it cannot be used to introduce subtle non-selectable mutations. To address this difficulty the basic replacement strategy has been further developed in the “Double Replacement” (Stacey *et al*, 1994) or “Tag and Exchange” methods (Askew *et al*, 1993) (Figure 1.6).

Both of these methods involve two separate rounds of gene targeting with two separate vectors, the outcome of which is the introduction of subtle non-selectable mutations into a target gene. The first step uses a normal  $\Omega$ -type vector with a positive selectable marker. The resultant clones are screened and any that have correctly undergone the first round of homologous recombination, are electroporated with a second vector. This vector replaces the previously introduced selectable marker in the target locus with sequence containing a non-selectable mutation via a second round of homologous recombination. The second recombination event is selected for using negative selection so that only clones which have lost the selective marker and gained the introduced mutation will survive.

Another variation on this theme is the “Plug and Socket” (Detloff *et al* 1994) (Figure 1.7). In this system the first round targeting vector introduces one functional and one crippled positive selection marker into the target locus via HR. The second round vector carries DNA sequences which undergo HR with the integrated first vector, resulting in the deletion of the functional positive selection gene, simultaneous reconstitution of the crippled marker and the introduction of any predetermined mutations into the target locus. Such clones can then be selected for on the basis of expression of the crippled marker gene. This system has the advantage that expression of the crippled marker gene is strictly dependent upon HR, unlike the double replacement or tag and exchange strategies in which loss of the negative selectable gene can occur by HR-independent mechanisms. Nevertheless, these methods do have the advantage of not leaving any marker sequence at the target

**Figure 1.5** – A Replacement Gene Targeting Strategy



Replacement type targeting vectors are linearised outwith the region of homology (hatched boxes). When such vectors are introduced into cells, a double crossover event mediated by homologous recombination between the chromosomal target sequence and the vector-derived region of the homology, results in the replacement of part of the target locus with the marker cassette and surrounding vector derived homologous sequence. This type of replacement targeting strategy is commonly used to insert selectable marker cassettes within the coding sequence of a target gene generating a null allele.

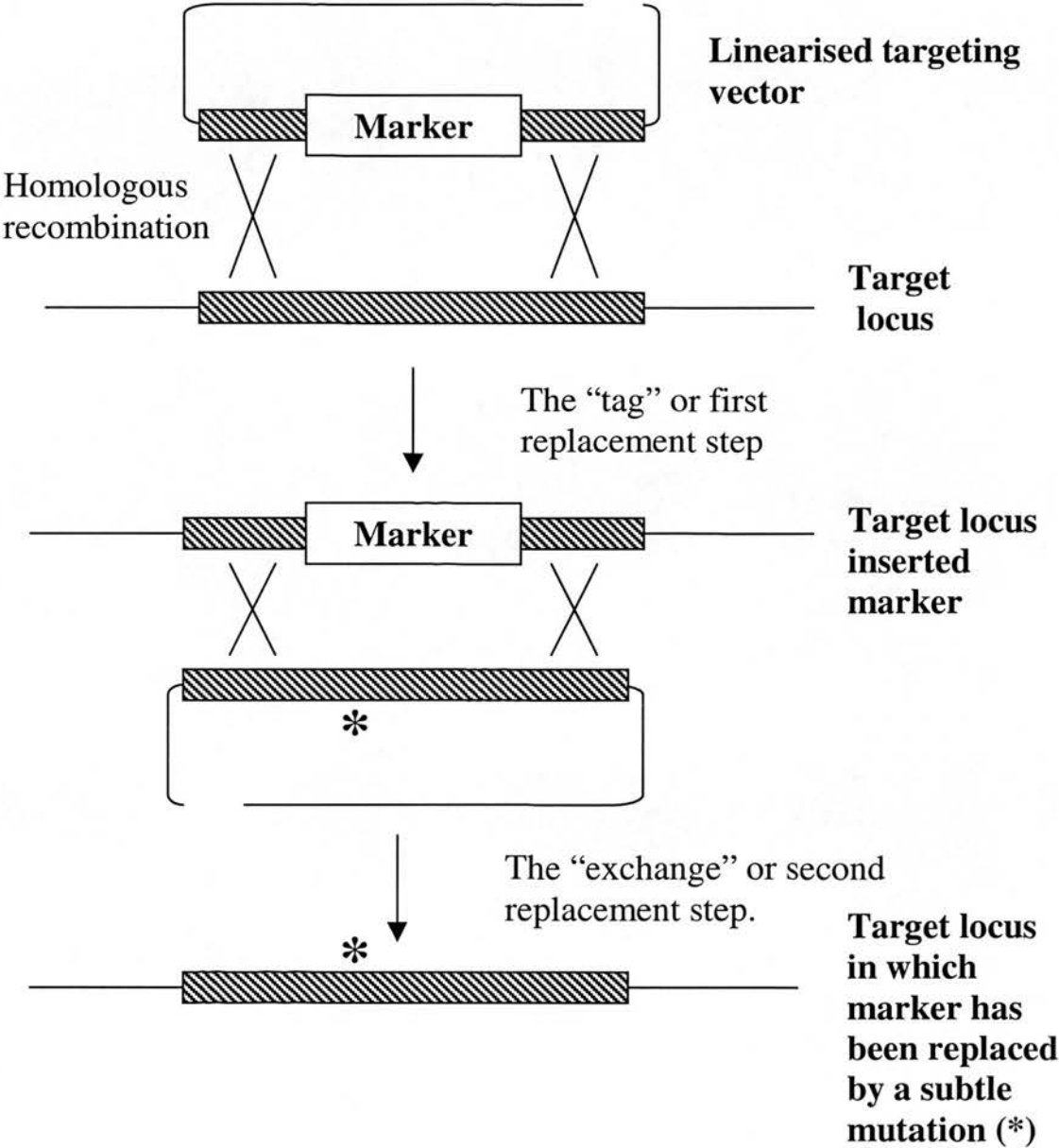


**Figure 1.6** – *Double Replacement and Tag and Exchange Gene Targeting*

Tag and Exchange gene targeting strategies are mediated by two rounds of replacement gene targeting (see also previous figure). In the “tag” or first replacement step a standard linearised replacement targeting vector is introduced into cells. The vector is linearised outwith the region of homology (hatched boxes) and a double crossover event mediated by homologous recombination between the chromosomal target sequence and the vector-derived region of the homology, results in the replacement of part of the target locus with the marker cassette and surrounding vector derived homologous sequence.

In the second replacement step, or “exchange”, another targeting vector is introduced into cells which are known to have undergone the first replacement step. A double crossover event mediated by homologous recombination then exchanges the chromosomally integrated marker gene for sequences derived from the second targeting vector. Importantly, if the second replacement vector was previously engineered to contain a subtle, non-selectable mutation this will be introduced into the target locus. The types of selectable markers used Tag and Exchange or Double Replacement targeting strategies are discussed in more detail in Section 1.2.2.6.

**Figure 1.6 – Double Replacement and Tag and Exchange Gene Targeting**



locus after completion of the second round of targeting whereas after the plug and socket strategy is complete the reconstituted crippled marker gene is retained.

The types of selectable markers that can be used in these strategies are discussed in more detail in Section 1.2.2.6.

#### **1.2.2.5. Factors Affecting Homologous Recombination**

Gene targeting takes advantage of the fact that HR will occur between introduced exogenous sequences and endogenous chromosomal sequences within mammalian cells. The ratio of HR events to random integrations in mammalian cells is about  $10^{-3}$  (Thomas & Capecchi, 1987) and while the exact molecular details of HR are unclear several key parameters that affect its efficiency have been defined.

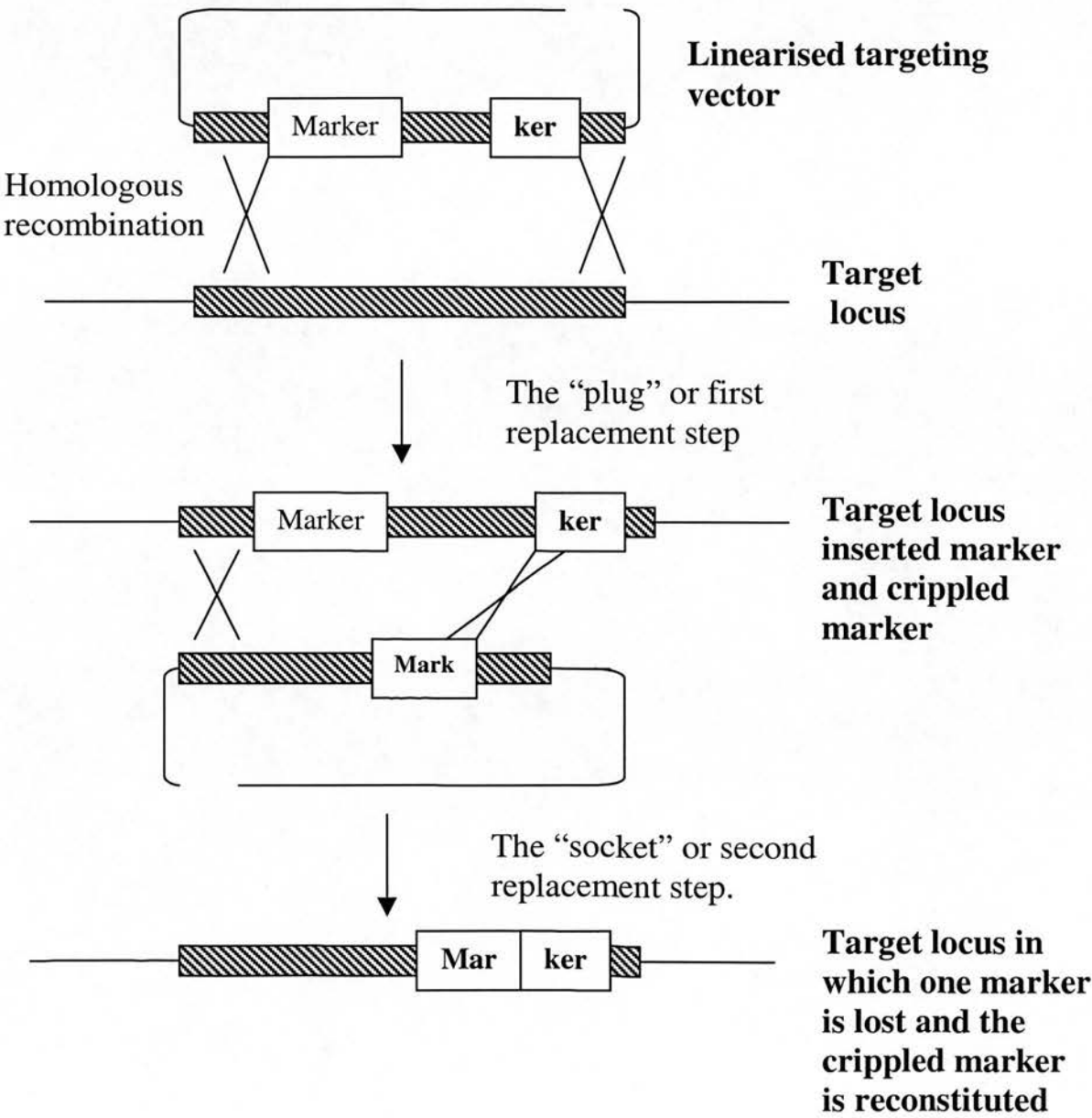
One significant factor is the extent of the homology between the targeting vector and the chromosomal DNA. In general, the greater the homology the more efficient the process (Thomas & Capecchi, 1987). Importantly, homologous recombination efficiency is unaffected by the length of non-homologous sequence introduced, for example, selectable markers included within the targeting vector (Mansour *et al*, 1990). When gene targeting was first developed it was thought that the rate limiting step in the process would be the search by the targeting vector for cognate homologous sequences within the chromosomal DNA. However, it has been demonstrated that targeting efficiencies are unaltered by both the number of target sequences in the genome (Zheng & Wilson, 1990) and the number of DNA molecules introduced into each cell (Thomas *et al*, 1986). Therefore, electroporation conditions have been optimised to result primarily in single-site, single-copy insertions of targeting vector DNA (Thomas & Capecchi, 1987). These conditions dramatically reduce the probability of homologous and non-homologous recombination events occurring within one cell without reducing the actual frequency of homologous recombination.

### **Figure 1.7- Plug and Socket Gene Targeting**

Plug and Socket gene targeting strategies are mediated by two rounds of replacement gene targeting in a manner analogous to Tag and Exchange targeting. The only difference between the two types of strategies is the selectable marker used. In the first replacement step or “plug”, a replacement targeting vector, linearised outwith the region of homology is introduced into cells. A double crossover event mediated by homologous recombination between the chromosomal target sequence and the vector-derived region of the homology, results in the replacement of part of the target locus with vector derived sequences. The vector-derived sequences introduced into the target locus include a functional positive selectable marker and a crippled positive selectable marker. It should be noted that a single crossover event and subsequent branch migration of the Holliday junction could equally well mediate this type of targeting event.

In the second replacement step, or “socket”, another targeting vector is introduced into cells that are known to have undergone the first replacement step. A double crossover event mediated by homologous recombination then exchanges the chromosomally integrated marker gene for sequences derived from the second targeting vector. This reaction simultaneously deletes the first positive selectable marker from the target locus and reconstitutes the second positive selectable maker. Hence, unlike Tag and Exchange the outcome of this type of strategy is the introduction of a marker cassette into the target locus rather than a subtle non-selectable mutation.

**Figure 1.7** – *Plug and Socket Gene Targeting*



The presence of DNA ends has also been shown to increase the frequency of recombination (Folger *et al*, 1982). This effect is concentration dependent, when high levels of plasmid DNA are introduced into mammalian cells the frequency of insertion is independent of the physical form of the DNA, supercoiled or linear. However, at lower DNA levels the frequency of linear plasmid DNA insertion was approximately 40 times greater than for supercoiled (Folger *et al*, 1982). These observations led to the hypothesis that linear DNA molecules may be an obligatory reaction intermediate for recombination to occur between host chromosomes and exogenous DNA hence linearised targeting vectors are used in gene targeting experiments.

Cell cycle position also alters the ability of a cell to mediate homologous recombination, a peak of activity has been reported in early S phase (Wong & Cappechi, 1987). Furthermore, the efficiency of gene targeting is also significantly affected by the cell cycle rate of an ES cell culture, higher efficiencies are observed in cultures with shorter mean doubling times (Udy *et al*, 1997). The effect of transcriptional activity at the target locus on recombination efficiency is unclear. Early reports showed that homologous recombination efficiencies were not significantly different between transcriptionally active and silent loci (Smithies *et al*, 1985) however contradictory evidence has subsequently been published (Nickoloff & Reynolds, 1990). Perhaps the major consideration about the transcriptional status of a target gene should be the type of selection system used, for example a targeting strategy based on the use of promoter-less selectable cassette can only be applied to genes that are actively expressed in ES cells (discussed in more depth in Section 1.2.2.6.d).

#### **1.2.2.6. Introducing Exogenous DNA into ES cells and Identifying Recombinants**

In order for recombination to occur between an exogenous DNA molecule and a chromosomal target it is first necessary to introduce the DNA into ES cells. As discussed above electroporation has become the method of choice. However,

because of the relatively low transfection efficiencies only a minority of cells will carry the introduced DNA (transformation frequencies of  $10^{-5}$  to  $10^{-2}$  have been reported, reviewed in Mansour, 1990). Therefore, it is necessary to select the successfully transfected cells, usually by the acquisition of a novel drug resistance, via the introduction of appropriate expression cassettes included in the targeting construct. The strategies used to select transfected cells can be grouped into three types, positive selection, positive/negative selection (PNS) and the use of promoter-less selectable genes. The relative advantages and limitations of all of these approaches are discussed below.

#### **1.2.2.6.a. Positive Selection**

All cells that acquire a positive selectable drug resistance gene should survive exposure to the corresponding drug at an appropriate concentration. Examples of this type of system include the bacterial *neomycin phosphotransferase* gene (*neo*) which confers resistance to the neomycin analogue G418 (Southern & Berg, 1982), the *hygromycin phosphotransferase* (*hyg*) and *puromycin N-acetyltransferase* (*pac*) genes which confer resistance to hygromycin B (Te Riele *et al*, 1990) and puromycin (Vara *et al*, 1985) respectively.

The electroporation of a targeting vector into a population of cells will result in the uptake and integration of that DNA molecule into the genome of a proportion of those cells. If one of the above positive selection markers was included in the introduced targeting vector then the exposure of the cell population to the corresponding drug will select for cells which have acquired the novel drug resistance. However, the introduced DNA may be incorporated into the cell genome in two ways. Firstly and most frequently, via random integration or secondly, via homologous recombination. This simple positive selection strategy is unable to distinguish between these two alternatives and has been superseded by the more sophisticated strategies discussed below.

#### **1.2.2.6.b. Positive/Negative Selection**

Positive/negative selection (PNS) was devised in an attempt to enrich the selected cell population for those in which HR-mediated rather than random integration events have occurred.

The PNS strategy relies on the observations that random integration proceeds through and preserves the ends of incoming, exogenous DNA vectors whereas HR does not require that the ends of the vector be homologous with the target sequence (Thomas *et al*, 1986). Therefore a PNS replacement vector carries an independently expressed positive selectable marker (Section 1.2.2.6.a) and a negative selectable marker that is placed within the plasmid backbone, outwith the region of homology used for HR. Random integration of the PNS vector will preserve the negative selectable marker and this can be used for counter-selection with an appropriate drug. During HR however, the negative selectable gene is lost as it is located distal to the region of homology between vector and target and so is excluded from the crossover event. The most frequently used negative drug selection marker is the Herpes simplex virus *thymidine kinase* gene (*HSV-tk*) (Mansour *et al*, 1988) although other genes such as a diphtheria toxin A (DT-A) have been used successfully (Yagi *et al*, 1990). The expression of *HSV-tk* renders cells sensitive to the nucleoside analogues FIAU (Borelli *et al*, 1988) and gancyclovir (Mansour *et al*, 1988) whereas the DT-A gene encodes an intrinsically toxic protein (Pappenheimer, 1977).

PNS has been used to target both ES cell expressed and non-expressed genes and has been reported to yield enrichments, from tenfold to 2,000-fold of HR relative to random integration events (Thomas & Capecchi, 1990; Mansour *et al*, 1988),

#### **1.2.2.6.c. Double Replacement/Tag and Exchange Targeting Strategies**

The second instance when the presence of a negative selection marker is required is during 'Double Replacement' or 'Tag and Exchange' targeting strategies (Section 1.2.2.4.b). Both of these methods use two separate rounds of targeting to introduce a subtle non-selectable mutation into the locus of interest. To achieve this a drug resistance marker is needed which can be both positively selected for after the first



round of targeting and negatively selected against after the second round. Two such selectable markers are the *Hprt* gene and *neo/HSV-tk* expression cassette.

Expression of the *Hprt* gene can be selected for by culturing cells in HAT medium (Littlefield, 1964). Importantly, selection for the expression of an exogenously introduced *Hprt* gene is dependent upon the host cell lacking any endogenous *Hprt* enzyme activity. Such ES cell lines are now available, for example the HM-1 ES cell line (Magin *et al*, 1992).

HAT medium selection relies on the role of the *Hprt* enzyme within the cellular purine metabolism pathway. Cells have two pathways to synthesise mononucleotides, the first is a salvage pathway in which *Hprt* operates and the second is *de novo* synthesis independent of *Hprt* status. HAT medium supplies hypoxanthine as a substrate for the salvage pathway while aminopterin is used to block the *de novo* synthesis route. The final component of HAT medium is thymidine, this is needed by cells to circumvent the aminopterin-dependent inhibition of the thymidylate synthase reaction. The outcome of this selection is that all cells will be unable to synthesise mononucleotides *de novo* due to aminopterin, but only those expressing *Hprt* will be able to take advantage of the supplied hypoxanthine via the *Hprt*-dependent salvage pathway.

To select against cells which express *Hprt* the drug 6-thioguanine (6-tG) is used (Stutts & Brockman, 1963). This guanine analog is a substrate for the *Hprt* enzyme and undergoes a phosphoribosylation reaction to generate 6-thioguanine monophosphate (6-thioGMP). High levels of 6-thioGMP within cells inhibit the biosynthesis of guanine nucleotides and this inhibition eventually results in the death of all cells that express *Hprt* (Miech *et al*, 1967).

The *neo/HSV-tk* expression cassette has also been used successfully in double replacement targeting strategies (Askew *et al*, 1993). The HR-mediated integration of the first round targeting vector is selected for using G418 (Southern & Berg,

1982). The HR-mediated exchange reaction at the target locus with the incoming second round vector is predicted to result in the loss of the *neo/HSV-tk* expression cassette and loss of the *HSV-tk* gene can be selected for using FIAU (Borelli *et al*, 1988) or gancyclovir (Mansour *et al*, 1988).

#### **1.2.2.6.d. Crippled Selectable Marker Genes**

An alternative strategy for the enrichment of HR events is to use a selectable marker gene in the construct lacking either a functional promoter (Doestchman *et al*, 1988), polyadenylation sequence (Schwartzberg *et al*, 1989) or that requires the trapping of an enhancer element (Jasin & Berg, 1988). In this type of strategy the expression of the positive selection marker is HR-dependent as it is unlikely that random integration will juxtapose appropriate activating sequences adjacent to the crippled selection cassette.

High targeting efficiencies have been reported with the use of promoter-less or otherwise crippled selectable genes. For example, the targeted disruption of an endogenous gene, *Hprt*, using selection with a promoter-less *neo* gene has been demonstrated in ES cells with a targeting frequency of 67% (Doestchman *et al*, 1988). Interestingly, this targeting frequency was higher than that reported by Thomas & Capecchi despite the fact that these authors targeted the same locus and used an insertion targeting vector containing a larger region of genomic homology (Thomas & Capecchi, 1988). The use of an enhancerless *xanthine guanine phosphoribosyltransferase* (*gpt*) gene has been reported to yield an estimated 100-fold enrichment for targeted integrations without direct selection at the target locus (Jasin & Berg, 1988). Homologous integrations accounted for 44% of the *gpt*<sup>+</sup> cells. As well as using HR recombination to insert crippled drug resistance genes into target loci the technique has also been used to insert histochemically detectable reporter genes. For example, a promoter-less *βgeo* gene, a fusion of the *neo* and *LacZ* genes (Friedrich & Soriano, 1991) was targeted into the Oct-4 locus (Mountford *et al*, 1994). This strategy not only resulted in a very high targeting efficiency (70-80%) but also placed *βgeo* expression under the control of the

endogenous *Oct-4* promoter allowing direct visualisation of promoter activity in *in vitro* and *in vivo* (Mountford *et al*, 1994).

The major consideration about the use of promoter-less or crippled positive selection marker genes is the expression levels of the target gene within ES cells. A promoter-less marker gene can only be used for gene targeting if the target gene is actively expressed in ES cells. The level of target gene expression must also be considered. For example, if the target gene is more strongly expressed in differentiated derivatives of the ES cells, the selection procedure may enrich for these at the expense of the pluripotent population (reviewed in Hooper, 1992).

### **1.3. Inducible Gene Targeting**

The advent of gene targeting has permitted the generation of numerous mouse strains that carry specifically engineered modifications in a gene of choice, knock-out mice. The technique has become an established methodology of reverse genetics, i.e. the determination of gene function by the ablation or modification of target gene expression *in vitro* or *in vivo* (Berg, 1993).

While standard gene targeting strategies have furthered our understanding of the function of many genes this approach is limited. Amongst the key problems is the phenomenon of embryonic lethality where target gene function is critical for the successful completion of the developmental program making it impossible to study loss of gene function in adult, differentiated tissues. Although embryonic lethality cannot be overcome with standard gene targeting, novel inducible gene targeting strategies now under development should allow conditional target gene expression and provide significant insights into gene function.

The aim of inducible gene targeting is to allow the experimenter to determine both the time and location at which gene function is ablated or restored. For example, genes can be switched off in the adult mouse, so circumventing the phenotype of embryonic lethality. The conditional control of gene expression in a tissue-specific

manner will also permit a dissection of the often complex phenotypes of knockout animals so increasing our understanding of the pleiotropic nature of gene function. For example, the ability to knockout genes in specific somatic tissues will provide a model system in which to study human somatically acquired genetic diseases such as cancer. This type of analysis is extremely difficult with standard gene targeting as both tumour suppressor genes and proto-oncogenes commonly have vital developmental roles, the absence of which can be incompatible with survival in the mutant mice. Finally, inducible gene targeting should also provide an *in vivo* model system for the study of gene therapy. Just as gene function can be specifically ablated in the adult mouse, expression could also be restored. This type of study should provide valuable data about both the feasibility and efficacy of gene therapy in humans.

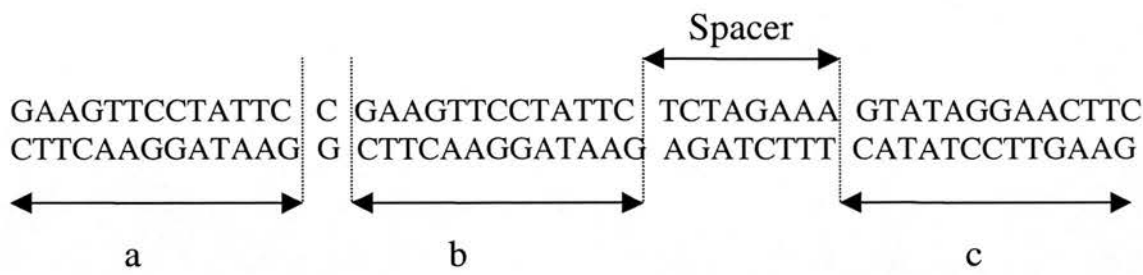
The main technologies used to achieve inducible gene targeting are the recombinase-based Cre/loxP (Abremski *et al*, 1983) and FLP/frt (Broach & Hicks, 1980) systems isolated from bacteriophage P1 and *Saccharomyces cerevisiae* respectively and are reviewed below.

### **1.3.1. The FLP/frt System : Background**

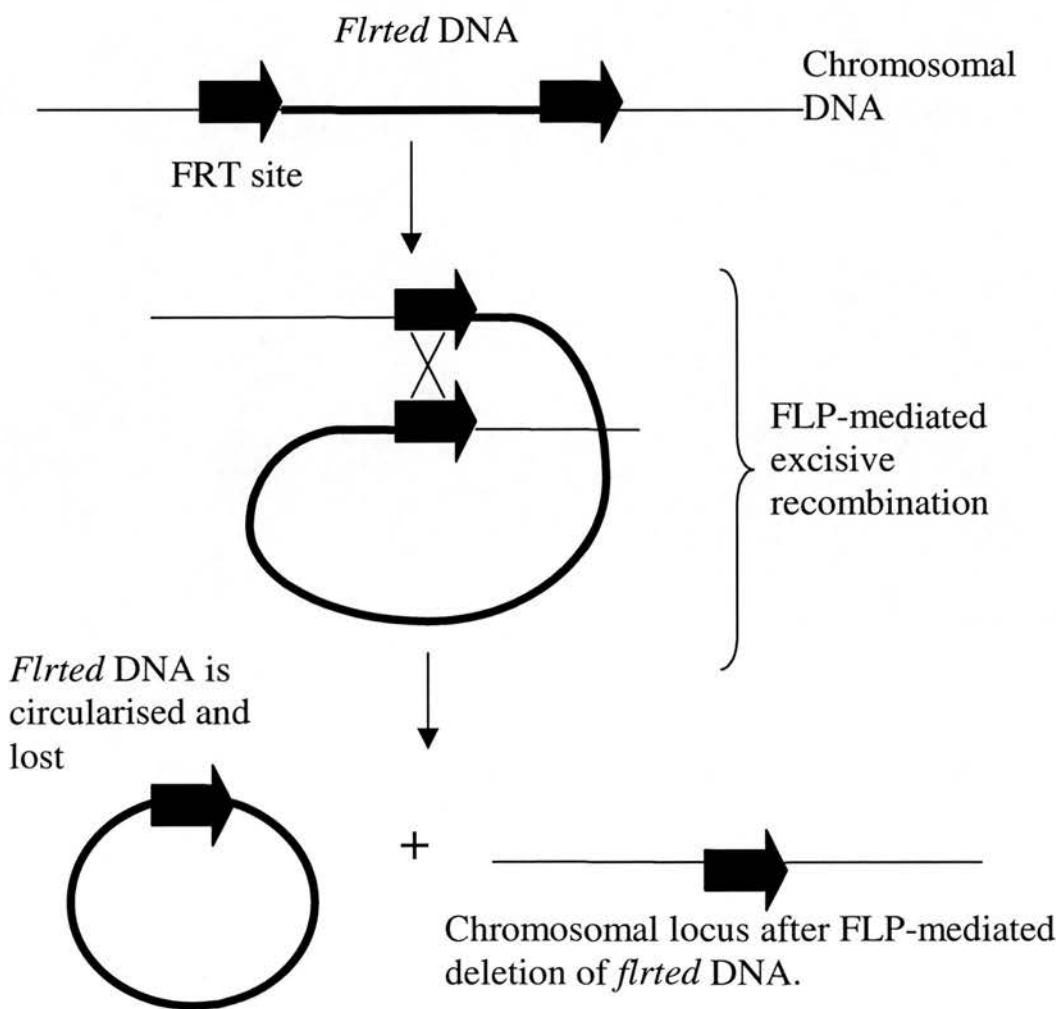
The FLP gene of the 2- $\mu$ m circle plasmid of *Saccharomyces cerevisiae* encodes a conservative site-specific DNA recombinase protein that is involved in the amplification of that plasmid (Volkert & Broach, 1986). Both FLP and Cre recombinases (Section 1.3.2.) are members of the integrase family of recombinases, all of which show a high level of sequence conservation within the catalytic domain and related catalytic mechanisms (Argos *et al*, 1986). FLP mediates a recombination event between two 48bp FRT sites (Meyer-Leon *et al*, 1984). Each FRT site includes two inverted 13bp symmetry elements (a and b) surrounding an 8bp core region and a third 13bp symmetry element (c) present in the direct orientation (Figure 1.8). The third 13bp symmetry element has been shown to be dispensable for recombination both *in vitro* and *in vivo* (Proteau *et al*, 1986). FLP molecules

**Figure 1.8 – The FLP Recombinase System**

A) An FRT site



B) FLP-mediated excisive recombination



binds to an FRT site in an ordered fashion; binding to the b element occurs first, then binding to a and finally to c (Andrews *et al*, 1987; Beatty & Sadowski, 1988). When two Flp molecules are bound to symmetry elements a and b, a bend of approximately 60° is introduced into the DNA, binding of a third protein to element c increases the DNA bend to greater than 144° (Schwartz & Sadowski, 1990). Intermolecular protein-protein interactions between the individual Flp molecules bring the two partner FRT sites together to form a synaptic complex (Amin & Sadowski, 1990). Site-specific cleavage results from a nucleophilic attack by Tyr343 on the phosphodiester backbone of DNA within the core of the FRT site (Jayaram, 1994). The Flp-mediated DNA bending is thought to be important in facilitating DNA strand separation and exchange in the core region (Zhu & Sadowski, 1998).

The Flp recombinase system has been shown to work efficiently in a number of experimental systems including the mouse. For example, several Flp-transgenic mouse strains have been developed. These include TgN(hACTB::Flp) in which Flp expression is driven from the global human  $\beta$ -actin promoter (Dymecki, 1996), Wnt1::Flp in which Flp expression is directed to the developing nervous system (Dymecki & Tomasiewicz, 1998) and rPOMC-Flp in which sequences from the rat pro-opiomelanocortin promoter were used to direct Flp expression to the pituitary gland (Vooijs *et al*, 1998). Furthermore, a ligand inducible Flp recombinase has also been developed allowing temporal as well as spatial control of gene expression (Logie & Stewart, 1995).

The Flp system has also been used in inducible gene targeting strategies. For example, the insertion of two FRT sites flanking exon 19 of the mouse retinoblastoma gene allowed its inducible inactivation *in vivo* and demonstrated the tumour-suppressor function of this gene (Vooijs *et al*, 1998). Flp has also been used to manipulate FRT-containing transgene arrays in zygotes (Ludwig *et al*, 1996) and to engineer large-scale chromosome manipulations *in vitro* (Aladjem *et al*, 1997).

### **1.3.2. The Cre/loxP System : Background**

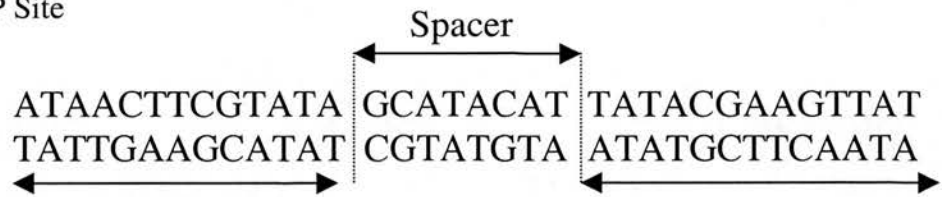
Cre recombinase (causes recombination) is an enzyme produced by bacteriophage P1. Within the bacteriophage Cre has two roles, firstly to circularise the viral genome should this fail to be carried out by host cell recombination machinery (Segev & Cohen, 1981) and secondly, to maintain correct unit copy segregation of the prophage by resolving any dimeric molecules into monomers prior to cell division (Austin *et al*, 1981). Cre does not act randomly throughout the bacteriophage genome but will only stimulate recombination at specific sequences encoded within loxP sites (locus of crossover (X)). A loxP site consists of 34 base pairs (bp) of DNA arranged in three components, two 13bp inverted repeats separated by an 8bp non-symmetrical spacer region (Hoess *et al*, 1982) (Figure 1.9). DNA footprinting studies have shown that one molecule of Cre binds to one 13bp repeat, so each complete loxP site is bound by two molecules of recombinase (Hoess & Abremski, 1984). Intriguingly, both Flp (Section 1.3.1.) and Cre recombinase have also been shown to bind single-stranded DNA molecules in a sequence specific manner (Zhu & Sadowski, 1998). The biological significance of these observations has yet to be determined.

X-ray crystallography techniques have been used to determine the exact macromolecular structures involved in Cre-mediated recombination (Guo *et al*, 1997). The reaction proceeds in a sequential manner with double strand exchange occurring after two rounds of single strand cleavage and re-ligation. The first step in this recombination event is the binding of two molecules of recombinase to one loxP site. A recombination synapse is then formed involving two loxP sites and four associated recombinase molecules. Within this synapse structure the recombinase molecules form a tetrameric ring around the central active site. The Cre tetramer holds the loxP sites in a square-planar layout by introducing a sharp bend within the 8 bp spacer region. In this conformational state the two spacer regions, the sites of cleavage and strand re-ligation during recombination, protrude into the active site. During the formation of the synapse a tyrosine residue conserved in all integrase family members (position 324 in Cre) from one of each pair of recombinases attacks the DNA substrate. This nucleophilic attack leads to the formation of a covalent

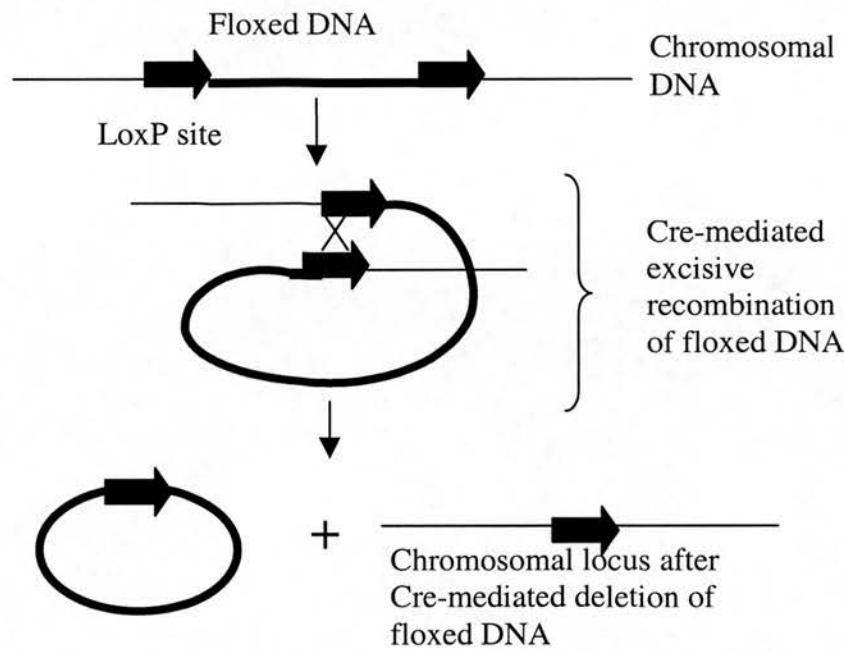


**Figure 1.9 – The Cre/LoxP System**

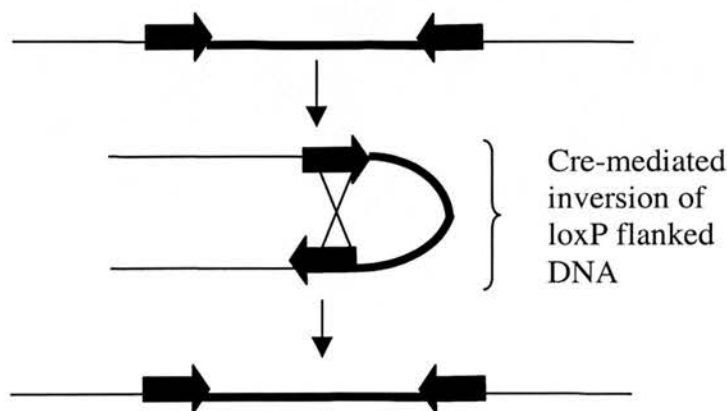
A) LoxP Site



B) DNA flanked (floxed) by two directly repeated loxP sites will undergo Cre-mediated excise recombination.



C) DNA flanked (floxed) by two inversely repeated loxP sites will undergo Cre-mediated inversion.





phosphotyrosine bond between one half of the loxP site and one molecule of Cre. Two free 5' ends of single stranded DNA are also formed as a result of this reaction. The free 5' ends of DNA then act as nucleophiles and attack the phosphotyrosine intermediates generated above. Importantly, the free end of DNA from one loxP site attacks the phosphotyrosine intermediate of the second loxP site, leading to strand exchange within a four-way Holliday junction structure. The four-way synapse is then resolved by a second round of cleavage and strand exchange reactions generating recombinant products.

Using the mechanism described above, the Cre/loxP system is able to carry out two types of recombination event depending on the relative orientation of the two loxP sites (Figure 1.9). As the two inverted repeats within a loxP site are palindromic it is the nonsymmetrical 8bp spacer that confers directionality. When the spacer regions of two loxP sites are directly repeated any intervening DNA (described as floxed) will be excised, whereas inversion will occur when the loxP sites are in opposite orientations. Interestingly, when the asymmetry of loxP sites is destroyed and symmetrical sites are constructed both excision and inversion recombination products result with equal frequency (Hoess *et al*, 1986).

The exciting potential of the Cre/loxP system became apparent when it was shown that the enzyme will catalyse recombination in the absence of ATP, co-factors or topoisomerase activity (Abremski & Hoess, 1984). Most importantly, the system will also function in eukaryotic cells (Sauer, 1987; Sauer & Henderson, 1988). These observations have subsequently been extended *in vivo* using transgenic mice and it was this work which first demonstrated the potential application of this system to conditional gene targeting (Orban *et al*, 1992; Lakso *et al*, 1992).

### **1.3.3. Applications of the Cre/loxP System: Inducible Gene Targeting**

To achieve conditional gene expression using Cre/loxP technology there are two basic requirements. The first is the ability to regulate the expression of Cre recombinase and the second is the generation of a floxed target gene.



Regulated expression of Cre can be achieved by several methods, the use of inducible or tissue specific promoters to drive the expression of Cre or viral delivery systems. All of these approaches have been demonstrated successfully *in vivo* and *in vitro* and are reviewed in the subsequent sections.

The generation of floxed target genes can also be achieved in a multitude of ways depending on the desired outcome of recombination, either target gene activation or inactivation. The types of strategy used can be grouped by the nature of the recombination event they are engineered to produce, either insertion or excision. All approaches designed to confer conditional gene expression are also reviewed in the subsequent sections.

### **1.3.3.1. Regulating the Activity of Cre Recombinase**

#### **1.3.3.1.a. Tissue-specific Promoters**

In order to achieve the conditional expression of a target gene within any given tissue of a transgenic mouse it is first necessary to be able to express Cre specifically within that tissue. With this aim in mind a variety of transgenic mice which express Cre from different tissue-specific promoters have been generated.

Adipose tissue-specific expression has been achieved by coupling Cre expression to the adipose protein 2 (aP2) gene regulatory element in transgenic mice (Barlow *et al*, 1997). Other somatic tissues to which Cre expression has been targeted include the mammary gland (Wagner *et al*, 1997; Selbert *et al*, 1998), basal cells of the skin (Tarutani *et al*, 1997), the heart (Agah *et al*, 1997), the forebrain (Tsien *et al*, 1996a), thymocytes (Orban *et al*, 1992), the kidney (Nelson *et al*, 1998), the pancreas (Ray *et al*, 1998) and the eye (Lakso *et al*, 1992).

Cre expression has also been targeted to the female germ line by placing it under the control of zona pellucida 3 (Zp3) gene regulatory elements (Lewandoski *et al*, 1997). The Zp3 promoter is normally only active in the oocyte prior to the first meiotic

division and as such Zp3-Cre transgenic animals do not show any expression of cre in somatic tissues. Likewise, expression of Cre recombinase has been targeted to the male germline using the mouse protamine 1 promoter (Prm1) (O’Gorman *et al*, 1997). The Prm1 promoter allows expression of Cre recombinase within the testis although some degree of ectopic expression was seen in all Prm1-Cre founder animals. The Synaptonemal Complex Protein 1 (Sycp1) promoter has also been used to generate testicular-specific expression of Cre recombinase (Vidal *et al*, 1998).

As well as the ability to express Cre in germ cells, expression has also be targeted to the earliest stages of embryogenesis using the adenovirus EIIa promoter (Lakso *et al*, 1996), the nestin promoter in the *balancer* strain (Betz *et al*, 1996) and the c-kit promoter (Bergqvist *et al*, 1998). Interestingly, the c-kit-Cre mice display homogenous chimerism in tissues of the same individual but varied between different individual offspring (Bergqvist *et al*, 1998). Recent publications have reported expression of Cre recombinase in a tissue-specific manner during embryogenesis, to areas such as the embryonic midbrain-hindbrain constriction region using the *Engrailed-2* promoter (Zinyk *et al*, 1998) and the developing neural tube using regulatory sequences from the *Wnt1* gene (Danielian *et al*, 1998).

Not all attempts at achieving tissue-specific expression of Cre recombinase are successful however. For example, a transgenic mouse strain engineered to express Cre under the control of the platelet endothelial cell adhesion molecule-1 promoter (PECAM-1) was predicted to express Cre only in endothelial cells (Terry *et al*, 1997). However when the PECAM-1/Cre mouse was crossed to a floxed mouse, the progeny were seen to have undergone recombination in all tissues. The conclusion from this work is that if the promoter is even briefly active during an early stage of development this can be sufficient to induce floxing in a non-tissue-specific manner. Other groups have also reported this problem, for example, the *balancer* strain described above was originally predicted to give central nervous system specific expression (Betz *et al*, 1996).

#### **1.3.3.1.b. Cre Fusion Proteins**

Several groups have demonstrated that the activity of cre recombinase can be controlled *in vivo* by generating fusion proteins between Cre and the ligand binding domains (LBD's) of various steroid receptors. In the absence of ligand the LBD suppresses recombination by a mechanism thought to involve steric hindrance through its association with members of the heat shock protein (HSP) family (Picard *et al*, 1990). Upon the addition of ligand the HSPs are displaced and the ligand binds the LBD. This binding then removes the steric constraints on Cre and the enzyme is once more able to catalyse recombination.

A number of different Cre-LBD fusions have been reported to date. For example, Cre fused to the LBD of the glucocorticoid receptor will respond to the steroids dexamethasone, aldosterone and the synthetic steroid RU486 (Dias *et al*, 1998). As this Cre fusion would respond to endogenous steroids in an *in vivo* setting it can only be used in cultured cells. However a mutant form of the LBD which is only activated in response to the synthetic inducers such as RU486 has been used to create a Cre fusion protein more suitable for use *in vivo* (Kellendonk *et al*, 1996; Brocard *et al*, 1999). Several groups have reported the generation of Cre fusion proteins with a mutated oestrogen receptor LBD of either mouse (Zhang *et al*, 1996) or human origin (Schwenk *et al*, 1998; Feil *et al*, 1997; Feil *et al*, 1996; Brocard *et al*, 1997). The mutated LBD in all of these constructs renders Cre activity dependent upon the addition of the synthetic inducer tamoxifen rather than upon endogenous oestrogens. The technology of inducible promoters has now been combined with tissue-specific promoters to permit simultaneous spatial and temporal regulation of Cre expression (Kellendonk *et al*, 1999).

#### **1.3.3.1.c. Inducible Promoters**

The use of inducible promoters permits temporal control over Cre expression but not usually tissue-specificity as global promoter activity occurs following induction. To date, there have only been two published reports of Cre expression being regulated via an inducible promoter. One group has generated a strain of transgenic mice

which express a tetracycline regulated Cre. In these animals Cre will be expressed only in the absence of tetracycline and expression can be abolished by the addition of tetracycline (St-Onge *et al*, 1996). A second group has generated transgenic mice expressing Cre under the control of the interferon alpha or  $\beta$  inducible promoter Mx-1 (Kuhn *et al*, 1995). Cre expression can be induced in these animals by intraperitoneal injection of interferon  $\alpha$  or  $\beta$  or the synthetic inducer pI-pC although there are variations in the efficiency of induction between different tissues.

#### **1.3.3.1.d. Global Promoters**

The technologies discussed above have focussed on methods to regulate Cre activity to specific timepoints or tissues, however, not all Cre transgenic strains are developed with this aim in mind. Several groups have developed strains of mice in which global promoters drive Cre expression from the earliest stages of development. For example, a hybrid control element containing the immediate early enhancer of the cytomegalovirus and the chicken  $\beta$ -actin promoter (CAG) directed Cre recombinase expression constitutively throughout development (Sakai & Miyazaki, 1997). As well as virally derived enhancer sequences viral promoters have also been used in the generation of Cre transgenics. The *deleter* strain produced in Rajewskys laboratory expresses Cre from a human cytomegalovirus minimal promoter in all tissues of the mouse (Schwenk *et al*, 1995). These authors suggest that such strains should serve as a useful tool for the introduction of prescribed genetic modifications into the mouse embryo at the zygote stage. Furthermore, the ability to express Cre in all tissues of the developing embryo should permit a comparison of the null phenotype with that arising from the recombined floxed allele engineered as part of an conditional gene inactivation targeting strategy.

#### **1.3.3.1.e. Viral Delivery**

Three groups first reported the development of recombinant adenoviruses which express Cre recombinase, AdCre (Anton & Gramham, 1995; Sakai *et al*, 1995; Kanegae *et al*, 1995), although similar technologies have been now been developed by other groups. All of these groups used the same basic strategy, in which sections

of the wild type virus genome, such as sequences encoding the E1 and E3 genes are replaced with a Cre expression construct. Such recombinant viruses are replication deficient but still capable of host cell infection. AdCre has several other advantages, the viruses can be generated at high titres ( $10^9$ - $10^{11}$  pfu/ml), they can infect dividing and non-dividing cells and they integrate only very rarely into the genomes of eukaryotic cells. As these viruses are non-replicating they will persist briefly as extrachromosomal molecules but will eventually be lost from dividing cells hence they offer only transient gene expression. However, as Cre recombinase is only needed to cause recombination its continued presence in a cell is unnecessary.

Since the development of AdCre it has been used successfully by many groups. As cultured cells can be exposed directly to the virus very high efficiencies of infection can be achieved, more so than with standard transient transfection techniques. For example, infection of CV1 cell lines with AdCre resulted in recombination mediated gene activation in up to 100% of cells (Kanegae *et al*, 1995). AdCre technology has also been used successfully *in vivo*. The commonest method of introducing AdCre into mice is by intravenous injection (IV) but this route does not lead to uniform infection of somatic tissues. When transgenic mice which contain a recombination reporter construct were infected with AdCre via IV injection high levels of recombination were seen in the liver and spleen but lower levels of recombination were detected in the kidney, heart and lung with trace levels found in the brain (Wang *et al*, 1996). However, the fact that the liver is the major site of infection in animals injected intravenously with Cre has been used to their advantage by several groups. For example, Cre-mediated liver specific activation of a Hepatitis C virus transgene was used to investigate the immune responses and pathogenesis of HCV infection (Wakita *et al*, 1998). Cre-mediated gene deletion specifically in the liver has also been reported using this method of infection (Rohlmann *et al*, 1998) but because of the low levels of infection described in tissues other than the liver this method is not strictly tissue specific. One way around this would be the development of a recombinant adenovirus that expressed Cre under the control of a liver specific promoter. A related development was recently reported, a recombinant adenovirus in



expression is driven from the  $\alpha$ -fetoprotein (AFP) promoter (Sato *et al*, 1998). While this adenovirus is able to infect the normal range of cell types, Cre is only expressed in cells that also express the carcinoembryonic antigen,  $\alpha$ -fetoprotein.

Intravenous injection is not the only way to introduce adenovirus *in vivo*. Because adenovirus will not diffuse far away from the site of injection it can be introduced into tissues directly, for example into the colorectum (Shibata *et al*, 1997), the heart (Agah *et al*, 1997) or by stereotaxic injection into the brain (Wang *et al*, 1996).

Despite all of the advantages of the AdCre system described above, it is not without its problems. *In vitro*, high doses of replication deficient adenoviruses can result in cytopathology and even cell death. *In vivo*, exposure of mice to adenovirus can initiate an inflammatory response, for example in the liver a lymphocytic infiltration characteristic of adenoviral infection (Yang *et al*, 1994). There is also evidence that cells infected by adenovirus can be eliminated by the immune system. For example, immunisation of mice with a recombinant LacZ expressing adenovirus elicited a cytotoxic T lymphocyte (CTL) response against both viral antigens and the transgene product,  $\beta$ -galactosidase (Yang *et al*, 1996). More recent evidence indicates that provided the mice are tolerant of the adenovirus-encoded transgene product persistence of expression can be achieved (Michou *et al*, 1997). However, as the Cre/LoxP system requires only transient expression to induce a heritable genetic change in the host cell not all cells which have undergone recombination will retain the non-replicating adenovirus and so should escape destruction by the host immune system.

Because of the potential side effects of AdCre discussed above it is important that appropriate controls are included during the analysis of phenotypes resulting from AdCre-mediated gene rearrangements.

As well as recombinant adenoviridae genetically engineered to express Cre recombinase other types of viruses have also been modified with this aim in mind. A

recombinant Cre-expressing retrovirus has been reported (Choulika *et al*, 1996) and focal delivery of the Herpes Simplex virus-Cre (HSV-Cre) into the dorsal hippocampus resulted in successful transgene recombination and detectable phenotypic alterations *in vivo* (Brooks *et al*, 1997). Such HSV amplicon vector technology can also be coupled with tissue specific promoters allowing even greater control of expression localisation than with focal delivery alone (Kaplitt *et al*, 1994).

#### **1.3.3.1.f. Other Cre Delivery Systems**

While the most frequently used methods of introducing Cre, *in vitro* or *in vivo*, have been discussed in the preceding sections several other methods have been used successfully by various research groups and are worthy of a brief mention. Standard gene targeting techniques were used to insert the human PrP coding sequence into the PrP locus in the mouse. Transient expression of Cre then resulted in the excision of the selectable marker cassette and the replacement of the endogenous gene with the human coding sequence, creating a “knock-in” mouse (Kitamoto *et al*, 1996). Transient Cre expression was achieved by the microinjection of a circular Cre encoding plasmid into pronuclei. These Cre-treated pronuclei were then transferred into pseudopregnant female mice and the progeny screened for the Cre-mediated recombination event at the target locus.

In a similar approach, targeted ES cells have also been treated directly with Cre recombinase. Several groups have reported the successful introduction of Cre into ES cells by electroporation with supercoiled Cre encoding plasmids (Zou *et al*, 1994; Gu *et al*, 1993; Li *et al*, 1996) and also calcium phosphate/DNA co-precipitation (Gagnetten *et al*, 1997).

#### **1.3.3.2. Inducible Control of Gene Expression Using the Cre/loxP System**

Having achieved regulated Cre expression the next step is the generation of the floxed substrate. Because the Cre/loxP system is able to catalyse three types of recombination event, namely, excisive recombination, site-specific insertion and



inversion several different strategies have been developed to allow conditional gene expression.

#### **1.3.3.2.a. Site-specific Insertion**

The presence of a single loxP site within a chromosome will act as a target for insertional recombination with any introduced exogenous DNA constructs that also contain a single loxP site. The target loxP site can be introduced via gene targeting into a specific location or positioned at random within the genome by illegitimate recombination. Whichever method is used the site of the target loxP site remains fixed such that any subsequent insertional recombination events will occur at this predetermined locus. This strategy of site-specific integration has been successfully demonstrated using loxP-*tk* (Sauer & Henderson, 1990) and loxP-*neo* constructs as well as a loxP-*lacZ* marker gene used to analyse the scale of position effect on marker gene expression (Fukushige & Sauer, 1992).

Because this technology provides a way to reproducibly insert exogenous DNA into defined chromosomal locations it has allowed significant advances to be made in the study of *cis*-acting control elements that regulate gene expression in relation to chromosomal context. For example, Cre-mediated site-specific insertion was used to gain insights into the poorly defined mechanism of action of the Locus Control Region (LCR) enhancer present within the human  $\beta$ -globin locus (Bouhassira *et al*, 1997). The ability to reproducibly insert expression constructs into a defined chromosomal location allowed the first rigorous assessment of transcriptional regulation by subdomains of the LCR demonstrating that these enhancer sequences act to increase both the probability of gene expression and the rate of transcription (Bouhassira *et al*, 1997).

The relative importance of chromosomal context and endogenous promoter activity can be separated with this approach circumventing the problem of position effect and allowing a more meaningful analysis of promoter activity. A construct which included the minimal human p53 promoter and the *chloramphenicol*

*acetyltransferase* (CAT) gene was co-transfected with a Cre-expression vector into mouse NIH 3T3 cells (Bethke & Sauer, 1997). Clones that represented single copy, stable integration events were selected and the levels of CAT expression were assayed in response to various genotoxic insults. The Cre-mediated site-specific insertion of the expression construct permitted a position effect-independent demonstration of strong p53 promoter induction after mitomycin C exposure (Bethke & Sauer, 1997).

#### **1.3.3.2.b. Site-specific Excisional Recombination of Exogenous DNA Sequences**

The ability of Cre to mediate excise recombination of exogenous DNA sequences has been used by many groups to achieve conditional gene expression all of whom used the same basic strategy. The target gene is placed under the control of a given promoter but the insertion of a floxed inactivating cassette between the transgene promoter and downstream coding sequence confers Cre-mediated control of expression. In the absence of Cre transgene expression is blocked by the presence of the inactivating cassette. After expression of Cre the floxed cassette is lost and transgene expression activated (reviewed in depth in Section 2.2).

#### **1.3.3.2.c. Site-specific Excisional Recombination of Endogenous DNA Sequences**

This type of strategy has been applied to achieve inducible inactivation of gene expression, for example, temporal specific or tissue-specific knockouts *in vitro* and *in vivo*. Whatever the target gene the basic approach is the same, the introduction of two directly repeated loxP sites into the gene of interest and then regulated expression of Cre recombinase.

To date, recombination-dependent gene inactivation has been demonstrated *in vivo* by several groups but varying degrees of success have been reported in obtaining mutant mice with relevant phenotypes. The mice reported so far range from having no observable phenotype to one of embryonic lethality. For example, the DNA polymerase  $\beta$  gene has been conditionally inactivated in T-cells (Gu *et al*, 1994) and

also in a temporally specific manner (Kuhn *et al*, 1995) but both of these conditional knockouts had no obvious phenotype. At the other end of the scale, mice homozygous for a floxed allele of the mitochondrial transcription factor A (TFAM) gene die prior to day E10.5 (Larsson *et al*, 1998). All of this work serves to highlight the fact that while Cre/loxP technology can offer a way to circumvent the problem of embryonic lethality both the target gene and the Cre recombinase delivery strategy must be chosen carefully. For example, in the TFAM experiments Cre expression was driven from the  $\beta$ -actin promoter so directing expression to the preimplantation embryo. As a result the floxed animals underwent recombination at an early stage in development making them little different from constitutively null animals which could have been generated using standard gene targeting techniques.

Despite these problems other groups have been more fortunate in both their choice of target gene and Cre delivery strategy. For example, Taruntani *et al*, used an inducible gene targeting strategy to construct a conditional allele of the murine X-linked *Phosphatidylinositolglycan class A (Pig-a)* gene (Tarutani *et al*, 1997). Somatically acquired mutation(s) in the PIG-A gene in humans are responsible for Paroxysmal Nocturnal Haemoglobinuria (Rosse & Ware, 1995) and *Pig-A* null ES cells are incapable of making a significant contribution to chimaeras thereby precluding the generation of a *Pig-A* knockout mouse (Takeda & Kinoshita, 1995). To create a conditional allele of the *Pig-A* gene two directly repeated loxP sites were inserted on either side of exon 6. The floxed mice were then mated with a second transgenic strain that expressed Cre recombinase under the control of the skin-specific keratin 5 promoter (Taruntani *et al*, 1997). Cre-mediated inactivation of the *Pig-A* gene in hemizygous floxed male animals resulted in death 1-3 days after birth, however lethality was not observed in the floxed female mice. Both sexes displayed altered skin characteristics relative to wild type including, scaly and wrinkly skin with a reduced lipid component. The application of this inducible gene targeting strategy to the *Pig-A* gene provided insights into gene function that were unobtainable with standard gene targeting.

A variety of other genes have also been analysed with this approach. LoxP sites were targeted into the N-methyl-D-aspartate receptor 1 gene (NMDAR1) and using forebrain specific expression of Cre the function of this receptor was ablated specifically in one region of the hippocampus (Tsien *et al*, 1996b). The Cre/loxP system also permitted the study of the developmentally important B cell antigen receptor (BCR) complex (Lam *et al*, 1997). Complete ablation of the BCR would lead to a total block in B cell production during early development precluding an analysis of its function in mature B cells. Using the Cre/loxP system mutant mice were generated in which BCR function could be specifically abolished in mature B cells providing the first direct evidence for the role of BCR expression and the persistence of mature B cells in the peripheral immune system.

This technology has been taken one step further to generate an allelic series of mutations at one given locus (Meyers *et al*, 1998). Using one round of standard gene targeting two FRT sites, for the Flp recombinase (Broach & Hicks, 1980), two loxP sites and a *neo* cassette were inserted into the *Fgf8* gene generating an *Fgf8<sup>neo</sup>* allele. When these mice were crossed to a strain which expressed Cre from the human  $\beta$ -actin promoter excisive recombination resulted in the generation of a null allele, *Fgf8<sup>Δ2,3n</sup>*. Mice with the null allele displayed a defect in gastrulation and hence embryonic lethality. This deletion phenotype was more severe than that displayed by mice that carried the *Fgf8<sup>neo</sup>* insertion allele, these animals showed perinatal lethality. This observation led to the classification of the *Fgf8<sup>neo</sup>* insertion allele as hypomorphic. The third allele that can be derived from the parental *Fgf8<sup>neo</sup>* was generated by crossing the mice to a second transgenic strain which express Flp. Flp mediated excisive recombination leads to the loss of the *neo* cassette from the *Fgf8<sup>neo</sup>* allele, two intronic loxP sites are retained but this allele, *Fgf8<sup>lox</sup>* is functionally equivalent to wild type. Finally, the *Fgf8<sup>lox</sup>* allele can be inactivated by subsequent expression of Cre giving the fourth possible allele in this allelic series.

Previously, gene targeting technologies have been directed at the creation of null alleles whereas the paper by Meyers *et al*, is the first to report the construction of an

allelic series of mutations all of which can be derived from one targeted progenitor mouse strain. This type of approach not only increases the productivity of gene targeting but also permits a more complete analysis of gene function. The ability to use Flp and Cre recombinases in parallel also increases the complexity of genetic modifications possible.

Another advantage of the Cre/loxP-based inducible gene targeting relative to standard targeting techniques is the ability to analyse specific splice variants. For example, the  $\alpha 6$  integrin gene encodes two mRNAs,  $\alpha 6A$  and  $\alpha 6B$  generated by alternative splicing. Conditional gene targeting was used to delete the  $\alpha 6A$  specific exon and a mild phenotype of altered cell migration resulted, demonstrating that the two splice variants are not functionally equivalent (Gimond *et al*, 1998). The same exon-specific knockout approach has also been used successfully to investigate the function of the  $\beta 1D$  integrin splice variant (Baudoin *et al*, 1998).

#### **1.3.3.2.d. Chromosomal Manipulations Using Cre/loxP**

The applications of Cre/loxP system are not limited to the manipulation of specific transgenic loci, the technology can also be applied to chromosome engineering. The feasibility of using Cre/loxP technology to engineer large-scale chromosomal manipulations into the eukaryotic genome was first demonstrated in plants (Qin *et al*, 1994) however this technology was rapidly applied to the mammalian genome.

For example, the human chromosome translocation t(6;9), associated with a specific subtype of acute myeloid leukaemia was modelled in ES cells using the Cre/loxP system. Two loxP sites of identical orientation were introduced by standard gene targeting techniques, one into each target chromosome. Transient expression of Cre recombinase in doubly targeted ES cell clones resulted in a site-specific reciprocal exchange of chromosome arms beyond the position of the loxP sites generating a balanced translocation between non-homologous chromosomes (van Deursen *et al*, 1995). An identical approach was also used to successfully engineer a t(12;15) translocation commonly found in mouse plasmacytomas in ES cells (Smith *et al*,

1995). As well as translocations the Cre/loxP system has also been used to introduce deletions into the genomes of ES cells, for example, deletions ranging from 90kb to 3-4cM have been successfully generated on mouse chromosome 11 (Ramirez-Solis *et al*, 1995).

#### **1.3.4. Historical Perspective**

This research project was initiated during the autumn of 1995. At this time the potential of the Cre and Flp recombinase systems was apparent but very little groundwork had been done. As the majority of the preliminary characterisation experiments were carried out in non-mammalian species few research tools were available. For example, only two Cre transgenic mouse had been published (Lakso *et al*, 1992, Orban *et al*, 1992) and none of the viral delivery methods had even been developed (Section 1.3.3.1.e). The first use of the Cre/loxP system in an inducible gene targeting strategy was published in the summer of 1994 (Gu *et al*, 1994) but it would be another 15 months before a second mouse was reported (Kuhn *et al*, 1995). This indicates that we were in the very early stages of the development of this technology and highlights the ambitious nature of this PhD project. The central aim of this project was to apply the Cre/loxP system to design a gene targeting strategy that would create a mouse with a conditional allele of the tumour suppressor gene p53 (Section 1.4). In order to achieve this, a novel mechanism of regulating both exogenous and endogenous gene expression was developed, the technical problems of Cre delivery were overcome and an inducible gene targeting strategy was designed and implemented. As there were few, if any, precedents in the literature for this type of work a significant proportion of the duration of this project was spent characterising and defining the limitations of the Cre/loxP system.

An introduction to the target gene for this project, murine p53, is given in the following section (Section 1.4) and the results of work with the Cre/loxP system are discussed in Chapters 2-5.

#### **1.4. p53**



From its ignominious beginning as a protein that stubbornly bound to SV40 large T antigen (TAG) (Lane & Crawford 1979), p53 has become the subject of worldwide research. Despite its initial classification as an oncogene the function of wild type p53 as a tumour suppressor gene has now been established. The fact that p53 is the most frequently mutated tumour suppressor gene in all human cancers testifies to its importance in tumourigenesis (Hollstein *et al*, 1994). Furthermore, human families with Li-Fraumeni syndrome have a germ line mutation of the p53 gene and display a predisposition to cancer (Malkin *et al*, 1990 and Srivastava *et al*, 1990) and p53 null mice generated by gene targeting are highly predisposed to malignancy (Donehower *et al*, 1992; Jacks *et al*, 1994; Purdie *et al*, 1994).

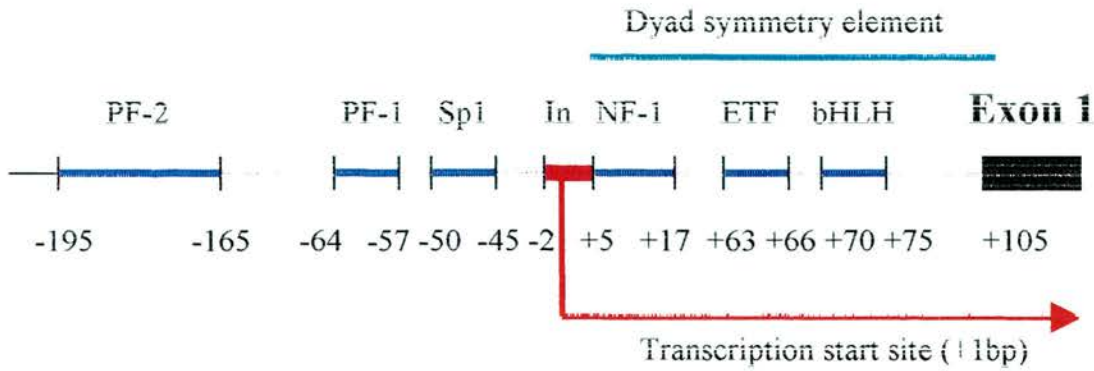
#### **1.4.1. Genomic Organisation and Transcriptional Regulation of p53**

The mouse p53 gene spans 12kb and lies on chromosome 11 (Rotter *et al*, 1984 and Czosnek *et al*, 1984). It consists of 11 exons of which 10 contribute to the translation product as exon 1 is transcribed but not translated (Bienz *et al*, 1984).

The promoter region of mouse p53 lies directly upstream of exon 1 and the regulatory motifs present within it stretch over approximately 300bp of DNA. The promoter lacks any of the standard consensus sequences commonly found in most eukaryotic promoters such as CAAT or TATA boxes, but contains sequence elements characteristic of a TATA-less promoter (Figure 1.10) including an initiator element (-2 to +5bp) required to position the start-site of transcription in TATA-less promoters (O'Shea-Greenfield & Smale, 1992). The promoter region of p53 also contains binding sites for a variety of general transcription factors. These include Sp1 (-44 to -50bp) (Bienz-Tadmor *et al*, 1985 and Dynan 1986), nuclear factor-1, NF-1, (+5 to +17 bp) (Ginsberg *et al*, 1990), ETF or an ETF-like factor (+63 to +66bp) (Hale & Braithwaite, 1995), PF-1 (-64 to -57bp) (Ginsberg *et al*, 1990) and the basic helix-loop-helix (bHLH) family of transcription factors (+70 to +75bp) (Ronen *et al*, 1991). Key members of the bHLH family are the transcription factors c-Myc and Max, which form a heterodimer and bind at this motif (Reisman *et al*, 1993) and USF which has been shown to enhance p53 transcription (Reisman &

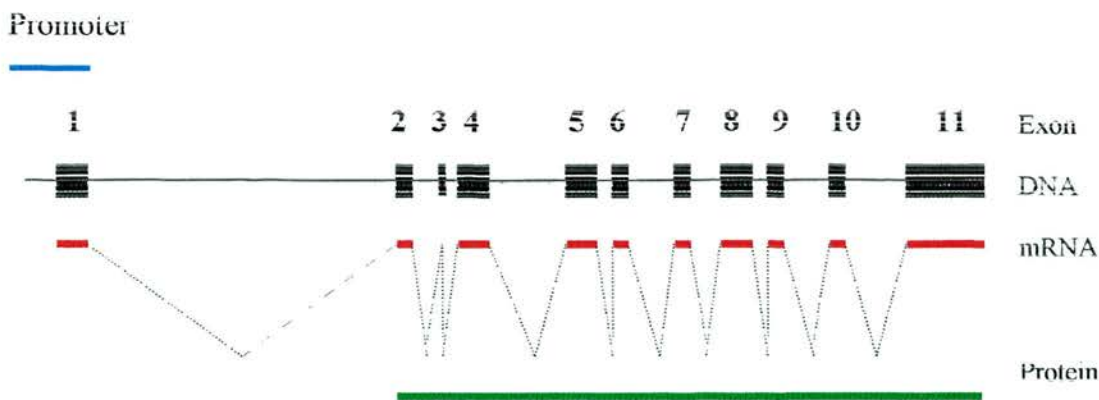
**Figure 1.10** – *The Promoter Structure and Genomic Organisation of the Murine p53 Gene*

A) Detailed p53 promoter structure (not to scale).



The p53 promoter spans 411bp and includes numerous protein binding sites (thick black lines). Transcription is initiated within the Initiator element (In) (-2 bp +5bp) (O'Shea-Greenfield & Smale, 1992) as indicated by the red arrow. To the 5' of the In element lie three protein binding sites, PF-2 (Hale & Braithwaite, 1995), PF-1 (Ginsberg *et al*, 1990) and Sp-1 (Bienz-Tadmor *et al*, 1985; Dynan, 1986). A further three protein binding sites lie downstream of the In, NF-1 (Ginsberg *et al*, 1990), ETF (Hale & Braithwaite, 1995) and bHLH (Ronen *et al*, 1991). The position of the proposed dyad symmetry element present in the 5' region of the p53mRNA is also indicated (+5-+108bp) (Bienz *et al*, 1984).

B) Genomic organisation of the murine p53 gene (not to scale).



The promoter region is indicated (blue line) as are the 11 exons (black boxes) and 10 intervening introns (thin black line). The mRNA (red line) and protein products (green line) expressed from this locus are also shown.



Rotter, 1993). The protein binding site PF-2 (approx. -195 to -169bp) has also been demonstrated to be absolutely required for the activity of the murine p53 promoter although the exact protein involved remains to be identified (Hale & Braithwaite, 1995).

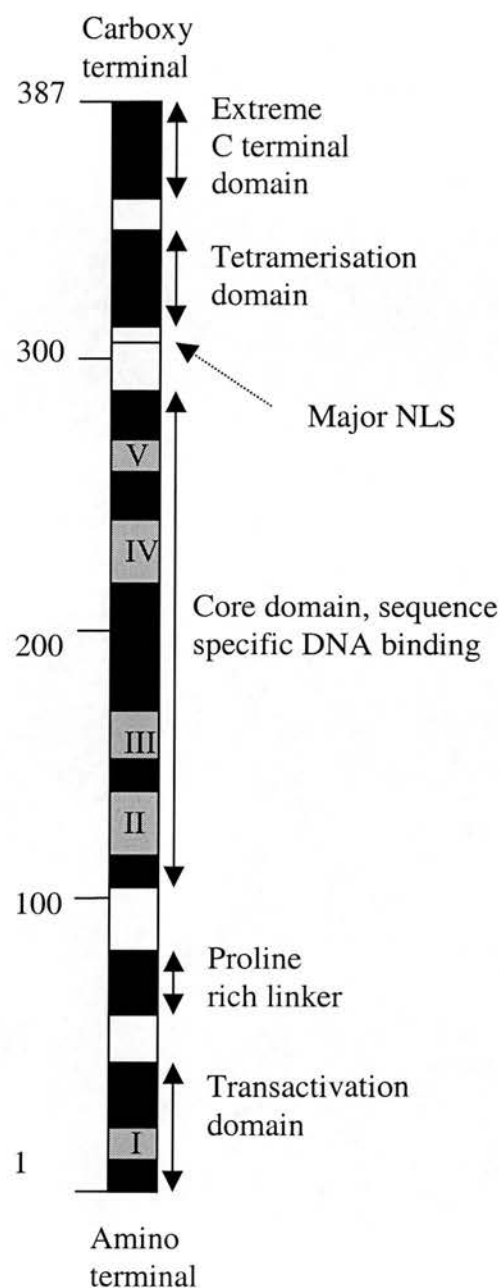
In addition to the protein binding sites described above, murine p53 also contains a putative stem loop structure within the 5' untranslated region (5'UTR) (Bienz *et al*, 1984). This region of dyad symmetry is highly conserved among species (Bienz-Tadmor *et al*, 1985) and has been postulated to mediate a regulatory interaction between the p53 protein and its own mRNA (Mosner *et al*, 1995).

Two intronic regulatory elements have also been described. In the human gene there is a strong promoter within intron 1 (Reisman *et al*, 1988) and an intron 1 initiated transcript is also seen from the mouse gene, but it is in the antisense orientation with respect to the coding p53 sequence (Knochbin & Lawrence, 1989). The second intronic regulatory element lies within intron 4 of the mouse p53 gene. p53 cDNA expression constructs lacking intron 4 showed an approximate 10 fold decrease in protein expression relative to genomic constructs or cDNAs including intron 4 (Hinds *et al*, 1989). This finding has since been extended to transgene constructs within mice (Lozano & Levine, 1991). The exact mechanism of action of this regulatory element is unclear however recent work has demonstrated the importance of a specific, but as yet uncharacterised, protein interaction with sequences within intron 4 (Beenken *et al*, 1994).

#### **1.4.2. p53 : Functional Domains and Structure**

The primary sequence of p53 is highly conserved between species and five domains, I to V, of the protein display particularly high levels of sequence conservation (Soussi *et al*, 1990). Domains I, III, IV and V are all contained in one exon each, respectively exons 2, 5, 7 and 8, while domain II is encoded by both exons 4 and 5. Domain I is located within the highly acidic amino terminus of p53 whereas II-V lie within the central core region of the protein. Various functional elements have been

**Figure 1.11** – *The Major Functional Domains of the Murine p53 Protein*



Schematic representation of the major functional domains of mouse p53. Black boxes indicate the relative position of each domain, the functions are indicated at the right hand side of the diagram. Grey boxes indicate the positions of the five (I-V) evolutionary conserved domains. Approximate amino acid numbers are shown at the left hand side of the diagram.

described within these domains and are discussed in the following sections and represented in Figure 1.11.

#### **1.4.2.1. p53: The Amino Terminus**

The transcriptional activation function of p53 was originally mapped to its acidic amino terminus (Fields & Jang, 1990) but this domain has since been more precisely defined as lying within amino acids 1-42 (Unger *et al*, 1992).

All transcriptional activators act as adaptor molecules, binding to both DNA and components of the transcription machinery thereby accelerating the association of such molecules with DNA and increasing the rate of transcriptional initiation.

Consistent with its function as a transcriptional transactivator, p53 has been shown to bind to several component of the cells transcription machinery. These include, TBP (Seto *et al*, 1992) and the human TAF's TAF<sub>II</sub>32 and TAF<sub>II</sub>70 (Thut *et al*, 1995) all of which are subunits of the general transcription factor TFIID. A p53 protein with mutations at residues 22 and 23 was unable to interact with TAF<sub>II</sub>32 and TAF<sub>II</sub>70 and was defective in transcriptional activation (Thut *et al*, 1995). Other proteins that interact with the amino terminus of p53 include the general transcription factor Sp-1 (Borellini & Glazer, 1993) and p62 subunit of the dual transcription/repair factor, TFIIF (Xiao *et al*, 1994). Weak binding has also been detected between p53 and TFIIB *in vitro* (Liu *et al*, 1993) although more recent evidence would seem to indicate that the p53/TFIIB interaction might be indirect (Liu & Berk, 1995).

As well as binding to components of the RNA polymerase II transcription system the N terminus of p53 has also been shown to bind to TFIIB (Chesnokov *et al*, 1996) and act as a general suppressor of RNA polymerase III transcription (Cairns & White, 1998). Furthermore, the binding site for the Mdm2 protein, a key negative regulator of p53 activity, has also been mapped to the N-terminal of p53. The biological significance of these interactions is discussed in more detail in Sections 1.4.5.1, 1.4.5.2. and 1.5.3.2 respectively.

#### 1.4.2.2. p53 : The Proline Rich Linker

The existence of a proline rich linker functional domain within the p53 molecule was first postulated after the observation that Pro-X-X-Pro motifs were present (amino acids 60-82 in mouse) and such motifs were already known to have functional implications in other proteins.

The use of deletion mutants demonstrated that the proline-rich linker was dispensable for the transactivation function of p53 but such mutants had severely compromised growth suppression activity (Walker & Levine, 1996). An explanation for this compromised growth suppression activity was provided by the discovery that the proline rich linker domain is necessary for the induction of p53-dependent apoptosis (Sakamuro *et al*, 1997).

Having demonstrated the functional importance of the proline-rich linker domain, the race was on to understand this function at the molecular level. The Pro-X-X-Pro motifs in the linker are characteristic of a Src homology 3 domain (SH3) (reviewed in Pawson, 1995). All known SH3 domains contain at least one Pro-X-X-Pro motif and all recognise proline-rich sequences, for example, other SH3 domains (Cohen *et al*, 1995). Therefore, it is reasonable to hypothesise that a cellular SH3 domain-containing protein must bind to the p53 SH3 domain. One candidate for the cellular SH3 domain-containing protein is the product of the *gas-1* gene. The *gas* genes (growth arrest specific) were originally identified by virtue of their increased expression in nonproliferating, G<sub>0</sub>, cells (Schneider *et al*, 1988). *gas-1* is a membrane-associated protein which, when ectopically expressed, blocks G<sub>0</sub>-S phase transition in a p53-dependent manner (Del Sal *et al*, 1995). It has since been shown that *gas-1* regulated growth suppression does not involve the sequence-specific transactivation function of p53 but is actually mediated by the proline-rich linker domain of p53 (Ruaro *et al*, 1997). As *gas-1* is an integral membrane protein, the growth suppression signal could be communicated to intracellular p53 by the hypothesised p53 SH3 domain binding protein.

#### 1.4.2.3. p53 : The Core Domain

The central core of p53 encompasses amino acids 100-300 and the evolutionarily conserved domains II to V lie within this region. The first function to be assigned to the core domain of p53 was sequence-specific DNA binding (Pavletich *et al*, 1993).

Once p53 is activated, for example in response to DNA damage, it binds DNA in a sequence specific manner. p53 recognises and binds to four copies of the consensus pentamer sequence 5'RRRCA/T 3' arranged in alternating orientations with variable distance between the two pairs ( $\rightarrow \leftarrow X \rightarrow \leftarrow$ , where each arrow represents one pentamer and X represents variable spacing) (El Diery *et al*, 1992). Consensus sequences have been identified within the promoters of many cellular genes and the binding of p53 to these sites stimulates their transcription. Both the mechanism of transcriptional transactivation (Section 1.4.2.1) and a review of p53 target genes (Section 1.4.5.1) are included elsewhere in this review.

The functional importance of this sequence specific DNA binding domain had been indicated by the observation that the vast majority of tumour-associated p53 mutations were clustered within this central core of the gene, particularly in the four highly conserved domains (Hollstein, 1994). It was only when the co-crystal structure of p53 bound to its cognate DNA binding site was solved, that the critical importance of these domains became apparent. Within the DNA-binding element of p53, which contacts both the major and minor grooves of the DNA, the residues most frequently mutated in cancer patients make critical contributions to sequence-specific DNA binding (Cho *et al*, 1994).

The original work delineating the p53 core domain also demonstrated that p53 was a zinc metalloprotein (Pavletich *et al*, 1993). The three dimensional structure of the DNA binding domain is maintained partly by a tetrahedrally co-ordinated zinc ion. This interaction is biologically important because if the ion is removed by metal chelating agents p53 conformation is altered and sequence specific DNA binding inhibited (Hainaut & Milner, 1993). The presence of the metal ion also confers

redox status sensitivity upon p53 and this topic is discussed in more detail in Section 1.4.3.4.

Interestingly, the core domain has also been shown to be the site of 3' to 5' exonuclease activity (Mummenbrauer *et al*, 1996). However, this exonuclease activity is specific to the latent form of p53 and the presence of such contrasting functions, sequence-specific DNA binding and DNA degradation illustrates the high level of regulation of p53 activity. Finally, the core domain is also a binding site for a variety of cellular and viral proteins and this will be discussed in Section 1.4.5.4.

#### **1.4.2.4. The Carboxy Terminus of p53**

The carboxy terminus of p53 contains can be functionally divided into three subdomains. A flexible linker connecting the core domain to the carboxy terminus (amino acids 300-317), a tetramerisation domain (amino acids 317-357) and, at the extreme end of the carboxy terminal, a small span of highly basic residues (amino acids 361-387 in the mouse protein).

The tetramerisation domain of p53 allows the protein to self-aggregate and form dimeric and tetrameric (dimers of dimers) species (Stenger *et al*, 1992). Truncation mutants lacking the last 47 amino acids fail to form tetrameric complexes (Milner *et al*, 1991). This interaction is biologically relevant as it is the tetrameric form of p53 that binds DNA sequence-specifically with the highest affinity (Hainaut *et al*, 1994).

The last thirty or so predominantly basic amino acids of p53 make up the extreme carboxy terminal subdomain. Despite its small size, multiple biological functions have been assigned to this subdomain. These include the regulation of the p53 activity as extensive data has confirmed that this span of basic amino acids acts as an autoinhibitory domain (See Section 1.4.3.1.a). and the regulation of the cellular localisation of p53 (Ostermeyer *et al*, 1996, and Section 1.4.3.1.b).

### **1.4.3. Mechanisms of p53 Activity Regulation**

#### **1.4.3.1. p53 in the Normal Cell**

Under normal circumstances, p53 levels within cells are low. This is due to the short half-life (approximately 15 minutes) of the protein (Kamijo *et al*, 1998). However, after DNA damage a rapid accumulation of p53 is observed within cells (Maltzman & Czyzyk, 1984). This occurs without altering the level of p53 mRNA and correlates with an increase in protein half-life (reviewed in Kubbutat & Vousden, 1998). The regulatory mechanisms responsible for the variable half-life of p53 are gradually being elucidated and this data is discussed below.

##### **1.4.3.1.a. Latent p53**

When human or mouse p53 is overexpressed as a heterologous protein in bacterial cells, the purified protein is predominantly in a latent, oligomeric state (Hupp *et al*, 1992). This protein is correctly folded and is not denatured but has a very low affinity for sequence specific DNA binding (Hupp & Lane, 1994b). Subsequent work has demonstrated that these latent p53 molecules are not simply an artefact of the expression system but do exist within normal cells. Furthermore, these latent molecules have functions discrete from those of active p53 (Wu *et al*, 1997). For example, the latent state-specific 3'-5' exonuclease activity of the p53 core domain (Mummenbrauer *et al*, 1996) and the various latent state-specific activities of the C-terminal domain. These include non-specific DNA binding (Wang *et al*, 1993), single strand nucleotide binding and RNA or DNA strand annealing (Oberosler *et al*, 1993), strand transfer (Bakalkin *et al*, 1994) and the recognition of one to three nucleotide long insertion or deletion mismatches in DNA repair (Lee *et al*, 1995). The nature of the latent state-specific activities of p53 has led to the proposal that this form of the protein may be involved in proofreading and regulating the repair of endogenous DNA damage (Wu *et al*, 1997).

The last 30 amino acids of the C-terminal of p53 form an autoinhibitory domain and are central to the regulation of the latent state. If these residues are deleted, bound by an antibody or phosphorylated, p53 is strongly stimulated to bind DNA in a sequence specific manner (Hupp *et al*, 1992; Halazonetis *et al*, 1993 and Takenaka *et al*,



1995). For example, the naturally occurring splice variant of mouse p53, ASp53, in which the wild type C-terminal amino acids are deleted (Arai *et al*, 1986) is constitutively active for sequence-specific DNA binding but lacks any non-specific binding activity (Bayle *et al*, 1995).

Because of the distal location of the C-terminal residues from the core DNA binding domain, allostery has been proposed as the mechanism of autoinhibition (Hainaut *et al*, 1994; Hupp & Lane, 1994b). According to the allosteric theory, in the latent state p53 is unable to bind DNA in a sequence-specific manner, this conformation is maintained by intramolecular (or intermolecular between different subunits of a tetramer) interactions between the C-terminal and other regions of the p53 protein. If phosphorylation or protein binding disrupts this physical interaction, p53 will be flipped into an alternative, active, conformation with increased sequence-specific DNA binding affinity. A large body of evidence exists which supports this hypothesis. For example, several authors have shown that the binding of synthetic peptides to the C-terminal of p53 activates sequence-specific DNA binding by p53 (for example, Hupp *et al*, 1995). Furthermore, using antibodies specific for different conformational states of p53 it has been demonstrated that different epitopes are exposed in latent relative to active forms of p53, suggesting the p53 protein may exist in one of at least three different conformational states of within cells (reviewed in Milner, 1995).

The existence of multiple conformational states of p53 is thought to account for the variable half-life observed for the protein. In normal cells, the vast majority of p53 is in the latent state and as such is subject to protease-mediated degradation. For example, p53 has recently been demonstrated to be a substrate of the  $\text{Ca}^{++}$  dependent neutral protease, calpain (Pariat *et al*, 1997). The strongest evidence for a role for calpain in p53 degradation comes from experiments showing that expression of calpastatin, a physiological inhibitor of calpain, leads to an elevated p53 level (Pariat *et al*, 1997). Interestingly, calpain activity is translocated into the nucleus just prior

to the onset of DNA synthesis suggesting that calpain-mediated p53 cleavage during G1 allows cells to enter S phase (Zhang *et al*, 1997).

Latent p53 is also subject to ubiquitin-dependent proteolysis via the proteasome in an Mdm-2-dependent regulatory pathway (Haupt *et al*, 1997; Kubbutat *et al*, 1997 and Section 1.4.3.2.)

In conclusion, latent p53 is subject to efficient protease-mediated degradation. However, when p53 is activated, for example after DNA damage, it undergoes a conformational change and is less efficiently targeted for protease-mediated degradation. This results in an increased protein half-life (approximately 75 minutes after  $\gamma$ -irradiation, Kamijo *et al*, 1998) and higher levels of p53 activity within such cells. The detailed mechanism of p53 induction and stabilisation and the role of Mdm2 in regulating p53 activity are discussed in Sections 1.4.4. and 1.4.3.2. respectively.

#### **1.4.3.1.b. Cellular Compartmentalisation**

Cellular compartmentalisation has also been proposed as a mechanism used by cells to regulate p53 activity. While p53 is usually thought of as a nuclear protein several groups have reported cytoplasmic p53 in both normal (Takahashi & Suzuki, 1994) and transformed cells (Moll *et al*, 1992). Subsequent experiments have provided tantalising evidence of the biological importance of these observations. For example, several groups have reported that the subcellular localisation of p53 varies during the cell cycle, with cytoplasmic sequestration during G1 and nuclear localisation once S phase has been initiated (Martinez *et al*, 1991; Takahashi & Suzuki, 1994). Impaired nuclear entry by p53 has also been implicated as a non-mutational mechanism to inactivate p53 function during tumourigenesis. In neuroblastoma-derived cell lines which express wild type p53 no nuclear accumulation is observed after treatment with DNA damaging agents which correlates with an impaired p53-mediated G1 arrest in these cells (Moll *et al*, 1996). In addition, mutant forms of p53 have allowed insights into the regulation of the cellular compartmentalisation of p53. For

example, one mutant has been identified that displays a dominant negative nuclear: cytoplasmic shuttling defect, resulting in nuclear exclusion, sufficient to confer transforming activity onto the protein (Crook *et al*, 1998). A temperature sensitive mutant p53 protein has also been identified, at the permissive temperature the protein is nuclear and confers G1 arrest on such cells, however when cells are shifted up to the restrictive temperature p53 becomes cytoplasmic and cell growth resumes (Gannon & Lane, 1991).

In order to understand the regulation of p53 localisation it has been necessary to identify other proteins involved. These can be divided into two populations, first, those that interact directly with p53 and maintain cellular compartmentalisation including several members of the heat shock protein family (Sephernia *et al*, 1996; Dasgupta & Momand, 1997). Second, those proteins that do not interact directly with p53, but may which may act to regulate p53 cellular compartmentalisation. For example, bcl-2 is known to inhibit p53-dependent apoptosis (Chiou *et al*, 1994) and one possible mechanism for this is bcl-2 mediated nuclear exclusion of p53 (Beham *et al*, 1997).

#### **1.4.3.2. Negative Autoregulation by Mdm2**

The mdm2 gene was originally identified because of its amplification in transformed mouse cell lines (Cahilly-Synder *et al*, 1987). Subsequent studies showed that the human homologue was also amplified in a significant number of tumours, for example sarcomas (Oliner *et al*, 1992). An insight into the underlying oncogenic mechanism of mdm2 was gained when its relationship with p53 was determined. It was demonstrated that mdm2 was able to bind p53 both *in vitro* and *in vivo* (Barak & Oren, 1992; Oliner *et al*, 1992) resulting in an inhibition of sequence specific transactivation by p53 (Momand *et al*, 1992; Oliner *et al*, 1993a). Two mechanisms have been proposed to explain this observation, first, that the binding of mdm2 to p53 prevents sequence specific DNA binding by p53 (Zauberman *et al*, 1993) or second, that the binding of mdm2 to p53 may prevent the interaction of p53 with

components of the cellular transcriptional machinery, for example TATA binding protein associated factors (TAF's) (Lu & Levine, 1995).

However, the most significant mdm2-mediated mechanism for the regulation of p53 activity involves the targeting of p53 for ubiquitin-directed proteolysis (Haupt *et al*, 1997; Kubbutat *et al*, 1997). For example, p53 accumulation was observed in a cell line defective in the ubiquitination process (Chowdary *et al*, 1994). Furthermore, in double transient transfection assays p53 is only stable in the presence of mdm2 mutants or after the addition of proteasome inhibitors such as MG132 or lactacystin (Midgeley *et al*, 1997). Mdm2 may function as a ubiquitin ligase, directly attaching the ubiquitin molecule to p53 (Honda *et al*, 1997). Alternatively, recent studies have demonstrated that mdm2 contains both nuclear localisation and nuclear export signals, and specific impairment of nuclear export reduces the ability of mdm2 to target p53 for degradation (Roth *et al*, 1998).

The observations that mdm2 is both a transcriptional target of p53 (Juven *et al*, 1993) and a promoter of p53 degradation led to a model in which p53 and mdm2 form an autoregulatory negative feedback loop. However, the existence of this feedback loop means that p53 stabilisation in response to genotoxic or other stress can only be achieved by interruption of this pathway. This implies a high level of regulation, and some of the molecular mechanisms involved have only recently been elucidated.

As the mdm2-targeted degradation of p53 relies on the physical interaction of the two proteins, an obvious way to regulate the pathway is to control this interaction. One potential method is by the regulation of the phosphorylation status of p53. Indeed recent data has demonstrated that DNA damage-dependent changes in site-specific phosphorylation of p53 do modulate the p53/mdm2 interaction (Shieh *et al*, 1997 and Section 1.4.3.3.a.).

An alternative mechanism used to regulate the p53/mdm2 interaction involves the tumour suppressor gene product p19<sup>ARF</sup>. p19<sup>ARF</sup> is expressed from the *INK4a* locus

and forced overexpression induces a p53-dependent cell cycle arrest (Quelle *et al*, 1995). Two groups have reported that p19<sup>ARF</sup> interacts with mdm2, an interaction which promotes the rapid degradation of mdm2 thereby inhibiting mdm2-targeted degradation of p53 and resulting in p53 stabilisation (Zhang *et al*, 1998; Pomerantz *et al*, 1998). An alternative model has also been suggested in which rather than promoting the degradation of mdm2, p19<sup>ARF</sup> blocks mdm2-mediated nuclear export of p53 (Kamijo *et al*, 1998).

The significance of the p53/mdm2 interaction at the biological level *in vivo* became apparent when mdm2 knockout mice were generated. Mdm2 null mice die early in development but this phenotype is fully rescued by the absence of p53 (Montes de Oca Luna *et al*, 1995; Jones *et al*, 1995), suggesting that the mdm2 null mouse dies because of its inability to down-modulate p53 during development. Conversely, the generation of mice that overexpressed mdm2 provided the first evidence for a p53-independent role for mdm2 in tumourigenesis (Jones *et al*, 1998).

The mdm2 gene can give rise to various transcripts that may differ in their abilities to interact with p53. The full length mdm2 protein has a predicted size of 52 kDa but migrates at 90kDa in SDS-PAGE however proteins ranging from 57 to 85 kDa have been observed in cells which overexpress mdm2 (Olson *et al*, 1993; Sigalas *et al*, 1996). The biological significance of these alternative transcripts and the proteins they encode is unclear as they have not been observed in nontransformed cells, normal tissues or during embryogenesis (Sigalas *et al*, 1996; Montes de Oca Luna *et al*, 1996). However, an mdm2 homologue MDMX has been identified (Shvarts *et al*, 1996). MDMX has significant homology to mdm2 particularly in the p53 binding domain and is able to inhibit the transactivation function of p53. Unlike mdm2 however, MDMX is not induced by DNA damage or by p53.

#### **1.4.3.3. Covalent Modification of p53**

The pleiotropic nature of p53 and the potency of its effects require the cell to tightly regulate p53 activity. Its function is controlled at the levels of transcription,

translation, protein turnover, cellular compartmentalisation and association with other proteins. p53 is also regulated by post-translational modifications including multi-site phosphorylation and acetylation. The effectors and biological consequences of these modifications are discussed below.

#### **1.4.3.3.a. Phosphorylation**

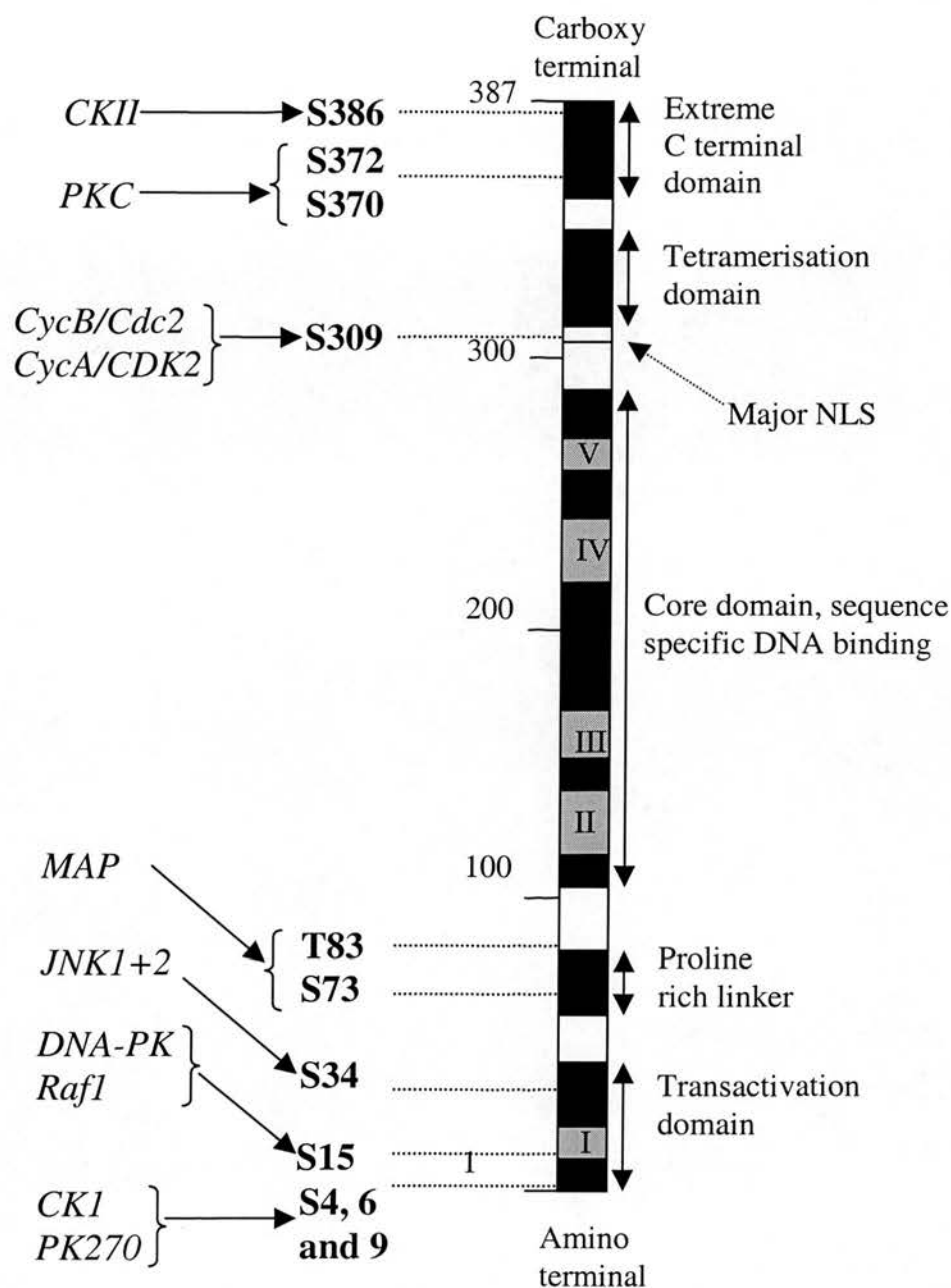
p53 contains two distinct phosphorylated regions, the amino and carboxy termini with the amino terminus being the most extensively phosphorylated part of the molecule (see Figure 1.12).

Three kinase target sites have been identified in the mouse p53 protein, Ser 4, 6 and 9 which are substrates for casein kinase 1 and the CK 1-like kinase, PK270 (Milne *et al*, 1992). Based on sequence homology the phosphorylation of human p53 on Ser 6 and 9 by the same kinases can also be predicted. Another kinase demonstrated to phosphorylate the N terminus of p53 *in vitro* is MAP kinase. Two sites have been identified in the mouse protein, Ser 73 and Thr 83, although no homologous sites exist in human p53 (Milne *et al*, 1994). MAP kinase is a member of the MAP kinase superfamily and another family member JNK1 also phosphorylates p53 *in vitro* and *in vivo* (Milne *et al*, 1995). JNK1 is an UV radiation-induced protein kinase which phosphorylates murine p53 at Ser 34 and based on sequence homology human p53 at Ser 37 (Milne *et al*, 1995). A second UV inducible kinase known to phosphorylate p53 at the N terminus is Raf-1 (Jamal & Ziff, 1995). The final p53 N terminus kinase identified to date is the double-stranded DNA-Dependent Protein Kinase (DNA-PK). DNA-PK is activated after binding to DNA containing nicks, gaps or double strand breaks and once activated is able to phosphorylate many regulatory proteins, including p53. The target sites within p53 have been identified as Ser 15 and 37 in the human protein and Ser 15 in mouse (Lees-Miller *et al*, 1992).

Three kinase target sites have been identified within the C terminus of p53. Firstly, casein kinase II (CKII) phosphorylates Ser 392 of human p53 and the equivalent residue, Ser 386 on the mouse protein (Hupp *et al*, 1992). This phosphorylation has



**Figure 1.12 – Phosphorylation Sites Within the Murine p53 Protein**



Relative positions of the major phosphorylation sites of murine p53. At the amino terminal there are seven residues that are targets for protein kinases, including serines 4, 6 and 9 which are substrates of casein kinase1 (CK1) and the related kinase PK270, serine 15 which is a substrate for both Raf1 and DNA-PK and serine 34, a substrate for JNK1 and JNK2. There are two residues which can be phosphorylated by MAPK within the proline rich linker domain, serine 73 and threonine 83. At the carboxy terminal of p53 serine 309, adjacent to the major nuclear localisation signal of p53, is a substrate for both CycB/Cdc2 and CycA/CDK2 complexes. Also serines 370 and 372 are substrates for protein kinase C (PKC) and serine 386 is phosphorylated by casein kinase II (CKII) and is also the site where a 5.8S rRNA molecule is covalently attached to the p53 protein.



been implicated in the regulation of p53 transcriptional repression (Hall *et al*, 1996) and in p53 induction in response to UV irradiation (Blaydes & Hupp, 1998).

Secondly, Ser 315 in human p53 (Ser 309 in mouse) is the target phosphorylation site for the cell cycle regulatory kinases cyclin B/Cdc2 and cyclin A/Cdk2 whereas this same site is only poorly phosphorylated by cyclin D/Cdk4 and cyclin E/Cdk2 complexes (Wang & Prives, 1995). The third kinase known to phosphorylate the carboxy terminal of p53, Ser 370 and 372, is protein kinase C (PKC) (Baudier *et al*, 1992).

Despite the large volume of work in this area the effects of p53 phosphorylation *in vivo* have proved difficult to define. However, a number of studies have generated insights into the mechanism of action of phosphorylation and these can be grouped into several areas. The first way in which phosphorylation has been proposed to act is by influencing the stability of p53. For example, the DNA damage-dependent phosphorylation events at Ser 15 and 37 in human p53 are carried out by DNA-PK (Shieh *et al*, 1997), a kinase only active in the presence of abnormal DNA structures (Gottlieb & Jackson, 1993). This phosphorylation event is thought to induce significant conformational changes in the p53 protein resulting in a decreased interaction with mdm2 and subsequent p53 stabilisation (Shieh *et al*, 1997). This phosphorylation-dependent mechanism is one way in which the mdm2/p53 negative autoregulatory feedback loop maybe overcome, for example, in response to genotoxic insult.

The phosphorylation status of p53 is also thought to regulate the DNA binding activity of the protein. For example, recombinant p53 has a low sequence-specific DNA binding activity but this can be increased by CK II phosphorylation *in vitro* (Hupp *et al*, 1992). Recombinant p53 can be activated into a DNA binding form by PKC (Takenaka *et al*, 1995) and phosphorylation of Ser 315 by cyclin B/Cdc2 or cyclin A/Cdk2 was found to selectively influence DNA binding capacity (Wang & Prives, 1995). The effects of phosphorylation on the DNA binding activity of p53 may be due to induced conformational changes. For example, two studies have

demonstrated that PKC phosphorylation alters the reactivity of p53 to conformational specific antibodies (Hupp *et al*, 1994a; Takenaka *et al*, 1995). These observations are consistent with the allosteric theory of p53 regulation, phosphorylation within the C terminus of p53 disrupts the action of the autoinhibitory domain, causing conformational changes and activating sequence-specific DNA binding.

Furthermore, phosphorylation status also modulates the transactivation activity of p53. For example, the N terminus of p53 is phosphorylated by Raf-1 and this potentiates p53-dependent transcriptional transactivation *in vivo* (Jamal & Ziff, 1995).

When considering the phospho-regulation of protein activity dephosphorylation is equally as important as phosphorylation. It has been demonstrated that p53 is specifically dephosphorylated at the PKC site *in vitro* by phosphatase 2A(PP2A) (Schiedtmann *et al*, 1991; Takenaka *et al*, 1995). Indeed, small t antigen inhibition of PP2A may be responsible for the increased p53 phosphorylation observed in SV40 transformed cells (Schiedtmann *et al*, 1991). The discovery that a target gene of p53, cyclin G interacts with a regulatory subunit of PP2A in a p53 dependent manner opens up the possibility of a feedback loop to regulate p53 activity involving these proteins (Okamoto *et al*, 1996).

Another important dephosphorylation event for human p53 is the ionising radiation (IR)-induced dephosphorylation of Ser376 (Waterman *et al*, 1998). The result of this dephosphorylation is the creation of a consensus binding site for 14-3-3 proteins. 14-3-3 proteins are so-called because of their particular migration pattern on two-dimensional DEAE-cellulose chromatography and starch gel electrophoresis. Many diverse functions have been attributed to members of this protein family, including the mediation of interactions between signal transduction molecules (reviewed in Aitken, 1996). However, in the case of p53, the binding of 14-3-3 to the C-terminal activates p53 sequence-specific DNA binding (Waterman *et al*, 1998).

In conclusion, when considering the biological effects of phosphorylation it is important to remember that the *in vivo* situation will be significantly more complex than isolated experiments *in vitro* can show. For example, the p53 molecule could be subject to multiple phosphorylations and dephosphorylations by several enzymes simultaneously. The consequences of multiple events could be significantly different to the effects of each kinase/phosphatase separately. Substantially more work is needed in this field before a definitive answer about the role of phosphorylation in regulating p53 stability and activity can be arrived at.

#### **1.4.3.3.b. Other Posttranslational Modifications of p53**

p300 and the closely related histone acetyltransferase (HATs) CBP are nuclear proteins that regulate transcription by acting as co-activators, they are found complexed with another HAT, PCAF (Yang *et al*, 1996). Both p300 and CBP have been shown to bind p53 *in vivo* (Gu *et al* 1997; Lill *et al*, 1997) and recently the acetylation of p53 *in vivo* by p300 has been demonstrated (Gu & Roeder, 1997). Furthermore, the physical association between p53 and p300 is required for transactivation of p53 target genes (Thomas & White, 1998) and influences the biological outcome of the p53 response (see Section 1.4.5.6.d. and Lee *et al*, 1998).

It is now thought that acetylation of p53 may occur as part of a cascade of post-translational modifications of the protein induced after genotoxic insult. An early response to UV or IR exposure is p53 phosphorylation, for example Ser15 phosphorylation by DNA-PK (Shieh *et al*, 1997). The phosphorylated protein is then preferentially and site-specifically acetylated, at Lys 382 in response to IR (by p300) and Lys320 and 382 (by PCAF and p300 respectively) in response to UV (Sakaguchi *et al*, 1998). The phosphorylation of Ser15 also promotes the interaction of p53 with, and acetylation by, CBP (Lambert *et al*, 1998). One proposed function of acetylation is to inhibit the latent state-specific, non-sequence-specific DNA binding activity of p53 and to promote sequence-specific DNA binding (Sakaguchi *et al*, 1998).

Finally, p53 is also subject to the covalent attachment of the 5.8S ribosomal RNA via a phosphodiester bond to Ser 386 (Fontoura *et al*, 1992 and Figure 1.12) although the biological significance of this interaction remains unclear.

#### **1.4.3.4. Redox Regulation**

In addition to the mechanisms discussed above p53 activity is also regulated by its redox and metal ion binding status. p53 must be in a reduced state to bind DNA (Hainaut & Milner, 1993) and have a metal ion, copper or zinc, bound for full DNA binding activity (Verhaegh *et al*, 1997; Hainaut *et al*, 1995).

The molecular machinery that regulates protein redox status is gradually being elucidated. For example, the protein Ref-1 was known to regulate the redox state of a number of proteins and has also been independently identified as a potent activator of latent p53. It is now known that Ref-1, which also functions as a DNA repair endonuclease, is a key regulator of p53 activity via both redox-dependent and independent means (Jayaraman *et al*, 1997).

#### **1.4.4. Induction of p53**

In normal cells levels of p53 activity are very low and the protein displays a short half-life and rapid turnover. However, in cells exposed to a genotoxic insult or environmental stress, much higher levels of p53 activity are observed with a concurrent increase in protein half-life, the so-called “p53 response”.

Numerous agents have been defined which can lead to the stabilisation of p53, these include exposure of cells to either ionising radiation (IR) or UV light generates both of which generate double strand breaks within the DNA, directly or indirectly. The presence of these dsDNA breaks is critical for the induction of p53 (Nelson & Kastan, 1994). In addition to its response to genotoxic stress, p53 has also been proposed to mediate a more general stress response to suboptimal growth conditions. Heat, starvation and hypoxic conditions induce p53 (Zhan *et al*, 1993; Graeber *et al* 1994). Another stimulus for p53 induction is depletion of ribonucleotide

triphosphates necessary for RNA synthesis the result of which is a reversible G1 cell cycle arrest in the absence of DNA damage (Linke *et al*, 1996). Furthermore, p53 can be induced by specific oncogenes such as adenovirus E1A (Lowe & Ruley, 1993) or Myc (Hermeking & Eick, 1994).

As these signals all induce high levels of nuclear p53 protein, they serve to demonstrate the ability of p53 to integrate signals emanating from diverse upstream stimuli. At least three distinct molecular pathways that result in p53 induction have been characterised. First, the induction of p53 in response to bulky DNA lesions such as those caused by UV irradiation. This pathway is thought to be mediated by the actions of multiple UV inducible kinases and has been recently reviewed elsewhere (Agarwal *et al*, 1998).

The second p53 induction pathway responds to DNA double strand breaks caused by IR exposure. A key molecule in this pathway is the Atm (Ataxia-telangiectasia mutated) gene product. Ataxia telangectasia (AT) is a human autosomal recessive disorder characterised by hypersensitivity to ionising radiation (IR), radioresistant DNA synthesis, cancer predisposition and progressive cerebellar ataxia (McKinnon, 1987). Cells derived from AT patients exhibit defective or delayed induction of p53 after IR indicating that Atm is required for the optimal transduction of the DNA damage signal to the p53 protein (Kastan *et al*, 1992). Further research has revealed that Atm is a kinase that phosphorylates and activates the nuclear protein c-Abl only after DNA damage (Baskaran *et al*, 1997). Phosphorylated c-Abl then binds to p53 enhancing its transcriptional activation function (Goga *et al*, 1995). Atm does not signal to p53 via the c-Abl route alone. As already mentioned, dephosphorylation of the Ser376 residue of human p53 occurs after exposure to IR, this event is Atm-dependent as it does not occur in cells from patients with AT (Waterman *et al*, 1998). The absence of this site-specific dephosphorylation prevents the interaction of p53 with the signal transduction mediator 14-3-3 proteins and may be causally related to the delayed kinetics of p53 induction seen in AT cells (Kastan *et al*, 1992). Furthermore, Atm is also able to signal directly to p53 as human p53 at least, is now



known to be phosphorylated at Ser15 by Atm in response to IR (Banin *et al*, 1998; Canman *et al*, 1998).

The third pathway results in the induction of p53 in response to oncogene expression and involves the p19<sup>ARF</sup> tumour suppressor protein. Thus, expression of adenovirus E1A induces p19<sup>ARF</sup> accumulation and the ability of E1A to bind and inactivate Rb solely contributes to p19<sup>ARF</sup> accumulation (de Stanchina *et al*, 1998). As already described in Section 1.4.3.2, an increase in p19<sup>ARF</sup> inhibits mdm2-directed degradation of p53 resulting in p53 stabilisation (Zhang *et al*, 1998; Pomerantz *et al*, 1998). Unlike the E1A protein which is thought to induce p19<sup>ARF</sup> by inhibiting Rb (de Stanchina *et al*, 1998), Myc induced p19<sup>ARF</sup> accumulation is thought to proceed by numerous mechanisms, one of which is a direct induction at the level of gene expression (Zindy *et al*, 1998).

Once p53 has become activated characteristic downstream events are initiated. The mechanism of action of activated p53 and the downstream events that make up the “p53 response” are discussed in the following sections.

#### **1.4.5. Biological Activities of p53**

##### **1.4.5.1. Transcriptional Activation by p53**

Muscle-specific creatine kinase (MCK) was the first mammalian gene identified as being transcriptionally activated by p53 (Weintraub *et al*, 1991). Subsequent work characterising MCK 5' regulatory sequences showed the presence of two p53 binding sequences (Kern *et al*, 1991). Since this initial discovery many more transcriptional targets of p53 have been identified.

The p21 gene (El-Diery *et al*, 1993; Harper *et al*, 1993; Xiong *et al*, 1993b) is probably the most well studied p53 response gene. p21 is a member of the Cip/Kip family of cyclin-CDK inhibitors. This protein forms part of a quaternary complex with cyclin/CDKs and PCNA (Xiong *et al*, 1993b) and at high concentrations is able to inhibit the function of CDKs, particularly those active during G1 (Harper *et al*,

1993). p21 is not the only component of the cell cycle machinery that is a target gene of p53, others include cyclin D1 (Chen *et al*, 1995), cyclin G (Okamoto & Beach, 1994), PCNA (Morris *et al*, 1996) and Rb (Osifchin *et al*, 1994).

Several other p53 target genes which play a role in mediating G1 arrest have subsequently been identified for example, GADD45 (Kastan *et al*, 1992; Lu and Lane *et al*, 1993) and Insulin-like growth factor binding protein 3 (IGF-BP3) (Buckbinder *et al*, 1996). GADD45 is thought to act by binding to the replication and repair factor PCNA, an interaction which may inhibit entry of the cell into S phase (Smith *et al*, 1994). IGF-BP3 is induced after DNA damage and encodes a secreted protein that binds IGF, a mitogenic growth factor. IGF signalling is inhibited by binding to IGF-BP3 so this antimitogenic action provides another pathway by which p53 can suppress growth. A novel member of this pro-G1 arrest class of p53 target genes has recently been identified as Siah, the human homologue of the *D. melanogaster* gene *seven in absentia* (Matsuzawa *et al*, 1998). p53-dependent Siah expression promotes G1 arrest and cells in which Siah activity is inhibited display a significant reduction in p53-induced growth arrest (Matsuzawa *et al*, 1998).

As well as inducing the transcription of genes involved in G1 arrest p53 also transactivates pro-apoptotic genes. For example, bax, a member of the bcl-2 family, is upregulated by p53 (Miyashita & Reed, 1995). While the proto-oncogene bcl-2 promotes cell survival and is anti-apoptotic, the bax gene product has an opposing pro-apoptotic effect (for review see White, 1996). The Fas/APO-1 gene, which encodes a cell surface receptor capable of transmitting an apoptotic signal upon ligand binding, is also a candidate p53 response gene. Fas expression can be increased by wild type p53 (Owen-Schaub *et al*, 1995) *in vitro*, and this correlation has also been observed *in vivo* (Reinke & Lozano, 1997). Another aptly named pro-apoptotic gene that is transcriptionally upregulated by p53 is KILLER/DR5 (Wu *et al*, 1997).



Recent work looking at gene induction occurring before the onset of outward morphological changes characteristic of apoptosis has described a whole new class of p53 inducible genes, PIG's (Polyak *et al*, 1997). Two of the fourteen PIG genes had already been identified as p53 response genes, p21 (see above) and Ei24 (Lehar *et al*, 1996) however the remaining 12 were newly identified p53 targets. Many of these genes were related to or encoded known proteins which could generate or respond to oxidative stress, for example PIG3 is a novel gene the closest relative of which is NADPH-quinone oxidoreductase (Rao *et al*, 1992). As NADPH-quinone oxidoreductase is a potent generator of reactive oxygen species (ROS) and ROS in turn are powerful inducers of apoptosis (Kroemer *et al*, 1997) the hypothesis has been put forward that p53-dependent apoptosis could be due to ROS production by PIG's.

A novel class of p53 target genes involved in neither G1 arrest or apoptosis are those that play a role in the control of angiogenesis. As normal cells progress toward malignancy they must switch to an angiogenic phenotype to attract the neovascularisation necessary for increased growth. The gain of an angiogenic phenotype is usually accompanied by loss of p53 function and in agreement with this two inhibitors of angiogenesis, thrombospondin-1 (Dameron *et al*, 1994) and BAI1 (Nishimori *et al*, 1997) have been identified as p53 target genes.

As well as the p53 target genes discussed so far, many more have been identified. These include Wig-1 (Varmeh-Ziaie *et al*, 1997), RGS-14 (Buckbinder *et al*, 1997), p22/PRG1 (Schafer *et al*, 1998), EGFR (Ludes-Meyer *et al*, 1996), FAC (Liebetrau *et al*, 1997), TGF $\alpha$  (Shin *et al*, 1995) and matrix metalloproteinase 2 (Bian & Sun, 1997). The list of p53 target genes has recently been dramatically expanded using a computer based approach to search sequence databases, 55 new p53 target genes were identified (Bourdon *et al*, 1997).

It is noteworthy that p53 also transactivates transcription of its own gene (Deffie *et al*, 1993) as well as that of its negative regulator, mdm2 (Juven *et al*, 1993) allowing tight control of intracellular p53 levels.

#### **1.4.5.2. Transcriptional Repression by p53**

The ability of wild type p53 to repress transcription is less well documented than the transactivation function of p53 although several authors have reported transcriptional repression of specific cellular genes. For example, *c-fos* (Ginsberg *et al*, 1991), interleukins 2, 4 and 6 (Pesch *et al*, 1996; Santhanam *et al*, 1991), PCNA (Mercer *et al*, 1991), MAP4 (Murphy *et al*, 1996) cyclin A (Yamamoto *et al*, 1994), the multi-drug resistance gene (MDR1) (Chin *et al*, 1992), the multidrug resistance-associated protein (MRP) gene (Wang & Beck, 1998) and the Werner's syndrome gene, (WRN) (Yamabe *et al*, 1998). The mechanism used by p53 to achieve this transcriptional repression is still the subject of research. It was originally proposed that p53 repressed transcription from promoters lacking a p53 response element and containing a TATA box sequence (Mack *et al*, 1993) through direct interaction with TBP (Seto *et al*, 1992). However, exceptions have been found to this rather simplistic rule (Shen & Shenk, 1994). More recent work has revealed that p53 actually interacts with TBP via two domains, an N-terminal region and a C-terminal region (Horikoshi *et al*, 1995). One model proposes that the N-terminal p53/TBP interaction is needed for transcriptional activation after sequence-specific DNA binding but both the N and C terminal regions of p53 are needed to interact with TBP to repress transcription (Horikoshi *et al*, 1995).

It is likely that p53 does not repress transcription solely by a pathway involving TBP, several researchers have obtained data implicating other mechanisms. For example, p53 binds to and inactivates TFIIB and acts as a general suppressor of RNA polymerase III transcription in cells (Cairns & White, 1998). Also, the interaction of p53 with CCAAT binding factor (CBF), a transcriptional activator, is necessary to repress transcription from the hsp70 promoter (Agoff *et al*, 1993). A final novel mechanism of transcriptional repression by p53 involves Hypoxia-inducible Factor

(HIF) stimulated transcription. p53 exerts its repressive activity via binding to a HIF/p300 complex and inhibiting the transcriptional activities of HIF (Blagosklonny *et al*, 1998).

A significant indicator of the biological importance of p53-mediated transcriptional repression was the demonstration that proteins that block p53-dependent apoptosis also inhibit the transcriptional repression function of p53 while leaving the transactivation function unaffected. Such proteins include WT-1 (Maheswaran *et al*, 1995), bcl-2 and the adenovirus E1B-19 kDa protein (Shen & Shenk, 1994).

#### **1.4.5.3. p53 and Translational Control**

As well as regulating gene expression at the level of transcription mounting evidence now exists that p53 is also able to regulate translation of specific genes (reviewed in Ewen & Miller, 1995a). For example, after TGF- $\beta$  exposure CDK4 mRNA fails to associate with polysomes and its translation is blocked in a p53 dependent manner (Ewen *et al*, 1995b). The exact mechanism of this p53-dependent translational inhibition is at present unclear. p53 is also thought to regulate the transcription of its own mRNA allowing rapid translation and increase in protein levels after genotoxic stress (Mosner *et al*, 1995).

#### **1.4.5.4. p53 : Direct Interactions With Other Proteins**

##### **1.4.5.4.a. Cellular Proteins**

In the previous sections, several of the proteins that interact directly have been mentioned, for example, mdm2, p300 and components of the cellular transcription machinery and these will not be discussed further in this section which will focus on other cellular binding partners of p53.

The Wilms' tumour suppressor gene product, WT1 binds p53 resulting in p53 stabilisation and increased DNA binding and transactivation capabilities of p53 (Maheswaran *et al*, 1993). Other tumour suppressor gene products known to bind p53 include BRCA1, which binds to the C-terminal of p53 and stimulates the

transcriptional transactivation activity of p53 (Zhang *et al*, 1998) and p33<sup>ING1</sup> (Garkavtsev *et al*, 1998). The growth suppression activity of p53 has been shown to depend on p33<sup>ING1</sup> expression, for example, interaction between the two proteins is absolutely necessary for p53-mediated p21 transactivation (Garkavtsev *et al*, 1998).

A specific subset of proteins with which p53 interacts are involved in DNA repair. For example, single-strand binding protein RPA (Dutta *et al*, 1993; He *et al*, 1993; Li & Botchan, 1993), TFIIH subunits p62, XPB, XPD (Xiao *et al*, 1994) the putative helicase, CSB (Wang *et al*, 1995) and human Rad51 (Sturzbecher *et al*, 1996). The binding of p53 to RPA has been reported to inhibit RPA function and this interaction is disrupted after UV damage to DNA providing a mechanism by which p53 could directly modulate nucleotide excision repair (NER) (Abramova *et al*, 1997). The XPB and XPD subunits of TFIIH also play a role in NER and p53 binding inhibits the helicase activity of both of these proteins (Wang *et al*, 1995). The XPB and XPD helicases have subsequently been shown to be essential members of the p53-dependent apoptotic pathway (Wang *et al*, 1996).

More recent work has revealed that p53 also interacts directly with another component of TFIIH, cyclin H (Schneider *et al*, 1998). Cyclin H, along with Cdk7 and Mat1 make up the heterotrimeric CAK kinase complex (Nigg, 1996). CAK kinase has two main roles, it phosphorylates and thereby activates the Cdk2/cyclin E kinase needed to ensure the G1/S transition (Nigg, 1996) and as a component of TFIIH phosphorylates RNA polymerase II to allow the elongation of transcription (Akoulichev *et al*, 1995). Interestingly, the interaction of p53 with cyclin H results in a significant downregulation of CAK kinase activity (Schneider *et al*, 1998).

A number of other cellular proteins that bind p53 have also been identified for which no obvious function has yet been ascribed. These include p53BP1 and 2 (Iwabuchi *et al*, 1994), Spot-1 (Elkind *et al*, 1995), trk kinase (Montano, 1997), p34<sup>cdc2</sup> (Wagner *et al*, 1998) and several as yet uncharacterised proteins (Maxwell & Roth, 1993).

#### 1.4.5.4.b. Viral Proteins

A number of different virally expressed proteins have been shown to bind p53 both *in vitro* and *in vivo* and directly modulate its function. A brief summary of these interactions is given below.

SV40 TAg binds to the core domain of p53 (Jenkins *et al*, 1988) and induces an increase in p53 stability (Oren *et al*, 1981). This binding blocks the transcriptional activation function of p53 (Bargonetti *et al*, 1991) and results in the abrogation of the apoptosis function of p53 *in vivo* (McCarthy *et al*, 1994).

The E6 protein from HPV employs multiple mechanisms to modulate p53 function. These include targeting the protein for ubiquitin-mediated degradation of p53 (Schneffer *et al*, 1993) and inhibiting the transactivating and transrepressing functions of p53 (Mietz *et al*, 1992; Lechner *et al*, 1992). The proposed mechanism for this inhibition of transcriptional control is thought to involve E6-mediated inhibition of sequence-specific DNA binding by p53 (Thomas *et al*, 1995).

Another viral protein known to bind directly to p53 is the 55kDa protein encoded by the adenovirus E1B gene (Sarnow *et al*, 1982). The binding of E1B 55kDa to p53 inhibits p53-mediated transcriptional activation but does not block sequence specific DNA binding by p53 (Yew & Berk, 1992). Instead it is thought that E1B 55kDa protein is a direct repressor of transcription targeted to the DNA by its interaction with p53 (Yew *et al*, 1994).

In addition to the well-characterised viral binding partners of p53 several less well understood interactions of viral proteins and p53 have also been described. These include the hepatitis B virus X protein (HBX) which has been shown to bind to p53 and inhibit the transcriptional activation function (Truant *et al*, 1995). The biological consequences of this interaction are still unclear. For example, HBX has been reported to block the nuclear import of p53 (Ueda *et al*, 1995) yet in other HBX test systems the p53 response appears to be functionally intact (Puisieux *et al*, 1995).

Other members of this newly identified group are the Epstein Barr Virus (EBV) proteins EBNA-5 (Szekely *et al*, 1993) and BZLF1 (Zhang *et al*, 1994). Finally, the IE84 protein of human cytomegalovirus can bind p53 and is capable of inhibiting the transactivation function of p53 (Speir *et al*, 1994).

#### **1.4.5.5. p53-dependent Apoptosis**

Apoptosis is a tightly regulated mechanism of cell death, distinct from necrosis, involving plasma membrane blebbing, loss of cell volume, chromatin condensation and DNA degradation (Wyllie *et al*, 1980). This complex process can be initiated by a variety of stimuli and both p53-dependent and independent apoptotic pathways have been described (reviewed in Liebermann *et al*, 1995). p53-dependent apoptosis can be triggered by a number of different stimuli including DNA damage (Clarke *et al*, 1993), oncogene activation (for example, see Hermeking & Eick, 1994), specific cytokine exposure or deprivation (Canman *et al*, 1995), hypoxia and heat shock (Graeber *et al*, 1994). Conversely, p53-dependent apoptosis can be inhibited by expression of bcl-2 or the E1B 19kDa protein from adenovirus (Debbas & White, 1993; Chiou *et al*, 1994) or by the exposure of cells to a variety of growth factors which act as positive survival signals (for example, see Canman *et al*, 1995).

Several groups have demonstrated the biological importance of p53-dependent apoptosis. For example, it acts to suppress transformation of oncogene-expressing cells (Lowe *et al*, 1994), inhibits tumour growth and progression *in vivo* (Symonds *et al*, 1994), and, in the embryo, is critical for the suppression of radiation-induced teratogenesis (Norimura *et al*, 1996).

One of the major controversies in the field of p53-dependent apoptosis is over the role of p53-mediated site-specific transcriptional activation (SST). For example, p53-dependent apoptosis can occur in the absence of RNA and protein synthesis (Caelles *et al*, 1994) and p53 SST mutants are capable of inducing apoptosis although at a slower rate than wild type p53 (Haupt *et al*, 1995). Conversely, other groups have reported that SST is critical for p53-dependent apoptosis (Sabbatini *et*



*al*, 1995). Further work now suggests that p53-dependent apoptosis can occur through both SST-dependent and -independent mechanisms, and that the requirement for either pathway is determined by the cell type (Haupt *et al*, 1996). However, even when apoptosis proceeds via SST-dependent mechanisms the transactivation of all p53 target genes is not equally important. One of the most significant pro-apoptotic p53 target genes is bax (Miyashita & Reed, 1995). For example, some tumour-derived p53 mutants that bind and activate transcription from the p21 promoter but are unable to activate bax and IGF-BP3 expression display compromised apoptotic activity (Ryan & Vousden, 1998). The development of the Death Cycle Model has provided an insight into the significance of bax expression in p53-mediated SST-dependent apoptosis (Hengartner, 1998). The stabilisation of p53 results in SST-dependent bax expression, this in turn induces depolarisation of the mitochondrial electropotential gradient ( $\Delta\Psi_m$ ) allowing the release of cytochrome *c* from mitochondrial membranes into the cytoplasm which leads to the activation of caspase-3 and results in apoptosis (Rosse *et al*, 1998). This pathway can be inhibited by the activation of KIT kinase which stabilises the mitochondrial  $\Delta\Psi_m$  and inhibits the production of reactive oxygen species (ROS) suggesting that these two processes are critical components of a p53-dependent death program (Lee, 1998). The significance of ROS in p53-mediated SST-dependent apoptosis is supported by the characterisation of the PIG genes, many of which encode proteins known to generate or respond to oxidative stress (Polyak *et al*, 1997)

In contrast, the pathway of p53-mediated SST-independent apoptosis is less well characterised although two domains of p53 have been implicated in this process, the proline-rich linker and the extreme C-terminal. Deletion of the proline-rich linker generates p53 molecules that are SST-competent, able to inhibit tumour cell growth and cell transformation but cannot induce apoptosis (Sakamuro *et al*, 1997). Whereas the mechanism of action of the C-terminal domain in SST-independent apoptosis has been proposed to involve its interaction with XPB and XPD (Wang *et al*, 1996). The observation of attenuated apoptosis induction by the ASp53 splice



variant which lacks the extreme C-terminal domain would support this hypothesis (Almog *et al*, 1997)

#### **1.4.5.6. Cell Cycle Control/Checkpoints and p53**

##### **1.4.5.6.a. p53-dependent G1 Arrest**

There is now considerable evidence that one of the most significant factors in the p53-dependent G1 arrest is the transactivation of p21. The up-regulation of p21 has pleiotropic effects within the cell including inhibition of cyclinE/cdk2 and cyclin A/Cdc2 kinases (Dulic *et al*, 1994) and binding to PCNA (Waga *et al*, 1994). The binding of p21 to PCNA is sufficient to inhibit SV40 DNA replication *in vitro* suggesting a similar p53-dependent mechanism might exist *in vivo* (Waga *et al*, 1994). Although p21 upregulation is observed during p53-dependent G1 arrest, the ability of p53 to induce G1 arrest is not totally dependent on p21 function as embryonic fibroblasts isolated from p21 null embryos are only partially deficient in G1 arrest after DNA damage (Deng *et al*, 1995; Brugarolas *et al*, 1995).

The p21-independent pathway of p53-mediated G1 arrest may involve other transcriptional target genes of p53. For example, GADD45 can bind to inhibit PCNA function thereby inhibiting entry into S phase (Smith *et al*, 1994) and p53-dependent Siah expression also promotes G1 arrest (Matsuzawa *et al*, 1998). Furthermore, the interaction of p53 with cyclin H in the CAK kinase complex has also been demonstrated to play a role in G1 arrest. p53 binds to and inhibits the action of CAK kinase, blocking the phosphorylation of its two substrates, RNA polymerase II and Cdk2. In turn, the inhibition of Cdk2 phosphorylation acts to block the activity of the cyclinE/Cdk2 complex and results in G1 arrest (Schneider *et al*, 1998).

Interestingly, as well as the p53-dependent G1 arrest after DNA damage, p53 has also been demonstrated to affect the cell cycle in the absence of DNA damage as a shortened G1 stage was observed in p53 null embryonic fibroblasts (Harvey *et al*, 1993).

#### **1.4.5.6.b. p53 and the G2/M Transition**

It has been proposed that while the onset of the G2 checkpoint is p53-independent, p53 may function as a secondary regulator (Guillouf *et al*, 1995) and play a role in the G2/M phase transition (Agarwal *et al*, 1995; Stewart *et al*, 1995). For example, it has been proposed that during the DNA damage-dependent G2 delay, p53 may regulate both double strand break repair and the post-repair exit from the G2 block (Schwartz *et al*, 1997).

The underlying molecular mechanisms and downstream targets used by p53 to regulate the G2/M arrest in response to DNA damage are currently unknown. However the discovery that cyclin G, a transcriptional target gene of p53, is an important negative regulator of this checkpoint provides the first insight (Shimizu *et al*, 1998).

#### **1.4.5.6.c. p53 and Other Cell Cycle Checkpoints**

A number of other cell cycle control functions have been ascribed to p53. For example, after the treatment of mouse embryonic fibroblasts (MEFs) with nocodazole, a spindle poison, p53 null MEFs fail to arrest and instead undergo another round of DNA synthesis in the absence of cell division (Cross *et al*, 1995). Based on this observation a mitotic checkpoint function was proposed for wild type p53. However, subsequent research has shown that p53 is not expressed during mitosis or required for mitotic arrest and expression occurs only after cells exit the mitotic arrest (Minn *et al*, 1996). This p53-dependent spindle checkpoint is now thought to occur when cells with damaged spindles enter a G1-like state in which the p53 dependent arrest would be identical to that seen after DNA damage (Lanni & Jacks, 1998). The role of p21 in this p53-dependent checkpoint is still under debate, some groups report an intact spindle checkpoint in the absence of p21 (Deng *et al*, 1995) while others demonstrate a requirement for functional p21 (Lanni & Jacks, 1998).

A role for p53 in centrosome homeostasis has also been proposed based on the observation that p53 null MEFs frequently acquire more than two centrosomes and undergo mitotic failure (Fukasawa *et al*, 1996). Although the mechanism involved remains to be identified, the physical association of p53 and MAP kinase with centrosomes (Brown *et al*, 1994; Wang *et al*, 1997), the knowledge that MAP kinase is important for centrosome homeostasis and that p53 is a MAP kinase substrate are suggestive observations (Milne *et al*, 1994).

#### **1.4.5.6.d. Growth Arrest or Apoptosis ?**

One of the fundamental questions in p53 research is how the choice is made between G1 arrest and apoptosis. It is only with the recent discovery of the functional interplay between p53 and p300 that the molecular mechanisms employed in this decision making process are becoming apparent (Avantaggiati *et al*, 1997).

p300 is a transcriptional activator and the binding of p53 to p300 is essential for p53-mediated transactivation of the p21 gene (Lee *et al*, 1998). p21 then augments the transcriptional transactivation function of the p300/p53 complex resulting in a positive feedback loop generating high levels of p21 expression leading to G1 arrest. In addition, the p53/p300 interaction allows cross-talk with the Rb/E2F-1 pathway as p300 also interacts with E2F-1, meaning that both p53 and E2F-1 are competing for the same cellular reservoir of p300. This competition between E2F-1 and p53 may explain why the ectopic expression of high levels of E2F-1 in cultured cells results in p53-dependent apoptosis (Wu & Levine, 1994). The high levels of E2F-1 sequester p300 preventing it binding to p53 and so blocking p53 transactivation of p21. The resultant low levels of p21 expression are insufficient to maintain a stable G1 arrest so the result is p53-dependent apoptosis.

Alongside p21, another gene product involved in the G1 arrest/apoptosis decision is mdm2 as the formation of the p53/p300 complex is also necessary for efficient transactivation of the mdm2 gene (Thomas & White, 1998). The adenovirus E1A protein binds to and sequesters p300 (Moran, 1993) and cells which express E1A

**Figure 1.13a** – *G1 Arrest or Apoptosis ?, the Interaction Between p53 and p300*

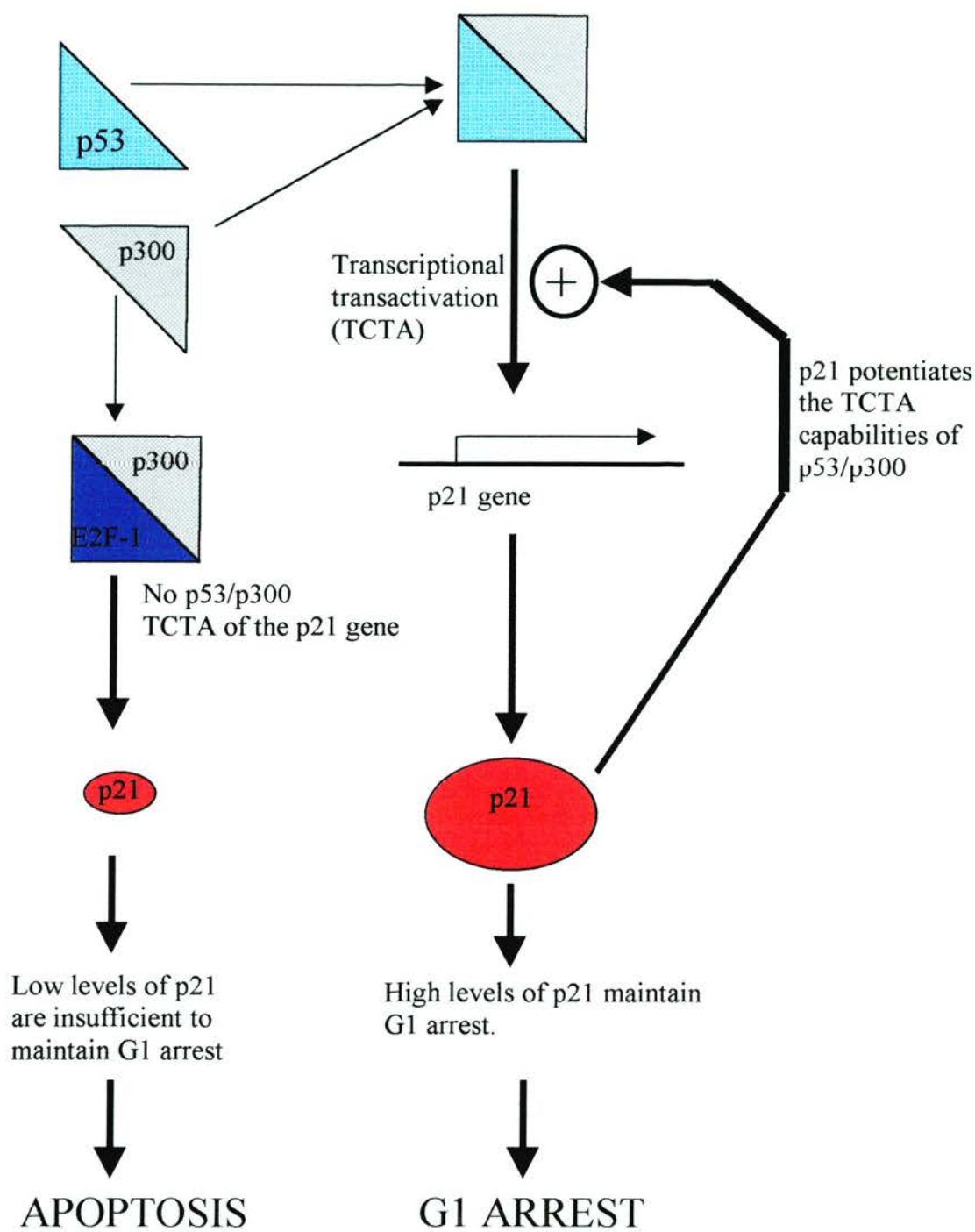
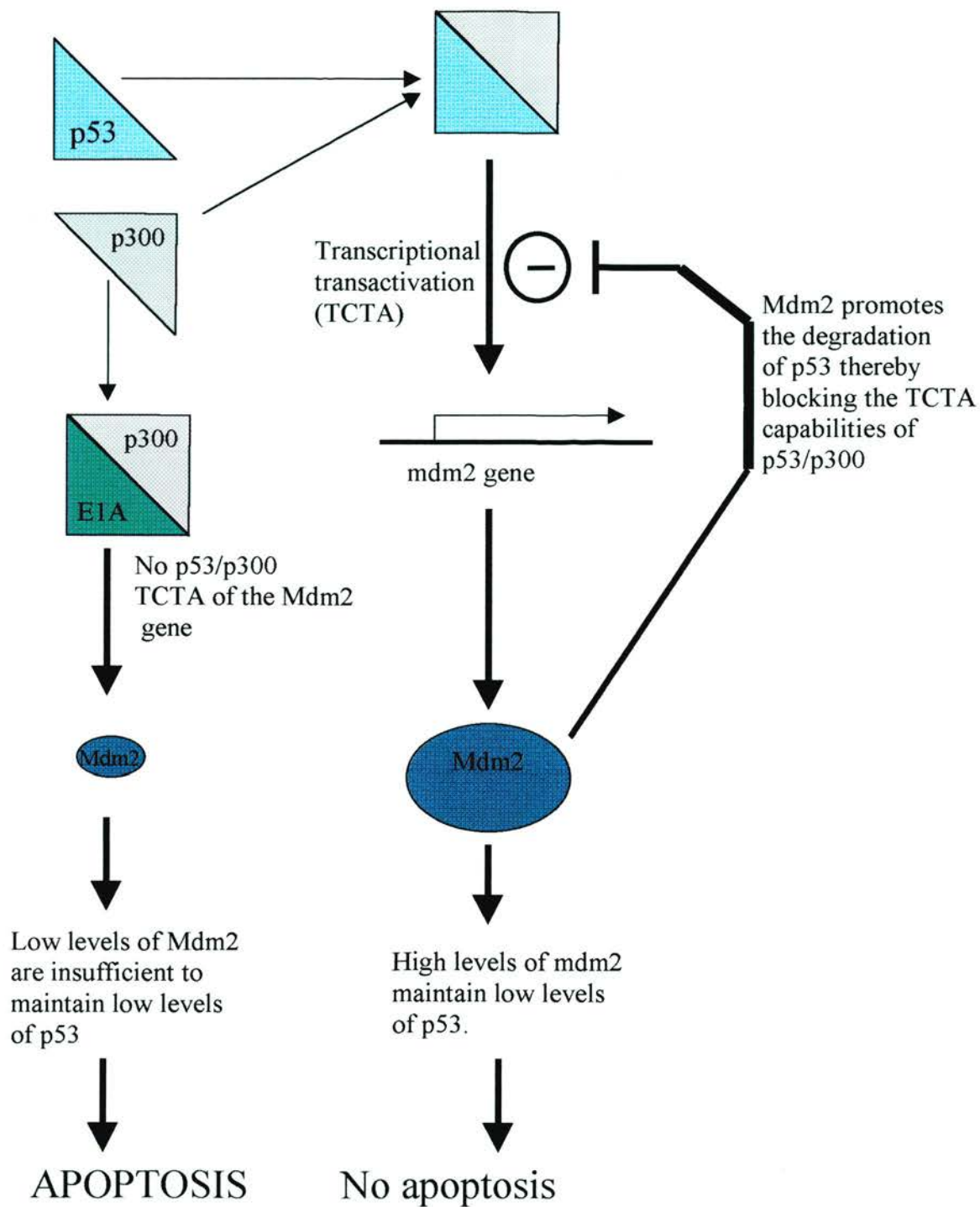


**Figure 1.13b** – *The Interaction Between p53 and p300.*



upregulate p53 but do not transactivate mdm2. The lack of mdm2 expression in such cells, means that p53 levels go unchecked leading to apoptosis (Thomas & White, 1998). The induction of p53-dependent apoptosis in E1A expressing cells may also be related to induction of p19<sup>ARF</sup> expression (see Section 1.4.4.).

In conclusion, p300 levels are critical in determining the nature of the outcome after p53 induction (Figure 1.13). If p300 is sequestered either by high E2F-1 levels or E1A expression then p53 will be unable to transactivate the expression of p21 or mdm2. Low levels of p21 will be insufficient to maintain G1 arrest and low mdm2 levels will be insufficient to inhibit p53 activity or efficiently target p53 for degradation. As such high levels of p53 will lead to apoptosis. This model is consistent with the earlier observation that the outcome of p53 induction is dependent on the level of p53 activity present in a cell (Chen *et al*, 1996).

The above section has focussed on the SST-dependent induction of apoptosis by p53 but p53 is known to induce apoptosis in an SST-independent manner. The mechanisms by which this is achieved are unclear although a tantalising glimpse has been provided by the demonstration of p53-facilitated Rb cleavage during apoptosis (Gottlieb & Oren, 1998).

The presence or absence of survival factors had been demonstrated by several groups to affect the G1arrest/apoptosis decision (Canman *et al*, 1995; Gottlieb *et al*, 1994). If cells from the interleukin 3 (IL-3) dependent haematopoietic cell-line DA-1 are exposed to DNA damage, p53 is activated. In the presence of IL-3, p53 activation results in G1 arrest but in the absence of IL-3 the outcome of p53 activation is apoptosis (Gottlieb *et al*, 1994). As such, the wild type p53 status of the cells is necessary to potentiate Rb cleavage but it is the survival factor withdrawal that actually turns on the Rb caspase activity (Gottlieb & Oren, 1998). These results were the first demonstration of a molecular mechanism for co-operation between p53 and survival factor withdrawal in the modulation of the p53 response.



#### **1.4.6. p53 in Development**

The development of gene targeting technology allowed the generation of mice with null p53 alleles (Donehower *et al*, 1992; Jacks *et al*, 1994; Purdie *et al*, 1994).

Homozygous null animals were originally reported as developmentally normal however a more detailed phenotypic examination has uncovered some problems. Predominantly female-associated defects in neural tube closure leading to exencephaly and subsequent anencephaly have been reported by two groups (Armstrong *et al*, 1995; Sah *et al*, 1995). p53 status has also been reported to influence skeletogenesis with p53 null E.17 (E.17 refers to embryos which have completed 17 days of development) embryos displaying delayed cartilage maturation (Ohyama *et al*, 1997).

Mdm2 null mice provided a further insight into the role of p53 during development. Homozygous null mdm2 animals generated by gene targeting display embryonic lethality at around E.5.5 unless they are doubly null for p53 expression also (Montes de Oca Luna *et al*, 1995). This result suggests that the primary role of mdm2 during development is to negatively regulate p53 hence dysregulated p53 expression is more detrimental to normal development than a total absence.

Because of the developmental defects observed in a percentage of p53 null embryos attempts have been made to define the role of p53 during embryogenesis.

Experiments looking at radiation induced teratogenesis in mouse embryos have demonstrated the protective function of wild type p53 against teratogenic defects (Norimura *et al*, 1996). Interestingly, the most frequent developmental defects induced by ionizing radiation (IR) in p53 null embryos affect the tail and limbs (Norimura *et al*, 1996) which are also the sites of maximal p53-SST induction after IR in wild type embryos (Gottlieb *et al*, 1997).

#### **1.4.7. p53 and Tumourigenesis**

Several lines of evidence indicated the importance of p53 in tumourigenesis. For example, mutation of the p53 gene is one of the most frequently observed genetic



alterations in carcinogenesis (reviewed in Hollstein *et al*, 1997). That p53 loss of function is important in tumour development was further supported by the phenotype of both mice and humans with compromised p53 function. Patients with Li-Fraumeni syndrome have a germline mutation in one p53 allele and display a predisposition to a range of cancers (Malkin *et al*, 1990; Srivastava *et al*, 1990) and p53 null mice generated by gene targeting are highly predisposed to malignancy (Donehower *et al*, 1992, Jacks *et al*, 1994; Purdie *et al*, 1994).

Because of the pleiotropic nature of p53 function and the multiple p53 inactivation mechanisms means that p53 loss of function is thought to facilitate tumour progression in many ways.

#### **1.4.7.1. Attenuated Apoptosis**

The use of transgenic mouse models has allowed insights into the role of p53-dependent apoptosis in tumour suppression. Mice which express HPV E7 protein (inactivates Rb function) in the lens and retina display high levels of apoptosis, inhibition of normal cell differentiation and enhanced cell proliferation (Pan & Griep, 1994). However, retinal or lens tumours were only seen when these mice were crossed to either p53 null animals or a strain expressing the HPV E6 protein (see Section 1.4.5.4.b) which correlated with a significant reduction in apoptosis in the affected tumour tissues (Pan & Griep, 1994).

The role of attenuated apoptosis in tumour progression was further demonstrated by another transgenic mouse model. Transgenic mice expressing a truncated SV40 large T antigen protein, capable of inactivating Rb function but not p53 developed slow growing tumours. However, when crossed onto a p53 null background these mice developed aggressive tumours with attenuated apoptosis (Symonds *et al*, 1994).

The discovery that hypoxia induces p53-dependent apoptosis provided more support for a role of apoptosis in tumour progression. Hypoxic conditions, common in areas within large tumours, select for cells with defects in the apoptotic pathway and in

particular p53 mutations. As a result high levels of apoptosis are observed in tumours with hypoxic regions and functional p53, but not in hypoxic regions of tumours that have lost wild type p53 function (Graeber *et al*, 1996).

#### **1.4.7.2. Increased Genomic Instability**

The association of p53 loss of function and increased genomic instability has been established *in vitro* (Livingstone *et al*, 1992; Cross *et al*, 1995). p53 mutations in a range of human tumours have also been associated with increased aneuploidy or genomic instability (for example see Blount *et al*, 1994). Mouse models have again provided more data to support this hypothesis. Transgenic mice that ectopically express the Wnt-1 oncogene in the mammary gland develop mammary cancer (Donehower *et al*, 1995). When these mice were crossed to p53-deficient mice tumours developed earlier, displayed a more anaplastic morphology and contained more chromosomal abnormalities (Donehower *et al*, 1995).

#### **1.4.7.3. Increased Proliferative Capacity**

Another mechanism by which loss of p53 function may contribute to tumour progression is enhanced cell proliferative capacity. For example, p53 null MEFs have shorter cell cycle times and higher proliferation rates *in vitro* than wild type MEFs (Harvey *et al*, 1993). This increased proliferative capacity may be partly explained by the loss of p53-dependent checkpoints within the cell cycle.

#### **1.4.7.4. Increased Invasiveness and Metastasis**

Both mouse and human data have suggested a link between loss of p53 function and the acquisition by a tumour of a malignant, metastatic phenotype but there is still debate over whether this is a direct result of p53 loss of function or an indirect consequence. For example, in human colorectal cancer the transition from localised adenoma to invasive carcinoma is often accompanied by p53 mutation (Fearon & Vogelstein, 1990) and in prostate cancer p53 mutations are associated with the metastatic forms of the disease (Bookstein, 1994). The application of the classic two stage skin carcinogenesis protocol to p53-deficient and normal mice, found that p53

null mice developed fewer benign papillomas and more malignant carcinomas in a shorter timespan than treated normal mice. Furthermore, the carcinomas observed in the p53 null mice tended to be poorly differentiated and more invasive (Kemp *et al*, 1993).

#### **1.4.7.5. Increased Angiogenesis**

In order to support tumour growth beyond the size of a few millimetres angiogenesis must occur within the tumour mass. The discovery that the transcriptional target genes of p53 include thrombospondin-1 (TSP-1) (Dameron *et al*, 1994) and BAI1 (Nishimori *et al*, 1997), both potent inhibitor of angiogenesis, placed p53 as a central regulator of angiogenesis. Preliminary evidence also indicates regulation of other anti-angiogenic genes by p53 (Van Meir *et al*, 1994). It is also worth noting that as well as mutation of p53 inhibiting the SST of anti-angiogenic genes specific mutant forms of p53 are able to transcriptionally upregulate bFGF, a potent angiogenic factor (Ueba *et al*, 1994).

#### **1.4.8. p53 Related Proteins**

Up until 1997 it was thought that p53 was a unique protein with no other related molecules. This myth was dispelled with the discovery of p73. Two splice variants of p73 were originally reported,  $\alpha$  and  $\beta$  (Kaghad *et al*, 1997), although more recent work has led to the identification of two new variants,  $\gamma$  and  $\delta$  (DeLaurenzi *et al*, 1998). All four splice variants differ only in their 3' sequence due to alternative exon splicing but have distinct activities. For example, p73 $\gamma$  can efficiently heterodimerise with all other p73 isoforms whereas p73 $\delta$  binds efficiently to the  $\alpha$  and  $\gamma$  isoforms only (DeLaurenzi *et al*, 1998). All of the p73 isoforms share a high level of sequence homology with p53, up to 63% in the core domain which suggests some level of functional redundancy (reviewed in Wiman, 1997). Indeed, p73 is able to transactivate p21 and induce apoptosis when overexpressed (Kaghad *et al*, 1997; Jost *et al*, 1997) although viral oncoproteins such as adenovirus E1B and SV40 TAg discriminate between p53 and p73 (Marin *et al*, 1998) and p73 is not induced after DNA damage (Kaghad *et al*, 1997).

The status of p73 as a tumour suppressor is still under debate. For example, the p73 gene is located on human chromosome 1p36 a region that is frequently deleted in a variety of human cancers although to date, no intragenic mutations have been identified in human cancer cells (Kaghad *et al*, 1997). It has been suggested that the p73 gene may be subject to imprinting while a role for epigenetic control of p53 expression cannot be excluded, there are currently no genetic data that firmly establish that p73 is a tumour suppressor (DeLaurenzi *et al*, 1998).

Since the publication of the p73 work a flurry of subsequent papers have described the identification of other p53 homologues. The newly discovered p53 homologues can be divided into two groups, depending on their C-terminal structure. The first includes p53 itself, p73 $\beta$  and p51A (Osada *et al*, 1998). The second group includes all proteins that have C-terminal extensions that at present are of unknown function. Members of this group are the squid (*Loligo forbesi*) p53 protein, the rat KET protein (Schmale & Bamberger, 1997) and p73 $\alpha$  (Kaghad *et al*, 1997). The absence of structural data prevents the assignment of the newly identified p73  $\gamma$  and  $\delta$  isoforms and another p53 homologue, NBPp53RE within the two groups described above (Zeng *et al*, 1998).

This already complex picture has been further complicated by the discovery of RB18A (Drane *et al*, 1997). This protein is not a true homologue of p53 but does share both antigenic and functional properties and is thought to be an upstream regulator of p53 activity (Drane *et al*, 1997).

#### **1.4.9. Conclusions**

In the twenty years since p53 was first discovered significant advances have been made in our understanding of this complex protein. The identification of both upstream regulators and downstream effectors has facilitated a more complete understanding of p53 function. Furthermore, the discovery that p53 plays a significant part in multiple molecular pathways and acts as an integration point for

many intracellular signals has greatly increased our understanding of the tumour suppressor function of this protein. However, it is testament to the pleiotropic nature of p53 function that after twenty years there are still unanswered questions.

## **1.5. Replicative Cellular Senescence**

### **1.5.1. Introduction**

Replicative cellular senescence describes the process of terminal growth cessation and morphological change displayed by normal animal cells after they have undergone a finite number of population doublings *in vitro* (Hayflick & Moorhead, 1961). Cellular senescence is not programmed cell death as these cells are viable in culture for long periods of time, remaining metabolically active, adherent to the growth surface (Matsumura *et al*, 1979) and resistant to apoptosis (Wang, 1995).

Cells display several novel characteristics upon entry into senescence. Senescent cells enter an irreversible cell cycle block and cannot initiate DNA synthesis in response to mitogenic stimulation (Cristofalo *et al*, 1989) although this is not due to a lack of DNA synthesis machinery (Gorman & Cristofalo, 1985). Furthermore, senescent cells acquire altered functions and morphology and have been likened to terminally differentiated cells (Goldstein, 1990).

Two models have been proposed to explain the phenomenon of replicative cellular senescence. In the first, the cell is seen as passive, simply accumulating mutations with each round of replication until a critical threshold is reached which triggers senescence. Conversely, in the programmed control or genetic hypothesis the cell is envisaged as actively regulating the onset of senescence via an intrinsic, genetically controlled process. Therefore, at the end of the proliferative life span of a normal cell an internal genetic programme may be activated which results in the characteristic morphological and growth arrest changes of replicative cellular senescence (Macieira-Coelho, 1988). The majority of the experimental evidence discussed in the following sections supports this second hypothesis.

### 1.5.2. Senescence *in vivo*

The first description of replicative cellular senescence was based on observations *in vitro* (Hayflick & Moorhead, 1961), however, evidence now exists which indicates that senescence is a true *in vivo* phenomenon and not an artefact of *in vitro* cell culture. Morphologically senescent cells have been observed (Bruce, 1991) and detected histochemically *in vivo* (Dimri *et al*, 1995). Serial cell transplantation experiments have demonstrated that normal cells, but not tumour cells, have a limited life span *in vivo* (Daniel *et al*, 1968) and cells aged *in vivo* or *in vitro* share certain biochemical characteristics (Heydari *et al*, 1993). The acceptance of senescence as a true *in vivo* phenomenon has stimulated research into the functions of this complex process and two roles have been proposed, in ageing and in neoplasia.

There are several lines of evidence that suggest that cellular senescence *in vitro* represents ageing at the cellular level *in vivo*. Firstly, the maximum cumulative population doubling that cultured, normal fibroblasts can achieve reflects the average life span of the species from which they are derived (Stanley *et al*, 1975). This observation suggests that the replicative lifespan of cells and the chronological lifespan of organisms may be controlled by overlapping or interacting genes (reviewed in Campisi, 1996). Secondly, there is an inverse relationship between the lifespan in culture and age of the organism from which the cultured cells were obtained suggesting that cells in renewable tissues may progressively exhaust their replicative lifespan *in vivo* during ageing (Martin, 1993). Furthermore, fibroblasts established from individuals with genetically linked ageing syndromes display a reduced proliferative capacity (Goldstein, 1969; Goldstein *et al*, 1989, see also Section 1.5.4.3.).

The proposed involvement of senescence in neoplastic development is related to the suppression of growth that occurs as cells enter senescence. The ability of this process to limit the proliferative capacity of normal cells has led to the hypothesis that it may act to suppress tumour formation *in vivo*. In support of this suggestion, the majority of tumour cell lines can be cultured indefinitely *in vitro* indicating that



they have escaped the constraints of replicative senescence (Leibovitz, 1986). However, not all primary tumours are capable of giving rise to immortal cell lines (Paraskeva *et al*, 1988). Therefore, although immortality alone is insufficient for neoplastic progression, immortal cells are more susceptible to spontaneous, oncogene-induced or carcinogen-induced progression (Barrett, 1987). In line with this hypothesis, certain oncogenes, both viral and cellular, also act to extend replicative lifespan (reviewed in Campisi, 1996). Furthermore, key genes involved in the establishment and maintenance of senescence include well known tumour suppressor genes such as p53 and RB.

### **1.5.3. Genetic Regulation of Senescence**

Senescence is characterised by a terminal growth arrest and several lines of evidence indicate that this arrest occurs in the G1 portion of the cell cycle. For example, stimulation of senescent cells with serum mitogens induces the expression of some genes associated with G1 progression in cycling cells but does not permit entry into S phase (Seshadri & Campisi, 1990). Furthermore, flow cytometric analysis has confirmed a G1 DNA content for the majority of cells in a senescent population (Sherwood *et al*, 1988). The conclusion that senescence-induced growth arrest occurs in G1 is supported by an analysis of key cell cycle regulatory molecules within these cells (reviewed in Vojta & Barrett, 1995)

As the cell cycle effector molecules used to implement and maintain this terminal growth arrest are the same as those required for reversible G1 arrest in normal, non-senescent cells, the key differences between the two processes must lie in their upstream regulation. The genetic regulation of senescence is discussed in the following sections.

#### **1.5.3.1. Chromosomal Localisation of Pro-senescence Genes**

The technique of somatic cell hybridisation has been instrumental in dissecting the genetic regulation of senescence. Fusions between different immortal cell lines can result in senescent hybrids, indicating that specific immortal cell lines differ in the



defects they possess in the senescence genetic pathway(s). Using this technique four different complementation groups have been identified, A, B, C and D (Pereira-Smith *et al*, 1988). In theory all the members of one complementation group will have a similar genetic alteration and so the endpoint of this work was to identify the specific genes involved. However, it should be noted that certain immortal cell lines can be assigned to more than one complementation group highlighting the complexity of senescence regulation (Duncan *et al*, 1993).

The first step towards the characterisation of individual pro-senescence genes was to identify which chromosomes carried pro-senescence activity. Microcell-mediated chromosome transfer has been used to map pro-senescence activity to human chromosomes 1 (Sugawara *et al*, 1990), 4 (Ning *et al*, 1991), 6 (Sandhu *et al*, 1994), 7 (Ogata *et al*, 1993), 11 (Koi *et al*, 1993), 18 (Sasaki *et al*, 1994) and X (Klein *et al*, 1991). The senescence-inducing activity of human chromosome 1 has since been assigned to complementation group C (Hensler *et al*, 1994), chromosome 4 to group B (Ning *et al*, 1991) and chromosome 7 to group D (Ogata *et al*, 1993). Subsequent research has led to the identification of two candidate regions, at 1q25 and 1q41-42, for a pro-senescence gene on chromosome 1 (Karlsson *et al*, 1996) and the discovery of the MORF4 (mortality factor 4) gene on chromosome 4 (Berube *et al*, 1998).

Recent mapping studies have also helped pinpoint the pro-senescence gene, termed SEN-6, present on human chromosome 6 (see also Section 1.5.4). One candidate for SEN6 is the AF6 gene known to be deleted and/or mutated in several TAg-expressing immortal HDF clones (Prasad *et al*, 1993). This gene is a tantalising candidate for SEN-6 as the gene product is known to participate in several signal transduction pathways and interacts with other cellular proteins such as *ras* and *Apc* (reviewed in Jha *et al*, 1998).

#### **1.5.3.2. Individual Pro-senescence Genes**

Experiments with SV40 large T antigen (TAg) have facilitated the dissection of the internal senescence-regulatory program and the identification of individual

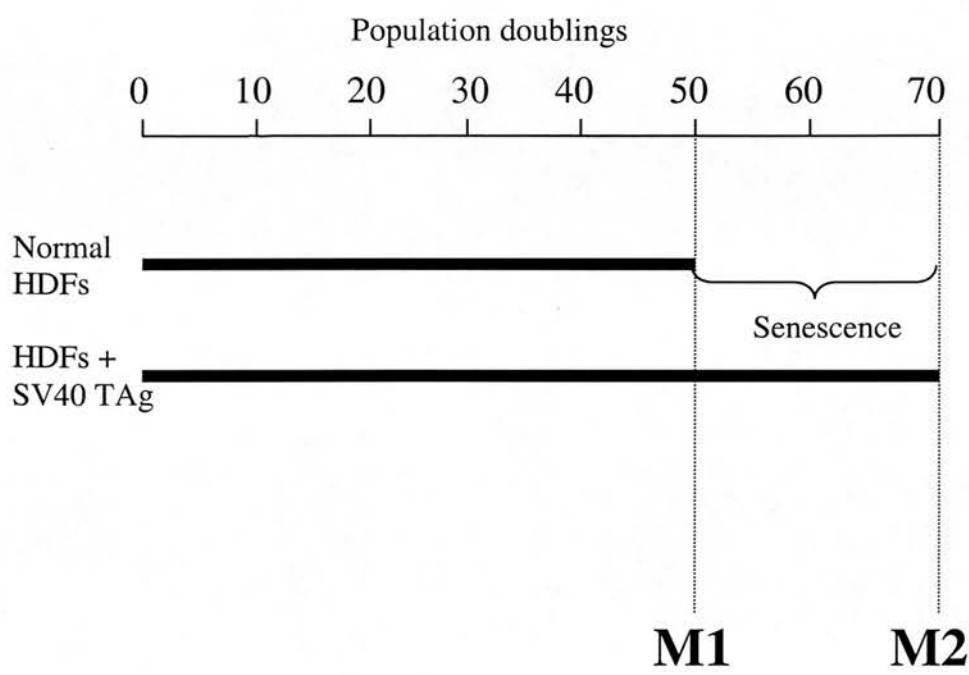
senescence regulatory genes. Briefly, normal human diploid fibroblasts (HDFs) proliferate for approximately 50 population doublings *in vitro* (Shay & Wright, 1989). After this point, named M1 or the first mortality checkpoint, the cells enter a characteristic senescent state. Transfection of HDFs with TAg extends their replicative lifespan beyond M1 and up to approximately 70 population doublings. Such TAg-expressing cultures then enter a state termed crisis or M2, the second mortality checkpoint. High levels of cell death are observed in a crisis culture but proliferation also occurs and rare immortal variants may emerge. These immortal clones have overcome both the first and second mortality checkpoints (reviewed in Jha *et al*, 1998; see Figure 1.14).

#### **1.5.3.2.a. RB**

The RB tumour suppressor gene product is a strong candidate as a pro-senescence regulatory gene as the reintroduction of RB into certain immortal cells is sufficient to induce a senescent phenotype (Xu *et al*, 1997).

The RB protein is found at similar levels in young and senescent cells but exists predominantly in the hypophosphorylated, growth inhibitory form in senescent cells (Stein *et al*, 1990). The growth inhibitory activity of the hypophosphorylated form of the RB protein is due to its ability to bind the E2F transcription factor complex (Nevins, 1992). This interaction sequesters E2F and inhibits the transcriptional transactivation function of the protein, it may also cause E2F to actively repress transcription (Weintraub *et al*, 1992). The absence of E2F-mediated transcriptional transactivation in senescent cells has several downstream effects. Genes which would normally be upregulated by E2F are not, for example, c-fos, which has two E2F binding sites within its promoter (Chellappan *et al*, 1991), is transcriptionally down-regulated in senescent cells (Seshadri & Campisi, 1990). Many other genes also contain E2F binding sites in their promoters, including cell proliferation genes whose expression is required to exit G1 (DeGregori *et al*, 1995). The abrogation of E2F-mediated transcriptional transactivation in senescent cells is likely to be one of several mechanism used by cells to maintain senescence as the restoration of E2F-1

**Figure 1.14 - Mortality Checkpoints and Replicative Cellular Senescence**



Normal human diploid fibroblasts (HDFs) will proliferate *in vitro* for approximately 50 population doublings until they reach the first mortality checkpoint (M1). Such cells then enter senescence. IF HDFs are stably transfected with SV40 TAg the replicative lifespan of the culture is extended beyond M1 for approximately 20 population doublings and such cells do not enter senescence. However, at the end of their lifespan, TAg-expressing cultures reach the second mortality checkpoint (M2) and enter crisis. Cell death and cell proliferation occur within crisis populations and rare immortal clones, which have bypassed M2 may arise (reviewed in Jha *et al*, 1998).

expression (a component of the E2F transcription complex) is insufficient to induce cell cycle re-entry in senescent cells (Dimri *et al*, 1994).

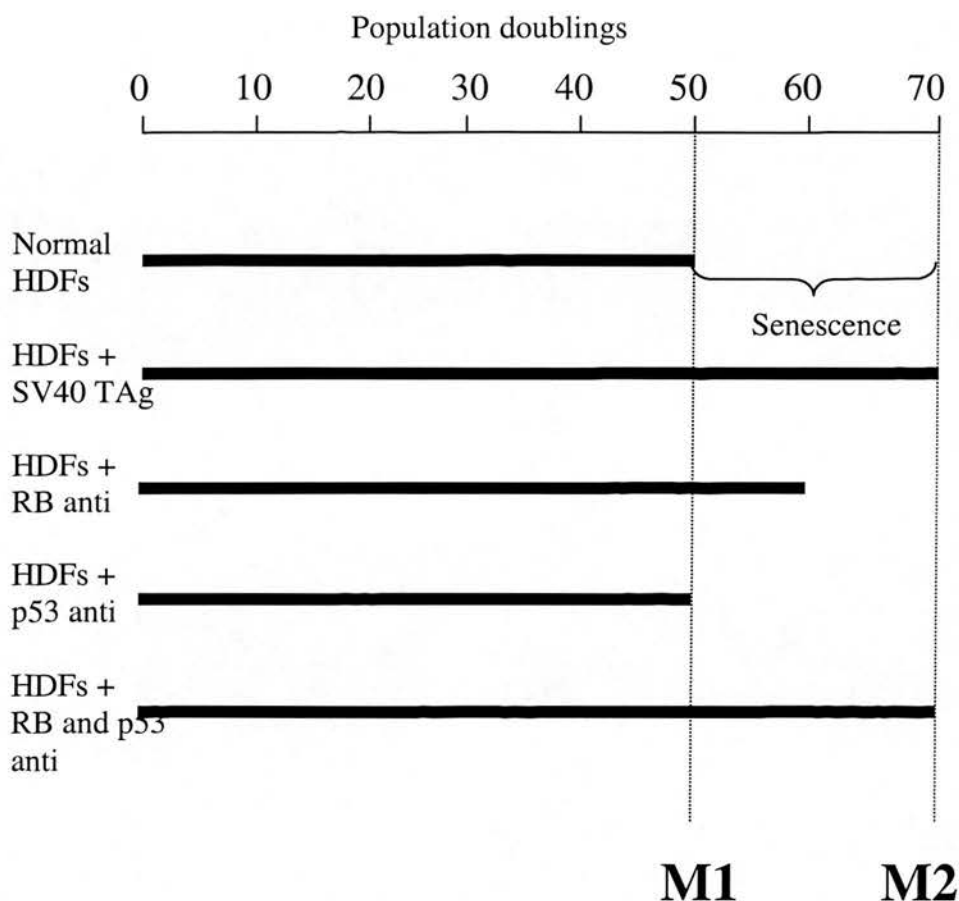
One mechanism by which RB is proposed to regulate senescence is by controlling the M1 checkpoint. For example, if HDFs are cultured in the presence of antisense oligonucleotides that inhibit the expression of RB, their lifespan is extended by approximately 10 population doublings beyond the normal M1 checkpoint (Hara *et al*, 1991 and Figure 1.15). Hence, while antisense-mediated reduction of RB expression can extend a cells replicative lifespan and delay the onset of M1, it is insufficient to allow cells to overcome M1 completely. The importance of RB in the regulation of M1 is further supported by the observation that SV40 TAg-mediated escape from M1 is dependent upon the inactivation of both RB and p53 (reviewed in Jha *et al*, 1998).

#### **1.5.3.2. p53**

As with the RB protein, work with SV40 TAg demonstrated a requirement for wild type p53 activity to maintain an intact first mortality checkpoint. Interestingly, HDFs cultured in the presence of antisense oligonucleotides that inhibited the expression of p53 did not have significantly different replicative lifespans to untreated HDFs, yet if such cells were exposed to both p53 and RB antisense oligonucleotides, M1 was abolished (Hara *et al*, 1991 and Figure 1.15). M1 dependence upon both functional p53 and RB was further supported by the observation that continued proliferation of post-M2, TAg-transfected immortal HDF clones was dependent upon continued SV40 TAg expression (Wright *et al*, 1989). Both the p53 and RB binding functions of TAg are required to maintain post-M2 proliferation demonstrating that a functional M1 checkpoint would otherwise be reconstituted that would be sufficient to induce senescence. The significance of p53 in regulating senescence was further confirmed by a report documenting senescence induction after the reintroduction of p53 into an immortal tumour cell line (Sugrue *et al*, 1997).

In addition, primary embryonic fibroblasts derived from p53 targeted animals

**Figure 1.15** – *Effects of Antisense Oligonucleotides on the Onset of Replicative Cellular Senescence*



Normal HDF's will proliferate in culture for approximately 50 population doublings after which point they reach M1 and enter replicative cellular senescence. HDF's stably transfected with SV40 TAg continue to proliferate for approximately 70 population doublings beyond M1 after which point they reach M2 and enter a crisis state. HDFs cultured in the presence of antisense RB oligonucleotides proliferate beyond the normal M1 point for approximately 10 population doublings before entering senescence. In contrast, no lifespan extension is observed when HDFs are cultured in the presence of p53 antisense oligonucleotides. However, if HDFs are cultured with both p53 and RB antisense oligonucleotides M1 is abolished and the cells behave identically to those stably transfected with Sv40 TAg (Hara *et al*, 1991). These experiments have formed the basis of the hypothesis that the M1 checkpoint is dependent on both p53 and RB function and although this work was carried out in human cells an analogous mechanism is thought to exist in murine cells.

display different growth characteristics relative to normal cells. p53 homozygous null EFs will proliferate for over 50 passages *in vitro* with no obvious senescent phase whereas both heterozygous and wild type fibroblasts enter senescence by approximately passage 20 (Harvey *et al*, 1993). While the constitutive absence of p53 expression can explain the prolonged proliferation of p53 null EFs past M1, continued growth of the culture must be dependent upon the acquisition of other mutations, this may correlate with the high levels of genetic instability reported in these cells (Harvey *et al*. 1993; see also Section 1.5.4).

It should be noted that although the levels of p53 transcription do not change as a cell approaches senescence, p53 activity increases as there is a shift from the latent to the active form of the molecule (Atadja *et al*, 1995).

#### **1.5.3.2.c. p21**

The p21 gene was first identified as it encoded an mRNA that was present at higher levels in senescent cells than in young cells (Noda *et al*, 1994). Subsequent work revealed that p21 forms a quaternary complex with cyclins, cyclin-dependent kinases (CDKs) and PCNA (Xiong *et al*, 1993). This interaction inhibits the activity of the complexed CDK; hence p21 acts to block CDK-mediated phosphorylation of the RB protein (Harper *et al*, 1993). Although re-expression of p21 in spontaneously immortalised, p53 null human fibroblasts is sufficient to induce senescence (Vogt *et al*, 1998), senescence is not strictly dependent on p21 expression (Medcalf *et al*, 1996). These seemingly contradictory results only serve to highlight the complexity of the multiple genetic pathways that are thought to regulate senescence.

#### **1.5.3.2.d. p16<sup>INK4a</sup>**

p16<sup>INK4a</sup> was originally identified as a protein that bound the cyclin dependent kinase CDK4 and it was subsequently shown to be a specific inhibitor of the kinase activities of both CDK4 and CDK6 (Serrano *et al*, 1993). One of the substrates of CDKs 4 and 6 is the RB protein (reviewed in Weinberg, 1995), the combination of high levels of p21 and p16<sup>INK4a</sup> in senescent cells should act in concert to maintain

RB in a growth inhibitory, hypophosphorylated form. As p16<sup>INK4a</sup> acts to negatively regulate cellular proliferation it was put forward as a candidate tumour suppressor gene. This was confirmed when high frequencies of hemizygous and homozygous deletions of the p16<sup>INK4a</sup> locus were observed in both primary tumours and tumour cell lines (reviewed in Larsen, 1996). In fact, of all of the genes which encode cell cycle components, the p16<sup>INK4a</sup> gene is the most frequently inactivated or mutated during tumorigenesis (reviewed in Hiram & Koeffler, 1995).

The accumulation of p16<sup>INK4a</sup> in senescent cells provided the first clue that this protein was also involved in the regulation of cellular senescence (Loughran *et al*, 1996). In addition, loss of p16<sup>INK4a</sup> facilitates immortalisation in many systems (Serrano *et al*, 1996), and the viral oncoprotein Tax from HTLV-1 inactivates p16<sup>INK4a</sup> by direct physical interaction and thereby promotes immortalisation (Suzuki *et al*, 1996). The recent demonstration that the restoration of p16<sup>INK4a</sup> expression in spontaneously immortalised fibroblasts is sufficient to induce senescence confirms the significance of this protein in the regulation of senescence (Vogt *et al*, 1998).

#### **1.5.3.2.e. p33<sup>ING1</sup>**

The p33<sup>ING1</sup> tumour suppressor gene was identified using a cloning strategy to distinguish genes whose expression is specifically reduced in cancer cells (Garkavtsev *et al*, 1996). Further research has revealed that p33<sup>ING1</sup> is a component of the p53 signalling pathway and that overexpression of p33<sup>ING1</sup> inhibits cell proliferation in a p53-dependent manner (Garkavtsev *et al*, 1998). The demonstration that p33<sup>ING1</sup> expression is specifically upregulated in senescent cells and that expression of antisense p33<sup>ING1</sup> mRNA in presenescent fibroblasts extends their replicative life span is strong evidence that another function of p33<sup>ING1</sup> is as a prosenescence gene (Garkavtsev & Riabowol, 1997).

#### **1.5.3.3. Anti-senescence Genes**

The above sections have focussed on genes whose actions are considered as pro-senescence. However, the existence of anti-senescence genes has also been



postulated. Werner's syndrome (WS) is a rare autosomal recessive genetic disorder characterised by symptoms of premature ageing (Epstein *et al*, 1966) and the development of rare cancers (Goto *et al*, 1996). Fibroblast cell strains established from individuals with WS display precocious senescence (Goldstein *et al*, 1989).

The gene responsible for WS, WRN, has been mapped to human chromosome 8p11-12 (Yu *et al*, 1996) and shown to function as a DNA helicase (Suzuki *et al*, 1997) although it is still unclear how the WRN gene product acts to regulate the onset of replicative senescence.

#### **1.5.4. Cellular Immortality - Bypassing M2**

Human cells undergo spontaneous immortalisation in culture at almost undetectable frequencies but such cells can be immortalised, albeit at low frequencies, by stable transfection with SV40 TAg (Shay & Wright, 1989). As already mentioned, any TAg-expressing immortal clones which arise must have bypassed both the M1 and M2 checkpoints. Although genes such as p53 and RB are thought to be involved in M1 regulation, the genetics of the M2 checkpoint are less well understood. However, one candidate location for an M2 checkpoint gene is human chromosome 6 (see also Section 1.5.3.1). Cells that have escaped senescence and bypassed M2 display non-random losses of this chromosome (Hubbard-Smith *et al*, 1992) and the introduction of chromosome 6 into post-crisis cells is sufficient to restore M2 and induce senescence (Sandhu *et al*, 1994).

The majority of the experiments relating to the M1/M2 model of senescence regulation discussed above have been done in human cells. While a checkpoint analogous to M1 is thought to exist in murine cells, the existence of a murine M2 checkpoint is still under debate. For example, human cells undergo spontaneous immortalisation in culture at almost undetectable frequencies (Shay & Wright, 1989) and are rarely immortalised by chemical carcinogens (McCormick & Maher, 1988). In direct contrast, murine cells are readily immortalised by chemical carcinogens and also undergo spontaneous immortalisation at a high frequency (McCormick &

Maher, 1988). The simplest interpretation of these observations is that mouse cells lack a functionally important M2, or that M2 can be inactivated by both genetic and epigenetic mechanisms (Wright *et al*, 1989). Further characterisation of the human M2 checkpoint should facilitate a fuller understanding of related mechanisms in the mouse.

In conclusion, a single mutation in any of the multiple senescence pathways is insufficient to permit escape from cellular replicative senescence. Immortality can only be achieved by the complete loss of function of all of these pathways and a senescent phenotype can be induced by the restoration of any single senescent pathway.

#### **1.5.5. Senescence Activation**

Activation of senescence pathways is likely to involve complex regulatory mechanisms. One such mechanism is thought to be a counting system which records the number of cell divisions, this was proposed to explain the observation that the proliferative life span of a cell correlates with the total number of divisions, independent of chronological time (Hayflick, 1976). To determine how a cell records the number of cell divisions that it has undergone, several studies were undertaken to compare specific physical parameters between young and near-senescent cells. One such study reported that telomere length shortens in normal cells as they approach senescence (Harley *et al*, 1990). Subsequent work has confirmed a strong correlation between telomere length and proliferative capacity (Allsopp *et al*, 1992).

Telomerase is the enzyme responsible for the extension of telomeres and is active in germline tissues and the majority of immortal cell lines but is undetectable in normal tissue (Kim *et al*, 1994). The correlation of both advanced stage malignancy and *in vitro* cellular immortality with telomerase activity provides additional support for the hypothesis that cellular immortalisation is required for extended tumour cell proliferation *in vivo*. Interestingly, it has recently been demonstrated that the restoration of RB expression in an immortal cell line is sufficient to induce

replicative senescence and that this correlates with an inhibition of telomerase activity (Xu *et al*, 1997). However, the role of telomerase and telomere length in the regulation of senescence *in vivo* is more complex, as evidenced by the generation of viable telomerase null mice (Blasco *et al*, 1997).

Another physical parameter that varies with cellular proliferation is DNA methylation. The level of methylated cytosine residues decreases in normal fibroblasts as they reach the end of their life span in culture. However, exposure of normal cells to 5-azacytidine doses which are sufficient to reduce methylation levels to lower than those seen in senescent cells is insufficient to induce growth arrest (Gray *et al*, 1991). The favoured interpretation of these results is that the demethylation that occurs in ageing cells must be site specific, not random as would be induced by 5-azacytidine. A potential target for site-specific demethylation in ageing cells is the CpG island in the p16<sup>INK4a</sup> gene (Merlo *et al*, 1995). As cells approach replicative senescence this site is demethylated and the result is an increase in p16<sup>INK4a</sup> expression (Vogt *et al*, 1998).

A possible mechanism for senescence-dependent demethylation has also become apparent. The methyltransferase enzyme and p21 both form separate and mutually exclusive complexes with PCNA (Chuang *et al*, 1996). Hence the accumulation of p21 in cells as they approach senescence could lead to the down-regulation of methyltransferase and explain the activation of p16<sup>INK4a</sup> during late senescence.

#### **1.5.6. Summary**

A substantial body of evidence now exists which supports the genetic hypothesis of replicative cellular senescence, which states that the process is regulated by an internal cellular program. It is probable that the onset of senescence can be triggered by several signals, of which telomere erosion and methylation status are examples. Cells are also able to use multiple pathways to reach the same endpoint, terminal growth cessation and immortality can only be achieved after the acquisition of mutations in all of the senescence pathways. While some of the senescence

regulatory genes and the pathways they function in have been identified many more are still unknown. Significant advances in our understanding of senescence will undoubtedly follow the cloning and analysis of the as yet unidentified gene products. Further in depth study of the better characterised senescence pathways should also facilitate a more in depth understanding. All of these lines of research should yield information on neoplastic progression, tumour suppression and ageing *in vitro* and *in vivo*.

# **Chapter 2**

## **Recombinase Activated Gene Expression**

## Chapter 2

### Recombinase Activated Gene Expression

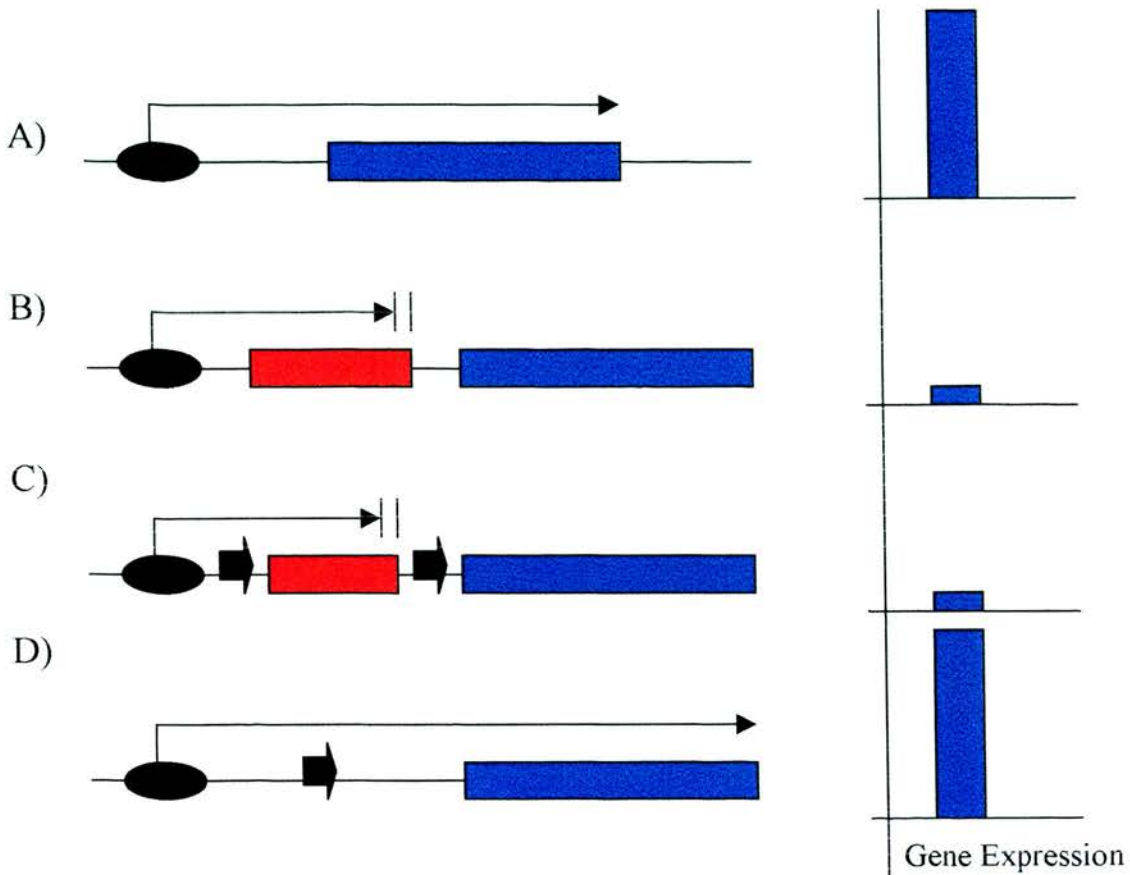
#### 2.1. Introduction

The basic strategy of recombinase activated gene expression (RAGE) has now been used by several different research groups, and although the exact molecular details differ between individual groups, the approach remains very similar.

RAGE strategies are closely related to the promoter-trap system (Figure 2.1). This approach takes advantage of the fact that linear pieces of DNA introduced into mammalian cells are capable of stably integrating into the genome. If the introduced DNA encodes a selectable marker gene, clones that have undergone an insertion event can be selected for. For example, cells transfected with the *neomycin phosphotransferase* gene (*neo*) will survive selection with the antibiotic G418 (Southern & Berg, 1982). In the promoter-trap strategy promoter-less selectable marker genes are transfected into mammalian cells and selected for on the basis of marker gene expression. As the introduced marker gene was promoter-less, expression can only result from the activity of an endogenous promoter adjacent to the site of integration (Gossler *et al*, 1989). Clones that survive selection are therefore predicted to represent integration events into the coding sequence of an endogenous gene. Such an integration event has two consequences; first, it places the selectable marker gene under the control of the endogenous promoter and second, it disrupts the regulation of the endogenous gene. As such, the downstream gene may no longer be transcribed or expressed because the insertion event renders it effectively promoter-less, so-called insertional mutagenesis (Figure 2.1).

It is this simple idea, that the insertion of a piece of DNA between the promoter and coding sequence of a gene will prevent the expression of that gene, which has been developed into novel floxed STOP technology.

**Figure 2.1** – *Mechanism of Action of Promoter Traps and Floxed STOP Cassettes*



A) If a constitutive promoter (black oval) is placed upstream of a marker gene (blue box) high levels of marker gene expression will result. This is represented by the graph at the left-hand side of the figure.

B) If a promoter trap construct (red box) is inserted between the promoter and coding sequence of the marker gene, marker gene expression is inhibited.

C) As with the promoter trap strategy represented in B), the insertion of a floxed STOP between the promoter and coding sequence of the marker gene inhibits expression.

D) In the presence of Cre recombinase the construct represented in C) will undergo excision. The outcome will be loss of the STOP sequence and one loxP site will be retained. Marker gene expression will be restored.



Normally, a promoter-trap insertion confers a total and irreversible block upon downstream gene expression, whereas the use of a floxed STOP strategy should permit conditional gene expression. This approach still relies on the insertion of DNA encoding a STOP sequence acting to abolish downstream gene expression, but additionally uses two directly repeated loxP sites on either side of the STOP sequence (i.e. floxed) to render the promoter-trap conditional. After expression of Cre recombinase, recombination will occur at the loxP sites resulting in excision of the STOP cassette with only one loxP site remaining. As the 34bp of DNA that comprise a loxP site are unlikely to affect transcription, the regulatory relationship between the promoter and downstream gene should be restored and expression of the downstream gene stimulated (see Figure 2.1).

## **2.2. Conditional Gene Expression – The Floxed STOP Approach**

One of the earliest reports of the application of floxed STOP technology to achieve conditional gene expression *in vivo* was in 1992 (Lakso *et al*, 1992). A transgene was designed which contained the SV40 large tumour antigen (TAg), the lens-specific murine  $\alpha$ -crystallin promoter (m $\alpha$ A) and a floxed STOP cassette. The floxed STOP cassette used in this work consisted of two loxP sites, stuffer DNA (a segment of the Yeast *His3* gene, included to increase the size of the construct rather than to encode an important function) and a polyadenylation signal (poly A). This floxed STOP cassette was inserted between the m $\alpha$ A and TAg sequences of the transgene and Cre-mediated excision was used to control the expression of TAg. In transgenic mice which carried the floxed STOP-TAg construct no TAg expression could be detected indicating that any transcripts which initiated from the upstream m $\alpha$ A promoter were being efficiently terminated within the STOP sequence. However, when these mice were mated with Cre-expressing mice efficient Cre-mediated excision was observed in the doubly transgenic progeny. This resulted in loss of the floxed STOP sequence and subsequent lens-specific expression of the TAg gene driven by the m $\alpha$ A promoter (Lakso *et al*, 1992). This paper demonstrated the feasibility of using of the Cre/loxP system in mammals as well as demonstrating Cre-mediated control of gene expression *in vivo*.

In more recent examples of floxed STOP cassettes the stuffer DNA has been replaced with promoter-less marker genes. This type of construct has several advantages, marker gene expression can allow direct selection of cells that contain the floxed STOP cassette and can also be used to assay the activity of the trapped promoter. Furthermore, this type of construct has been demonstrated to work efficiently by several research groups. Examples of promoter-less marker genes used in floxed STOP cassettes include the *chloramphenicol acetylase transferase* (CAT) gene (Araki *et al*, 1995), the *neo* gene (Kellendonk *et al*, 1996; Feil *et al*, 1997), the *neotk* fusion gene (Russ *et al*, 1996) and the *puromycin N-acetyltransferase* (*pac*) gene (Dias *et al*, 1998).

While the inclusion of a promoter-less marker gene within floxed STOP cassettes is now standard, the success of Lakso *et al* (Lakso *et al*, 1992) has demonstrated that it is not essential for the function of these constructs. As such the basic requirements of a functional floxed STOP cassette are a poly A to efficiently terminate transcription and two directly repeated loxP sites. This minimal floxed STOP cassette lacking a marker gene or stuffer DNA and comprising of only a poly A and loxP sites has been used successfully (Wagner *et al*, 1997; Gagnetten *et al*, 1997).

There are two major concerns that must be addressed when using a floxed STOP. The first is how efficiently the floxed DNA will be excised from the genome and the second is how well the STOP sequence will function in abolishing downstream gene expression. Notably, of the several groups that have used this approach few have reported problems in either of these two areas. The efficiency of Cre-mediated excisive recombination is not quantified by all authors as the process is normally very efficient. In support of this, two published reports cite recombination frequencies of over 90% for floxed STOP-containing transgenes as determined by Southern blot analysis (O’Gorman *et al*, 1997; Orban *et al*, 1992). Several publications have also reported the successful control of gene expression using various different floxed STOP cassettes. FDCP1 haematopoietic precursor cells are strictly dependent on interleukin 3 (IL-3) for survival and as such provide an excellent model system in

which to study floxed STOP-regulated IL-3 expression (Russ *et al*, 1996). FDCP1 cells that contain a floxed STOP IL-3 transgene did not express IL-3 in the absence of Cre recombinase as determined by sensitive survival assays. However, subsequent expression of Cre within these cells caused excisive recombination and resulted in the loss of the floxed STOP cassette. Such cells were then able to express high levels of IL-3 and continued to proliferate despite the withdrawal of IL-3 from the culture medium. Within the limitations of this assay system, both the absence of leaky expression, and the efficient induction of expression after Cre recombinase-mediated excision of the floxed STOP cassette were demonstrated (Russ *et al*, 1996).

### **2.3. Aims**

- a) Design and construct a floxed STOP cassette suitable for the regulation of both exogenous and endogenous gene expression.
- b) Demonstrate that the floxed STOP cassette is a functional substrate for Cre recombinase.
- c) Construct a test plasmid with which to assay the efficiency of floxed STOP-mediated control of gene expression.
- d) Introduce the test plasmid into cells and optimise a Cre delivery strategy
- e) Analyse the effects of Cre expression upon floxed STOP-regulation of marker gene expression.

### **2.4. Construction of pFloxSTOP**

A relatively small body of literature exists concerning the use of floxed STOP cassettes. Although several authors have reported the successful use of such cassettes to regulate exogenous gene expression *in vitro*, there are no published reports of floxed STOP-mediated control of endogenous gene expression *in vivo*. However, when an analogous strategy using Flp recombinase and FRT sites flanking a STOP cassette was applied to the *fgf8* gene, a 45% reduction in gene expression from the unrecombined targeted allele relative to wild type was observed (Meyers *et al*, 1998). Therefore, although this particular STOP cassette was not working with 100% efficiency the experiment has demonstrated the feasibility of this approach.

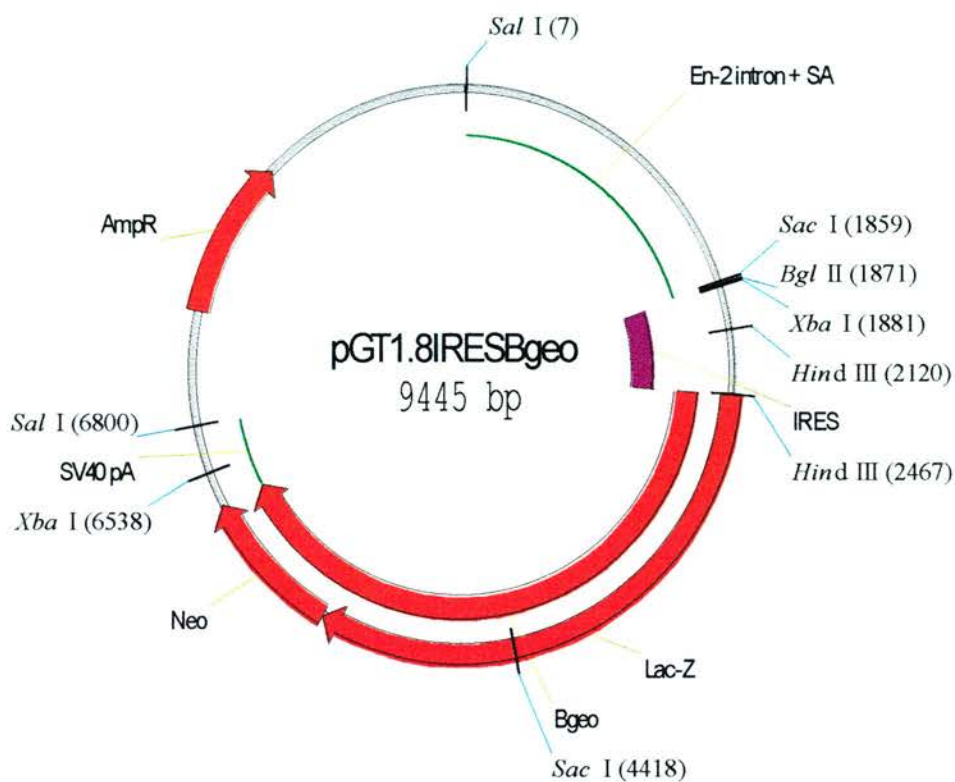
The STOP cassette used by Meyers *et al*, consisted of a *neo* gene, a promoter and two directly repeated FRT sites, “flrtd” (Meyers *et al*, 1998). Although this fulfils the minimum requirements for floxed or flrtd STOP cassettes, one possible way to increase the efficacy of the approach is to develop a novel STOP cassette that can be used to control both exogenous and endogenous gene expression. The design, construction and testing of this cassette, pFloxSTOP, are discussed below.

#### **2.4.1. The pGT1.8IRES $\beta$ geo Plasmid**

The starting point for the creation of the floxed STOP used in these studies, pFloxSTOP, was the vector pGT1.8IRES $\beta$ geo. This plasmid was constructed by Peter Mountford and obtained from the Centre For Genome Research, Edinburgh (Figure 2.2). pGT1.8IRES $\beta$ geo was originally designed as a promoter-trap vector and has five main components, a splice acceptor from the *engrailed 2* gene (En-2SA), an internal ribosomal entry site (IRES), a  $\beta$ geo gene which is a fusion of the *LacZ* and *neo* genes, a polyadenylation signal from SV40 and a backbone derived from the pUC19 plasmid (Mountford *et al*, 1994).

The En-2SA is a 1.8kb fragment derived from a genomic clone of the mouse *engrailed 2* gene that includes the splice acceptor from exon 7 of this gene (Logan *et al*, 1992). The En2SA sequences were present to enable pGT1.8IRES $\beta$ geo to be used as a promoter-trap vector. As discussed in Section 2.1, promoter traps work by the integration of a reporter construct adjacent to an endogenous promoter whereby successful promoter trapping is usually dependent upon the integration of the construct into exonic sequences. The efficiency of promoter trapping can be increased by the inclusion of a splice acceptor such that, after intronic insertion the reporter gene, e.g.  $\beta$ geo, would be expressed following appropriate splicing. Experiments have shown that constructs lacking a splice acceptor generate 12-fold less  $\beta$ geo expressing clones than otherwise identical constructs which carry the splice acceptor (Gossler *et al*, 1989).

**Figure 2.2** – *The pGT1.8IRESβgeo Plasmid*



The pGT1.8IRESβgeo plasmid was the starting point for the construction of pFloxSTOP. This plasmid was designed as a promoter-trap vector and was constructed by Peter Mountford.

The next functional domain of pGT1.8IRES $\beta$ geo is the 600bp Internal Ribosomal Entry Site (IRES) derived from the 5' UTR of the Encephalomyocarditis virus (ECMV) (Ghattas *et al*, 1991). IRES sequences allow the constructs which carry them to express marker genes such as  $\beta$ geo, independently of the translation frame or the coding/noncoding status of the insertion locus. The marker gene present in pGT1.8IRES $\beta$ geo is the fusion gene  $\beta$ geo, generated by placing the *neo* gene (Beck *et al*, 1982) in-frame at the 3' end of the LacZ gene (Kalnins *et al*, 1983). During the construction of  $\beta$ geo the LacZ gene used was engineered to include an ATG codon which can serve as an initiator of translation in eukaryotic cells (Friedrich & Soriano, 1991). The final functional element of pGT1.8IRES $\beta$ geo is the SV40 polyadenylation signal (polyA) (Mountford *et al*, 1994).

The following construction strategy was developed to convert the pGT1.8IRES. $\beta$ geo plasmid into a functional floxed STOP cassette.

- a) Retain the En2SA splice acceptor, the  $\beta$ geo reporter gene and the SV40 poly A signal.
- b) Delete the IRES sequence (see also Figure 4.2).
- c) Replace the plasmid backbone and insert two directly repeated loxP sites.

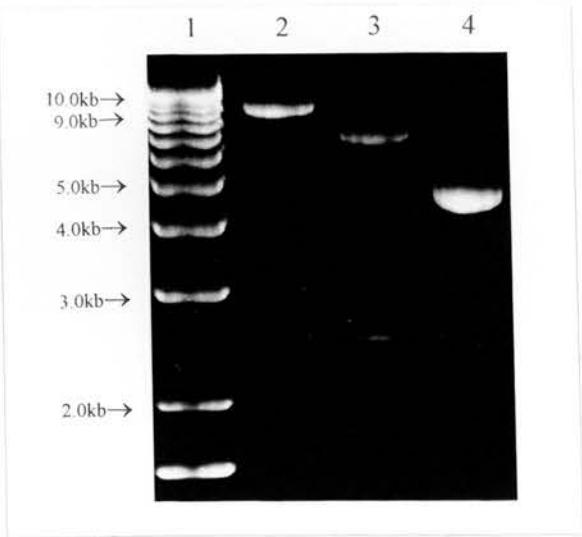
This work is discussed in subsequent sections.

#### **2.4.1.1. Removal of the IRES From pGT1.8IRES $\beta$ geo**

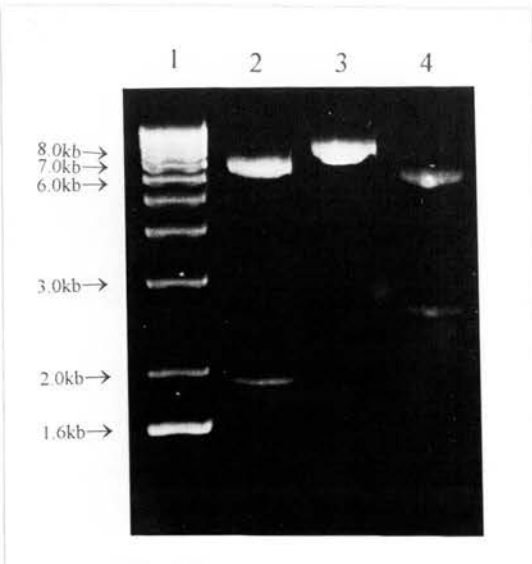
IRES removal was achieved via double digestion of pGT1.8IRES $\beta$ geo with the restriction enzymes *Bgl II* and *Hind III* (Figure 2.3). After this digest had gone to completion a 596bp fragment spanning the IRES was lost and non-compatible single strand DNA (ssDNA) overhangs are generated. To permit the recircularisation of the linearised plasmid the 5' ssDNA overhangs were blunted with Klenow fragment and then ligated. The ligation reaction was used to transform competent bacteria and resultant clones were screened for successful deletion of the IRES sequence by restriction digest analysis (Figure 2.3).



**Figure 2.3** – Deletion of the IRES Sequence From the pGT1.8IRESβgeo Plasmid



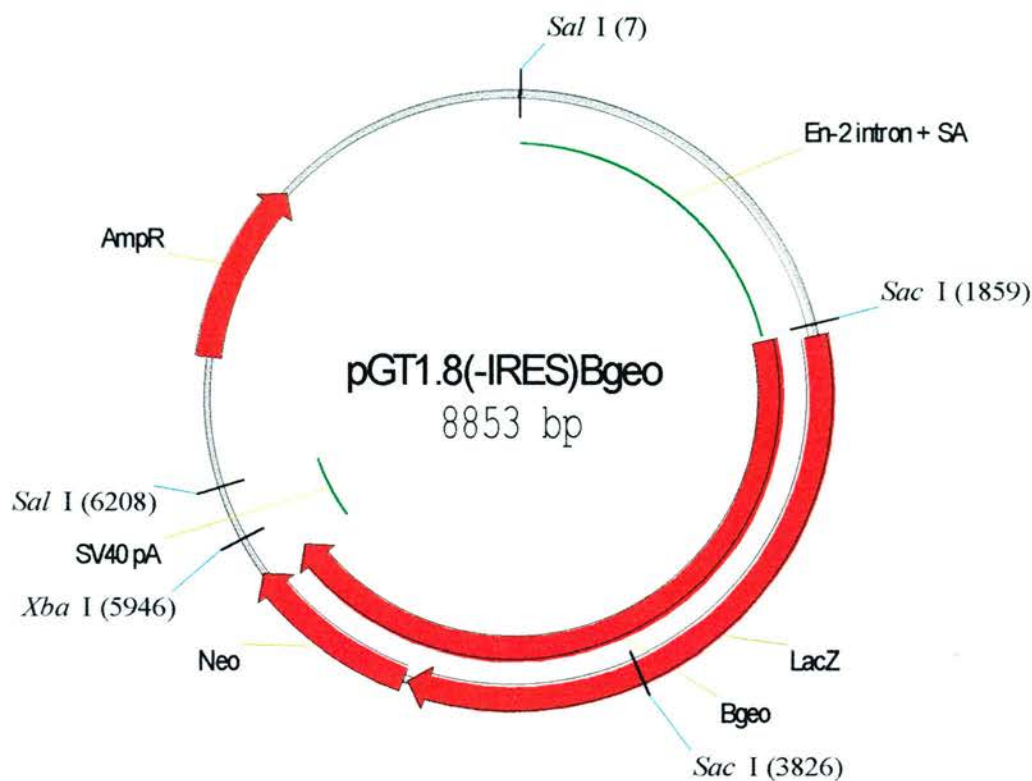
1.0% agarose/ethidium bromide gel. Lane 1, molecular weight markers. Lane 2, pGT1.8IRESβgeo cut with *Bgl II* and *Hind III* generates two products, 8849bp and 569bp. Lane 3, the products of pGT1.8IRESβgeo cleavage by *Sac I*, 2559bp and 6886bp. Lane 4, the products of *Xba I* cleavage of pGT1.8IRESβgeo, 4657bp and 4788bp. These bands are so close in size that on this gel they run as an unresolved doublet.



1.0% agarose/ethidium bromide gel. Lane 1, molecular weight markers. Lane 2, *Sac I* digestion of pGT1.8(-IRES)βgeo. The removal of the IRES sequence brings the two *Sac I* sites closer together hence one cleavage product, 1963bp, is 596bp shorter than in the parental plasmid pGT1.8IRESβgeo (parental product is 2559bp). The other *Sac I* digest product of this plasmid, 6886bp, is unaffected by the IRES deletion. Lane 3, *Xba I* digestion of pGT1.8(-IRES)βgeo. The deletion of the IRES removes one *Xba I* site from this plasmid so this enzyme now cuts once only generating a single band at 8853bp. Lane 4, *Sal I* cleavage of pGT1.8(-IRES)βgeo. This enzyme cuts twice in this plasmid generating two cleavage products of 2652bp and 6201bp. The latter of these products contains all the components of a STOP cassette and was subcloned during the construction of pFloxSTOP.



**Figure 2.4** – The pGT1.8(-IRES) $\beta$ geo Plasmid



The pGT1.8(-IRES) $\beta$ geo plasmid shown above is the end result after the IRES sequence was deleted from the parental pGT1.8IRES $\beta$ geo plasmid (Figure 2.2)

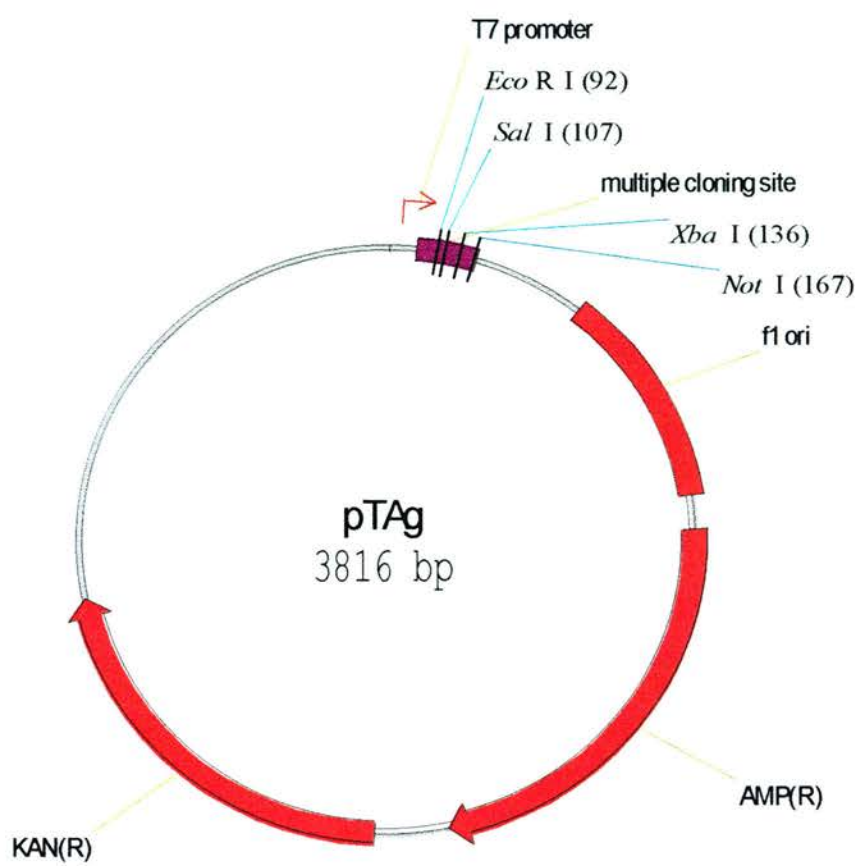
Having successfully deleted the IRES sequence, pGT1.8(-IRES) $\beta$ geo has all the basic components of a STOP cassette (Figure 2.4). The final stage in the construction of a floxed STOP from this plasmid was the insertion of two directly repeated loxP sites flanking the STOP cassette. This was achieved by the replacement of the pUC19 backbone of pGT1.8(-IRES) $\beta$ geo with a modified pTAg backbone.

#### **2.4.2. The pTAg Plasmid**

The pTAg plasmid is a commercially available plasmid designed for the cloning of PCR products (R&D Systems). It was supplied as a linear molecule with 3' overhangs of one molecule of the base thymine. Conversely, PCR products generated using standard *Taq* polymerase have 3' overhangs of one adenine molecule added in a template-independent manner by the polymerase. These complementary ssDNA overhangs allow PCR products to insert efficiently into the pTAg vector. Because of the 3' overhangs on the linear pTAg plasmid it cannot recircularise except in the presence of PCR derived inserts. However, the extremely useful polylinker of the pTAg plasmid makes this molecule an attractive substrate for cloning reactions involving none-PCR derived inserts. In order to obtain sufficient pTAg plasmid for frequent use in standard cloning reactions it was necessary to construct a circular form of the plasmid as the linearised molecule supplied commercially cannot be propagated in bacteria. Because the pTAg plasmid had been specifically designed not to circularise in the absence of insert, the non-complementary 3' overhangs were blunted with T4 DNA polymerase and then ligated. This blunting reaction altered none of the restriction sites within pTAg and the result was a plasmid with a very useful polylinker used in several of the cloning steps described in this thesis (Figure 2.5).

Once the pTAg plasmid had been circularised two other modifications were needed to produce the floxed plasmid backbone used in the construction of pFloxSTOP. The first was the insertion of two directly repeated loxP sites and the second was the disruption of a *Not I* site in the polylinker to facilitate later subcloning steps.

**Figure 2.5 – The pTAg Plasmid**



The circular form of the pTAg plasmid generated after the use of T4 polymerase to blunt the commercially supplied linear molecule. Relevant restriction sites within the polylinker are shown.

#### 2.4.2.1. Introducing the LoxP Sites

Two directly repeated loxP sites were introduced into the polylinker of pTAg in two separate cloning steps. Both loxP sites were obtained as pairs of HPLC purified oligonucleotides that were 5' phosphorylated during manufacture (Cruachem). All four oligonucleotides were 40 bases in length, 34 bases of which encoded one strand of a standard loxP site and 6 bases of which comprised one half of a specific restriction enzyme recognition sequence. The full sequences of all four oligonucleotides are shown in Figure 2.6.

The loxP sites were introduced sequentially and each pair of component oligos was annealed prior to ligation. To insert the first loxP site, pTAg was digested with the restriction enzymes *EcoRI* and *Sal I*. In case of incomplete double digestion the linearised plasmid was also dephosphorylated using Shrimp Alkaline Phosphatase (SAP, Amersham) to reduce background due to vector recircularisation. The SAP treated linearised plasmid was then mixed with the appropriate pair of annealed oligos, ligated and transformed into competent bacteria. As the insertion of a pair of loxP oligonucleotides into the pTAg backbone introduced no new restriction sites and the presence of an extra 40bp of DNA is not readily detectable on a standard agarose gel, all clones were sequenced. DNA sequencing was also important to identify and rule out any clones with concatemeric insertion events.

When one clone had been identified which contained the correctly inserted loxP sequence, pTAg(ESloxP), the second loxP site was then cloned in. This was achieved using a direct repeat of the process above except that the substrate plasmid, pTAg(ESloxP) was digested with the restriction enzymes *Sal I* and *Xba I* and then SAP dephosphorylated. As before, DNA sequencing was used to screen recombinant plasmids resulting from this cloning step. The outcome of these cloning steps was the production of a pTAg-derived plasmid that contained two directly repeated loxP sites separated by one *Sal I* site, this plasmid was named pFloxpTAg (Figure 2.6).

**Figure 2.6 – Inserting *LoxP* Sites into the Backbone of the pTAg Plasmid**

LoxP Pair 1

*Eco RI*

**AAT TCA TAA CTT CGT ATA GCA TAC** ATT ATA CGA AGT TAT G

GT ATT GAA GCA TAT CGA ATG TAA TAT GCT TCA ATA **CAG CT**

*Sal I*

LoxP Pair 2

*Sal I*

**TCG ACA TAA CTT CGT ATA GCA TAC** ATT ATA CGA AGT TAT T

GT ATT GAA GCA TAT CGA ATG TAA TAT GCT TCA ATA **AGA TC**

*Xba I*

Each loxP site was composed of two 40 bp oligonucleotides. The oligos annealed in a staggered fashion generating 4bp 5' ssDNA overhangs. Each 5' overhang was designed as one half of a restriction digest cleavage site, the relevant sequences are in bold text with the specific restriction enzyme site indicated. The two loxP sites were cloned into the pTAg backbone sequentially, generating the pFloxpTAg plasmid with a polylinker structure as shown below.

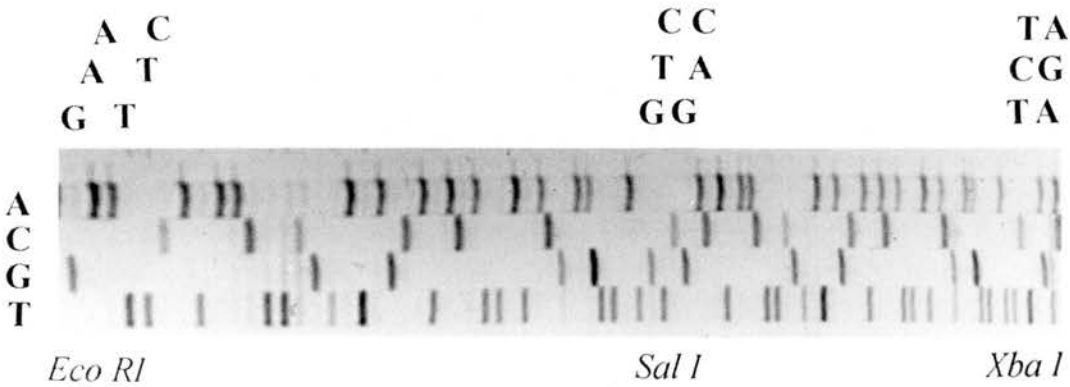
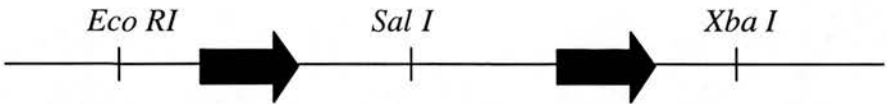


**Figure 2.7- Destruction of the Unique NotI Site in the pTAg Polylinker**

**A) Not I Linkers**

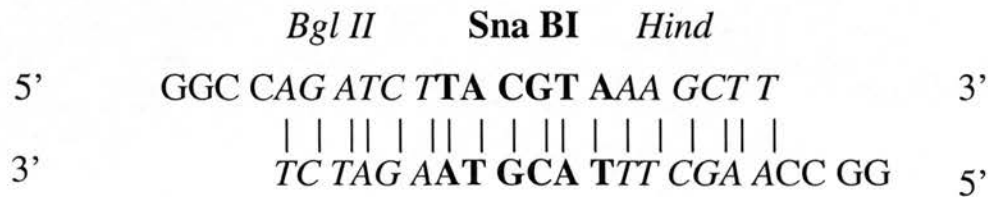
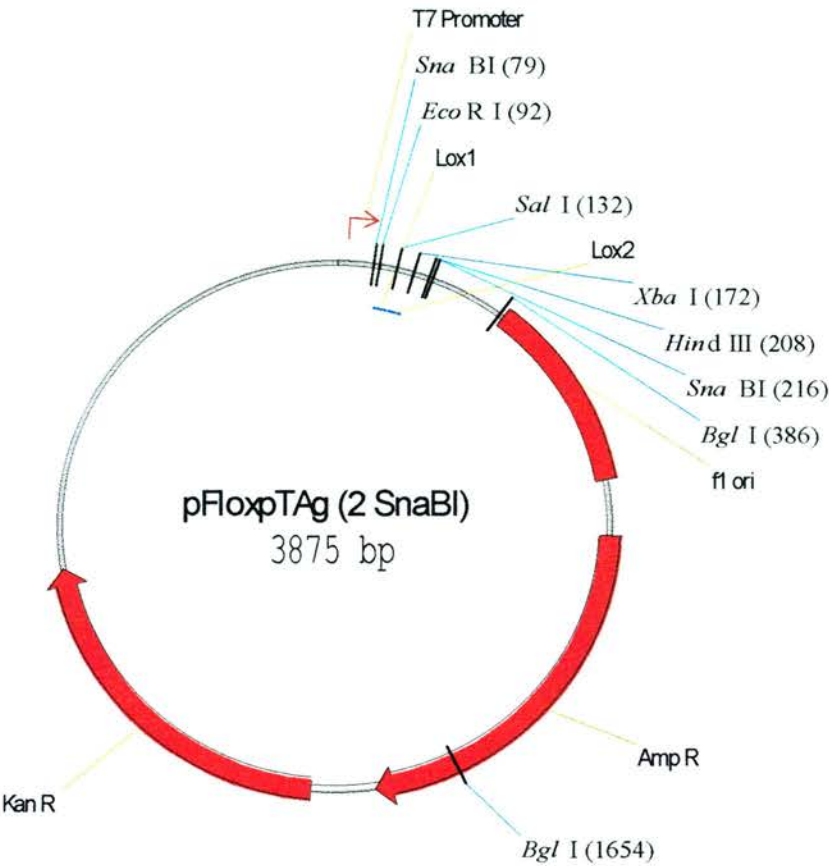


**Figure 2.8** – *The pFloxpTag(2 Sna BI) Plasmid*



The pFloxpTag(2*Sna BI*) plasmid shown above is the product of the cloning steps described in Sections 2.3.2.1 and 2.3.2.2. The plasmid contains two directly repeated loxP sites and contains the Not I linkers thereby introducing a second Sna BI site in the polylinker.



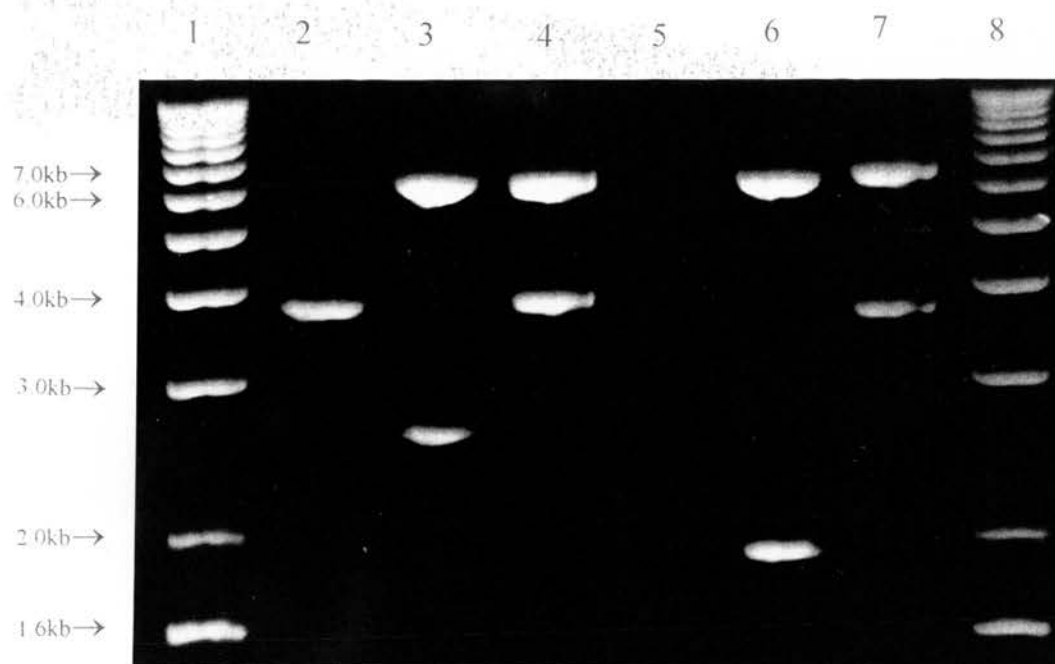
#### 2.4.2.2. Modifying the pFloxPTag Polylinker

The unique *Sal I* site between the two loxP sites was designed to allow the subcloning of selected DNA segments. The two directly repeated loxP sites will then flank or “flox “ the inserted DNA. To allow easy removal of the floxed DNA sequences a simple digest strategy was needed to cut out with the two loxP sites. It was originally intended to use a double digest of *Sna BI* and *Not I* but while the blunt end generated by *Sna BI* is ideal for further subcloning reactions the overhangs generated by *Not I* cleavage are more difficult to work with. To remove the *Not I* site and replace it with a more useful cleavage site a pair of oligonucleotides were designed (see Figure 2.7). As with the loxP oligonucleotides these were also supplied with 5' phosphate groups (Cruachem) and were annealed prior to subcloning. To insert the oligonucleotide pair into the *Not I* site the pFloxPTag plasmid was digested to completion with *Not I*, dephosphorylated and then ligated with the annealed oligonucleotides. The insertion event was designed to destroy the *Not I* site and replace it with a *Bgl II*, a *HindIII* and a second *Sna BI* site (Figure 2.7A). The correct integration of the oligonucleotides into the *Not I* site was demonstrated by the acquisition of a novel *Bgl II* cleavage site and resistance to *Not I* digestion (Figure 2.7B) generating pFloxPTag(2*Sna BI*) (Figure 2.8).

#### 2.4.3. Inserting the STOP Cassette into pFloxPTag(2*Sna BI*)

The final cloning step in the construction of pFloxSTOP was the insertion of the STOP sequence derived from pGT1.8(-IRES) $\beta$ geo into the pFloxPTag(2*Sna BI*) polylinker. The pFloxPTag(2*Sna BI*) vector was linearised by *Sal I* digestion and the STOP cassette-containing insert was also prepared by *Sal I* digestion of pGT1.8(IRES) $\beta$ geo. These two components were ligated, transformed into bacteria and resultant clones screened by restriction digest analysis. Insertion of the STOP cassette was demonstrated via digestion with *Sal I* and the orientation of the insert was established with *Sac I* digestion (Figure 2.9). The resultant plasmid was termed pFloxSTOP (Figure 2.10a). The complete floxed STOP cassette in pFloxSTOP can subsequently be excised with a single *Sna BI* (Figure 2.10b). Two blunt ended

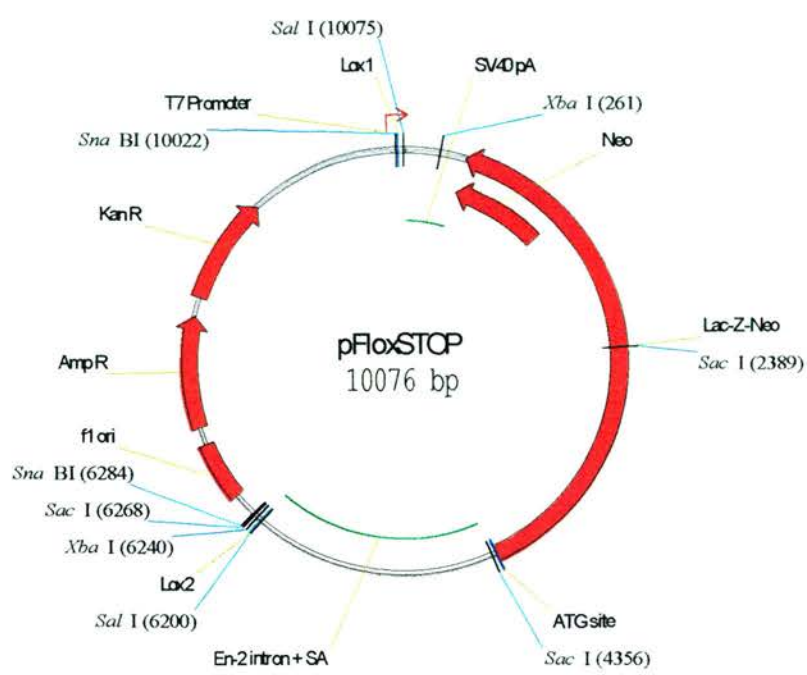
**Figure 2.9** – Constructing *pFloxSTOP*; Inserting the *STOP* Cassette into the *pFloxpTAg(2Sna BI)* Backbone



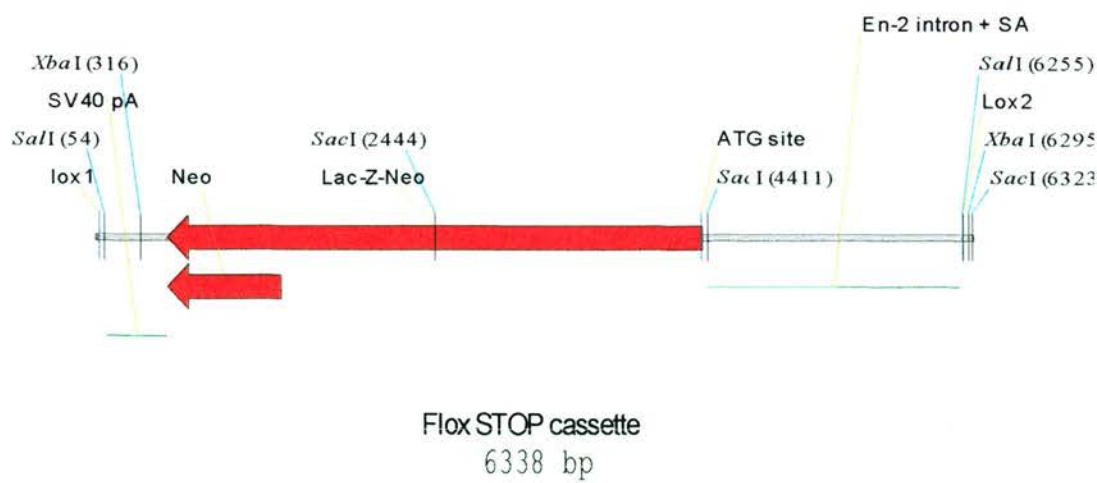
1.0% agarose/ethidium bromide gel. Lane 1, molecular weight markers. Lane 2, *Sal I* digestion of *pFloxpTAg(2Sna BI)* generating a linear 3875bp vector backbone. Lane 3, *Sal I* digestion of *pGT1.8(-IRES)βgeo* generates two products a 2652bp and a 6201bp *STOP* sequence-containing fragment. To construct *pFloxSTOP* the 6201bp *STOP* fragment was subcloned into the *pFloxpTAg(2Sna BI)* plasmid. *Sal I* digestion was used to screen the resultant clones. *Sal I* digestion of the *pFloxSTOP* plasmid generates two cleavage products. A 3875bp pTAg backbone-derived fragment and a 6201bp *STOP* cassette-derived fragment (Lane 4). Lane 6, *Sac I* digestion was used to determine the orientation of the *STOP* cassette. The sample shown in lane 6 has the *STOP* in the reverse orientation giving *Sac I* cleavage products of 6197bp, 1967bp and 1912bp. The latter two products run as an unresolved doublet. The *pFloxSTOP* plasmid and corresponding *Sac I* sites are illustrated in Figure 2.11. Lane 7, *Sna BI* cleavage of *pFloxSTOP* results in two products, a 3738bp product derived from the pTAg backbone and a 6338bp product which includes the complete floxed *STOP* cassette.

**Figure 2.10 – The pFloxSTOP Plasmid and Complete Floxed STOP Cassette**

a)



b) Below is a linear representation of the floxed STOP cassette which is excised from pFloxSTOP upon *Sna BI* digestion.



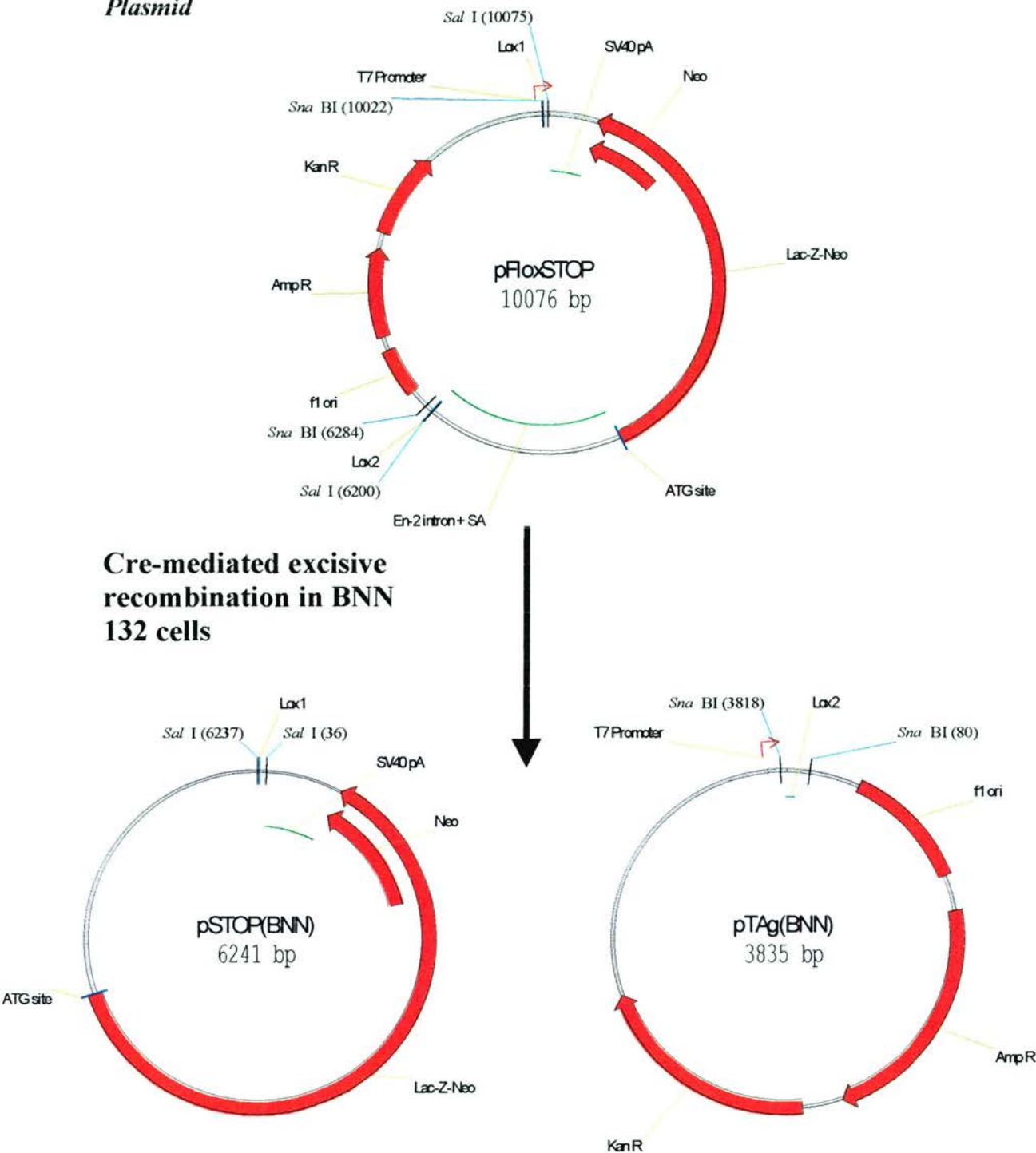
cleavage products are generated; a 3738bp derived from the pTAg backbone and a 6338bp band that includes the complete floxed STOP (Figure 2.9).

## **2.5. Is pFloxSTOP a Functional Substrate For Cre Recombinase ?**

### **2.5.1. Excisive Recombination in BNN 132 Cells**

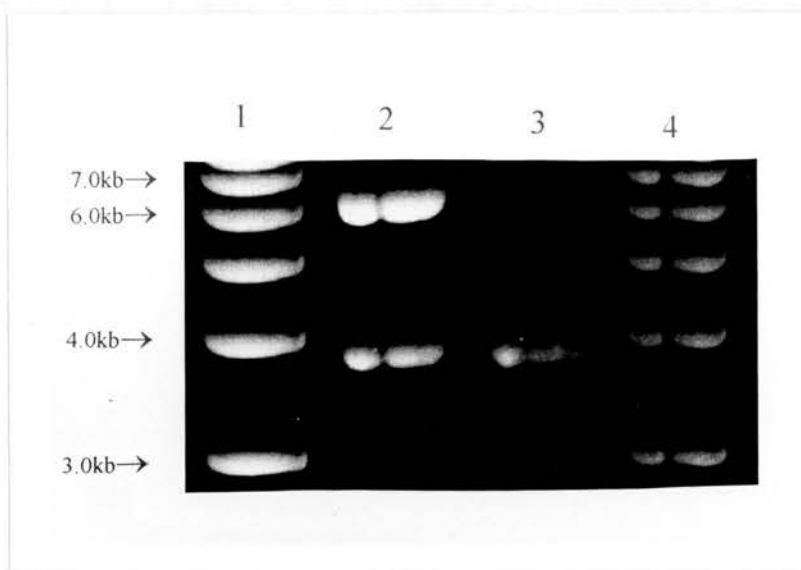
The availability of bacterial strains that constitutively express Cre recombinase allows loxP site containing plasmids to be tested for recombination competence prior to any lengthy *in vitro* or *in vivo* characterisation (Buchholz *et al*, 1996b). One such commercially available Cre-expressing bacterial strains, BNN 132 (MoBiTec), was used to test pFloxSTOP and related plasmids. Cultures of BNN132 cells were grown up and competent cells generated using a standard calcium chloride protocol (Sambrook *et al*, 1989). Competent BNN 132 bacteria were transformed with the pFloxSTOP plasmid and plated onto LB-agar plates supplemented with the antibiotic ampicillin (50µg/ml). The predicted outcome of Cre-mediated recombination will be the generation of two plasmid species from the parental pFloxSTOP plasmid. First, pTAg(BNN) which will be derived from the pFloxTAg(2*Sna BI*) backbone and contain one loxP site and second, pSTOP(BNN) which will be derived from the STOP cassette and also contain one loxP site (Figure 2.11). However, as the ampicillin resistance gene is present only on the pTAg(BNN) plasmid, only this species will be represented in clones produced from the transformation of BNN 132 cells after selection with ampicillin. These predicted results were confirmed by restriction digest analysis of ampicillin resistant (amp<sup>R</sup>) clones arising after the transformation of BNN 132 cells with pFloxSTOP. Figure 2.12, lane 2 shows the products of *Sna BI* digestion of pFloxSTOP, a 6338bp band containing the floxed STOP cassette and a 3738bp band derived from pTAg backbone. *Sna BI* digestion of plasmid DNA isolated from clones that resulted from the transformation of BNN 132 cells with pFloxSTOP generated only two cleavage products of 3738bp and 97bp, only the former is visible in Figure 2.12, lane 3. This result is consistent with Cre-mediated excision of the STOP cassette having occurred within BNN 132 bacteria.

**Figure 2.11 – The Outcome of Cre-mediated Recombination on the pFloxSTOP Plasmid**



When the pFloxSTOP plasmid is transformed into BNN 132 cells Cre-mediated excision occurs. The result of this is two plasmid species, the first, pSTOP(BNN), contains one loxP site and all of the STOP cassette. The second species, pTAg(BNN), is derived from the plasmid backbone and also contains one loxP site. Only pTAg(BNN) contains an ampicillin resistance gene so this should be the only plasmid species represented in clones arising from the transformation.

**Figure 2.12** – *Restriction Digest Analysis To Confirm That The pFloxSTOP Plasmid Has Undergone Cre-mediated Excisive Recombination*



1.0% agarose/ethidium bromide gel. Lane 1, molecular weight markers. Lane 2, *Sna* *BI* digestion of pFloxSTOP. Two products are seen, a 6338bp band which constitutes the floxed STOP cassette and a 3738bp band comprising the pTag backbone. Lane 3, *Sna* *BI* digestion of pTag(BNN) results in one band of 3835bp. This plasmid is the outcome of pFloxSTOP transformation into BNN 132 cells. The absence of the 6338bp band in this lane demonstrates that pFloxSTOP is a substrate for Cre recombinase.



## 2.6. Summary

The work discussed above has reported the successful completion of the first two aims of this chapter. First, the design and construction of a novel floxed STOP cassette, pFloxSTOP. Second, the demonstration pFloxSTOP is a functional substrate for Cre recombinase and undergoes excisive recombination in BNN 132 bacteria. The next sections of work focus on testing the capabilities of pFloxSTOP to regulate exogenous gene expression *in vitro*.

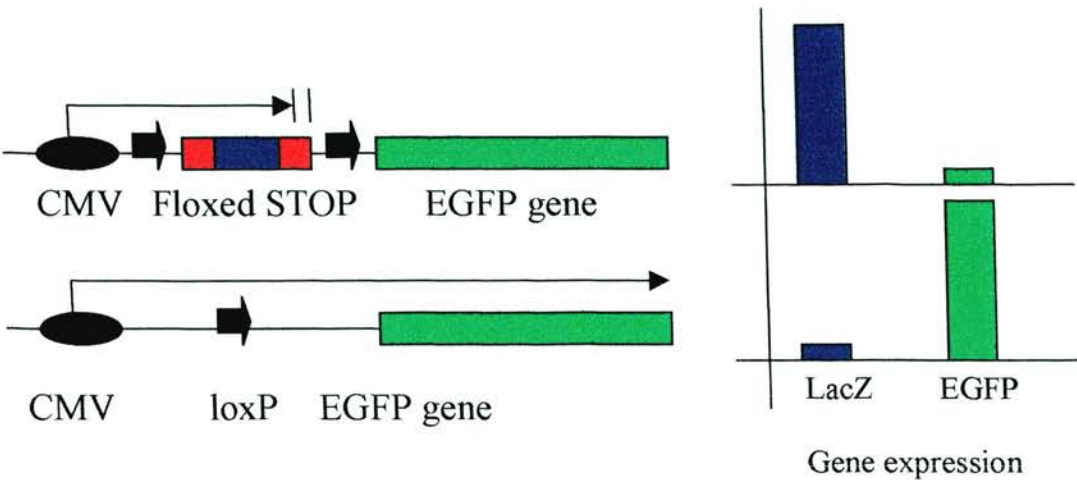
## 2.7. Inducible Control of Gene Expression *in vitro*

In order to investigate the transcriptional control functions of the floxed STOP cassette derived from pFloxSTOP a test construct, pFloxEGFP, was designed and built. In the pFloxEGFP plasmid the floxed STOP cassette from pFloxSTOP was inserted between the promoter and downstream coding sequence of a marker gene thereby permitting an analysis of Cre recombinase-mediated conditional marker gene expression (see Figure 2.13). The marker gene used in pFloxEGFP was the Enhanced Green Fluorescent Protein gene (EGFP) and the basic experimental strategy is illustrated in Figure 2.13.

The presence of the floxed STOP cassette in pFloxEGFP should block expression of the EGFP marker gene in the absence of Cre recombinase. Transcription will initiate from the upstream CMV<sub>IE</sub> promoter and read through the floxed STOP cassette before hitting the SV40 polyadenylation signal and terminating. While this should prevent EGFP expression, the  $\beta$ geo gene within the floxed STOP will be transcribed and expressed. As a result cells that contain the unrecombined plasmid will be neo<sup>R</sup> and should stain positively for  $\beta$ -galactosidase expression (Friedrich & Soriano, 1991). After Cre mediated excisive recombination the  $\beta$ geo containing-floxed STOP cassette should be lost from both constructs. Cells that contain a recombined form of the pFloxEGFP plasmid will no longer be neo<sup>R</sup> or stain positively for  $\beta$ -galactosidase but should now express the EGFP marker gene.



**Figure 2.13** – *Research Strategy For the pFloxEGFP Plasmid*



The pFloxEGFP plasmid. In the unrecombined state the CMV<sub>IE</sub> promoter (black oval) is positioned upstream of the floxed STOP cassette (black arrows flanking the red and blue boxes). This arrangement is predicted to prevent the expression of the EGFP marker gene (green box) although the  $\beta$ geo gene should be expressed from within the floxed STOP cassette (dark blue box within red box). The relative levels of gene expression are represented in the bar chart to the right of the figure.

The second figure illustrates the pFloxEGFP plasmid structure after Cre-mediated excision of the floxed STOP cassette. The loss of the floxed STOP cassette is predicted to abolish expression of  $\beta$ geo and stimulate expression of the second marker gene, EGFP.

### 2.7.1. The Enhanced Green Fluorescent Protein Gene

The EGFP gene (Cormack *et al*, 1996) is derived from the green fluorescent protein (GFP) gene of the jellyfish *Aequorea victoria* (Prasher *et al*, 1992). The GFP gene encodes a 238 amino acid protein able to fluoresce in a wide variety of cell types without the need of any co-factors. The fluorescence is emitted from a chromophore consisting of a cyclic tripeptide derived from Ser-Tyr-Gly in the primary protein sequence of GFP (Cody *et al*, 1993). Nascent GFP is not fluorescent as chromophore formation occurs post-translationally during cyclization and oxidation reactions (Heim *et al*, 1994). GFP emits a green fluorescence ( $\lambda_{\text{max}}$  508nm) in living cells after stimulation with UV light (major absorbance peak 395nm, minor peak at 470nm). Another significant property of the GFP protein is that fusions can be made to either its C- or N- termini without affecting its fluorescent properties (Wang & Hazelrigg, 1994) and indeed commercial vectors are now available with this aim in mind (Clontech).

Since the original GFP gene became widely available it has undergone several refinements and improvements the result of which is the EGFP gene. EGFP encodes a red-shifted variant of wild type GFP achieved by introducing two amino acid substitutions, Phe64 to leucine and Ser65 to threonine into the wild type primary sequence (Cormack *et al*, 1996). EGFP has an excitation peak at 488nm and an emission maximum at 507nm making it ideally suited to the argon lasers used in flow cytometry and for use with FITC filter sets for UV microscopy. These mutations also confer other advantages, the fluorescence is brighter and the altered excitation wavelengths mean that the fluorescence is more stable and less susceptible to photobleaching. In addition to the two amino acid substitutions in the EGFP sequence more than 190 silent base changes have been made which correspond to human codon-usage preferences (Haas *et al*, 1996). This and the addition of a Kozak sequence (Kozak, 1987) were designed to increase the expression of EGFP in mammalian cells.

### 2.7.2. Construction of pFloxEGFP

The pFloxEGFP vector was built with a simple one-step cloning reaction. The pEGFP expression vector, pEGFP-C1 (Clontech, Figure 2.14), was linearised with the blunt cutting restriction enzyme, *Eco 47III* and dephosphorylated with SAP. The aim was to insert the floxed STOP cassette excised from pFloxSTOP into the *Eco47III* site. The linear floxed STOP insert was prepared by digestion of the pFloxSTOP plasmid with the restriction enzyme *Sna BI*. This generates two cleavage products, a 3738bp pTAg backbone-derived fragment and a 6338bp fragment that includes the floxed STOP cassette. The higher molecular weight fragment comprising the floxed STOP cassette was then excised from the gel, purified and ligated into the blunt, dephosphorylated pEGFP-C1 vector. Competent bacteria were transformed with the ligation reaction mix and restriction digest analysis used to identify those clones which contained the recombinant pFloxEGFP plasmid (Figure 2.15).

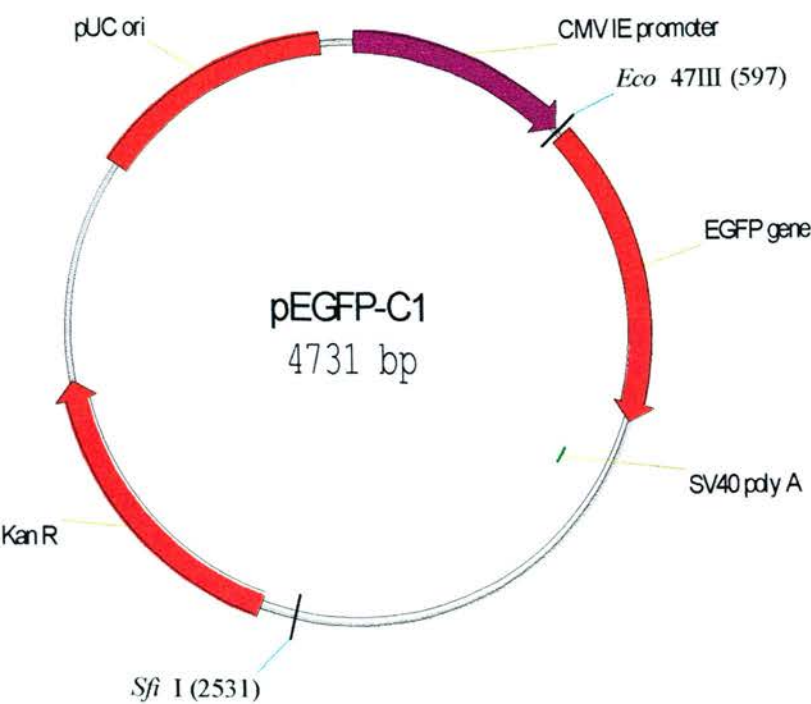
Having successfully constructed pFloxEGFP (Figure 2.16) the next step was to introduce it into mammalian cells and assay the effects of Cre recombinase on marker gene expression.

### **2.7.3. Introduction of pFloxEGFP into ES Cells**

ES cells were chosen as the test system for this plasmid for several reasons. Extensive culture experience was available locally, standardised protocols for electroporation and transient transfection of DNA were already in existence and published work had shown that the Cre/loxP system worked well in this cell type (for example, Smith *et al*, 1995).

The pFloxEGFP plasmid was electroporated into passage 19 HM-1 ES cells (Magin *et al*, 1992). Prior to electroporation the pFloxEGFP plasmid was linearised via digestion with the restriction enzyme *Sfi I*. This enzyme cuts at a unique site within the plasmid backbone of pFloxEGFP, distal to important functional domains of the plasmid such as the CMV<sub>IE</sub> promoter or EGFP coding sequence (Figure 2.16). This

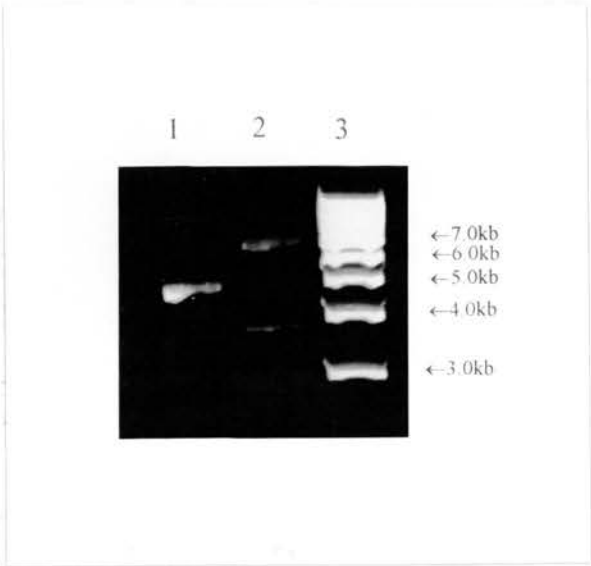
**Figure 2.14** – *The EGFP-C1 Plasmid (Clontech)*



pEGFP-C1, the commercially supplied EGFP expression vector (Clontech). The Eco 47III site into which the floxed STOP cassette was inserted is indicated as is the unique Sfi I site.

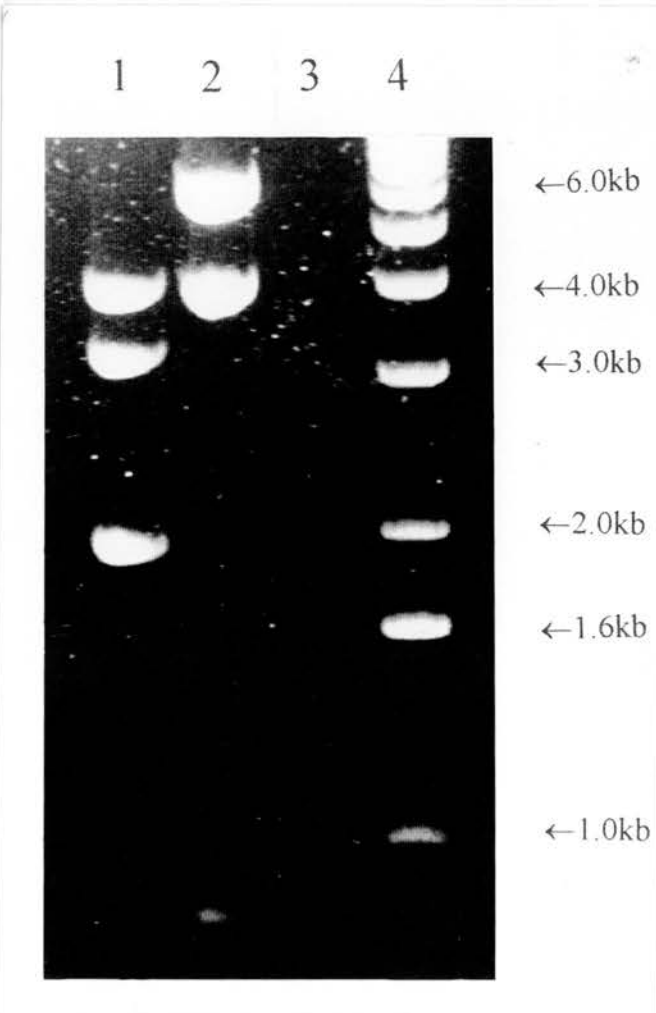
**Figure 2.15 – Construction of the pFloxEGFP Plasmid**

A)



1.0% agarose/ethidium bromide gel. Lane 1, *Eco 47III* digestion of the pEGFP-C1 plasmid generates a single 4731bp cleavage product. Lane 2, *Sna BI* digestion of the pFloxSTOP plasmid generates two cleavage products, 3738bp and 6338bp. Lane 3, molecular weight markers

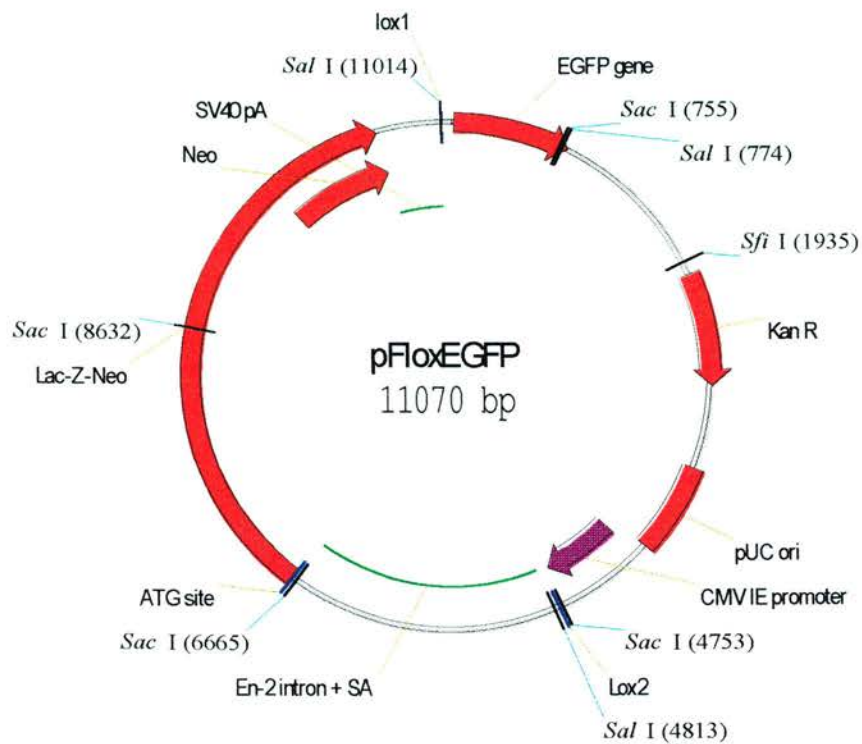
B)



1.0% agarose/ethidium bromide gel. Lane 1, *Sac I* digestion of pFloxEGFP was used to orientate the floxed STOP cassette insert. In the correct orientation four cleavage products should be seen, 3998bp, 3193bp, 1912bp and 1967bp (last two are seen as an unresolved doublet). Lane 2, *Sal I* digestion of pFloxEGFP. Three cleavage products are observed, 6201bp, 4039bp and 830bp. Lane 3, blank. Lane 4, molecular weight markers.

The *Sal I* and *Sac I* digests both confirmed that the floxed STOP cassette was in the correct orientation in pFloxEGFP. The complete plasmid is shown in Figure 2.16.

**Figure 2.16 – The pFloxEGFP Plasmid**



The pFloxEGFP vector in which a floxed STOP cassette has been inserted between the promoter, CMV<sub>IE</sub> and the EGFP marker gene. The orientation of the floxed STOP cassette was confirmed by restriction digest analysis (Figure 2.15b) as it will function correctly only in the orientation shown above. The *Sfi* I site used to linearise this plasmid prior to introduction into mammalian cells is also shown.



is significant as during the electroporation procedure linearised plasmids may be subject to degradation at the ends of the molecule.

Following electroporation the cells were put into medium containing 200µg/ml G418 and G418<sup>R</sup> clones became visible to the naked eye after 10-14 days. Over two hundred clones were picked and expanded prior to analysis.

### **2.7.3.1. Analysis of G418<sup>R</sup> Clones**

#### **2.7.3.1.a. $\beta$ -galactosidase Expression**

Of the first 64 G418<sup>R</sup> clones analysed,  $\beta$ -gal activity was only detectable in 14 (22%). Of the 14 clones, 10 expressed high levels of  $\beta$ -gal while the remaining 4 expressed only low levels with a high degree of mosaicism. However, the successful identification of 10  $\beta$ -gal positive clones meant that the remaining G418<sup>R</sup> clones were not subjected to further analysis.

#### **2.7.3.1.b. EGFP Marker Gene Status**

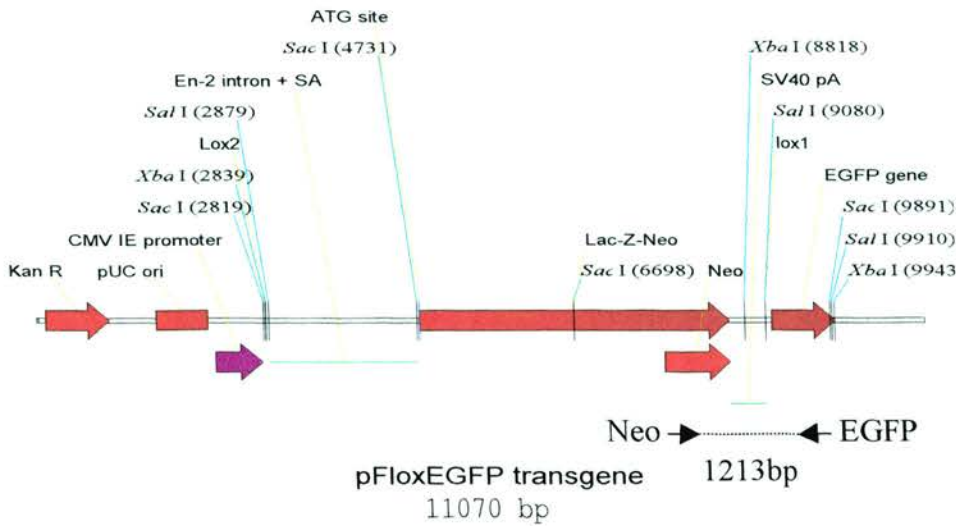
Integration of the linear pFloxEGFP construct into the genome of HM-1 ES cells introduces two novel marker genes. The first of these is the  $\beta$ geo fusion gene that confers resistance to the antibiotic G418 and expression of  $\beta$ -gal. As the clones arising from electroporation of HM-1 cells with pFloxEGFP had survived exposure to 200µg/ml of G418 and 14 of the 64 clones analysed expressed histochemically detectable  $\beta$ -gal, the only marker gene which could not be assayed directly at this stage was the EGFP gene. The presence of the floxed STOP cassette in pFloxEGFP abolishes EGFP expression but it was vital to establish whether or not the full length EGFP coding sequence was present in the  $\beta$ geo positive clones.

With this aim in mind a PCR was designed with primers that anneal within the  $\beta$ geo gene of the floxed STOP and at the extreme 3' end of the EGFP gene (Figure 2.17a). Genomic DNA samples were prepared from the 10 G418<sup>R</sup>/ $\beta$ gal positive clones and subjected to PCR analysis, the results are shown in Figure 2.17b. The presence of



**Figure 2.17 – PCR Screening For the Presence of the Full-length pFloxEGFP Plasmid**

a)



The structure of the intact pFloxEGFP-derived transgene. The respective positions of the neo and EGFP PCR primers and predicted product size are indicated.

b)



1.0% agarose/ethidium bromide gel showing the neo-EGFP PCR results. Lanes 1 and 14, MW, molecular weight markers. Lanes 2-11 each represent one clone, the number of which is listed above. All clones except FE62 and FE63 contain the full length EGFP sequence as determined by PCR. Lane 12, PCR blank. Lane 13, PCR positive control (1:10,000 dilution of pFloxEGFP plasmid).

the 1213bp PCR product identified those clones that contained the full-length EGFP sequence and of the 10 clones examined the full-length EGFP coding sequence could be detected in 8. One such clone, FE13 which was PCR positive and expressed high levels of  $\beta$ -gal was selected for further analysis.

## **2.8. Clone FE13 – Introducing Cre Recombinase**

The aim of this next section of work was to develop a strategy to express Cre recombinase within FE13 cells and to analyse the effects upon marker gene expression. The first method considered was the transient transfection of FE13 cells with Cre-encoding plasmids. However, only relatively low transfection efficiencies were achieved, using both lipofection and electroporation, and Cre-mediated recombination could not be detected (data not shown). Another reason for the poor results obtained with transient transfection could be low levels of Cre expression from the introduced plasmid, Cre-5 a gift from Dr. T. Gardner (see Appendix 1). Two alternatives were considered in parallel in an attempt to overcome this problem, first, the construction of another Cre expression vector with an alternative promoter sequence (Section 2.8.1) and second, the use of replication-defective recombinant adenoviridae (Section 2.8.2).

### **2.8.1. Characterisation of an ES Cell Differentiation State-Specific Promoter Sequence**

#### **2.8.1.1. Background**

As discussed above, one approach to permit the expression of Cre recombinase in FE13 cells was to develop a new vector that would drive high levels of Cre expression in ES cells. As part of this work, in collaboration with Dr. J. Quinn and Dr. C. Fiskerstrand from the Department of Veterinary Pathology, Edinburgh University, the promoter activity of a novel region of the rat preprotachykinin gene (rPPT) was characterised in murine ES cells. Dr. C. Fiskerstrand constructed and supplied all plasmids and prepared the protein extracts from transfected cells, however the ES cell culture was carried out by myself.

The rPPT gene encodes the neuropeptides substance P, neurokinin A, neuropeptide K and neuropeptide  $\gamma$ , which are derived by alternative splicing and post translational processing of the peptide precursors (Maggio, 1988). Sequences derived from the promoter of this gene have already been demonstrated to restrict expression to neuronal cells *in vitro* but do not support transgene expression *in vivo* (Mulderry *et al*, 1993). Therefore, it was of interest to characterise the enhancer activity of a novel intronic domain within the rPPT gene, consisting of a CCCT repeat motif, which had not been previously characterised due to a high level of genetic instability. This domain was cloned upstream of a luciferase marker gene and basal promoter (pGL3p, Promega) and the resultant plasmid, CCCT-pGL3p, was then transfected into HeLa and ES cells and the levels of luciferase expression quantified.

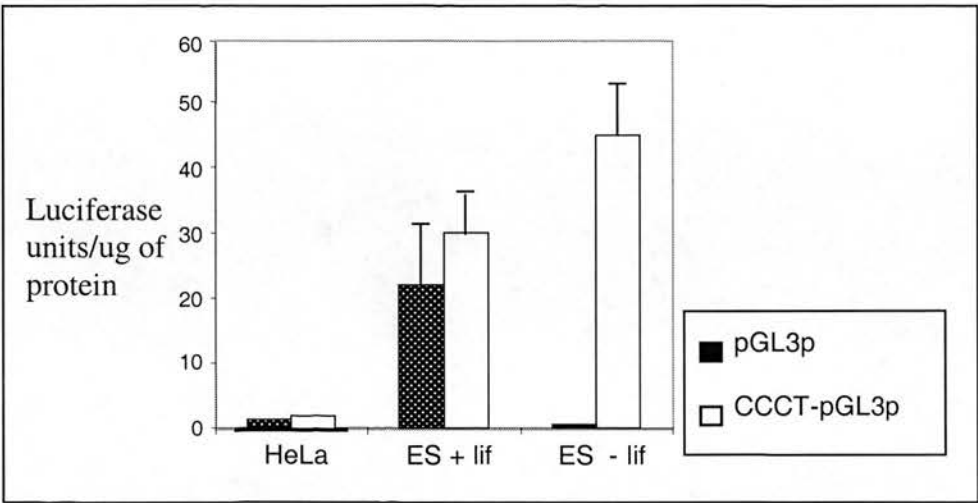
ES cells are pluripotent and undifferentiated however, the maintenance of this stem cell phenotype is an active process. Several protocols have been developed which promote the differentiation of ES cells (reviewed in Hooper, 1982). As certain elements of the rPPT promoter had already been shown to restrict marker gene expression to differentiated cells it was of interest to compare the enhancer activity of the novel CCCT repeat motif in undifferentiated and differentiating ES cells. There are two basic protocols to stimulate ES cell differentiation, first, the withdrawal of LIF and second, the addition of retinoic acid (RA). The withdrawal of LIF induces the differentiation of ES cells into a mixture of visceral and parietal endoderm-like and mesoderm-like cells (Mummery *et al*, 1990). Neuronal cells constitute only a small percentage of the cell types observed after LIF withdrawal, although this yield can be increased by exposure to RA (Gajovic *et al*, 1997). Hence, ES cells were transfected in the presence or absence of LIF and RA (all trans RA, dissolved in ethanol, over the range 0-500 $\mu$ M) and luciferase expression quantified.

#### **2.8.1.2. Results**

As shown in Figure 2.18A the level of luciferase expression driven from both the pGL3p and CCCT-pGL3p plasmids was cell type specific. Low levels of luciferase

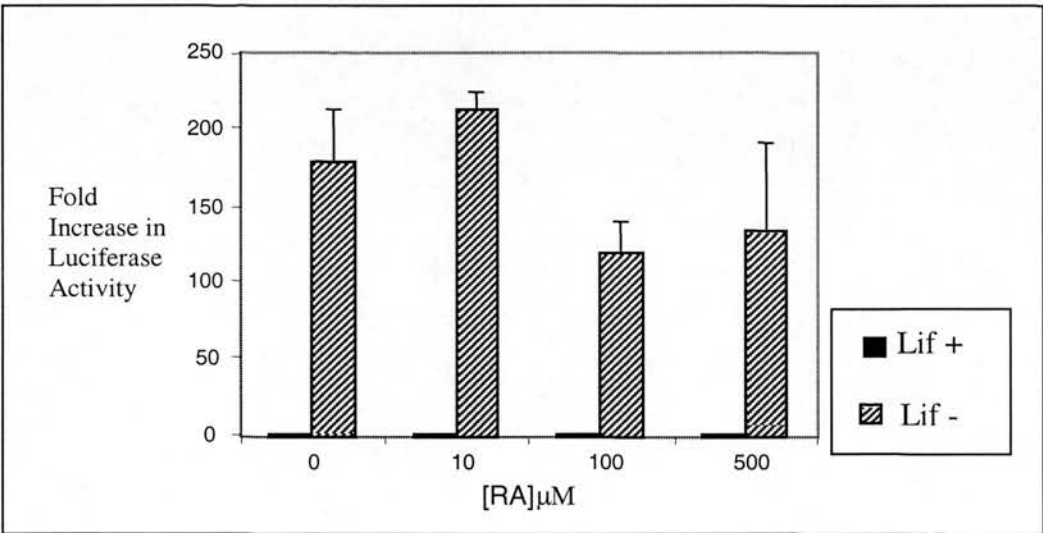
**Figure 2.18** – Investigation of the Enhancer Activity of the CCCT Repeat Motif From the Rat Preprotachykinin Gene

A)



Luciferase expression from cells transfected with either the basal luciferase expression vector (pGL3p) or the vector with the CCCT putative enhancer present (CCCT-pGL3p). Luciferase units are normalised using RSVCAT expression in each sample to correct for transfection efficiencies. A similar number of HeLa and ES cells were used in each experiment and transfections were carried out in triplicate (error bars are standard error of the mean).

B)



The enhancer activity of the rPPT Intron 2 CCCT element is shown as the increase in luciferase units over the basal activity of the expression vector. Results are corrected for transfection efficiencies. Data is shown as + and – LIF at increasing retinoic acid concentrations from 0-500 $\mu\text{M}$  (error bars are standard error of the mean).

were expressed from both plasmids after transfection into HeLa cells. Higher, but not significantly different levels of luciferase expression were detected when both plasmids were transfected into undifferentiated ES cells cultured in the presence of LIF. However, the withdrawal of LIF over the 64-hour period of transient transfection resulted in a 150-fold increase of luciferase expression from the CCCT-pGL3p plasmid relative to the control plasmid. Hence the molecular changes initiated in ES cells by the withdrawal of LIF were sufficient to permit the CCCT repeat motif to prevent the inhibition of luciferase expression observed with the control plasmid. One interpretation of these data is that the CCCT element is able to act as a transcriptional enhancer, an effect not further enhanced by exposure of transfected cells to a variety of RA doses.

In conclusion, the rPPT-derived CCCT element can permit high levels of marker gene expression in differentiating ES cells. However, no attempts were made to utilise this enhancer for the expression of Cre recombinase as the recombinant adenovirus approach, investigated in parallel, yielded encouraging results. This work is discussed in the following section.

### **2.8.2. Replication-defective Recombinant Adenoviridae**

Several groups have developed replication-defective recombinant adenoviridae and all are constructed along similar lines but differ in the heterologous protein that they have been engineered to express. The virus is rendered replication-defective by the insertion of an expression cassette and simultaneous deletion of endogenous genes that are essential for replication. One such virus in which the E1 region has been replaced with a Cre recombinase expression cassette, AdCre, was obtained from M. Anton and FL. Graham (Anton & Graham, 1995).

The adenovirus approach has several advantages, the virus is able to efficiently infect a wide variety of cell types, both replicating and quiescent, at a high efficiency. Once inside cells the constitutive promoter, human CMV<sub>IE</sub> drives high levels of Cre recombinase expression from the expression cassette present in AdCre. Because

AdCre is non-replicating the virus behaves as an episomal molecule and will be gradually lost from dividing cells and in this respect AdCre acts as a high efficiency method of transiently transfecting mammalian cells with Cre recombinase.

At the time of this work only one publication had reported the successful use of adenovirus to infect murine ES cells (Aladjem *et al*, 1998). The authors had indicated that very high titres of virus were needed to infect undifferentiated ES cells (at least  $5 \times 10^9$  particles per  $5 \times 10^5$  cells) but no data were included in this paper about the actual multiplicity of infection (m.o.i.) used. For this reason it was necessary to determine an optimal adenovirus m.o.i that resulted in a high level of infection without any obvious cytopathic effects.

#### **2.8.2.1. Determination of the Optimum Adenovirus Titre for ES Cell Infection**

Because the AdCre recombinant adenovirus does not express any readily detectable marker genes, the optimum titre of adenovirus for efficient infection of ES cells was determined using an alternative recombinant adenovirus, AdLacZ which expresses  $\beta$ -gal, also obtained from M. Anton and FL. Graham (Anton & Graham, 1995).

Undifferentiated HM-1 ES cells were plated out at identical densities and each sample was then infected with a different titre of AdLacZ, either 50 m.o.i, 200 m.o.i or 1000 m.o.i. Twenty-four hours after infection the cells were fixed and stained for  $\beta$ -gal expression (Figure 2.19). At both 50 m.o.i. and 1000 m.o.i, a similar number of  $\beta$ -gal positive cells were present. However, the majority of  $\beta$ -gal positive cells were in fact differentiated ES cells that make up a percentage of the ES cell population in any given culture. It is only when the efficiency of infection of undifferentiated ES cells was examined that differences between the AdLacZ titres become apparent. No undifferentiated ES cell infection was seen in the two lower titres used in this experiment (Figure 2.19A). It is only at 1000m.o.i. AdLacZ that small numbers of  $\beta$ -gal positive undifferentiated ES cells can be visualised (Figure 2.19B). In support of this observation, the preferential infection of differentiated ES cells has been reported elsewhere (Aladjem *et al*, 1998). However, rather than use



**Figure 2.19 - Histochemical Detection of  $\beta$ -gal Activity; Results of AdLacZ-infection of Undifferentiated ES Cells**

1)  $\beta$ -gal staining results after undifferentiated ES cells exposed to 50 m.o.i. of AdLacZ.

- A) Photograph taken without phase at x100 magnification. Blue staining cells are clearly visible.
- B) Duplicate photograph of the cells shown in 1A) but taken here with phase at x100 magnification. In this image morphological details of the cells can be seen. In the centre of the image a group of undifferentiated ES cells can be seen. By comparison with image 1A), such cells do not express histochemically detectable  $\beta$ -gal activity and have therefore not been infected with AdLacZ. At the extremities of the photograph large cells with irregular size and morphology are seen, these are differentiated ES cells. By comparison with image 1A), such cells express high levels of  $\beta$ -gal and have therefore been infected by AdLacZ.

Therefore, at 50 m.o.i., only differentiated ES cells are infected by the recombinant adenovirus, AdLacZ.

2)  $\beta$ -gal staining results after undifferentiated ES cells exposed to 1000 m.o.i. of AdLacZ.

- A) Photograph taken without phase at x100 magnification. Blue staining cells are clearly visible.
- B) Duplicate photograph of the cells shown in 2A) but taken here with phase at x100 magnification. In this image morphological details of the cells can be seen. In the centre of the image a group of undifferentiated ES cells can be seen. By comparison with image 2A), a percentage of such cells do express histochemically detectable  $\beta$ -gal activity and have therefore been infected with AdLacZ. At the extremities of the photograph large cells with irregular size and morphology are seen, these are differentiated ES cells. By comparison with image 2A), such cells express high levels of  $\beta$ -gal and have therefore been infected by AdLacZ.

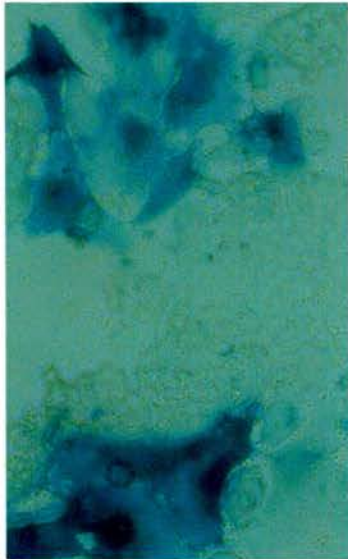
Therefore, at 1000 m.o.i., both differentiated and undifferentiated ES cells are infected by the recombinant adenovirus, AdLacZ. However, even at this relatively high viral titre a low efficiency of undifferentiated ES cell infection is observed.



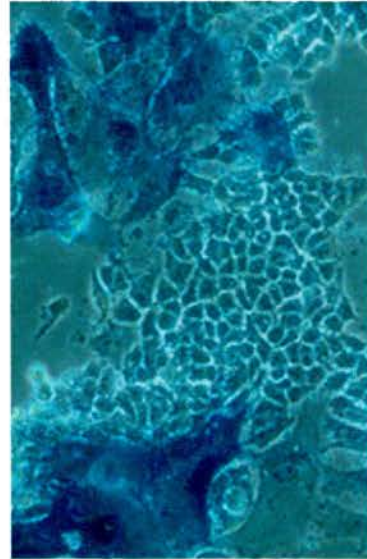
**Figure 2.19** - *Histochemical Detection of  $\beta$ -gal Activity; Results of AdLacZ-infection of Undifferentiated ES Cells*

1) With 50 m.o.i AdLacZ (x100)

A) (Bright field)

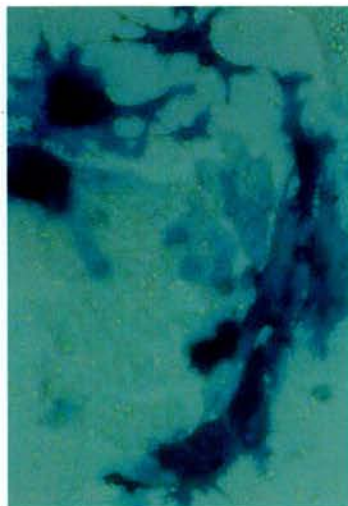


B) (With phase)

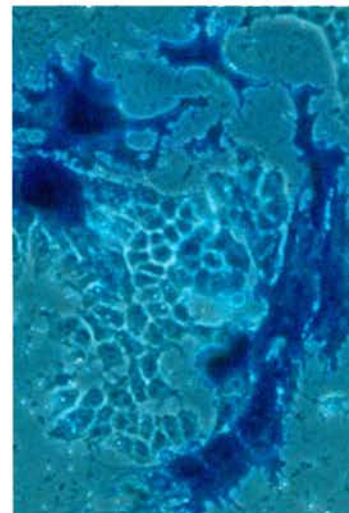


2) With 1000 m.o.i. AdLacZ (x100)

A) (Bright field)



B) (With phase)



extremely high titres of adenovirus to infect undifferentiated FE13 cells it was decided to deliberately differentiate ES cells in culture prior to adenovirus infection.

#### **2.8.2.2. AdCre Infection of Differentiated of FE13 ES Cells**

FE13 cells were differentiated according to standard procedures (reviewed in Keller, 1995). The cells were then infected with 50 m.o.i of AdCre and control plates of differentiated HM-1 and FE13 ES cells and were mock-infected. Immediately after infection zero hour time-points of mock infected HM-1 and FE13 cells were harvested. Seventy-two hours after infection, the infected cells and the mock-infected control samples were also harvested. At each time-point the harvested cells were divided into multiple samples for analysis including protein extract preparation, samples for FACS and UV microscopy, preparation of genomic DNA and total RNA.

##### **2.8.2.2.a. Episomal AdCre Detection**

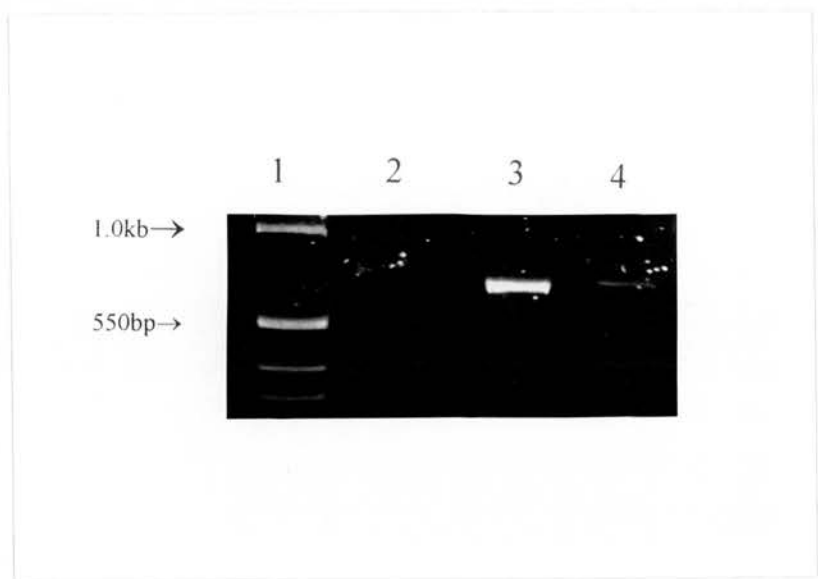
Adenoviridae only rarely integrate into the host genome and are instead thought to persist as extrachromosomal molecules (Stratford-Perricaudet *et al*, 1992). The presence of these episomal molecules in DNA extracts prepared from infected cells can be detected by PCR, using primers that anneal within the Cre expression cassette of AdCre (designed by Dominic Rannie). The 660bp band visible in Figure 2.20, lane 4 suggests the successful infection of differentiated FE13 cells.

Having demonstrated that AdCre is capable of infecting FE13 cells the next step was to demonstrate that the recombinant virus was expressing functional Cre recombinase. This was achieved by examining the recombination status of the pFloxEGFP transgene in FE13 cells.

##### **2.8.2.2.b. pFloxEGFP Recombination Status**

Genomic DNA was prepared from FE13 cells harvested at 0hrs, 72hrs(mock infected) and finally 72hrs(AdCre-infected) and the recombination status of the transgene present in the genome of FE13 cells was analysed by both PCR and Southern blot.

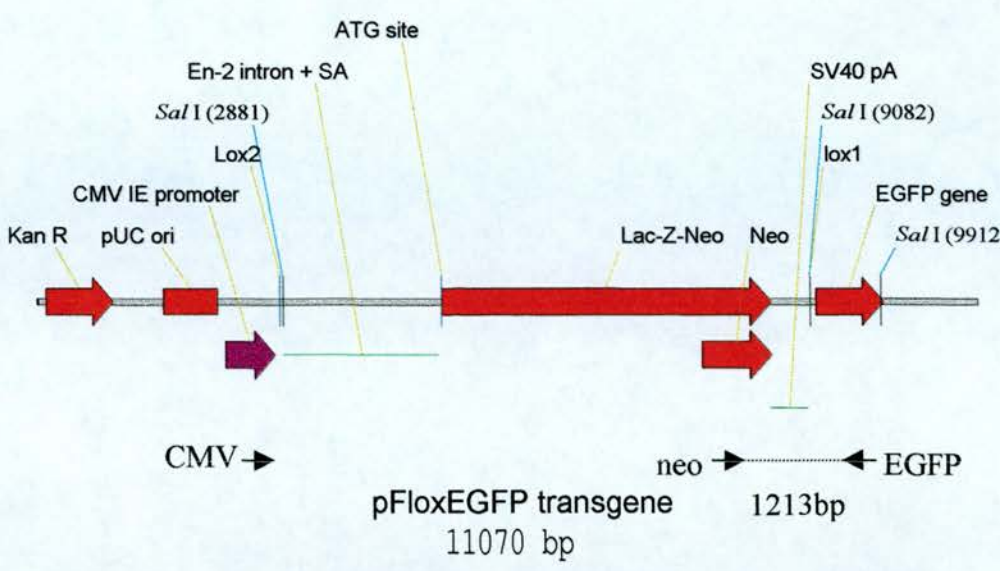
**Figure 2.20** – *PCR Detection of Episomal Adenovirus Molecules*



2.0% agarose/ethidium bromide gel. Lane 1, molecular weight markers. Lane 2, DNA sample from uninfected FE13 cells. Lane 3, positive control sample supplied by D. Rannie of DNA extracted from cells known to be infected with AdCre. Lane 4, DNA sample prepared from AdCre infected FE13 cells (72hr timepoint). The 660bp band diagnostic of the presence of episomal AdCre molecules within genomic DNA can be seen in both lanes 3 and 4.

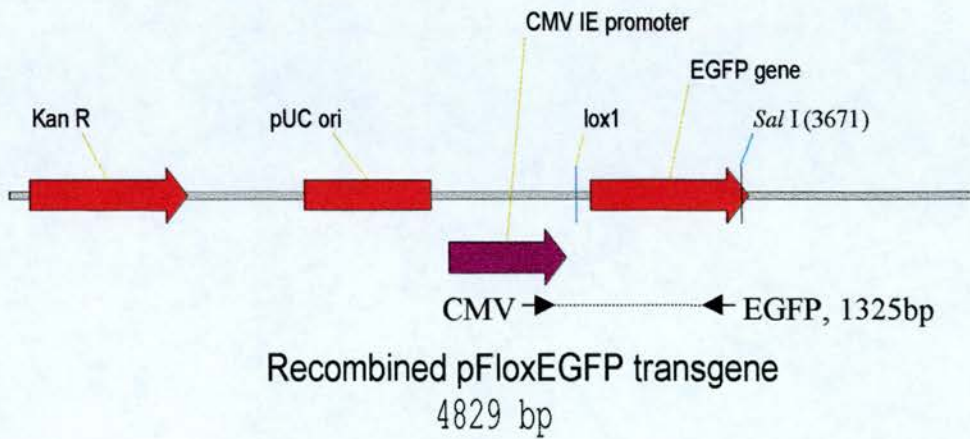
**Figure 2.21 – Recombination Status-Specific PCR For The pFloxEGFP Plasmid**

A)



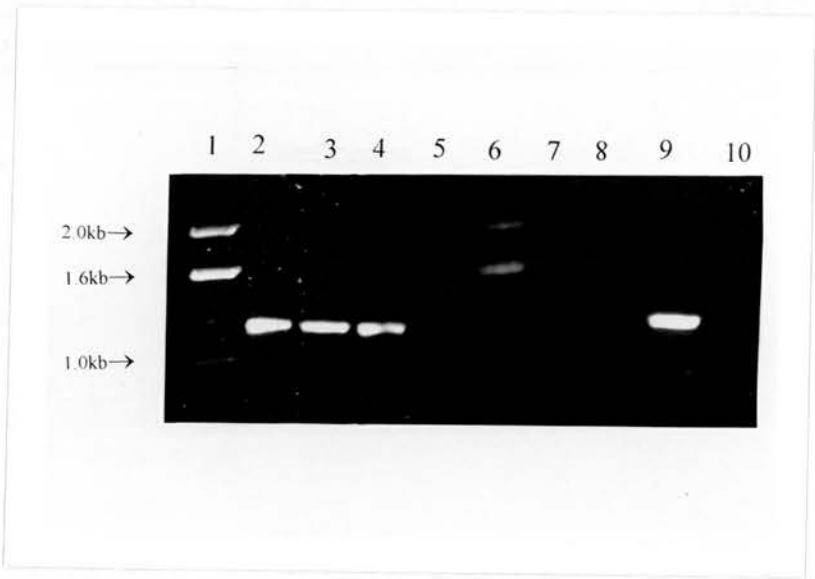
The structure of the complete pFloxEGFP transgene with the relative positions of the CMV, neo and EGFP primers indicated. Prior to Cre-mediated excisive recombination only the neo and EGFP primers function to generate a 1213bp product.

B)



After excisive recombination has occurred the neo primer binding site is lost and the alternative upstream primer, CMV together with the EGFP primer, generates a recombination specific 1325bp product.

**Figure 2.22** – Results of the *pFloxEGFP Recombination Status-Specific PCR*



1.0% agarose/ethidium bromide gel. Lane 1, molecular weight markers. Lane 2, the 1213bp PCR product amplified from genomic DNA harvested from cells at the 0hrs. uninfected timepoint. Lane 3, the 1213bp PCR product amplified from genomic DNA harvested from cells at the 72hrs. uninfected timepoint. Lane 4, the 1213bp PCR product amplified from genomic DNA harvested from cells at the 72hrs. AdCre infected timepoint. Lane 5, negative control (water). Lane 6, molecular weight markers. Lane 7, blank, no 1325bp recombination-specific is amplified from genomic DNA harvested from cells at the 0hrs. uninfected timepoint. Lane 8, blank, no 1325bp recombination-specific is amplified from genomic DNA harvested from cells at the 72hrs. uninfected timepoint. Lane 9, the 1325bp recombination-specific PCR product amplified from genomic DNA harvested from the 72hrs AdCre infected timepoint. Lane 10, negative control (water).



### **i) PCR Strategy**

A PCR strategy was designed which generated recombination status-specific products (Figure 2.21). In the unrecombined state, the primer pair *neo* and *EGFP* are predicted to generate a 1213bp product from the integrated transgene present in FE13 cells (Figure 2.21). However, after Cre-mediated recombination has occurred the floxed STOP cassette is excised and the *neo* primer binding site lost. The third primer *CMV* then pairs with *EGFP* to generate a recombination specific 1325bp PCR product.

These two PCR reactions were carried out on genomic DNA harvested from AdCre- or mock-infected FE13 cells and the results are shown in Figure 2.22. The *neo/EGFP* primer pair gives rise to a 1213bp band from all DNA samples indicating that the unrecombined transgene is still present even in AdCre-infected FE13 cells. However, the 1325bp recombination-specific *CMV/EGFP* product is only amplified from genomic DNA prepared from AdCre-infected cells (Figure 2.22, lane 9). The presence of this 1325bp PCR product is diagnostic that Cre-mediated excisive recombination has occurred only in AdCre-infected cells and demonstrates the production of functional Cre recombinase by AdCre. However, this PCR reaction is not quantitative and cannot be used to assess the efficiency of Cre-mediated recombination in FE13 cells.

### **ii) Southern Blot Strategy**

FE13 genomic DNA was digested with the restriction enzyme *Hind III*. This enzyme was selected as it generates recombination status-specific cleavage products, a 7090bp product from the unrecombined transgene (Figure 2.23A) and an 849bp digest product from the recombined transgene (Figure 2.23B). These digest products were detected by hybridisation with a radiolabelled EGFP-derived probe, the relative location of the probe sequence is shown on Figure 2.23. The EGFP probe used was a 600bp PCR product amplified from the EGFP gene using the primers *CAP* and *EGFP* (see Chapter 6, Section 6.1.14.3.b). The result of this Southern blot strategy is shown in Figure 2.24.

**Figure 2.23** – Southern Strategy for the pFloxEGFP Plasmid

A)

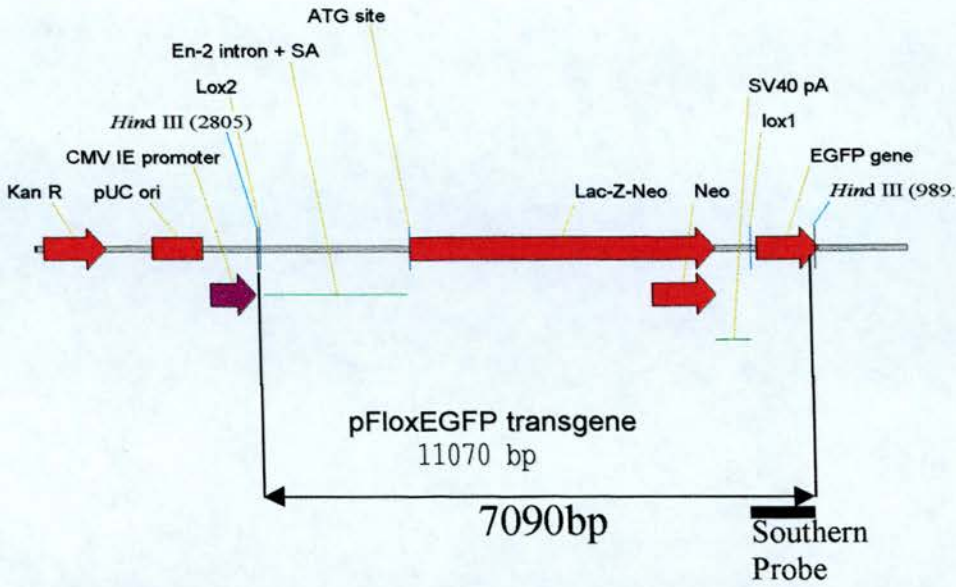
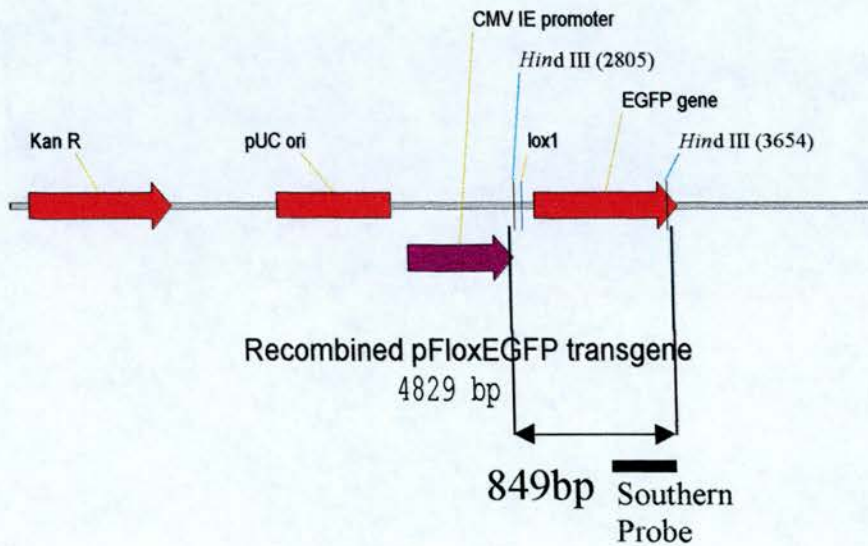


Diagram to illustrate the Southern blot strategy to monitor Cre-mediated excisive recombination in FE13 cells. Digestion of genomic DNA from FE13 cells with *Hind* III should generate a 7090bp band which will hybridise with the EGFP probe indicated (thick black line).

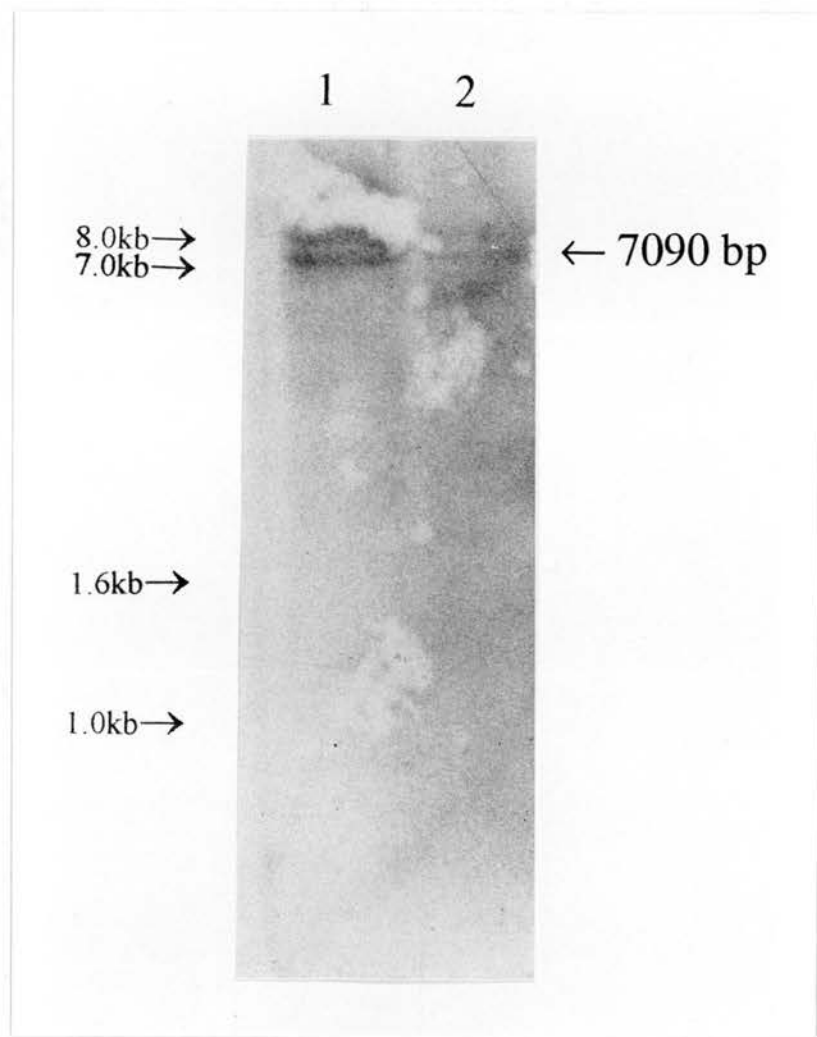
B)



After Cre-mediated excisive recombination has occurred, digestion of FE13 genomic DNA with *Hind* III is predicted to yield an 849bp band which will hybridise with the EGFP Southern probe indicated.



**Figure 2.24 – FE13 Southern Blot Result**



Photograph of autoradiograph obtained from Hind III-digested FE13 genomic DNA, transferred onto a filter and then probed with a radiolabelled EGFP probe. Lane 1, genomic DNA harvested from control uninfected FE13 cells. Two bands are visible, the 7090bp digest product derived from the unrecombined pFloxEGFP transgene and a +8 kb digest product which presumably represents incomplete digestion of the genomic DNA. Lane 2, genomic DNA harvested from AdCre-infected (50 m.o.i) FE13 cells. As in lane 1, two bands are visible, the 7090bp digest product derived from the unrecombined pFloxEGFP transgene and the +8kb incomplete digest product. However, the 849bp digest product derived from the recombined pFloxEGFP transgene was not detected in this lane. Approximate size markers are shown at the left-hand side of the photograph, these were calculated from the positions of molecular weight markers on the original agarose gel (not shown).

The 7090bp digest product generated from the unrecombined pFloxEGFP transgene was detected in both the FE13 mock-infected and FE13 AdCre-infected genomic DNA samples (indicated on Figure 2.24). Both lanes also contain a higher molecular weight band (approximately 8-9kb) which probably represents incomplete digestion of the genomic DNA. However, the 849bp digest product diagnostic of Cre-mediated excisive recombination was not detected in genomic DNA isolated from AdCre-infected FE13 cells. The possible reasons for this are discussed further in Section 2.9.

#### **2.8.2.2.c. EGFP Expression Data**

If the floxed STOP cassette present in pFloxEGFP functions as predicted, in the absence of Cre recombinase EGFP expression should be inhibited. However, after Cre-mediated loss of the floxed STOP cassette high levels of EGFP should be expressed (see Figure 2.13). Three methods were used to monitor levels of EGFP expression, Fluorescence Activated Cell Sorting (FACS), UV microscopy and RT-PCR.

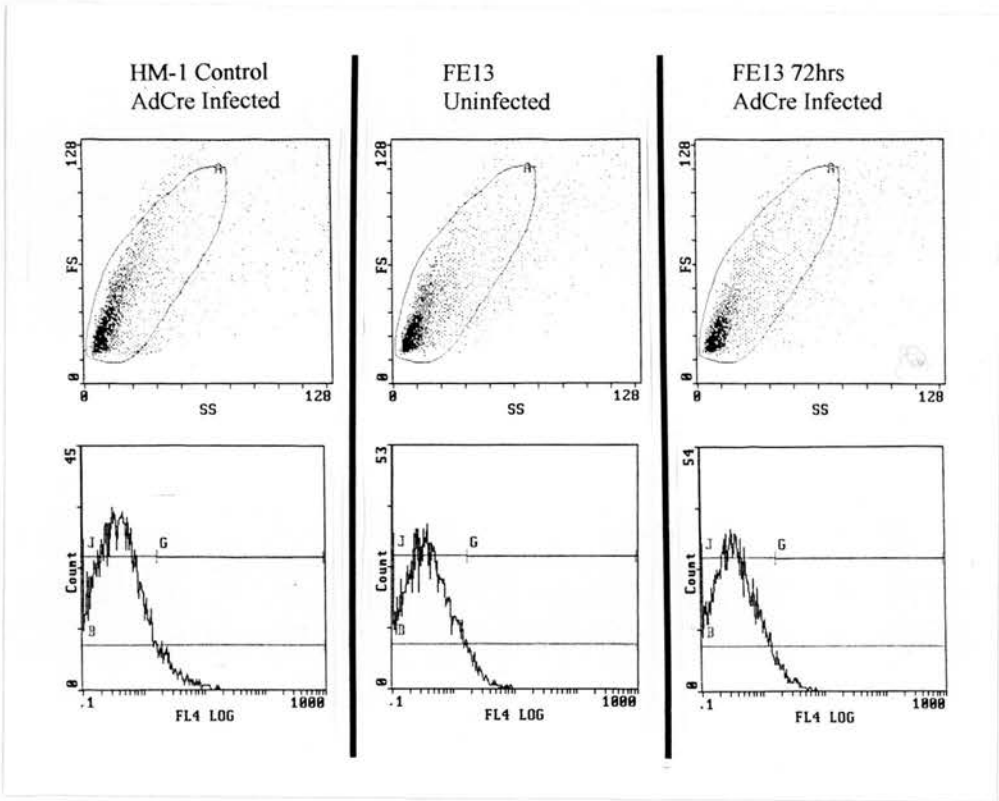
##### **i) FACS and UV Microscopy Data**

As already mentioned FE13 cells were infected with AdCre and control FE13 and HM-1 cells were simultaneously mock infected. Cell samples were harvested at 0hr and 72hr timepoints, and were transferred to storage at -70°C. Prior to FACS analysis all cell samples were defrosted simultaneously, washed in PBS and then resuspended in PBS. A small aliquot of cells from each sample were transferred onto chamber slides and visualised by UV microscopy (FITC filter set). Positive control cells transiently transfected with the pEGFP-C1 plasmid (Figure 2.14) were immediately obvious when viewed using a UV microscope, however, no fluorescent cells were seen in the FE13 samples. This observation was supported by FACS data.

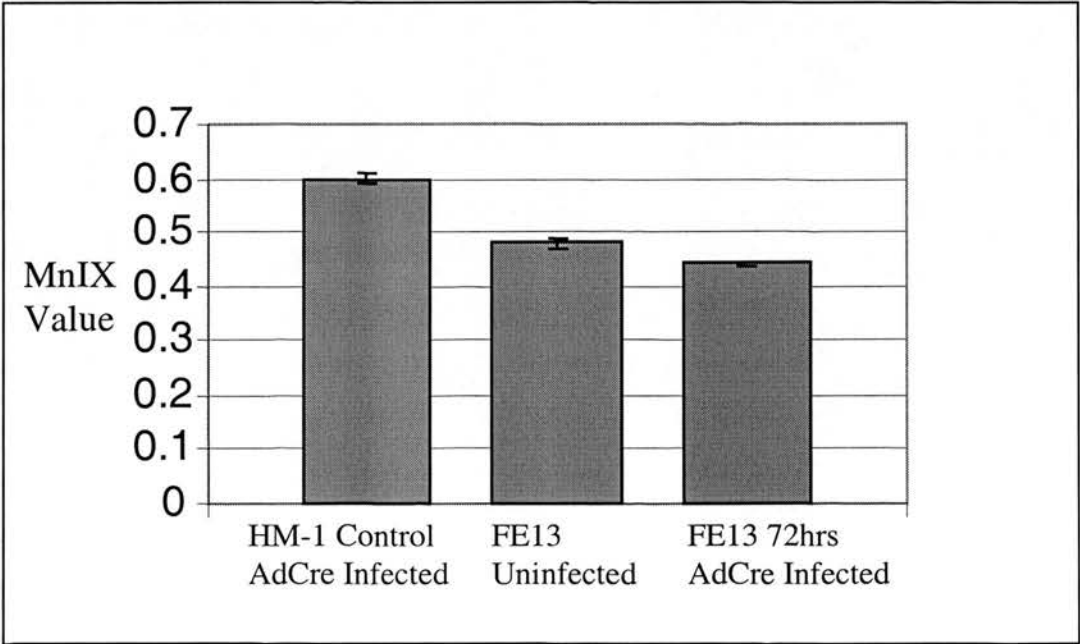
The remaining cells from each sample were not fixed and so were subjected to FACS analysis immediately. Ten thousand cells from each sample were analysed in triplicate using a Coulter EPICS XL-MCS flow cytometer measuring the

**Figure 2.25 – EGFP Expression Data**

A) FACS data



B) Bar chart of the MnIX values from triplicate samples of HM-1 control AdCre infected, FE13 72hrs uninfected and FE13 72hrs AdCre infected.



fluorescence emitted by each cell in a 488nm argon laser. The forward scatter (FS), side scatter (SS) and fluorescent light emissions of the samples were measured between the wavelengths of 489nm-700nm. The data was then presented as a scatter plot and histogram as shown in Figure 2.25A.

The excitation maximum of the EGFP protein is 488nm and the emission maximum is 507nm, these characteristics make it an ideal fluorescent marker gene for use in flow cytometry. However, when the mean fluorescence (MnIX value) of the three cell populations represented in Figure 2.25A, HM-1 mock infected, FE13 mock-infected and FE13 AdCre-infected, is plotted as in Figure 2.25B no increase in MnIX value is observed in the FE13 AdCre-infected cell population. There is no significant difference between the MnIX values of any of the cell populations shown in Figure 2.25 ( $p > 0.05$ , Mann-Whitney U test, two-tailed).

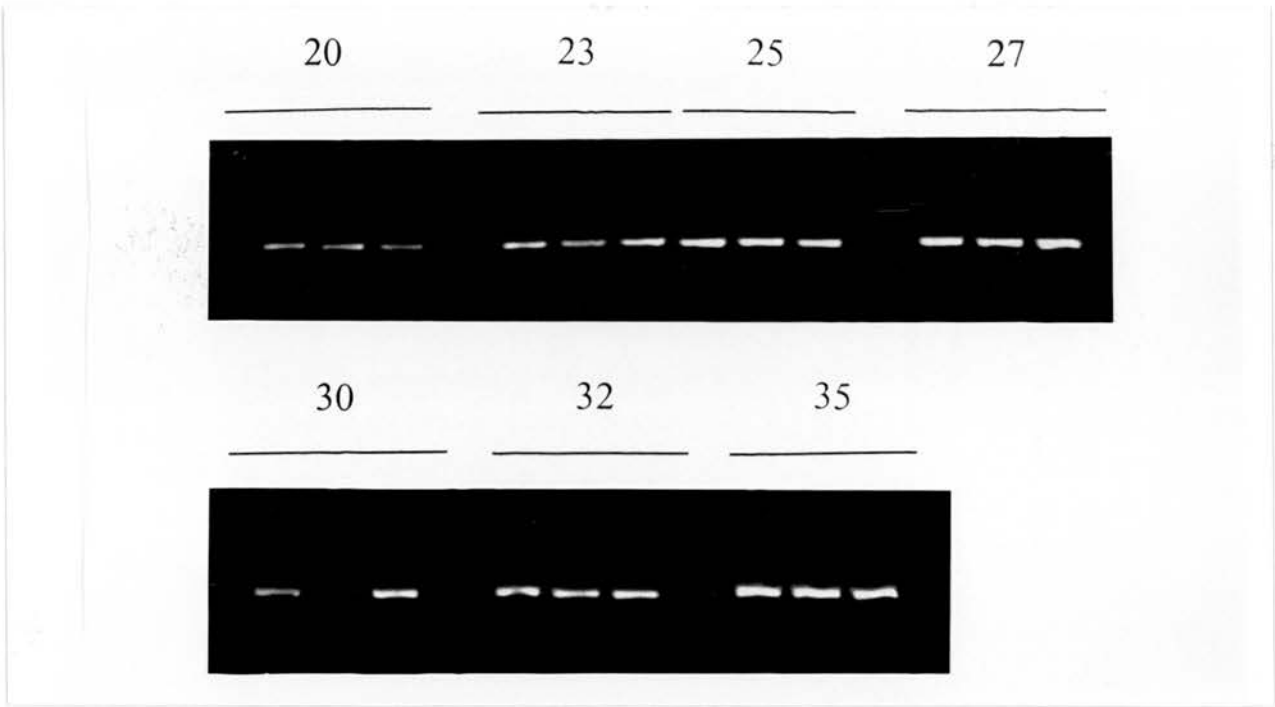
## **ii) Semi-quantitative RT-PCR Detection of EGFP mRNA**

As expression of the EGFP protein from the recombined pFloxEGFP transgene could not be demonstrated by UV microscopy or FACS analysis an RT-PCR strategy was designed in an attempt to quantify, within the limitations of this technique, the levels of EGFP transcription. Two pairs of PCR primers were used, firstly, *BA4* and *BA15* which generate a 440bp band from the mouse  $\beta$ -actin cDNA and secondly *CAP* and *EGFP* which generate a 600bp band from the EGFP cDNA.

In order for PCR to be quantitative the reaction must terminate during the log phase of product amplification. During this phase, the product concentration has a log linear relationship with the original template concentration. To determine the log phase of the EGFP PCR reaction, 21 reaction mixes were prepared as described in Chapter 6, Section 6.1.14.3.b and three tubes were removed after 20, 23, 25, 27, 30, 32 and 35 of the programme thermal cycles had been completed. The PCR products were then electrophoresed through a 2% agarose gel and the relative intensity of all of the products analysed with EASY Analysis gel documentation software. In conclusion, cycle number 30 of the EGFP PCR was determined as being within the

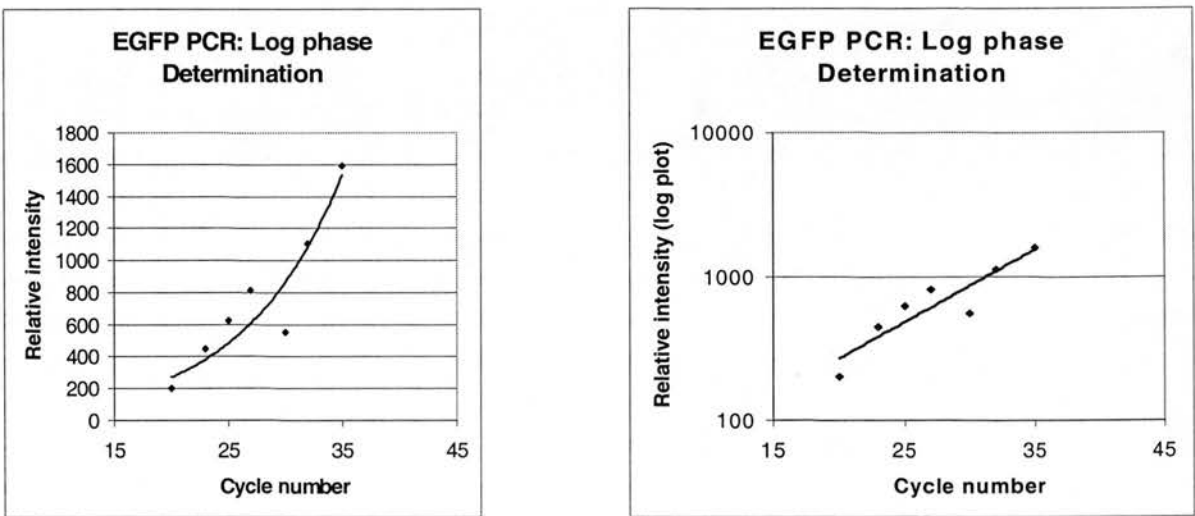
**Figure 2.26 – Determination of the Log Phase of the EGFP/CAP PCR Reaction**

A)



2.0% agarose/ethidium bromide gel. Three sample tubes were removed from the thermal cycler at each of the cycle numbers indicated above the gel. 10 $\mu$ l of each product for cycles 20-27 and 5 $\mu$ l for cycles 30-35, was then loaded on the above gel.

B)



Linear and logarithmic plots of the relative intensities of the PCR products shown in the above gel after standardisation for gel loading.

log phase, these results are shown in Figure 2.26A and B. As the log phase for the  $\beta$ -actin PCR had already been determined as cycle number 31 it was unnecessary to repeat this process for this PCR reaction (Wallace, 1997).

Total RNA was harvested from FE13 AdCre-infected and control cells and equal amounts of RNA from each sample were converted to cDNA via reverse transcription. The cDNA produced in these reactions was then used as a template for both the  $\beta$ -actin and EGFP PCR reactions. The thermal cycler programmes for each reaction were amended to terminate within the pre-determined log phase cycle number. PCR products were then electrophoresed through a 2.0% agarose gel and the relative intensity of the products was quantified using EASY Analysis gel documentation software. Triplicate samples of RNA harvested from FE13 mock-infected cells (0hr and 72hr timepoints) and AdCre-infected FE13 cells (72 hr timepoint) were analysed in this manner and the results are shown in Figure 2.27.

A 440bp  $\beta$ -actin PCR product was amplified efficiently from all cDNA samples. However, the 600bp EGFP PCR product can was also detected in all cDNA samples irrespective of the exposure of the cells to AdCre. This result indicates that the floxed STOP cassette present in the pFloxEGFP transgene within FE13 cells does not block transcription of the EGFP marker gene with 100% efficiency. If the ratio of  $\beta$ -actin to EGFP PCR products present in Figure 2.27A is calculated an approximate two-fold induction of EGFP mRNA is seen in the AdCre infected cells (Figure 2.27B,  $p < 0.05$ , Mann-Whitney U test, two-tailed).

### **iii) Confirmation of the Absence of EGFP protein**

As discussed above, the infection of FE13 cells with AdCre resulted in Cre-mediated excisive recombination, as detected by PCR, and a small but significant upregulation of EGFP mRNA. However, no fluorescent EGFP protein was detected by FACS analysis or UV microscopy. To confirm this surprising observation a repeat AdCre-infection (50 m.o.i) using a new viral stock, was carried out on differentiated FE13 cells. Twenty-four hours after infection cells were harvested and half of the sample



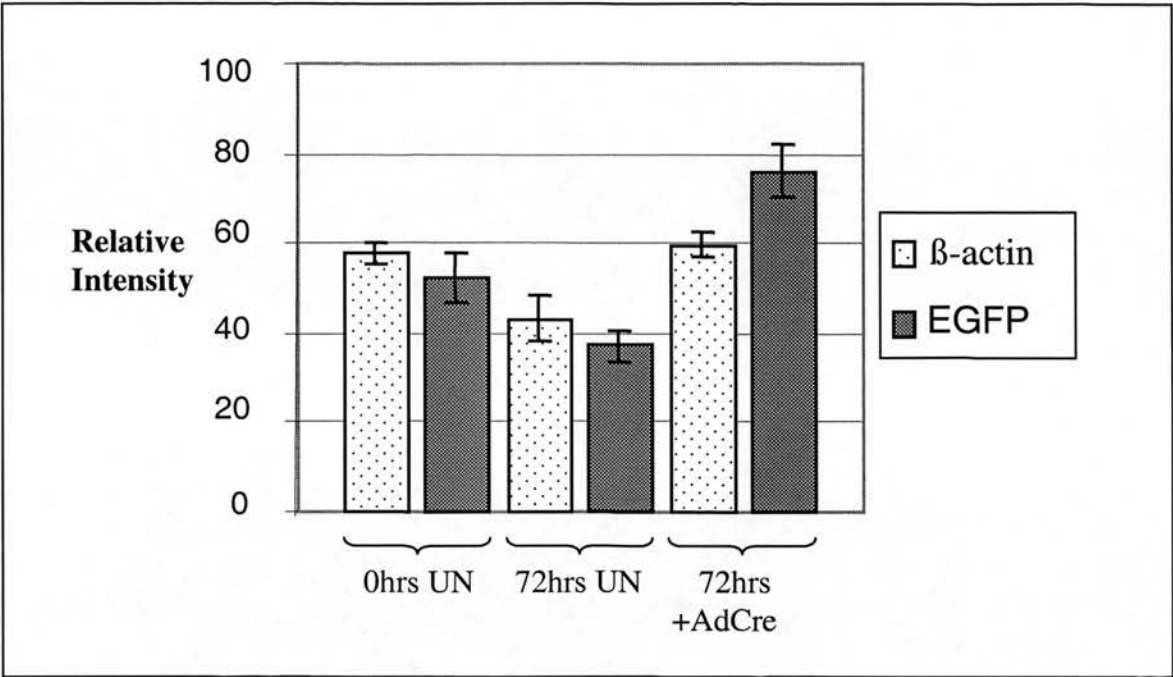
**Figure 2.27** – *qRT-PCR Data on  $\beta$ -actin and EGFP Expression*

A)

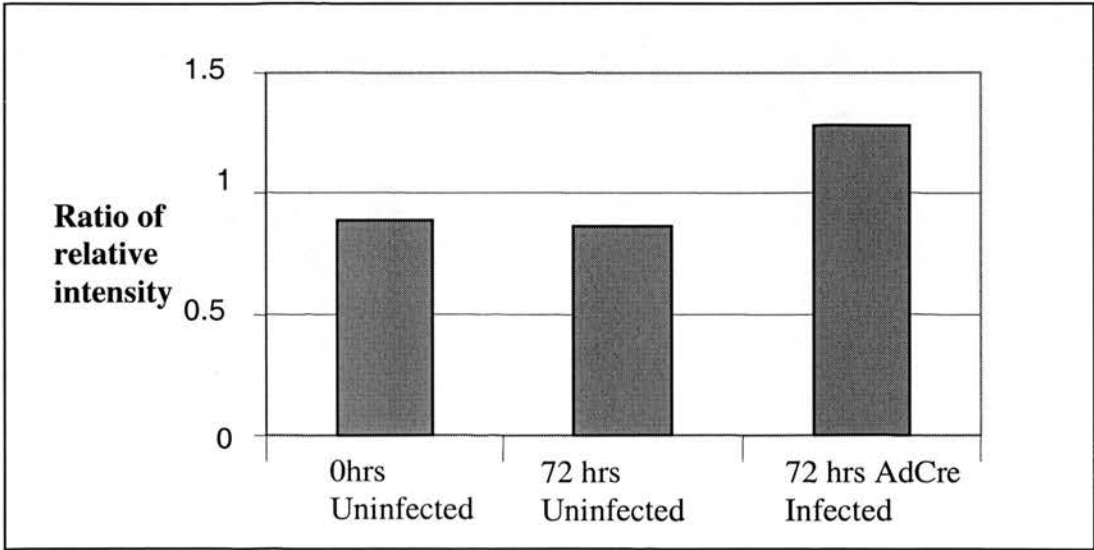


Top gel, 10ul of the 440bp  $\beta$ -actin PCR product amplified from cDNA templates prepared from three cell samples, FE13 0hr uninfected, FE13 72 hr uninfected and FE13 72hr AdCre infected. Lower gel, 10 $\mu$ l of the 600bp PCR product amplified from cDNA templates prepared from three cell samples, FE13 0hr uninfected, FE13 72 hr uninfected and FE13 72hr AdCre infected.

B) Bar chart illustrating the mean relative intensities of the  $\beta$ -actin and EGFP PCR products shown in Figure 2.26A.



C) Bar chart illustrating the ratio of the relative intensities of the  $\beta$ -actin and EGFP PCR products amplified from cDNA prepared from the three timepoints, FE13 0hrs and 72 hrs uninfected and FE13 72 hrs after AdCre infection.



used for protein extract preparation while the remaining cells were examined by UV microscopy. A comparable decrease in  $\beta$ -gal activity was seen between the AdCre- and mock-infected cells (from 57 $\mu$ U/ $\mu$ g to 20 $\mu$ U/ $\mu$ g after AdCre infection, detailed data not shown) as shown in Figure 2.28 indicating a similar efficiency of infection had occurred. However, when samples from both populations of cells were examined under UV light no fluorescent cells were visible. This experiment confirmed the observation that Cre-mediated excision of the floxed STOP cassette from pFloxEGFP plasmid is insufficient to permit the upregulation of EGFP protein.

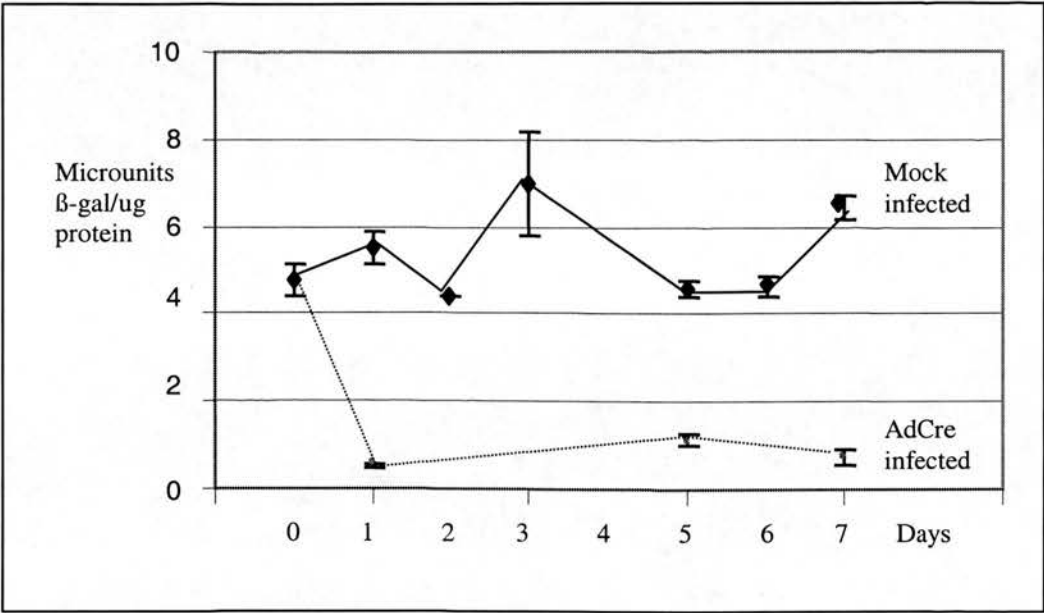
#### **2.8.2.2.d. $\beta$ -galactosidase Expression Data**

As shown in Figure 2.13, the recombination status of pFloxEGFP influences the expression of two marker genes, the fusion gene  $\beta$ geo, encoding the  $\beta$ -gal and *neo* genes, and EGFP. In the absence of Cre-mediated recombination, the constitutive CMV<sub>IE</sub> promoter should drive high levels of expression of the  $\beta$ geo fusion gene. After excisive recombination, the floxed STOP cassette will be lost, the  $\beta$ geo gene deleted, and expression abolished. The  $\beta$ -galactosidase Enzyme Assay Kit (Promega) was used to quantify the levels of  $\beta$ -gal activity in protein extracts prepared from FE13 cells exposed to or mock treated with AdCre. However, a comparison of  $\beta$ -gal activity levels in protein extracts prepared from uninfected control cells and those from AdCre-infected cells revealed only a small decrease (data not shown). There were two possible explanations, first that Cre-mediated recombination had occurred at a low frequency within the FE13 cells or second, that the stability of the bacterial  $\beta$ -gal protein in mammalian cells resulted in its retention in cells even after expression had been abolished (Yang *et al*, 1995). To determine which of these factors was responsible a second AdCre infection was set up and the levels of  $\beta$ -gal activity in FE13 cells were analysed daily for one week after infection.

##### **i) $\beta$ -gal Activity**

The amount of  $\beta$ -gal activity present in the total protein extracts prepared from FE13 cells exposed to AdCre or mock-infected was measured using the  $\beta$ -galactosidase

**Figure 2.28** -  *$\beta$ -galactosidase Expression Data Over a 7 day Timecourse*



Graph illustrating the levels of  $\beta$ -gal activity (microunits/ $\mu$ g of total protein) in control uninfected FE13 cells and FE13 cells infected with AdCre.  $\beta$ -gal activity was determined using a  $\beta$ -galactosidase Enzyme Assay Kit (Promega) and standardised for protein concentration. Triplicate samples were analysed and mean  $\beta$ -gal activity values are plotted.

Enzyme Assay Kit (Promega). The results are shown in Figure 2.28. The average level of  $\beta$ -gal activity in the control cells remains at approximately 53 $\mu$ U/ $\mu$ g over 7 days. However, a significant decrease in  $\beta$ -gal activity was seen in the AdCre-infected cells. Twenty four hours after infection the level of  $\beta$ -gal activity has decreased from 47.9 $\mu$ U/ $\mu$ g to 5.12 $\mu$ U/ $\mu$ g (approx. 90% decrease). This significantly reduced level of expression was maintained over 7 days ( $p < 0.05$ , Mann-Whitney U test, two-tailed). Note, AdCre-infected cells displayed a slight growth impairment and therefore a minimum number of timepoints were analysed (Days 1, 5 and 7). In the mock treated sample it was possible to harvest material daily.

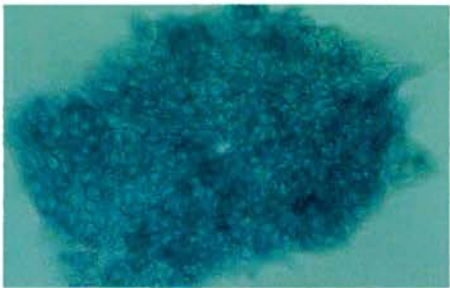
## ii) Histochemical $\beta$ -gal Detection and Scoring

As well as quantifying the level of  $\beta$ -gal expression in FE13 cells using the above protein assay,  $\beta$ -gal expression was also monitored via histochemical visualisation and scoring. Cells harvested over the 7-day period were transferred onto 100mm culture dishes and allowed to grow until small, discrete clones (approximately 50-100 cells) became visible. These were then fixed and stained. A 5-Bromo-4-chloro-3-indolyl galactopyranoside (X-gal) based stain was used as the cleavage of the X-gal substrate by the  $\beta$ -gal enzyme produces a local blue precipitate. The number of blue clones and white clones visible on each culture dish was then scored. It should be noted that mosaicism was observed in all cultures of FE13 cells. Other groups using the  $\beta$ geo marker gene have also reported this observation (Friedrich & Soriano, 1991). For this reason the stained populations of clones were divided into four groups, those which were uniformly dark blue staining, those which were uniformly pale blue staining, those which displayed mosaic staining and finally clones which were completely white. Photographs of a representative clone from each of these groups are shown in Figure 2.29.

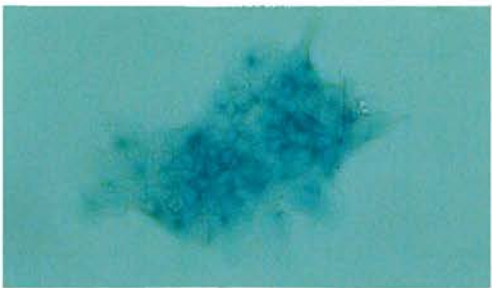
The number of each of the above four clone types in the AdCre-infected, and mock treated FE13 cultures, was scored in order to determine their relative proportions. It was necessary to establish a running mean to determine the minimum number of clones to count in order to produce accurate data. As shown in Figure 2.30, the

**Figure 2.29** - *Photographs of the Four Clone Types Scored After  $\beta$ -gal Staining of FE13 Cells*

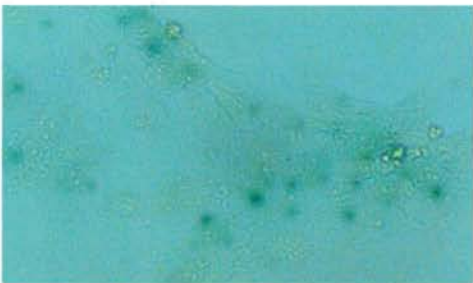
1) Navy Blue (x100)



2) Pale Blue (x100)



3) Mosaic (x100)

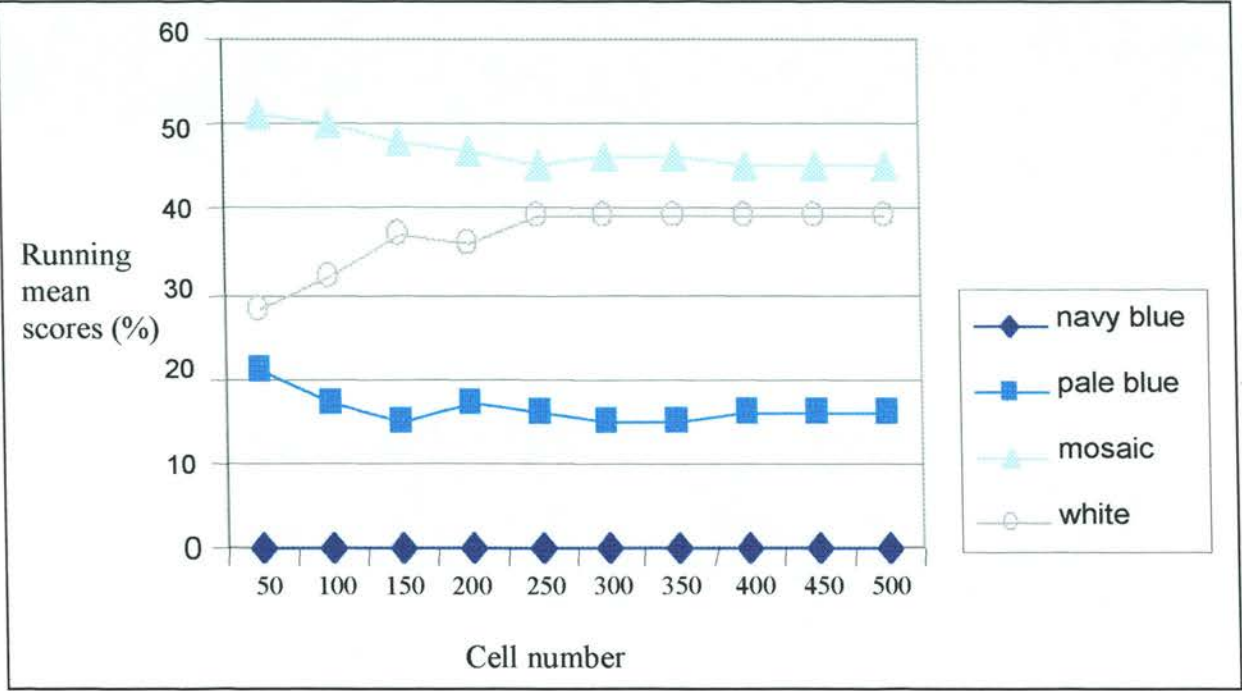


4) White (x100)



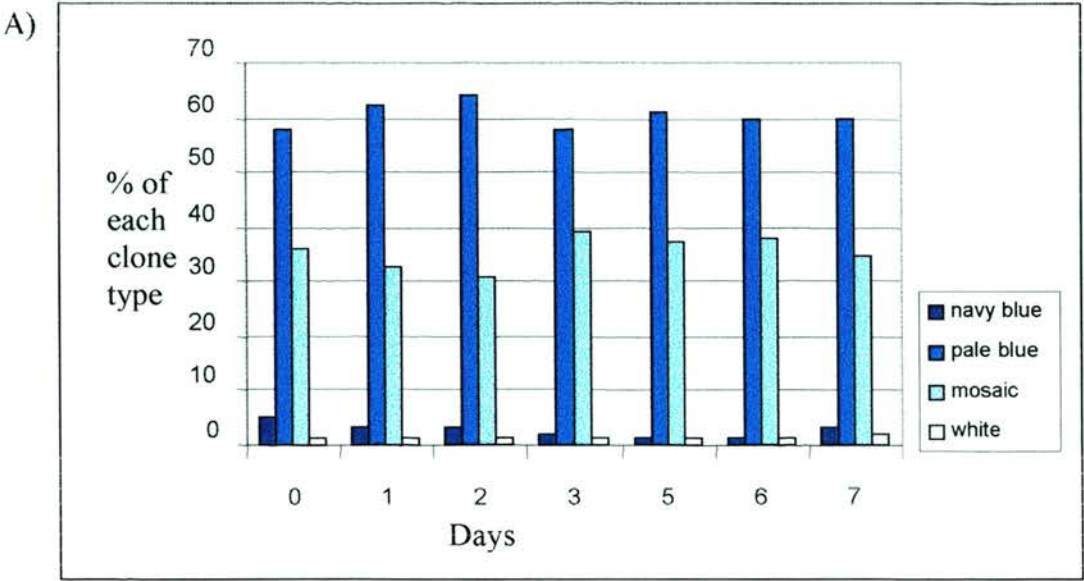


**Figure 2.30** – *An Example of the Running Mean Data Obtained for One Sample of AdCre-infected FE13 Cells*

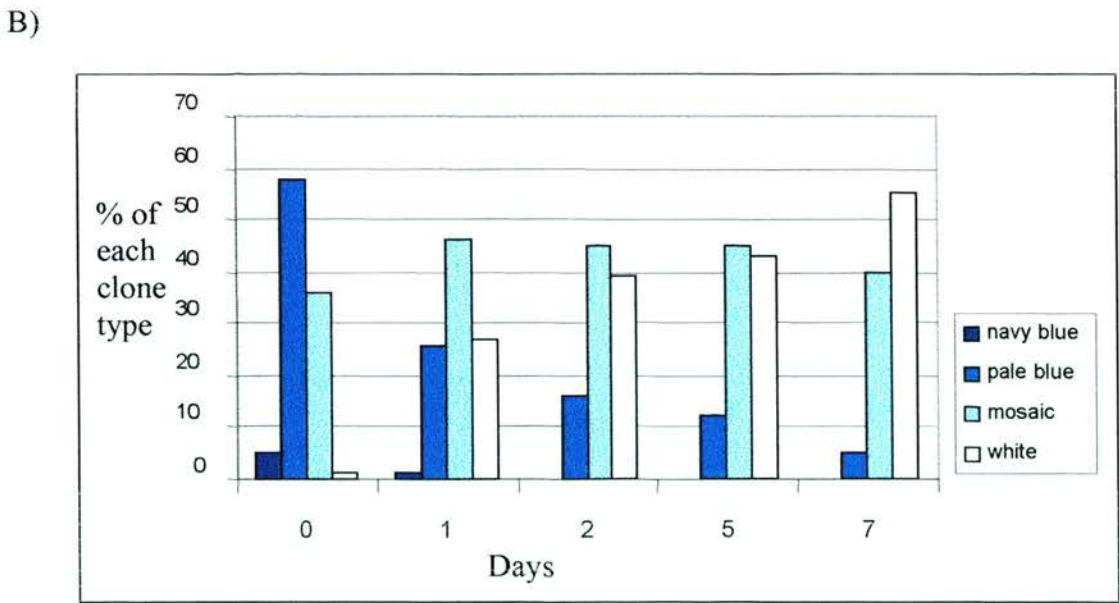


An example of the data generated when the numbers of navy blue, pale blue, mosaic and white clones present in FE13 cells 2 days after infection with AdCre were scored as a running mean. Each point represents the running mean (%) of that clone type when 50-60 clones were scored. When the mean value stabilised, i.e. when the inclusion of counts from the next set of 50-60 clones were included and the mean remained unchanged, no further clones were scored.

**Figure 2.31** – *Percentage of Clone Subtypes in Control and AdCre-infected FE13 Cells*



This graph shows the % of each clone type (see legend) present in samples from control mock infected FE13 cells over a 7 day period. The numbers of each clone type were scored as explained in Figure 2.30.



This graph illustrates the % of each clone type (see legend) present in samples from FE13 cells infected with AdCre at Day 0. The numbers of each clone type were scored as explained in Figure 2.30.

running mean value for each clone type stabilised after 500 clones had been scored, therefore a minimum of 500 clones were counted from each subsequent sample. Figure 2.31A illustrates the characteristic staining pattern of mock treated FE13 clones, consisting of approximately 5% navy blue, 58% pale blue, 36% mosaic and 1% white clones, this remains essentially unchanged over the 7 day period of analysis.

However, as shown in Figure 2.31B, a notable change in the relative proportions of the four clone types was seen in FE13 cells infected with the AdCre virus. A gradual shift can be seen, navy blue clones are no longer apparent by 48 hours after AdCre infection. While the level of mosaic clones did not change dramatically, a steady decrease in pale blue clones and concomitant increase in white clones was observed. These data suggest that Cre-mediated excision of the floxed STOP abolishes  $\beta$ geo expression, leading to progressively lower levels of histochemically detectable  $\beta$ -gal in AdCre-infected FE13 cells.

## 2.9. Discussion

A relatively small body of literature exists on the application of floxed STOP-based technology to achieve conditional gene expression. However, many of these publications report that floxed STOP cassettes function well and allow the efficient and tight regulation of exogenous gene expression (reviewed in Section 2.2). Because of these reports it was decided to develop a novel floxed STOP cassette designed to regulate both endogenous and exogenous gene expression *in vitro* and *in vivo*. As discussed in Section 2.1, floxed STOP cassettes are analogous to promoter traps, hence the logical starting point for the construction of a floxed STOP cassette was a previously characterised promoter trap vector such as pGT1.8IRES $\beta$ geo (Mountford *et al*, 1994).

To generate an effective floxed STOP cassette from pGT1.8IRES $\beta$ geo the IRES sequence was removed and two directly repeated loxP sites were introduced. Before the pFloxSTOP plasmid was introduced into cells it was necessary to determine

whether the introduced loxP sites were functional substrates for Cre recombinase. The pFloxSTOP plasmid was transformed into cells of the bacterial strain BNN132 that had been engineered to constitutively express Cre recombinase (Clontech). Restriction digest analysis of resultant transformants indicated that the pFloxSTOP plasmid underwent efficient Cre-mediated excisive recombination.

To determine the ability of the floxed STOP cassette to regulate downstream gene expression the test plasmid pFloxEGFP was built. This plasmid contained the CMV<sub>IE</sub> promoter and the EGFP marker gene separated by the floxed STOP cassette. In theory, the  $\beta$ geo marker gene present within the floxed STOP cassette should only be expressed from the unrecombined plasmid whereas expression of the EGFP marker gene should be dependent upon Cre-mediated excisive recombination. To test this theory the plasmid was linearised and electroporated into HM-1 ES cells. Clones that arose were then analysed to determine whether the complete pFloxEGFP plasmid had stably integrated. First, the ability of clones to survive selection in 200 $\mu$ g/ml of G418 demonstrated that the *neo* component of the  $\beta$ geo fusion gene was being expressed at a level commensurate with function. However, not all such G418<sup>R</sup> clones also expressed  $\beta$ -gal, of 64 clones screened,  $\beta$ -gal expression was histochemically detectable in 14 (22%) only 10 of which expressed significant levels (16%). As the  $\beta$ geo gene is a fusion gene it is perhaps surprising that all G418<sup>R</sup> clones do not also stain positively for  $\beta$ gal expression, however this observation is in agreement with earlier work on the  $\beta$ geo gene (Friedrich & Soriano, 1991). These authors suggested that differences in the sensitivity of the detection systems, i.e. clones which express low levels of  $\beta$ geo will survive G418 selection but the  $\beta$ -gal activity may be below threshold detectable with an X-gal based stain, were responsible for the observed variation (Friedrich & Soriano, 1991). An alternative explanation for clonal heterogeneity in  $\beta$ -gal staining is variation in the methylation status of the integrated transgene (MacGregor *et al*, 1987).

To determine whether the full-length pFloxEGFP transgene was present in the 10 G418<sup>R</sup>,  $\beta$ -gal positive FE clones, a PCR strategy was designed. The full-length

EGFP gene could be detected in 8 clones and one such clone, FE13 was chosen for further analysis (Figure 2.17). Two methods were considered for the introduction of Cre recombinase into FE13 ES cells. First, the transient transfection of Cre-encoding plasmids into FE13 cells and second, the infection of cells with a recombinant, replication defective adenovirus engineered to express Cre recombinase (Anton & Graham, 1995).

As part of the work examining the feasibility of transiently transfecting FE13 cells with Cre-encoding plasmids a novel ES cell differentiation state-specific enhancer element was characterised. In collaboration with Dr C. Fiskerstrand from the Department of Veterinary Pathology, University of Edinburgh the enhancer activity of a previously unidentified intronic region of the rat preprotachykinin gene was analysed (Fiskerstrand *et al*, 1999). The ~1kb of novel sequence was cloned upstream of a basal promoter and a luciferase marker gene, plasmid pGL3p (Promega), and the resultant plasmid, pGL3p-CCCT was transiently transfected into ES cells. When the two plasmids were introduced into undifferentiated ES cells no significant differences in the levels of luciferase expression were observed. However, when they were introduced into ES cells cultured in the absence of LIF, approximately 150-fold more luciferase was expressed from the pGL3p-CCCT plasmid than the control pGL3p plasmid. These ES cells had been cultured in the absence of LIF for approximately 64 hours after transfection. While this was insufficient time for gross morphological changes to be visible, changes at the molecular level can be detected as early as 36 hours after LIF withdrawal (Nemetz & Hocke, 1998). These data would seem to indicate that changes in the components of the intracellular pool of transcription factors, induced by LIF withdrawal, facilitated a dramatic increase in the enhancer capabilities of the CCCT intronic element.

In conclusion, this work has reported the successful characterisation of a novel enhancer element isolated from the rPPT gene. This element was shown to permit high levels of marker gene expression in differentiating, but not undifferentiated, ES cells. However, this technology was not adapted for use as part of a Cre delivery



strategy. There are several publications reporting the successful expression of Cre recombinase using various transient transfection techniques (for example, calcium phosphate, Bethke & Sauer, 1997; lipofection, Dias *et al*, 1998). However, attempts to introduce Cre-encoding plasmids into FE13 cells by both electroporation and lipofection yielded poor transfection efficiencies and no Cre-mediated recombination was detected. Furthermore, encouraging results obtained with the adenovirus system investigated in parallel precluded any further optimisation of transfection protocols.

When using adenovirus it is crucial to determine the optimal titre (multiplicity of infection, m.o.i) for infection. Too little and a low efficiency of infection will result, too much and cytopathic effects may occur. To determine the optimal m.o.i for the infection of ES cells a second recombinant adenovirus, AdLacZ, which had been engineered to express the bacterial  $\beta$ -gal enzyme, was used. Cultures of ES cells were exposed to a range of AdLacZ titres and preferential infection of differentiated ES cells was observed. This phenomenon has been previously reported (Aladjem *et al*, 1998). The efficient infection of differentiated ES cells was observed even at the lowest adenovirus titre used, 50 m.o.i, whereas the infection of undifferentiated ES cells was only observed at 1000 m.o.i. Even with this high virus titre a very low efficiency of infection was seen. For this reason the decision was taken to deliberately differentiate ES cells *in vitro* prior to infection with AdCre.

Therefore, in all experiments described below FE13 cells were differentiated *in vitro* and then infected with 50 m.o.i of AdCre. A PCR strategy was then used to determine whether any episomal adenovirus molecules were present in the genomic DNA extracted from infected cells. The 660bp band amplified from the Cre-expression cassette within AdCre was produced only from adenovirus-exposed cells demonstrating that the AdCre was successfully infecting the differentiated FE13 ES cells (Figure 2.20). A second PCR strategy was used to monitor the recombination status of the pFloxEGFP transgene integrated within FE13 cells (Figure 2.21). A 1213bp product was amplified from the unrecombined transgene in both AdCre-infected and uninfected FE13 cells. However, the recombination-specific 1325bp



product was only amplified from genomic DNA harvested from AdCre-infected FE13 cells (Figure 2.22). This result demonstrated that Cre-mediated excisive recombination was occurring specifically within AdCre-infected FE13 cells but because the PCR reaction was not quantitative, the exact level of recombination could not be determined.

In order to quantify the amount of Cre-mediated excisive recombination occurring within AdCre-infected FE13 cells a Southern blot strategy was designed. The 7090bp *HindIII* genomic DNA digest product derived from the unrecombined pFloxEGFP transgene was detected in both AdCre- and mock-infected cells. However, the 849bp recombination specific *HindIII* digest product was not identified (Figure 2.24). This is in direct contrast with the results obtained from recombination state-specific PCR discussed above. However, others have observed disparities between the sensitivity of PCR and Southern blotting for the detection of Cre-mediated recombination in this research group (D. Rannie, unpublished obs.). Therefore, although the level of Cre-mediated recombination was sufficient to be detected by PCR it was below the sensitivity threshold of this specific Southern blot.

The failure to induce high levels of Cre-mediated recombination in response to AdCre exposure is also in direct contrast with published observations. For example, when the mouse myoblast cell line C2C12, stably transfected with a floxed STOP/ $\beta$ -gal reporter construct, was infected with AdCre upregulation of  $\beta$ -gal expression was histochemically detectable in 90-100% of cells (Sakai *et al*, 1995). Furthermore, AdCre has been used successfully *in vivo*, with high recombination frequencies reported by several authors (for example, Wakita *et al*, 1998). The most logical interpretation of the observed low recombination frequency is a low efficiency of adenovirus infection. The implications of this conclusion are discussed in more depth at the end of this section.

Having demonstrated that Cre mediated recombination was occurring within AdCre-infected FE13 cells, albeit at a low frequency, the next step was to analyse its effects

upon marker gene expression. First, was Cre-mediated excision of the floxed STOP cassette causing an upregulation of EGFP expression? The level of EGFP expression was quantified by flow cytometry but no significant difference between the fluorescence of mock- and AdCre-infected FE13 cells was observed (Figure 2.25). Because the presence of the full length EGFP gene had been shown by PCR, it was unclear why it was not being expressed after Cre-mediated recombination. An RT-PCR strategy was designed to determine whether or not the EGFP gene was transcriptionally active. Preliminary results indicated that the EGFP mRNA was present in both mock- and AdCre-infected FE13 cells demonstrating that transcription was occurring from the unrecombined transgene. The RT-PCR strategy was then made quantitative in an attempt to determine whether the floxed STOP cassette exerted any control over EGFP expression. Results from the qRT-PCR demonstrated that although leaky EGFP expression was occurring from the unrecombined transgene, an approximate 2-fold induction in EGFP mRNA was seen in FE13 cells after AdCre infection (Figure 2.27).

The FACS and RT-PCR data discussed above generated three key results. First, the demonstration that the floxed STOP cassette within the pFloxEGFP plasmid permits leaky expression of the EGFP gene at the level of transcription. The majority of floxed STOP cassettes described in the literature are not reported to permit leaky expression of the target gene. However, others have observed this phenomenon. For example, two groups (Agah *et al*, 1997; Anton & Graham, 1995) have reported leaky expression from a floxed STOP-luciferase vector. Both groups suggested that spontaneous homologous recombination between the two loxP sites and resultant excision of the intervening floxed STOP cassette was responsible for leaky expression in the absence of Cre recombinase although this has not been demonstrated. Spontaneous recombination would be expected to occur at the same frequency in both mock- and AdCre-infected FE13 cells. However, the inability to amplify the 1325bp recombination-specific PCR product from genomic DNA extracted from mock-infected FE13 cells indicates that if spontaneous recombination was occurring it was at an undetectably low frequency. It is therefore improbable

that it was responsible for the leaky EGFP mRNA expression in mock-infected cells. An alternative suggestion to explain the leaky EGFP expression observed in FE13 cells is position effect. It may be that the linear pFloxEGFP vector has integrated into a transcriptionally active region of the genome that is preventing maximal inhibition of transcription by the floxed STOP cassette. One possible way to test this theory would be the examination of EGFP expression in other FE clones that presumably represent alternative integration events. Time constraints precluded this analysis.

The second key result generated by this work is the absence of detectable EGFP expression at the protein level. Although fluorescent cells could be visualised by UV microscopy in the positive control sample, none were seen in the mock- or AdCre-infected FE13 cells. Flow cytometric analysis confirmed this observation. Interestingly, the inability to upregulate downstream gene expression after Cre-mediated excision of the floxed STOP cassette has been described elsewhere. For example, in the floxed STOP-LacZ mouse developed by Agaki *et al* (Agaki *et al*, 1997) silencing of the transgenic locus after recombination and juxtaposition of the LacZ gene adjacent to the promoter was observed (Krimpenfort *et al*, 1998). Conversely, the successful upregulation of EGFP expression using constructs analogous to pFloxEGFP has been reported by two independent research groups (He & Thomas, 1998; Gaur & Rajewsky, 1998).

The possibility that the EGFP gene had been silenced by methylation was eliminated after the RT-PCR data shown in Figure 2.27 demonstrated that the gene was transcriptionally active. Another possibility was that the levels of EGFP mRNA, although detectable by RT-PCR, may have been too low permit the expression of sufficient EGFP protein to be detected by UV or FACS analysis. This option cannot be ruled out and is discussed in more depth at the end of this section. A third option was that during the construction of pFloxEGFP, or the generation of the FE13 clone, a point mutation could have arisen within the EGFP coding sequence abolishing the fluorescence of the protein. No sequencing of the RT-PCR products was undertaken

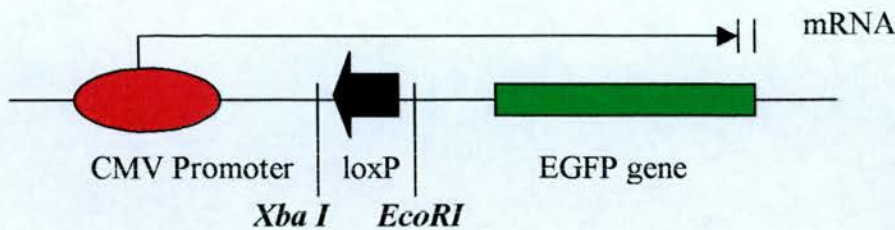
so this option cannot be ruled out. The fourth possible explanation is the “Reverse loxP Problem” which was first suggested by B. Sauer, one of the original Cre/loxP researchers (reviewed in Sauer, 1998). As shown in Figure 2.32, when a loxP site is present in the reverse orientation two false translation start signals, ATG codons, are introduced. This is only problematic if the loxP site lies between a promoter and downstream coding sequence. In the pFloxEGFP vector the loxP site retained after Cre-mediated excisive recombination is in the reverse orientation and does lie between the CMV<sub>IE</sub> promoter and the EGFP gene. Therefore, three translation start codons lie immediately downstream of the 5' end of the mRNA (numbers 1,2 and 3 on Figure 2.32). If translation is initiated at either codons 1 or 2 (loxP site-derived) then a frameshift will be introduced into the protein product. Only translation initiation at codon 3 will give rise to the fluorescent EGFP protein. This is only a theoretical model and false translation initiation at a loxP-derived start codon has not been reported, nonetheless it is an attractive hypothesis to explain some of the results obtained with clone FE13.

The third key result generated from the FACS and RT-PCR data discussed above is that only a low level of EGFP mRNA induction, 2-fold, was observed in the AdCre-infected FE13 cells relative to the mock-infected controls. There are two possible explanations, first, that the low level of induction may be due to the almost complete failure of the floxed STOP cassette to regulate transcription. Hence, the presence or absence of the floxed STOP cassette would have little or no effect upon EGFP transcription. The second possible explanation for the low EGFP mRNA induction observed, is a low efficiency of AdCre infection that would generate a concomitant low level of Cre-mediated recombination. Therefore, the amount of EGFP expression being driven from the recombined transgene would be almost indistinguishable from the leaky expression off the unrecombined pFloxEGFP transgene. The latter explanation is the most probable as there is a small but significant ( $p < 0.05$ , Mann-Whitney U test) increase in EGFP transcription after Cre-



**Figure 2.32 – The Reverse loxP Problem**

A) The structure of the recombined pFloxEGFP transgene



B) Sequence data

5' TCA GAT CCG CTA GCG TAA GAT CTG GCC GCG AGC TCG GGC CCC  
3' AGT CTA GGC GAT CGC ATT CTA GAC CGG CGC TCG AGC CCG GGG

Xba I 1    2

CAC ACG TGT GGT **CTA GA** *A TAA CTT CGT ATA* **ATG TATGCT**  
GTG TGC ACA CCA **GAT CT** *T ATT GAA GCA TAT TAC ATA CGA*

Eco RI

*ATA CGA AGT TAT* **GAA TTC** TGG ATC CGA TAC GCTACC GGT  
*TAT GCT TCA ATA* **CTT AAG** ACC GAG GCT ATG CGA TGG CCA

3

CGC CAC C **ATG** GTG 3'  
GCG GTG G **TAC** CAC 5'

Above is the sequence from the extreme 5' end of the EGFP mRNA initiated within the CMV promoter. The loxP sequence is shown in italics. The two restriction sites which flank the loxP, *Xba I* and *Eco RI* are indicated in bold text. The numbers 1-3 mark the multiple translation initiation codons (ATG) present in this mRNA. Positions 1 and 2 are encoded in the loxP site spacer region, whereas position 3 is the intended translation initiation signal with surrounding Kozak consensus sequence underlined.

mediated excisive recombination and a low efficiency AdCre-infection has been implied by other data.

Changes in the expression of two marker genes EGFP and  $\beta$ geo were examined during the work described in this chapter. As already discussed, Cre-mediated excision of the floxed STOP cassette in pFloxEGFP did permit a small but significant upregulation of EGFP mRNA. To determine whether a concomitant decrease in  $\beta$ geo expression occurred, two methods were used to quantify  $\beta$ -gal activity in FE13 cells, a quantitative  $\beta$ -gal activity assay and direct histochemical detection. Differentiated FE13 cells were either mock- or AdCre-infected (50 m.o.i) and protein extracts prepared 72 hours later. When the levels of  $\beta$ -gal activity were compared between the 72 hours mock- and AdCre-infected extracts only a small decrease was observed. There are two possible explanations for this observation, first that a low level of infection has occurred or second, that the long half-life of  $\beta$ -gal results in its retention within cells. To distinguish these two alternatives a repeat AdCre-infection was set up and protein extracts and cultures for histochemical analysis were prepared over the 7 day period after infection.

When the levels of  $\beta$ -gal activity were analysed in AdCre-infected cells relative to controls significant differences were observed. Twenty-four hours after infection the level of  $\beta$ -gal activity had decreased from  $47.9\mu\text{U}/\mu\text{g}$  to  $5.12\mu\text{U}/\mu\text{g}$  (approx. 90% decrease) (Figure 2.28). This reduced level of expression was maintained over the 7-day experimental period but did not decrease any further. The significant decrease in  $\beta$ -gal expression after AdCre-infection is also supported by data generated from scoring FE13 clones after histochemical detection of  $\beta$ -gal activity. The numbers of four species of clones, navy blue, pale blue, mosaic and white were scored blind in cultures arising from mock- and AdCre-infected FE13 cells. In the control cells no significant alterations are seen in the relative proportions of each clone type over the seven-day experimental period (Figure 2.31A). However, in the AdCre-infected cells notable changes are seen (Figure 2.31B). By 48 hours after infection no navy blue clones are seen and a large increase in mosaic clones is seen. Over the seven-day



period, the number of pale blue clones in the AdCre-infected cultures also decreases but there is a gradual increase in the proportion of white clones until they constitute over 50% of the total. These data indicate that Cre-mediated exciseive recombination of the floxed STOP cassette does indeed efficiently abolish expression of  $\beta$ -gal from the  $\beta$ geo marker gene. The successful abolition of floxed gene expression after Cre-mediated excision has been reported by numerous other groups using floxed STOP technology (for example, O’Gorman *et al*, 1997). In all cases the efficiency is proportional to the efficiency of Cre-mediated exciseive recombination.

In the data reviewed above one recurring explanation for some of the results is a low efficiency of AdCre-infection. For example, the difficulty in detecting the recombination-specific *HindIII* genomic digest product by Southern blot, the small increase in EGFP mRNA in AdCre-infected cells and the small decrease in  $\beta$ -gal activity in AdCre-infected relative to mock-infected control cells over the original seventy two-hour timecourse. When the AdCre-infection was repeated using a fresh stock of recently titred adenovirus and  $\beta$ -gal levels assayed over one week, a much larger decrease in  $\beta$ -gal activity was detected in both protein assays and with the use of histochemical staining techniques. Therefore, these data would seem to suggest that the levels of  $\beta$ -gal activity within differentiated FE13 ES cells decrease in proportion with efficiency of Cre-mediated excision of the floxed STOP cassette, exactly as reported in other publications (for example, O’Gorman *et al*, 1997).

As already mentioned, one possible explanation for the absence of EGFP protein in AdCre-infected FE13 cells was a low level of mRNA. Therefore, even if translation was occurring normally the level of EGFP protein in such cells may remain below the threshold detectable by FACS analysis or UV microscopy. This would be a particular problem if AdCre-infection was submaximal giving a concurrent low efficiency of Cre-mediated recombination. To establish if this problem had occurred in FE13 cells, in parallel with the repeat infection for  $\beta$ -gal activity analysis discussed above, a second AdCre-infection (50 m.o.i) was also carried out to confirm the EGFP data. The second adenovirus infection was carried out using a fresh stock

of recently titred virus and twenty four hours after infection a cell sample was removed for UV microscopy and a protein extract prepared for use in determining  $\beta$ -gal activity. This timepoint was chosen as the data illustrated in Figure 2.28 demonstrated that a significant decrease in  $\beta$ -gal activity within FE13 cells occurred twenty four hours after AdCre-infection. However, despite a sizeable reduction in  $\beta$ -gal activity within the repeat infected FE13 cells, when they were examined by UV microscopy no fluorescent cells were seen.

In conclusion, it is probable that the first time the EGFP status of FE13 cells was examined only a small percentage of cells had been successfully infected with AdCre hence the small scale of EGFP mRNA induction, the inability to identify the 849bp recombination-specific *Hind III* digest product by Southern and the low level of  $\beta$ -gal activity decrease over the original seventy two hour time course. However, in the repeat experiment a higher efficiency of Cre-mediated recombination was almost certainly induced as evidenced by the concurrent decrease of  $\beta$ -gal activity. Yet in both experiments no fluorescent cells were detected. This observation sheds further light on the question of why no EGFP protein could be detected in FE13 cells. Three hypotheses were originally proposed, first that the levels of EGFP mRNA, even in the AdCre-exposed cells, were too low to permit the expression of sufficient EGFP protein to be detected by UV or FACS analysis. This hypothesis has become less probable due to the absence of detectable EGFP protein in cells that have almost certainly undergone a high efficiency of AdCre-infection. Instead either the acquisition of a mutation in the EGFP gene or the Reverse loxP Problem discussed above may better explain the absence of fluorescent cells.

These proposed variations in adenovirus infection efficiencies can be most simply explained by variations in the viability and titre of the virus. Therefore, although all AdCre infections were apparently carried out using a titre of 50 m.o.i in reality, cells were probably exposed to different viral titres. Errors could have been introduced at several stages including the initial titration of the stock. Furthermore, repeat freeze-thaw cycles are known to significantly affect viral titres (Croyle *et al*, 1998).

Nonetheless, this work did indicate a potential problem with the pFloxEGFP vector, that is the absence of EGFP protein expression. As this vector was originally designed to provide a simple, visual indicator of Cre-mediated excision no further experiments were carried out using it. Instead, bearing in mind the problems with encountered during the construction and testing of pFloxEGFP an alternative vector, pICDP(for) was developed. This work is discussed in Chapter 3.

# **Chapter 3**

## **RAGE-Based Strategies to Achieve Conditional Upregulation of the Murine p53 Gene *in vitro***

## Chapter 3

### RAGE-Based Strategies to Achieve Conditional Upregulation of the Murine p53 Gene *in vitro*

#### 3.1. Introduction

Replicative cellular senescence has been reviewed in depth elsewhere in this thesis (Section 1.5). Briefly, at the end of a cells replicative lifespan it enters a state of terminal G1 arrest. This event is thought to be regulated by an internal genetic program via two regulatory mortality checkpoints, M1 and M2 (Wright & Shay, 1992). Immortality can only be achieved by cells able to overcome both M1 and M2, therefore escaping the constraints of replicative cellular senescence.

A key molecule involved in the regulation of senescence and in particular, the M1 checkpoint is the tumour suppressor gene p53. The majority of the work investigating the role of p53 in this process has been carried out using the SV40 TAg protein (see Section 1.5.3.2). A significant drawback to this approach is the pleiotropic nature of TAg function. First, SV40 TAg binds to RB, dissociating RB-E2F complexes within cells (Stein *et al*, 1990), and the RB-related proteins p107 and p130 (Knudsen & Wang, 1998). Second, a novel anti-apoptotic domain has been identified within TAg (amino acids 525-541) with uncharacterised cellular binding partners (Conzen *et al*, 1997). Third, the C-terminal (amino acids 351-450 and 533-626) of TAg binds to the core domain of p53 (amino acids 94-293) (Ruppert *et al*, 1993) and inhibits the sequence-specific DNA binding activity of p53 (Bargonetti *et al*, 1991). Each of these functional domains has the ability to transiently bypass senescence but individually, are insufficient to permit immortality (Jha *et al*, 1998). Therefore when using SV40 TAg it may be difficult to separate the individual contributions of these domains to the abrogation of senescence.

Antisense technology is a second approach that has been much used during the investigation of the genetic regulation of senescence. The culturing of HDFs in the

presence of RB or p53 antisense oligonucleotides was shown to have functional consequences in terms of the onset of senescence (Hara *et al*, 1991). However, in all of these experiments the precise extent of reduction of target gene expression is unclear, for example, it is highly unlikely that p53 expression has been completely abolished in cells exposed to p53 antisense oligonucleotides. Therefore experiments based on antisense technology need careful interpretation.

One way around the problems inherent in TAg- or antisense-based experiments is to approach it from the opposite direction namely, to directly regulate target gene expression. The power of this approach was demonstrated when a tetracycline inducible p53 construct was introduced into a p53 null bladder carcinoma cell line. Re-expression of p53 was sufficient to induce the onset of replicative senescence in these cells (Sugrue *et al*, 1997).

Several different strategies for the regulated expression of p53 have been reported including inducible promoters (Sugrue *et al*, 1997) and recombinant adenoviridae (Aladjem *et al*, 1998). There are several important considerations when using such approaches including the stability, delivery or toxicity of inducing agents for some inducible promoters, differences in the sensitivity to adenovirus and potential cytopathic cellular response to infection. To provide an alternative tool for the regulation of p53 expression, it was decided to construct a floxed STOP-regulated p53 expression vector, pICDP(for).

A large proportion of the work investigating replicative cellular senescence has been done in human diploid fibroblasts (HDFs). However, the availability of numerous knock-out mouse strains with targeted null mutations in potential senescence regulatory genes makes murine cells an attractive model system. One possible reason why full advantage has not been taken of the mouse system is the absence of a convenient senescence-specific biomarker. In contrast, expression of the novel biomarker Senescence Associated  $\beta$ -galactosidase (SA $\beta$ -gal) has been reported in human cells (Dimri *et al*, 1995). Previously senescent cells, such as primary



fibroblasts, were distinguished *in vitro* using morphological criteria. Senescent fibroblasts have enlarged nuclei, elongated cellular processes, increased size and a flattened appearance (Hayflick & Moorehead, 1961). However, these criteria were very difficult to apply *in vivo* making the identification of such cells very difficult. The discovery of SA $\beta$ -gal permitted an analysis of human cell senescence *in vitro* and *in vivo* for the first time. To facilitate an analysis of senescence in murine cells an analogous biomarker was required however, no SA $\beta$ -gal expression was originally detected in rodent cells (Dimri *et al*, 1995). This is discussed further in Section 3.3.

### 3.2.Aims

- a) Identify and characterise SA $\beta$ -gal expression in primary mouse fibroblasts and mouse skin sections.
- b) Design and construct a vector in which expression of the p53 cDNA can be upregulated in response to Cre-mediated excision of the floxed STOP cassette from the pFloxSTOP plasmid.
- c) Develop a method for the stable transfection of p53 null primary mouse fibroblasts.
- d) Characterise primary mouse fibroblast system in terms of feasibility of Cre-mediated upregulation of p53 expression and effects on SA $\beta$ -gal expression.

### 3.3. Do Primary Mouse Fibroblasts Express SA $\beta$ -gal ?

#### 3.3.1. Human Senescence Associated $\beta$ -galactosidase

$\beta$ -galactosidase ( $\beta$ -gal) activity can be detected histochemically using the synthetic substrate 5-Bromo-4-chloro-3-indolyl galactopyranoside (X-gal), which forms a local blue precipitate upon cleavage (Miller, 1972). All human cells express a lysosomal  $\beta$ -galactosidase enzyme with a pH optimum of 4 (Moreau *et al*, 1989). A neutral, pH 7,  $\beta$ -gal activity has also been described in mammalian tissues (Kuo & Wells, 1978). However, no change in the activity of either of these enzymes has been reported as cells approach replicative senescence. In contrast, SA $\beta$ -gal has a pH optimum of 6 and is detected primarily in senescent human cells with a perinuclear staining pattern (Dimri *et al*, 1995).

### 3.3.2. Murine $\beta$ -galactosidases

SA $\beta$ -gal was originally described in human cells and indeed the original authors stated that SA $\beta$ -gal activity could not be detected in murine fibroblasts (Dimri *et al*, 1995). Because the availability of a murine senescence-specific biomarker was such a desirable tool it was decided to re-examine the possibility of mouse SA $\beta$ -gal.

Detailed SA $\beta$ -gal and lysosomal  $\beta$ -gal protocols were kindly supplied by J. Campisi (J. Campisi, pers. comm.) and tested on mouse embryonic fibroblasts (MEFs).

However, in line with previous work (Dimri *et al*, 1995), no positively staining cells were detected. It should be noted that SA $\beta$ -gal histochemical visualisation was attempted with MEFs that had been maintained *in vitro* for a range of different times and no positive cells were observed even in the oldest cultures (data not shown).

However, when MEFs were treated with the lysosomal  $\beta$ -gal stain solution, prepared as described by J. Campisi, all cells were positive independent of length of time in culture. A typical MEF that stained positively for lysosomal  $\beta$ -gal activity is shown in Figure 3.1A.

However, a second novel SA- $\beta$ gal stain solution was also used in parallel with that recommended by J. Campisi. When MEF cultures were exposed to this stain solution positively staining cells were observed. The vast majority of positively staining cells also displayed morphological changes characteristic of replicative cellular senescence (see Section 3.1). Typical SA $\beta$ -gal positive MEFs are shown in Figure 3.1.B and C. The perinuclear staining pattern observed in SA $\beta$ -gal positive MEFs is identical to that described in human cells (Dimri *et al*, 1995) and obviously distinct to that observed in lysosomal  $\beta$ -gal positive cells (compare the three morphologically senescent cells in Figure 3.1).

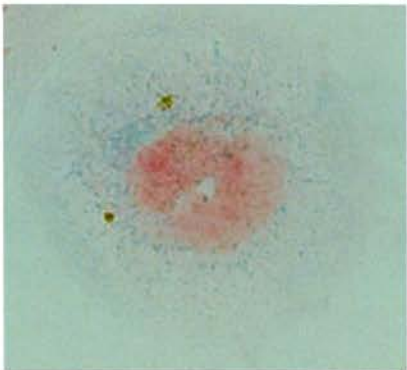
Also in agreement with the original report of Dimri *et al*, was the observation of SA $\beta$ -gal positive cells that were not morphologically senescent. Such cells are rare

**Figure 3.1 - Histochemical Detection of Lysozomal and Senescence-Associated  $\beta$ -galactosidase Expression**

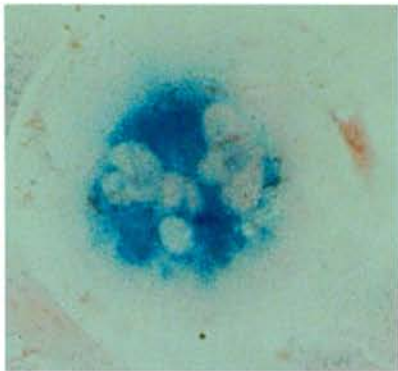
- A) Photograph taken at x400 magnification of a morphologically senescent cell showing positive staining for lysozomal  $\beta$ -gal expression (pH 4.0) and counterstained with Neutral Red. The dispersed, granular blue deposits are characteristic of lysozomal  $\beta$ -gal activity.
- B) Photograph taken at x400 magnification of a morphologically senescent cell showing positive staining for Senescence-Associated  $\beta$ -gal (pH 6.0) expression and counterstained with Neutral Red. The intense perinuclear blue deposit is identical to that described by Dimri *et al*, in senescent human cells (Dimri *et al*, 1995).
- C) Another example of the staining pattern charactersitic of SA  $\beta$ -gal expression as described in B).

**Figure 3.1** -Histochemical Detection of Lysozomal and Senescence -associated  $\beta$ -galactosidase Expression

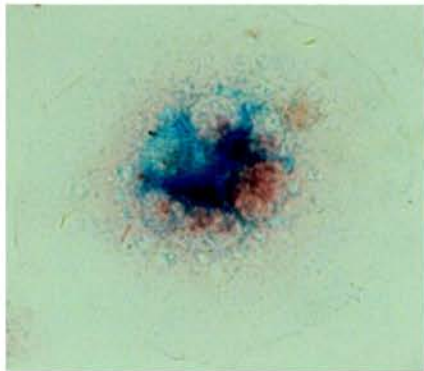
A)



B)



C)



in both human (Dimri *et al*, 1995) and mouse early passage cultures and an explanation for this observation has yet to be proposed.

### **3.3.3. Does The Expression of SA $\beta$ -gal Correlate With Passage Number ?**

In an attempt to further characterise the SA $\beta$ -gal positivity observed in MEFs *in vitro*, a continuous culture experiment was set up from which cell samples from wild type and p53 null cultures were removed at regular intervals and stained for SA $\beta$ -gal activity.

#### **3.3.3.1. Continuous Passaging of MEFs**

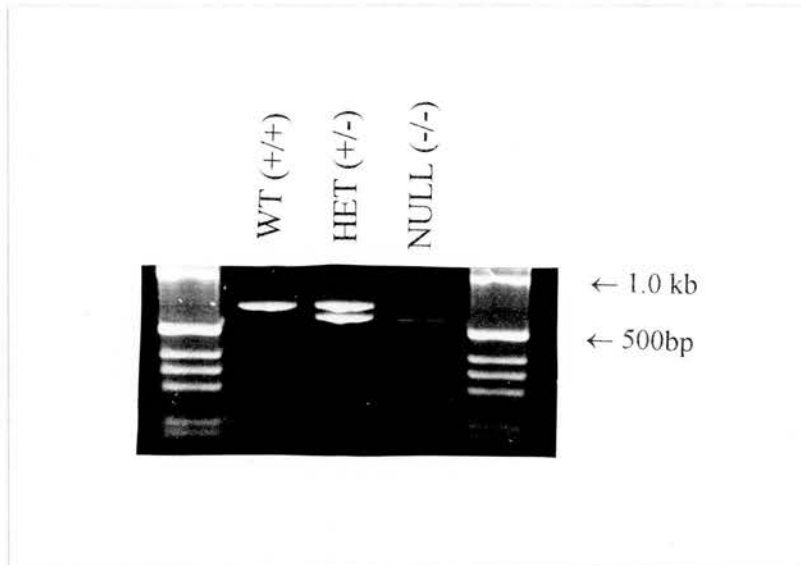
Embryos were harvested from p53 +/- and -/- matings and embryonic fibroblasts were prepared as described (Todaro & Green, 1963). The following day cells were harvested by trypsinisation and transferred to storage at -80°C, such cells were referred to as passage 1 (P1). A small aliquot of cells was removed and genomic DNA prepared. This DNA was used as a template for a PCR reaction to determine the p53 genotype of the individual cultures (Figure 3.2).

The standard EF culture regime is referred to as 3T3, in which  $1 \times 10^6$  cells are plated per 100mm tissue culture dish and passaged every 3 days (Todaro & Green, 1963). Once the p53 genotype of the cells had been established, wild type and p53 null MEFs were seeded at  $1 \times 10^6$  cells per 100mm dish and maintained in approximate accordance to the 3T3 regime such that cells were plated at 40% confluence every three days as this corresponded to the cell density observed when  $1 \times 10^6$  cells were originally plated out per 100mm dish. Cell samples were removed regularly and stained for SA $\beta$ -gal expression, counterstained with Neutral Red and mounted. SA $\beta$ -gal positivity was then scored via a running mean method and the results are illustrated in Figure 3.3.

#### **3.3.3.2. SA $\beta$ -galactosidase Timecourse Results**

Wild type MEFs were maintained in culture according to the passaging regime described above for 11 passages (P11). During this culture period the level of SA-

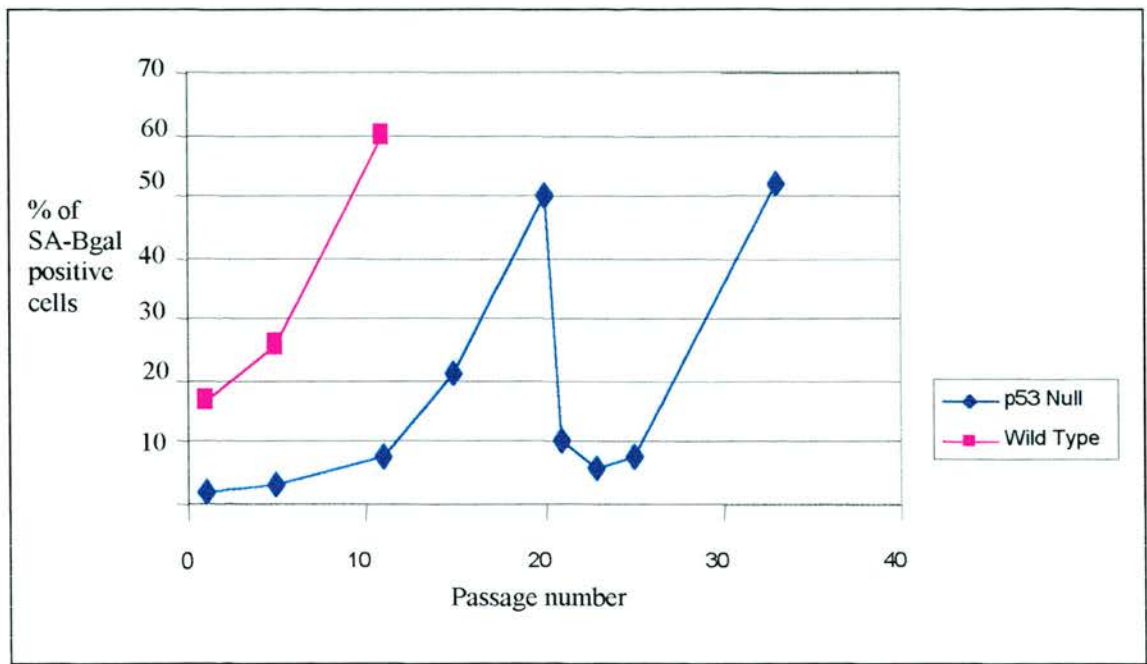
**Figure 3.2** – *PCR Genotyping of Primary Mouse Embryonic Fibroblasts*



4.0% agarose/ethidium bromide gel. Lane 1, molecular weight markers. Lane 2, the 642bp PCR product amplified from the wild type p53 allele. Lane 3, the 642bp PCR product amplified from the wild type allele and the 510bp PCR product amplified from the targeted allele of p53, therefore this embryo was heterozygous for p53. Lane 4, the 510bp PCR product amplified from the targeted allele of p53, therefore this embryo was homozygous null for p53. Lane 5, molecular weight markers.



**Figure 3.3** – Graph Illustrating the Number of SA-βgal Positive Cells in p53 Null and Wild Type MEF Cultures After Repeat Passaging



This graph illustrates the changes in SA-βgal positivity in wild type and p53 null MEFs after repeat passaging in culture. All samples were scored using a running mean method.

$\beta$ gal positivity increased from 17% at P1 to 60% at P11. At this point there were no overt signs of proliferation as no change in cell density was observed in the three days subsequent to passaging and the majority of cells displayed the morphological changes characteristic of senescence. In contrast, p53 null MEFs were maintained in culture for over 30 passages. Even at this late passage the cells were actively proliferating and had not entered replicative cellular senescence. A substantially reduced number of SA- $\beta$ gal positive cells were observed in the p53 null cultures relative to wild type at all timepoints. For example, at P1 only 2% of p53 null cells expressed detectable levels of SA- $\beta$ gal and this increased to 50% by P20. Interestingly, two peaks of SA- $\beta$ gal expression are seen in the p53 null cultures, at P20 and at P33. These results are discussed further in Section 3.7.

#### **3.3.4. Murine SA $\beta$ -gal *in vivo***

When the discovery of SA $\beta$ -gal was originally reported, positively staining human cells were detected *in vitro* and *in vivo* (Dimri *et al*, 1995). Having successfully demonstrated the existence of murine SA $\beta$ -gal *in vitro* the next step was to investigate whether this enzyme activity could also be detected *in vivo*. Two mice were killed, one was six weeks of age and the second was 2 years of age. A patch of skin on the back of the mice was shaved and a skin sample removed. The tissue sample was then snap frozen in liquid nitrogen. Frozen sections from the two skin samples were then fixed and incubated with SA $\beta$ -gal staining solutions. Duplicate sections were incubated with both the stain solution described by J. Campisi and the stain developed by myself. After 24 hours the sections were counterstained with eosin, mounted and viewed. A frozen section of mouse skin stained with haematoxylin and eosin is shown in Figure 3.4. Relevant structures within the section are indicated. Typical SA $\beta$ -gal staining results from frozen skin sections are shown in Figure 3.5.

No SA- $\beta$ gal positive cells were seen in the sections of skin harvested from the 6 week old mouse exposed to either stain solution. However, in the old mouse positive staining is associated with hair follicles, sebaceous glands and eccrine glands. This

**Figure 3.4 - *Haematoxylin and Eosin Counterstained Mouse Skin Section (x200)***

A mouse was killed, an area of back skin exposed by shaving and a sample removed and snap frozen. The skin sample was then mounted and frozen sections cut. The sections were transferred onto poly-lysine coated microscope slides and fixed with Macrodex before being stained with haematoxylin and eosin, mounted, viewed microscopically and photographed.

**Key**

E – epidermis

C – collagenous layer

HF – hair follicles

SDF – subdermal fat layer

ED – eccrine duct

**Figure 3.4 - Haematoxylin and Eosin Counterstained Mouse Skin Section (x200)**

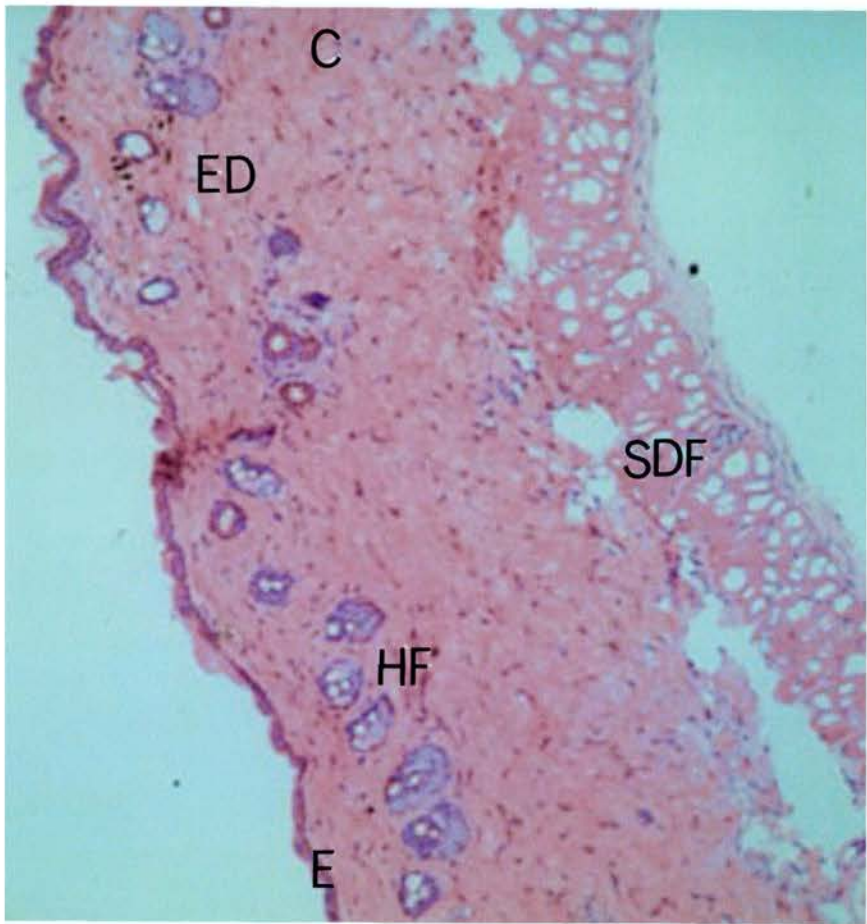


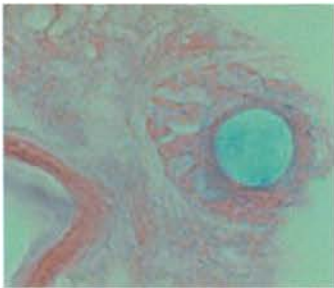
**Figure 3.5** – *SA- $\beta$ gal Staining in Mouse Skin Sections Counterstained With Eosin (x400)*

Two mice were killed, the first six weeks of age and the second, two years of age. An area of skin on the back of each mouse was shaved, a sample removed, transferred into a sterile eppendorf and then snap frozen. The skin samples were mounted in OCT and frozen sections cut which were then transferred onto poly-lysine coated microscope slides. Immediately after cutting the sections were immersed into SA- $\beta$ gal stain solution and incubated at 37°C overnight. The following day the sections were rinsed, fixed with MacroDEX, counterstained with eosin, mounted, viewed microscopically and photographed.

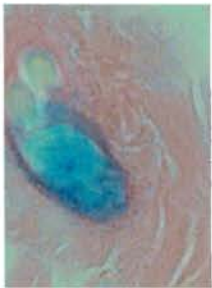
- A) SA- $\beta$ gal staining in an eccrine gland within the skin of the two year old mouse (x400).
- B) SA- $\beta$ gal staining within a hair follicle and associated gland structure within the skin of the two year old mouse (x400).
- C) SA- $\beta$ gal staining in two hair follicle structures within the skin of the two year old mouse (x400).
- D) Skin section taken from six week old mouse. The photograph includes several hair follicles and associated ducts, notice the absence of SA- $\beta$ gal staining in these structures (x400).

**Figure 3.5** - SA $\beta$ -gal Staining in Mouse Skin Sections Counterstained With Eosin (x400)

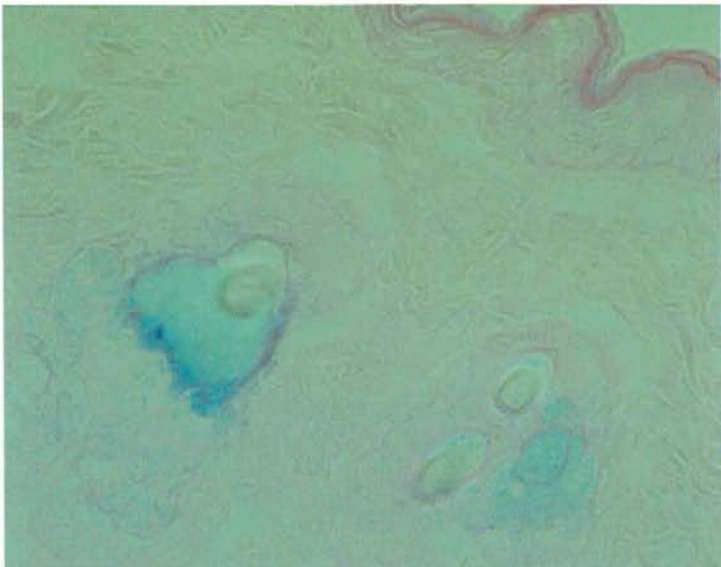
A)



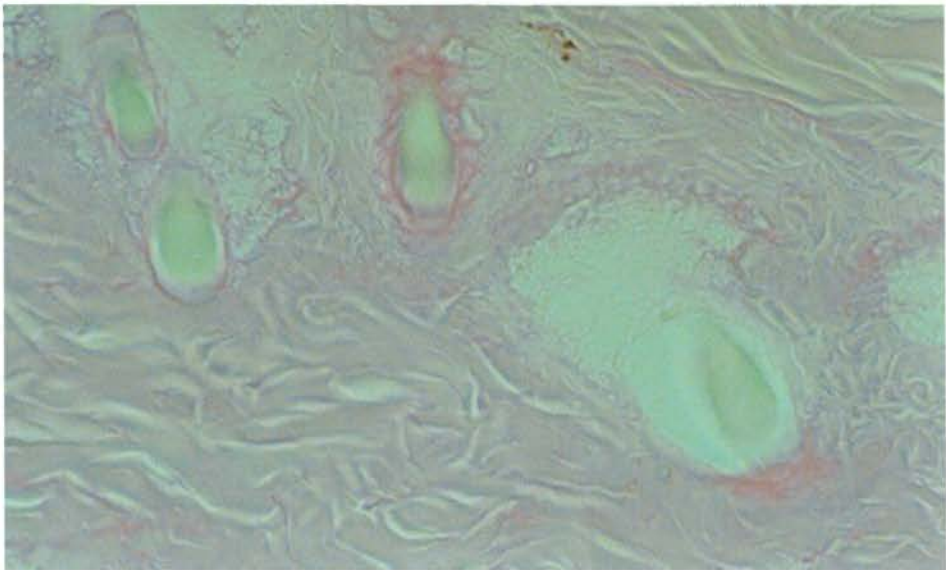
B)



C)



D)





staining pattern was seen in sections exposed to both staining solutions. Intriguingly, this is similar to observations reported by Dimri *et al* (Dimri *et al*, 1995). In human skin sections positive cells were always observed in hair follicles and associated sebaceous glands and in eccrine glands and ducts. However, in human skin samples, this staining occurred independently of donor age. A second pattern, which was absent in the mouse, was positively staining cells within the dermis and epidermis of skin sections taken from old donors only (Dimri *et al*, 1995).

### **3.3.5. Summary**

The first aim of this section of work was to determine whether SA $\beta$ -gal expression could be detected in murine cells. A novel SA $\beta$ -gal stain solution was developed which permitted the detection of murine SA $\beta$ -gal positive cells *in vitro* for the first time. SA $\beta$ -gal positive cells were not detected *in vivo*.

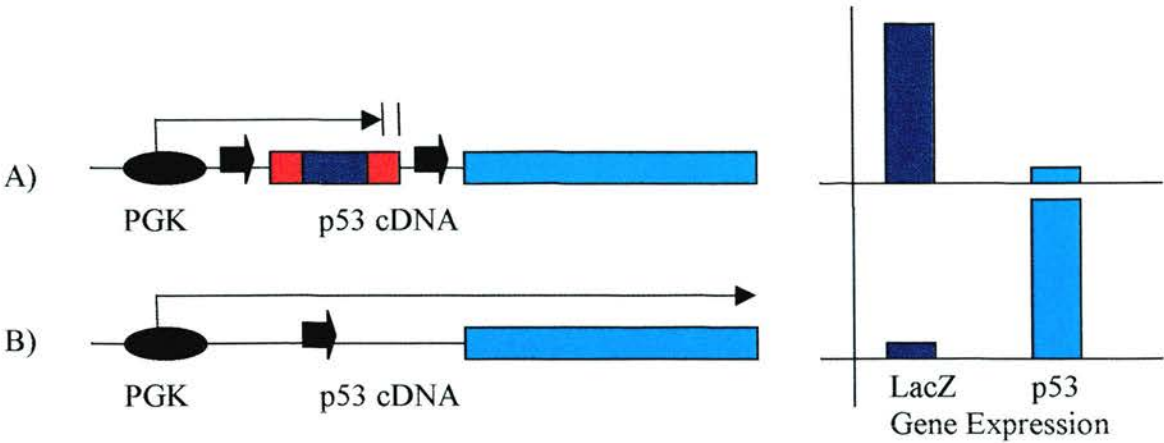
## **3.4. Design of a Conditional p53 Expression Vector**

### **3.4.1. Basic Strategy**

The second aim of this section of work was to design and construct a vector in which expression of the p53 cDNA is upregulated in response to Cre-mediated excision of the floxed STOP cassette from the pFloxSTOP plasmid. To achieve this the pICDP(for) plasmid was developed.

The pICDP(for) plasmid has three key functional domains that are represented in Figure 3.6. Firstly, the constitutive promoter, PGK, secondly, the floxed STOP cassette subcloned from the pFloxSTOP vector (Section 2.4, Figure 2.10) and finally the mouse wild type p53 cDNA. When the pICDP(for) plasmid is in the unrecombined state as represented in Figure 3.6.A, the floxed STOP cassette should block expression of p53. Instead, the constitutive PGK promoter should drive high levels of expression of the  $\beta$ geo fusion gene present in the floxed STOP cassette. After Cre-mediated recombination has occurred the floxed STOP cassette should be excised. The structure of the recombined pICDP(for) plasmid is shown in Figure

**Figure 3.6** – Basic Strategy To Achieve Conditional Upregulation of p53 Expression



The pICDP(for) plasmid.

A) In the absence of Cre recombinase the floxed STOP is predicted to prevent the expression of the p53 cDNA (pale blue box). However, the  $\beta$ geo gene is expressed from within the floxed STOP cassette (dark blue box within red box). The relative expression levels of both of these genes from the unrecombined plasmid are represented in the bar chart at the right hand side of the figure.

B) The structure of the pICDP(for) plasmid after Cre-mediated excisive recombination has occurred. The floxed STOP cassette has been excised abolishing expression of the  $\beta$ geo gene and the p53 cDNA is now directly downstream of the PGK promoter. This plasmid structure is predicted to drive high levels of p53 expression. The relative levels of gene expression after Cre-mediated recombination are represented in the bar chart to the right of the figure.

3.6B. As the  $\beta$ geo gene has been lost, LacZ expression is abolished and the PGK promoter should instead drive high levels of p53 expression.

### **3.5. Construction of pICDP(for)**

#### **3.5.1. The p53 cDNA**

The p53 cDNA used in the construction of pICDP(for) was constructed by Dr. R. Malcomson (Malcomson, 1996). The cDNA encodes the wild type sequence of the mouse p53 protein with the only alterations being the inclusion of an SV40 intron sequence and associated splice donor and acceptor sites and the replacement of the endogenous polyadenylation signal with an SV40 polyadenylation signal (Figure 3.7). The full length cDNA was sequenced after construction to confirm that it encoded the wild type p53 protein.

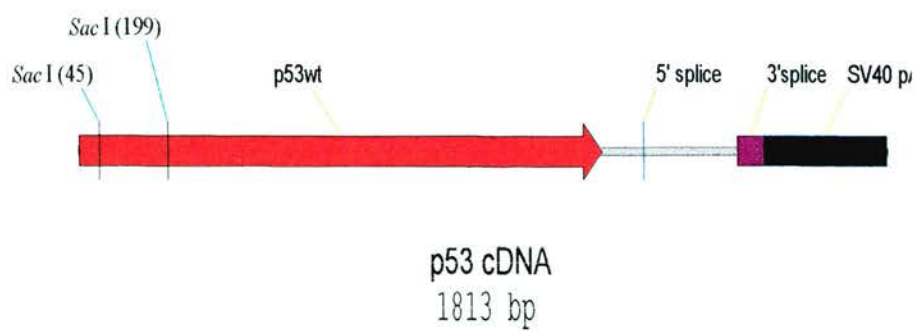
The p53 cDNA was originally subcloned into the pTETOp53HYG vector constructed by Dr. S. Lyons (Lyons, 1999) and this vector was used as the starting point for the construction of pICDP(for). Digestion of the pTETOp53HYG plasmid with the restriction enzyme *Eco RI* releases a 1.9kb cleavage product that includes the p53 cDNA sequence. The 1.9kb band was gel extracted, purified and ligated into an *Eco RI* site within the polylinker of the pTAg plasmid (see Section 2.4.2, Figure 2.5) to generate the recombinant p53pTAg plasmid (Figure 3.8B). Several recombinant clones were identified as a result of this approach and the orientation of the cDNA insert was determined by digestion of the plasmids with the restriction enzyme *Bam HI* (Figure 3.8.A).

Having successfully identified a clone in which the p53 cDNA had been inserted in the reverse orientation within the pTAg polylinker the next step was to insert the constitutive promoter, PGK into the p53pTAg plasmid (Figure 3.8B).

#### **3.5.2. Inserting PGK Promoter into p53pTAg**

The PGK promoter used for the construction of the pICDP(for) vector was subcloned from a vector constructed by Dr. C. Cooper, pPGK (Cooper, 1999). The polylinker

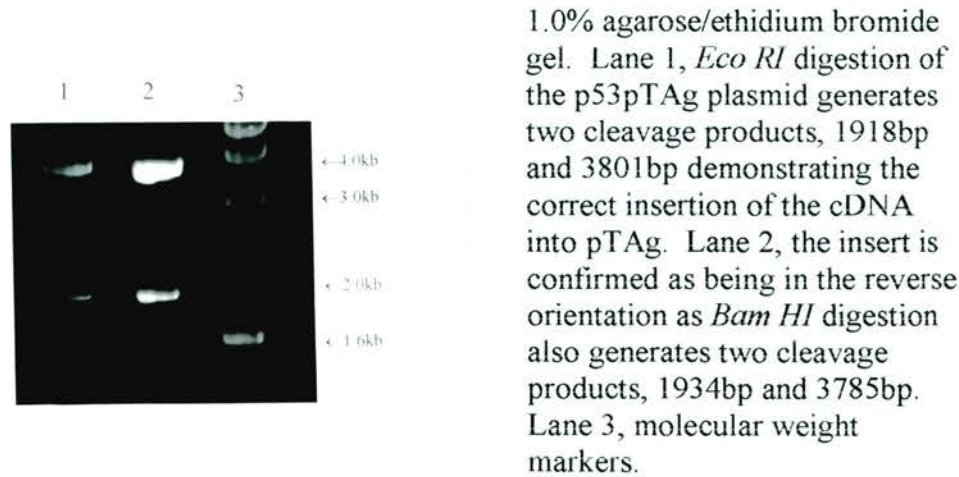
**Figure 3.7** – *Structure of the p53 cDNA*



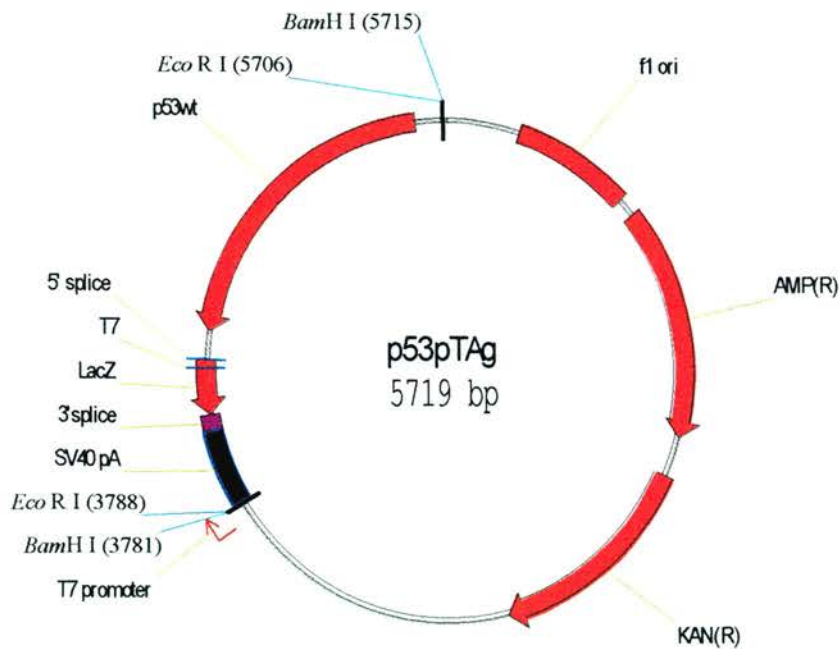
The p53 cDNA cassette. The relative positions of the mouse wild type p53 cDNA sequence, splice sites and polyadenylation signal are shown. This cDNA sequence was constructed by Dr. R. Malcomson.

**Figure 3.8 – Subcloning the p53 cDNA To Generate the p53pTAg Plasmid**

A)



B)



The p53pTAg plasmid with the cDNA (p53wt) inserted in the reverse orientation as determined by *Bam HI* digestion.

of the pPGK plasmid had been modified to allow excision of the PGK promoter with a single *Apa I* digest. Digestion of pPGK with this restriction enzyme generates two cleavage products, a 903bp fragment which includes the PGK sequence and a 2745bp fragment derived from the plasmid backbone (lane 3, Figure 3.9). The 903bp *Apa I* fragment was excised from the gel, purified and ligated into *Apa I* linearised p53pTAg (lane 4, Figure 3.9). Several clones were identified as a result of this approach and screened for the correct insertion event via digestion with the restriction enzyme *Bam HI* (lane 5, Figure 3.9). The recombinant plasmid, pPGKp53 is shown in Figure 3.9.B.

### 3.5.3. Inserting the Floxed STOP into pPGKp53

The next step was the insertion of the floxed STOP cassette from pFloxSTOP between the PGK promoter and downstream p53 cDNA present in pPGKp53. The pPGKp53 plasmid was linearised via digestion with the restriction enzyme *Bst XI* (Figure 3.9.B) which cleaves at a site between the promoter and cDNA sequences. The 3' single stranded DNA overhangs generated by *Bst XI* digestion of pPGKp53 were removed using T4 DNA polymerase. The 6338bp floxed STOP cassette excised from pFloxSTOP via digestion with the restriction enzyme *Sna BI* (lane 4, Figure 3.10A) was then cloned into the linear, blunt ended pPGKp53 plasmid. Resultant clones were screened and insertion and orientation of the floxed STOP cassette was confirmed by *Sac I* digestion of recombinant plasmids (lane 5, Figure 3.10A). The outcome of this cloning step was the vector pIcDNA(rev) as shown in Figure 3.10B.

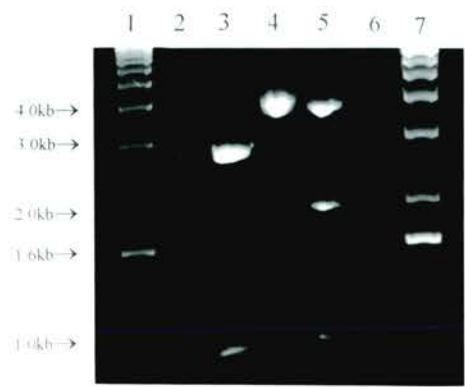
### 3.5.4. Testing pIcDNA(rev) in BNN 132 Cells

Having inserted the floxed STOP cassette from pFloxSTOP into the pPGKp53 vector to produce the plasmid pIcDNA(rev), the ability of the plasmid to act as a substrate for Cre recombinase was tested in BNN 132 bacteria (see also Section 2.4.1). Bacteria of the strain BNN 132 have been engineered to constitutively express Cre recombinase (MoBiTech) and can be used as a convenient test system in which to assay the functionality of loxP-site containing vectors (Bucholz *et al*, 1996).



**Figure 3.9** – Inserting the PGK Promoter into p53pTAg

A)



1.0% agarose/ethidium bromide gel. Lane 1, molecular weight marker. Lane 2, blank. Lane 3, *Apa I* digestion of the pPGK plasmid generates two cleavage products, a 903bp fragment which encompasses the PGK promoter and a 2745bp backbone-derived fragment. Lane 4, *Apa I* digestion of the p53pTAg plasmid linearises the molecule generating a 5719bp band. Lane 5, *Bam HI* digestion was used to orientate the PGK insert introduced into p53pTAg. In the orientation as shown in Figure 2.32b the digestion products are, 943bp, 1934bp and 3753bp. Lane 6, blank. Lane 7, molecular weight marker.

B)

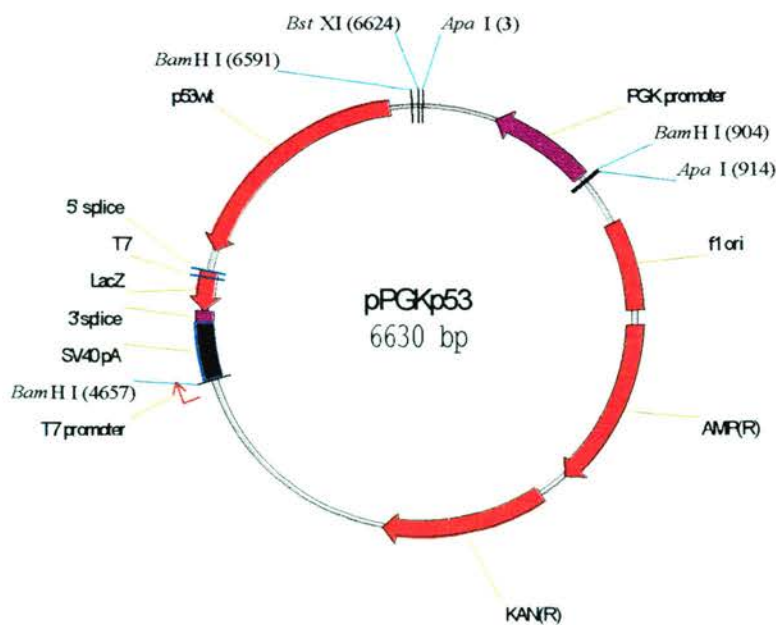
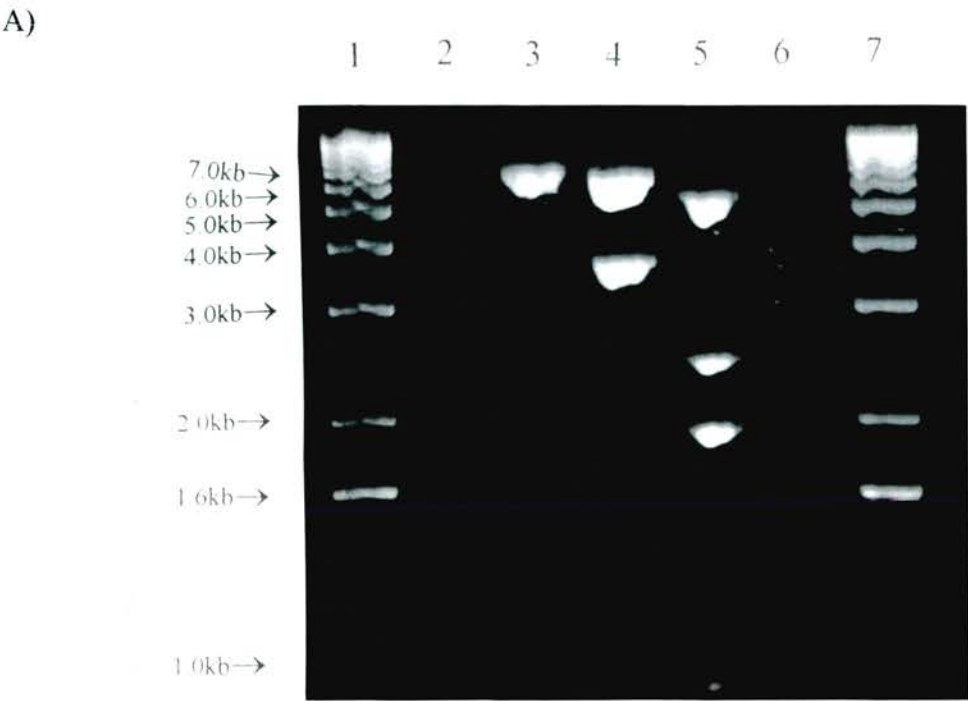


**Figure 3.10** – *Inserting the Floxed STOP Cassette into the pPGKp53 Plasmid*



1.0% agarose/ethidium bromide gel. Lane 1, molecular weight markers. Lane 2, blank. Lane 3, Bst XI linearisation of the pPGKp53 plasmid generates a 6630bp band. Lane 4, Sna BI digestion of pFloxSTOP generates two cleavage products, the floxed STOP encompassing 6338bp fragment and the 3738bp plasmid backbone-derived fragment. Lane 5, Sac I digestion of the plcDNA(rev) plasmid generates 6 cleavage products of 5368bp, 2621bp, 1967bp, 1912bp, 942bp and 154bp. All but the latter are visible. Lane 6, blank. Lane 7, molecular weight markers.

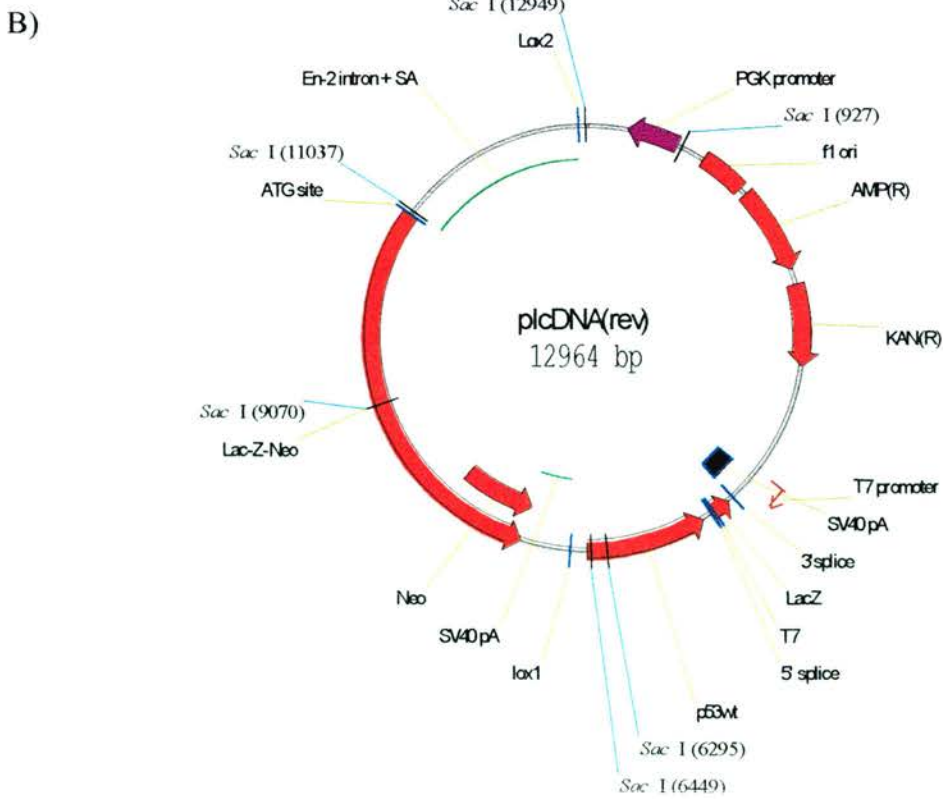
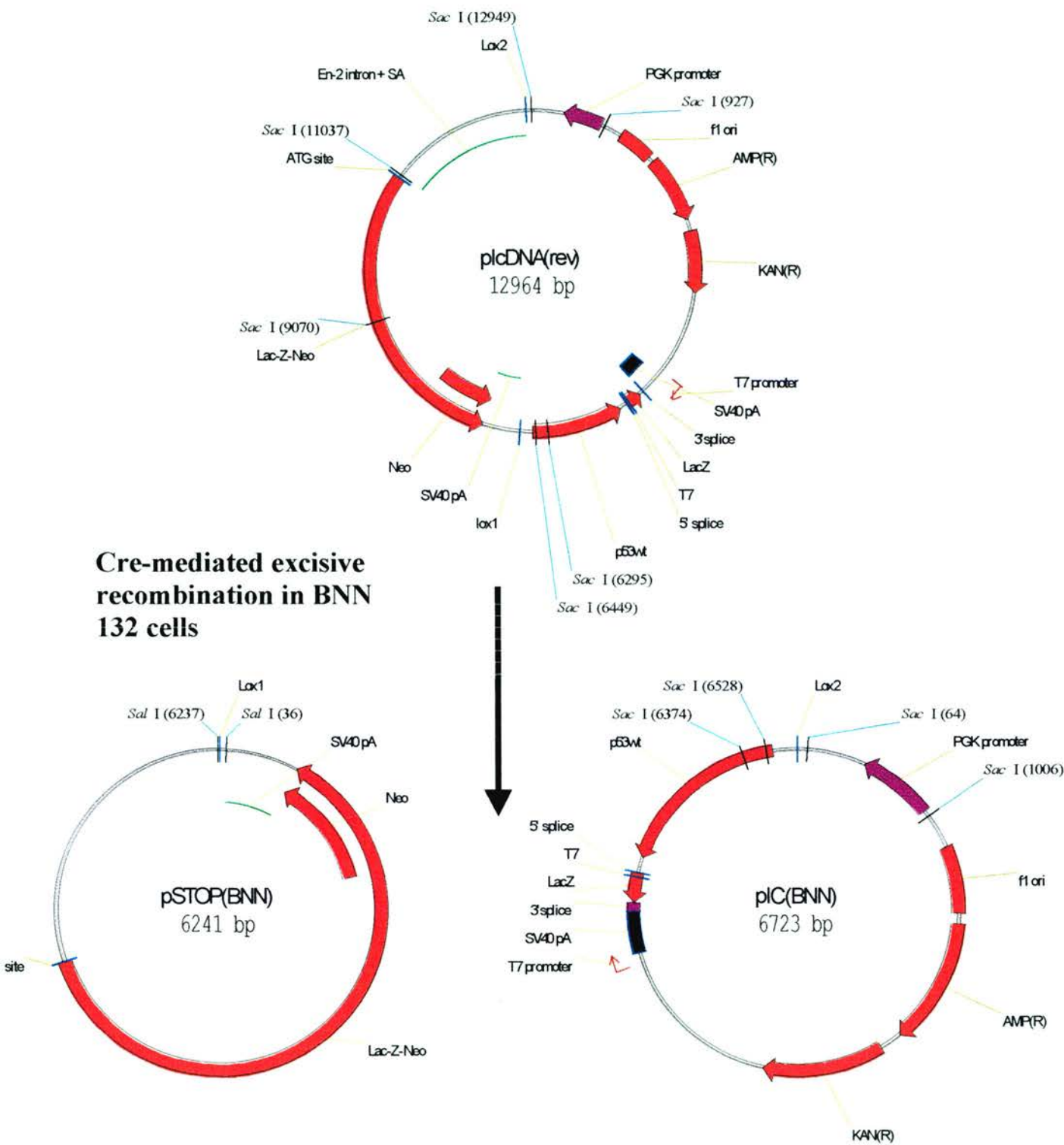
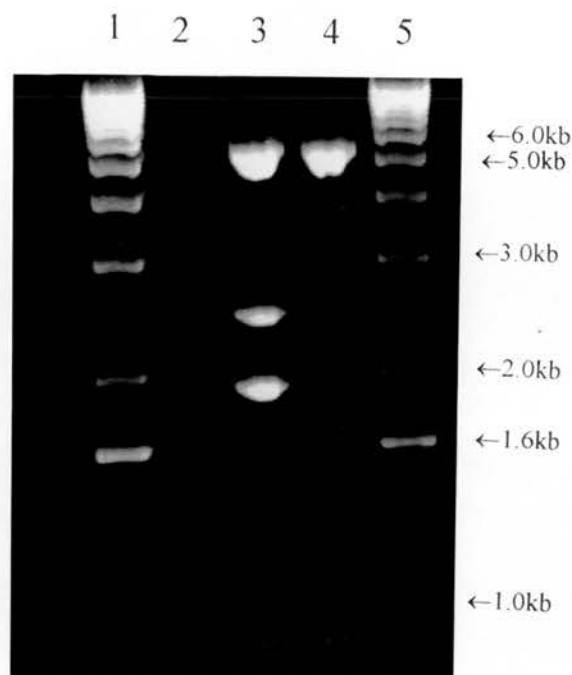


**Figure 3.11** – Predicted Outcome After the *plcDNA(rev)* Plasmid has Undergone Cre-mediated Excisive Recombination



When the *plcDNA(rev)* plasmid is transformed into BNN 132 cells Cre-mediated excisive recombination occurs. The result of this is two plasmid species, the first, *pSTOP(BNN)*, contains one loxP site and all of the STOP cassette. The second species, *pIC(BNN)*, is derived from the plasmid backbone and also contains one loxP site. Only *pIC(BNN)* contains an ampicillin resistance gene so this is the only plasmid species represented in clones arising from the transformation.

**Figure 3.12** – *Restriction Digest Analysis to Demonstrate That the pIcDNA(rev) Plasmid Has Undergone Cre-mediated Excisive Recombination*



1.0% agarose/ethidium bromide gel. Lane 1, molecular weight markers. Lane 2, blank. Lane 3, *Sac I* digestion of pIcDNA(rev) generates six cleavage products of 5368bp, 2621bp, 1967bp, 1912bp, 942bp and 154bp(the latter is too small to be seen above). Lane 4, *Sac I* digestion of the pIC(BNN) plasmid generates four cleavage products of 5368bp, 942bp, 280bp and 154bp (the latter are too small to be seen above). Lane 5, molecular weight markers.

The bacteria were grown up to an appropriate volume, made competent using a standard calcium chloride-based protocol (Sambrook *et al*, 1989) and transformed with the pIcDNA(rev) plasmid. Clones that resulted from this transformation were grown up as minipreps and plasmid DNA subjected to restriction digest analysis. Cre-mediated recombination would be expected to generate two plasmid species, first, the excised and circularised floxed STOP component, pSTOP(BNN) and second, the pIcDNA(rev) backbone-derived pIC(BNN) plasmid (Figure 3.11). As the BNN132 cells are selected in ampicillin after transformation only the second plasmid species will be represented in surviving clones. *Sac I* digestion of plasmid DNA extracted from Amp<sup>R</sup> clones confirmed this prediction (Figure 3.12).

### **3.5.5. Substitution of the Floxed STOP Cassette Within pIcDNA(rev)**

After the construction of pIcDNA(rev) had been completed it was decided to replace the floxed STOP cassette present in this plasmid. The original floxed STOP cassette present, subcloned from the pFloxSTOP plasmid (Chapter 2, Figure 2.10) contains two directly repeated loxP sites that are in the reverse orientation according to standard nomenclature. The possible implications of leaving a reverse loxP site between a promoter and coding sequence have been discussed in Chapter 2 and to avoid this problem it was considered necessary to rebuild the floxed STOP cassette and the pIcDNA(rev) plasmids.

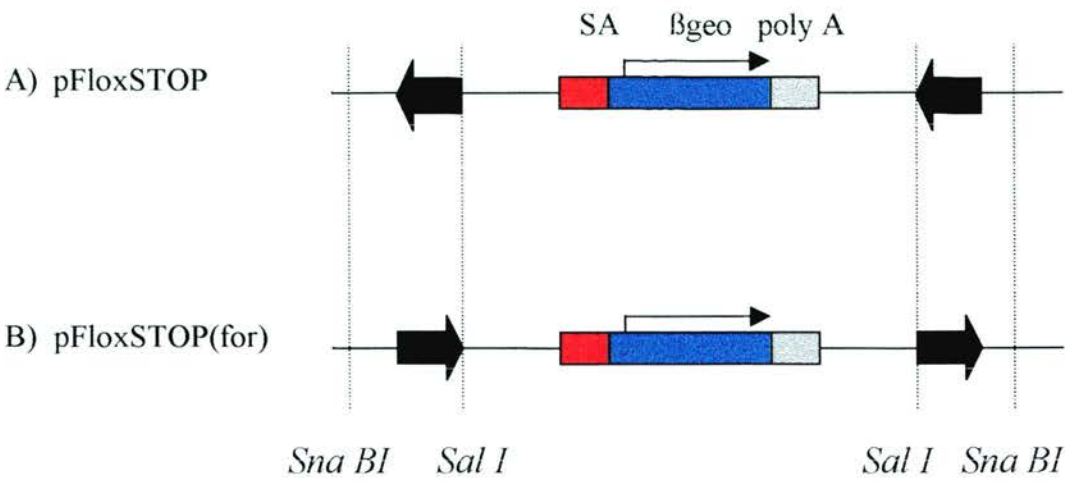
#### **3.5.5.1. Construction of pFloxSTOP(for)**

The relative orientations of the functional components of the pFloxSTOP and pFloxSTOP(for) plasmids are shown in Figure 3.13.

The pFloxSTOP(for) plasmid was constructed from the parental pFloxSTOP plasmid. As shown in Figure 3.13, digestion of pFloxSTOP with the restriction enzyme *Sal I* excises the STOP cassette from the floxed pTAg backbone. Therefore, to reverse the orientation of the loxP sites relative to the STOP cassette pFloxSTOP was digested with *Sal I* and then re-ligated. The ligation reaction was then transformed into bacteria and plasmid DNA extracted from resultant clones



**Figure 3.13** – *Relative orientations of the STOP Cassettes Within the pFloxSTOP and pFloxSTOP(for) Plasmids*

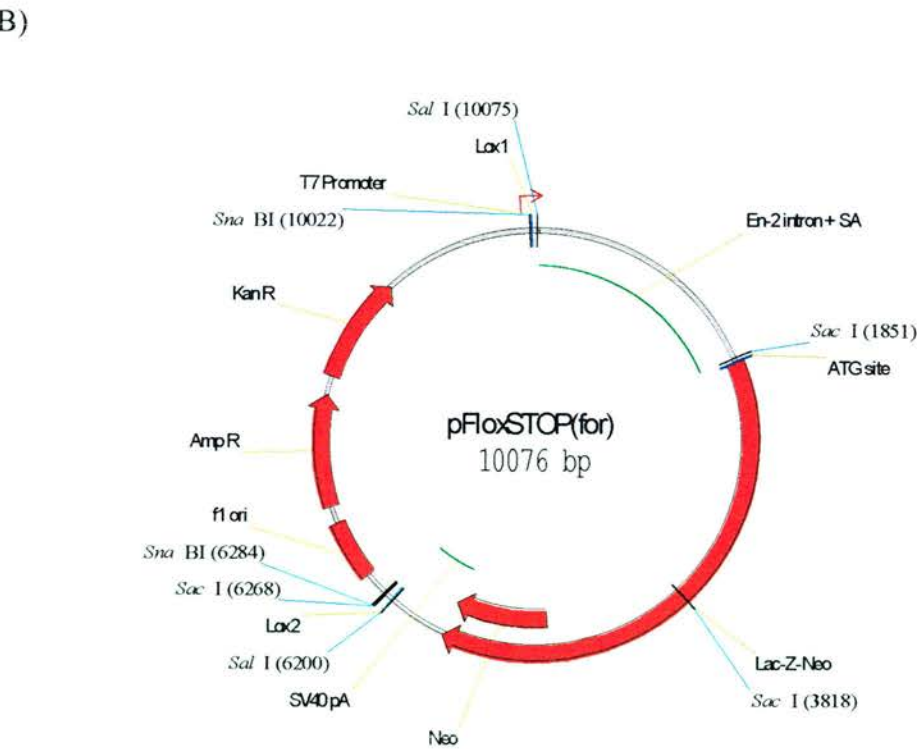
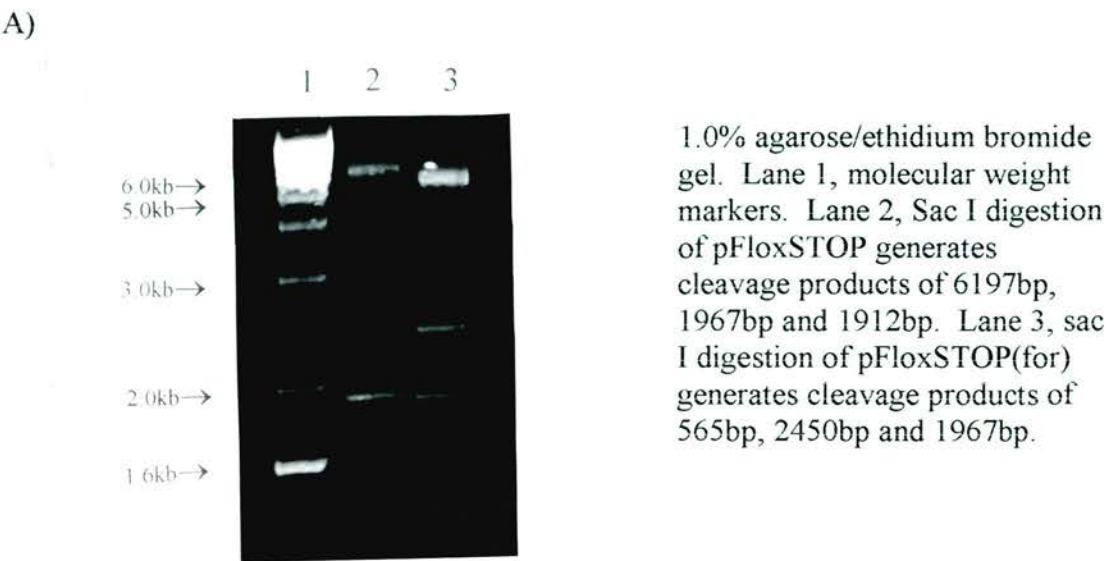


Schematic representation of the two plasmids pFloxSTOP and pFloxSTOP(for).

- A) The original plasmid, pFloxSTOP contains the STOP cassette in the opposite orientation to the loxP sites (black arrows). This was the floxed STOP cassette structure used for the construction of pFloxEGFP and pIcDNA(rev).
- B) The pFloxSTOP(for) plasmid contains the STOP cassette in the same, forward orientation as the loxP sites. This plasmid was used for the construction of pIcDNA(for).



**Figure 3.14** – Construction of pFloxSTOP(for); Restriction Digest Analysis to Determine the STOP Cassette Orientation



The pFloxSTOP(for) plasmid in which both the directly repeated loxP sites and the STOP cassette are in the forward orientation. The floxed STOP cassette can be excised from this plasmid via digestion with the restriction enzyme, *Sna BI*.

subjected to restriction digest analysis. Three plasmid species were predicted to arise after *Sal I* digestion and re-ligation of the pFloxSTOP plasmid. Firstly, a 3875bp plasmid species derived from the floxed plasmid backbone (the pFloxTag(2 *SnaBI*), Figure 2.8), secondly, a 10076bp species in which the STOP cassette has inserted into the floxed plasmid backbone in the reverse orientation (equivalent to the parental plasmid, pFloxSTOP, Figure 3.13.A) and finally a 10076bp species in which the STOP cassette has inserted into the floxed plasmid backbone in the forward orientation (the desired outcome, Figure 3.13B). These three alternatives were distinguished by digestion of plasmid DNA with the restriction enzyme *Sac I* (Figure 3.14).

As with the parental plasmid, pFloxSTOP, the floxed STOP cassette present in pFloxSTOP(for) can be excised from its plasmid backbones via digestion with the restriction enzyme, *Sna BI* (Figure 3.13).

#### **3.5.5.2. Inserting the Floxed STOP Cassette From pFloxSTOP(for) into pPGKp53**

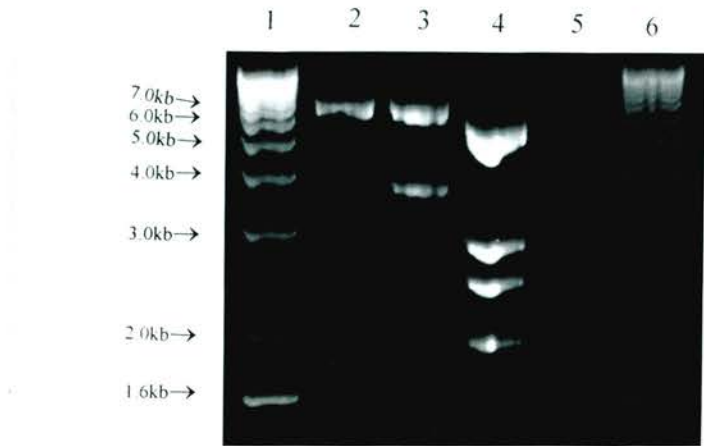
The pPGKp53 plasmid was linearised via digestion with the restriction enzyme *Bst XI* (Figure 3.9B) which cleaves at a site between the PGK promoter and p53 cDNA. The 3' single stranded DNA overhangs generated by *Bst XI* digestion of pPGKp53 were removed using T4 DNA polymerase. The 6338bp floxed STOP cassette excised from pFloxSTOP(for) via digestion with the restriction enzyme *Sna BI* was then ligated into the linear, blunt ended pPGKp53 plasmid. The ligation reaction was then used to transform bacteria and plasmid DNA isolated from resultant clones was screened for insertion and orientation of the floxed STOP cassette by digestion with the restriction enzyme *Sac I*. The outcome of this cloning step was the vector pIcDNA(for) as shown in Figure 3.15.B.

#### **3.5.6. Inserting the Puromycin Resistance Gene (*pac*) into pIcDNA(for)**

The presence of the  $\beta$ geo gene within the floxed STOP cassette of pIcDNA(for) would normally have been sufficient to allow the selection of cells that contain

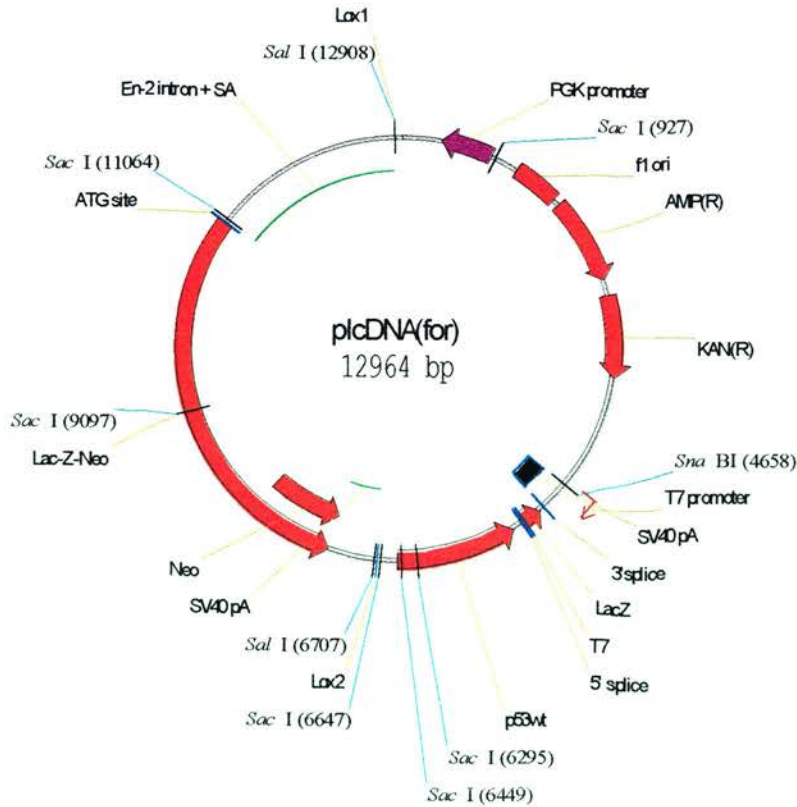
**Figure 3.15** - Inserting the Floxed STOP Cassette From pFloxSTOP(for) Into pPGKp53

A)



1.0% agarose/ethidium bromide gel. Lane 1, molecular weight markers. Lane 2, *Bst* XI digestion of pPGKp53 linearises the plasmid giving a single digest product of 6630bp. Lane 3, *Sna* BI digestion of pFloxSTOP(for) generates two digest products of 6338bp and 3738bp. Lane 4, *Sac* I digestion of plcDNA(for) with the floxed STOP cassette inserted in the correct orientation generates seven digest products of 5368bp, 2827bp, 2450bp, 1967bp, 1912bp, 198bp and 154bp. The latter two products are not seen in the above gel.

B)



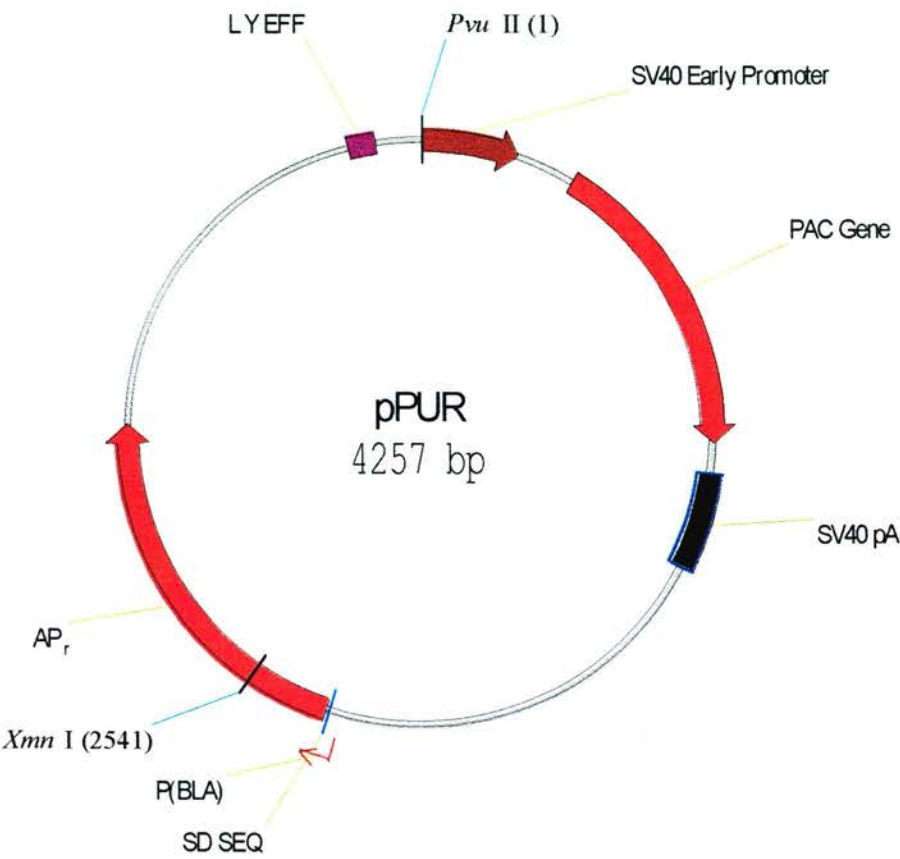
stably integrated copies of pIcDNA(for). However, the aim was to introduce the pIcDNA(for) vector into p53 null cells generated by gene targeting which are already G418<sup>R</sup> as a consequence of the targeting event (Purdie *et al*, 1994). For this reason it was necessary to introduce a second selectable marker into the construct and the puromycin N-acetyltransferase gene, *pac*, from the commercially available pPUR plasmid (Clontech) was chosen (Figure 3.16).

The pIcDNA(for) plasmid was linearised via digestion with the restriction enzyme *Sna* *BI*. The *pac* expression cassette was excised from pPUR (Figure 3.16) using a double digest, with the enzymes *Xmn* *I* and *Pvu* *II*, that generated two cleavage products, a 1716bp backbone-derived fragment and a 2541bp fragment which encompassed the *pac* cassette. All of the restriction enzymes used in this cloning step generate blunt ended cleavage fragments so that the 2541bp *pac* fragment was ligated directly into the *Sna* *BI*-linearised pIcDNA(for) plasmid. The ligation reaction was used to transform bacteria and plasmid DNA isolated from resultant clones was screened by restriction digestion analysis. The *pac* cassette can insert into the pIcDNA(for) plasmid in two possible orientations, these two plasmid species, pICDP(for) and pICDP(rev), were differentiated by digestion with the restriction enzyme *Sal* *I* (Figure 3.17A) and both outcomes are illustrated in Figure 3.17C.

### 3.5.7. Summary

This section has described the successful construction of the pICDP(for) plasmid that has been designed to permit the conditional upregulation of p53 expression. The first version of the plasmid, pIcDNA(rev) contained the floxed STOP cassette derived from the pFloxSTOP plasmid which was the same as that used for the construction of the pFloxEGFP plasmid described in Chapter 2. As one possible explanation for the results obtained with the pFloxEGFP plasmid was the orientation of the loxP sites, it was decided to rebuild both the floxed STOP cassette and pIcDNA(rev). The outcome was pICDP(for) in which, after Cre-mediated

**Figure 3.16** – *The Commercially Available pPUR Plasmid*

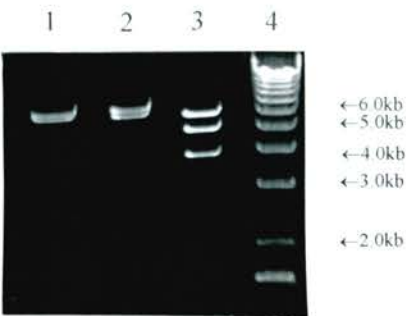


The pPUR plasmid was obtained from a commercial supplier (Clontech). The puro expression cassette was excised via double digestion with the restriction enzymes, Xmn I and Pvu II (cleavage sites indicated above).



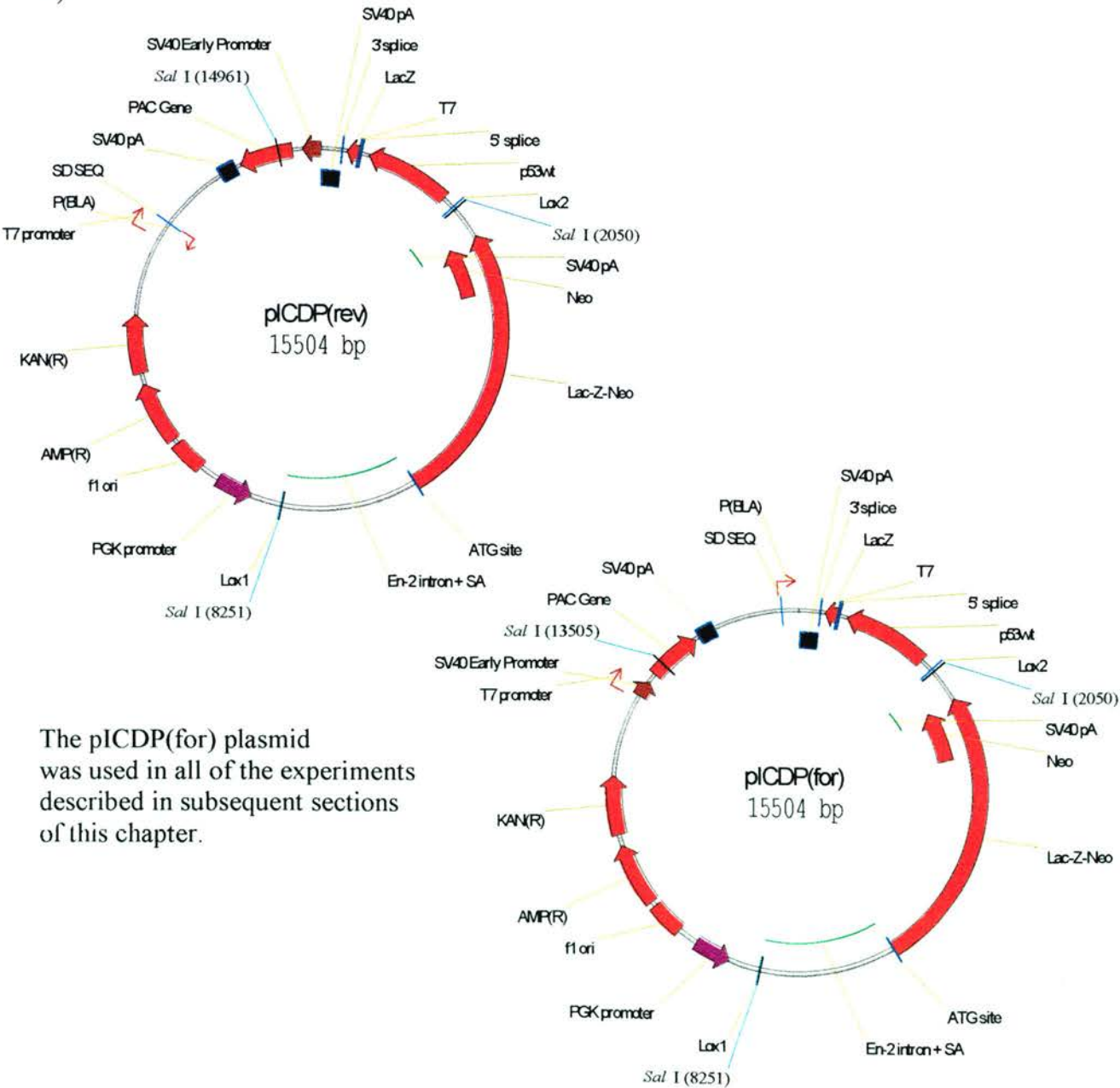
**Figure 3.17** – Constructing of *pICDP(for)*; Inserting the *pac* Gene Into the *pICDNA(for)* Plasmid

A)



1.0% agarose/ethidium bromide gel. Lane 1, Sal I digestion of *pICDP(rev)* generates three cleavage products of 6710bp, 6201bp and 2593bp. Lane 2, Sal I digestion of *pICDNA(for)*, the parental species, generates cleavage products of 6763bp and 6201bp. Lane 3, Sal I digestion of *pICDP(for)* generates three cleavage products of 6201bp, 5254bp and 4049bp. Lane 4, molecular weight markers.

B)



The *pICDP(for)* plasmid was used in all of the experiments described in subsequent sections of this chapter.



recombination has occurred, one loxP site will be retained but in the forward orientation.

### **3.6. Introducing pICDP(for) Into p53 Null Mouse Embryonic Fibroblasts by Calcium Phosphate Transfection**

Previous sections of this chapter have described the generation of two useful tools, the identification of a novel murine senescence-specific biomarker and the design and construction of a p53 conditional expression. This next section of work examines the feasibility of combining these two tools, i.e. stably introducing the pICDP(for) plasmid into EFs, expressing Cre in the transfected cells, quantifying p53 upregulation and examining its effect on senescence and SA $\beta$ -gal expression.

#### **3.6.1. Determination of Puromycin Sensitivity of p53 Null EFs**

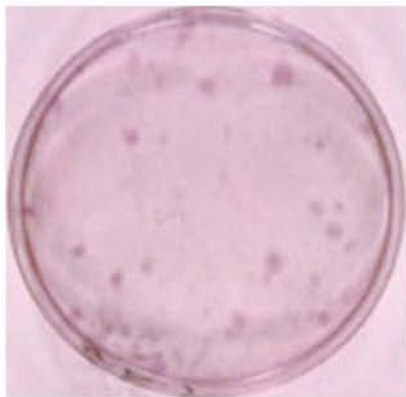
As no data were available, it was necessary to determine the puromycin sensitivity of p53 null MEFs. Equal numbers of the cells were plated onto 100mm culture dishes and exposed to doses of puromycin over the range of 0.5 $\mu$ g/ml to 2.5 $\mu$ g/ml for 14 days. At the end of this time the surviving clones at each dose were stained with GIEMSA (Sigma) and then scored (data not shown). This work established that the optimal concentration of puromycin with which to select stable *pac* transformants of p53 null MEFs is 2.5 $\mu$ g/ml.

#### **3.6.2. Stable Transfection of MEFs**

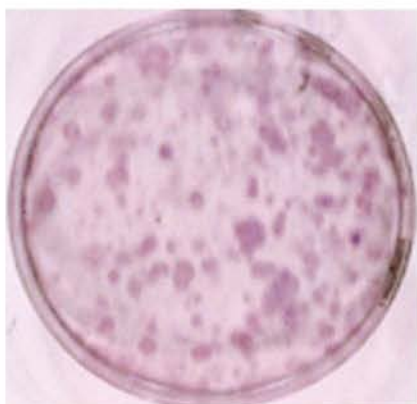
There are no publications reporting the stable introduction of plasmid DNA into primary MEFs. One significant reason for this is the short replicative lifespan of the cells, usually between 15 and 20 passages in culture (Harvey *et al*, 1993) hence the cultures will have reached senescence before the selection period (10-14 days) after stable transfection has elapsed. However, because I intended to work with p53 null EFs, which had been reported not to enter senescence (Harvey *et al*, 1993) stable transfection was a realistic option. It was decided to attempt to introduce DNA into these cells using a modified calcium phosphate precipitation protocol (Chen & Okayama, 1987). For two days after transfection the cells were maintained in non-

**Figure 3.18** - *GIEMSA Visualisation of Stably Transfected MEF Clones*

A) Untransfected control MEFs exposed to 2.5ug/ml of puromycin for 18 days. Cells then stained with GIEMSA (100mm culture dish).



B) MEFs transfected with the pPUR vector (Clontech) and cultured in the presence of 2.5ug/ml of puromycin for 18 days. Cells then stained with GIEMSA (100mm culture dish).



selective medium, after which they were transferred into medium containing 2.5µg/ml puromycin. Clones became visible after 15-20 days in selection and were then harvested and subjected to further analysis. Figure 3.18 illustrates the number of clones visible on a control and a transfected plate after 15 days in selection (visualised with GIEMSA).

### **3.6.3. Introduction of Cre Recombinase into MEF/pICDP(for) Clones**

As with the pFloxEGFP system already described, expression of Cre in MEFs was achieved by their infection with a recombinant adenovirus engineered to express Cre recombinase, AdCre (Anton & Graham, 1995; also Section 2.5.4). At the time of this experiment no data had been published relating to the feasibility of infecting MEFs with adenovirus. For this reason it was necessary to establish the optimal titre (measured in multiplicity of infection, m.o.i, units) for infection as described below.

#### **3.6.3.1. Determination of Optimal Adenovirus Titre For MEF Infection**

Equal numbers of p53 null MEFs were plated out into three wells, each sample of cells were then infected with either 1 m.o.i, 10 m.o.i or 50 m.o.i of AdLacZ (Anton & Graham, 1995). Twenty-four hours after infection the cells were fixed and β-galactosidase activity was visualised histochemically (Figure 3.19). Infection of MEFs with 1m.o.i of AdLacZ resulted in the successful infection of 1-5% of cells, in contrast, at 50m.o.i almost 100% of cells are infected and no obvious cytopathological side-effects were observed. After this preliminary experiment all subsequent adenovirus infections of MEF cells were carried out using 50 m.o.i of virus.

#### **3.6.3.2. Infection of MEF/pICDP(for) Cells With AdCre**

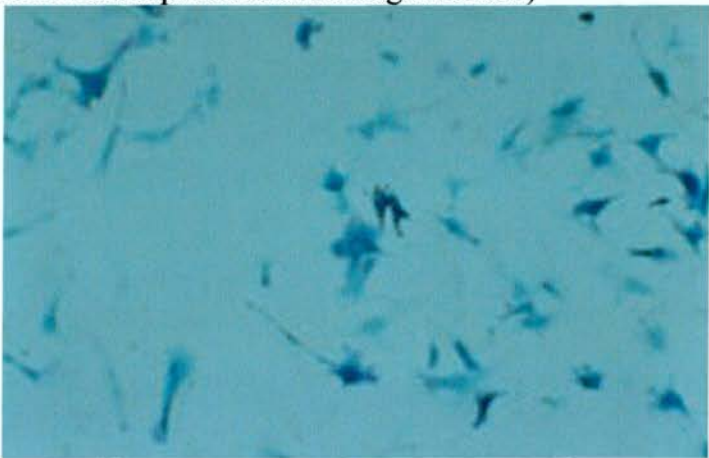
p53 null MEF cells, which had been stably transfected with the pICDP (for) plasmid, were plated onto chamber slides. The slides of cells were then divided into two groups, one group were infected with AdCre at 50 m.o.i, and the other half were infected with the control adenovirus DL-70 at 50 m.o.i.(Sallenave *et al*, 1998). The DL-70 adenovirus has been engineered to be replication defective but does not

**Figure 3.19** - *Infection of Primary MEFs With a Range of AdLacZ Titres*

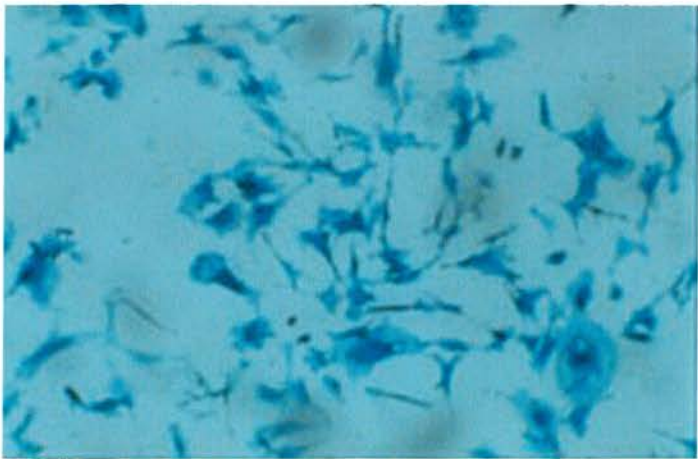
A) 1 m.o.i (taken without phase at x100 magnification)



B) 10 m.o.i (taken without phase at x100 magnification)



C) 50 m.o.i (taken without phase at x100 magnification)



express any heterologous proteins and is referred to as “empty” (Sallenave *et al*, 1998). Forty-eight hours after infection, 1 slide from each group was UV irradiated ( $10 \text{ j/m}^2$ ) to facilitate the immunohistochemical detection of p53. This was necessary as the p53 protein has a very short half-life within normal cells and is not readily detectable by immunohistochemistry in the un-induced state (half-life approximately 15 minutes, Kamijo *et al*, 1998). Six hours after UV irradiation all cells were harvested. Genomic DNA was isolated from cells infected with either DL-70 or AdCre and the remaining cells were fixed and stored at  $-70^\circ\text{C}$  prior to immunohistochemical visualisation of p53 status.

### **3.6.4. PCR-Based Analysis of MEF Clones**

#### **3.6.4.1. PCR Detection of Episomal Adenovirus Molecules**

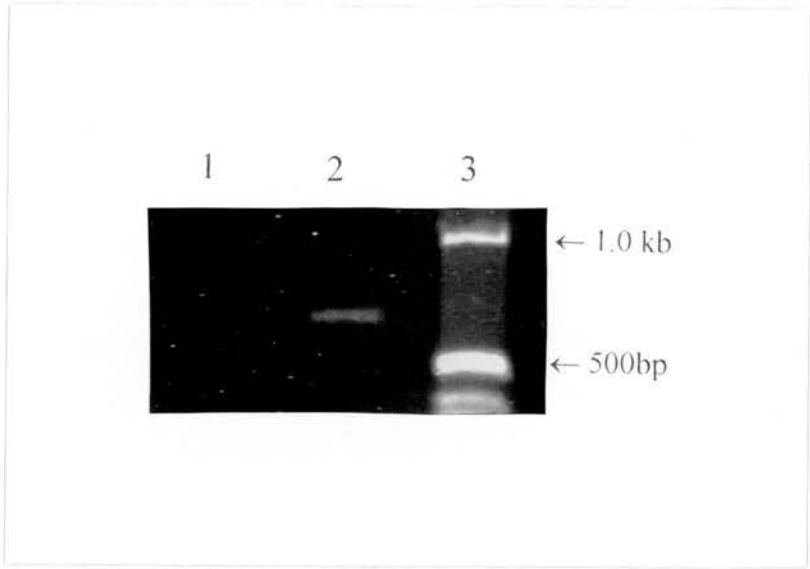
Adenoviridae only rarely integrate into the host genome and are instead thought to persist as extrachromosomal molecules (Stratford-Perricaudet *et al*, 1992). The presence of these episomal molecules in DNA extracts prepared from infected cells can be detected by PCR, using primers that anneal within the Cre expression cassette of AdCre (designed by Dominic Rannie). The 660bp band visible in Figure 3.20, confirms the successful infection of MEF cells.

#### **3.6.4.2. Recombination-Specific PCR Strategy**

A PCR strategy was designed which generated recombination-specific PCR products from the pICDP(for)-derived transgene present in the MEF cells (Figure 3.21). In the unrecombined state the *neo* and *SENIII* primers anneal to the transgene and generate a 2291bp product. However, after Cre-mediated recombination, the floxed STOP is excised from the transgene, deleting the *neo* primer binding site and a novel upstream primer, *PGK*, is needed. The *PGK/SEN III* primer combination cannot generate a product from the unrecombined transgene but in the presence of the recombined transgene a 1887bp product is produced.

As shown in Figure 3.22, the 2291bp product generated from the unrecombined pICDP(for) construct can be amplified from genomic DNA harvested from control

**Figure 3.20** – *PCR Detection of Episomal AdCre Molecules*

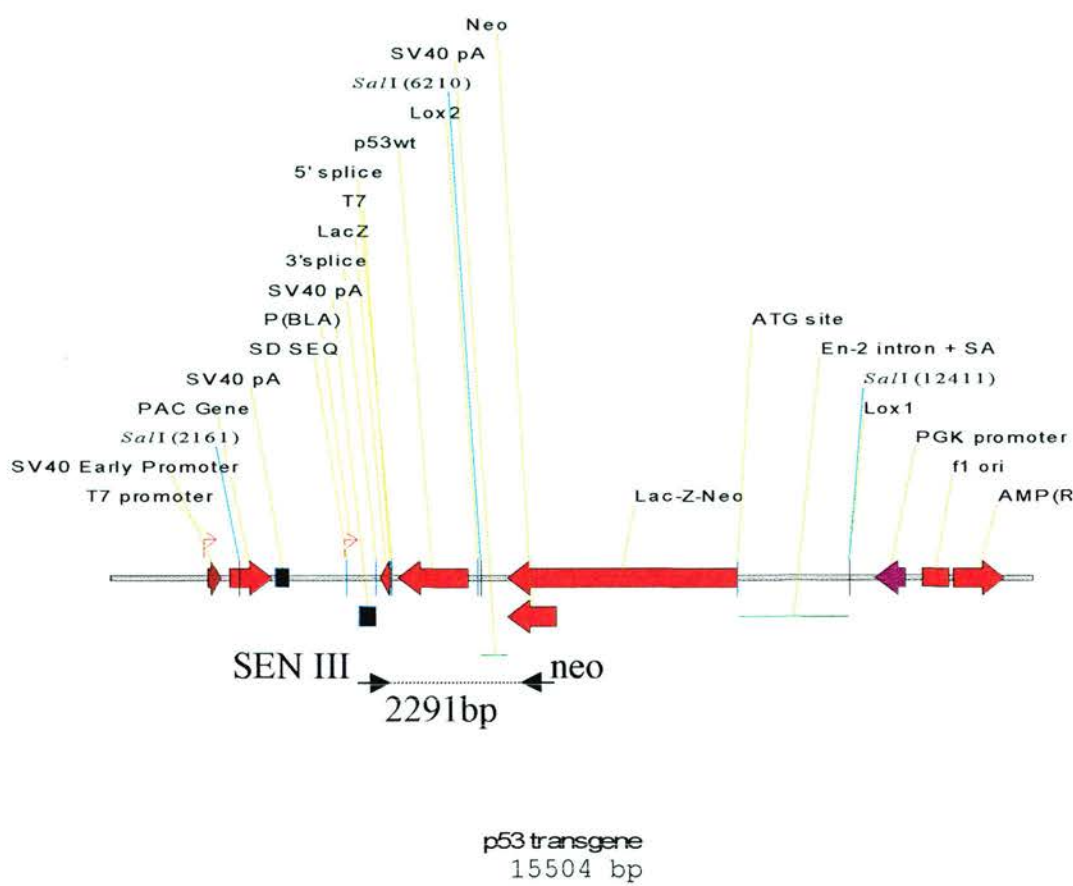


4% agarose/ethidium bromide gel. Lane 1, blank. Lane 2, the 660bp PCR product amplified from genomic DNA harvested from AdCre-infected EF cells. Lane 3, molecular weight markers.



**Figure 3.21** – *Recombination Status-Specific PCR Strategy For the pICDP(for) Plasmid*

A) Structure of the unrecombined pICDP(for) plasmid in EF cells and relative PCR primer positions.



B) Structure of the p53 transgene in EF cells after Cre-mediated recombination has occurred. The PCR primers PGK and SEN III should give rise to a 1887bp recombination-specific PCR product.

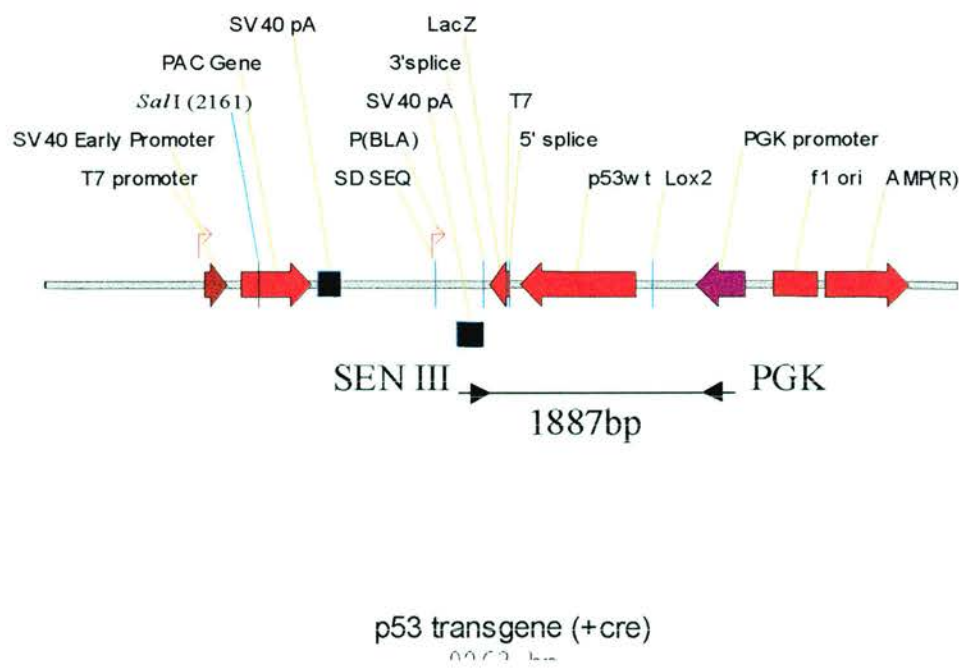
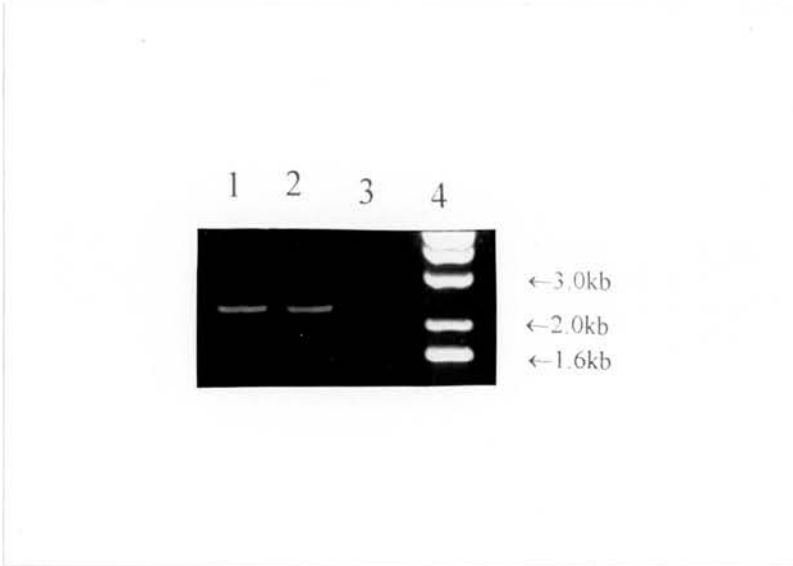


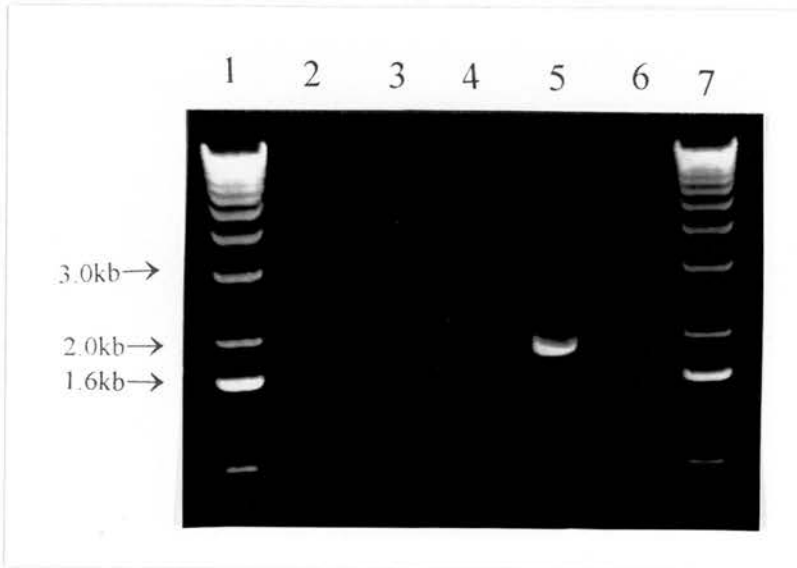
**Figure 3.22 – Recombination Status-Specific PCR Results**

A)



1.0% agarose/ethidium bromide gel. Lane 1, the 2291bp product amplified from genomic DNA harvested from DL-70-infected EF cells. Lane 2, the 2291bp product amplified from genomic DNA harvested from AdCre-infected EF cells. Lane 3, blank. Lane 4, molecular weight markers.

B)



1.0% agarose/ethidium bromide gel. Lane 1, molecular weight markers. Lane 2, PCR result when genomic DNA harvested from DL-70-infected EF cells was used as the template for the *PGK/SENIII* PCR reaction. Lane 3, PCR result when genomic DNA harvested from AdCre-infected EF cells was used as the template for the *PGK/SENIII* PCR reaction. Lane 4, blank. Lane 5, the 1887bp recombination status-specific PCR product amplified from a positive control plasmid.

DL-70 and AdCre-infected MEF cells. This confirms that the plasmid has been stably integrated into the genome of these cells. However, when the recombination-specific *PGK/SENIII* primer pair were used the characteristic 1877bp band was amplified from the positive control DNA but not the MEF genomic DNA (Figure 3.22B).

### 3.6.5. Immunohistochemical Detection of p53 Status

The successful detection of episomal adenovirus molecules in genomic DNA from AdCre-infected MEF cells confirms that the virus was entering these cells. Furthermore the PCR results shown in Figure 3.22A demonstrate that the pICDP(for) plasmid has stably integrated into the genome of the transfected MEFs. However, the 1887bp recombination-specific PCR product could not be amplified from the same genomic DNA samples. Therefore, the predicted recombined plasmid structure shown in Figure 3.21 was not present and so low levels of p53 upregulation are expected in these cells. Nevertheless, p53 immunohistochemistry was undertaken on the various transfected MEF samples to provide data on two aspects of the pICDP(for) plasmid. First, whether any leaky expression from the integrated, but unrecombined pICDP(for) plasmid, be detected in transfected but DL-70 infected cells as was indicated by the analogous pFloxEGFP system. Second, whether the predicted low level of p53 upregulation can be detected in the AdCre-infected population of cells. Immunohistochemistry was carried out on AdCre- and DL-70-infected cell samples, one unirradiated and a second UV irradiated ( $10\text{J/m}^2$ ) sample, as well as appropriate positive and negative controls.

An example of the typical nuclear staining pattern observed after p53 has been UV stabilised in a wild type EF is shown in Figure 3.23A. In comparison, no p53 expression can be detected in p53 null MEFs after UV irradiation (Figure 3.23B). However, rare p53 positive cells were seen in the pICDP(for) transfected-MEF cells that had been infected with AdCre and UV irradiated (approximately 1-2%). Two examples are shown in Figure 3.23C and 3.23D. No positive cells were observed in

**Figure 3.23 - Immunohistochemical Detection of p53 in MEFs**

A) Positive staining wild type cell demonstrating nuclear p53 accumulation after UV irradiation (x400, haematoxylin counterstaining).



B) Negative staining in p53 null MEFs after UV irradiation (x400, haematoxylin counterstaining).



C) Positive staining p53 null MEF cells after stable transfection with pICDP(for), infection with AdCre and subsequent UV irradiation (x400, haematoxylin counterstaining).

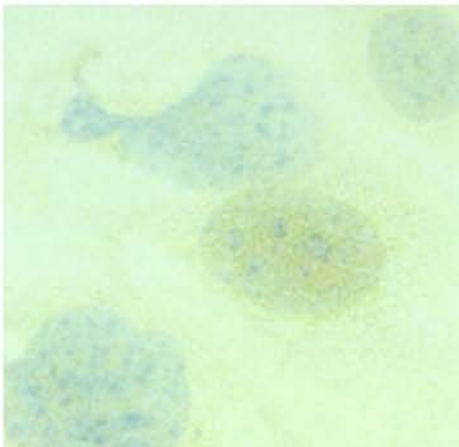
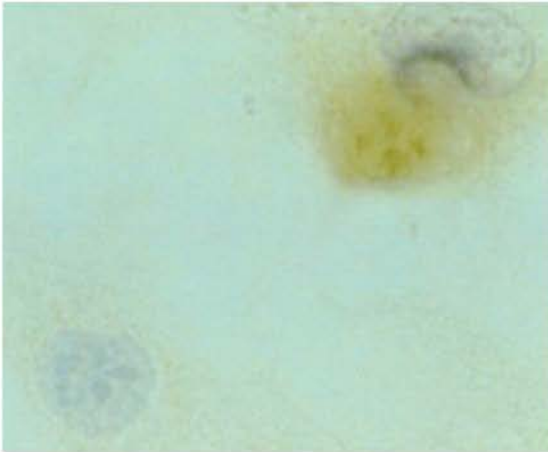
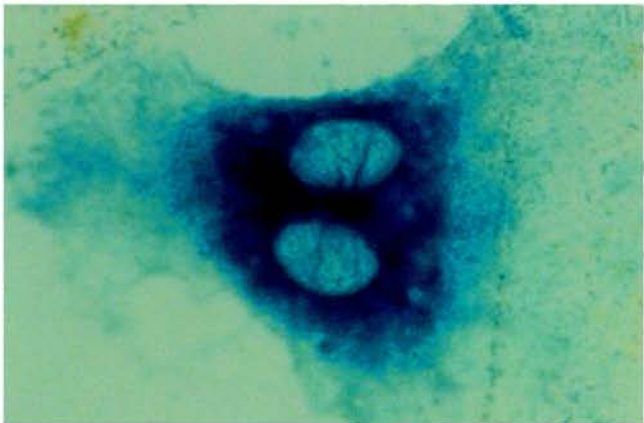
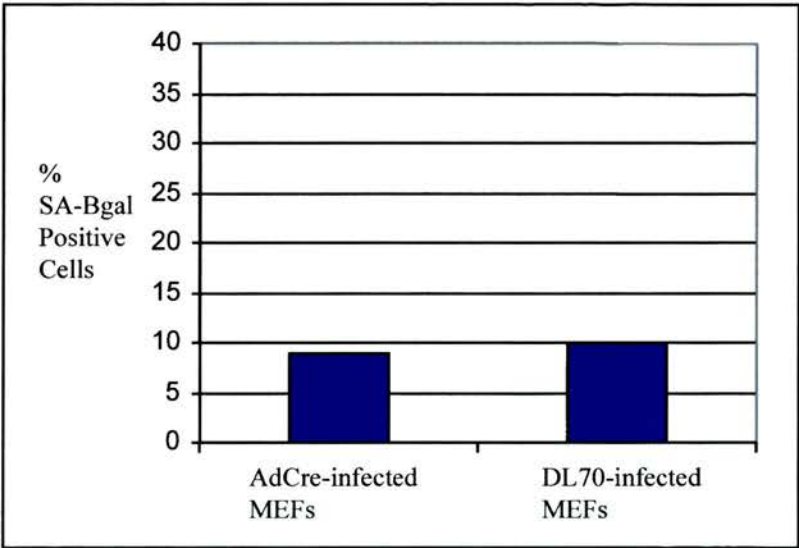


**Figure 3.24** - *SA $\beta$ -gal Scoring in AdCre-infected, pICDP(for) transfected MEFs*

A) Typical SA $\beta$ -gal Positive Cell (x400)



B) Numbers of SA $\beta$ -gal positive cells in control DL70-infected and AdCre-infected pICDP(for) transfected MEFs scored via running mean.



the control DL-70-infected cells or in the unirradiated AdCre-infected cells (data not shown).

### 3.6.6. SA- $\beta$ gal Detection

After adenoviral infection of the transfected MEF cells samples were removed for both immunohistochemistry and the histochemical detection of SA- $\beta$ -gal expression. The low level of p53 upregulation in the AdCre-infected cell population would be predicted to have no significant effect on the level of SA- $\beta$ -gal expression. In line with this prediction, when the numbers of SA- $\beta$ -gal positive cells in both the AdCre- and DL-70-infected samples was scored no significant difference was observed (Figure 3.24).

## 3.7. Discussion

The availability of a senescence-specific biomarker for use in murine cells was such a desirable tool it was decided to re-examine the possibility of SA- $\beta$ -gal expression in MEFs. A novel stain solution was developed which, for the first time, permitted the visualisation of SA- $\beta$ -gal expression in MEFs *in vitro* (Figure 3.1). However, unlike the system developed by Dr. J. Campisi and colleagues for use with human samples (Dimri *et al*, 1995), the murine stain solution failed to identify SA- $\beta$ -gal positive cells *in vivo* (Figure 3.5).

To check the validity of the murine SA- $\beta$ -gal detection system *in vitro* a continuous culture experiment was initiated. Wild type and p53 null MEFs were maintained according to the 3T3 culture regime (Todaro & Green, 1963). Cells samples were removed at regular intervals, fixed, stained and scored via a running mean for SA- $\beta$ -gal expression. As shown in Figure 3.3 substantial differences became apparent in the SA- $\beta$ -gal positivity detectable in p53 null and wild type cultures. At passage 1, SA- $\beta$ -gal expression was detectable in 17% of wild type MEFs but in only 2% of p53 null MEFs. The consistently higher level of SA- $\beta$ -gal expression in the wild type cells was maintained up to passage 11, at which point the culture was not obviously proliferating and was judged to have entered replicative cellular senescence. This



conclusion was supported by the observation that 60% of such cells expressed histochemically detectable SA- $\beta$ gal activity. In contrast, at passage 11 only 8% of p53 null MEFs were SA- $\beta$ gal positive. Interestingly, two peaks of SA- $\beta$ gal positivity were observed in the p53 null cultures, the first at P20 with 50% staining and the second at P33 with 52% of cells staining positively for SA- $\beta$ gal expression. No changes in cell proliferation, such as a crisis phase, or morphology were noticed that correlated with the increased SA- $\beta$ gal positivity at P20 and the correct interpretation of this observation is at present unclear and at P33 the p53 null MEFs were still actively proliferating.

The successful development of a murine SA- $\beta$ gal detection system arose fortuitously. Having unsuccessfully tried the protocol provided by J. Campisi on primary MEFs, it was decided to vary individual components of the stain solution. The basic ingredients of all  $\beta$ -gal stain solutions are, X-gal which acts as a visible indicator of enzyme activity, the potassium ferro- and ferricyanide mixture which acts as an oxidation catalyst to help localise the stain and intensify the colour of the reaction, a buffer to maintain pH, and sodium and magnesium ions which act as activator and co-factor, respectively, of the  $\beta$ -gal enzyme (Yarborough *et al*, 1967). The first component varied in the new stain was the magnesium ion concentration, this was increased 100 fold. When this new stain was tested on primary MEFs, cells that stained positively for SA- $\beta$ gal expression were detected. Therefore, the only significant difference between the SA- $\beta$ gal stain protocol developed by J. Campisi and colleagues and the one developed during the course of this PhD is the concentration of magnesium. This may reflect an underlying biochemical difference in the requirement for the magnesium ion co-factor between the human and murine forms of the  $\beta$ -galactosidase enzyme.

The experimental data illustrated in Figure 3.3 also highlighted the different proliferative capacities of the wild type and p53 null MEFs. Wild type MEFs could only be maintained in culture for 11 passages. With other authors reporting vastly different MEF replicative lifespan values, from 20 passages (Harvey *et al*, 1993) to 4

passages (Jha *et al*, 1998) there is obviously significant variation in this value. This may be due to differences between the mouse strain from which the primary MEFs were established or culture conditions. However, the continued proliferation and failure of p53 null MEFs to enter senescence is exactly in line with previous reports (Harvey *et al*, 1993). p53 null MEFs were maintained according to the 3T3 regime for over 30 passages and even at this point displayed no signs of reduced proliferation.

As p53 status conferred such different growth capabilities on MEFs it was decided to generate tools to facilitate the understanding of the role of p53 in the regulation of replicative senescence. The first such tool was the pICDP(for) vector, designed to permit Cre-mediated conditional upregulation of p53 expression. This vector was initially constructed using the floxed STOP cassette from the pFloxSTOP plasmid. However, in the light of results obtained with the pFloxEGFP vector (Chapter 2), it was decided to rebuild both the floxed STOP cassette and the p53 expression vector. The outcome of these cloning steps was the pICDP(for) vector.

Having built the conditional p53 expression vector it was then necessary to develop and optimise a protocol for the introduction of plasmid DNA into primary MEFs. This had not previously been reported. Techniques including electroporation were tried, although eventual success was achieved when stable transformants were generated using a modified calcium phosphate protocol (Chen & Okayama, 1987). The successful amplification of a vector-derived 2291bp PCR product from the genomic DNA of transfected MEFs confirmed that the pICDP(for) plasmid had indeed stably integrated into these clones (Figure 3.22).

The Cre delivery method selected for use with the MEFs was the recombinant adenovirus, AdCre (Anton & Graham, 1995). However, no publications had reported the use of adenoviridae with this cell type so it was necessary to determine the optimal virus titre for infection. MEFs were infected with a range of three viral titres, 1 m.o.i, 5 m.o.i and 50 m.o.i of the AdLacZ virus (Anton & Graham, 1995)

and  $\beta$ -gal expression was detected histochemically (Figure 3.19). The infection efficiency with 1 m.o.i of virus was less than 5%, however, when MEFs were exposed to 50 m.o.i. of AdLacZ 100% of cells were infected with no obvious cytopathic effects. Therefore, all further adenovirus infections of MEF cells were carried out at this titre.

After the successful infection of MEFs with AdCre was confirmed by the PCR detection of episomal adenovirus molecules, the next step was to analyse the consequences of Cre expression. First, a recombination status-specific PCR strategy was designed and implemented. The presence of the unrecombined pICDP(for) plasmid in MEFs was confirmed, but the predicted recombination-specific PCR product could not be amplified from genomic DNA harvested from AdCre-infected MEFs (Figure 3.22).

There are several possible explanations for this result. First, that Cre-mediated excisive recombination was not actually occurring within these cells. This is improbable as episomal adenovirus molecules were detected by PCR in the genomic DNA of AdCre-infected MEFs indicating successful infection. Furthermore, the virus stock used was freshly prepared and its ability to express Cre recombinase had been confirmed by other research workers (D. Rannie, data not shown). Alternatively, a mutation may have arisen in one of the loxP sites in pICDP(for) which could prevent Cre-mediated excisional recombination. This is also improbable as the integrity of the loxP sites in pICDP(for) were confirmed by DNA sequencing. Therefore, it is probable that Cre-mediated excisive recombination was occurring within these cells, and that the failure to detect it, was due to the transfection method used.

When high concentrations of plasmid DNA are introduced into cells, extrachromosomal homologous recombination (ECR) results in the production of large tandem arrays in which the DNA molecules are joined in a head-to-tail arrangement. Tandem arrays can only be formed by ECR taking place between

**Figure 3.25** – *Mechanisms of Chromosomal Integration of Calcium Phosphate Transfected DNA*

A) Productive Insertion Events

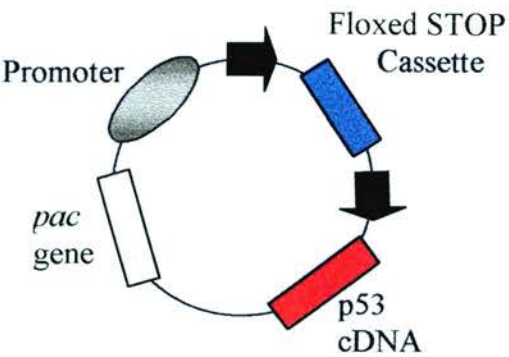
i) A schematic representation of the pICDP(for) plasmid. ii) When this plasmid is introduced into cells it undergoes random linearisation, in this example at a site within the plasmid backbone. iii) ECR between the linear and circular species of the plasmid then results in the production of large tandem arrays. The tandem arrays then integrate into the genome of the transfected cell. Dotted lines in iii) delineate the individual repeat units that comprise this tandem array. iv) After cre-mediated recombination all floxed DNA is excised and the result is the transgene structure shown. This transgene structure can be detected using a recombination state-specific PCR reaction which amplifies a 1887bp product and should permit the upregulation of p53 expression.

B) Non-productive insertion events

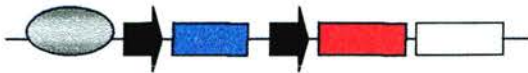
i) A schematic representation of the pICDP(for) plasmid. ii) When this plasmid is introduced into cells it undergoes random linearisation, in this example at a site within the functional domains of the plasmid. iii) ECR between the linear and circular species of the plasmid then results in the production of large tandem arrays. The tandem arrays then integrate into the genome of the transfected cell. Dotted lines in iii) delineate the individual repeat units that comprise this tandem array. iv) After cre-mediated recombination all floxed DNA is excised and the result is the transgene structure shown. The 1887bp recombination-specific PCR product cannot be amplified from this transgenes of this structure, furthermore, they will not support the upregulation of p53 expression.

**Figure 3.25A** – Mechanism of Chromosomal Integration of Calcium Phosphate Transfected DNA; Productive Insertion

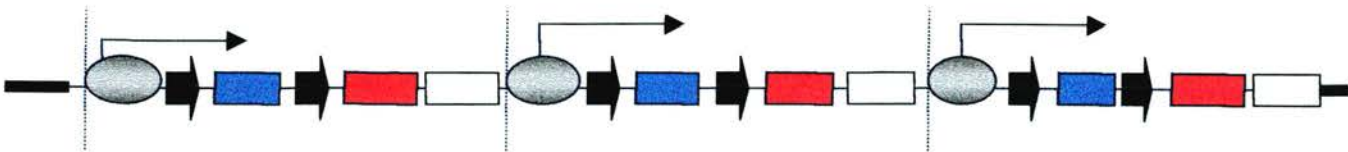
i) Simplified pICDP(for) Structure



ii) After Random Linearisation



iii) Tandem Array (Head-to-Tail Structure)



iv) Tandem Array After Cre-mediated Excisive Recombination

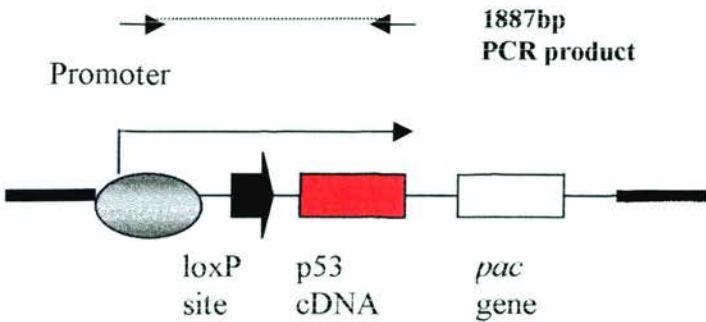
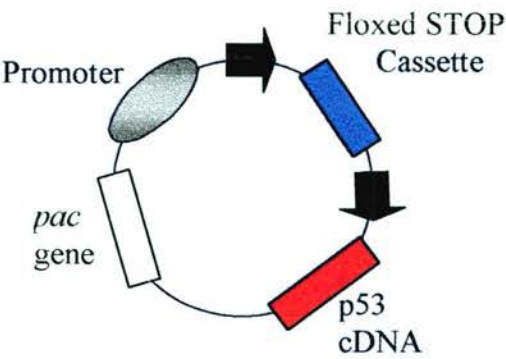


**Figure 3.25B** – Mechanism of Chromosomal Integration of Calcium Phosphate Transfected DNA; Non-productive Insertion

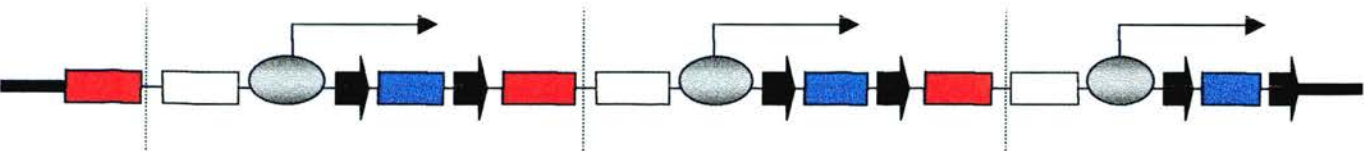
i) Simplified pICDP(for) Structure



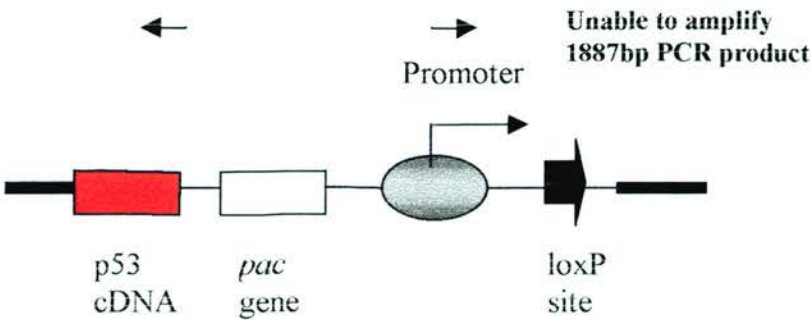
ii) After Random Linearisation



iii) Tandem Array (Head-to-Tail Structure)



iv) Tandem Array After Cre-mediated Excisive Recombination





linear and circular forms of the introduced plasmid DNA (reviewed in Bishop & Smith, 1989). However, as the DNA used for calcium phosphate transfection is circular, linearisation occurs randomly. The results of random pICDP(for) linearisation can be divided into two groups. First, productive insertion which occurs as a result of linearisation within the plasmid backbone as shown in Figure 3.25. If ECR occurs between the linear and circular plasmid forms shown in Figure 3.25A a tandem array will be formed (Figure 3.25A, iii), dotted lines on the diagram delineate the functional domains within the array). Such arrays then integrate randomly into host chromosomes. After Cre-mediated excisive recombination has occurred all floxed sequences are deleted and the functional plasmid structure is reconstituted (Figure 3.25A, iv). The recombined structure should then be detectable by PCR and should support p53 upregulation.

The second type of insertion event that occurs after the random linearisation of plasmids introduced into cells by calcium phosphate transfection is non-productive (see Figure 3.25B). Such events are due to linearisation occurring within a functional domain of the plasmid (see Figure 3.25B, ii). If the pICDP(for) plasmid is randomly linearised, forms tandem arrays and then undergoes Cre-mediated excisive recombination, the outcome is the structure as shown in Figure 3.25B, iii). In this example, the recombined plasmid structure will not be detectable by PCR and will not permit the upregulation of p53 expression (Figure 3.25B, iv).

The probability of productive and non-productive events can be estimated by comparing the relative length of functional plasmid domains to the length of the plasmid backbone. pICDP(for) is 15kb, key functional domains span 11kb and the remaining 4kb are plasmid backbone structures. Therefore, if linearisation occurs randomly, approximately 24% of linearisation sites will result in productive insertion events and 76% of linearisation sites will generate non-productive transgenes after Cre-mediated excisive recombination. However, the exact percentage of pICDP(for)-transfected MEFs that can upregulate p53 expression in response to AdCre-infection is dependent upon the AdCre-infection efficiency. For example, the predicted 24%

maximal induction is dependent upon 100% infection efficiency. As shown in Figure 3.19, at 50 m.o.i. up to 100% infection efficiencies were seen when MEFs were infected with AdLacZ. However, variations in the viability of viral stocks could result in lower infection efficiencies. For example, repeated freeze/thaw cycles are known to be deleterious to virus viability (Croyle *et al*, 1998).

The failure to detect recombined plasmid structures that have arisen from productive insertion events may also be explained by non-random plasmid linearisation. If linearisation events were occurring preferentially within the functional domain-containing regions of pICDP(for) then substantially fewer productive insertion events would be observed. The recombination state-specific *PGK/SEN III* PCR can only amplify a 1887bp product from the recombined pICDP(for) plasmid structures that result from productive insertion events (Figure 3.25). The failure to amplify this PCR product from genomic DNA isolated from AdCre-infected MEFs (Figure 3.22) may suggest that significantly fewer than predicted productive insertion events have occurred within the transfected MEFs. The presence of non-productive insertion events could not be confirmed by either Southern blot analysis, due to limitations on experimental material availability or, by PCR, due to the multiple possible linearisation sites and subsequent tandem array structures.

In concordance with the failure to detect Cre-mediated recombination products by PCR, when the AdCre- and control DL70-infected MEFs were subject to p53 immunohistochemistry a very low level of p53 upregulation was observed (approximately 1-2%). As the pICDP(for) plasmid was specifically rebuilt to avoid the potential Reverse loxP Problem, this is not a valid explanation for these data. Furthermore, it is improbable that a mutation has arisen within the coding sequence of the p53 gene as some p53 expressing cells were successfully detected by immunohistochemistry (Figure 3.23). However, a contributory factor to the low level of p53 upregulation may be the potential for a small number of untransfected clones to survive selection in 2.5µg/ml of puromycin. As shown in Figure 3.18 a small minority of untransfected MEF cells can survive puromycin selection. The continued

survival of such cells would further reduce the percentage of MEFs capable of p53 upregulation after AdCre-infection. Unfortunately, higher doses of puromycin could not be used as they compromised the survival of *pac* expressing cells (data not shown); furthermore, a puromycin concentration of 2.5µg/ml was already significantly higher than the maximum recommended by the manufacturer (Boehringer Mannheim).

In conclusion, the failure to detect recombined pICDP(for) transgene structures and the low level of p53 upregulation are interrelated observations. Minor variations in AdCre titre, and a small number of untransfected MEFs surviving puromycin selection may have contributed to a lower frequency of p53 upregulation than predicted. However, these data may also be explained as artefacts of the calcium phosphate precipitation method used to stably transfect the p53 null MEFs, if for example non-random plasmid linearisation was occurring.

Despite the low level of p53 upregulation observed after AdCre-infection of transfected MEFs, a key result was obtained with the pICDP(for)/MEF system. That is the absence of detectable leaky p53 expression from the unrecombined tandem arrays. For example, a maximum of 24% of all linearisation events would be predicted to result in the reconstitution of productive plasmid structures after Cre-mediated recombination. However, independent of the linearisation site all tandem arrays, which are predicted to comprise up to 100% of calcium phosphate-mediated insertion events (reviewed in Bishop & Smith, 1988), should contain functional units. Therefore, if leaky expression was occurring from the unrecombined plasmid arrays, as suggested by data from the pFloxEGFP plasmid, then p53 expression should be immunohistochemically detectable in the UV irradiated, DL70-infected control cells. This was not observed which would seem to indicate that the floxed STOP cassette was efficiently stopping marker gene expression.

Another explanation for the absence of leaky expression from the proposed unrecombined tandem arrays is the phenomenon of repeat-induced gene silencing

(Garrick *et al*, 1998). These authors demonstrated that the presence of multiple homologous copies of a transgene within a tandem array can have a repressive effect upon gene expression. Therefore, the introduction of the pFloxEGFP plasmid into ES cells via electroporation probably resulted in single-copy insertion at a unique locus (reviewed in Hooper, 1992), a situation which may permit leaky expression. In contrast the pICDP(for) plasmid is probably present in MEFs as a tandem array in which leaky expression could be limited by repeat-induced gene silencing (Garrick *et al*, 1998). Unfortunately, as already mentioned, the limited availability of experimental material prevented a Southern analysis of the nature of the integration events occurring within pICDP(for)-transfected MEFs.

As well as attempting to develop tools for the conditional upregulation of p53 expression, this section of work has also addressed the phenomenon of replicative cellular senescence. One area of particular interest was the role of p53 in regulating the onset of senescence and coincident expression of the novel murine senescence-specific biomarker, SA $\beta$ -gal. Therefore, as well as examining the p53 status of pICDP(for)-transfected MEFs after DL70- or AdCre-infection, SA $\beta$ -gal expression was also quantified. As shown in Figure 3.24, there was no significant difference in the number of SA $\beta$ -gal positive cells in the DL70- and AdCre-infected samples (~10% in both). This was expected as only a low level of p53 upregulation was achieved in the AdCre-infected cells. Hence, the levels of SA- $\beta$ gal expression are below any of those recorded in wild type MEFs (Figure 3.3), therefore independent of AdCre exposure, the pICDP(for)-transfected MEFs are effectively still p53 null.

The problem of both productive and non-productive insertion events occurring within calcium phosphate transfected cells could have been overcome if a method were developed to permit the introduction of linear, rather than supercoiled DNA. The plasmid could then be linearised by digestion with a restriction enzyme that cuts at a known position within the backbone, for example, *Eco NI* for the pICDP(for) plasmid. In theory, all integration events that arise from the transfection should then be productive.

Several alternative transfection strategies were considered. First, lipofection, but this was not attempted as no publications or technical literature from various suppliers had reported the successful application of this technology to the stable transfection of primary cells. Second, the use of a calcium phosphate protocol to introduce the pICDP(for) plasmid after linearisation by digestion with the restriction enzyme *Eco*NI. However, after transfection with the linear DNA no MEF clones were observed after 18 days in selection with 2.5µg/ml of puromycin (data not shown). This observation is in agreement with other reports stating that linear DNA cannot be used in calcium phosphate precipitation (Chen & Okayama, 1987). The third strategy used in an attempt to introduce linear DNA into MEFs was electroporation. Using conditions recommended by the manufacturer of the electroporation equipment (BioRad), MEFs were electroporated with linear pICDP(for) plasmid DNA. However, following the electroporation, no MEF clones became visible after 18 days in selection with 2.5µg/ml of puromycin (data not shown).

In conclusion, the only successful strategy for the stable transfection of primary MEFs was the calcium phosphate protocol using supercoiled DNA (Chen & Okayama, 1987). Unfortunately, this method brings with it the potential for both productive and non-productive insertion events. One final option for the introduction of pICDP(for) into MEFs is the generation of transgenic mice. The conditional p53 expression transgene could then be bred onto a p53 null background and primary cultures established from embryos. This method has the advantage that the pICDP(for) plasmid would be present in all cells within the culture avoiding the need for transfection. Furthermore, this section of work has demonstrated the simplicity of using AdCre to infect MEF cultures. Transgene positive cultures could be infected at approximately 100% efficiency allowing maximal induction of p53 expression and a thorough analysis of the effects of p53 expression on the onset of replicative senescence. Unfortunately, time and budget constraints rendered such an approach unfeasible within the duration of this project.

# **Chapter 4**

## **Inducible Gene Targeting of the Murine p53 Gene**



## Chapter 4

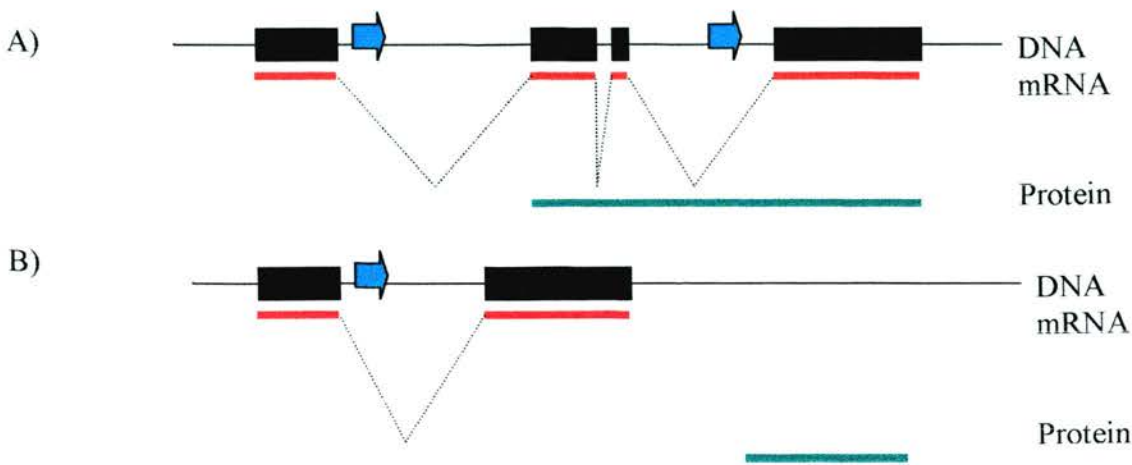
### Inducible Gene Targeting of the Murine p53 Gene

#### 4.1. Introduction – Inducible Gene Targeting

Standard gene targeting allows the generation of knockout mice, that is mice with engineered deletions introduced into specific endogenous genes. While this type of approach has resulted in significant advances in the field of reverse genetics the technique does have limitations. One of the most significant problems is that target gene function is ablated or at least modulated in all tissues of the mouse throughout development. Furthermore, not all knockout mice are viable; the absence of expression of certain gene products is incompatible with the successful completion of normal embryogenesis and development, hence precluding further analysis of target gene function (reviewed in Copp, 1995). The ability to spatially and temporally regulate endogenous gene expression within transgenic mice, so-called inducible gene targeting (IGT), should allow a more informative analysis of gene function. It was with this aim in mind that the two technologies of gene targeting and the Cre/loxP system have been brought together. Both of these systems have been described in detail elsewhere in this thesis (see Sections 1.1-1.3) and the aim of this introduction is to explain how they can be combined to generate an allele of a target gene from which conditional expression can be achieved.

The minimum components of a replacement type targeting vector are a substantial length of DNA homologous to the target locus, a positive selectable marker and a unique restriction site outwith the region of homology with which to linearise the vector. Replacement targeting strategies utilise the intracellular homologous recombination machinery to replace sections of the endogenous target gene with sequences from the linearised targeting vector. The vector-derived sequences may encode selectable markers or mutated versions of the target gene depending on the type of replacement strategy used. The outcome is either the creation of a null allele,

**Figure 4.1** – Inducible Gene Targeting Strategies to Permit the Conditional Inactivation of Gene Expression



Strategy to achieve conditional inactivation of gene expression. A) The insertion of two directly repeated loxP sites (blue arrows) within the intronic sequence (narrow black line) of a gene should not affect expression as shown by normal mRNA production (broken red line) and protein expression (green line). B) After Cre-mediated excisive recombination the floxed segment of DNA, including two exons (solid black boxes) is deleted. A truncated mRNA and protein product are expressed from this allele.

if for example wild type sequences are deleted and replaced with an exogenous selectable marker, or the creation of a subtle mutant allele (see Section 1.2.2.4.b).

The basic replacement gene targeting strategy can be adapted for use in IGT. The only significant design consideration is whether the desired outcome of the IGT strategy is conditional activation or inactivation of target gene expression. The method of choice to achieve conditional inactivation of target gene expression is to use a replacement targeting vector to remove an area of the target gene and replace it with a copy that includes two directly repeated loxP sites (Figure 4.1). This type of approach has been used successfully by several groups to achieve conditional inactivation of endogenous gene expression (discussed in more detail in Section 1.3.3.2.c).

In contrast to conditional gene inactivation, no publications have reported the use of the Cre/loxP system to achieve conditional activation of endogenous gene expression. Yet in theory the same replacement targeting strategies used above can be modified to allow the insertion of a floxed STOP cassette within the coding sequence of an endogenous gene. In the absence of Cre expression the floxed STOP cassette should prevent target gene expression. After Cre-mediated excision recombination has occurred only one 34bp loxP site will be retained within the target gene. To allow gene expression from the recombined allele it is vital that the retained loxP site does not lie within the coding sequence of the target gene. The simplest way to ensure this is to insert the floxed STOP cassette within an intron. Two types of insertion event can be envisaged with this approach, directly downstream of the target gene promoter or alternatively within a more 3' intron. Both of these strategies and their predicted effects on gene expression are shown in Figure 4.2.

Recently, the application of an analogous strategy using FLP recombinase and a STOP cassette flanked by FRT sites has been reported (Meyers *et al*, 1998). These authors inserted a flrtd STOP cassette, a neo gene and polyA signal, into intron 1 of

**Figure 4.2** – *The Predicted Effects of Floxed STOP Insertion and Subsequent Excision on Gene Expression*

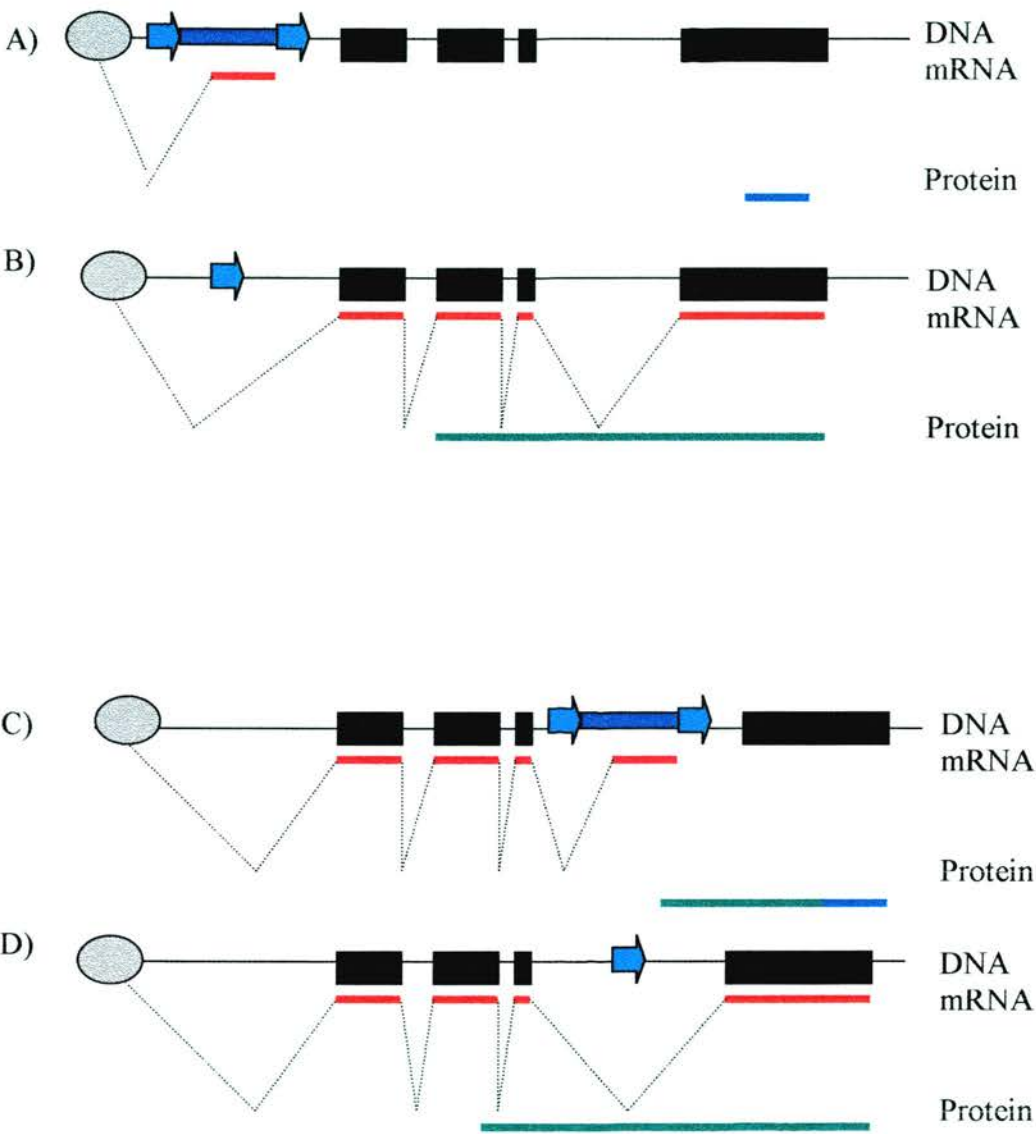
- A) The insertion of a floxed STOP cassette between the promoter (grey circle) and downstream coding sequence of a gene (black boxes) blocks target gene expression. However, any marker genes present within the floxed STOP cassette should be transcribed (broken red line) and translated (blue line).

Note that both the transcription and translation of the exogenous marker gene are under the control of the trapped endogenous promoter. However, latent p53 negatively regulates the translation of its own mRNA (Mosner *et al*, 1995).

Therefore to place the  $\beta$ geo marker gene under both the transcriptional and translational control of p53 it was necessary to delete the IRES cassette from the original pGT1.8IRES $\beta$ geo vector (described in Sections 2.4.1 and 2.4.1.1.). Had the IRES cassette been retained it may have permitted IRES-mediated translation initiation of the p53/ $\beta$ geo fusion transcript under conditions when latent p53 was inhibiting CAP-mediated translation of this mRNA.

- B) Cre-mediated excisive recombination results in the excision of the floxed STOP cassette and the retention of one loxP site. Normal transcription of the target gene is restored and the full-length protein product should be expressed (green line).
- C) The insertion of a floxed STOP cassette within a more 3' intron of the target gene also disrupts transcription (broken red line) and protein expression. A fusion protein is produced (blue/green line) made up of target gene-derived sequence and any marker genes present within the floxed STOP. The possible expression of a truncated target gene is an important consideration when choosing between this strategy and that shown in A).
- D) Cre-mediated excisive recombination results in the excision of the floxed STOP cassette and the retention of one loxP site in the third intron. Normal transcription is restored and the full-length protein product is expressed.

**Figure 4.2** – *The Predicted Effects of Floxed STOP Insertion and Subsequent Excision on Gene Expression*



the mouse *fgf8* gene via homologous recombination. Gene expression was reduced by over 50% from the targeted allele relative to wild type but was restored to normal after Flp-mediated excisive recombination (Meyers *et al*, 1998). This confirms that STOP cassettes can be used to regulate both exogenous and endogenous gene expression *in vivo* and demonstrates the feasibility of this approach.

## **4.2. Inducible Gene Targeting Of The Murine p53 Gene**

The central objective of this chapter was to apply IGT technology to the murine p53 gene. Details on the target locus and the design and implementation of an IGT strategy are discussed in the following sections.

### **4.2.1. Structure of the p53 Locus**

The mouse p53 gene spans 12kb and lies on chromosome 11 (Rotter *et al*, 1984; Czosnek *et al*, 1984). It consists of 11 exons of which 10 contribute to the translation product as exon 1 is transcribed but not translated (Bienz *et al*, 1984). The structure of the endogenous promoter and genomic organisation of the murine p53 locus are represented in Figure 4.3.

### **4.2.2. Targeting Strategy**

As shown in Figure 4.2 the floxed STOP insertion site can have significant effects on target gene expression from the unrecombined allele. To avoid the possibility of expression of a truncated p53 protein from the unrecombined targeted allele it was decided to target the floxed STOP cassette into intron 1, directly downstream of exon 1 and the promoter. The chosen floxed STOP cassette-insertion site lies downstream of the transcription start site but upstream of the translation initiation point. This has the advantage that the  $\beta$ geo marker gene present in the floxed STOP cassette should be expressed under the control of the endogenous murine p53 promoter while simultaneously abolishing expression of the p53 gene itself.



**Figure 4.3** – *The Promoter Structure and Genomic Organisation of the Murine p53 Gene*

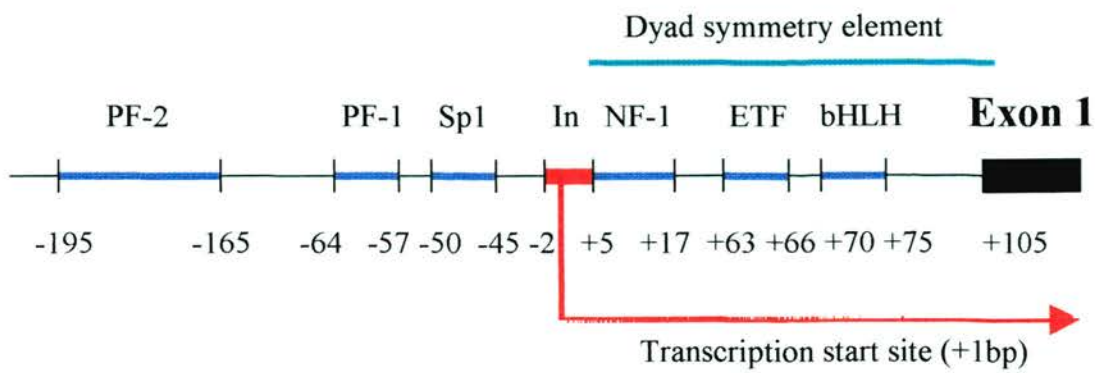
A) Detailed p53 promoter structure (not to scale). The p53 promoter spans 411bp and includes numerous protein binding sites (thick black lines). Transcription is initiated within the Initiator element (In) (-2 bp +5bp) (O'Shea-Greenfield & Smale, 1992) as indicated by the red arrow. To the 5' of the In element lie three protein binding sites, PF-2 (Hale & Braithwaite, 1995), PF-1 (Ginsberg *et al*, 1990) and Sp-1 (Bienz-Tadmor *et al*, 1985; Dynan, 1986). A further three protein binding sites lie downstream of the In, NF-1 (Ginsberg *et al*, 1990), ETF (Hale & Braithwaite, 1995) and bHLH (Ronen *et al*, 1991). The position of the proposed dyad symmetry element present in the 5' region of the p53mRNA is also indicated (+5-+108bp) (Bienz *et al*, 1984).

The aim of this diagram is only to provide an overview of the p53 promoter structure, a detailed discussion can be found elsewhere (Section 1.3.1).

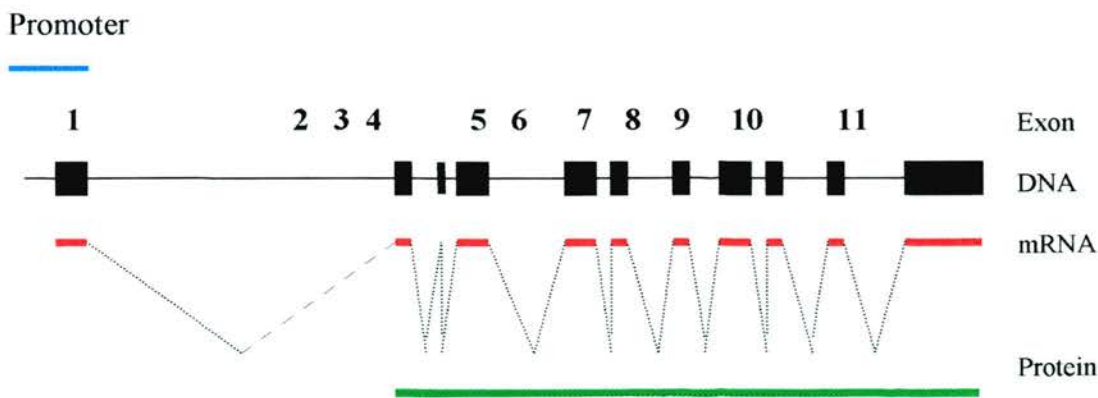
B) Schematic representation of the murine p53 genomic locus (not to scale). The promoter region is indicated (blue line) as are the 11 exons (black boxes) and 10 intervening introns (thin black line). The mRNA (red line) and protein products (green line) expressed from this locus are also shown.

**Figure 4.3** – Genomic Organisation and Promoter Structure of the Murine p53 Locus

A) Detailed p53 Promoter Structure (not to scale)



B) Genomic organisation of the murine p53 gene (not to scale).



### **4.3. Aims**

- a) The isolation and/or construction of a genomic clone spanning the promoter region of p53.
- b) The construction of a targeting vector, pIGTV, designed to permit the insertion of the floxed STOP cassette from pFloxSTOP into intron 1 of the murine p53 gene.
- c) Demonstration that pIGTV is a functional substrate for Cre recombinase.
- d) The introduction of pIGTV into ES cells and the development of a screening strategy allowing the identification of successfully targeted clones.

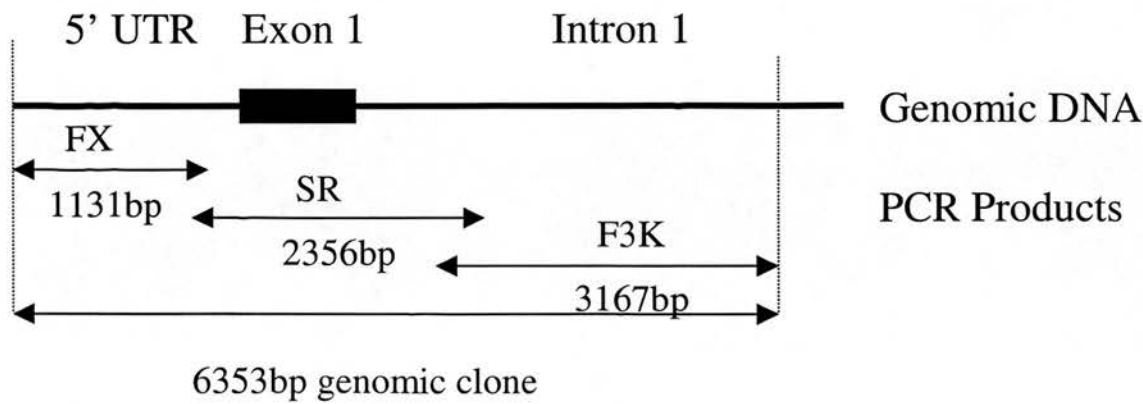
### **4.4. IGT Vector Construction**

#### **4.4.1. Obtaining a Genomic Clone Homologous to the Target Locus**

The variables which affect targeting efficiency at a given locus have been discussed in depth elsewhere (Section 1.2.2.5.). The only one of these factors relevant to this discussion is the extent of homology between the target locus and the targeting vector as this is roughly proportional to the recombination frequency observed (reviewed in Capecchi, 1989). For this reason it is desirable to use regions of homology in targeting vectors which are as long as reasonably practical. The standard method of obtaining genomic clones that are homologous to specific loci is via the screening of genomic libraries. However, a suitable genomic clone spanning the 5' end of the p53 gene was not successfully identified after the screening of two genomic libraries (see Lyons, 1999). Therefore, it was decided to try to obtain a genomic clone by PCR. Three PCR reactions were designed, the products of which span the site to be targeted in the p53 genomic locus (see Figure 4.4). Two of the three PCR reactions, FX and F3K were designed and optimised by Dr. S. Lyons (Lyons, 1999). These two PCR products were cloned into the Bluescript plasmid backbone generating the pFXF3K plasmid which was obtained as a kind gift from Dr. S. Lyons (Figure 4.5). All PCR products were amplified from genomic DNA harvested from HM-1 ES cells as the completed IGT vector was to be introduced into that ES cell strain.

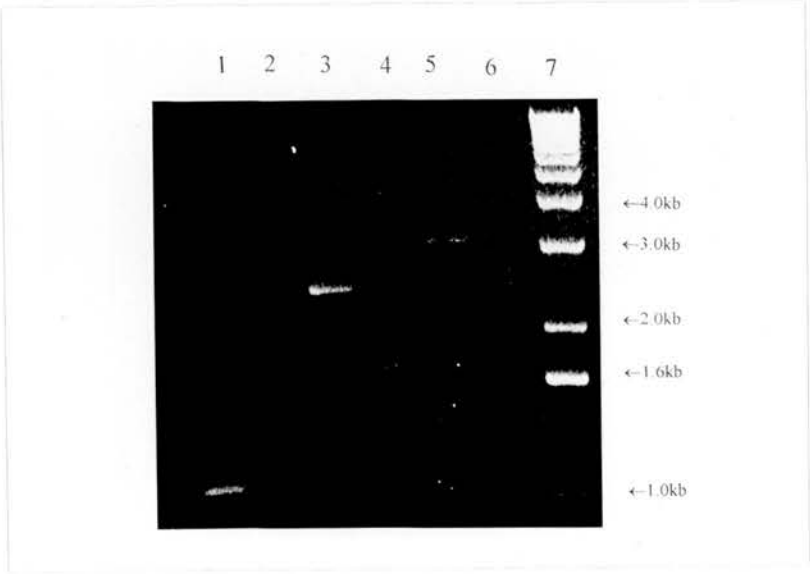
**Figure 4.4** – *The Relative Sizes and Locations of the FX, SR and F3K PCR Products*

A)



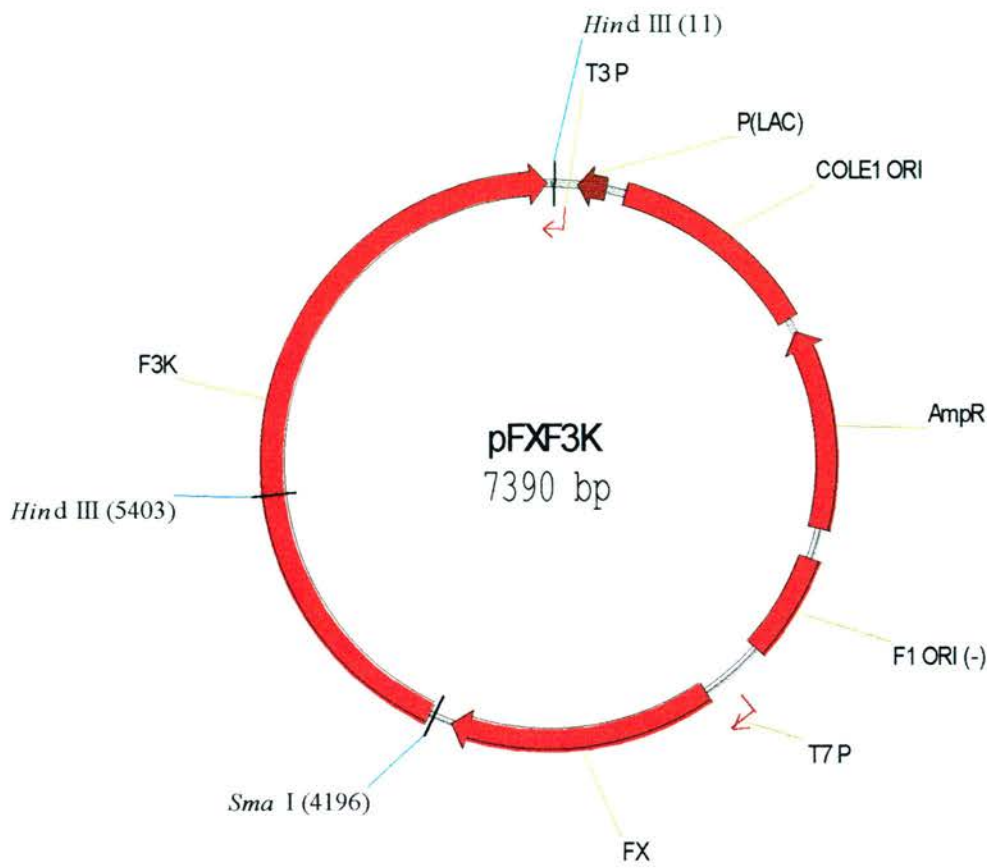
A diagram of the 5' end of the mouse p53 locus (black line and box, not to scale) with the three overlapping PCR products also shown (arrows). The construction of the complete genomic clone is discussed in Section 4.5.1.

B)



1.0% agarose/ethidium bromide gel. Lane 1, the 1158bp band generated during the FX PCR reaction. Lane 2, blank. Lane 3, the 2300bp band generated during the SR PCR reaction. Lane 4, blank. Lane 5, 3200bp band generated during the F3K PCR reaction. Lane 6, blank. Lane 7, molecular weight markers.

**Figure 4.5** – The *pFXF3K* Plasmid



The *pFXF3K* plasmid was obtained as a kind gift from Dr. S. Lyons. This plasmid contains both the FX and F3K PCR products and these are indicated on the above diagram. The *Sma* I site was used during the *in vivo* cloning and this work is discussed in more detail in Section 3.3.1.1.

The pFXF3K vector was the starting point for the construction of a continuous genomic clone spanning the promoter, exon 1 and the 5' end of intron 1 of the mouse p53 gene. However, while the FX and F3K PCR products are separated by only a few base pairs in the pFXF3K plasmid their genomic homologues are actually separated by over 2 kilobases in the p53 locus (Figure 4.4.A). To generate a continuous genomic clone spanning the region of interest it was necessary to insert a third PCR product, SR between FX and F3K. However, the absence of suitable restriction enzyme cleavage sites meant that this could not be accomplished using standard cloning techniques, therefore the relatively new technique of *In Vivo* Cloning (IVC) was used.

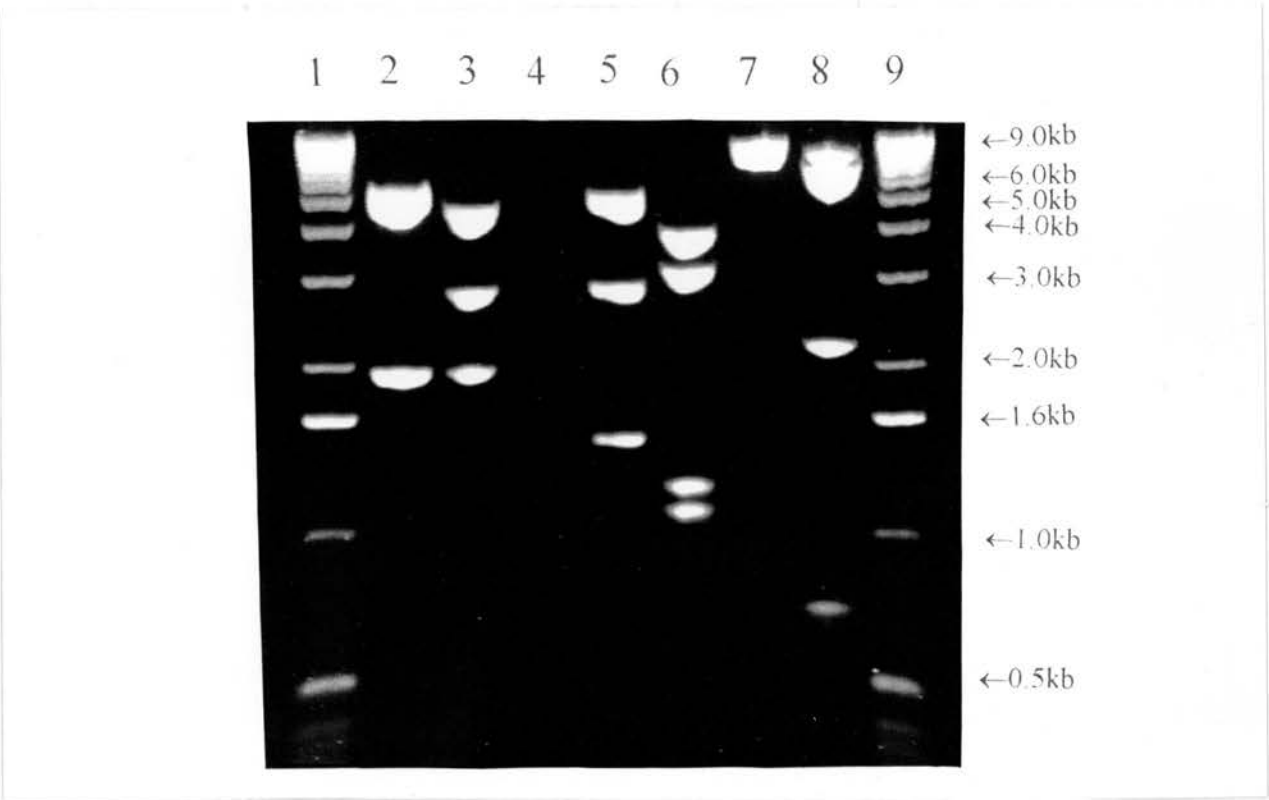
#### **4.4.1.1. *In Vivo* Cloning**

The standard method used to construct recombinant plasmids from multiple DNA molecules involves restriction digestion of parental molecules and subsequent ligation of component fragments. However, appropriate restriction enzyme cleavage sites cannot always be found for every cloning step and this was the case with the SR/pFXF3K step. Conventional cloning techniques would not have permitted the seamless joining of the SR PCR product between the cloned FX and F3K products in the pFXF3K vector. For this reason the continuous genomic clone was generated using IVC (Oliner *et al*, 1993; Bubeck *et al*, 1993).

Specific *E. coli* strains can repair gapped plasmids via intramolecular homologous recombination (Kobayashi & Takahashi, 1988) and the IVC technique is based on the subsequent demonstration that certain of these strains can also perform intermolecular homologous recombination (Oliner *et al*, 1993; Bubeck *et al*, 1993). If two pieces of linear DNA are co-transformed in to the bacteria homologous recombination can occur between the two to generate one circular molecule, provided there is sufficient homology at the ends of both molecules. Cloning efficiency is roughly proportional to the extent of homology between the components with 10 base pair overlaps being a practical minimum (Bubeck *et al*, 1993).



**Figure 4.6** – Construction of the pIVC4 Plasmid and Restriction Digest Analysis of the p53 Genomic Clone



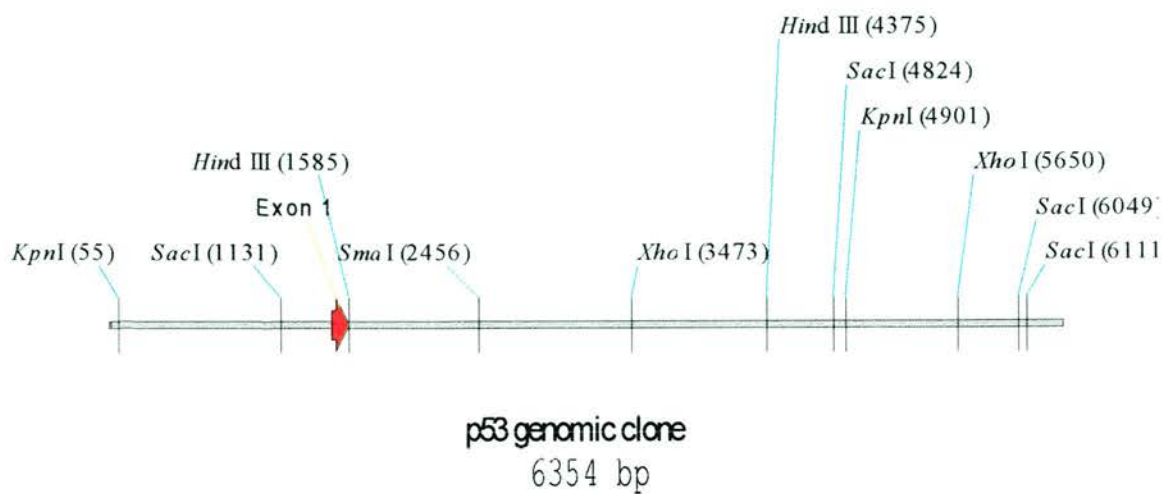
1.0% agarose/ethidium bromide gel. Lane 1, molecular weight markers. Lane 2, Hind III digestion of pFXF3K plasmid generates two cleavage products of 5392bp and 1998bp. Lane 3, Hind III digestion of the pIVC plasmid generates three products, 1998bp, 2790bp and 4556bp. Lane 4, blank. Lane 5, Kpn I digestion of pIVC gives a 103bp fragment (too small to be visible), a 1512bp, a 2883bp and 4846bp cleavage products. Lane 6, Sac I digestion of pIVC. Six cleavage products are generated, two of 62bp and 33bp are too small to be visible on this gel. The other four products of 1173bp, 1225bp, 3158bp and 3693bp are all seen. Lane 7, Sma I cleaves the pIVC plasmid at one unique site generating a single band of 9344bp. Lane 8, Xho I digestion of pIVC generates three cleavage products of 744bp, 2177bp and 6423bp. Lane 9, molecular weight markers.

The relative positions of cleavage sites for the above restriction enzymes are shown in the 6354bp genomic clone below (Figure 4.6.A) and in the complete pIVC plasmid in Figure 4.7.

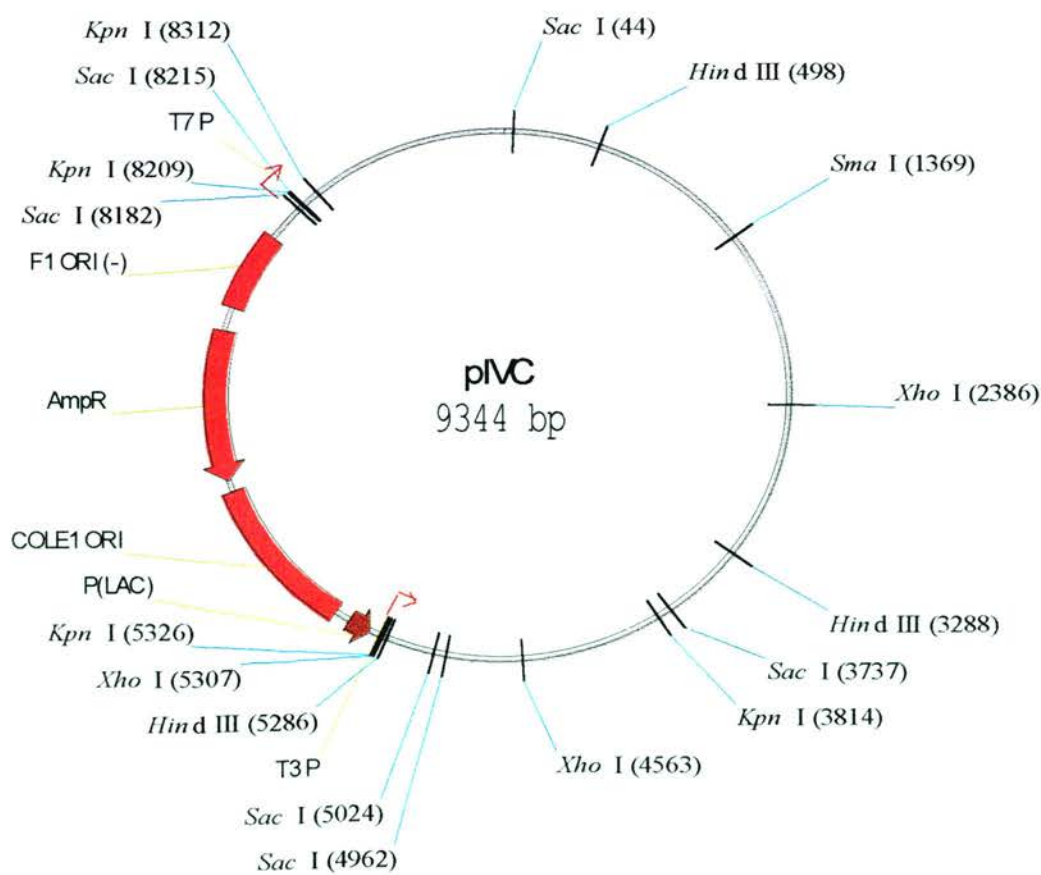
Taking this into consideration the SR PCR reaction was designed to generate a product that overlapped the cloned FX and F3K PCR products by a minimum of 40bp at both ends. The SR PCR reaction was carried out using a blend of high fidelity Taq polymerases (the Expand<sup>TM</sup> system, Boehringer Mannheim). The Pwo polymerase in this blend possesses a 3'-5' exonuclease proof-reading activity which has been reported to result in a 3-fold increased fidelity of DNA synthesis ( $8.5 \times 10^{-6}$  error rate) compared to normal Taq DNA polymerase ( $2.6 \times 10^{-5}$  error rate) (Barnes, 1994). This reduced error rate was significant as the SR PCR product includes exonic sequences whereas the FX and F3K products are composed of intronic sequences only. The pFXF3K plasmid was linearised by overnight digestion with the restriction enzyme Sma I. This digest was used as Sma I cleaves the pFXF3K plasmid at a unique site within the polylinker between the cloned PCR products (site indicated on Figure 4.5). The digest reaction was then electrophoresed through a 0.8% agarose gel and the linear 7.3kb plasmid band excised and purified from the gel. The SR PCR product was also prepared for IVC via gel electrophoresis and subsequent excision and purification of the 2.3kb band. Both of the linear DNA molecules were mixed and then used to transform competent bacteria of the strain DH5 $\alpha$  (Life Technologies). The transformed bacteria were plated onto L-amp plates (50 $\mu$ g/ml of ampicillin) and resultant clones screened by restriction digest analysis. *Hind III* digestion of the parental pFXF3K plasmid generates two cleavage products of 1998bp and 5392bp in size (Figure 4.6, lane 2). However, if the SR PCR product has been inserted into this plasmid via IVC, generating the plasmid pIVC, the *Hind III* cleavage pattern is altered and three cleavage products are seen (Figure 4.6, lane 3). To confirm that the SR PCR product had been correctly introduced into the pFXF3K plasmid in the predicted location, the pIVC plasmid was subjected to digestion with numerous restriction enzymes (Figure 4.6, lanes 5-8). All of these restriction digest analyses yielded products of exactly the sizes predicted from Figure 4.7 suggesting that the pIVC plasmid did contain a 6354bp continuous genomic clone spanning the 5' end of the murine p53 gene although this was not confirmed by direct DNA sequencing.

**Figure 4.7** – Plasmid Maps of the p53 Genomic Clone Contained in the pIVC4 Plasmid

A) A map of the 6354bp continuous genomic clone created by In Vivo Cloning



B) The pIVC plasmid



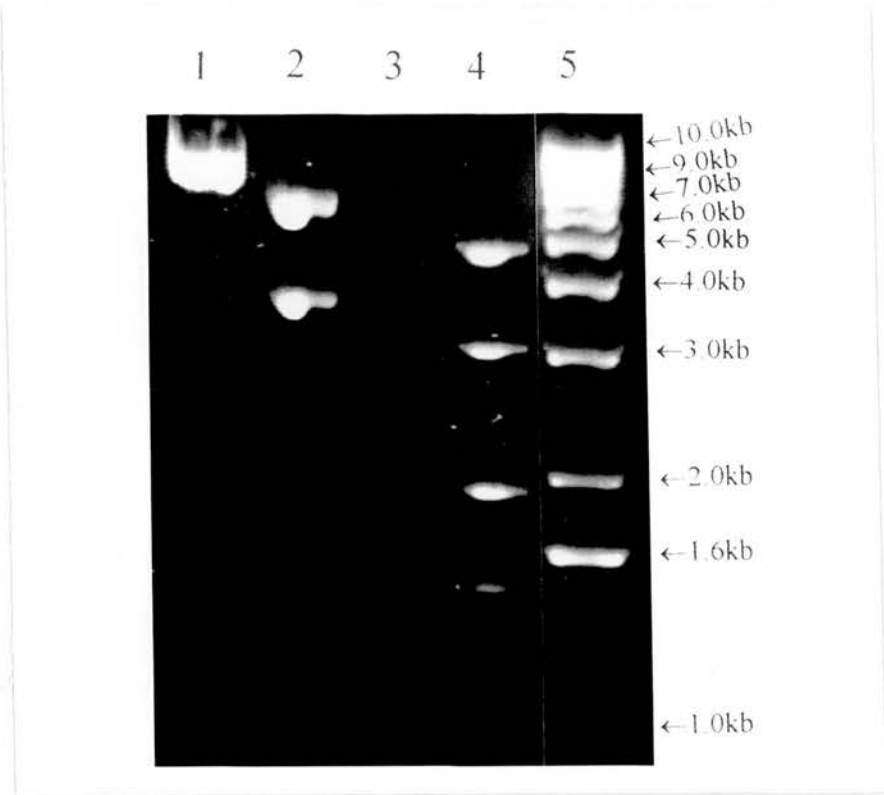
#### 4.4.2. Inserting the Floxed STOP Cassette into pIVC

To generate the complete targeting vector the final construction step was the insertion of the floxed STOP cassette from pFloxSTOP into pIVC. The pIVC plasmid was linearised using the restriction enzyme *Sma I* (Figure 4.8, lane 2). Digestion of pIVC with *Sma I* has several advantages, cleavage with *Sma I* generates blunt ends which facilitates insertion of the floxed STOP cassette and the unique cleavage site lies downstream of exon 1 within intron 1-derived sequences in the p53 genomic clone present in pIVC. As already discussed in Section 4.2.2, the desired insertion site of a floxed STOP cassette is downstream of the target promoter and within intronic sequences. The correct insertion and orientation of the floxed STOP cassette into pIVC was confirmed by *Sac I* restriction digest analysis (Figure 4.8, lane 5). The completed targeting vector, pIGTV, is shown in Figure 4.9. A linear representation of the p53 genomic clone containing the correctly inserted floxed STOP cassette is also shown in Figure 4.9.

#### 4.4.3. Testing pIGTV in BNN 132 Cells

Before the pIGTV vector was introduced into mammalian cells the ability of the vector to undergo Cre-mediated excisive recombination was tested using the bacterial strain BNN 132 (Clontech, see also Section 2.5.1.). Cultures of BNN 132 cells were grown and competent cells generated using a standard calcium chloride protocol (Sambrook et al, 1989). Competent BNN 132 bacteria were transformed with the pIGTV plasmid and plated onto LB-agar plates supplemented with the antibiotic ampicillin (50µg/ml). The predicted outcome of Cre-mediated recombination will be the generation of two plasmid species from the parental pIGTV plasmid. First, the pBluescript(BNN) plasmid which should be derived from the pBluescript backbone and contain the p53 genomic clone and one retained loxP site. Second, the pSTOP(BNN) plasmid which should be derived from the STOP cassette and contain the second loxP site (Figure 4.10). However, as the ampicillin resistance gene is present only in the pBluescript(BNN) plasmid only this species will be represented in clones produced from the transformation of BNN 132 cells after selection with ampicillin. These predicted results were confirmed by restriction

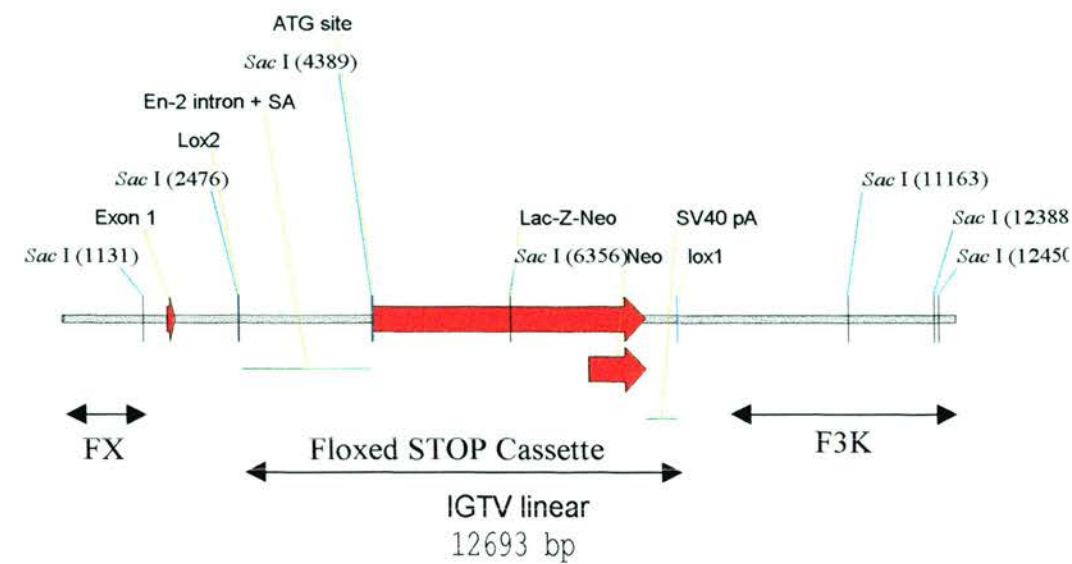
**Figure 4.8** – *Generation of pIGTV; Insertion of the Floxed STOP Cassette into pIVC4*



1% agarose gel with ethidium bromide. Lane 1, molecular weight markers. Lane 2, Sma I digestion of the pIVC plasmid generates one band of 9344bp. Lane 3, Sna BI digestion of pFloxSTOP produces two cleavage products of 3738bp and 6339bp. Lane 4, blank. Lane 5, sac I digestion was used to orientate the floxed STOP cassette present in pIGTV. The cleavage products shown above, 4807bp, 3158bp, 1967bp and 1913bp (which run as an unresolved doublet), 1345bp, 1225bp and 1173bp are those obtained when the floxed STOP cassette is inserted in the correct orientation as shown in Figure 4.9.

**Figure 4.9 – Plasmid Maps of the Inducible Gene Targeting Vector, pIGTV**

A) A linear representation of the p53 genomic clone and inserted floxed STOP cassette present in the pIGTV plasmid shown below.



B) The complete pIGTV vector. The relative positions of all Sac I cleavage sites are shown. This vector was linearised via digestion with Sac II, this site is also indicated.

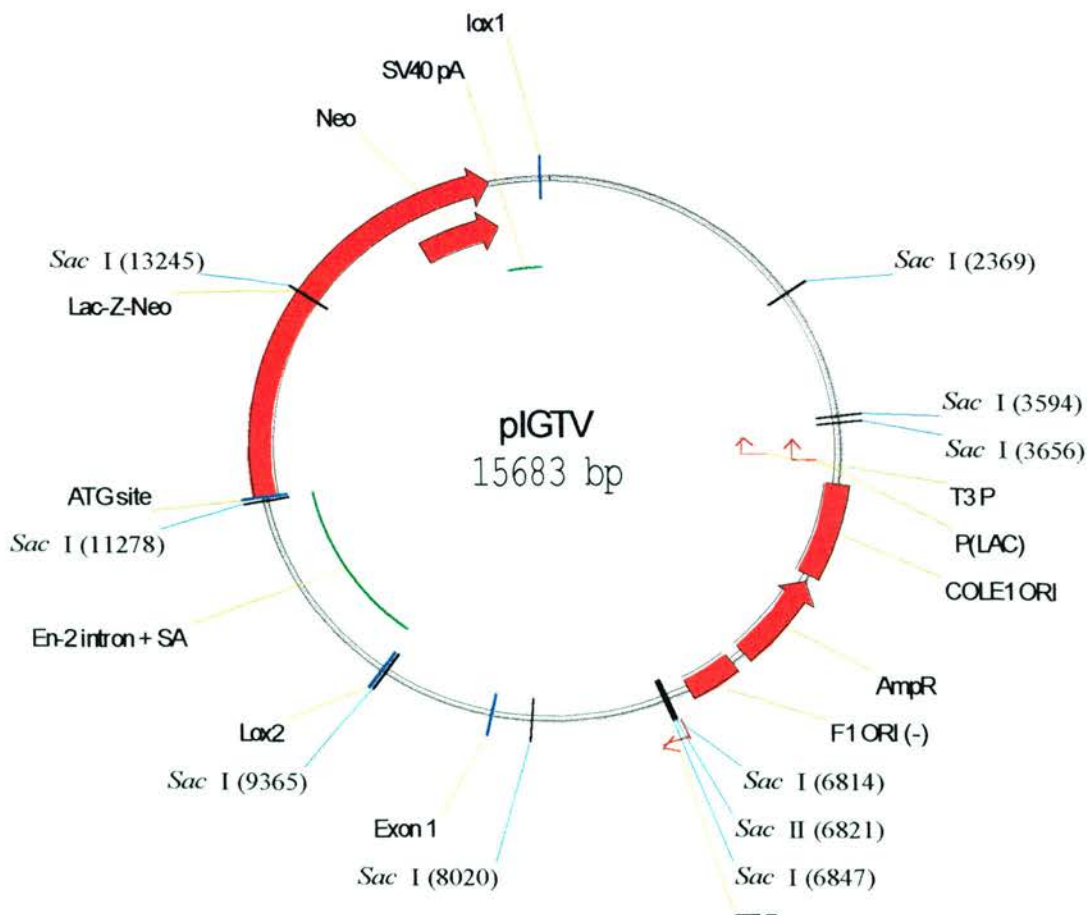
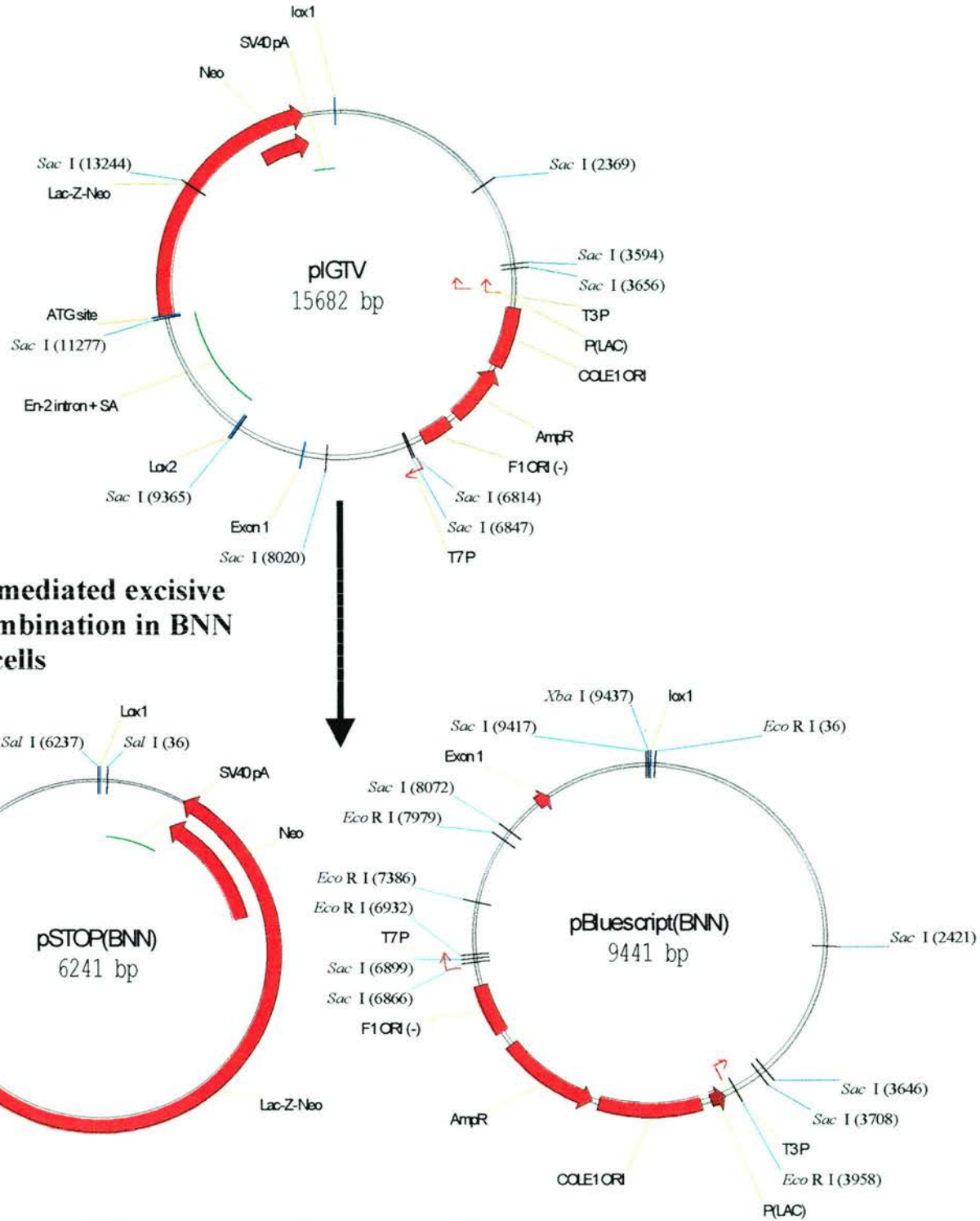


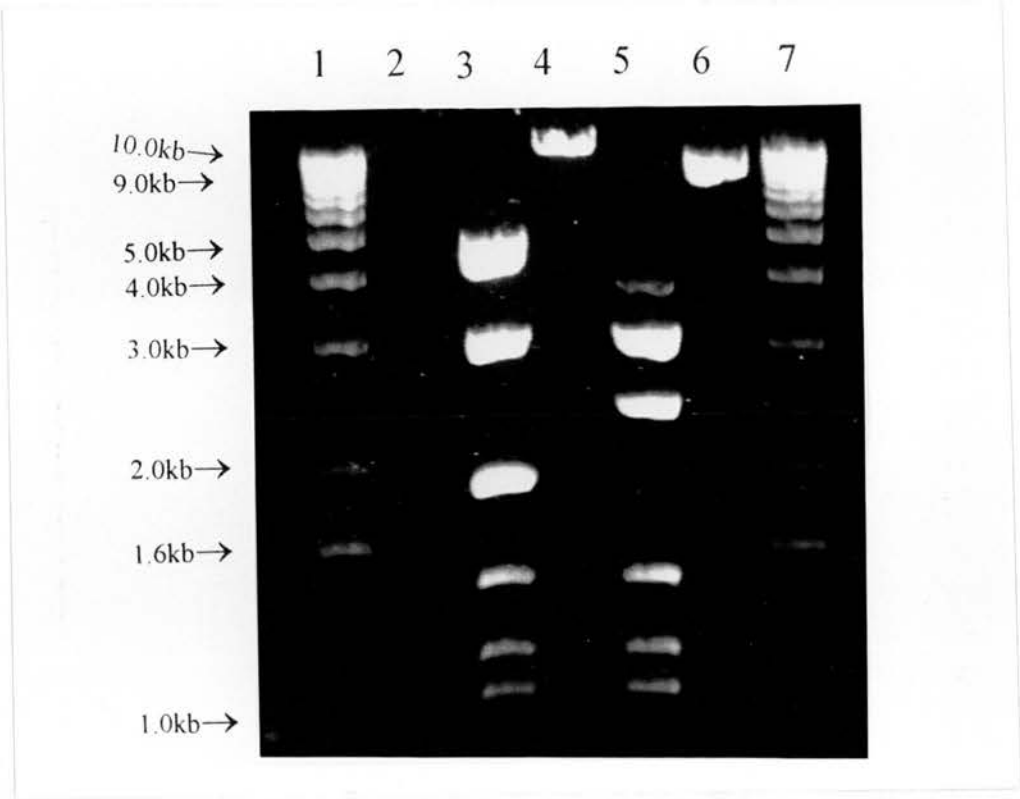


**Figure 4.10** – *The Outcome of Cre-mediated Excisive Recombination on the pIGTV Plasmid*



When the pIGTV plasmid is transformed into BNN 132 cells Cre-mediated excisive recombination occurs. The result of this is two plasmid species, the first, pSTOP(BNN), contains one loxP site and all of the STOP cassette. The second species, pBluescript(BNN), is derived from the plasmid backbone and p53 genomic clone and also contains one loxP site. Only pTAg(BNN) contains an ampicillin resistance gene so this should be the only plasmid species represented in clones arising from the transformation.

**Figure 4.11** – *Restriction Digest Analysis to Confirm pIGTV Has Undergone Cre-mediated Excisive Recombination*



1.0% agarose/ethidium bromide gel. Lane 1, molecular weight markers. Lane 2, blank. Lane 3, *Sac* I digestion of pIGTV. Cleavage with this enzyme generates nine digestion products, 4807bp, 3158bp, 1912bp and 1967bp (which run as an unresolved doublet), 1345bp, 1225bp, 1173bp, 62bp and 33bp bands, the last two of which are too small to be seen in the above gel. Lane 4, *Sal* I digestion of pIGTV generates a single cleavage product of 15682bp. Lane 5, *Sac* I digestion of the pBluescript(BNN) plasmid generates seven cleavage products of 3158bp, 2445bp, 1345, 1225bp, 1173bp, 62bp and 33bp. All but the latter two bands are visible above. Lane 6, *Sal* I digestion of pBluescript(BNN) generates a single cleavage product of 9441bp. Lane 7, molecular weight markers.

digest analysis of ampicillin resistant (Amp<sup>R</sup>) clones that arose from the transformation of BNN 132 cells with pIGTV plasmid (Figure 4.10).

#### **4.5. Summary**

The work described in the above sections represents the successful completion of the first three aims of this chapter. A continuous genomic clone spanning the 5' region of the murine p53 gene has been constructed, furthermore the floxed STOP cassette from the pFloxSTOP plasmid has been inserted into this clone generating the IGT vector pIGTV. Finally, the efficient Cre-mediated excisive recombination of this floxed STOP cassette from pIGTV has been demonstrated in BNN132 cells.

#### **4.6. Inducible Gene Targeting**

##### **4.6.1. Introducing pIGTV Into ES Cells**

The completed targeting vector, pIGTV, was linearised by digestion with *Sac II* (Figure 4.9B). The linear DNA was then introduced into ES cells by electroporation (300µF, 0.8Kv, time constant 0.1secs, Biorad Pulse Generator) and the cells selected in medium containing 200µg/ml of G418 (Southern & Berg, 1982). After 10-14 days clones were picked into individual wells. The clones were then grown up and divided into duplicate wells. Genomic DNA was prepared from one well while the duplicate sample of each clone was transferred into storage at -80°C. The genomic DNA from each clone was analysed by Southern blot to determine the mechanism of targeting vector integration, either random or via homologous recombination. This work is discussed in the following sections.

##### **4.6.2. The Screening Strategy**

A screening strategy is needed to allow the differentiation of ES cell clones in which pIGTV has integrated randomly from those clones in which represent insertion events mediated by homologous recombination. To determine which of these two outcomes has occurred a Southern blot-based strategy is required in which the wild type structure of the target locus can be differentiated from that of a correctly targeted locus. Ideally two screening strategies should be designed, one for each end of the

targeting vector to confirm that vector-derived sequences have indeed been inserted into the target locus by homologous recombination. The Southern blot strategy designed to identify ES cell clones in which the floxed STOP cassette had been introduced into intron 1 of the murine p53 gene is discussed below.

#### **4.6.2.1. Southern Blot Analysis**

The restriction enzyme used for Southern analysis of clones that arose from the electroporation of ES cells with linearised pIGTV was *Bst XI*. In the wild type p53 allele, digestion with *Bst XI* generates a 4894bp product whereas the digestion of the targeted allele is predicted to yield a 5699bp product. Both of these digest products share the same 3' sequences and it is to this region that the probe hybridises. The probe designed for use in this strategy was a 224bp PCR product amplified from within intron 1 of the p53 gene. Importantly, the intronic sequence from which the probe is amplified lies beyond the 3' end of sequences incorporated into the targeting vector.

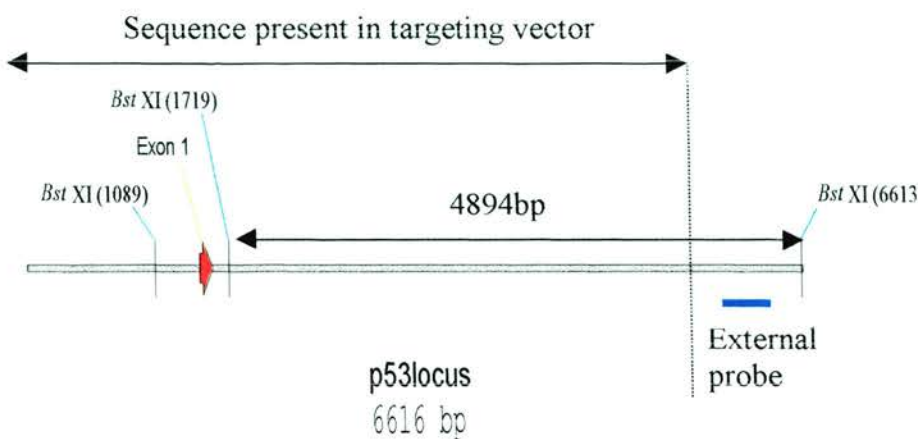
The PCR primers and reaction conditions were designed and optimised by Dr. S. Lyons (Lyons, 1999). The PCR product was then cloned into the commercial pCR 2.1 vector (Invitrogen) generating the plasmid pProbe. The p53 probe was excised from pProbe by digestion with the restriction enzyme *Eco RI*. The reaction mixture was then electrophoresed through a 2% agarose gel and the 241bp band containing the probe sequence was excised from the gel and the DNA extracted. Southern blots were hybridised with probe overnight, washed and then exposed to X-ray film for 10-14days at -80°C before developing (Kodak Hyperprocessor). A typical blot is shown in Figure 4.13.

#### **4.6.2.2. Targeting Frequency**

Over 200 G418<sup>R</sup> clones which arose after the electroporation of HM-1 ES cells with the linearised pIGTV vector were picked and expanded for further analysis. Genomic DNA prepared from individual clones was subjected to the Southern blotting regime described above. The numbers of clones with wild type or targeted

**Figure 4.12 – Southern Blot Screening Strategy for the Identification of Targeted Clones**

A) Structure of the exon1 and intron1 region of the wild type p53 genomic locus. The positions of the relevant *Bst* *XI* sites, boundary of targeting vector-derived sequences (dotted line) and probe (blue line) are all indicated.



B) Structure of the targeted locus after the floxed STOP cassette has been inserted into intron 1 of the p53 gene. As above the positions of the relevant *Bst* *XI* sites, extent of vector-derived sequences (dotted line) and probe (blue line) are all indicated. Note, the two diagrams are not at the same scale.

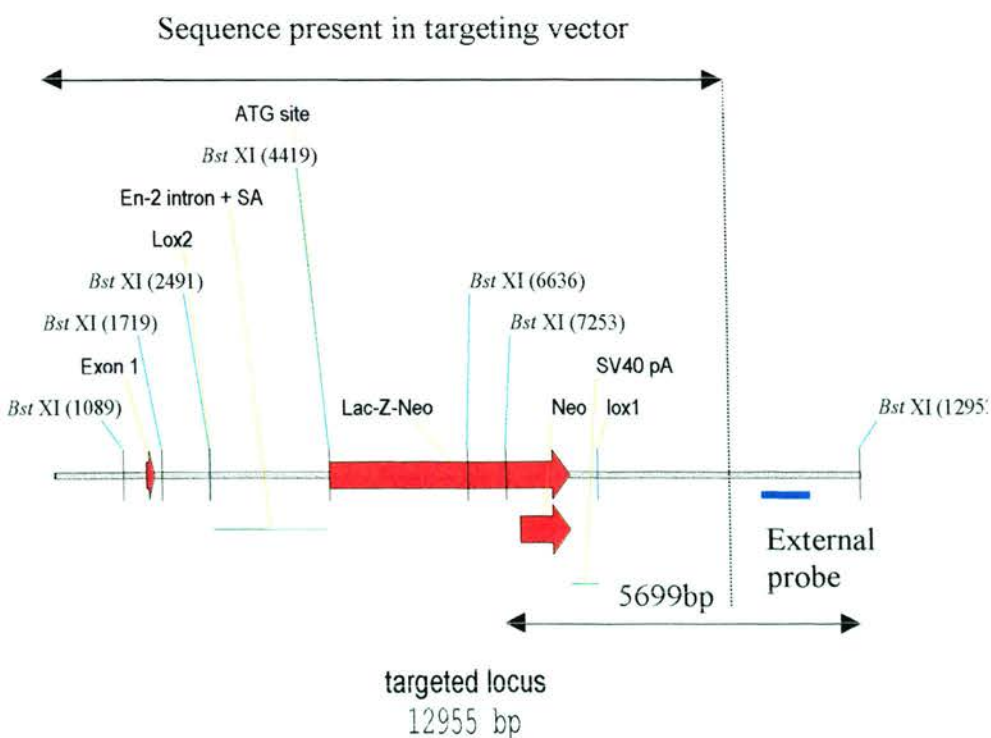
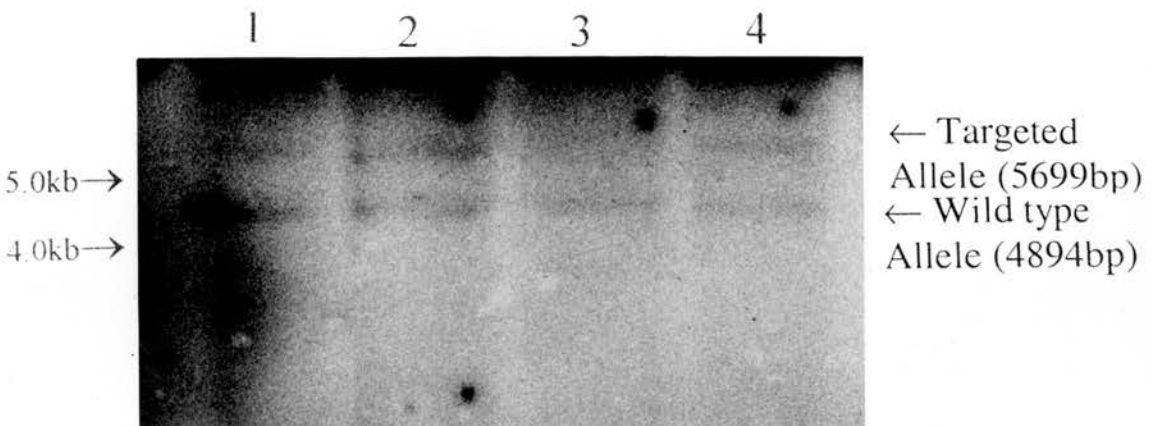


**Figure 4.13** –p53 Southern Blot Result



Photograph of autoradiograph obtained from *Bst*XI digested-genomic DNA transferred onto a filter and probed with a radiolabelled p53 probe. Lane 1, two bands are visible, the 4894bp digest product diagnostic of a wild type p53 allele and the 5699bp digest product diagnostic of a targeted p53 allele. Lane 2, as with lane 1. Lane 3, only one digest product is visible, the 4894bp digest product which indicates that both p53 alleles in this clone are wild type. Lane 4, as with lanes 1 and 2.



alleles were then scored and a targeting frequency of 48% observed (from 31 clones, 15 were scored as being correctly targeted). That is, in 48% of the G418<sup>R</sup> clones analysed the linear pIGTV vector had undergone homologous recombination rather than random insertion into the genome.

#### **4.6.3. Cre-mediated Excisive Recombination**

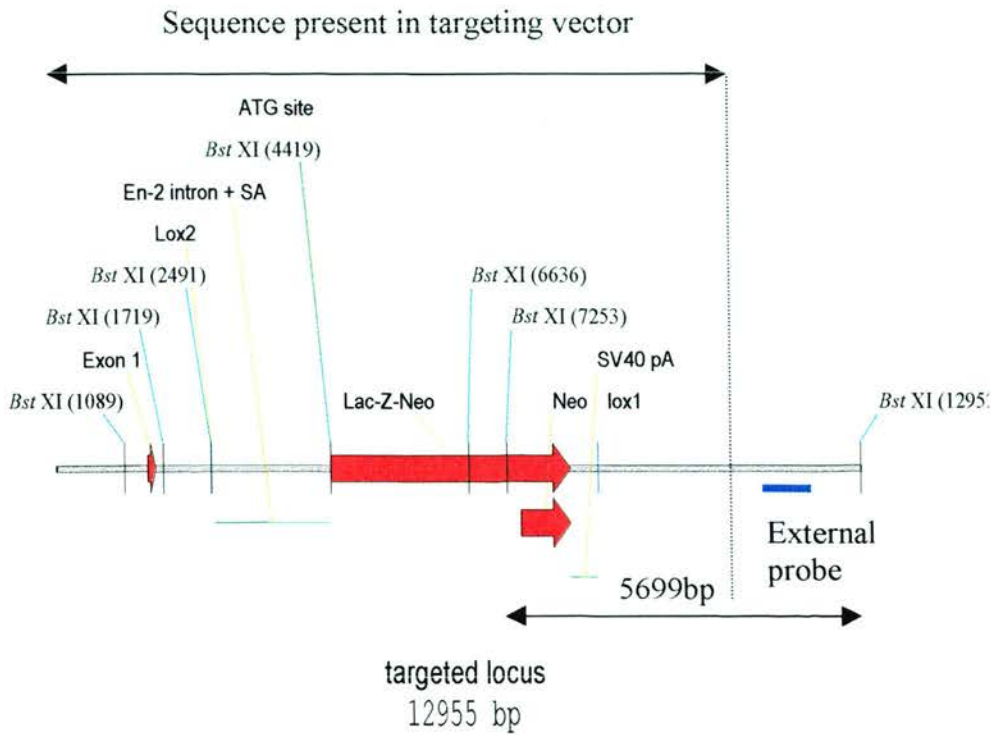
As mentioned in Section 4.5.2, it is desirable to design two Southern blot screening strategies, one for each end of the targeting vector to confirm that vector-derived sequences have indeed been inserted into the target locus by homologous recombination. However, the extreme 5' end of the murine p53 gene is composed of entirely unknown and unmapped sequence. For that reason it was impossible to obtain a probe which was external to the 5' of the targeting vector integration site. Furthermore, repeated attempts to map this region of the gene using internal vector sequences as Southern probes were unsuccessful (data not shown). Therefore, in an attempt to further characterise targeted clones identified by the Southern strategy discussed in Section 4.6.2.1, a recombination state-specific Southern blot strategy was designed. As shown in Figure 4.14, digestion of the correctly targeted allele with the restriction enzyme *Bst* XI yields a 5699bp product. However, if this allele has undergone Cre-mediated excisive recombination *Bst* XI digestion is predicted to yield a 4220bp product. Unfortunately, time constraints prevented the implementation of this Southern strategy and further characterisation of the clones identified in Section 4.6.2.1.

#### **4.7. Discussion**

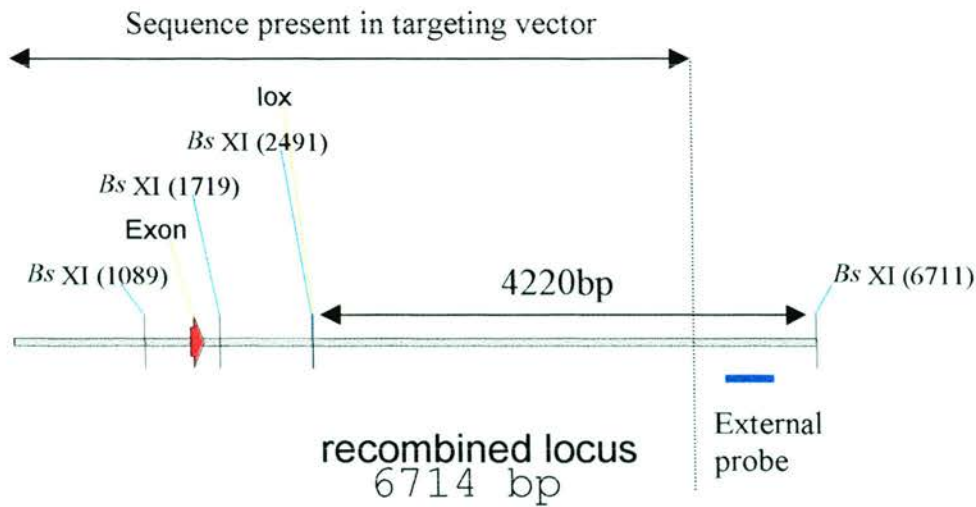
This chapter has focussed on the design and implementation of an inducible gene targeting strategy for the mouse p53 gene. The vast majority of IGT strategies are designed to permit the conditional inactivation of gene expression (see Figure 4.1). In an attempt to broaden the applications of Cre/loxP technology it was decided to develop an IGT strategy for the conditional activation of p53 expression, a floxed STOP approach. The application of floxed STOP technology to the murine p53 gene was also biologically relevant. p53 is the most frequently mutated tumour

**Figure 4.14** – *Recombination State-Specific Southern Blot Screening Strategy*

A) Structure of the targeted locus after the floxed STOP cassette has been inserted into intron 1 of the p53 gene. The positions of the relevant *Bst* XI sites, extent of vector-derived sequences (dotted line) and probe (blue line) are all indicated.



B) Structure of the targeted locus after the floxed STOP cassette has been inserted into intron 1 of the p53 gene via homologous recombination and then undergone Cre-mediated excisive recombination. As above the positions of the relevant *Bst* XI sites, extent of vector-derived sequences (dotted line) and probe (blue line) are all indicated. Note, the two diagrams are not on the same scale.



suppressor gene in all human cancers (Hollstein *et al*, 1994) and a variety of data indicate its central importance in tumourigenesis (reviewed in section 1.4, Chapter 1). However, relatively little is known about the biological consequences of restoring p53 function to a previously p53 null cell. For example, whether a tumour that arose in a p53 null mouse, would continue to survive if wild type levels of p53 expression were restored. This type of question is directly relevant when considering the potential of the p53 gene for use in gene therapy protocols and could be addressed using a floxed STOP-p53 mouse.

Numerous publications have reported the use of floxed STOP cassettes to regulate exogenous gene expression *in vitro* (reviewed in Chapter 2). In these examples the floxed STOP cassette is simply inserted between the promoter and target gene. However, floxed STOP cassettes can also be used to achieve conditional endogenous gene expression *in vivo*. With this aim in mind, there are two alternative floxed STOP cassette-insertion sites, within an intron directly downstream of the promoter, or within a more three prime intron (Figure 4.2). Both options are predicted to abolish target gene expression, although the use of a more three prime insertion site may result in a truncated protein product being expressed from the target locus. Because of the pleiotropic nature of p53 function the possible expression of truncated protein forms was regarded as undesirable. Therefore it was decided to attempt to introduce the floxed STOP cassette from the pFloxSTOP plasmid into intron 1 of the p53 gene, directly downstream of the endogenous promoter.

To achieve this, the first requirement was the isolation of a continuous genomic clone spanning the extreme 5' end of the mouse p53 gene. The failure to obtain such a clone after the screening of two genomic libraries resulted in the use of a PCR-based strategy. The successful generation of a PCR-derived 6.3kb genomic clone spanning the region of interest using an *In Vivo* Cloning strategy is reported. A potential drawback that must be considered when using a PCR-based strategy is the risk of introducing mutations into the amplified products. However, over 95% of the genomic clone obtained is composed of intronic sequences which contain no known

regulatory functions (reviewed in Section 1.4.1, Chapter 1). Furthermore, the SR PCR product, which contains exon 1 and the p53 promoter, was amplified using High Fidelity™ Taq polymerase (Boehringer Mannheim) which has a three-fold greater level of fidelity than standard Taq polymerases (Barnes, 1994). However, DNA sequencing was not undertaken so the possibility of introduced mutations in any of the three PCR products used cannot be ruled out.

The final step in the construction of an IGT vector was the insertion of the floxed STOP cassette from the pFloxSTOP vector into the p53 genomic clone to generate the vector pIGTV. Prior to introduction into ES cells this vector was shown to undergo efficient Cre-mediated excisive recombination in BNN132 cells.

The linearised pIGTV vector was then electroporated into passage 19 HM-1 ES cells. The cells were selected with the antibiotic G418 (Southern & Berg, 1982), resistance to this drug is encoded by the *neo* component of the  $\beta$ geo fusion gene. Importantly, the  $\beta$ geo gene is promoter-less so random integration of the linear pIGTV plasmid should not permit  $\beta$ geo expression. Theoretically, the majority of G418<sup>R</sup> clones that survive selection should represent homologous recombination-mediated insertion events of the pIGTV plasmid. In this situation the  $\beta$ geo gene should be integrated directly downstream of the endogenous p53 promoter and its expression regulated by this same promoter. Therefore, targeting strategies that use promoter-less selectable marker genes are predicted to yield high targeting efficiencies, a phenomenon that has been reported by other authors. For example, the targeted disruption of an endogenous gene, *Hprt*, using selection with a promoter-less *neo* gene has been demonstrated in ES cells with a targeting frequency of 67% (Doestchman *et al*, 1988). The use of an enhancerless *xanthine guanine phosphoribosyltransferase* (*gpt*) gene resulted in a targeting frequency 44% of the *gpt*<sup>+</sup> cells (Jasin & Berg, 1988) and the use of a promoter-less  $\beta$ geo gene for during the targeted disruption of the Oct-4 locus gave rise to a targeting efficiency of 70-80% (Mountford *et al*, 1994). The 48% targeting frequency obtained with the pIGTV vector described in this chapter is comparable with these reports.

The work described in this chapter has reported the successful completion of all of the original aims laid out in Section 4.3. However, the direction of future work is obvious. First, the completion of the Southern analysis detailed in Figure 4.13 on all clones identified as being correctly targeted at the 3' end of the allele. Second, the microinjection of correctly targeted ES cell clones into blastocysts and the breeding of any subsequent chimaeric offspring to establish a targeted mouse line. Although time constraints prevented the completion of these steps within the duration of this research project they will hopefully be completed by other research workers.

# **Chapter 5**

## **Discussion**



## Chapter 5

### Discussion

This thesis has examined the feasibility of using floxed STOP-based strategies to achieve conditional gene expression *in vitro* and *in vivo*. I have reported the successful design, construction and testing of a novel floxed STOP cassette. The ability of the cassette to regulate the expression of two marker genes, the EGFP gene and the p53 cDNA, has been tested *in vitro*. This work succeeded in demonstrating a two-fold upregulation of EGFP transcription and a low level of p53 upregulation after Cre-mediated excisive recombination of the floxed STOP cassette.

Furthermore, an inducible gene targeting strategy was designed and implemented to permit the insertion of the floxed STOP cassette into intron 1 of the endogenous murine p53 gene. Unfortunately, despite the identification of correctly targeted ES cell clones, time constraints prevented the generation of a targeted mouse line.

Finally, a new histochemical detection protocol was optimised permitting an examination of SA- $\beta$ gal expression in primary MEFs. However, during this work a number of problems were encountered.

These included, the failure to observe upregulation of EGFP expression at the protein level after Cre-mediated excisive recombination of the floxed STOP cassette from the plasmid pFloxEGFP. Four potential explanations were considered in an attempt to rationalise this observation. First, that the pFloxEGFP transgene had been inactivated by methylation during the generation of the FE13 cell line. However, this possibility was eliminated by RT-PCR data that demonstrated that the introduced EGFP gene was transcriptionally active within FE13 cells. The second explanation was that a mutation had arisen spontaneously in the EGFP coding sequence during the construction of the pFloxEGFP vector. This option could not be ruled out. The third possibility was that AdCre-infection was occurring at such a low efficiency that the level of EGFP mRNA and therefore protein, were below that detectable using either UV microscopy or FACS detection systems. This option was ruled out by a

repeat infection of FE13 ES cells using a new and more accurately titred AdCre stock that also failed to induce detectable EGFP expression. The fourth and final possibility was the so-called Reverse loxP Problem, an idea first proposed last year (Sauer, 1998). This author theorised that the presence two ATG codons in the spacer region of a loxP site in the reverse orientation could interfere with downstream gene expression. It should be noted that this idea is purely theoretical and has never been demonstrated in an experimental system.

In conclusion, the failure to observe EGFP expression in the pFloxEGFP experimental system may be due to the acquisition of a point mutation within the EGFP coding sequence or the “Reverse loxP Problem” discussed above. However, by ensuring that any loxP sites retained after Cre-mediated recombination are in the forward orientation the potential problem can be avoided altogether. It was for this reason that the pICDP(for) plasmid discussed in Chapter 3, was rebuilt using the floxed STOP cassette derived from the pFloxSTOP(for) plasmid.

The second problem encountered with the pFloxEGFP experimental system was leakiness, i.e., it was possible to detect expression of EGFP mRNA in the absence of Cre-mediated excisive recombination. Although other authors have theorised that leakiness from floxed STOP cassettes is due to spontaneous homologous recombination between loxP sites (Agah *et al*, 1997; Anton & Graham, 1995), this phenomenon was not detected with the pFloxEGFP plasmid. The most probable explanation is that rather than transcription splicing onto the splice acceptor within the STOP cassette, splicing around occurred, thereby permitting EGFP expression. It should be noted that both the observation of leaky target gene expression, and the failure to upregulate target gene expression after floxed STOP cassette excision are not without precedent in the literature. For example, a recent meeting abstract produced by the laboratory of Prof. A. Berns detailed numerous problems with a floxed STOP-LacZ transgenic mouse strain, including failure to upregulate LacZ gene expression after Cre-mediated excision of the floxed STOP cassette (Krimpenfort *et al*, 1998). Furthermore, two independent research groups have

reported leaky expression from a floxed STOP-luciferase vector (Agah *et al*, 1997; Anton & Graham, 1995).

The other challenge encountered during the work discussed in Chapter 2 was the development of a Cre-delivery strategy. The first approach tested was the transient transfection of cells with Cre-encoding plasmids. However, variations in transfection efficiencies and the failure to detect Cre-mediated recombination curtailed this line of investigation. Nonetheless, as part of this work a novel ES cell differentiation state-specific enhancer element was characterised (Fiskerstrand *et al*, 1999). The second Cre-delivery strategy investigated was the use of replication-defective recombinant adenoviridae (Anton & Graham, 1995). It was demonstrated that undifferentiated ES cells are resistant to adenoviral infection, confirming previous reports (Aladjem *et al*, 1997), although efficient infection of differentiated ES cells was achieved. Having optimised an adenovirus-infection protocol, the next step was to obtain reproducible infection efficiencies. Variations in adenoviral infection efficiencies were probably due to variations in viral titre, a problem that was almost certainly responsible for some of the observed variations in marker gene expression reported in Chapter 2. However, the sensitivity of adenoviral stocks to storage conditions is well documented (for example see, Croyle *et al*, 1998) and the majority of these problems were overcome by small alterations to laboratory practice. These included the aliquoting of viral stocks and increasing the accuracy of titration experiments. These changes facilitated not only the more successful application of recombinant adenoviral technology at other points in this thesis, but also by other members of the laboratory.

As already mentioned the data obtained from the pFloxEGFP plasmid was used to redesign and rebuild the pICDP(for) plasmid. To avoid the possibility of the Reverse loxP Problem preventing expression of the p53 cDNA, the plasmid was rebuilt so that after Cre-mediated excisive recombination the single retained loxP site was in the forward orientation. The next step was to introduce the pICDP(for) plasmid into cells. The most significant factor in the selection of the cells to be transfected was

that they should be p53 null. Therefore, the predicted Cre-mediated upregulation of p53 expression from the introduced cDNA should be readily detectable by immunohistochemistry. The chosen cells were primary murine embryonic fibroblasts (MEFs) that were isolated from embryos which contained a targeted mutation in the endogenous p53 gene (Purdie *et al*, 1994).

It was necessary to optimise a protocol for the stable transfection of MEFs as this had not previously been reported. Generally, the short lifespan *in vitro* of wild type MEFs had precluded prolonged selection experiments. However, the increased lifespan of p53 null MEFs permitted prolonged selection and the isolation of stable transformants. Two transfection methods were tested on p53 null MEFs, electroporation and calcium phosphate precipitation. No clones were obtained after the electroporation of p53 null MEFs with linearised pICDP(for) plasmid, and success was only achieved using a modified calcium phosphate transfection protocol (Chen & Okayama, 1987). The central aim of the work with the pICDP(for) plasmid was to attempt to develop a new tool for the conditional expression of p53, thereby facilitating an analysis of p53 function. Therefore by developing and optimising new MEF transfection methods the long-term aim was to permit the investigation of the role of p53 in replicative cellular senescence.

However, before this work could begin it was necessary to identify a murine senescence-specific biomarker. This goal was achieved within the duration of the project after the development of a histochemical detection system permitting the visualisation of murine senescence-associated  $\beta$ gal (SA- $\beta$ gal) expression. The existence of SA- $\beta$ gal was first demonstrated in human cells where SA- $\beta$ gal positivity displayed an inverse correlation with DNA synthesis as detected by [ $^3$ H] thymidine labelling (Dimri *et al*, 1995). However, this thesis reports the first description of SA- $\beta$ gal expression in mouse cells and the first analysis of SA- $\beta$ gal expression in both wild type and p53 null MEFs over the duration of a continuous culture experiment. The only significant difference in the stain solution developed in this thesis and that developed by Dr. J. Campisi (Dimri *et al*, 1995) is the magnesium ion concentration,

the murine SA- $\beta$ gal stain reported here contains a 100 times greater concentration of magnesium. This ion is known to function as an essential cofactor for the  $\beta$ -gal enzyme and the difference between the two stains may represent an underlying biochemical difference in the magnesium requirements of the murine and human forms of  $\beta$ -gal.

Despite the successful isolation of pICDP(for)-transfected MEF cells and the identification of murine SA- $\beta$ gal, further problems were encountered. First, when pICDP(for)-transfected MEFs were infected with AdCre, or the control DL70 virus, a recombination state-specific PCR failed to detect the presence of any recombined plasmid structures. As episomal AdCre molecules were detected in the cells, and the integrity of the loxP sites within the pICDP(for) plasmid had been confirmed by DNA sequencing, recombination was almost certainly occurring in these cells.

Two contributory factors may have been responsible for the failure to detect Cre-mediated excisive recombination. First, small variations in AdCre titre and subsequent infection efficiencies, therefore, all cells which contained productive insertion events may not have been infected by AdCre and second, limitations of the transfection system. That is, the random linearisation events that occur during calcium phosphate precipitation which render a large proportion of integration events non-productive. Due to the size and complexity of the pICDP(for) vector, random linearisation events are predicted to have generated non-productive insertion events in 76% of clones. However, at the time of this work, no publications had reported the stable transfection of primary MEFs and the successful transfection reported here was only accomplished using a modified calcium phosphate transfection protocol and could not be achieved using an alternative strategy *in vitro*. As discussed in Chapter 3, an obvious solution to the problem of MEF transfection was the generation of pICDP(for)-transgenic mice strains. Unfortunately, this was outwith the temporal and financial constraints of this research project.

The second problem experienced with the pICDP(for) system was the low level of p53 upregulation observed after Cre-mediated recombination . Because the pICDP(for) plasmid was specifically rebuilt to avoid the potential Reverse loxP Problem, this not a valid explanation for these data. Furthermore, it is improbable that the p53 cDNA had acquired a mutation during the construction of pICDP(for) as a low frequency of p53 upregulation was successfully detected by immunohistochemistry. This observation, and that of the failure to amplify the recombination-specific PCR product are linked. Although contributing factors such as the survival of non-transfected MEFs and variations in AdCre titre I believe that both may best be explained as limitations of the transfection system. That is, only pICDP(for) plasmids which have undergone productive insertion events give rise to recombined plasmid structures which both permit the upregulation of p53 expression, and the amplification of the recombination-specific PCR product. It may be that a significantly smaller percentage than the predicted 24% of clones, represented productive insertion events. However, the absence of scientific literature on this field, and the small amount of experimental material available, which prevented Southern analysis of transfected MEFs, makes it very difficult to prove this theory.

The final area of research was an examination of the feasibility of using floxed STOP cassettes to regulate endogenous gene expression *in vivo*. As part of this work an inducible gene targeting strategy was applied to the murine p53 gene. A targeting vector, pIGTV, was constructed to permit the insertion of a floxed STOP cassette into intron 1 of this gene via homologous recombination in ES cells. The long-term aim of this work was to use any targeted ES cells for the generation of mice that carried the floxed STOP cassette within intron 1 of their p53 gene. Such mice could then be used to investigate the biological consequences of restoring p53 function to a previously null cell, for example, as part of a study assessing the efficacy of p53-based gene therapy protocols.

Using a Southern blot-based screening strategy successfully targeted ES cell clones were identified and a targeting efficiency of 45% was recorded. Unfortunately, the



injection of targeted ES cells into blastocysts and subsequent generation of chimaeric progeny were not completed within the time limits of this research project. As germ-line chimaeras and targeted mice were not obtained an investigation of floxed STOP-mediated regulation of p53 gene expression *in vivo* could not be completed.

Only one other paper has reported the use of an analogous system, a flrtd STOP cassette, to regulate gene expression *in vivo* (Meyers *et al*, 1998). However, these authors only detected an approximate 50% reduction in gene expression from the targeted allele indicating that the flrtd STOP cassette was not working at maximal efficiency. The STOP cassette used by Meyers *et al*, did not contain a splice acceptor and this may have been responsible for the significant frequency of splicing around observed. It would have been interesting to compare this level of leaky expression to that observed after the insertion of the floxed STOP cassette from the pFloxSTOP plasmid into intron 1 of the p53 gene.

The work described in this thesis has explored the feasibility of using Cre/loxP-based technologies to regulate gene expression both *in vitro* and *in vivo*. By overcoming numerous technical problems the limitations of this novel technology have been explored. Although the basic floxed STOP strategy is theoretically straightforward, this work has highlighted the potential pitfalls. In conclusion, floxed STOP-based approaches to achieve conditional gene expression offer an extremely exciting opportunity. However, this technology is not as straightforward as a cursory glance at the literature might indicate, and should be approached with substantial thought and consideration.

# **Chapter 6**

## **Materials and Methods**

## Chapter 6

### Materials and Methods

#### 6.1. Manipulation of DNA

##### 6.1.1. Transformation of Bacteria With Plasmid DNA

A 5µl aliquot of Epicurian Coli XL-2 Blue ultracompetent cells ( $5 \times 10^9$  cfu/µg pUC18 DNA, Stratagene) was removed from storage at  $-70^{\circ}\text{C}$  and thawed on ice. Plasmid DNA was added directly onto the cells and then mixed by pipetting. The cells and the DNA were incubated on ice for 30 minutes, heat shocked at  $42^{\circ}\text{C}$  for 45 seconds and returned to ice for a further 2 minutes. After which 80µl of Luria Broth (LB) was added and the tube incubated at  $37^{\circ}\text{C}$  for 1 hour in an orbital incubator at 225rpm. The transformed bacteria were then plated onto LB-agar plates containing appropriate antibiotics to select for transformants.

<b>Luria Broth:</b>	Bactotryptone	10g/l
	Yeast Extract	5g/l
	NaCl	0.17mM
	Made up with ddH <sub>2</sub> O and autoclaved, supplemented with 1.2% w/v Bactoagar for plates	

##### 1000 X Antibiotic Selection Concentrations:

Ampicillin	50mg/ml in H <sub>2</sub> O	Stored at $-20^{\circ}\text{C}$
Kanamycin	10mg/ml in H <sub>2</sub> O	Stored at $-20^{\circ}\text{C}$

Note, when transforming ligation reactions (Section 7.1.7) 15µl aliquots of ultracompetent cells were used and mixed with no more than 1.5µl of a 20µl ligation reaction mix.

##### 6.1.2. Calcium Chloride Preparation of Competent BNN 132 Cells

The following protocol using calcium chloride to make competent bacteria is based on the standard method (see Sambrook *et al*, 1989). A 5ml starter culture of LB and 50µg/ml of kanamycin was inoculated with a single BNN 132 cell clone and grown

overnight at 37°C in an orbital incubator at 225rpm. The following day 100µl of this culture was added to 100mls of LB-Kanamycin and grown at 37°C, 225rpm until the OD<sub>600</sub> was approximately 0.3 units. The culture was then cooled to 4°C before being split between two 50ml Oakridge tubes and spun down at 4000rpm for 10 minutes. The supernatant was removed and the pellets placed on ice. The bacteria were kept on ice during resuspension of the pellet in 10mls of ice cold sterile 0.1M CaCl<sub>2</sub>. The 0.1M CaCl<sub>2</sub> used was prepared freshly each time from a 1M stock stored at -20 °C. The bacteria were then centrifuged at 2,500xg for 10 minutes, the supernatant removed and the pellet resuspended in 1ml of CaCl<sub>2</sub>. At this point the cells were divided into 200µl aliquots which could be used directly for transformation. Alternatively aliquots could be stored at 4°C for up to 24 hours but these cells did not store well at -70°C.

**6.1.3. Preparation of Bacterial Glycerol Stocks**

A clone picked from a plate of transformed bacteria was used to inoculate 5ml of LB (supplemented with appropriate antibiotics) and grown at 37°C overnight in an orbital incubator. Cells were harvested by centrifuging for 3 minutes at 13,000rpm in a microfuge and the pellet resuspended in 750µl of sterile 50% LB: 50% glycerol. The bacteria were transferred in CryoTube™ vials (Nunc) and stored at -70°C.

**6.1.4. Small Scale Preparation of Plasmid DNA**

This “miniprep” method is a modification of the procedures described in Sambrook *et al.* (Sambrook *et al.*, 1989). A single bacterial clone was picked from an LB-agar plate using a sterile P200 pipette tip. The clone was then transferred into a Falcon 2059 tube containing 5 ml of LB supplemented with appropriate antibiotics and incubated in an orbital incubator (225rpm) at 37°C overnight. The following day the cells were harvested by centrifugation for 2 minutes at 10,000xg in a microfuge. The supernatant was removed and the pellet resuspended in 200ul of Solution 1.

<b>Solution 1:</b>	Tris-HCl, pH7.5	50mM
	EDTA	10mM
	RNase A	100mg/ml

The cells were then lysed by the addition of 200µl of Solution 2.

<b>Solution 2:</b>	NaOH	0.2M
	SDS	1.0%

The lysis reaction was then neutralised with 200ul of Solution 3.

<b>Solution 3:</b>	Potassium acetate, pH 4.8	1.32M
--------------------	---------------------------	-------

A protein precipitate became visible after Solution 3 was added and this was removed by centrifugation for 3 minutes in a microfuge, the supernatant was then transferred to a fresh tube. Any proteins remaining in the sample were removed by the addition of 2 volumes of a 50% phenol: 48% chloroform: 2% isoamyl alcohol mix. The samples were mixed by inversion and then centrifuged for a further 3 minutes. After centrifugation the sample was present in two phases, the aqueous top layer was removed and the DNA precipitated by the addition of 2 volumes of ethanol and 0.1 volumes of 10M Ammonium acetate. During the precipitation the samples were stored at -70°C for 20-30 minutes and then centrifuged at 10,000g, 4°C for 20 minutes. The pellet was rinsed twice in 100µl of 70% ethanol, air-dried and finally redissolved in 20ul of TE pH 8.0 (store DNA at -20°C) .

<b>TE Buffer:</b>	Tris-HCl, pH 8.0	10mM
	EDTA	1mM

### 6.1.5. Large Scale Preparation of Plasmid DNA

The large-scale isolation of plasmid DNA was carried out using a Plasmid Maxi Kit (QIAGEN) according to the manufacturers instructions. A flask containing 100ml of LB, supplemented with the appropriate antibiotics, was inoculated with bacteria containing the chosen plasmid. Maxipreps can be inoculated using bacteria from glycerol stocks (Section 6.1.3), miniprep cultures (Section 6.1.4) or with individual

clones from LB-agar plates. The bacteria were then grown for 12- 16 hours in an orbital incubator. The following morning the cells were harvested by centrifugation at 2,500xg for 10 minutes at 4°C (Sorvall GSA rotor, Centrikon H-401B). The cells were resuspended and lysed just as for the miniprep method (Section 7.1.4) and the protein precipitate was removed by centrifugation at 20,000xg for 30 minutes at 4°C (Sorvall GSA rotor, Centrikon H-401B). The need for an organic extraction was avoided by adding the supernatant directly onto a QIAGEN-tip that contains a DNA-binding resin. The QIAGEN-tip column and bound DNA were then washed twice before the DNA was eluted and precipitated by the addition of 0.7 volumes of room temperature isopropanol. The sample was then centrifuged immediately at 16,000xg for 30 minutes at 4°C (Sorvall SS-34 rotor, Centrikon H-401B). The DNA pellet was washed once in 5ml of 70% ethanol, air-dried for 5 minutes and finally resuspended in 0.5 ml of TE and stored at -20°C.

#### **6.1.6. Restriction Digest Analysis of Plasmid DNA**

Depending on the downstream applications planned varying amounts of DNA were digested. For example less than 1µg of DNA would be digested when analysing miniprep DNA whereas up to 100µg would be used in some applications, such as electroporation (Section 6.2.6). In all cases a suitable amount of DNA was mixed with 0.1 volumes of 10X reaction buffer (supplied by the manufacturer) and 0.1 volumes of 10X Bovine serum albumen (10X BSA at 1mg/ml). Finally, 0.1 volumes of restriction endonuclease were added to the reaction mix and any remaining volume was made up with ddH<sub>2</sub>O. The digests were then incubated for 1-24hrs at the temperature recommended by the manufacturer (in all cases, New England Biolabs). To visualise digest patterns samples were run out on agarose gels.

#### **6.1.7. Agarose Gel Electrophoresis of DNA**

Agarose gel electrophoresis can be carried out using gels that contain varying amounts of agarose depending on the size of the DNA molecules to be resolved. All gels were prepared identically, an appropriate weight of agarose was added to 1X TBE, for example, 1g in 100mls 1X TBE to produce a 1% gel. The agarose/1X TBE



mixture was then heated in a microwave for 2-3 minutes. A small amount of the fluorescent dye ethidium bromide (10mg/ml) was added directly to the liquefied gel mix and the gel then poured into a casting tray.

<b>10X TBE Buffer:</b>	Tris base	108g
	Boric acid	55g
	0.5M EDTA, pH 8.0	40ml
	(Made up to one litre)	

Samples to be run were mixed with Orange G loading buffer and then loaded directly into the gel. Molecular weight markers, for example, 1kb Ladder (Life Technologies) were also diluted in identical loading buffer and loaded into the gel. Electrophoresis was carried out in 1X TBE at 50-100V.

<b>Loading Buffer:</b>	Orange G	0.35% (w/v)
	Sucrose	30% (w/v)

#### **6.1.8. Extraction of DNA Fragments From Agarose Gels**

The QIAEX II Gel Extraction Kit (QIAGEN) was used for the purification of DNA fragments from agarose gels. DNA was digested with appropriate restriction endonucleases, after the digest had gone to completion the sample was run out on an agarose-TBE gel containing ethidium bromide. The bands were visualised quickly with UV light (Herolab, gel documentation equipment) and excised from the gel with a scalpel. The gel slice was then weighed and an appropriate volume of solubilisation buffer and DNA-binding resin were added to the sample according to the manufacturers instructions. After solubilisation and adsorption of the DNA to the resin the sample was centrifuged at 10,000g for 30 secs. The resin pellet was washed three times and then air-dried for 15 minutes. To elute the DNA, the pellet was resuspended in 20µl of water and incubated at room temperature for 5 minutes before centrifuging at 10,000g for 30 secs. The purified DNA was present in the supernatant. DNA samples extracted from gels in this manner were stored at -20°C.

**6.1.9. DNA Ligation**

To ligate an insert into a vector differing ratios of both DNA fragments were mixed together, see below (Table 6.1). The exact yield of each of these components was never precisely quantified but for most ligations was between 10-50ng/μl.

**Table 6.1. Relative proportions of vector and insert DNA in standard ligation reactions**

Tube	Vector DNA/μl	Insert DNA/μl	Water/μl
IO	0	6	14
V2	2	6	12
V4	4	4	12
V6	6	2	12
V0	6	0	14

The IO tube is included as any colonies that arise from the transformation of this ligation reaction must represent plasmid backbone contamination of the insert. This can become a particular problem when large fragments are being inserted into smaller vectors. The V0 tube is included to provide a guide to the level of background due to vector recircularisation occurring, this can be dramatically reduced by treating the linear vector DNA with Shrimp Alkaline Phosphatase (Section 6.1.10). The total volume of all the reaction mixes was 20μl, this was then added directly into a tube of dehydrated Ready-To-Go™ T4 DNA ligase (Pharmacia Biotech). The ligation reaction was incubated at room temperature for 5 minutes, mixed by gentle pipetting and then transferred to a 16°C water bath for 30 minutes. After this time the ligation is complete, the ligase can be inactivated by heating to 70°C for 10 minutes and the sample used to transform bacteria.

<b>Ready-To-Go T4 DNA ligase:</b>	
FPLCpure™	6 Weiss units
T4 DNA ligase	
Tris-HCl (pH 7.6)	66mM
MgCl <sub>2</sub>	6.6 mM
ATP	0.1 mM

Spermidine	0.1 mM
Dithiothreitol	10 mM
(End concentrations when diluted in 20 µl)	

### 6.1.10. Dephosphorylation of Vectors

The removal of 5' terminal phosphate groups from linearised vector DNA prevents vector recircularisation in a ligation reaction. This was achieved by incubating the DNA with 1 unit of Shrimp Alkaline Phosphatase (SAP, United States Biochemical) for a minimum of 30 minutes at 37°C. The SAP was added directly into the restriction digest reaction as it is compatible with most enzyme buffers and will be removed in the subsequent gel purification of the vector DNA. Alternatively, linear DNA can be SAP treated after gel extraction. In the absence of any restriction enzyme reaction buffer, such as after the DNA has been extracted from a gel and resuspended in ddH<sub>2</sub>O, the SAP reaction should be carried out in the presence of 0.1 volumes of 10X SAP reaction buffer.

#### 10X SAP Reaction Buffer:

Tris-HCl, pH 8.0	200mM
MgCl <sub>2</sub>	100mM

It is crucial to ensure that all SAP activity is removed before a treated DNA sample is used in a ligation reaction otherwise other reaction components could also be dephosphorylated preventing efficient ligation. This was achieved by incubation of SAP reaction mixtures at 65°C for 10 minutes.

### 6.1.11. Blunting 3' and 5' Overhangs of Linear DNA

#### 6.1.11.1. Klenow Reaction

The large fragment of DNA polymerase I, Klenow enzyme (United States Biochemical), retains 5' to 3' polymerase activity but lacks any exonuclease activity. This polymerase was used to blunt 5' overhangs of DNA generated by restriction enzyme cleavage when needed. The enzyme (1-5 units, depending on reaction volume) and 0.1 volumes of 0.5mM dNTP mix can be added directly to a restriction

digest and incubated at 37°C for 30 minutes. The blunted DNA sample was then run out on a gel to check no degradation had occurred. If the blunted DNA was to be used in subsequent ligations the correct size band was excised from the gel, purified (Section 6.1.8.) and SAP treated if necessary.

**6.1.11.2. T4 DNA Polymerase**

T4 DNA polymerase catalyses the synthesis of DNA in the 5' to 3' direction so, like Klenow fragment, can be used to fill in 5' overhangs. However, T4 DNA polymerase also has a 3' to 5' exonuclease activity that will remove any 3' overhangs generated by certain restriction enzymes to leave blunt ends. As with Klenow, the enzyme and other reaction components were added directly to restriction digests after they had gone to completion. Each reaction contained 3 units of polymerase (New England Biolabs)/μg of DNA, 0.1 volumes of 1mM each NTP mix (Pharmacia Biotech), 0.1 volumes of 0.5mg/ml BSA and 0.1 volumes of T4 reaction buffer.

**1X T4 DNA Polymerase Reaction Buffer:**

50mM	NaCl
10mM	Tris-HCl
10mM	MgCl <sub>2</sub>
1mM	DTT
(pH 7.9 at 25°C)	

The blunting reactions were incubated at 12°C for 20 minutes after which point the enzyme was heat inactivated at 75°C for 10 minutes.

**6.1.12. DNA Sequence Analysis**

**6.1.12.1. DNA Template Preparation**

DNA was sequenced directly supercoiled plasmids (Hattori & Sakaki, 1986). In order to successfully sequence double stranded template a small excess of template was needed, 3-5μg of plasmid per primer, which was then denatured in alkali. 5ug of DNA were diluted to a final volume of 45μl in ddH<sub>2</sub>O and 5μl of freshly prepared Denaturing Solution was added.

**Denaturing Solution:**

NaOH	2M
EDTA	2mM

The DNA was incubated for 5 minutes at room temperature with the Denaturing Solution after which the reaction was neutralised with 5 $\mu$ l of 2M ammonium acetate (pH 4.6, filter sterilised). The DNA was then precipitated by the addition of 185 $\mu$ l of absolute ethanol and storage at -70°C for 30 minutes. The denatured plasmid was recovered by centrifugation at 10,000g for 20 minutes in a microfuge at 4°C. The supernatant was discarded and the pellet washed with 200 $\mu$ l of ice cold 70% ethanol. The DNA was then dried under vacuum and resuspended in 6 $\mu$ l ddH<sub>2</sub>O. This denatured template can be stored at -20°C for up to one week or used immediately in the sequencing reactions described below.

**6.1.12.2. Dideoxy Sequencing**

Chain-termination sequencing (Sanger *et al*, 1977) was carried out using the T7 Sequenase® Version 2.0 system (United States Biochemical) according to the manufacturer's instructions. Briefly, template prepared as described in Section 7.1.12.a was mixed with 1pmol of a selected sequencing primer, 2 $\mu$ l of 5X Sequenase Reaction Buffer and the total volume made up to 10 $\mu$ l with dd H<sub>2</sub>O.

**5X Sequenase Reaction Buffer:**

Tris-HCl, pH 7.5	200mM
MgCl <sub>2</sub>	100mM
NaCl	250mM

The template and primer mixture was incubated at 65°C for 2 minutes before being cooled to approximately 37°C over a period of 30 minutes to allow primer annealing. The tube was then placed on ice prior to the labelling reaction. To each 10 $\mu$ l volume of template/primer 1 $\mu$ l of 0.1M DTT, 2 $\mu$ l of labelling mix (diluted 1:5 in ddH<sub>2</sub>O) and 0.5 $\mu$ l of [ $\alpha$ -<sup>35</sup>S] dATP (10 $\mu$ Ci/ $\mu$ l, ICN Biochemicals) was added.

<b>Labelling Mix:</b>	dGTP, dCTP, dTTP	7.5 $\mu$ M each
-----------------------	------------------	------------------

To start the labelling reaction 2 $\mu$ l (3.25 units) of Sequenase T7 DNA polymerase (diluted 1:8 in Enzyme Dilution Buffer) was added and the reaction incubated at room temperature for 5 minutes.

**Enzyme Dilution Buffer:**

Tris-HCl, pH 7.5	10mM
Dithiothreitol	5mM
EDTA	0.1mM
Acetylated BSA	0.5mg/ml

Reactions were then terminated by placing 3.5 $\mu$ l of template/primer mix into each of four tubes warmed to 37°C, containing one of four (A, C, G or T) termination mixes. The tubes were then incubated for a further 5 minutes at 37°C and the reaction was stopped by the addition of 4 $\mu$ l of Stop Solution.

**Termination Mixes:** All four mixes contain,

dATP	80 $\mu$ M
dCTP	80 $\mu$ M
dGTP	80 $\mu$ M
dTTP	80 $\mu$ M
NaCl	50mM

In addition the 'A' mix contains 8 $\mu$ M ddATP, the 'C' mix 8 $\mu$ M ddCTP etc.

**Stop Solution:**

Formamide	95% v/v
EDTA	20mM
Bromophenol Blue	0.5g/l
Xylene Cyanol FF	0.5g/l

The completed sequencing reactions can be stored at -20°C otherwise the samples were heat denatured at 90°C for 2-3 minutes and immediately run on a 6% polyacrylamide, 6M urea 0.4mm sequencing gel.

**Gel Solution:**

Urea	250g
19:1, 40% acrylamide stock	75mls
10 X TBE	50mls
ddH <sub>2</sub> O	175mls



The acrylamide/urea gel solution was stored at 4°C in a dark bottle. For each sequencing gel, 60mls of the above solution was mixed with 60µl of TEMED and 60µl of 25% Ammonium persulphate (made fresh for each use) and poured immediately. The gel was left for one hour at room temperature to polymerise or can be wrapped up and stored overnight at room temperature. Prior to loading any samples, the gel was pre-run at 70W for one hour or until the gel reached approximately 50°C. Electrophoresis was carried out using 1X TBE electrophoresis buffer. After pre-warming the gel, the samples were loaded and electrophoresed at 70W for 1-4 hours. Upon completion of electrophoresis, the gel was fixed by two washes in 10% methanol, 10% acetic acid and blotted onto Whatman 3MM paper. The gel was dried under vacuum at 80°C for two hours and exposed to autoradiography film overnight (Kodak BioMax MR film, Eastman Kodak Company). The autoradiography film was developed (Amersham Hyperprocessor) and interpreted the next day.

### **6.1.13. Southern Blotting**

#### **6.1.13.1. Preparation of DNA**

10 µg of genomic DNA was digested with an appropriate restriction enzyme. Once the digest had gone to completion the sample was run out on a 0.8% agarose gel. The gel was then prepared for blotting onto nylon membrane. If the fragments of interest were predicted to be larger than 15kb, transfer of the DNA to the nylon membrane was improved by partially depurinating the DNA prior to transfer. Depurination was achieved by soaking the gel for 10 minutes 0.2M HCl. The gel was then rinsed in deionised water and the DNA was transferred immediately.

#### **6.1.13.2. DNA Transfer**

The DNA was transferred from the gel onto a positively charged nylon membrane, Zeta-Probe® GT, Bio-Rad) according to the manufacturers instructions using 0.4M Sodium hydroxide as the transfer buffer. After blotting overnight the membrane was rinsed in 2XSSC and air-dried.

<b>20X SSC:</b>	NaCl	3M
	Trisodium citrate	0.3M
	pH to 7.0 with 1M HCl	

The nylon membrane was then baked at 80°C for 30 minutes and stored between Whatman 3MM paper at room temperature until needed.

#### **6.1.13.3. Prehybridisation**

UltraHYB™ (Ambion) hybridisation buffer was heated to 68°C to ensure complete solubilisation of all components. 10 mls was then removed and added into a hybridisation tube containing the baked nylon membrane. The membrane and UltraHYB™ buffer were then incubated at 42°C for 1 hour in a hybridisation oven (Hybaid).

#### **6.1.13.4. Generation of Radiolabelled Probes**

50ng of appropriate DNA was radiolabelled to a high specific activity with [ $\alpha$ -<sup>32</sup>P] dCTP (ICN Biochemicals Inc.) using Prime-It RmT Random Primer Labelling Kit (Stratagene) according to the manufacturers protocol. Labelled probe was separated from unincorporated nucleotides using a Sephadex G50 Column (Pharmacia). The probe was mixed with 20µl of carrier salmon sperm DNA (10mg/ml) and added to the top of the column. 400µl of TE was then added and the column eluate collected in tube 1. A further 400µl of TE was added and the eluate collected in tube 2. Tube 2 should contain the radiolabelled probe. The level of [ $\alpha$ -<sup>32</sup>P] dCTP incorporation was assessed by comparing the counts from the column to those from tube 2 and the probe only used if greater than 50% incorporation was achieved.

#### **6.1.13.5. Hybridisation**

After the membrane had been incubated with prehybridisation buffer at 42°C for 1 hour the probe, denatured by boiling for 5 minutes, was added. Hybridisation proceeded overnight at 42°C and the membrane was washed the following morning.

**Wash 1:** 2X SSC, 0.1% SDS  
**Wash 2:** 0.1X SSC, 0.1% SDS

After the final wash the filter(s) were removed from the hybridisation tube, sealed in a plastic bag and exposed to Hyperfilm™ MP (Amersham) with intensifying screens at -70°C for 2 - 5 days. The autoradiography films were then developed (Amersham Hyperprocessor).

**6.1.14. Polymerase Chain Reaction**

Unless otherwise stated all PCR reactions were carried out using Taq Polymerase and accompanying reaction buffer, 1% WI and 50mM Magnesium chloride were supplied by Life Technologies. Pharmacia Biotech supplied all nucleotides and the oligonucleotides were synthesised by Cruachem.

**6.1.14.1. p53-Based PCR Strategies**

**6.1.14.1.a. FX PCR**

This primer pair and the reaction conditions were designed and optimised by Dr. S. Lyons (Lyons, 1999).

**Table 6.2: Primer sequences and annealing temperatures**

	Primer sequences (written 5' to 3')	Annealing temperature	Product size/ base pairs
<b>PIN 1</b>	gAggCACCggTTCAAAGTCTgTAT	64°C	1200
<b>P1</b>	gCTCTgTgCTCTTTCCTATCCAg		

<b>Reaction conditions:</b>	Primers (10pmol/μl)	4μl EACH
	50mM MgCl <sub>2</sub>	1.5μl
	10X Reaction Buffer	5μl
	1% WI detergent	2.5μl
	1.25mM dNTP stock mix	2μl
	ddH <sub>2</sub> O	26.5μl

2μl of mouse genomic DNA template and 2.5μl (1.5U) of Taq DNA polymerase (Life Technologies) was added to give a total volume of 50μl.

<b>PCR Thermal Cycler Programme:</b>	94°C, 2 min.	Hot start
	94°C, 45 secs	
	64°C, 1 min.	Repeated for 10
	72°C, 2 min.	cycles.
	94°C, 45 secs	Repeated for 20
	64°C, 1 min.	cycles with
		20sec.
	72°C, 2 min, 20secs.	increments
		added.
	72°C, 10 min.	One cycle at the
		end of the
		programme.

6.1.14.1.b. F3K PCR

This primer pair and the reaction conditions were also designed and optimised by Dr. S. Lyons (Lyons, 1999).

Table 6.3: Primer sequences and annealing temperatures

	Primer sequences (written 5' to 3')	Annealing temperature	Product size/ base pairs
p3KX	TCATCTAgAgCTTACATATgACCCTg	58°C	3200
p3KE	gCAgAATTCTCTTgCAATCAgCTAgA		

<b>Reaction conditions:</b>	Primers (10pmol/μl)	4μl EACH
	50mM MgCl <sub>2</sub>	1.5μl
	10X Reaction Buffer	5μl
	1% WI detergent	2.5μl
	1.25mM dNTP stock mix	2μl
	ddH <sub>2</sub> O	26.5μl

2μl of genomic DNA template and 2.5μl (1.5U) of Taq DNA polymerase (Life Technologies) was added to give a total volume of 50μl.

<b>PCR Thermal Cycler Programme:</b>	94°C, 2 min.	Hot start
	94°C, 45 secs	
	58°C, 1 min.	Repeated for 10
	72°C, 2 min.	cycles.

94°C, 45 secs	Repeated for 20 cycles with 20sec. increments added.
58°C, 1 min.	
72°C, 2 min, 20secs.	
72°C, 10 min.	One cycle at the end of the programme.

### 6.1.14.1.c. SR PCR

This PCR proved refractory to optimisation using standard Taq polymerase so the Expand<sup>TM</sup> High Fidelity blend of Taq and Pwo DNA polymerases (Boehringer Mannheim) was used instead.

**Table 6.4: Primer sequences and annealing temperatures**

	Primer sequences (written 5' to 3')	Annealing temperature	Product size/ base pairs
<b>LizIn1</b>	CTgTAgCAgCAggTTATCTTgTg	58°C	2317
<b>Son1</b>	gATggCTATgACTATCTAgCTgg		

<b>Reaction Conditions:</b> Primers (10pmol/μl)	2.5μl EACH
50mM MgCl <sub>2</sub>	4μl
10X Reaction Buffer	5μl
1.25mM dNTP stock mix	8μl
ddH <sub>2</sub> O	23.5μl

2μl of genomic DNA template and 2.5μl (2.6U) of Expand<sup>TM</sup> High Fidelity enzyme mix (Boehringer Mannheim) was added to give a total volume of 50μl.

<b>PCR Thermal Cycler Programme:</b> 94°C, 1 min.	
58°C, 1 min.	Repeated for 35 cycles.
68°C, 2 min.	
68°C, 10 min.	One cycle at the end of the programme.

### 6.1.14.1.d. PCR to Genotype the p53 Status of Embryonic Fibroblasts

The generation of mice with a *neo* cassette inserted into the p53 genomic sequence has been described (Clarke *et al*, 1993). The genotype of progeny was assigned using PCR designed by Dr J. Armstrong. Three primers were used in this PCR reaction, the first and second are common to both wild type and targeted alleles, the third is specific to the targeted allele. In wild type mice a single product of 642 base pairs is generated, in heterozygotes two products of 642 and 510 base pairs are generated and finally in homozygous nulls only one band of 510 base pairs is seen.

**Table 6.4: Primer sequences and annealing temperatures**

	Primer sequences (written 5' to 3')	Annealing temperature	Product size/ base pairs
Exon 6	gTggTggTACCTTATgAgCC	60	642 and 510
Intron 7	CAAAGAgCgTTgggCATgTg		
Neo	CATCgCCTTCTATCgCCTTC		

<b>Reaction Conditions:</b> Primers (10pmol/μl)	2.5μl EACH
50mM MgCl <sub>2</sub>	2μl
10X Reaction Buffer	5μl
1.25mM dNTP stock mix	8μl
DMSO	2.5μl
ddH <sub>2</sub> O	23μl

2μl of genomic DNA template and 2.5μl (1.5U) of Taq DNA polymerase (Life Technologies) were added to give a total volume of 50μl.

<b>PCR Thermal Cycler Programme:</b> 94°C, 2min.	Hot start
94°C, 1 min.	
62°C, 1 min.	Repeated for 30 cycles.
72°C, 1 min.	
72°C, 10 min.	One cycle at the end of the programme.

**6.1.14.1.e. p53 cDNA PCR**



As with the FX and F3K PCR reactions the primers used here were also designed by Scott Lyons (Lyons, 1999). However, the original reaction conditions were re-optimised by myself to increase the efficiency and yield of this PCR.

**Table 6.5: Primer sequences and annealing temperatures**

	Primer sequences (written 5' to 3')	Annealing temperature	Product size/ base pairs
cDNAIII	ATgCTACAgAggAgTCTggA	55	537
SenIII	gATCATgAACAgACTgTgAg		

<b>Reaction Conditions:</b> Primers (10pmol/μl)	2.5μl EACH
50mM MgCl <sub>2</sub>	2μl
10X Reaction Buffer	5μl
1.25mM dNTP stock mix	8μl
1% WI detergent	2.5μl
ddH <sub>2</sub> O	23μl

To this end volume of 45.5μl was added 2μl of genomic DNA template and 2.5μl (1.5U) of Taq DNA polymerase (Life Technologies).

<b>PCR Thermal Cycler Programme:</b> 94°C, 1min.	Hot start
94°C, 1 min.	
55°C, 1 min.	Repeated for 35 cycles.
72°C, 1min.	
72°C, 10 min.	One cycle at the end of the programme.

**6.1.14.1.f. neo/In PCR**

This PCR was designed to look at the recombination status of the pIGTV targeting vector, and subsequently, the targeted mouse genomic p53 locus. The first primer anneals within the neo gene of the floxed STOP and the second, downstream primer, anneals within intron 1. This PCR will generate a 1525bp band only from an unrecombined locus.

**Table 6.6: Primer sequences and annealing temperatures**

	Primer sequences (written 5' to 3')	Annealing temperature	Product size/ base pairs
Neo	TCgCCTTCTATCgCCTTC	58°C	1525bp
LizIn1	CTgTAgCAgCAgTTATCTTgTg		

<b>Reaction Conditions:</b>	Primers (10pmol/μl)	2.5μl EACH
	50mM MgCl <sub>2</sub>	2μl
	10X Reaction Buffer	5μl
	1.25mM dNTP stock mix	8μl
	1% WI detergent	2.5μl
	ddH <sub>2</sub> O	23μl

2μl of genomic DNA template and 2.5μl (1.5U) of Taq DNA polymerase (Life Technologies) were added to give an end volume of 50μl.

<b>PCR Thermal Cycler Programme:</b>	94°C, 1min.	Hot start
	94°C, 1 min.	
	58°C, 1 min.	Repeated for 35 cycles.
	72°C, 1min, 30secs.	
	72°C, 10 min.	One cycle at the end of the programme.

#### 6.1.14.1.g. Southern Probe PCR

This PCR was designed and optimised by Dr. S. Lyons to generate a small PCR product that can be used as a Southern blot probe to identify targeted clones that have integrated the targeting vector, pIGTV, via homologous rather than random integration mechanisms.

**Table 6.7: Primer sequences and annealing temperatures**

	Primer sequences (written 5' to 3')	Annealing temperature	Product size/ base pairs
Pro3A	AgCCTgTgACgCACTAgATT	60°C	224
Pro3B	CAGCAAAggCAAgCATTTTC		

<b>Reaction Conditions:</b> Primers (10pmol/μl)	2μl of Pro3A only
50mM MgCl <sub>2</sub>	1.5μl
10X Reaction Buffer	5μl
1.25mM dNTP stock mix	8μl
1% WI detergent	2.5μl
ddH <sub>2</sub> O	24.5μl

2μl of genomic DNA template, 2.5μl (1.5U) of Taq DNA polymerase (Life Technologies) and 2μl of heat denatured Pro3B (94°C, 10min) were added to give an end volume of 50μl.

<b>PCR Thermal Cycler Programme:</b> 94°C, 1 min.	Hot start
94°C, 1 min.	
60°C, 45 secs.	Repeated for 30 cycles.
72°C, 1min.	
72°C, 10 min.	One cycle at the end of the programme.

6.1.14.2. Other PCR Strategies

6.1.14.2.a. neo-EGFP PCR

This PCR reaction was designed as one of a pair to monitor recombination status of the plasmid pFloxEGFP (see 6.1.14.2.b.). This reaction gives rise to products from the unrecombined transgene.

**Table 6.8: Primer sequences and annealing temperatures**

	Primer sequences (written 5' to 3')	Annealing temperature	Product size/ base pairs
Neo	TCgCCTTCTATCgCCTTC	55°C	1213
EGFP	CAGCAGgACCATgTgATC		

<b>Reaction Conditions:</b> Primers (10pmol/μl)	2.5μl EACH
50mM MgCl <sub>2</sub>	2μl
10X Reaction Buffer	5μl
1.25mM dNTP stock mix	8μl
1% WI detergent	2.5μl
DMSO	2.5μl

ddH<sub>2</sub>O 20.5µl

2µl of genomic DNA template and 2.5µl (1.5U) of Taq DNA polymerase (Life Technologies) were added to give an end volume of 50µl.

<b>PCR Thermal Cycler Programme:</b>	94°C, 1min.	Hot start
	80°C, 1 min.	
	94°C, 1 min.	
	55°C, 1 min.	Repeated for 40 cycles.
	72°C, 1min.	
	72°C, 10 min.	One cycle at the end of the programme.

6.1.14.2.b. CMV-EGFP PCR

This PCR is the second of the pFloxEGFP pair and will only generate a product after the pFloxEGFP template has undergone Cre-mediated excisive recombination.

Table 6.9: Primer sequences and annealing temperatures

	Primer sequences (written 5' to 3')	Annealing temperature	Product size/ base pairs
CMV	ggAgTTCCgCgTTACATA	55°C	1325
EGFP	CAGCAggACCATgTgATC		

<b>Reaction Conditions:</b> Primers (10pmol/µl)	2.5µl EACH
50mM MgCl <sub>2</sub>	1µl
10X Reaction Buffer	5µl
1.25mM dNTP stock mix	8µl
1% WI detergent	2.5µl
DMSO	2.5µl
ddH <sub>2</sub> O	21.5µl

2µl of genomic DNA template and 2.5µl (1.5U) of Taq DNA polymerase (Life Technologies) were added to give an end volume of 50µl.

<b>PCR Thermal Cycler Programme:</b> 94°C, 1min.	Hot start
--	-----------

80°C, 1 min.	
94°C, 1 min.	
55°C, 1 min.	Repeated for 40 cycles.
72°C, 1min.	
72°C, 10 min.	One cycle at the end of the programme.

#### 6.1.14.2.c. Episomal Adenovirus Detection PCR

The PCR primers used here were designed by Dominic Rannie and anneal within the Cre coding sequence of AdCre (Anton & Graham, 1995). This PCR reaction was used to demonstrate the successful adenovirus infection of cells as a product will only be seen if adenoviridae are present as episomes in infected cells.

**Table 6.10: Primer sequences and annealing temperatures**

	Primer sequences (written 5' to 3')	Annealing temperature	Product size/ base pairs
<b>Cre360FOR</b>	AAACgTTgATgCCggTgAACg	55°C	660
<b>Cre3'REV</b>	CTAATCgCCATCTTCCTgCAgg		

<b>Reaction Conditions:</b> Primers (10pmol/μl)	2.0μl EACH
50mM MgCl <sub>2</sub>	1.5μl
10X Reaction Buffer	5μl
1.25mM dNTP stock mix	8μl
1% WI detergent	2.5μl
ddH <sub>2</sub> O	24.5μl

To this end volume of 45.5μl was added 2μl of genomic DNA template and 2.5μl (1.5U) of Taq DNA polymerase (Life Technologies).

<b>PCR Thermal Cycler Programme:</b> 94°C, 1min.	Hot start
94°C, 45 secs.	
55°C, 1 min.	Repeated for 30 cycles.
72°C, 1min.	

72°C, 10 min.	One cycle at the end of the programme.
---------------	--

6.1.14.3. RT-PCR Strategies

6.1.14.3.a. Mouse β-actin RT-PCR

This PCR reaction was designed and optimised to yield a product from the murine β-actin cDNA generated by reverse transcription (Section 7.5.2).

Table 6.11: Primer sequences and annealing temperatures

	Primer sequences (written 5' to 3')	Annealing temperature	Product size/ base pairs
BA4	CgTAgATgggCACAgTg	55°C	440
BA15	CTCCggCATgTgCAAAg		

<b>Reaction Conditions:</b> Primers (10pmol/μl)	2.5μl EACH
50mM MgCl <sub>2</sub>	1.5μl
10X Reaction Buffer	5μl
1.25mM dNTP stock mix	8μl
1% WI detergent	2.5μl
ddH <sub>2</sub> O	23.5μl

To this end volume of 45.5μl was added 2μl of cDNA template and 2.5μl (1.5U) of Taq DNA polymerase (Life Technologies).

PCR Thermal Cycler Programme: 94°C, 1min. Hot start

94°C, 1 min.	
55°C, 1 min.	Repeated for 31 cycles.
72°C, 1min.	
72°C, 10 min.	One cycle at the end of the programme.

6.1.14.3.b. EGFP RT-PCR



This PCR reaction was designed to allow the detection of EGFP expression at the mRNA level.

**Table 6.12: Primer sequences and annealing temperatures**

	Primer sequences (written 5' to 3')	Annealing temperature	Product size/ base pairs
CAP	CgTAAACggCCACAAGTT	55°C	660
EGFP	CAGCAggACCATgTgATC		

<b>Reaction Conditions:</b>	Primers (10pmol/μl)	2.5μl EACH
	50mM MgCl <sub>2</sub>	1μl
	10X Reaction Buffer	5μl
	1.25mM dNTP stock mix	8μl
	1% WI detergent	2.5μl
	ddH <sub>2</sub> O	24.μl

To this end volume of 45.5μl was added 2μl of cDNA template and 2.5μl (1.5U) of Taq DNA polymerase (Life Technologies).

<b>PCR Thermal Cycler Programme:</b>	94°C, 1min.	Hot start
	94°C, 1 min.	
	55°C, 1 min.	Repeated for 30 cycles.
	72°C, 1min.	
	72°C, 10 min.	One cycle at the end of the programme.

**6.2. Embryonic Stem Cell Culture**

**6.2.1. Media Preparation**

ES cells were cultured in Glasgow MEM (BHK 21) medium (Life Technologies) supplemented with the following per 500ml.

<b>Media supplements:</b>	
Foetal Calf Serum (Sigma)/Neonatal Calf Serum (Life Technologies)	5%v/v each

$\beta$ -mercaptoethanol (Sigma)	0.1mM
100X MEM Non-essential Amino Acids (Life Technologies)	5ml
100mM Sodium Pyruvate (Life Technologies)	5ml
200mM L-Glutamine (Life Technologies)	5ml
LIF (Leukaemia-inhibiting Factor)	0.5ml

LIF was prepared by the transfection of Cos-7 cells and subsequent harvesting of the conditioned medium (Smith *et al*, 1988).

### 6.2.2. Culture Conditions

ES cells were routinely cultured by growing in supplemented BHK 21 medium on tissue culture treated plastic (Falcon, Nunc or Costar) coated with swine skin gelatin (Sigma). A solution of 1% gelatin was prepared and autoclaved twice. This was then diluted 1:10 in ddH<sub>2</sub>O and tissue culture plastic was coated by covering the surface with the 0.1% gelatin solution and leaving the plate or flask at room temperature for a minimum of 5 minutes. Cultures were kept at a temperature of 37°C, in a humidified atmosphere of 5% CO<sub>2</sub>, 95% air. Medium was changed as appropriate, usually every day or every other day, and cells were passaged when 70-80% confluence was reached.

### 6.2.3. Passaging ES cells

Fresh medium was used to feed the cells about 2hrs prior to trypsinisation. After this time the medium was aspirated and the cultures washed twice with an appropriate volume of sterile phosphate buffered saline (PBS, 1ml for a 25cm<sup>2</sup> flask, 3ml for a 50cm<sup>2</sup> flask) (Life Technologies).

<b>10X PBS:</b>	KCl	2.0g/l
	KH <sub>2</sub> PO <sub>4</sub>	2.0g/l
	NaCl	80.0g/l
	Na <sub>2</sub> HPO <sub>4</sub> .7H <sub>2</sub> O	21.60g/l

The PBS was then aspirated off and Trypsin-EDTA (Life Technologies) added to the cells. To trypsinise a 25cm<sup>2</sup> flask of cells 1ml of trypsin was used and the volume

was increased up to 5mls for a 175cm<sup>2</sup> flask. The cells and trypsin were then incubated at 37°C for 1-2 minutes.

<b>1X Trypsin-EDTA:</b>	Trypsin	0.5g
	EDTA	2.0g
(Made up to 1l with Modified Puck's Saline A)		

Cells were disaggregated into a single cell suspension by tapping the side of the flask and further digestion was prevented by the addition of a minimum of two volumes of culture medium. The cells were then diluted as appropriate with medium and transferred into fresh plastic-ware coated with 0.1% gelatin. The ES cells were then refed after 4hrs to remove any debris from the trypsinisation process.

#### 6.2.4. Freezing ES Cells

Cells were trypsinised as described in Section 6.2.3 but once the trypsin had been neutralised by the addition of culture medium the cell suspension was transferred into a sterile universal and centrifuged at 800xg for 3 minutes. The supernatant was removed by aspiration and the cell pellet resuspended in freezing medium.

<b>Freezing Medium:</b>	Supplemented BHK 21 medium	40% v/v
	Foetal Calf Serum	50% v/v
	Dimethyl Sulfoxide	10% v/v
	(Acidified by the addition of a few drops of 1M HCl and subsequently filter sterilised.)	

The resuspended cells were then aliquoted into CryoTube™ vials (Nunc) and cooled at an approximate rate of 1°C/minute to -70°C then moved into storage over liquid nitrogen the next day.

### 6.2.5. Defrosting ES cells

To bring frozen cells back into culture the CryoTube™ vials (Nunc) were defrosted as quickly as possible. The cells were then transferred into 5mls of supplemented BHK 21 medium and centrifuged at 800xg for 3 minutes. The supernatant was removed by aspiration and the cell pellet resuspended in an appropriate volume of

fresh culture medium before transferring the cells to fresh plasticware coated with 0.1% gelatin. The ES cells were then refed after 4hrs.

#### **6.2.6. ES Cell Electroporation**

ES cells were transformed by electroporation using a BioRad Gene Pulser.  $10^8$  cells (approximately 1 confluent 175 cm<sup>2</sup> tissue culture flask) were fed with fresh medium about 4hrs prior to harvesting. After trypsinisation the cell suspension was centrifuged at 800xg for 3minutes and the cell pellet resuspended in 10mls of sterile PBS. The exact number of cells was then quantified by counting with a haemocytometer. The cells were pelleted by centrifugation at 800xg for 3 minutes and then resuspended in 0.7 mls of PBS before being transferred into an electroporation cuvette (BioRad, path length 0.4cm). 10µg of linearised DNA (verified by agarose gel electrophoresis, Section 7.1.7), resuspended in 100µl of PBS, was then added. The electric pulse, 3µF, 800V, time constant 0.1 secs, was applied immediately to minimise DNA degradation. The cells were then removed from the cuvette and diluted in culture medium before being plated out onto gelatinised 100mm tissue culture dishes ( $5 \times 10^6$  cells/100mm plate). The following day G418-sulphate (200µg/ml) selective medium was added and selection maintained for 10 days or until clones were visible to the naked eye.

<b>1000X G418-sulphate:</b>	2mg/ml dissolved in PBS stored at -20°C in
1ml	aliquots.

#### **6.2.7. Picking and Maintaining Clones**

After about 10 days clones which are visible to the naked eye are present on the culture dishes. The clones were picked using a sterile P200 pipette (Gilson) and filter tips. To separate the clone into single cells it was added to trypsin pre-aliquoted into a 96 well plate, mixed vigorously by pipetting and finally transferred into one well of a 24 well plate containing 1.5mls of medium. Each electroporation resulted in 200-300 clones picked in this manner. During work to introduce the pFloxEGFP plasmid into ES cells the clones were grown up and then trypsinised back into the same wells. A small amount of cells were removed and transferred into a gelatinised 96 well

plate, after 4 hours these cells were fixed and stained to visualise  $\beta$ -galactosidase activity (see Section 6.3.1.1.). However, during targeting experiments described in Chapter 4 the clones were grown up and duplicated, one sample was frozen down at -70°C and genomic DNA was extracted from the other.

**6.2.8. Extraction of Genomic DNA from ES cells**

Prior to genomic DNA extraction cells were rinsed twice with sterile PBS to remove all traces of culture medium. The cells were then lysed with an appropriate volume of Lysis Buffer, 3mls for a 25cm<sup>2</sup> flask or 500µl / well of a 24 well plate for 3-5hrs at 37°C.

<b>Lysis Buffer:</b>	Tris-HCl (pH 8.5)	100mM
	EDTA	5mM
	SDS	0.2%
	NaCl	200mM
	100µg of Proteinase K/ml	

To precipitate the genomic DNA an equal volume of isopropanol was added and the samples shaken for 15 minutes on an orbital shaker until a white DNA precipitate became visible. The precipitate and a small volume of solution were then removed by pipette and centrifuged to pellet out the genomic DNA ( 10,000xg , 5 minutes). The pellet was then washed twice in 70% ethanol, air-dried and finally resuspended in TE.

**6.2.9. Karyotyping of ES Cells**

A culture of ES cells was seeded into a 25cm<sup>2</sup> flask, the aim was to have the cells growing exponentially and to reach about 50% confluence on the day they were to be harvested. The cells were then harvested by trypsinisation, centrifuged, 800xg for 3 minutes, and the pellet resuspended in 5mls of hypotonic 0.56% KCl. The cells were centrifuged once more and the supernatant removed. The pellet was then resuspended in 5mls of ice cold fix, added dropwise, while vortexing the whole sample very gently. The fix used consisted of 3:1 methanol to acetic acid made up fresh each time. The centrifugation and fixing steps were repeated three times and

after the final fix cells can be stored at 4°C for up to 24 hours. To produce the metaphase spreads the cells were pelleted by centrifugation and most of the supernatant was removed leaving only a small volume with which to make a cell suspension. The cell suspension was then dropped onto microscope slides and left to dry. The slides were then stained with GIEMSA (Sigma) for 5-10 minutes before being viewed on the HOME microscope.

#### **6.2.10. Infection of ES and EF Cells with Recombinant Adenovirus**

Infection of both ES and embryonic fibroblasts (EF) cells with the adenovirus were carried out as described below. All adenoviruses were cultured and maintained by Dominic Rannie. They were supplied as a stock solution of known titre and an appropriate volume of virus was removed and mixed well with tissue culture medium. The amount of virus required depended upon the desired multiplicity of infection (m.o.i) for each experiment. The medium into which the virus was added contained only 1% serum as this had been shown to facilitate the efficient infection of cells (D. Rannie, unpublished observations). The volume of adenovirus-containing medium added to the cells was kept as small as possible, for example, 1ml for a 25cm<sup>2</sup> flask or 200µl for each well of a double chamber slide. Once the adenovirus had been added to the cells, the cultures were transferred to storage at 37°C, 5% CO<sub>2</sub> for one hour. During this incubation the flasks or chamber slides were rocked gently every 5 minutes. After one hour the adenovirus-containing medium was aspirated off, the cells were then rinsed in sterile PBS before normal culture medium was added back. For safety purposes all work involving adenovirus was carried out in microbiological safety cabinet (Class II), wearing lab coats and gloves. Any contaminated glass and plastic-ware were immersed in a 1000ppm Presept solution (Johnson & Johnson) prior to disposal. After use, the safety hood was UV irradiated overnight.

### **6.3. Detection of Marker Gene Expression**

#### **6.3.1. $\beta$ -galactosidase Histochemical Detection**

##### **6.3.1.1. Histochemical Detection of Bacterial $\beta$ -gal (pH7.0)**



This stain was used to detect the expression of the enzyme  $\beta$ -galactosidase ( $\beta$ -gal) from the bacterial LacZ gene within mammalian cells. LacZ is a commonly used marker gene, for example  $\beta$ -gal is expressed from the LacZ component of  $\beta$ geo fusion gene present within pFloxSTOP. This stain has been optimised to specifically detect  $\beta$ -gal activity with a pH optimum of pH7.0, a characteristic unique to the bacterial enzyme as the endogenous lysosomal  $\beta$ -gal of mammalian cells has a pH optimum at pH 4.0 (see next section and Moreau *et al*, 1989).

Prior to staining ES cells were rinsed in PBS and then fixed for 5 minutes in 0.05% glutaraldehyde diluted in PBS. This fix was made up fresh each time from a 3% stock kept at 4°C. After fixing cells were rinsed two more times in PBS, with the second wash being left on for 10 minutes. An appropriate volume of Stain Solution was then added, for example 2mls/25cm<sup>2</sup> flask, and the cells were left overnight at 37°C in a sealed humid box. After staining was complete the cells were stored at 4°C under PBS or fix.

<b>Stain Solution:</b>	20mM	NaH <sub>2</sub> PO <sub>4</sub>
	80mM	Na <sub>2</sub> HPO <sub>4</sub>
	1.3mM	K <sub>3</sub> Fe(CN) <sub>6</sub>
	3mM	K <sub>4</sub> Fe(CN) <sub>6</sub>
	1mg/ml	X-gal

### 6.3.1.2. Histochemical Detection of the Endogenous Mammalian $\beta$ -gal (pH4.0)

The majority of mammalian cells express a lysosomal  $\beta$ -gal that is optimally active at pH 4.0 (Moreau *et al*, 1989). Prior to staining all traces of culture medium were removed from the cells by two washes with PBS. The cells were then fixed in 3% formaldehyde (diluted in PBS) for 3 minutes and then washed twice more with PBS. The cells were incubated overnight at 37°C in the presence of an appropriate volume of stain solution, for example 2mls/25cm<sup>2</sup> flask or 500 $\mu$ l for a chamber slide. Although positively stained cells become visible after 2-4hrs, the reaction was usually allowed to proceed overnight.

<b>Stain Solution :</b>	150mM	NaCl
	2mM	MgCl <sub>2</sub>
	5mM	K <sub>3</sub> Fe(CN) <sub>6</sub>
	5mM	K <sub>4</sub> Fe(CN) <sub>6</sub>
	40mM	Citric acid buffer (see below)
	1mg/ml	X-gal
<b>Citric acid buffer:</b>	36.85ml	0.1M Citric acid Monohydrate
	63.15ml	0.2M NaH <sub>2</sub> PO <sub>4</sub>

This gives a total volume of 100mls and after mixing, the stain solution pH should be adjusted to pH 4.0. The fixation procedure and stain solution are as described by Dimri *et al* (Dimri *et al*, 1995).

### 6.3.1.3. Histochemical Detection of Mammalian Senescence-associated-βgal (pH6.0)

#### 6.3.1.3.a. SA-βgal *in vitro*

The identification of a senescence-associated β-gal (SA-βgal) activity in human cells was first reported in 1995 (Dimri *et al*, 1995). The stain used to detect this activity in human cells was known not to work in mouse cells (J. Campisi, pers. comm) but the following solution can be used to successfully detect SA β-gal in mouse EFs. Prior to staining the cells were washed twice in PBS, fixed for 3 minutes with 3% formaldehyde and washed two further times. The cells were then incubated overnight at 37°C in the presence of an appropriate volume of stain solution.

<b>Stain Solution :</b>	150mM	NaCl
	200mM	MgCl <sub>2</sub>
	5mM	K <sub>3</sub> Fe(CN) <sub>6</sub>
	5mM	K <sub>4</sub> Fe(CN) <sub>6</sub>
	40mM	Citric acid/PBS buffer (see below)
	1mg/ml	X-gal

**Citric acid/PBS buffer:** 0.1M Citric acid monohydrate dissolved in PBS rather than ddH<sub>2</sub>O, pH adjusted to 6.0.

#### **6.3.1.3.b. SA- $\beta$ gal *in vivo***

Mice were killed and an area of back skin exposed by shaving. A sample was excised, transferred into a sterile Eppendorf and then snap frozen in liquid nitrogen. The skin sections were then mounted in OCT (Bayer) and frozen sections cut. The sections were then transferred onto poly-L-lysine coated microscope slides (Sigma). Immediately after cutting the frozen sections were fixed in 1% glutaraldehyde for 1 minute at room temperature, rinsed in PBS and then immersed in SA- $\beta$ gal stain solution (as described in Section 6.3.1.3.a) and incubated overnight at 37°C. The following day the sections were rinsed in PBS, counterstained with eosin and mounted.

### **6.3.2. $\beta$ -galactosidase Activity Quantification**

To quantify the level of soluble  $\beta$ -gal activity within cells the  $\beta$ -galactosidase Enzyme Assay System (Promega) was used according to the manufacturers recommendations. Not all solution compositions were disclosed by the manufacturer and these are omitted from the subsequent text.

#### **6.3.2.1. Protein Extract Preparation**

ES cells were harvested by trypsinisation and the cell pellet was rinsed thoroughly with PBS. The final PBS wash was removed by pipette and sufficient 1X Reporter Lysis Buffer was added to cover the cells (e.g. 400 $\mu$ l/60mm culture plate or 900 $\mu$ l/100mm plate). The samples were then incubated at room temperature for 15 minutes to allow complete sample lysis. The cell lysate was then transferred into a fresh Eppendorf tube. The lysate was vortexed briefly and centrifuged at 10,000 g for 2 minutes at 4°C to pellet any cell debris. The supernatant was then transferred into a fresh Eppendorf tube and stored at -20°C for up to 2 months.

#### **6.3.2.2. Protein Concentration Assay**

The protein concentrations of cell extracts prepared by the above method were determined using a Bio-Rad Protein Assay (Bio-Rad). 10-50 $\mu$ l of the extracts were diluted in water up to a total volume of 800 $\mu$ l. After the addition of 200 $\mu$ l of the 5X

assay dye reagent, the tubes were vortexed briefly and left for a minimum of 10 minutes to allow the colour change to stabilise. The absorbance of each sample was then measured at 595nm and compared to a standard curve. Standard curves were set up for each assay using Bovine Serum Albumin over a concentration range of 1-10µg of protein.

#### **6.3.2.3. $\beta$ -gal Enzyme Assay**

This assay was carried out in 96 well tissue culture plates that allowed the simultaneous testing of numerous samples. Between 10 and 50µl of protein extract was added to each well, the exact amount depending on the protein concentration of each sample (as determined in Section 6.3.2.2.). The final volume of each sample was made up to 50µl with 1X Reporter Lysis Buffer. All samples were assayed in triplicate. 50µl of 2X Assay Buffer was then added to each well and the samples incubated at 37°C for up to 2 hours. A standard curve was also set up in duplicate for each assay with a range of  $\beta$ -galactosidase activities from 500 milliunits to 0.05 milliunits. A stock of  $\beta$ -gal was supplied with the kit (1u/µl in 50 mM Bicine Buffer, pH 7.5, with 100µg/ml of BSA). All reactions were stopped by the addition of 150µl of 1M Sodium Carbonate. Ideally the absorbance of the samples should be read at 420nm, however the only available plate reader (Dynatech MR5000) was unable to read at this wavelength so 405nm was used instead, this is within the range of suitable wavelengths recommended by Promega. The absorbance data was analysed using Bioline v2.0 software and a standard curve was plotted and used to determine the number of units of  $\beta$ -galactosidase in each sample. By correlating this with protein concentration the number of units  $\beta$ -gal/µg of protein was then be calculated.

#### **6.3.3. EGFP Marker Gene Detection**

##### **6.3.3.1. Flow Cytometric Analysis of EGFP Expression in ES Cells**

All flow cytometric analysis was carried out using a Coulter EPICS XL-MCL flow cytometer. The cells were excited at 488nm in an argon laser beam and the fluorescent forward scatter (FS), side scatter (SS) and fluorescent light emissions

recorded. The fluorescent light emissions were collected using an FL4 filter set (660-700nm). ES cells, which were to be subjected to flow cytometric analysis, were harvested by trypsinisation and then pelleted by centrifugation at 800xg for 3 minutes. The cell pellet was rinsed twice in PBS then diluted in 3-6 mls of PBS. The cells were not fixed prior to analysis and so were stored on ice and assayed immediately.

**6.4. Embryonic Fibroblast Culture**

**6.4.1. Isolation Of Primary Embryonic Fibroblasts**

Primary fibroblast cultures were derived from 12-14d.p.c. embryos (Todaro & Green, 1963). Pregnant mice were killed and uteri removed and transferred into Petri dishes containing 5mls of sterile PBS. Individual embryos were dissected out of the uterus and the placenta and yolk sac removed. The embryo was then decapitated before being dipped into 70% ethanol and transferred to a sterile universal. The tissue was homogenised using scissors and incubated at 37°C for twenty minutes after the addition of 2mls of 2.5% trypsin/PBS (DIFCO). After twenty minutes the trypsinisation reaction was neutralised with 5mls of EF culture medium and the cell suspensions were centrifuged for 3 minutes at 800xg .

**EF Culture Medium:**

Glasgow MEM (BHK 21) medium (Life Technologies)	500mls
Foetal Calf Serum (Sigma) and Neonatal Calf Serum (Life Technologies)	5%v/v each
100X MEM Non-essential Amino Acids (Life Technologies)	5ml
100mM Sodium Pyruvate (Life Technologies)	5ml
200mM L-Glutamine (Life Technologies)	5ml

After centrifugation the supernatant was removed and the cell pellet resuspended in 25mls of culture medium. The cells and medium were transferred into a sterile 75cm<sup>2</sup> tissue culture flask and incubated at 37°C, in a humidified atmosphere of 5% CO<sub>2</sub>, 95% air. The following day the cell medium was replaced to remove any

remaining embryo debris. EF cells were treated identically to ES cells (Section 6.2) for passaging, freeze/thawing and the preparation of genomic DNA.

#### **6.4.2. Calcium Phosphate Transfection of Murine EFs**

A modified high efficiency calcium phosphate transfection technique was used to introduce the pICDP(for) plasmid into primary EFs (Chen & Okayama, 1987). The EFs were genotyped by PCR immediately after their isolation and only cells that were identified as p53 null were grown on for transfection. Twenty-four hours prior to transfection the EFs were harvested by trypsinisation (as described in Section 7.2.3), counted and  $5 \times 10^5$  cells were plated out on each 100mm-culture dish).

The DNA to be introduced was also prepared 24hrs prior to transfection.

Transfections were always done over a range of three DNA concentrations, 10µg/100mm dish, 20µg/100mm dish and 30µg/100mm dish as the optimum DNA concentration could not be determined. The total amount of DNA needed for each transfection was calculated and an appropriate volume of plasmid (Section 6.1.5.) was ethanol precipitated overnight (Section 6.1.4.). The following morning the DNA was pelleted by microcentrifugation, 10,000g at 4°C for 30 minutes. The pellet was rinsed with 70% ethanol and then allowed to air dry in sterile conditions. Once the pellet of DNA had dried it was resuspended in sterile water to give a final concentration of 1µg/µl. The DNA was allowed to resuspend thoroughly prior to use for transfection.

For each 100mm dish of cells to be transfected an individual mix of DNA/calcium phosphate was prepared. 10-30µl of the sterile DNA was aliquoted into a sterile universal and 250µl of 2.5M CaCl<sub>2</sub> solution was added. The CaCl<sub>2</sub> solution was prepared in advance, filtered sterilised and stored at -20°C until needed. Lastly, 250µl of 2XBBS was added to each universal to give an end volume of 500µl.



<b>2X BBS:</b>	BES	50mM
	NaCl	280mM
	Na <sub>2</sub> HPO <sub>4</sub>	1.5mM
	Adjust to pH 6.95 with conc. HCl, store at -20°C	

After the addition of 2XBBS, the DNA/calcium phosphate mix was left at room temperature for 20 minutes. During this 20-minute incubation the cells to be transfected were refed with fresh medium (9mls/100mm dish) before the addition of one individual 500µl DNA/calcium phosphate mix to each dish of cells. The culture dishes were then transferred into an incubator at 35°C. The cultures were also kept in low CO<sub>2</sub>, 3%, to allow the calcium phosphate/DNA complex to form slowly overnight. After overnight exposure to the precipitate the cells were rinsed thoroughly with PBS then refed with fresh non-selective media. The cells were kept in non-selective medium and returned to standard culture conditions, 37°C with 5%CO<sub>2</sub>, for the next 48 hours. After 48 hours had elapsed the non-selective medium was replaced with selective medium containing 2.5µg/ml of puromycin (Sigma). Clones became apparent after 15-20 days and at this point the cells were harvested for further analysis. The concentration of puromycin used to select transfected cells, 2.5µg/ml, was determined as described in Section 3.5.2.2.

#### **6.4.3. Immunohistochemical Detection of p53 Protein in EFs**

The half-life of p53 protein is approximately 15 minutes and it is normally below the threshold for immunodetection (Kamijo *et al*, 1998). However, p53 can be stabilised in cells by exposing them to a variety of insults, for example UV irradiation. The half-life of the stabilised protein is then increased to approximately 75 minutes and it becomes localised in the nucleus (Kamijo *et al*, 1998). Therefore to facilitate the detection of p53 expression in transfected primary fibroblasts the cells were exposed to 10J/m<sup>2</sup> of UV irradiation 6 hours prior to fixation (UV Crosslinker, Spectronics Corporation).

After 6 hours had elapsed the cells, growing on two-well chamber slides (Nunc), were rinsed with PBS and the slides then immersed in ice-cold 50:50 methanol:

acetone and kept at -20°C for 5 minutes. After fixation was complete the slides were air-dried, wrapped in foil and stored at -70°C.

When the slides were removed from storage they were covered with TBS-Tween.

<b>TBS-Tween:</b>	Tris-HCl, pH 7.6	0.5M
	NaCl	0.15M
	Tween	0.1%

The TBS-Tween was poured off and the slides placed in a rack and transferred into 0.5% hydrogen peroxide (diluted in methanol) for 15 minutes with gentle shaking. The slides were removed from the hydrogen peroxide solution and rinsed twice with water. After thorough rinsing the slides were removed from the rack, and covered with TBS-Tween. The TBS-Tween was then poured off and the slides were incubated in normal swine serum (Sigma) diluted 1:5 with TBS-Tween for 20 minutes at room temperature in a humid chamber. The swine serum was removed and the primary antibody added to the slides. The p53 primary antibody used was the rabbit polyclonal CM5 antibody (Novocastra) which was diluted 1:500 with 1:5 swine serum: TBS-Tween solution (300µl/well). The slides were incubated with the primary antibody in a humid chamber at room temperature for 1 hour. During this incubation the ABC complex was prepared, this consists of 5mls of ABC buffer (Tris-HCl, pH7.6) to which 1 drop of streptavidin solution and 1 drop of biotinylated horse radish peroxidase solution were added (the latter two are kit components of undisclosed concentration, DAKO).

<b>ABC Buffer:</b>	Tris	0.2M
	HCl	0.1M
	Adjust to pH 7.6	

The primary antibody solution was drained off the slides and they were washed three times at 5 minute intervals in TBS-Tween. After the last wash had been poured off the secondary antibody was added. The secondary antibody used was a biotinylated swine anti-rabbit immunoglobulin (DAKO). This antibody was diluted 1:400 with

1:5 swine serum: TBS-Tween solution and 300µl was added to each well of the chamber slide. The samples were incubated for 30 minutes at room temperature with the secondary antibody. After this incubation had been completed the slides were washed for three, five minute intervals with TBS-Tween before the ABC complex made previously was added (300µl/well). The slides were then incubated for a further 30 minutes at room temperature in a humid chamber. The ABC complex was washed off the slides with three, 5 minute washes in TBS-Tween. HRP activity was visualised with diaminobenzidine (DAB). 100µl aliquots of DAB (25mg/ml) were made up and stored at -20°C. One DAB aliquot was defrosted and mixed with 4.9mls of DAB buffer.

<b>DAB Buffer:</b>	Tris	0.2M
	HCl	0.1M
	Imidazole	0.01M
	Adjust to pH 7.6	

300µl of the DAB/Buffer mix was added to each well of a chamber slide and the reaction allowed to proceed for 10 minutes. The transfer of the slides into water stopped the reaction. The slides were then counterstained with haematoxylin and mounted.

## 6.5. Manipulation of RNA

### 6.5.1. RNA Extraction

RNA was extracted from cells using the High Pure RNA Isolation Kit (Boehringer Mannheim) according to the manufacturers protocol. Briefly, cells were harvested by trypsinisation and pelleted by centrifugation at 800xg, 3 minutes. The cell pellet was then resuspended in 200µl of PBS and lysed by the addition of 400µl of Lysis/Binding buffer. A High Pure filter tube was then fitted into a collection tube (both supplied with the kit) and the sample added directly onto the filter. The tubes were then spun for 15 secs. at 8,000xg and the flow-through discarded. At this point both the DNA and RNA components of the cell extract are bound to the High Pure filter. Genomic DNA was then removed by the addition of 90µl of DNase

incubation buffer and 10µl of DNase I directly onto the filter. Digestion was allowed to proceed for 15 minutes at room temperature. Further impurities were removed from the RNA by two subsequent wash steps before elution of the RNA in 50µl of nuclease free, sterile ddH<sub>2</sub>O. RNA samples extracted by the method were stored at -70°C. RNA concentrations were determined spectrophotometrically (GeneQuant, Pharmacia Biotech).

**6.5.2. Reverse Transcription**

An appropriate amount of RNA, 0.1-1µg was diluted in a total volume of 10µl with nuclease-free water and 1µl of oligo dT primer (500µg/ml, Cruachem) was added. This procedure was carried out in nuclease-free, sterile 0.5ml Eppendorfs which also facilitated the use of thermal cycler heating blocks during the protocol.

The sample was heated to 70°C for 10 minutes then transferred onto ice. After 1 minute on ice the sample tube was centrifuged briefly to collect all fluid. To the 11µl sample volume a further 4µl of 5X First Strand Buffer, 2µl of 0.1M Dithiothreitol and 2µl of dNTP mix (10mM each) was added.

<b>5X First Strand Buffer:</b>	Tris-HCl, pH8.3	250mM
	KCl	375mM
	MgCl <sub>2</sub>	15mM

The samples were then mixed gently and transferred back to the thermal cycler. After heating the samples to 42°C for 2 minutes, 1µl (200 U) of Superscript™ II RNase H- Reverse Transcriptase (Life Technologies) was added to each tube. The reaction was then allowed to proceed at 42°C for a further 50 minutes before the enzyme was heat inactivated by a 15 minute incubation at 70°C. The cDNA synthesis was then complete and the products can be used as templates of the RT-PCR reactions described in Section 6.1.14.3.

# References

## References

- Abramova NA, Russell J, Botchan M, Li R. (1997). Interaction between replication protein A and p53 is disrupted after UV damage in a DNA repair-dependent manner. *Proc. Natl. Acad. Sci. USA*. **94**, 7186-7191.
- Abremski K, Hoess RH, Sternberg N. (1983). Studies on the properties of P1 site-specific recombination : evidence for topologically unlinked products following recombination. *Cell* **32**, 1301-1311.
- Abremski K, & Hoess RH. (1984). Bacteriophage P1 site-specific recombination. Purification and properties of the Cre recombinase protein. *J. Biol. Chem.* **259**, 1509-1514.
- Adair GM, Nairn RS, Wilson JH, Seidman MM, Brothman KA, Mackinnon C, Scherer JB. (1989). Targeted homologous recombination at the endogenous adenine phosphoribosyltransferase locus in Chinese Hamster cells. *Proc. Natl. Acad. Sci. USA* **86**, 4574-4579.
- Afshari CA, Vojta PJ, Bivins HB, Annab LA, Willard TB, Futreal PA, Barret JC. (1993). Investigation of the role of G1/S cell cycle mediators in cellular senescence. *Exp. Cell Res.* **209**, 231-237.
- Agah R, Frenkel PA, French BA, Michael LH, Overbeek PA, Schneider MD. (1997). Gene recombination in postmitotic cells, targeted expression of cre recombinase provokes cardiac site-specific rearrangement in adult ventricular muscle in vivo. *J. Clin. Invest.* **100**(1), 169-179.
- Agarwal ML, Agarwal A, Taylor WR, Strak GR. (1995). P53 controls both the G2/M and the G1 cell cycle checkpoints and mediates reversible growth arrest in human fibroblasts. *Proc. Natl. acad. Sci. USA*. **92**, 8493-8497.
- Agarwal ML, Taylor WR, Chernov MV, Chernova OB, Stark GR. (1998). The p53 network. *J. Biol. Chem.* **1**(2),1-4.
- Agoff SN, Hou J, Linzer DIH, Wu B. (1993). Regulation of the human hsp70 promoter by p53. *Science* **259**, 84-87.
- Aitken A. (1996). 14-3-3 and its possible role in co-ordinating multiple signalling pathways. *Trends In Cell Biol.* **6**, 341-347.
- Akoulitchiev S, Makela TP, Weinberg RA, Reinberg D. (1995). Requirement for TFIID kinase activity in transcription by RNA polymerase II. *Nature* **377**, 557-560.
- Aladjem MI, Brody LL, O'Gorman S, Wahl GM. (1997). Positive selection of FLP-mediated unequal sister chromatid exchange products in mammalian cells. *Mol. Cell. Biol.* **17**(2), 857-861.



Aladjem MI, Spike BT, Rodewald LW, Hope TJ, Klemm M, Jaenisch R, Wahl GM. (1998). ES cells do not activate p53-dependent stress responses and undergo p53-independent apoptosis in response to DNA damage. *Curr. Biol.* **8**, 145-155.

Allsopp RC, Vaziri H, Patterson C, Goldstein S, Younglai EV, Fletcher AB, Grider CW, Harley CB. (1992). Telomere length predicts replicative capacity of human fibroblasts. *Proc. Natl. Acad. Sci. USA* **89**, 10114-10118.

Almog N, Li R, Peled A, Schwartz D, Wolkowicz R, Goldfinger N, Pei H, Rotter V. (1997). The murine C-terminally alternatively spliced form of p53 induces attenuated apoptosis in myeloid cells. *Mol. Cell. Biol.* **17**(2), 713-722.

Amin AA, & Sadowski PD. (1990). Synaptic intermediates promoted by FLP recombinase. *J. Mol. Biol.* **214**, 55-72.

Andrews BJ, Beatty LG, Sadowski PD. (1987). Isolation of intermediates in the binding of the FLP recombinase from the yeast 2 $\mu$ M circle to its target sequence. *J. Mol. Biol.* **193**, 345-358.

Anton M, Graham FL. (1995). Site specific recombination mediated by an adenovirus vector expressing the cre recombinase protein : a molecular switch for control of gene expression. *J. Virol.* **69**(8), 4600-4606.

Araki K, Araki M, Miyazaki J-I, Vassalli P. (1995). Site-specific recombination of a transgene in fertilised eggs by transient expression of Cre recombinase. *Proc. Natl. Acad. Sci. USA*. **92**, 160-164.

Arai N, Nomura D, Yokota K, Wolf D, Brill E, Shohat O, Rotter V. (1986). Immunologically distinct p53 molecules generated by alternative splicing. *Mol. Cell. Biol.* **6**, 3232-3239.

Argos P, Landy A, Abremski K, Egan JB, Haggard-Ljungquist E, Hoess RH, Kahn ML, Kalionis B, Narayana SVL, Pierson III LS, Sternberg N, Leong JM. (1986). The integrase family of site-specific recombinases : regional similarities and global diversity. *EMBO J.* **5**(2), 433-440.

Armstrong JF, Kaufman MH, Harrison DJ, Clarke AR. (1995). High-frequency developmental abnormalities in p53-deficient mice. *Current Biol.* **5**(8), 931-936.

Askew GR, Doetschman T, Lingrel JB. (1993). Site-directed point mutations in embryonic stem cells : a gene targeting tag and exchange strategy. *Mol. Cell. Biol.* **13**(7), 4115-24.

Atadja P, Wong H, Garkatsev I, Veillette C, Riabowol K. (1995). Increased activity of p53 in senescing fibroblasts. *Proc. Natl. Acad. Sci. USA* **92**, 8348-8352.

Austin S, Zieses M, Sternberg N. (1981). A novel role for site-specific recombinases in the maintenance of bacterial replicons. *Cell* **25**, 729-736.

Avantaggiati ML, Ogryzko V, Gardner K, Giordano A, Levine AS, Kelly K. (1997). Recruitment of p300/CBP in p53-dependent signal pathways. *Cell* **89**, 1175-1184.

- Bakalkin G, Yakovleva T, Selivanova G, Magnusson KP, Szekzly L, Kiseleva E, Klein G, terenius L, Wiman KG. (1994). p53 binds single strand DNA ends and catalyzes DNA renaturation and strand transfer. *Proc. Natl. Acad. Sci. USA*. **91**, 413-417.
- Banin S, Moyal L, Shieh S-Y, Taya Y, Anderson CW, Chessa L, Smorodinsky NI, Prives C, Reiss Y, Shiloh Y, Ziv Y. (1998). Enhanced phosphorylation of p53 by Atm in response to DNA damage. *Science* (in press).
- Barak Y, & Oren M. (1992). Enhanced binding of a 95kDa protein to p53 in cells undergoing p53-mediated growth arrest. *EMBO J.* **11**, 2115-2121.
- Bargonetti J, friedman PN, Kern SE, Vogelstein B, Prives C. (1991). Wild type but not mutant p53 immunopurified proteins bind to sequences adjacent to the SV40 origin of replication. *Cell* **65**, 1083-1091.
- Barlow C, Schroeder M, lekstrom-Himes J, Kylefjord H, Deng C-X, Wynshaw-Boris A, Spiegelman BM, Xanthopoulos KG. (1997). Targeted expression of cre recombinase to adipose tissue of transgenic mice directs adipose-specific excision of loxP-flanked gene segments. *Nucleic Acids Res.* **25(12)**, 2543-2545.
- Barnes WM. (1994). PCR amplification of up to 35kb of DNA with high fidelity and high yield from lambda bacteriophage templates. *Proc. Natl. Acad. Sci. USA* **91**, 2216-2220.
- Barrett JC & Fletcher WF. (1987). Mechanisms of environmental carcinogenesis: multistep models of carcinogenesis. (Barrett JC ed.). **2**, 73-116. CRC Press, Boca Raton.
- Baskaran R, Wood LD, Whitaker LL, Canman CE, Morgan SE, Xu Y, Barlow C, Baltimore D, Wynshaw-Boris A, Kastan MB, Wang JY. (1997). Ataxia telangiectasia mutant protein activates c-Abl tyrosine kinase in response to ionizing radiation. *Nature* **387**, 516-519.
- Baudier J, Delphin C, Grunwald D, Knochbin S, Lawrence JJ. (1992). Characterisation of the tumour suppressor protein p53 as a protein kinase C substrate and a S100b-binding protein. *Proc. Natl. Acad. Sci. USA*. **89**, 11627-11631.
- Bayle JH, Elenbaas B, Levine AJ. (1995). The carboxyl-terminal domain of the p53 protein regulates sequence-specific DNA binding through its non-specific nucleic acid binding activity. *Proc. Natl. Acad. Sci. USA*. **92**, 729-733.
- Beatty LG, Sadowski PD. (1988). The mechanism of loading of the FLP recombinase onto its DNA target sequence. *J. Mol. Biol.* **204**, 283-294.
- Beck E, Ludwig G, Auerswald EA, Reiss B, Schaller H. (1982). Nucleotide sequence and exact localisation of the neomycin phosphotransferase gene from transposon Tn5. *Gene* **19**, 327-336.
- Beenken SW, Karsenty G, Raycroft L, Lozano G. (1994). An intron binding protein is required for transformation ability of p53. *Nucleic Acids Res.* **19(17)**, 4747-4752.
- Beham A, Marin C, Fernandez A, Hermann J, Brisbay S, Tari UM, Lopez-Bernstein G, Lozano G, Sarkiss M, McDonnell TJ. (1997). Bcl-2 inhibits p53 nuclear import following DNA damage. *Oncogene* **15**, 2767-2772.

- Berg P. (1993). Co-chairmans remarks : reverse genetics: directed modification of DNA for functional analysis. *Gene* **135**, 261-264.
- Bergqvist I, Eriksson B, Eriksson M, Holmberg D. (1998). Transgenic cre recombinase expression in germ cells and early embryogenesis directs homogeneous and ubiquitous deletion of loxP-flanked gene segments. *FEBS Lett.* **438**, 76-80.
- Berube NG, Smith JR, Pereira-Smith OM. (1998). Insights from model systems. The genetics of cellular senescence. *Am. J. Hum. Genet.* **62**, 1015-1019.
- Bethke B, & Sauer B. (1997). Segmental genomic replacement by cre-mediated recombination : genotoxic stress activation of the p53 promoter in single-copy transformants. *Nucleic Acid Res.* **25(14)**, 2828-2834.
- Betz UKA, Voßhenrich CAJ, Rajewsky K, Muller W. (1996). Bypass of lethality with mosaic mice generated by Cre-loxP mediated recombination. *Current Biol.* **6(10)**, 1307-1316.
- Bian J, & Sun Y. (1997). Transcriptional activation by p53 of the human type IV collagenase (gelatinase A or matrix metalloproteinase2) promoter. *Mol. Cell. Biol.* **17(11)**, 6330-6338.
- Bienz B, Zakut-Houri R, Givol D, Oren M. (1984). Analysis of the gene coding for the murine cellular tumour antigen p53. *EMBO J.* **3(9)**, 2179-2183.
- Bienz-Tadmor B, Zakut-Houri R, Libresco S, Givol D, Oren M. (1985). The 5' region of the p53 gene: evolutionary conservation and evidence for a negative regulatory element. *EMBO J.* **4(12)**, 3209-3212.
- Bishop JO, & Smith P. (1989). Mechanism of chromosomal integration of microinjected DNA. *Mol. Biol. Med.* **6**, 283-298.
- Blagosklonny MV, An WG, Romanova LY, Trepel J, Fojo T, Neckers L. (1998). P53 inhibits hypoxia-inducible factor stimulated transcription. *J. Biol. Chem.* **273(20)**, 11995-11998.
- Blasco MA, Lee H-W, Hande MP, Samper E, Lansdorp PM, DePinho RA, Greider CW. (1997). Telomere shortening and tumour formation by mouse cells lacking telomerase RNA. *Cell* **91**, 25-34.
- Blaydes JP, & Hupp TR. (1998). DNA damage triggers DRB-resistant phosphorylation of human p53 at the CK2 site. *Oncogene* **17**, 1045-1052.
- Blount PL, Galipeau PC, Sanchez CA, Neshat K, Levine DS, Yin J, Suzuki H, Abraham JM, Meltzer SJ, Reid BJ. (1994). 17p allelic losses in diploid cells of patients with Barrett's oesophagus who develop aneuploidy. *Cancer Res.* **54**, 2292-2295.
- Bollag RJ, Waldman AS, Liskay RM. (1989). Homologous recombination in mammalian cells. *Ann. Rev. Genet.* **23**, 199-225.

- Bookstein R. (1994). Tumour suppressor genes in prostatic oncogenesis. *J. Cell. Biochem. (suppl.)* **19**, 217-223.
- Borrellini E, Heyman R, His M, Evans RM. (1988). Targeting of an inducible toxic phenotype in animal cells. *Proc. Natl. Acad. Sci. USA* **85**, 7572-76.
- Borrellini F, & Glazer RI. (1993). Induction of Sp1-p53 DNA binding heterocomplexes during granulocyte/macrophage colony-stimulating factor-dependent proliferation in human erythroleukaemia cell line TF-1. *J. Biol. Chem.* **268**, 7923-28.
- Bouhassira EE, Westerman K, Leboulch P. (1997). Transcriptional behaviour of LCR enhancer elements integrated at the same chromosomal locus by recombinase mediated cassette exchange. *Blood* **90**(9), 3332-3344.
- Bourdon J-C, Deguin-Chambon V, Lelong J-C, Dessen P, Debuire B, May E. (1997). Further characterisation of the p53 responsive element – identification of new candidate genes for transactivation by p53. *Oncogene* **14**, 85-94.
- Bradley A, Evans M, Kaufman MH, Robertson E. (1984). Formation of germ-line chimaeras from embryo-derived teratocarcinoma cell lines. *Nature* **309**, 255-256.
- Broach JR, & Hicks JB. (1980). Replication and recombination functions associated with yeast plasmid 2 $\mu$ M circle. *Cell* **21**, 501-8.
- Brocard J, Warot X, Wendling O, Messadeq N, Vonesch J-L, Chambon P, Metzger D. (1997). Spatio-temporally controlled site-specific somatic mutagenesis in the mouse. *Proc. Natl. Acad. Sci. USA*. **94**, 14559-14563.
- Brocard J, Feil R, Chambon P, Metzger D. (1999). A chimeric cre recombinase inducible by synthetic, but not by natural ligands of the glucocorticoid receptor. *Nucleic Acids Res.* **26**(17), 4086-4090.
- Brooks AI, Mukherjee B, Panahian N, Cory-Slechta D, Federoff HJ. (1997). Nerve growth factor somatic mosaicism produced by herpes virus-directed expression of cre recombinase. *Nature Biotech.* **15**, 57-62.
- Brown CR, Doxsey SJ, White E, Welch WJ. (1994). Both viral (adenovirus E1B) and cellular(hsp 70 and p53) components interact with centrosomes. *J. Cell. Physiol.* **160**, 47-60.
- Bruce S. (1991). Ultrastructure of dermal fibroblasts during development and ageing: relationship to in vitro senescence of dermal fibroblasts. *Exp. Gerontol.* **26**, 3-16.
- Brugarolas J, Chandrasekaran C, Gordon JI, Beach D, Jacks T, Hannon GJ. (1995). Radiation induced cell cycle arrest compromised by p21 deficiency. *Nature* **377**, 552-557.
- Bubeck P, Winkler M, Bautsch W. (1993). Rapid cloning by homologous recombination in vivo. *Nucleic Acids Res.* **21**(15), 3601-3602.

- Bucholz F, Angrand P-O, Stewart A.F. (1996). A simple assay to determine the functionality of Cre or FLP recombination targets in genomic manipulation constructs. *Nucleic Acids Res.* **24(15)**, 3118-3119.
- Buckbinder L, Talbott R, Velasco-Migule S, Takenaka I, Faha B, Seizinger BR, Kley N. (1996). Induction of the growth inhibitor IGF-binding protein 3 by p53. *Nature* **377**, 646-649.
- Buckbinder L, Velasco-Miguel S, Chen Y, Xu N, Talbott R, Gelbert L, Gao J, Seizinger BR, Gutkind JS, Kley N. (1997). The p53 tumour suppressor targets a novel regulator of G protein signalling. *Proc. Natl. Acad. Sci. USA.* **94(15)**, 7868-7872.
- Caelles C, Helmberg A, Karin M. (1994). P53 dependent apoptosis in the absence of transcriptional activation of p53 target genes. *Nature* **370**, 220-223.
- Cahilly-Snyder L, Yang-Feng T, Francke U, George DL. (1987). Molecular analysis and chromosomal mapping of amplified genes isolated from a transformed mouse 3T3 cell line. *Som. Cell Mol. Genet.* **13**, 235-244.
- Cairns CA, & White RJ. (1998). P53 is a general repressor of RNA polymerase III transcription. *EMBO J.* **17(11)**, 3112-3123.
- Campisi J. (1996). Replicative senescence: An old wives tail ? *Cell* **84**, 497-500.
- Canman CE, Gilmer TM, Coutts SB, Kastan MB. (1995). Growth factor modulation of p53-mediated growth arrest versus apoptosis. *Genes Dev.* **9**, 600-611.
- Canman CE, Lim D-S, Cimprich KA, Taya Y, Tamai K, Sakaguchi K, Apella E, Kastan MB, Siliciano JD. (1998). Activation of the atm kinase by ionising radiation and phosphorylation of p53. *Science* (in press).
- Castle WE & Allen GM. (1903). The heredity of albinism. *Proc. Am. Acad. Arts Sci.* **38**, 603-621.
- Chellappan SP, Hiebert S, Mudryj M, Horowitz JM, Nevins JR. (1991). The E2F transcription factor is a cellular target for the RB protein. *Cell* **65**, 1053-61.
- Chen C & Okayama H. (1987). High-efficiency of mammalian cells by plasmid DNA. *Mol. Cell. Biol.* **7**, 2745-2752.
- Chen X, Bargonetti J, Prives C. (1995). p53, through p21(WAF1/CIP1), induces cyclin D1 synthesis. *Cancer Res.* **55(19)**, 4257-4263.
- Chen X, Ko LJ, Jayaraman L, Prives C. (1996). P53 levels, functional domains and DNA damage determine the extent of the apoptotic response of tumour cells. *Genes & Dev.* **10**, 2438-2451.
- Chesnokov I, Chu WM, Botchan MR, Schmid CW. (1996). P53 inhibits RNA polymerase III-directed transcription in a promoter dependent manner. *Mol. Cell. Biol.* **16**, 7084-7088.



- Chin K-V, Ueda K, Pastan I, Gottesman MM. (1992). Modulation of activity of the promoter of the human MDR1 gene by ras and p53. *Science* **255**, 459-462.
- Chiou SK, Rao L, White E. (1994). Bcl-2 blocks p53-dependent apoptosis. *Mol. Cell. Biol.* **14**(4), 2556-2563.
- Cho Y, Gorina S, Jeffrey PD, Pavletich NP. (1994). Crystal structure of a p53 tumour suppressor-DNA complex : understanding tumourigenic mutations. *Science* **265**, 346-355.
- Chouluka A, Guyot V, Nicolas J-F. (1996). Transfer of single gene containing long terminal repeats into the genome of mammalian cells by a retroviral vector carrying the cre gene and the LoxP site. *J. Virol.* **70**(3), 179-1798.
- Chowdary DR, Dermody JJ, Jha KK, Ozer HL. (1994). Accumulation of p53 in a mutant cell line defective in the ubiquitin pathway. *Mol. Cell. Biol.* **14**, 1997-2003.
- Chuang LS-H, Ian HI, Koh T-W, Ng H-H, Xu G, Li BFL. (1996). Human DNA-(cytosine-5) methyltransferase-PCNA complex as a target for p21<sup>WAF1</sup>. *Science* **277**, 1996-2000.
- Church GM, & Gilbert W. (1984). Genomic sequencing. *Proc. Natl. Acad. Sci. USA* **81**, 1991-5.
- Clarke AR, Purdie CA, Harrison DJ, Morris RG, Bird CC, Hooper ML, Wyllie AH. (1993). Thymocyte apoptosis induced by p53-dependent and independent pathways. *Nature* **362**, 849-851.
- Cody CW, Prasher DC, Westler WM, Prendergast FG, Ward WW. (1993). Chemical structure of the hexapeptide chromophore of *Aequorea* green-fluorescent protein. *Biochemistry* **32**, 1212-1218.
- Cohen GB, Ren R, Baltimore D. (1995). Modular binding domains in signal transduction proteins. *Cell* **80**, 237-248.
- Conzen SD, Snay CA, Cole CN. (1997). Identification of a novel antiapoptotic functional domain in simian virus 40 large T antigen. *J. Virol.* **71**, 4536-4543.
- Cooper C. (1999). Thesis submitted for the degree of Doctor of Philosophy, Department of Pathology, University of Edinburgh.
- Cormack B, (1996). FACS optimised mutants of the green fluorescent protein. *Gene* **173**, 33-38.
- Cristofalo VJ, Phillips PD, Sorger T, Gerhard G. (1989). Alterations in the responsiveness of senescent cells to growth factors. *J. Gerontol.* **44**, 55-59.
- Crook T, Parker GA, Rozycza M, Crossland S, Allday MJ. (1998). A transforming p53 mutant which binds DNA, transactivates and induces apoptosis reveals a nuclear:cytoplasmic shuttling defect. *Oncogene* **16**(11), 1429-1441.
- Cross SM, Sanchez CA, Morgan CA, Schimke MK, Ramel S, Idzerda RL, Raskind WH, Reid B. (1995). A p53-dependent mouse spindle checkpoint. *Science* **267**, 1353-1356.



Croyle MA, Roessler BJ, Davidson BL, Hilfinger JM, Amidon GL. (1998). Factors that influence stability of recombinant adenoviral preparations for human gene therapy. *Pharm. Dev. Technol.* **3**(3), 373-383.

Czosnek HH, Bienz B, Givol D, Zakut-Houri R, Pravtcheva DD, Ruddle RH, Oren M. (1984). The gene and the pseudogene for mouse p53 cellular tumour antigen are located on different chromosomes. *Mol. Cell. Biol.* **4**, 1638-40.

Dameron KM, Volpert OV, Tainsky MA, Bouck N. (1994). Control of angiogenesis in fibroblasts by p53 regulation of thrombospondin-1. *Science* **265**(5178), 1582-1584.

Damjanov I, Solter D, Skreb N. (1971). Teratocarcinogenesis as related to the age of embryos grafted under the kidney capsule. *Roux Arch. Dev. Biol.* **173**, 228-234.

Daniel CW, DeOme KB, Young JT, Blair PB, Faulkin LJ Jr. (1968). The in vivo lifespan of normal and preneoplastic mouse mammary glands : a serial transplantation study. *Proc. Natl. Acad. Sci. USA.* **61**, 53-60.

Danielian PS, Muccino D, Rowitch DH, Michael SK, McMahon AP. (1998). Modification of gene activity in mouse embryos in utero by a tamoxifen-inducible form of Cre recombinase. *Curr. Biol.* **8**, 1323-1326.

Dasgupta G, & Momand J. (1997). Geldanamycin prevents nuclear translocation of mutant p53. *Exp. Cell. Res.* **237**(1), 29-37.

Debbas M, & White E. (1993). Wild-type p53 mediates apoptosis by E1A, which is inhibited by E1B. *Genes & Dev.* **7**, 546-554.

Deffie A, Wu H, Reinke V, Lozano G. (1993). The tumour suppressor gene p53 regulates its own transcription. *Mol. Cell. Biol.* **13**, 3415-3423.

DeGregori J, Kowalik T, Nevins JR. (1995). Cellular targets for activation by the E2F1 transcription factor include DNA synthesis- and G1/S-regulatory genes. *Mol. Cell. Biol.* **15**(8), 4215-4224.

Del Sal G, Ruaro E, Utrera R, Cole CN, Levine AJ, Schneider CJ. (1995). Gas-1 induced growth suppression requires a transactivation-independent p53 function. *Mol. Cell. Biol.* **15**(12), 7152-7160.

Demers GW, Halbert CL, Galloway DA. (1994). Elevated wild-type p53 protein levels in human epithelial cell lines immortalised by human papillomavirus type 16 E7 gene. *Virology* **198**, 169-174.

Deng C, Zhang P, Harper JW, Elledge SJ, Leder P. (1995). Mice lacking p21CIP1/WAF1 undergo normal development but are defective in G1 checkpoint control. *Cell* **82**, 675-684.

Desdouets C, Ory C, Matesic G, Soussi T, Brechot C, Sobczak-Thépot J. (1996). ATF/CREB site mediated transcriptional activation and p53 dependent repression of the cyclin A promoter. *FEBS Lett.* **385**, 34-38.

- de Stanchina E, McCurrach ME, Zindy F, Shieh SY, Fereyre G, Samuelson AV, Prives C, Roussel MF, Sherr CJ, Lowe SW. (1998). E1A signalling to p53 involves the p19ARF tumour suppressor. *Genes & Dev.* **12**, 2434-2442.
- Detloff PJ, Lewis J, John SWM, Shehee WR, Langenbach R, Maeda N, Smithies O. (1994). Deletion and replacement of the mouse adult  $\beta$ -globin genes by a "plug and socket" repeated targeting strategy. *Mol. Cell. Biol.* **14**(10), 6939-6943.
- De Laurenzi V, Costanzo A, Barcaroli D, Terrinoni A, Falco M, Annicchiarico-Petruzzelli M, Levrero M, Melino G. (1998). Two new p73 splice variants, gamma and delta, with different transcriptional activity. *J. Exp. Med.* **188**(9), 1763-8.
- Dias JM, Go NF, Hart CP, Mattheakis LC. (1998). Genetic recombination as a reporter for screening steroid receptor agonists and antagonists. *Anal. Biochem.* **258**, 96-102.
- Di Leonardo A, Linke SP, Clarkin K, Wahl GM. (1994). DNA damage triggers a prolonged G1 arrest and long-term induction of Cip1 in normal human fibroblasts. *Genes & Dev.* **8**, 2540-2551.
- Di Leonardo A, Khan SH, Linke SP, Greco V, Seidita G, Wahl GM. (1997). DNA replication in the presence of mitotic spindle inhibitors in human and mouse fibroblasts lacking either p53 or RB function. *Cancer Res.* **57**, 1013-1019.
- Dimri DP, Hara E, Campisi JC. (1994). Regulation of two E2F-related genes in senescent and presenescent fibroblasts. *J. Biol. Chem.* **269**, 16180-16186.
- Dimri GP, Lee X, Basile G, Acost M, Scott G, Roskelley C, Medrano EE, Linskens M, Rubeli I, Pereira-Smith O, Peacocke M, Campisi J. (1995). A biomarker that identifies senescent human cells in culture and in aging skin in vivo. *Proc. Natl. Acad. Sci. USA* **92**, 9363-9367.
- Diwan SB, & Stevens LC. (1976). Development of teratomas from ectoderm of mouse egg cylinders. *J. Natl. Cancer Inst.* **57**, 937-942.
- Doetschman T, Maeda N, Smithies O. (1988). Targeted mutation of the Hprt gene in mouse embryonic stem cells. *Proc. Natl. Acad. Sci. USA* **85**, 8583-8587.
- Donehower LA, Harvey M, Slagle BL, McArthur MJ, Montgomery CA, Butel JS *et al.* (1992). Mice deficient for p53 are developmentally normal but susceptible to spontaneous tumours. *Nature* **356**, 215-221.
- Donehower LA, Godley LA, Aldaz CM, Pyle R, Shi Y-P, Pinkel D, Gray J, Bradley A, Medina D, Varmus HE. (1995). Deficiency of p53 accelerates mammary tumourigenesis in Wnt-1 transgenic mice and promotes chromosomal instability. *Genes & Dev.* **9**, 882-895.
- Doolittle DP, Davisson MT, Guidi JN, Green MC. (1996). Catalogue of mutant genes and polymorphic loci. In *Genetic variants and strains of the laboratory mouse*, 3<sup>rd</sup> ed. (eds. Lyon MF, Rastan S, Brown SDM.), pages 17-854. Oxford University Press, Oxford, UK.

Drane P, Barel M, Balbo M, Frade R. (1997). Identification of RB18A, a 205kDa new p53 regulatory protein which shares antigenic and functional properties with p53. *Oncogene* **15**, 3013-3024.

Dulic V, Kaufman WK, Wilson SJ, Tlsty TD, Lees E, Harper JW, Elledge SJ, Reed SI. (1994). P53-dependent inhibition of cyclin-dependent kinase activities in human fibroblasts during radiation-induced G1 arrest. *Cell* **76**, 1013-1023.

Duncan EL, Whitaker NJ, Moy EL, Reddel RR. (1993). Assignment of SV40-immortalised cells to more than one complementation group for immortalisation. *Exp. Cell Res.* **205**, 337-344.

Dutta A, Ruppert SM, Aster JC, Winchester E. (1993). Inhibition of DNA replication factor RPA by p53. *Nature* **365**, 79-82.

Dymecki SM. (1996). Fp recombinase promotes site-specific DNA recombination in embryonic stem cells and transgenic mice. *Proc. Natl. Acad. Sci. USA* **93**, 6191-6196.

Dymecki SM, & Tomasiewicz H. (1998). Using Flp-recombinase to characterise expansion of Wnt1-expressing neural progenitors in the mouse. *Dev. Biol.* **201**, 57-65.

Dynan WS. (1986). Promoters for housekeeping genes. *Trends Genet.* **2**, 196-197.

el Diery WS, Kinzler SE, Pietenpol JA, Kinzler KW, Vogelstein B. (1992). Definition of a consensus sequence binding site for p53. *Nature Genet.* **1**, 45-47.

el-Diery WS, Tokino T, Velculescu VE, Levy DB, Parsons R, Trent JM, Lin D, Mercer WE, Kinzler KW, Vogelstein B. (1993). WAF1, a potential mediator of p53 tumour suppression. *Cell* **75**, 817-825.

Elkind NB, Goldfinger N, Rotter V. (1995). Spot-1, a novel NLS-binding protein that interacts with p53 through a domain encoded by p(CA)<sub>n</sub> repeats. *Oncogene* **11**, 841-851.

Epstein CJ, Martin GM, Schultz AL, Motulsky AG. (1966). Werner's syndrome a review of its symptomatology, natural history, pathologic features, genetics and relationship to the natural aging process. *Medicine (Baltimore)* **45**, 177-221.

Evans MJ, & Kaufman MJ. (1981). Establishment in culture of pluripotential cells from mouse embryos. *Nature* **292**, 154-156.

Evans MJ, Bradley A, Kuehn M, Robertson EJ. (1985). The ability of EK cells to form chimaeras after selection of clones in G418 and some observations on the integration of retroviral vector proviral DNA into EK cells. *Cold spring Harbour Symp. Quant. Biol.* **50**, 685-689.

Ewen ME, & Miller SJ. (1995a). p53 and translational control. *Biochim. Biophys. Acta* **1242**, 181-184.

Ewen ME, Oliver CJ, Sluss HK, Miller SJ, Peeper DS. (1995b). p53 dependent replication of CDK4 translation in TGF- $\beta$  induced G1 cell cycle arrest. *Genes & Dev.* **9**, 204-217.

- Farmer G, Bargonetti J, Zhu H, Friedman P, Prywes R, Prives C. (1992). Wild-type p53 activates transcription *in vitro*. *Nature* **358**, 83-86.
- Fearon ER, & Vogelstein B. (1990). A genetic model for colorectal tumourigenesis. *Cell* **61**, 759-767.
- Feil R, Brocard J, Mascrez B, LeMeur M, Metzger D, Chambon P. (1996). Ligand-activated site-specific recombination in mice. *Proc. Natl. Acad. Sci. USA*. **93**, 10887-10890.
- Feil R, wagner J, Metzger D, Chambon P. (1997). Regulation of cre recombinase activity by mutated estrogen receptor ligand binding domains. *Biochem. Biophys. Res. Comm.* **237**, 752-757.
- Fields S, & Jang S. (1990). Presence of a potent transcription activating sequence in the p53 protein. *Science* **249**, 1046-1049.
- Fisher JP, Hope SA, Hooper ML. (1989). Factors influencing the differentiation of embryonal carcinoma and embryo-derived stem cells. *Exp. Cell Res.* **182**, 403-414.
- Fiskerstrand CE, Lovejoy EA, Gerrard L, Quinn JP. (1999). An intronic domain within the rat Preprotachykinin gene containing a CCCT repetitive motif acts as an enhancer in differentiating embryonic stem cells. *Neuroscience Lett.* In press.
- Folger KR, Wong EA, Wahl G, Cappechi MR. (1982). Patterns of integration of DNA microinjected into cultured mammalian cells : evidence for homologous recombination between injected plasmid DNA molecules. *Mol. Cell. Biol.* **2**, 1372-1387.
- Fontoura BA, Sorokina EA, David E, Carroll RB. (1992). P53 is covalently linked to 5.8S rRNA. *Mol. Cell. Biol.* **12**, 5145-5151.
- Friedrich G, & Soriano P. (1991). Promoter traps in embryonic stem cells : a genetic screen to identify and mutate developmental genes in mice. *Genes & Dev.* **5**, 1513-1523.
- Fuchs B, O'Connor D, Fallis L, schiedtmann KH, Lu X. (1995). p53 phosphorylation mutants retain transcriptional activity. *Oncogene* **10**, 789-793.
- Fukasawa K, Choi T, Kuriyama R, Rulong S, Vande Woude GF. (1996). Abnormal centrosome proliferation in the absence of p53. *Science* **271**, 1744-1747.
- Fukushige S, & Sauer B. (1992). Genomic targeting with a positive-selection lox integration vector allows highly reproducible gene expression in mammalian cells. *Proc. Natl. Acad. Sci. USA*. **89**, 7905-7909.
- Gagneten S, Le Y, Miller J, Sauer B. (1997). Brief expression of a GFPcre fusion gene in embryonic stem cells allows rapid retrieval of site-specific genomic deletions. *Nucleic Acid Res.* **25(16)**, 3326-3331.
- Gajovic S, St-Onge L, Yokota Y, Gruss P. (1997). Retinoic acid mediates Pax6 expression during in vitro differentiation of embryonic stem cells. *Differentiation* **62**, 187-192.

- Gannon JV, & Lane DP. (1991). Protein synthesis required to anchor a mutant p53 protein which is temperature-sensitive for nuclear transport. *Nature* **349**, 802-806.
- Garkavtsev I, Kazarov A, Gudkov A, Riabowol K. (1996). Suppression of the novel growth inhibitor p33<sup>ING1</sup> promotes neoplastic transformation. *Nat. Genet.* **14**, 415-420.
- Garkavtsev I, & Riabowol K. (1997). Extension of the replicative life span of human diploid fibroblasts by inhibition of the p33<sup>ING1</sup> candidate tumour suppressor. *Mol. Cell. Biol.* **17**(4), 2014-2019.
- Garkavtsev I, Grigorian IA, Ossovskaya VS, Chernov MV, Chumakov PM, Gudkov AV. (1998). The candidate tumour suppressor p33<sup>ING1</sup> cooperates with p53 in cell growth control. *Nature* **391**, 295-298.
- Garrick D, Fiering S, Martin DIK, Whitelaw E. (1998). Repeat induced gene silencing in mammals. *Nature Genet.* **18**, 56-59.
- Gaur A, & Rajewsky K. (1998). T-cell specific inducible gene targeting. Abstract. Conditional Gene Expression Technologies Meeting, Cold Spring Harbour.
- Gearing PD, Gough NM, King JA, Hilton DJ, Nicola NA, Simpson RJ, Nice EC, Kelso A, Metcalf D. (1987). Molecular cloning and expression of the cDNA encoding a murine myeloid leukemia inhibitory factor (LIF). *EMBO J.* **6**, 3995-4002.
- Ghattas IR, Sanes JR, Majors JE. (1991). The encephalomyocarditis virus internal ribosome entry site allows efficient co-expression of two genes from a recombinant provirus in cultured cells and in embryos. *Mol. Cell. Biol.* **11**, 5848-5859.
- Ginsberg D, Oren M, Yaniv M, Piette J. (1990). Protein-binding elements in the promoter region of the mouse p53 gene. *Oncogene* **5**, 1285-1290.
- Ginsberg D, Mechta F, Yaniv M, Oren M. (1991). Wild-type p53 can down-modulate the activity of various promoters. *Proc. Natl. Acad. Sci. USA.* **88**, 9979-9983.
- Goga A, Liu X, Hambuch TM, Senechal K, Major E, Bek AJ, Witte ON, Sawyers CL. (1995). P53-dependent growth suppression by the c-Abl nuclear tyrosine kinase. *Oncogene* **11**, 791-799.
- Goldstein S. (1969). Lifespan of cultured cells in progeria. *Lancet* **1**, 424-427.
- Goldstein S, Murano S, Benes H, Moerman EJ, Jones RA, Thewatt R, Shmookler Reis RJ, Howard BH. (1989). Studies on the molecular genetic basis of replicative senescence in Werners syndrome and normal fibroblasts. *Exp. Gerontol.* **24**, 461-468.
- Goldstein S. (1990). Replicative senescence: the human fibroblast comes of age. *Science* **249**, 1129-1133.
- Golic KG, & Lindquist S. (1989). The FLP recombinase of yeast catalyses site specific recombination in *Drosophila* genome. *Cell* **59**, 499-509.



Gordon JW, Scangos GA, Plotkin DJ, Barbosa JA, Ruddle FH. (1980). Genetic transformation of mouse embryos by microinjection of purified DNA. *Proc. Natl. Acad. Sci. USA* **77**, 7380-84.

Gorina S, & Pavletich NP. (1996). Structure of the p53 tumour suppressor bound to the ankyrin and SH3 domains of 53BP2. *Science* **274**, 1001-1005.

Gorman SD, & Cristofalo VJ. (1985). Reinitiation of cellular DNA synthesis in BrdU-selected nondividing senescent WI-38 cells by simian virus 40 infection. *J. Cell. Physiol.* **125**, 122-126.

Gossler A, Doetschman T, Korn R, Serfling E, Kemler R. (1986). Transgenesis by means of blastocyst-derived embryonic stem cells lines. *Proc. Natl. Acad. Sci. USA.* **83**, 9060-9065.

Gossler A, Joyner AL, Rossant J, Skarnes WC. (1989). Mouse embryonic stem cells and reporter constructs to detect developmentally regulated genes. *Science* **244**, 463-465.

Goto M, Miller RW, Ishikawa Y, Sugano H. (1996). Excess of rare cancers in Werner syndrome (adult progeria). *Cancer Epidemiol. Biomarkers Prev.* **5**, 239-246.

Gottlieb E, Haffner R, von Ruden T, Wagner EF, Oren M. (1994). Down-regulation of wild type p53 activity interferes with apoptosis of IL-3-dependent haematopoietic cells following IL-3 withdrawal. *EMBO J.* **13**, 1368-1374.

Gottlieb E, Haffner R, King A, Asher G, Gruss P, Lonai P, Oren M. (1997). Transgenic mouse model for studying the transcriptional activity of the p53 protein: age- and tissue-dependent changes in radiation-induced activation during embryogenesis. *EMBO J.* **16**(6), 1381-1390.

Gottlieb E, & Oren M. (1998). P53 facilitates pRb cleavage in IL-3 deprived cells: novel pro-apoptotic activity of p53. *EMBO J.* **17**(13), 3587-3596.

Gottlieb TM, & Jackson SP. (1993). The DNA-dependent protein kinase: requirement for DNA ends and association with Ku antigen. *Cell* **72**, 131-142.

Graeber TG, Peterson JF, Tsai M, Monica K, Fornace Jr AJ, Giaccia AJ. (1994). Hypoxia induces p53, but activation of a G1 checkpoint by low oxygen conditions is independent of p53 status. *Mol. Cell. Biol.* **14**, 6264-6277.

Graeber TG, Osmanian C, Jacks T, Housman DE, Koch CJ, Lowe SW, Giaccia AJ. (1996). Hypoxia-mediated selection of cells with diminished apoptotic potential in solid tumours. *Nature* **379**, 88-91.

Graham FL, Smiley J, Russel WC, Nairn R. (1977). Characteristics of a human cell line transforme by DNA from human adenovirus type 5. *J. Gen. Virol.* **36**, 59-72.

Gray MD, Jesch SA, Stein GH. (1991). 5-azacytidine-induced demethylation of DNA to senescent levels does not block the proliferation of human fibroblasts. *J. Cell. Physiol.* **149**, 477-484.



Groden J, Thilveris A, Samowitz W, Carlson M, Gelbert L, Albertsen H, Joslyn G, Stevens J, Spirio L, Robertson M, Sargeant L, Krapcho K, Wolf E, Burt R, Hughes JP, Warrington J, McPherson J, Wasmuth J, Le Paslier D, Abderrahim H, Cohen D, Leppert M, White D. (1991). Identification and characterisation of the familial adenomatous polyposis coli gene. *Cell* **65**, 589-600.

Gu H, Zou Y-R, Rajewsky K. (1993). Independent control of immunoglobulin switch recombination at individual switch regions evidenced through cre-loxP mediated gene targeting. *Cell* **73**, 115-1164.

Gu H, Marth JD, Orban PC, Mossmann H, Rajewsky K. (1994). Deletion of a DNA polymerase  $\beta$  gene segment in T cells using cell type specific gene targeting. *Science* **265**, 103-106.

Gu W, & Roeder RG. (1997). Activation of p53 sequence-specific DNA binding by acetylation of the p53 C-terminal domain. *Cell* **90**, 595-606.

Gu W, Shi X-L, Roeder RG. (1997). Synergistic activation of transcription by CBP and p53. *Nature* **387**, 819-823.

Guillouf C, Rosselli F, Krishnaraju K, Moustacchi E, Hoffman B, Lieberman DA. (1995). P53 involvement in control of G2 exit of the cell cycle : role in DNA damage-induced apoptosis. *Oncogene* **10**, 2263-2270.

Guo F, Gopaul DN, van Duyne GD. (1997). Structure of cre recombinase with DNA in a site-specific recombination synapse. *Nature* **389**, 40-46.

Haas J, Park EC, Seed B. (1996). Codon usage limitation in the expression of HIV-1 envelope glycoprotein. *Curr. Biol.* **6**, 315-324.

Hainaut P, & Milner J. (1993). A structural role for metal ions in the "wild-type" conformation of the tumour suppressor protein p53. *Cancer Res.* **53**, 1739-1742.

Hainaut P, Hall A, Milner J. (1994). Analysis of p53 quaternary structure in relation to sequence specific DNA binding. *Oncogene* **9**, 299-303.

Hainaut P, Rolley N, Davies M, Milner J. (1995). Modulation by copper of p53 conformation and sequence specific DNA binding: role for  $\text{Cu(I)}/\text{Cu(II)}$  redox mechanism. *Oncogene* **10**, 27-32.

Halazonetis TD, Davis LJ, Kandil AN. (1993). Wild-type p53 adopts a "mutant" like conformation when bound to DNA. *EMBO J.* **12**, 1021-1028.

Halazonetis TD, & Kandil AN. (1993). Conformational shifts propagate from the oligomerisation domain of p53 to its tetrameric DNA binding domain and restore DNA binding to select p53 mutants. *EMBO J.* **12**, 5057-5064.

Hale TK, & Braithwaite AW. (1995). Identification of an upstream region of the mouse p53 promoter critical for transcriptional expression. *Nucleic Acids Res.* **23(4)**, 663-669.

- Hall SR, Campbell LE, Meek DW. (1996). Phosphorylation of p53 at the casein kinase II site selectively regulates p53-dependent transcriptional repression but not transactivation. *Nucleic Acids Res.* **24**(6), 1119-1126.
- Hara E, Tsurui H, Shinozaki A, Nakada S, Oda K. (1991). Cooperative effect of antisense-Rb and antisense-p53 oligomers on the extension of lifespan in human diploid fibroblasts, TIG-1. *Biochem. Biophys. Res. Comm.* **179**, 528-534.
- Harley CB, Futcher AB, Grieder CW. (1990). Telomeres shorten during the ageing of human fibroblasts. *Nature* **345**, 458-460.
- Harper JW, Admai GR, Wei N, Keyomarsi K, Elledge SJ. (1993). The p21 Cdk-interacting protein Cip1 is a potent inhibitor of G1 cyclin dependent kinases. *Cell* **75**, 805-816.
- Harvey M, Sands AT, Weiss RS, Hegi ME, Wiseman RW, Pantazis P, Giovanella BC, Tainsky MA, Bradley A, Donehower LA. (1993). *In vitro* growth characteristics of embryo fibroblasts isolated from p53-deficient mice. *Oncogene* **8**, 2457-2467.
- Hasty P, Ramirez-Solis R, Krumlauf R, Bradley A. (1991). Introduction of a subtle mutation into the Hox-2.6 locus in embryonic stem cells. *Nature* **350**, 243-246.
- Hattori M. & Sakaki P. (1986). Dideoxy sequencing method using denatured plasmid templates. *Anal. Biochem.* **152**, 232-238.
- Haupt Y, Rowan S, Shaulian E, Vousden K, Oren M. (1995a). Induction of apoptosis in HeLa cells by transactivation deficient p53. *Genes & Dev.* **9**, 2170-2183.
- Haupt Y, Rowan S, Oren M. (1995b). p53 mediated apoptosis in HeLa cells can be overcome by excess pRB. *Oncogene* **10**, 1563-1571.
- Haupt Y, Barak Y, Oren M. (1996). Cell type-specific inhibition of p53-mediated apoptosis by mdm2. *EMBO J.* **15**, 1596-1606.
- Haupt Y, Maya R, Kazaz A, Oren M. (1997). Mdm2 promotes the rapid degradation of p53. *Nature* **387**, 296-299.
- Hayflick L, & Moorhead PS. (1961). The serial cultivation of human diploid cell strains. *Exp. Cell Res.* **25**, 585-621.
- Hayflick L. (1976). The cell biology of human ageing. *N. Engl. J. Med.* **295**, 1302-1308.
- He X, & Thomas ML. (1998). Generation of transgenic mice using the Cre/loxP system. Abstract, Conditional Gene Expression Technologies Meeting, Cold Spring Harbour.
- He Z, Brinton BT, Greenblatt J, Hassell JA, Ingles CJ. (1993). The transactivator proteins VP16 and GAL4 bind replication factor A. *Cell* **73**, 1223-1232.

- Heim R, Prasher DC, Tsien RY. (1994). Wavelength mutations and post-translational autooxidation of green fluorescent protein. *Proc. Natl. Acad. Sci. USA*. **91**, 12501-504.
- Helin K, Lees JA, Vidal M, Dyson N, Harlow E, Fattaey A. (1992). A cDNA encoding a pRB-binding protein with properties of the transcription factor E2F. *Cell* **70**, 337-350.
- Hengartner MO. (1998). Apoptosis, death cycle and swiss army knives. *Nature* **391**, 441-442.
- Hensler PJ, Annab LA, Barret JC, Pereira-Smith OM. (1994). A gene involved in the control of human cellular senescence on human chromosome 1q. *Mol. Cell. Biol.* **14**, 2291-2297.
- Hermeking H, & Eick D. (1994). Mediation of c-Myc induced apoptosis by p53. *Science* **265**, 2091-2093.
- Heydari AR, Wu B, Takahashi R, Strong R, Richardson A. (1993). Expression of hsp70 is altered by age and diet at the level of transcription. *Mol. Cell. Biol.* **264**, 12037-12045.
- Hinds P, Finlay C, Levine AJ. (1989). Mutation is required to activate the p53 gene for co-operation with the ras oncogene and transformation. *J. Virol.* **63**(2), 739-46.
- Hirama T, & Koeffler HP. (1995). Role of cyclin-dependent kinase inhibitors in the development of cancer. *Blood* **86**(3), 841-854.
- Hoess RH, Ziese M, Sternberg N. (1982). P1 site-specific recombination : nucleotide sequence of the recombining sites. *Proc. Natl. Acad. Sci. USA*. **79**, 3398-3402.
- Hoess RH, & Abremski K. (1984). Interaction of the bacteriophage P1 recombinase cre with the recombining site loxP. *Proc. Natl. Acad. Sci. USA*. **81**, 1026-1029.
- Hoess RH, Wierzbicki A, Abremski K. (1986). The role of the spacer region in P1 site-specific recombination. *Nucleic Acids Res.* **14**, 2287-2300.
- Hogan B, Costantini F, Lacy E. (1986). Manipulating the Mouse Embryo: a laboratory manual. Cold Spring Harbour, NY: Cold Spring Harbour Laboratory.
- Holliday R. (1964). A mechanism for gene conversion in fungi. *Genet Res.* **5**, 282-304.
- Hollstein M, Rice K, Greenblatt MS, Soussi T, Fucks R, Sorlie T, Hovig E, Smith-Sorenson B, Montesano R, Harris CC. (1994). Database of p53 gene somatic mutations in human tumours and cell lines. *Nucleic Acids Res.* **22**, 3551-3555.
- Hollstein M, Soussi T, Thomas G, von Brevern MC. (1997). P53 gene alterations in human tumours: perspectives for cancer control. *Recent Results in Cancer Res.* **143**, 369-389.
- Honda R, Tanaka H, Yasuda H. (1997). Oncoprotein mdm2 is a ubiquitin ligase for tumour suppressor p53. *FEBS Lett.* **420**, 25-27.

Hooper MI, Hardy K, Handyside A, Hunter S, Monk M. (1987). HPRT-deficient (Lesch-Nyhan) mouse embryos derived from germ-line colonisation by cultured cells. *Nature* **326**, 292-294.

Hooper ML. (1992). Embryonal stem cells; introducing planned changes into the animal germline. Volume 1, Modern Genetics. Eds. Evans HJ. Harwood Academic Publishers.

Horikoshi N, Usheva A, Chen J, Levine AJ, Weinmann R, Shenk T. (1995). Two domains of p53 interact with the TATA-binding protein, and the adenovirus 13S E1A protein disrupts the association relieving p53-mediated transcriptional repression. *Mol. Cell. Biol.* **15**(1), 227-234.

Hubbard-Smith K, Patsalis P, Pardinas JR, Jha KK, Henderson AS, Ozer HL. (1992). Altered chromosome 6 in immortal human fibroblasts. *Mol. Cell. Biol.* **12**, 2273-2281.

Hupp TR, Meek DW, Midgeley CA, Lane DP. (1992). Regulation of the specific DNA binding function of p53. *Cell* **71**, 875-886.

Hupp TR, & Lane DR. (1994a). Regulation of the cryptic sequence-specific DNA-binding function of p53 by protein kinases. *Cold Spring Harbour Symp. Quant. Biol.* **59**, 195-206.

Hupp TR, & Lane DP. (1994b). Allosteric activation of latent p53 tetramers. *Curr. Biol.* **4**, 865-875.

Hupp TR, Sparks A, Lane DP. (1995). Small peptides activated the latent sequence specific DNA binding activity of p53. *Cell* **83**, 237-245.

Iwabuchi K, Bartel PL, Li B, Maraccino R, Fields S. (1994). Two cellular proteins that bind to wild type but not mutant p53. *Proc. Natl. Acad. Sci. USA.* **91**, 6098-6102.

Jacks T, Remington L, Williams BO, Schmitt EM, Halachmi S, Bronson RT, Weinberg RA. (1994). Tumour spectrum analysis in p53 mutant mice. *Curr. Biol.* **4**, 1-7.

Jaenisch R, Mintz B. (1974). Simian virus 40 sequences in DNA of healthy adult mice derived from preimplantation blastocysts injected with viral DNA. *Proc. Natl. Acad. Sci. USA* **71**, 1250-54.

Jamal S, & Ziff EB. (1995). Raf phosphorylates p53 in vitro and potentiates p53-dependent transactivation in vivo. *Oncogene* **10**, 2095-2101.

Jasin M, & Berg P. (1988). Homologous integration in mammalian cells without target gene selection. *Genes Dev.* **2**, 1353-1363.

Jayaram M. (1994). Phosphoryl transfer in FLP recombination: a template for strand transfer mechanism. *Trends Biochem. Sci.* **19**, 78-82.

Jayaram M. (1997). Identification of redox/repair protein Ref-1 as a potent activator of p53. *Genes & Dev.* **11**(5), 558-70.

- Jenkins JR, Chumakov P, Addison C, Sturzbecher H-W, Wade-Evans A. (1988). Two distinct regions of the murine p53 primary amino acid sequence are implicated in stable complex formation with SV40 T antigen. *Mol. Cell. Biol.* **62**, 3903-3906.
- Jha KK, Satnam B, Palejwala V, Ozer HL. (1998). SV40-mediated immortalisation. *Exp. Cell Res.* **245**, 1-7.
- Jones SN, Roe AE, Donehower LA, Bradley A. (1995). Rescue of embryonic lethality in mdm2-deficient mice by absence of p53. *Nature* **378**, 206-208.
- Jones SN, Hancock AR, Vogel HN, Donehower LA, Bradley A. (1998). Overexpression of mdm2 in mice reveals a p53-independent role for mdm2 in tumourigenesis. *Proc. Natl. Acad. Sci. USA* **95**, 15608-12.
- Jost CA, Marin MC, Kaelin WG Jr. (1997). p73 is a human p53-related protein that can induce apoptosis. *Nature* **389**, 191-194.
- Juven T, Barak Y, Zaubermann A, George DL, Oren M. (1993). Wild-type p53 can mediate sequence specific transactivation of an internal promoter within the mdm2 gene. *Oncogene* **8(12)**, 3411-3416.
- Kaghad M, Bonnet H, Yang A, Creancier L, Biscan J-C, Valent A, Minthy A, Chalon P, Lelias J-M, Dumon X, Ferrara P, McKeon F, Caput D. (1997). Monoallelically expressed gene related to p53 at 1p36 is frequently deleted in neuroblastoma and other human cancers. *Cell* **90**, 809-819.
- Kalnins A, Otto K, Ruther U, Muller-Hill B. Sequence of the *LacZ* gene of *Escherichia coli*. *EMBO J.* **2(4)**, 593-597.
- Kamijo T, Weber JD, Zambetti G, Zindy F, Roussel MF, Sherr CJ. (1998). Functional and physical interactions of the ARF tumour suppressor with p53 and Mdm2. *Proc. Natl. Acad. Sci. USA* **95**, 8292-8297.
- Kanegae Y, Lee G, Sato Y, Tanaka M, Nakai M, Sakaki T, Sugano S, Saito I. (1995). Efficient gene activation in mammalian cells by using recombinant adenovirus expressing site specific cre recombinase. *Nucleic Acid Res.* **23(19)**, 3816-3821.
- Kaplitt MG, Kwong AD, Kleopoulos SP, Mobbs CV, Rabkin SD, Pfaff DW. (1994). Preproenkephalin promoter yields region-specific and long term expression in adult brain after direct in vivo gene transfer via a defective herpes simplex viral vector. *Proc. Natl. Acad. Sci. USA* **91**, 8979-8983.
- Karlsson C, Stenman G, Votja PJ, Bongcam-Rudloff E, Barrett JC, Westermarck B, Paulsson Y. (1996). Escape from senescence in hybrid cell clones involves deletions of two regions located on human chromosome 1q. *Cancer Res.* **56**, 241-245.
- Kastan MB, Zhan Q, El-Diery WE, Carrier F, Jacks T, Walsh WV, Plunkett BS, Vogelstein B, Fornace Jr AJ. (1992). A mammalian cell cycle checkpoint utilising p53 and GADD45 is defective in ataxia-telangiectasia. *Cell* **71**, 587-597.



- Kellendonk C, tronche F, Monaghan AP, Angrand PO, Stewart F, Schutz G. (1996). Regulation of cre recombinase activity by the synthetic steroid RU 486. *Nucleic Acids Res.* **24**(8), 1404-1411.
- Kellendonk C, Tronche F, Casanova E, Anlag K, Opherk C, Schutz G. (1999). Inducible site-specific recombination in the brain. *J. Mol. Biol.* **285**, 175-182.
- Keller GM. (1995). In vitro differentiation of embryonic stem cells. *Curr. Op. Cell Biol.* **7**, 862-869.
- Kemp CJ, Donehower LA, Bradley A, Balmain A. (1993). Reduction of p53 gene dosage does not increase initiation or promotion but enhances malignant progression of chemically induced skin tumours. *Cell* **74**, 813-822.
- Kemp CJ, Wheldon T, Balmain A. (1994). p53-deficient mice are extremely susceptible to radiation-induced tumorigenesis. *Nature Genet.* **8**, 66-69.
- Kern SE, Kinzler KW, Bruskin A, Jarosz D, Friedman P, prives C, Vogelstein B. (1991). Identification of p53 as a sequence-specific DNA-binding protein. *Science* **252**, 1708-1711.
- Kim NW, Piatszek MA, Prowse KR, Harley CB, West MD, Ho PLC, Coviello GM, Wright WE, Weinrich SL, Shay JW. (1994). Specific association of human telomerase activity with immortal cells and cancer. *Science* **266**, 2011-2015.
- Kitamoto T, Nakamura K, Mankao K, Shibuya S, Shin R-W, Gondo Y, Katsuki M, Tateishi J. (1996). Humanised prion protein knock-in by cre-induced site-specific recombination in the mouse. *Biochem. Biophys. Res. Comm.* **222**, 742-747.
- Klein CB, Conway K, Wang XW, Bhamra RK, Lin X, Cohen MD, Anaab L, Barrett JC, Costa M. (1991). Senescence of nickel transformed cells by an X chromosome: possible epigenetic control. *Science* **51**, 796-799.
- Knochbin S, & Lawrence J-J. (1989). An antisense RNA involved in p53 mRNA maturation in murine erythroleukemia cells induced to differentiate. *EMBO J.* **8**, 4107-4114.
- Knudsen ES, & Wang JY. (1998). Hyperphosphorylated p107 and p130 bind to T-antigen: identification of a critical regulatory sequence present in RB but not in p107/p130. *Oncogene* **16**(3), 1655-63.
- Kobayashi I, & Takahashi N. (1988). Double-stranded gap repair of DNA by gene conversion in *Escherichia coli*. *Genetics* **119**, 751-757.
- Koi M, Johnson LA, Kalikin LM, Little PFR, Nakamura Y, Feinberg AP. (1993). Tumour cell growth arrest caused by subchromosomal transferable DNA fragments from chromosome 11. *Science* **260**, 361-364.
- Kozak M. (1987). An analysis of 5' non-coding sequences from 699 vertebrate mRNAs. *Nucleic Acid Res.* **15**, 8125-8148.



- Kozak M. (1989). The Scanning Model for translation: an update. *J. Cell Biol.* **108**, 229-241.
- Kroemer G, Zamzami N, Susin SA. (1997). Mitochondrial control of apoptosis. *Immunol. Today* **18**, 45-51.
- Krimpenfort P, Jonkers J, Miceli F, Voojis M, Berns A. (1998). Conditional gene modification: a need for reliable reporter mice. Abstract, Conditional Gene Expression Technologies Meeting, Cold Spring Harbour.
- Kubbutat MHG, Jones SN, Vousden KH. (1997). Regulation of p53 stability by mdm2. *Nature* **387**, 299-300.
- Kubbutat MHG, & Vousden KH. (1998). Keeping an old friend under control: regulation of p53 stability. *Mol. Med. Today* **7**, 250-256.
- Kuehn M, Bradley A, Robertson EJ, Evans MJ. (1987). A potential animal model for Lesch-Nyhan syndrome through the introduction of HPRT mutations in mice. *Nature* **326**, 295-298.
- Kuhn R, Schwenk F, Aguet M, Rajewsky K. (1995). Inducible gene targeting in mice. *Science* **269**, 1427-1429.
- Kuo C, & Wells W. (1978). Beta-galactosidase from rat mammary gland. Its purification, properties, and role in the biosynthesis of 6beta-O-D-galactopyranosyl myo-inositol. *J. Biol. Chem.* **253**, 3550-3556.
- Lane DP, Crawford LV. (1979). T antigen is bound to a host protein in SV40-transformed cells. *Nature* **278**, 261-263.
- Lakso M, Sauer B, Mosinger Jr. B, Lee EJ, Manning RW, Yu SH, Mulder KL, Westphal H. (1992). Targeted oncogene activation by site-specific recombination in transgenic mice. *Proc. Natl. Acad. Sci. USA* **89**, 6232-6236.
- Lakso M, Pichel JG, Gorman JR, Sauer B, Okamoto Y, Lee Y, Alt FW, Westphal H. (1996). Efficient in vivo manipulation of mouse genomic sequences at the zygote stage. *Proc. Natl. Acad. Sci. USA* **89**, 5860-5.
- Lam K-P, Kuhn R, Rajewsky K. (1997). In vivo ablation of surface immunoglobulin on mature B cells by inducible gene targeting results in rapid cell death. *Cell* **90**, 1073-1083.
- Lambert PF, Kashanchi F, Radonovich MF, Shiekhata R, Brady JN. (1998). Phosphorylation of p53 serine 15 increases interaction with CBP. *J. Biol. Chem.* **273**, 33048-53.
- Lanni JS, & Jacks T. (1998). Characterization of the p53-dependent postmitotic checkpoint following spindle disruption. *Mol. Cell. Biol.* **18**(2), 1055-1064.
- Larsen C-J. (1996). p16<sup>INK4a</sup>: a gene with a dual capacity to encode unrelated proteins that inhibit cell cycle progression. *Oncogene* **12**, 2041-2044.

- Larsson N-G, Wang J, Wilhelmsson H, Oldfors A, Rusitn P, Lewandoski M, Barsh GS, Clayton DA. (1998). Mitochondrial transcription factor A is necessary for mtDNA maintenance and embryogenesis in mice. *Nature Genet.* **18**, 231-236.
- Lechner MS, Mack DH, Finicle AB, Crook T, Vousden KH, Laimins LA. (1992). Human papillomavirus E6 proteins bind p53 in vivo and abrogate p53-mediated repression of transcription. *EMBO J.* **11**(8), 3045-3052.
- Lee C-W, Sorenson TS, Shikama N, La Thangue NB. (1998). Functional interplay between p53 and E2F through the co-activator p300. *Oncogene* **16**, 2695-2710.
- Lee JM. (1998). Inhibition of p53-dependent apoptosis by the KIT tyrosine kinase: regulation of mitochondrial permeability transition and reactive oxygen species. *Oncogene* **17**, 1653-1662.
- Lee S, Elenbaas B, Levine A, Griffith J. (1995). P53 and its 14kDa domain recognise primary DNA damage in the form of insertion/deletion mismatches. *Cell* **81**, 1013-1020.
- Lees-Miller SP, Sakaguchi K, Ullrich SJ, Apella E, Anderson CW. (1992). Human DNA-activated protein kinase phosphorylates serine 15 and 37 in the amino terminal transactivation domain of human p53. *Mol. Cell. Biol.* **12**(11), 5041-5049.
- Lehar SM, Nacht M, Jacks T, Vater CA, Chittenden T, Guild BC. (1996). Identification and cloning of Ei24, a gene induced by p53 in etoposide-treated cells. *Oncogene* **12**, 1181-1187.
- Leibovitz A. (1986). Development of tumour cells. *Cancer Genet. Cytogenet.* **19**, 11-19.
- Lewandoski M, wassarman KM, Martin GR. (1997). Zp3-cre, a transgenic mouser line for the activation or inactivation of loxP-flanked target genes specifically in the female germ line. *Current Biol.* **7**, 148-151.
- Li R, & Botchan MR. (1993). The acidic transcriptional activation domains of VP16 and p53 bind the cellular replication protein A and stimulate in vitro BPV-1 DNA replication. *Cell* **73**, 1207-1221.
- Li Z-W, Stark G, Gotz J, Rulicke T, Muller U, Weissmann C. (1996). Generation of mice with a 200kb amyloid precursor protein gene deletion by cre recombinase mediated site specific recombination in ES cells. *Proc. Natl. Acad. Sci. USA.* **93**, 6158-6162.
- Liebermann DA, Hoffman B, Steinman RA. (1995). Molecular controls of growth arrest and apoptosis : p53 dependent and independent pathways. *Oncogene* **11**, 199-210.
- Liebetrau W, Budde A, Savoia A, Grummt F, Hoehn H. (1997). P53 activates Fanconi anaemia group C gene expression. *Hum. Mol. Genet.* **69**(2), 277-283.
- Lill NL, Grossman SR, Ginsberg D, DeCaprio J, Livingston DM. (1997). Binding and modulation of p53 by p300/CBP coactivators. *Nature* **387**, 823-827.

- Linke SP, Clarkin KC, DiLeonardo A, Tsou A, Wahl GM. (1996). A reversible G0/G1 cell cycle arrest induced by ribonucleotide depletion in the absence of detectable DNA damage. *Genes Dev.* **10**, 934-947.
- Littlefield JW. (1964). Selection of hybrids from matings of fibroblasts in vitro and their presumed recombinants. *Science* **145**, 709-710.
- Liu X, Miller CW, Koeffler PH, Berk AJ. (1993). The p53 activation domain binds the TATA box-binding polypeptide in holo-TFIID, and a neighbouring p53 domain inhibits transcription. *Mol. Cell. Biol.* **13**(6), 3291-3300.
- Liu X, & Berk AJ. (1995). Reversal of in vitro p53 squelching by both TFIIB and TFIID. *Mol. Cell. Biol.* **15**(11), 6474-6478.
- Livingstone LR, White A, Sprouse J, Livanos J, Jacks T, Tlsty TD. (1992). Altered cell cycle arrest and gene amplification potential accompany loss of wild-type p53. *Cell* **70**, 923-935.
- Logan C, Hanks MC, Noble-Topham S, Nallainathan D, Provart NJ, Joyner AL. (1992). Cloning and sequence comparison of the mouse, human and chicken engaged genes reveal potential functional domains and regulatory regions. *Dev. Genet.* **13**, 345-358.
- Logie C, & Stewart AF. (1995). Ligand-regulated site-specific recombination. *Proc. Natl. Acad. Sci. USA* **92**, 5940-5944.
- Loughran O, Malliri A, Owens D, Gallimore PH, Stanley MA, Ozanne B, Frame MC, Parkinson EK. (1996). Association of CDKN2A/ p16<sup>INK4a</sup> with human head and neck keratinocyte replicative senescence: relationship of dysfunction to immortality and neoplasia. *Oncogene* **13**, 561-568.
- Lovejoy EA, Clarke AR, Harrison DJ. (1996). Animal models and the molecular pathology of cancer. *J. Path.* **181**, 130135.
- Lowe S, & Ruley HE. (1993). Stabilisation of the p53 tumour suppressor is induced by adenovirus 5 E1A and accopianies apoptosis. *Genes & Dev.* **7**, 535-545.
- Lowe SW, Schmitt EM, Smith SW, Osborne BA, Jacks T. (1993). P53 is required for radiation-induced apoptosis in mouse thymocytes. *Nature* **362**, 847-849.
- Lowe SW, Jacks T, Housman DE, Ruley HE. (1994). Abrogation of oncogene associated apoptosis allows transformation of p53-deficient cells. *Proc. Natl. Acad. Sci. USA*. **91**, 2026-2030.
- Lozano & levine, 1991.
- Lu H, & Levine AJ. (1995). Human TAF31 protein is a transcriptional coactivator of the p53 protein. *Proc. Natl. Acad. Sci. USA* **92**, 5154-5158.
- Lu X, and Lane DP. (1993). Differential induction of transcriptionally active p53 following UV or ionising radiation : defect in chromosome instability syndromes ?. *Cell* **75**, 765-778.

- Ludes-Meyers JH, Subler MA, Shivakumar CV, Munoz RM, ianf P, Bigger JE, Brown DR, Deb SP, Deb S. (1996). Transcriptional activation of the human epidermal growth factor receptor promoter by human p53. *Mol. Cell. Biol.* **16**(11), 6009-6019.
- Ludwig DL, Stringer JR, Wight DC, Doetschman HC, Duffy JJ. (1996). FLP-mediated site-specific recombination in micro-injected murine zygotes. *Transgenic Res.* **5**(6), 385-395.
- Lyons SK. (1999). Thesis submitted for the degree of Doctor of Philosophy, Department of Pathology, University of Edinburgh.
- Macieira-Coelho A. (1988). *Interdisciplinary Topics in Gerontology* **132**, 1-212. Editor, von Hang HP. S Karger, Basel.
- Mack DH, Vartikar J, Pipas JM, Laiminis LA. (1993). Specific repression of TATA-mediated transcription by wild type p53. *Nature* **363**, 281-283.
- Magin TM, McWhir J, Melton DW. (1992). A new mouse embryonic stem cell line with good germ-line contribution and gene targeting frequency. *Nucleic Acids Res.* **20**(14), 3795-3796.
- Maheswaran S, Park S, Bernard A, Morris JF, Rauscher F, Hill DE, Haber DA. (1993). Physical and functional interaction between WT1 and p53 proetins. *Proc. Natl. Acad. Sci. USA.* **90**, 5100-5104.
- Maheswaran S, Englebert C, Bennet P, Heinrich G, Haber DA. (1995). The WT1 gene product stabilises p53 and inhibits p53-mediated apoptosis. *Genes Dev.* **9**, 2143-2156.
- Malcomson RGD. (1996). Thesis submitted for the degree of Doctor of Philosophy, Department of Pathology, University of Edinburgh.
- Malkin D, Li FP, Strong LC, Fraumeni JF, Nelson CE, Kim DH, Kassel J, Gryka MA, Bischoff FZ, Tainsky MA, Friend SH. (1990). Germ line p53 mutations in a familial syndrome of breast cancer, sarcomas and other neoplasms. *Science* **250**, 1233-1238.
- Maltzman W, & Czyzyk L. (1984). UV irradiation stimulates levels of p53 cellular tumour antigen in nontransformed mouse cells. *Mol. Cell. Biol.* **4**, 1689-1694.
- Mansour SL, Thomas KR, Capecchi MR. (1988). Disruption of the proto-oncogene int-2 in mouse embryo derived stem cells: a general strategy for targeting mutations to non-selectable genes. *Nature* **336**, 348-352.
- Mansour SL. (1990). Gene targeting in murine embryonic stem cells: Introduction of specific alterations into the mammalian genome. *GATA.* **7**(8), 219-227.
- Mansour SL, Thomas KR, Deng CX, Capecchi MR. (1990). Introduction of a LacZ reporter gene into the mouse Int-2 locus by homologous recombination. *Proc. Natl. Acad. Sci. USA.* **87**, 7688-7692.

- Marin MC, Jost CA, Irwin MS, DeCaprio JA, Caput D, Kaelin Jr WG. (1998). Viral oncoproteins discriminate between p53 and the p53 homolog p73. *Mol. Cell. Biol.* **18**(11), 6316-6324.
- Martin GM. (1993). Clonal attenuation: causes and consequences. *J. Gerontol.* **48**, 171-172.
- Martin GR. (1981). Isolation of a pluripotent cell line from early mouse embryos cultured in medium conditioned by teratocarcinoma stem cells. *Proc. Natl. Acad. Sci. USA.* **78**, 7634-7636.
- Martinez J, Georgoff I, Martinez J, Levine AJ. (1991). Cellular localisation and cell cycle regulation by a temperature-sensitive p53 protein. *Genes & Dev.* **5**, 151-159.
- Matsumura T, Zerrudo Z, Hayflick L. (1979). DNA synthesis in the human diploid cell strain WI-38 during in vitro ageing: An autoradiographic study. *J. Gerontol.* **34**, 328-334.
- Matsuzawa S, Takayama S, Froesch BA, Zapata JM, Reed JC. (1998). P53-inducible human homologue of Drosophila seven in absentia (Siah) inhibits cell growth: suppression by BAG-1. *EMBO J.* **17**(10), 2736-2747.
- Maxwell SA, & Roth JA. (1993). Binding of cellular proteins to a conformational domain of tumour suppressor protein p53. *Oncogene* **8**, 3421-3426.
- Mayr GA, Reed M, Wang P, Wang Y, Scweds JF, Tegtmeier P. (1995). Serine phosphorylation in the NH2 terminus of p53 facilitates transactivation. *Cancer Res.* **55**, 2410-2417.
- McCarthy SA, Symonds HS, Van DT. (1994). Regulation of apoptosis in transgenic mice by SV40 T antigen mediated inactivation of p53. *Proc. Natl. Acad. Sci. USA.* **91**, 3979-3983.
- McCormick JJ, & Maher VM. (1988). Towards an understanding of the malignant transformation of diploid human fibroblasts. *Mutat. Res.* **199**, 273-291.
- McKinnon PJ. (1987). Ataxia-telangiectasia: an inherited disorder of ionising-radiation sensitivity in man. *Hum. Genet.* **75**, 197-208.
- McKusick VA. (1978). *Mendelian Inheritance in Man*. 5<sup>th</sup> edn., John Hopkins Press, Baltimore.
- Medcalf ASC, Klein-Szanto AJP, Cristofalo VJ. (1996). Expression of p21 is not required for senescence of human fibroblasts. *Cancer Res.* **56**, 4582-4585.
- Mercer W, Shields M, Lin D, Apella E, Ullrich S. (1991). Growth suppression induced by wild type p53 protein is accompanied by selective downregulation of proliferating cell nuclear antigen. *Proc. Natl. Acad. Sci. USA* **88**, 1958-1962.
- Merlo A, Herman JG, Mao L, Lee DJ, Gabrielson E, Burger PC, Baylin SB, Sidransky D. (1995). 5' CpG island methylation is associated with the transcriptional silencing of p16CDKN2/MTS1 in human cancers. *Nature Med.* **1**, 692-695.



- Meselson MS, & Radding CM. (1975). A general model for genetic recombination. *Proc. Natl. Acad. Sci. USA* **72**, 358-361.
- Metzger D, Clifford J, Chiba H, Chambon P. (1995). Conditional site specific recombination in mammalian cells using a ligand dependent chimeric cre recombinase. *Proc. Natl. Acad. Sci. USA*. **92**, 6991-6995.
- Meyer-Leon L, Senecoff JF, Bruckner RC, Cox MM. (1984). Site specific genetic recombination promoted by the FLP protein of the yeast 2 $\mu$ M plasmid *in vitro*. *Cold Spring Harbour Symp. Quant. Biol.* **49**, 797-804.
- Meyers EN, Lewandoski M, Martin GR. (1998). An *Fgf8* mutant allelic series generated by Cre- and Flp- mediated recombination. *Nature Genet.* **18**, 136-141.
- Michou AI, Santoro L, Christ M, Julliard V, Pavirani A, Mehtali M. (1997). Adenovirus-mediated gene transfer: influence of transgene, mouse strain and type of immune response on persistence of transgene expression. *Gene Therapy* **4**, 473-482.
- Midgeley CA, Owens B, Briscoe CV, Brynmor T, Lane DP. (1995). Coupling between gamma irradiation, p53 induction and the apoptotic response depends upon cell type *in vivo*. *J. Cell. Sci.* **108**, 1843-1848.
- Midgeley CA, & Lane DP. (1997). P53 protein stability in tumour cells is not determined by mutation but is dependent on mdm2 binding. *Oncogene* **15**, 1179-1185.
- Miech RP, Parks Jr RE, Anderson Jr JH, Sartorelli AC. (1967). An hypothesis on the mechanism of action of 6-thioguanine. *Biochem. Pharmacol.* **16**, 2222-2227.
- Mietz JA, Unger T, Huibregtse JM, Howley PM. (1992). The transcriptional transactivation function of wild-type p53 is inhibited by SV40 large T-antigen and by HPV-16 E6 protein. *EMBO J.* **11**(13), 5013-5020.
- Miller J. (1972). *Experiments in Molecular Genetics*. Cold Spring Harbour Lab. Press, Plainview, NY.
- Milne DM, Palmer RH, Campbell DG, Meek DW. (1992). Phosphorylation of the p53 tumour suppressor protein at three N terminal sites by a novel Casein Kinase 1-like enzyme. *Oncogene* **7**, 1361-1369.
- Milne DM, Campbell DG, Caudwell FB, Meek DW. (1994). Phosphorylation of the tumour suppressor protein p53 by mitogen-activated protein kinases. *J. Biol. Chem.* **269**, 9253-9260.
- Milne DM, Campbell LE, Campbell DG, Meek DW. (1995). P53 is phosphorylated *in vitro* and *in vivo* by an ultraviolet radiation induced protein kinase characteristic of the c-Jun kinase, JNK-1. *J. Biol. Chem.* **270**, 551-5518.
- Milner J, Medcalf EA, Cook AC. (1991). Tumour suppressor p53: analysis of wild type and mutant p53 complexes. *Mol. Cell. Biol.* **11**, 12-19.



- Milner J. (1994). Forms and functions of p53. *Semin. Cancer Biol.* **5**, 211-219.
- Milner J. (1995). Flexibility: the key to p53 function. *Trends Bioch. Sci.* **20**, 49-51.
- Minn AJ, Boise LH, Thompson CB. (1996). Expression of Bcl-x<sub>L</sub> and loss of p53 can cooperate to overcome a cell cycle checkpoint induced by mitotic spindle damage. *Genes & Dev.* **10**, 2621-2631.
- Mintz B, & Illmensee K. (1975). Normal genetically mosaic mice produced from malignant taeratocarcinoma cells. *Proc. Natl. Acad. Sci. USA.* **72**, 3585-3589.
- Miyashita T, & Reed JC. (1995). Tumour suppressor p53 is a adirect transcriptional activator of the human bax gene. *Cell* **80**, 293-299.
- Moll UM, Riou G, Levine AJ. (1992). Two distinct mechanisms alter p53 in breast cancer : Mutation and nuclear exclusion. *Proc. Natl. Acad. Sci. USA* **89**, 7262-7266.
- Moll UM, Ostermeyer AG, Haladay R, Winkfield B, Frazier M, Zambetti G. (1996). Cytoplasmic sequestration of wild type p53 protein impairs the G1 checkpoint after DNA damage. *Mol. Cell. Biol.* **16**(3), 1126-1137.
- Mommand J, Zambetti GP, Olson DC, George D, Levine AJ. (1992). The mdm2 oncogene product forms a complex with the p53 protein and inhibits p53-mediated transactivation. *Cell* **69**, 1237-1245.
- Montano X. (1997). P53 associates with trk tyrosine kinase. *Oncogene* **15**, 245-256.
- Montes de Oca Luna R, Wagner DS, Lozano G. (1995). Rescue of ebryonic lethality of mdm2 deficient mice by deletion of p53. *Nature* **378**, 203-206.
- Moran E. (1993). DNA tumour virus transforming proteins and the cell cycle. *Curr. Opin. Genet. Dev.* **3**, 63-70.
- Moreau H, Galjart NJ, Gillemans N, Wellemsen R, van der Horst GT, D'Azzo A. (1989). Alternative splicing of the  $\beta$ -galactosidase mRNA generates the classic lysozomal enzyme and a  $\beta$ -galactosidase related protein. *J. Biol. Chem.* **264**, 20655-20663.
- Morris GF, Bischoff JR, Mathews MB. (1996). Transcriptional activation of the human proliferating cell nuclear antigen promoter by p53. *Proc. Natl. Acad. Sci. USA.* **93**(2), 895-899.
- Moser AR, Pitot HC, Dove WF. (1990). A dominant mutation that predisposes to multiple intestinal neoplasia in mice. *Science* **247**, 322-324.
- Mosner J, Mummenbrauer T, Bauer C, Sczakiel G, Grosse F, Deppert W. (1995). Negative feedback regulation of wild-type p53 biosynthesis. *EMBO J.* **14**(18), 4442-4449.
- Mountford PS, Zevnik B, Duwel A, Nichols J, Li M, Dani C, Robertson M, Chambers I, Smith A. (1994). Dicistronic targeting constructs : Reporters and modifiers of mammalian gene expression. *Proc. Natl. Acad. Sci. USA.* **91**, 4303-4307.

- Mountford PS, Smith AG. (1995). Internal ribosome entry sites and dicistronic RNAs in mammalian transgenesis. *Trends in Genet.* **11**(5), 179-184.
- Mulderry PK, Chapman KE, Lyons V, Harmar AJ. (1993). 5'-flanking sequences from the rPPT gene direct high-level expression of a reporter gene in adult rat sensory neurons transfected in culture by microinjection. *Mol. Cell. Neurosci.* **4**, 164-172.
- Mummenbrauer T, Janus F, Muller B, Wiesmuller L, Deppert W, Grosse F. (1996). P53 protein exhibits 3'-to-5' exonuclease activity. *Cell* **85**, 1089-1099.
- Mummery CL, Feyen A, Freund E, Shen S. (1990). Characteristics of embryonic stem cell differentiation: A comparison with two embryonal carcinoma cell lines. *Cell Diff. Dev.* **30**, 195-206.
- Murphy M, Hinman A, Levine AJ. (1996). Wild-type p53 negatively regulates the expression of a microtubule-associated protein. *Genes & Dev.* **10**, 2971-2980.
- Nelson RD, Stricklett P, Gustafson C, Stevens A, Ausiello D, Brown D, Kohan DE. (1998). Expression of an AQP2 cre recombinase transgene in kidney and male reproductive system of transgenic mice. *Am. J. Physiol.* (1 Pt 1), C216-C226.
- Nelson WG, & Kastan MB. (1994). DNA strand breaks : The DNA template alterations that trigger p53-dependent DNA damage response pathways. *Mol. Cell. Biol.* **14**, 1815-1823.
- Nemetz C, & Hocke GM. (1998). Transcriptional factor Stat5 is an early marker of differentiation of murine embryonic stem cells. *Diff.* **62**(5), 213-220.
- Nevins JR. (1992). E2F: a link between the RB tumour suppressor and viral oncoproteins. *Science* **258**, 424-430.
- Nichols J, Evans EP, Smith AG. (1990). Establishment of germ-line competent embryonic stem (ES) cells using differentiation inhibiting activity. *Development* **110**, 1341-1348.
- Nickoloff JA, & Reynolds RJ. (1990). Transcription stimulates homologous recombination in mammalian cells. *Mol. Cell. Biol.* **10**, 4837-4845.
- Nigg EA. (1996). Cyclin dependent kinase 7: at the crossroads of transcription, DNA repair and cell cycle control ? *Curr. Opin. Cell. Biol.* **8**, 312-317.
- Ning Y, Weber JL, Killary AM, Ledbetter DH, Smith JR, Pereira-Smith OM. (1991). Genetic analysis of indefinite cell division in human cells: evidence for a cell senescence related gene(s) on human chromosome 4. *Proc. Natl. Acad. Sci. USA.* **88**, 5635-5639.
- Nishimori H, Shiratsuchi T, Urano T, Kimura Y, Kiyono S, Tatsumi K, Yoshida S, Ono M, Kuwano M, Nakamura Y, Tokino T. (1997). A novel brain-specific p53 target gene, BAI1, containing thrombospondin type I repeats inhibits experimental angiogenesis. *Oncogene* **15**, 2145-2150.

Noda A, Ning Y, Venable SF, Pereira-Smith OM, Smith JR. (1994). Cloning of senescent cell-derived inhibitors of DNA synthesis using an expression screen. *Exp. Cell Res.* **211**, 90-98.

Norimura T, Nomoto S, Katsuki M, gondo Y, Kondo S. (1996). P53-dependent apoptosis suppresses radiation-induced teratogenesis. *Nature Med.* **2**, 577-580.

Nyhan WL. (1973). The Lesch-Nyhan syndrome. *A. Rev. Med.* **24**, 41-60.

Oberosler P, Hloch P, Ramsperger U, Stahl H. (1993). P53 catalysed annealing of complementary single stranded nucleic acids. *EMBO J.* **12**, 2389-2396.

Ogata T, Ayusawa D, Namba M, Takahashi E, Oshimura M, Oishi M. (1993). Chromosome 7 suppresses indefinite division of non-tumourigenic immortalised human fibroblast cell lines KMST-6 and SUSM-1. *Mol. Cell. Biol.* **13**, 6036-6043.

O'Gorman S, Dagenais NA, Qian M, Marchuk Y. (1997). Protamine-Cre recombinase transgenes efficiently recombine target sequences in the male germ line of mice, but not in embryonic stem cells. *Proc. Natl. Acad. Sci. USA* **94**, 14602-14607.

Ohtsubo M, & Roberts JM. (1993). Cyclin dependent regulation of G1 in mammalian fibroblasts. *Science* **259**, 1908-1912.

Ohyama K, Chung CH, Chen E, Gibson CW, Misof K, Fratzl P, Shapiro IM. (1997). P53 influences mice skeletal development. *J. Craniofac. Genet. Dev. Biol.* **17(4)**, 161-171.

Okamoto K, Beach D. (1994). Cyclin G is a transcriptional target of the p53 tumour suppressor protein. *EMBO J.* **13**, 4816-4822.

Okamoto K, Kamibayashi C, Serrano M, Prives C, Mumby MC, Beach D. (1996). P53-dependent association between cyclin G and the B' subunit of protein phosphatase 2A. *Mol. Cell. Biol.* **16(11)**, 6593-6602.

Oliner JD, Kinzler KW, Meltzer PS, George DL, Vogelstein B. (1992). Amplification of a gene encoding a p53-associated protein in human sarcomas. *Nature* **358**, 80-83.

Oliner JD, Pietenpol JA, Thiagalingham S, Gyuris J, Kinzler KW, Vogelstein B. (1993a). Oncoprotein mdm2 conceals the activation domain of tumour suppressor p53. *Nature* **362**, 857-860.

Oliner JD, Kinzler KW, Vogelstein B. (1993b). In vivo cloning of PCR products in *E. coli*. *Nucleic Acids Res.* **21(22)**, 5192-5197.

Olson DC, Marechal V, Mommand J, Chen J, Romocki C, Levine AJ. (1993). Identification and characterisation of multiple mdm-2 proteins and mdm-2-p53 protein complexes. *Oncogene* **8**, 2353-2360.

Orban PC, Chui D, Marth JD. (1992). Tissue and site-specific DNA recombination in transgenic mice. *Proc. Natl. Acad. Sci. USA* **89**, 6861-6865.

Oren M, Maltzman W, Levine AJ. (1981). Post-translational regulation of 54K cellular tumour antigen in normal and transformed cells. *Mol. Cell. Biol.* **1**, 101-110.

Orr-Weaver T, Szostak JW, Rothstein RJ. (1981). Yeast transformation : a model system for the study of recombination. *Proc. Natl. Acad. Sci. USA* **78**, 6354-6358.

Osada M, Ohba M, Kawahara C, Ishioka C, Kanamaru R, Katoh I, Ikawa Y, Nimura Y, Nakagawara A, Obinata M, Ikawa S. (1998). Cloning and functional analysis of human p51, which structurally and functionally resembles p53. *Nature Med.* **4**(7), 839-843.

O'Shea-Greenfield A & Smale ST. (1992). Roles of TATA and initiator elements in determining the start site location and direction of RNA polymerase II transcription. *J. Biol. Chem.* **267**, 1391-1402.

Osifchin NE, Jiang D, Ohtani-Fujita N, Carroza M, Kim SJ, Sakai T, Robbins PD. (1994). Identification of a p53 binding site in the human retinoblastoma susceptibility gene promoter. *J. Biol. Chem.* **269**(9), 6383-6389.

Ostermeyer AG, Runko E, Winkfield B, Ahn B, Moll UM. (1996). Cytoplasmically sequestered wild-type p53 protein in neuroblastoma is relocated to the nucleus by a C-terminal peptide. *Proc. Natl. Acad. Sci. USA* **93**, 15190-15194.

Owen-Schaub LB, Zhang W, Cusack JC, Angelo LS, Santee SM, Fujiwara T, Roth JA, Deisseroth AB, Zhang WW, Kruzel E, Radinsky R. (1995). Wild-type human p53 and a temperature-sensitive mutant induce fas/APO-1 expression. *Mol. Cell. Biol.* **15**, 3032-3040.

Palmiter RD, & Brinster RL. (1986). Germline transformation of mice. *Annu. Rev. Genet.* **20**, 465-499.

Pan H, & Griep AE. (1994). Altered cell cycle regulation in the lens of HPV-16 E6 or E7 transgenic mice: implications for tumour suppressor gene function in development. *Genes & Dev.* **8**, 1285-1299.

Pappenheimer AM Jr. (1977). Diphtheria toxin. *Annu. Rev. Biochem.* **46**, 69-94.

Paraskeva C, Finerty S, Powell S. (1988). Immortalisation of a human colorectal adenoma cell line by continuous in vitro passage: possible involvement of chromosome 1 in tumour progression. *Int. J. Cancer* **41**, 908-912.

Pariat M, Carillo S, Molinari M, Salvat C, debusche L, Braco L, Milner J, Piechaczyk. (1997). Proteolysis by calpains : a possible contribution to the degradation of p53. *Mol. Cell. Biol.* **17**, 2806-2815.

Pavletich NP, Chambers KA, Pabo CO. (1993). The DNA-binding domain of p53 contains the four conserved regions and the major mutation hot spots. *Genes & Dev.* **7**, 2556-2564.

Pawson T. (1995). Protein modules and signalling networks. *Nature* **373**, 573-580.

Peacock JW, Chung S, Brstow RG, Hill RP, Benchimol S. (1995). The p53 G1 checkpoint is retained in tumourigenic REF clones transformed by the HPV16 E7 gene and EJ-ras. *Mol. Cell. Biol.* **15**, 1446-1454.

Pelletier J, & Sonenberg N. (1988). Internal initiation of translation of eukaryotic mRNA directed by a sequence derived from poliovirus mRNA. *Nature* **334**, 320-325.

Pereira-Smith OM, Smith JR. (1988). Genetic analysis of indefinite division in human cells: identification of four complementation groups. *Proc. Natl. Acad. Sci. USA.* **85**, 6042-6046.

Pesch J, Brehm U, Staib C, Grummt F. (1996). Repression of interleukin-2 and interleukin-4 promoters by tumour suppressor protein p53. *J. Interferon Cytokine Res.* **16**(8), 595-600.

Picard D, Khursheed B, Garabedian MJ, Fortin MG, Lindquist S, Yamamoto KR. (1990). Reduced levels of hsp90 compromise steroid receptor action *in vivo*. *Nature* **348**, 166-168.

Polyak K, Xia Y, Zweier JL, Kinzler KW, Vogelstein B. (1997). A model for p53-induced apoptosis. *Nature* **389**, 300-305.

Pomerantz J, Schrieber-Agus N, Liegeois NJ, Silverman A, Alland L, Chin L, Potes J, Chen K, Orlow I, Lee H-W, Cordon-Cardo C, DePinho RA. (1998). The Ink4a tumour suppressor gene product, p19<sup>Arf</sup>, interacts with mdm2 and neutralises mdm2's inhibition of p53. *Cell* **92**, 713-723.

Prasad R, Gu Y, Adler H, Nakamura T, Canaani O, Sato H, Huebner K, Gale RP, Nowell PC, Kuriyama K, Miyazaki Y, Croce CM, Canaani E. (1993). Cloning of the ALL-1 fusion partner, the AF-6 gene, involved in acute myeloid leukemia with the t(6;11) chromosome translocation. *Cancer Res.* **53**, 5624-5628.

Prasher DC, Eckenrode VK, Ward WW, Prendergast FG, Cormier MJ. (1992). Primary structure of the *Aequorea victoria* green-fluorescent protein. *Gene* **111**, 229-233.

Proteau G, Sidenberg D, Sadowski P. (1986). The minimal duplex DNA sequence required for site-specific recombination promoted by the FLP protein of yeast *in vitro*. *Nucleic Acids Res.* **14**(12), 4787-4802.

Puisieux A, Ji JW, Guillot G, Legros Y, Soussi T, Isselbacher K, Oztruk M. (1995). P53 mediated cellular response to DNA damage in cells with replicative Hepatitis B virus. *Proc. Natl. Acad. Sci. USA.* **92**, 1342-1346.

Purdie CA, Harrison DJ, Peter A, Dobbie L, White S, Howie SEM, Salter DM, Bird CC, Wyllie AH, Hooper ML, Clark AR. (1994). Tumour incidence, spectrum and ploidy in mice with a large deletion in the p53 gene. *Oncogene* **9**, 3313-3322.

Qin M, Bayley C, Stockton T, Ow DW. (1994). Cre recombinase mediated site specific recombination between plant chromosomes. *Proc. Natl. Acad. Sci. USA.* **91**, 1706-1710.

Quelle DE, Zindy F, Ashmun R, Sherr CJ. (1995). Alternative reading frames of the INK4a tumour suppressor gene encode two unrelated proteins capable of inducing cell cycle arrest. *Cell* **83**, 993-1000.



- Raff MC. (1992). Social controls on cell death and survival. *Nature* **356**, 397-400.
- Ramirez-Solis R, Liu P, Bradley A. (1995). Chromosome engineering in mice. *Nature* **378**, 720-724.
- Rao PV, Krishna CM, Zigler JS. (1992). Identification and characterisation of the enzymatic activity of zeta-crystallin from guinea pig lens. A novel NADPH: quinone oxidoreductase. *J. Biol. Chem.* **267**, 96-102.
- Ray MK, Fagan SP, Moldovan S, DeMayo FJ, Brunicardi FC. (1998). A mouse model for beta cell-specific ablation of target gene(s) using the cre/loxP system. *Biochem. Biophys. Res. Comm.* **253**, 65-69.
- Redhead NJ, Selfridge J, Wu CL, Melton DW. (1996). Mice with adenine phosphoribosyltransferase deficiency develop fatal 2,8-dihydroxyadenine lithiasis. *Hum. Gene Ther.* **7(13)**, 1491-502.
- Reinke V, & Lozano G. (1997). The p53 targets mdm2 and Fas are not required as mediators of apoptosis in vivo. *Oncogene* **15**, 1527-1534.
- Reisman D & Rotter V. (1993). The helix-loop-helix-containing transcription factor, USF, binds to and transactivates the promoter of the p53 tumour suppressor gene. *Nucleic Acids Res.* **21**, 345-350.
- Reisman D, Greenberg M, Rotter V. (1988). Human p53 oncogene contains one promoter upstream of exon 1 and a second, stronger promoter in intron 1. *Proc. Natl. Acad. Sci. USA.* **85**, 5146-5150.
- Reisman D, Elkind NB, Roy B, Beamon J, Rotter V. (1993). C-Myc transactivates the p53 promoter through a required downstream CACGTG motif. *Cell Growth Differ.* **4**, 57-65.
- Rohlmann A, Gotthardt M, Hammer RE, Herz J. (1998). Inducible inactivation of hepatic LRP gene by cre-mediated recombination confirms role of LRP in clearance of chylomicron remnants. *J. Clin. Invest.* **101(3)**, 689-695.
- Ronen D, Rotter V, Reisman D. (1991). Expression from the murine p53 promoter is mediated by factor binding to a downstream helix-loop-helix recognition motif. *Proc. Natl. Acad. Sci. USA* **88**, 4128-4132.
- Rosse WF, & Ware RE. (1995). The molecular basis of paroxysmal nocturnal haemoglobinuria. *Blood* **86**, 3277-3286.
- Rosse T, Olivier R, Monney L, Rager M, Conus S, Fellay I, Jansen B, Borner C. (1998). Bcl-2 prolongs survival after Bax-induced release of cytochrome c. *Nature* **391**, 496-499.
- Roth J, Dobbelstein M, Freedman DA, Shenk T, Levine AJ. (1998). Nucleo-cytoplasmic shuttling of the hdm2 oncoprotein regulates the levels of the p53 protein via a pathway used by the human immunodeficiency virus rev protein. *EMBO J.* **17**, 554-564.



- Rotter V, Wolf D, Pravtcheva D and Ruddle FH. (1984). Chromosomal assignment of the murine gene encoding the transformation related protein p53. *Mol. Cell. Biol.* **4**, 1638-1640.
- Rotter V, Aloni-Grinstein R, Schwartz D, Elkind NB, Simons A, Wolkowicz R, Lavigne M, Beserman P, Kapon A, Goldfinger N. (1994). Does wild type p53 play a role in normal cell differentiation? *Semin. Cancer Bio.* **5**, 229-236.
- Ruaro EM, Collavin L, Del Sal G, Haffner R, Oren M, Levine AJ, Schneider C. (1997). A proline-rich motif in p53 is required for transactivation-independent growth arrest as induced by Gas-1. *Proc. Natl. Acad. Sci. USA.* **94**, 4675-4680.
- Ruppert JM, & Stillman B. (1993). *Mol. Cell. Biol.* **13**, 3811-3820.
- Russ AP, Friedel C, Ballas K, Kalina U, Zahn D, Strebhardt K, von Melchner H. (1996). Identification of genes induced by factor deprivation in hematopoietic cells undergoing apoptosis using gene-trap mutagenesis and site-specific recombination. *Proc. Natl. Acad. Sci. USA.* **93**, 15279-15284.
- Russell LB, Humsicker PR, Cacheiro NLA, Bangham JW, Russell WL, Shelby MD. (1989). Chlorambucil effectively induces mutations in mouse germ cells. *Proc. Natl. Acad. Sci. USA* **86**, 3704-3708.
- Ryan KM, & Vousden KH. (1998). Characterisation of structural p53 mutants which show selective defects in apoptosis but not cell cycle arrest. *Mol. Cell. Biol.* **18**(7), 3692-3698.
- Sabbatini P, Lin J, Levine AJ, White E. (1995). Essential role for p53-mediated transcription in E1A induced apoptosis. *Genes & Dev.* **9**, 2184-2192.
- Sah VP, Attardi LD, Mulligan GJ, Williams BO, Bronson RT, Jacks T. (1995). A subset of p53-deficient embryos exhibit exencephaly. *Nature Genet.* **10**, 175-179.
- Sakaguchi K, Herrera JE, Saito S, Miki T, Bustin M, Vassilev A, Anderson CW, Appella E. (1998). DNA damage activates p53 through a phosphorylation-acetylation cascade. *Genes & Dev.* **12**, 2831-2841.
- Sakai K, Mitani K, Miyazaki J-I. (1995). Efficient regulation of gene expression by adenovirus vector mediated delivery of the cre recombinase. *Biochem. Biophys. Res. Comm.* **217**(2), 393-401.
- Sakai K, & Miyazaki J. (1997). A transgenic mouse line that retains cre recombinase activity in mature oocytes irrespective of the cre transgene transmission. *Biochem. Biophys. Res. Comm.* **237**, 318-324.
- Sakamuro D, Sabbatini P, White E, Prendergast GC. (1997). The polyproline region of p53 is required to activate apoptosis but not growth arrest. *Oncogene* **15**(8), 887-898.
- Sallanave JM, Xing Z, Simpson AJ, Graham FL, Gauldie J. (1998). Adenovirus-mediated expression of an elastase-specific inhibitor (elafin): a comparison of different promoters. *Gene Ther.* **5**(3), 352-60.

- Sambrook J, Fritsch EF, Maniatis T. (1989). *Molecular Cloning: A Laboratory Manual*. Cold Spring Harbour Press.
- Sandhu AK, Hubbard K, Kaur GP, Jha KK, Ozer HL, Athwal RS. (1994). Senescence of immortal human fibroblasts by introduction of normal human chromosome 6. *Proc. Natl. Acad. Sci. USA*. **91**, 5498-5502.
- Sanger F, Niklen S, Coulson AR. (1977). DNA sequencing with chain terminating inhibitors. *Proc. Natl. Acad. Sci. USA* **74**, 5463-5467.
- Santhanam U, Ray A, Sehgal PB. (1991). Repression of the interleukin 6 gene promoter by p53 and the retinoblastoma susceptibility gene product. *Proc. Natl. Acad. Sci. USA* **88**, 7605-7609.
- Sarnow P, Sullivan CA, Levine AJ. (1982). Adenovirus E1B-58kDa tumour antigen and SV40 large T antigen are physically associated with the same 54kDa cellular protein in transformed cells. *Cell* **28**, 387-394.
- Sasaki M, Honda T, Yamada H, Wake N, Barrett JC, Oshimura M. (1994). Evidence for multiple pathways to senescence. *Cancer Res.* **54**, 6090-6093.
- Sato Y, Tanaka K, Lee G, Kanegae Y, Sakai Y, Kaneko S, Nakabayashi H, Tamaoki T, Saito I. (1998). Enhanced and specific gene expression via tissue-specific production of cre recombinase using adenovirus vector. *Biochem. Biophys. Res. Comm.* **244**, 455-462.
- Sauer B. (1987). Functional expression of the cre-lox site-specific recombination system in the yeast *Saccharomyces cerevisiae*. *Mol. Cell. Biol.* **7**, 2087-2096.
- Sauer B, & Henderson N. (1988). Site-specific DNA recombination in mammalian cells by the Cre recombinase of bacteriophage P1. *Proc. Natl. Acad. Sci. USA* **85**, 5166-5170.
- Sauer B, & Henderson N. (1990). Targeted insertion of exogenous DNA into the eukaryotic genome by the cre recombinase. *New Biol.* **2(5)**, 4410449.
- Sauer B. (1998). Inducible gene targeting in Mice Using the Cre/loxP system. *Methods Enzym.* **14**, 381-392.
- Savatier P, Lapillonne H, van Grunsven LA, Rudkin BB, Samarut J. (1995). Withdrawal of differentiation inhibitory activity/leukaemia inhibitory factor up-regulates D-type cyclins and cyclin-dependent kinase inhibitors in mouse embryonic stem cells. *Oncogene* **12**, 309-322.
- Schafer H, Trauzold A, Sebens T, deppert W, Folsch UR, Schmidt WE. (1998). The proliferation associated early response gene p22/PRG1 is a novel p53 target gene. *Oncogene* **16**, 2479-2487.
- Scheffner M, Huibregtse JM, Vierstra RD, Howley PM. (1993). The HPV-16 E6 and E6-AP complex functions as a ubiquitin-protein ligase in the ubiquitination of p53. *Cell* **75**, 495-505.

Schiedtmann KH, Mumby MC, Rundell K, Walter G. (1991). Dephosphorylation of SV40 large T antigen and p53 protein by protein phosphatase 2A : inhibition by small t antigen. *Mol. Cell. Biol.* **11**, 1996-2003.

Schmale H, & Bamberger C. (1997). A novel protein with strong homology to the tumour suppressor p53. *Oncogene* **15**, 1363-1367.

Schneider C, King R, Philipson L. (1988). Genes specifically expressed at growth arrest of mammalian cells. *Cell* **54**, 787-793.

Schneider E, Montenarh M, Wagner P. (1998). Regulation of CAK kinase activity by p53. *Oncogene* **17**, 2733-2741.

Schwartz CJ, & Sadowski PD. (1990). FLP 2 $\mu$ M circle plasmid of yeast induces multiple bends in the FLP recognition target site. *J. Mol. Biol.* **216**, 289-298.

Schwartz D, Goldfinger N, Rotter V. (1993). Expression of p53 protein in spermatogenesis is confined to the tetraploid pachytene primary spermatocytes. *Oncogene* **8**, 1487-1494.

Schwartz D, Almog N, Peled A, Goldfinger N, Rotter V. (1997). Role of wild type p53 in the G2 phase : regulation of the  $\gamma$ -irradiation-induced delay and DNA repair. *Oncogene* **15**, 2597-2607.

Schwartzberg PL, Goff SP, Robertson EJ. (1989). Germ-line transmission of a c-abl mutation produced by targeted gene disruption in ES cells. *Science* **246**, 799-803.

Schwenk F, Baron U, Rajewsky K. (1995). A cre-transgenic mouse strain for the ubiquitous deletion of loxP-flanked gene segments including deletion in germ cells. *Nucleic Acids Res.* **23**(24), 5080-5081.

Schwenk F, Kuhn R, Angrand P-O, Rajewsky K, Stewart AF. (1998). Temporally and spatially regulated somatic mutagenesis in mice. *Nucleic Acid Res.* **26**(6), 1427-1432.

Segev N, & Cohen G. (1981). Control of circularisation of bacteriophage P1 DNA in *Escherichia coli*. *Virology* **114**, 333-342.

Selbert S, Efficient BLG-Cre mediated gene deletion in the mammary gland. (1998). *Transgenic Res.* **7**(5), 387-96.

Sephernia B, Paz IB, Dasgupta G, Momand J. (1996). Heat shock protein 84 forms a complex with mutant p53 protein predominantly within a cytoplasmic compartment of the cell. *J. Biol. Chem.* **271**(25), 15084-15090.

Serrano M, Hannon GJ, Beach D. (1993). A new regulatory motif in cell cycle control causing specific inhibition of cyclin D/CDK4. *Nature* **366**, 704-706.

Serrano M, Lee H-W, Chin L, Cordon-Cardo C, Beach D, DePinho RA. (1996). Role of the INK4A locus in tumour suppression and cell mortality. *Cell* **85**, 27-37.

Seshadri T, & Campisi J. (1990). Repression of c-fos transcription and an altered genetic program in senescent human fibroblasts. *Science* **247**, 205-209.

Seto E, Usheva A, Zambetti GP, Momand J, Horikoshi N, Weinmann R, Levine AJ, Shenk T. (1992). Wild type p53 binds to the TATA-binding protein and represses transcription. *Proc. Natl. Acad. Sci. USA*. **89**, 12028-12032.

Shay JW, & Wright WE. (1989). Quantitation of the frequency of immortalisation of normal human diploid fibroblasts by SV40 T antigen. *Exp. Cell. Res.* **184**, 109-118.

Shen Y, & Shenk T. (1994). Relief of p53-mediated transcriptional repression by the adenovirus E1B 19 kDa protein or the cellular bcl-2 protein. *Proc. Natl. Acad. Sci. USA*. **91**, 8940-8944.

Sherwood SW, Rush D, Ellsworth JL, Shimke RT. (1988). Defining cellular senescence in Imr 90 cells: a flow cytometric analysis. *Proc. Natl. Acad. Sci. USA*. **85**, 9086-9090.

Shibata H, Toyama K, Shioya H, Ito M, Hirota M, Hasegawa S, Matsumoto H, Takano H, Akiyama T, Toyoshima K, Kanamaru R, Kanegae Y, Saito I, Nakamura Y, Shiba K, Noda T. (1997). Rapid colorectal adenoma formation initiated by conditional targeting of the Apc gene. *Science* **278**, 120-123.

Shieh SY, Ikeda M, Taya Y, Prives P. (1997). DNA damage induced phosphorylation of p53 alleviates inhibition by mdm2. *Cell* **91**, 325-334.

Shimizu A, Nishida J, Ueoka Y, Kato K, Hachiya T, Kuriaki Y, Wake N. (1998). Cyclin G contributes to G2/M arrest of cells in response to DNA damage. *Biochem. Biophys. Res. Comm.* **242**, 529-533.

Shin TH, Paterson AJ, Kudlow JE. (1995). P53 stimulates transcription from the human transforming growth factor alpha promoter: a potential growth-stimulatory role for p53. *Mol. Cell. Biol.* **15**(9), 4694-4701.

Shvarts A, Steegenga WT, Riteco N, van Laar T, Dekker P, Bazuine M, van Ham RCA, van der Houven van der Oordt W, Hateboer G, van der Eb AJ, Jochemsen AG. (1996). MDMX: a novel p53-binding protein with some functional properties of mdm2. *EMBO J.* **15**, 5349-5357.

Sigalas I, Clavert AH, Anderson JJ, Neal DE, Lunec J. (1996). Alternatively spliced mdm2 transcripts with loss of p53 binding domain sequences: transforming ability and frequent deletion in human cancer. *Nature Med.* **2**, 912-917.

Slebos RJC, Lee MH, Plunkett BS, Kessis TD, Williams BO, Jacks T, Hedrick L, Kastan MB, Cho KR. (1994). P53-dependent G1 arrest involves pRb related proteins and is disrupted by the human papillomavirus 16 E7 protein. *Proc. Natl. Acad. Sci. USA*. **91**, 5320-5324.

Smith AG & Hooper ML. (1987). Buffalo Rat Liver cells produce a diffusible activity which inhibits the differentiation of murine embryonal carcinoma and embryonic stem cells. *Dev. Biol.* **121**, 1-9.

- Smith AG, Heath JK, Donaldson DD, Wong GC, Moreau J, Stahl M, Rogers D. (1988). Inhibition of pluri-potential ES cell differentiation by purified polypeptides. *Nature* **336**, 688-690.
- Smith AG. (1992). Mouse embryo stem cells; their identification , propagation and manipulation. *Semin. Cell Biol.* **3**, 385-399.
- Smith AJH, De Sousa MA, Kwabi-Addo B, Heppell-Parton A, Impey H, Rabbitts P. (1995). A site directed chromosomal translocation induced in embryonic stem cells by cre-loxP recombination. *Nature Genet.* **9**, 376-385.
- Smith ML, Chen I-T, Zhan Q, Bae I, Chen C-Y, Gilmer TM, Kastan MB, O'Connor PM, Fornace Jr AJ. (1994). Interaction of the p53-regulated protein GADD45 with proliferating cell nuclear antigen. *Science* **266**, 1376-1380.
- Smithies O, Gregg RG, Boggs SS, Karalewski MA, Kucherlapati RS. (1985). Insertion of DNA sequences into the human chromosomal  $\beta$ -globin locus by homologous recombination. *Nature* **317**, 230-234.
- Solter D, Skreb N, Damjanov I. (1970). Extrauterine growth of mouse egg cylinders results in malignant teratoma. *Nature* **227**, 503-504.
- Southern PJ, & Berg P. (1982). Transformation of mammalian cells to antibiotic resistant with a bacterial gene under the control of the SV40 early region promoter. *J. Mol. Appl. Genet.* **1**, 327-341.
- Soussi T, Caron de Fromentel C, May P. (1990). Structural aspects of the p53 protein in relation to gene evolution. *Oncogene* **5**, 945-952.
- Speir E, Modali R, Huang ES, Leon MB, Shawl F, Finkel T, Epstein SE. (1994). Potential role of human CMV and p53 interaction in coronary restenosis. *Science* **265**, 391-394.
- Srinivasan R, & Maxwell SA. (1996). A cellular protein activates the sequence-specific DNA-binding of p53 by interacting with the central conserved region. *Oncogene* **12**, 193-200.
- Srivastava S, Zou Z, Pirollo K, Blattner W, Chang EH. (1990). Germ-line transmission of a mutated p53 gene in a cancer-prone family with Li-Farumeni syndrome. *Nature* **348**, 110-115.
- Stacey A, Schnieke A, McWhir J, Cooper J, Colman , Melton DW. (1994). Use of double-replacement gene targeting to replace the murine alpha-lactalbumin gene with its human counterpart in embryonic stem cells and mice. *Mol. Cell. Biol.* **14**(2), 1009-1016.
- Stanley JF, Pye D, MacGregor A. (1975). Comparison of doubling numbers attained by cultured animal cells with lifespan of species. *Nature* **255**, 150-159.
- Steegenga WT, Shvarts A, van Laar T, van der EB AJ, Jochemsen AG. (1995). Altered phosphorylation and oligomerisation of p53 in adenovirus type 12-transformed cells. *Mol. Cell. Biol.* **16**, 2101-2109.



- Stein GH. (1985). SV40 transformed human fibroblasts: evidence for cellular ageing in precrisis cells. *J. Cell. Physiol.* **125**, 36-44.
- Stein GH, Beeson M, Gordon L. (1990). Failure to phosphorylate the retinoblastoma gene product in senescent human fibroblasts. *Science* **249**, 666-669.
- Stenger JE, Mayr GA, Mann K, Tegtmeyer P. (1992). Formation of stable p53 homotetramers and multiples of tetramers. *Mol. Carcinog.* **5**, 102-106.
- Stewart CL. (1982). Formation of viable chimaeras by aggregation between teratocarcinomas and preimplantation mouse embryos. *J. Embryol. Exp. Morphol.* **67**, 167-179.
- Stewart CL, Vanek M, Wagner EF. (1985). Expression of foreign genes from retroviral vectors in mouse teratocarcinoma chimaeras. *EMBO J.* **4**, 3701-3709.
- Stewart N, Hicks GG, Paraskevas F, Mowat M. (1995). Evidence for a second cell cycle block at G2/M by p53. *Oncogene* **10**, 109-115.
- Stewart TA, & Mintz B. (1981). Successive generations of mice produced from an established culture line of euploid teratocarcinoma cells. *Proc. Natl. Acad. Sci. USA* **78**, 6314-6318.
- St-Onge L, Furth PA, Gruss P. (1996). Temporal control of the cre recombinase in transgenic mice by a tetracycline responsive promoter. *Nucleic Acids Res.* **24**(19), 3875-3877.
- Stratford-Perricaudet LD, Makeh I, Perricaudet M, Briand P. (1992). Widespread long-term gene transfer to mouse skeletal muscle and heart. *J. Clin. Invest.* **90**, 626-630.
- Sturzbecher H-W, Donzelmann B, Henning W, Knippschild U, Buchop S. (1996). P53 is linked directly to homologous recombination processes via RAD51/RecA protein interaction. *EMBO J.* **15**, 1992-2002.
- Stutts P, & Brockman RW. (1963). A biochemical basis for the resistance of L1210 mouse leukaemia to 6-thioguanine. *Biochem. Pharmacol.* **12**, 97-104.
- Sugawara OM, Oshimura M, Koi M, Annab L, Barrett JC. (1990). *Science* **247**, 707-710.
- Sugrue MM, Shin DY, Lee SW, Aaronson SA. (1997). Wild-type p53 triggers a rapid senescence program in human tumour cells lacking functional p53. *Proc. Natl. Acad. Sci. USA* **94**, 9648-9653.
- Suzuki T, Kitao S, Matsushime H, Yoshida M. (1996). HTLV-1 Tax protein interacts with the cyclin dependent kinase inhibitor p16<sup>INK4a</sup> and counteracts its inhibitory activity towards CDK4. *J. Virol.* **71**, 1956-62.
- Suzuki N, Shimamoto A, Imamura O, Kuromitsu J, Kitao S, Goto M, Furuichi Y. (1997). DNA helicase activity in Werner's syndrome gene product synthesized in a baculovirus system. *Nucleic Acid Res.* **25**, 2973-2979.



- Symonds H, Krall L, Remington L, Saenz-Robles M, Lowe S, Jacks R, Van Dyke T. (1994). p53-dependent apoptosis suppresses tumour growth and progression *in vivo*. *Cell* **78**, 703-711.
- Szekely L, Selivanova G, Magnuson KP, Klein G, Wiman KG. (1993). EBNA-5, an Epstein Barr virus encoded nuclear antigen, binds to the Rb and p53 proteins. *Proc. Natl. Acad. Sci. USA* **90**, 5455-5459.
- Takahashi K, & Suzuki K. (1994). DNA synthesis-associated nuclear exclusion of p53 in normal human breast epithelial cells in culture. *Oncogene* **9**, 183-188.
- Takeda J, & Kinoshita T. (1995). GPI-anchor biosynthesis. *Trends in Biochem. Sci.* **20**, 367-371.
- Takenaka I, Morin F, Seizinger BR, Kley N. (1995). Regulation of the sequence-specific DNA binding function of p53 by protein kinase C and protein phosphatases. *J. Biol. Chem.* **270**, 5405-5411.
- Tan T-H, Wallis J, Levine AJ. (1986). Identification of the p53 protein domain involved in formation of SV40-p53 protein complexes. *J. Virol.* **59**, 574-583.
- Tarutani M, Itami S, Okabe M, Ikawa M, Tezuka T, Yoshikawa K, Kinoshita T, Takeda J. (1997). Tissue-specific knockout of the mouse *Pig-a* gene reveals important roles for the GPI-anchored proteins in skin development. *Proc. Natl. Acad. Sci. USA* **94**, 7400-7405.
- Te Riele H, Maandag ER, Clarke A, Hooper M, Berns A. (1990). Consecutive inactivation of both alleles of the *pim-1* proto-oncogene by homologous recombination in embryonic stem cells. *Nature* **348**, 649-651.
- Terry RW, Kwee L, Baldwin S, Labow MA. (1997). Cre-mediated generation of a VCAM-1 null allele in transgenic mice. *Transgenic Res.* **6**, 349-356.
- Thomas A, & White E. (1998). Suppression of the p300-dependent mdm2 negative-feedback loop induces the p53 apoptotic function. *Genes & Dev.* **12**, 1975-1985.
- Thomas KR, Folger KR, Capecchi MR. (1986). High frequency of targeting of genes to specific sites in the mammalian genome. *Cell* **44**, 419-428.
- Thomas KR, & Capecchi MR. (1987). Site-directed mutagenesis by gene targeting in mouse-embryo derived stem cells. *Cell* **51**, 503-512.
- Thomas KR, Capecchi MR. (1990). Targeted disruption of the murine *int-1* proto-oncogene resulting in severe abnormalities in midbrain and cerebellar development. *Nature* **346**, 847-850.
- Thomas M, Massimi P, Jenkins J, Banks L. (1995). HPV-18 E6 mediated inhibition of p53 DNA binding activity is independent of E6 induced degradation. *Oncogene* **10**, 261-268.

- Thukral SK, Blain GC, Chang KH, Fields S. (1994). Distinct residues of human p53 implicated in binding to DNA, SV40 T antigen, 53BP1 and 53BP2. *Mol. Cell. Biol.* **14**, 8315-8321.
- Thut C, Chen JL, Klemm R, Tijan R. (1995). p53 transcriptional activation mediated by coactivators TAFII40 and TAFII60. *Science* **267**, 100-104.
- Todaro GJ, & Green H. (1963). Quantitative studies of the growth of mouse embryo cells in culture and their development into established lines. *J. Cell. Biol.* **17**, 299-313.
- Tomida M, Yamamoto-Yamaguchi Y, Hozumi M. (1984). Purification of a factor inhibiting differentiation of mouse myeloid leukemic M1 cells from conditioned medium of mouse fibroblast L929 cells. *J. Biol. Chem.* **259**, 10978-10982.
- Truant R, Antunovic J, Greenblatt J, Prives C, Cromlish JA. (1995). Direct interaction of HBx protein with p53 leads to inhibition by HBx of p53 response element-directed transactivation. *J. Virol.* **69**, 1851-1859.
- Tsien JZ, Chen DF, Gerber D, Tom C, Mercer EH, Anderson DJ, Mayford M, Kandel ER, Tonegawa S. (1996a). Sub-region- and cell type-restricted gene knockout in mouse brain. *Cell* **87**, 1317-1326.
- Tsien JZ, Huerta PT, Tonegawa S. (1996b). The essential role of hippocampal CA1 NMDA receptor-dependent synaptic plasticity in spatial memory. *Cell* **87**, 1327-1338.
- Udy GB, Parkes BD, Wells DN. (1997). ES cell cycle rates affect gene targeting frequencies. *Exp. Cell. Res.* **231**, 296-301.
- Ueba T, Nosaka T, Takahashi JA, Shibata F, Florkiewicz RZ, Vogelstein B, Oda Y, Kikuchi H, Hatanaka M. (1994). Transcriptional regulation of bFGF gene by p53 in human glioblastoma and hepatocellular carcinoma cells. *Proc. Natl. Acad. Sci. USA* **91**, 9009-9013.
- Ueda H, Ullrich SJ, Gangemi JD, Kappel CA, Ngo L, Feitelson MA, Jay G. (1995). Functional inactivation but not structural mutation of p53 causes liver cancer. *Nature Genet.* **9**, 41-47.
- Unger T, Nau MM, Segal S, Minna JD. (1992). p53: a transdominant regulator of transcription whose function is ablated by mutations in human cancer. *EMBO J.* **11**, 1383-1390.
- Valancius V, Smithies O. (1991). Testing an "in-out" targeting procedure for making subtle genomic modifications in mouse embryonic stem cells. *Mol. Cell. Biol.* **11**(3), 1402-1408.
- Van Deursen J, Fornerod M, van Rees B, Grosveld G. (1995). Cre mediated site specific translocation between nonhomologous mouse chromosomes. *Proc. Natl. Acad. Sci. USA* **92**, 7376-7380.
- Van Meir EG, Polverini PJ, Chazin VR, Su Huang H-J, de Tribolet N, Caveness W. (1994). Release of an inhibitor of angiogenesis upon induction of wild type p53 expression in glioblastoma cells. *Nature Genet.* **8**, 171-176.

- Vara J, Malpartida F, Hopwood DA, Jimenez A. (1985). Cloning and expression of a puromycin N-acetyltransferase gene from *Streptomyces albaniger* in *Streptomyces lividans* and *Escherichia coli*. *Gene* **33**, 197-206.
- Varmeh-Ziaie S, Okan I, Wang Y, Magnusson KP, Warthoe P, Strauss M, Wiman KG. (1997). Wig-1, a new p53-induced gene encoding a zinc finger protein. *Oncogene* **15**, 2699-2704.
- Verhaegh GW, Richard MJ, Hainaut P. (1997). Regulation of p53 by metal ions and by antioxidants : dithiocarbamatedown-ergulates p53 DNA-binding activity by increasing the intracellular level of copper. *Mol. Cell. Biol.* **17**(10), 5699-5706.
- Vidal F, sage J, Cuzin F, Rassoulzadegan M. (1998). Cre expression in primary spermatocytes: a tool for genetic engineering of the germ line. *Mol. Repro. Dev.* **51**, 274-280.
- Vogt M, Haggbloom C, Yeargin J, Christiansen-Weber T, Haas M. (1998). Independent induction of senescence by p16<sup>INK4a</sup> and p21 in spontaneously immortalised human fibroblasts. *Cell Growth Diff.* **9**, 139-146.
- Vojta PJ, & Barrett JC. (1995). Genetic analysis of cellular senescence. *Biochim. Biophys. Acta.* **1242**, 29-41.
- Volkert FC, & Broach JR. (1986). Site specific recombination promotes plasmid amplification in yeast. *Cell* **46**, 541-550.
- Vooijs M, van der Valk M, te Riele H, Berns A. (1998). Flp-mediated tissue-specific inactivation of the retinoblastoma tumour suppressor gene in the mouse. *Oncogene* **17**, 1-12.
- Waga S, Hannon GJ, Beach D, Stillman B. (1994). The p21 inhibitor of cyclin dependent kinases controls DNA replication by interaction with PCNA. *Nature* **369**, 574-578.
- Wagner KU, Wall RJ, St-Onge L, Gruss P, Wynshaw-Boris A, Garrett L, Li M, Furth PA, Henninghausen L. (1997). Cre-mediated deletion in the mammary gland. *Nucleic Acid Res.* **25**(21), 4323-4330.
- Wagner P, Fuchs A, Gotz C, Nastainczyk W, Montenarh M. (1998). Fine mapping and regulation of the association of p53 with p34<sup>cdc2</sup>. *Oncogene* **16**, 105-111.
- Wakita T, Taya C, Katsume A, Kato J, Yonekawa H, Kanegae Y, Saito I, Hayashi Y, Koike M, Kohara M. (1998). Efficient conditional transgene expression in hepatitis C virus cDNA transgenic mice mediated by the cre/loxP system. *J. Biol. Chem.* **273**(15), 9001-9006.
- Walker KK, Levine AJ. (1996). Identification of a novel p53 functional domain that is necessary for efficient growth suppression. *Proc. Natl. Acad. Sci. USA* **93**, 15335-40.
- Wallace M (1997).

Thesis submitted for the degree of BSc (Hons), Department of Pathology, University of Edinburgh.

Wang E. (1995). Senescent human fibroblasts resist programmed cell death and failure to suppress bcl-2 is involved. *Cancer Res.* **55**, 2284-92.

Wang Q, & Beck WT. (1998). Transcriptional suppression of the multidrug resistance-associated protein (MRP) gene expression by wild type p53. *Cancer Res.* **58(24)**, 5762-9.

Wang S, & Hazelrigg T. (1994). Implications for bcd mRNA localisation from spatial distribution of exu protein in *Drosophila* oogenesis. *Nature* **369**, 400-403.

Wang WM, Zhai Y, Ferrell JE Jr. (1997). A role for MAPK in the spindle assembly checkpoint in XTV cells. *J. Cell Biol.* **137**, 433-443.

Wang XW, Yeh H, Schaeffer L, Roy R, Moncollin V, Egly J-M, Wang Z, Friedberg EC, Evans MK, Taffe BG, Bohr VA, Weeda G, Hoejmakers JHJ, Forrester K, Harris CC. (1995). p53 modulation of TFIIH-associated nucleotide excision repair activity. *Nature Genet.* **10**, 188-193.

Wang XW, Vermeulen W, Couuren JD, Gibson M, Lupold SE, Forrester K, Xu G, Elmore L, Yeh H, Hoejmakers JHJ, Harris CC. (1996). The XPB and XPD DNA helicases are components of the p53-mediated apoptosis pathway. *Genes & Dev.* **10**, 1219-1232.

Wang Y, Reed M, Wang P, Stenger JE, Mayr G, Anderson ME, Schwedes JF, Tegtmeier P. (1993). P53 domains : identification and characterisation of two autonomous DNA-binding regions. *Genes & Dev.* **7**, 2575-2586.

Wang Y, & Prives C. (1995). Increased and altered DNA binding of human p53 by S and G2/M but not G1 cyclin-dependent kinases. *Nature* **376**, 88-91.

Wang Y, Krushel LA, Edelman GM. (1996). Targeted DNA recombination *in vivo* using an adenovirus carrying the cre recombinase gene. *Proc. Natl. Acad. Sci. USA.* **93**, 3932-3936.

Waterman MJF, Stavridi ES, Waterman JLF, Halazonetis TD. (1998). ATM-dependent activation of p53 involves dephosphorylation and association with 14-3-3 proteins. *Nature Genet.* **19**, 175-178.

Weinberg RA. (1995). The retinoblastoma protein and cell cycle control. *Cell* **81**, 323-330.

Weintraub H, Hauschka S, Tapscott SJ. (1991). The MCK enhancer contains a p53 responsive element. *Proc. Natl. Acad. Sci. USA.* **88**, 4570-4571.

Weintraub SJ, Prater CA, Dean DC. (1992). RB protein switches the E2F site from a positive to negative element. *Nature* **358**, 259-261.

White E. (1996). Life, death and the pursuit of apoptosis. *Genes & Dev.* **10**, 1-15.

Williams RL, Hilton DJ, Pease S, Wilson TA, Stewart CL, Gearing DP, Wagner EF, Metcalf D, Nicola NA, Gough GM. (1988). Myeloid leukaemia inhibitory factor maintains the developmental potential of embryonic stem cells. *Nature* **336**, 684-688.

Wiman KG. (1997). P53: emergency brake and target for cancer therapy. *Exp. Cell Res.* **237**, 14-18.

Wobus AM, Grosse R, Schineich J. (1988). Specific effects of nerve growth factor on the differentiation pattern of the mouse embryonic stem cells in vitro. *Biomed. Biophys. Acta* **47**, 965-973.

Wolkowicz R, Peled A, Elkind NB, Rotter V. (1995). Augmented DNA binding activity of p53 protein encoded by a carboxyl-terminal alternatively spliced mRNA is blocked by p53 protein encoded by the regularly spliced form. *Proc. Natl. Acad. Sci. USA* **92**, 6842-6846.

Wong EA, & Cappechi MR. (1987). Homologous recombination between coinjected DNA sequences peaks in S phase. *Mol. Cell. Biol.* **5**, 2599-2607.

Wright WE, Pereira-Smith OM, Shay JW. (1989). Reversible cellular senescence: implications for immortalisation of normal human diploid fibroblasts. *Mol. Cell. Biol.* **9**, 3088-3092.

Wright WE, & Shay JW. (1992). The two stage mechanism controlling cellular senescence and immortalisation. *Exp. Gerontol.* **27**, 383-389.

Wu GS, Burns TF, McDonald ER 3<sup>rd</sup>, Jiang W, Meng R, Krantz ID, Kao G, Gan DD, Zhou JY, Muschel R, Hamilton SR, Spinner NB, Markowitz S, Wu G, el-Deiry WS. (1997). KILLER/DR5 is a DNA damage-inducible p53-regulated death receptor gene. *Nat. Genet.* **17**(2), 141-143.

Wu L, Bayle JH, Elenbaas B, Pavletich NP, Levine AJ. (1995). Alternatively spliced forms in the carboxy-terminal domain of the p53 protein regulate its ability to promote annealing of complementary single strands of nucleic acids. *Mol. Cell. Biol.* **15**, 497-504.

Wu X, & Levine AJ. (1994). Growth suppression by p18, a p16INK4/MTS1- and p14INK4B/MTS2-related CDK6 inhibitor correlates with wild type Rb function. *Proc. Natl. Acad. Sci. USA.* **91**, 3602-3606.

Wu Y, Liu Y, Lee L, Miner Z, Kulesz-Martin M. (1994). Wild type alternatively spliced p53 : binding to DNA and interaction with the major p53 protein in vitro and in cells. *EMBO J.* **13**, 4823-4830.

Wu Y, Huang H, Miner Z, Kulesz-Martin M. (1997). Activities and response to DNA damage of latent and active sequence-specific DNA binding forms of mouse p53. *Proc. Natl. Acad. Sci. USA.* **94**, 8928-8987.

Wyllie AH, Kerr JFR, Currie AR. (1980). Cell death : the significance of apoptosis. *Int. Rev. Cytol.* **68**, 251-306.



- Xiao H, Pearson A, Coulombe B, Truant R, Zhang S, Regier JL, Triezenberg SJ, Reinberg D, Flores O, Ingles CJ, Greenblatt J. (1994). Binding of basal transcription factor TFIID to the acidic activation domains of VP16 and p53. *Mol. Cell. Biol.* **14**, 7013-7024.
- Xiong Y, Hannon GJ, Zhang H, Casso D, Kobayashi R, Beach D. (1993). P21 is a universal inhibitor of cyclin kinases. *Nature* **366**, 701-704.
- Xu H-J, Zhou Y, Ji W, Perng G-S, Kruzelock R, Kong C-T, Bast RC, Mills GB, Li J, Hu S-X. (1997). Reexpression of the retinoblastoma protein in tumour cells induces senescence and telomerase inhibition. *Oncogene* **15**, 2589-2596.
- Yagi T, Ikawa Y, Yoshida K, Shigetani Y, Takeda N, Mabuchi I, Yamamoto T, Aizawa S. (1990). Homologous recombination at c-fyn locus of mouse embryonic stem cells with use of diphtheria toxin A-fragment gene in negative selection. *Proc. Natl. Acad. Sci. USA*. **87**, 9918-9922.
- Yamabe Y, Shimamoto A, Goto M, Yokota J, Sugawara M, Furuichi Y. (1998). Sp1-mediated transcription of the Werner helicase gene is modulated by Rb and p53. *Mol. Cell. Biol.* **18**(11), 6191-6200.
- Yamamoto M, Yoshida M, Ono K, Fujita T, Ohtani-Fujita N, Sakai T, Nikaido T. (1994). Effect of tumour suppressors on cell cycle regulatory genes : RB suppresses p34 expression and normal p53 suppresses cyclin A expression. *Exp. Cell. Res.* **210**, 94-101.
- Yang S, Veide A, Enfors SO. (1995). Proteolysis of fusion proteins: stabilisation and destabilisation of staphylococcal protein A and Escherichia coli beta-galactosidase. *Biotechnol. Appl. Biochem.* **22**(Pt 2), 145-59.
- Yang X-J, Ogryzko VV, Nishikawa J-I, Howard BH, Nakatani Y. (1996). A p300/CBP associated factor that competes with the adenoviral oncoprotein E1A. *Nature* **382**, 319-324.
- Yang Y, Nunes FA, Berenski K, Furth EE, Gonczol E, Wilson JM. (1994). Cellular immunity to viral antigens limits E1-deleted adenoviruses for gene therapy. *Proc. Natl. Acad. Sci. USA* **91**, 4407-4411.
- Yang Y, Jooss KU, Su Q, Ertl HCJ, Wilson JM. (1996). Immune responses to viral antigens versus transgene product in the elimination of recombinant adenovirus-infected hepatocytes in vivo. *Gene Therapy* **3**, 137-144.
- Yarborough DJ, & Meyer OT, Dannenberg AM, Pearson B. (1967). *J. Reticuloendothel. Soc.* **4**, 390-408.
- Yew PR, & Berk AJ. (1992). Inhibition of p53 transactivation required for transformation by adenovirus E1B protein. *Nature* **357**, 82-85.
- Yew PR, Liu X, Berk AJ. (1994). Adenovirus E1B oncoprotein tethers a transcriptional repression domain to p53. *Genes & Dev.* **8**, 190-202.



Yu CE, Oshima J, Fu YH, Wijsman EM, Hisama F, Alisch R, Matthews J, Nakura T, Miki T, Ouais S, Martin GM, Mulligan J, Schellenberg GD. (1996). Positional cloning of the Werner's syndrome gene. *Science* **272**, 258-262.

Zauberman A, Lubp A, Oren M. (1995). Identification of p53 target genes through immune selection of genomic DNA : The cyclin G gene contains two distinct 53 binding sites. *Oncogene* **10**, 2361-2366.

Zeng X, Levine AJ, Lu H. (1998). Non-p53, p53RE binding protein, a human transcription factor functionally analogous to p53. *Proc. Natl. Acad. Sci. USA*. **95(12)**, 6681-6686.

Zhan Q, Pan S, Bae I, Guillouf C, Lieberman DA, O'Connor PM, Fornace Jr AJ. (1993). Induction of bax by genotoxic stress in human cells correlates with normal p53 status and apoptosis. *Oncogene* **9**, 3743-3751.

Zhang H, Somasundaram K, Peng Y, Tian H, Zhang H, Bi D, Weber BL, El-Diery WS. (1998). BRCA1 physically associates with p53 and stimulates its transcriptional activity. *Oncogene* **16**, 1713-1721.

Zhang Q, Gutsch D, Kenney S. (1994). Functional and physical interaction between p53 and BZLF1: implications for EBV latency. *Mol. Cell. Biol.* **14**, 1929-1938.

Zhang W, Lu Q, Xie ZJ, Mellgren RL. (1997). Inhibition of the growth of WI-38 fibroblasts by benzyloxycarbonyl-Leu-Leu-Tyr diazomethyl ketone: evidence that cleavage of p53 by a calpain-like protease is necessary for G1 to S phase transition. *Oncogene* **14**, 255-263.

Zhang Y, Riesterer C, Ayrall A-M, Sablitsky F, Littlewood TD, Reth M. (1996). Inducible site-directed recombination in mouse embryonic stem cells. *JOURNAL??* **24(4)**, 543-548.

Zhang Y, Xiong Y, Yarbrough WG. (1998). ARF promotes mdm2 degradation and stabilises p53: ARF-INK4a locus deletion impairs both the Rb and p53 tumour suppression pathways. *Cell* **92**, 725-734.

Zheng H, & Wilson JH. (1990). Gene targeting in normal and amplified cell lines. *Nature* **344**, 170-173.

Zhu X-D, Sadowski PD. (1998). The role of single-stranded DNA in Flp-mediated strand exchange. *J. Biol. Chem.* **273(9)**, 4921-4927.

Zimmerman L, Lendahl U, Cunningham M, McKay R, Parr B, Gavin B, Mann J, Vassileva G, McMahon M. (1994). Independent regulatory elements in the nestin gene direct transgene expression to neural stem cells or muscle precursors. *Neuron* **12**, 11-24.

Zinyk DL, Mercer EH, Harris E, Anderson DJ, Joyner AL. (1998). Fate mapping of the mouse midbrain-hindbrain constriction using a site-specific recombination system. *Curr. Biol.* **8**, 665-668.

# **Appendix 1**

## **Publications**

## REVIEW ARTICLE

# ANIMAL MODELS AND THE MOLECULAR PATHOLOGY OF CANCER

ELIZABETH A. LOVEJOY, ALAN R. CLARKE AND DAVID J. HARRISON

*Department of Pathology, University Medical School, Teviot Place, Edinburgh, EH8 9AG, U.K.*

### INTRODUCTION

The pathogenesis of cancer is a multistep process characterized by the accumulation of critical genetic lesions within the cell. The rate of mutation accumulation is influenced by both external environmental factors and the genotype of the cell. To date, many studies have described a bewildering variety of molecular genetic abnormalities, the significance of which to pathogenesis is often obscure. Indeed, it is probable that many of these abnormalities are epiphenomenal rather than of crucial importance.

### HISTORICAL BACKGROUND

Epidemiological and genetic studies have led to substantial advances in our understanding of the pathogenesis of cancer. Naturally occurring germline mutations in humans, manifesting as heritable cancer predisposition syndromes, provided an insight into the molecular genetics of tumour suppressor genes. For example, familial adenomatous polyposis coli (FAP) is transmitted as an autosomal dominant trait with incomplete penetrance.<sup>1</sup> FAP patients develop multiple adenomatous polyps, especially within the colon and rectum, and show a high incidence of colorectal adenocarcinoma. FAP patients also show a predisposition to other neoplasms including osteomas, fibromas, desmoid tumours, and hepatoblastomas.<sup>2</sup> The tumour suppressor gene affected in FAP<sup>3</sup> was localized to human chromosome 5 and it has since been shown that inactivating mutations in the adenomatous polyposis coli (APC) gene are present in the majority of cases of colon cancer, both sporadic and familial.

Mutation of the tumour suppressor genes p53 and RB is responsible for two other cancer predisposition syndromes seen in humans. Germline heterozygosity for a mutated p53 allele characterizes Li–Fraumeni syndrome,<sup>4,5</sup> which predisposes to a variety of neoplasms, of which breast and brain are the most common. Human retinoblastomas are childhood cancers and can occur spontaneously or as an autosomal dominant familial form. Of people with a mutated RB allele, more than 90

per cent will develop retinoblastoma and about 15 per cent will also develop osteosarcoma.<sup>6</sup> Somatic mutation and subsequent loss of RB allele function are also seen in sporadic lung, breast, prostate, and bladder carcinomas, although no increase in the incidence of these tumours is observed in the germline heterozygotes.

The study of DNA tumour viruses has facilitated an understanding of the second class of genes involved in neoplasia. These oncogenic viruses carry mutated forms of normal cellular genes which may be truncated or carry an activating point mutation. The cellular copies of such genes are referred to as proto-oncogenes and most are involved with the regulation of growth and division of the normal cell. Mutations present in viral oncogenes mimic those arising spontaneously in proto-oncogenes during malignant progression; both lead to aberrant activity of these important regulatory molecules.

Despite the value of these approaches, they are limited and essentially descriptive. Thus, considerable effort and resources have been directed towards creating accurate animal models of this complex disease. Although animal models may never provide exact representations of a human disease, they do permit dissection of specific molecular and biochemical pathways which may be involved. Furthermore, they allow a variety of genetic manipulations that would be technically and ethically impracticable with human tissues.

### MOUSE MODELS OF HUMAN NEOPLASIA

Since the production of the first murine models of human neoplasia, technological advances and refinement of the concept being examined have led to increasingly accurate and informative models. Initial work on chemical carcinogens in rats and mice demonstrated that exposure results in DNA mutation and then progression to tumour. This led to the concepts of initiation and promotion of tumours.

As individual genes important in neoplasia were identified, the newer technologies of gene targeting and transgenic mouse production allowed a more directed analysis of the molecular function of such gene products. This increased the complexity of the model of carcinogenesis from a simple linear progression to a network of interacting factors. The latest advances with

Addresssee for correspondence: Elizabeth A Lovejoy, Department of Pathology, University Medical School, Teviot Place, Edinburgh, EH8 9AG, Scotland, U.K.

and tissue-specific gene targeting and transgenesis can only serve to increase the usefulness of the transgenic model system.

### *Intestinal carcinogenesis*

The first association between exposure to chemical carcinogens and the induction of cancer was made in 1915. Subsequent work has shown that the same carcinogens are able to induce tumours in animals. However, treatment of mice with standard carcinogen regimens produce significant variations in tumour incidence, and the age of onset between animals of different strains. It is implicit from such heterogeneity that inter-strain extrapolation is fraught with error. For example, the treatment of rats initiates a sequence of focal hyperplastic changes in pancreatic acinar cells, the end result of which is the development of carcinomas.<sup>7</sup> These carcinomas bear little histological similarity to the majority of human pancreatic carcinomas, which are ductal in histology, and little genetic similarity; K-*ras* mutations are seen in more than 80 per cent of human pancreatic carcinomas,<sup>8</sup> whereas no K-*ras* or H-*ras* mutations can be detected in the azaserine-induced carcinomas.<sup>9</sup>

Tumours which arise in humans and animals in response to chemical carcinogens are comparable, in that they both arise due to carcinogen-induced DNA mutations. However, the precise molecular genetic pathology is often uncharacterized and in most cases, similarities between the two are assumed but not proved. It is unjustified to accept that because one carcinogen induces cancer in both mice and humans, such cancers have identical or similar genetic alterations.

### *Germline mutagenesis*

The implementation of the carcinogen-based strategy was first achieved by the use of random mutagenesis. Here, carcinogens are exploited to induce random mutations within the germline of mice, which are then mated and the progeny examined for phenotypic abnormalities. Any progeny displaying a phenotype of interest are then further characterized, eventually leading to the identification of the mutant gene.

This approach led to the identification of a mouse model of the human cancer predisposition syndrome, familial adenomatous polyposis, one of the pedigrees established after random mutagenesis with *N*-ethyl-nitrosourea displayed a progressive adult-onset anaemia.<sup>10</sup> Examination revealed numerous adenomas within the small and large intestines of the anaemic mice; adenoma *in situ* was seen in some older animals. This syndrome was described as multiple intestinal neoplasia (Min mice). Further work revealed that the syndrome is heterozygous for a nonsense mutation at codon 50 of the *Apc* gene, the mouse homologue of APC,<sup>11</sup> the gene affected in FAP. The exact number of adenomas which Min mice develop depends on the genetic background of the strain and the effects of modifier loci such as *Mom-1*.<sup>12</sup> Although all cells

within the organism are +/– for *Apc*, not all intestinal epithelial cells form adenomas. Thus, heterozygosity at the *Apc* locus is necessary but not sufficient for the Min phenotype. Further genetic events must occur, including the loss of the remaining wild-type *Apc* allele, before adenomas develop and subsequently progress to carcinoma.

Although at the molecular level, human FAP patients and the Min mouse have mutations in homologous genes, the phenotypes are not identical. Firstly, mutation of the APC gene in humans is predominantly associated with colorectal neoplasia, whereas Min mice demonstrate adenomas preferentially in the small intestine. Secondly, progression to locally invasive carcinoma occurs in almost 100 per cent of untreated FAP patients, yet in the mouse progression is relatively rare. This difference may arise either as a consequence of a higher adenoma burden in FAP patients, or due to the predilection for small intestinal involvement in the mouse, or because of other differences in the genetics of progression between mice and humans.

### *Reverse genetics—transgenic mice*

The Min mouse was identified by analysis of phenotype and the genotype responsible was subsequently identified. Reverse genetics<sup>13</sup> refers to the technique of analysing gene function by modulating or ablating gene expression either *in vivo* or *in vitro* and then studying the resultant phenotype.

#### *Transgenic mice generated by pronuclear injection—*

The first generation of transgenic mice was generated using simple pronuclear injection of DNA. For example, in an attempt to model human pancreatic neoplasia, mice have been produced which are characterized by pancreatic acinar cell specific expression of an activated form of a human H-*ras* transgene.<sup>14</sup> While H-*ras* transgenic mice developed acinar tumours in the fetal pancreas, no pancreatic tumours of ductal morphology (the predominant human tumour type associated with *ras* mutations) were observed. These experiments support the conclusion that overexpression of mutant *ras* is capable of causing cancer. However, this bears little resemblance to spontaneously occurring human pancreatic cancer.

This first generation of transgenic mice is of limited value and they are not faithful models of human neoplasia. They do have the significant advantages of relative simplicity and low cost of production, compared with the targeted mice discussed later. The major disadvantages are limited control of transgene copy number and expression and the lack of control of site of integration, bringing with it the risk of insertional mutagenesis. A further limitation is that the transgene must be dominant to produce an observable phenotype, as new genetic material can only be added to the existing genotype.

*Transgenic mice generated by gene targeting*—The advent of stem cell technology led to a second generation of transgenic mice, circumventing some of the



above problems. Embryonic stem (ES) cells were first isolated in the early 1980s<sup>15,16</sup> and are pluripotent cell lines derived from the inner cell mass of mouse blastocysts. They can be cultured *in vitro* indefinitely, genetically manipulated, and then reintroduced into blastocysts. Once back inside the new blastocyst, they are able to contribute to all lineages of the resulting chimaeric embryo, including the germline. Progeny may constitutively carry any mutations introduced into the ES cells during culture. These mutations will subsequently be inherited in a stable Mendelian fashion. The standard approach to gene targeting relies upon the introduction of exogenous DNA constructs which replace their endogenous counterparts via homologous recombination. Alterations such as mutation, interruption, or truncation into the targeted gene are now commonplace.<sup>17</sup>

Knockout mice, in which the function of a specific gene is ablated in all tissues of the mouse, have provided an ideal framework for the study of the role of tumour suppressor genes. For example, p53 null mice were generated independently by four groups.<sup>18–20</sup> Homozygous null mice have reduced viability<sup>21</sup> and develop tumours, predominantly thymic T-cell lymphomas, during the first 6 months of life. The tumour spectrum observed is strain-dependent and mimics only approximately the tumour spectrum observed in the human equivalent, Li-Fraumeni syndrome. Both Li-Fraumeni patients and p53 +/– mice display a cancer predisposition that would be predicted due to their heterozygosity for this important tumour suppressor gene. Variations within the tumour spectra observed may represent differences in the molecular control of oncogenesis in mice and humans, as well as differences in environment.

Similar techniques were applied to permit analysis of the retinoblastoma gene product, Rb-1.<sup>22–24</sup> These studies have shown Rb-1 function to be essential for normal development, as Rb-1 homozygous null embryos die mid-gestation. Unexpectedly, animals heterozygous for Rb-1 function failed to develop retinal tumours. Instead, they have a high incidence of pituitary adenomas. Thus, Rb-1 deficiency in the mouse does model malignancy, but with a clearly different tissue specificity from that seen in humans.

### EXISTING MOUSE MODELS—LIMITATIONS AND LESSONS

While the p53 or Rb-1 knockout mice were of only limited success in modelling human diseases, they did provide an unequivocal definition of a tumour suppressor gene—that loss of function will result in increased tumour incidence. This important result is taken as the paradigm for all putative tumour suppressor genes.

The phenotypic differences observed between mice and humans with analogous genetic mutations, such as in the retinoblastoma gene, originally called into question the validity of mouse models of human diseases. However, subsequent work to rationalize and understand the causes of these differences has led to significant

advances in our understanding of the molecular mechanisms of such gene products. Some variations in type may be due to interspecies differences in function, but others arise as a result of differences in functional redundancy of a specific gene product. Redundancy may vary spatially, for example in a specific manner, and temporally, such as in relation to critical windows of gene function during development. A comparison of the Rb-1 mouse and human retinoblastoma patients illustrates both of these concepts of redundancy. Loss of function of both *RB* alleles within human retina will result in retinoblastoma, indicating that within these cells, *RB* is non-redundant and activating mutations predispose to neoplastic transformation. Similarly, within the mouse pituitary, compensation of Rb-1 function results in the development of pituitary adenomas.<sup>22–24</sup> Thus, a major phenotypic variation between mouse and human is explained by tissue-specific differences in the functional redundancy of the retinoblastoma gene product. The Rb-1-related gene products p107 and p130 are able to compensate for loss of Rb-1 function in the murine retina. Preliminary data are showing that ablation of these genes in an Rb-1 background results in retinoblastoma in the mouse.

Differences in molecular controls within mouse and human cells complete the explanation of the Rb-phenotype. Rb-1 –/– cells in the murine retina are deleted via p53-dependent apoptosis,<sup>25</sup> preventing progression to retinoblastoma; such cells in the human retina are not. If the viral SV40 TAg is expressed in murine retinal cells, thereby inactivating both p107 and p130, Rb function, retinoblastoma is the outcome<sup>26</sup> and in –/–, Rb +/– animals retinal dysplasia is commonly observed, but not actual retinoblastoma.<sup>27</sup> Hence, Rb-1 is essential for normal development of the retina, indicating that p107 and p130 do not display complete functional redundancy.

The constitutive absence of Rb-1 and many other tumour suppressor genes or proto-oncogenes during mouse embryonic development frequently leads to lethality of the embryo and is a significant limitation of strategies to produce targeted mice. In direct contrast to the problems of embryonic lethality, complete functional redundancy can result in knockout mice with no obvious phenotype. For example, with *N-ras* knockout mice<sup>28</sup> no differences between –/–, +/– and wild-type animals could be identified, leading some authors to conclude that there is significant redundancy within the *ras* family. Thus, with any gene targeted for study, it is not always possible to predict the phenotype accurately. The information gained, while still valuable, may not be immediately applicable to specific human types in man. In some regards, gene knockout mice raise more questions than they answer.

### INDUCIBLE GENE TARGETING

#### Potential and benefits

Gene targeting is now an accepted methodology in reverse genetics and the approach has become a routine. While present targeting strategies do pro-

work within which many questions have been addressed, the problems discussed above will not be solved with the technology as it stands. Inducible targeting strategies now under development will allow significant refinements to be made to the basic tools of gene targeting. Conditional knockouts, in which gene function is ablated after embryological development in the adult, somatic tissue, should overcome the problem of embryonic lethality in homozygous mice. Such animals should also better reflect the process of tumorigenesis in humans, since most cancers do not have an inherited germline susceptibility. In contrast to conditional knockouts, inducible targeting can also be used to restore the function of genes which were previously inactive, with temporal and spatial control over this activation, so-called 'knock-on'. These new advances are now past the initial development and characterization stages and are being incorporated into current targeting protocols.

### Inducible promoters

Gene expression at the level of transcription is governed by promoter elements within the DNA sequence. A variety of promoters exist in both prokaryotes and eukaryotes that can alter levels of transcription in response to the presence or absence of specific inducers. If an inducible promoter is positioned upstream of a target gene in place of the normal promoter, then expression of the target gene can be controlled externally by the inducer. Both eukaryotic and prokaryotic promoters have been used in an attempt to provide inducible expression of mammalian genes, with varying degrees of success. Early attempts with mammalian promoter systems using inducers such as heat shock, heavy metal ions, or aromatic hydrocarbons encountered problems with pleiotropic gene induction, restricted temporal specificity, toxicity or carcinogenicity of inducing agents, and small scale of induction.<sup>29</sup> Characterization of mammalian promoters has led to the discovery of promoters more suited to inducible control of gene expression, such as the murine *Mx* gene promoter which is induced in response to interferon or virus exposure.<sup>30</sup> The inherent complexity of mammalian transcription regulation means that these endogenous systems are not ideal for induction of one specific experimental gene. To avoid these problems altogether, transcriptional tools from bacteria were adapted for use in mammals. Much recent effort has concentrated on *Escherichia coli* tetracycline responsive promoters,<sup>31-33</sup> with considerable success. For any of the inducible promoters which have been developed to make a significant contribution to the modelling of human neoplasia, it must be demonstrated that they allow tight control of gene expression and that they are able to regulate expression of genes important in neoplasia. Tetracycline-inducible luciferase expression has since been demonstrated in transgenic mice and expression of a marker gene was shown to be highly inducible, specific, and without any tetracycline side-effects.<sup>34</sup> As no *in vivo* work with tetracycline-regulated oncogenes or tumour suppressor genes has been published,

but *in vitro* studies have demonstrated that the expression of such genes can be controlled in this way. For example, a tetracycline-inducible p53 was used in the human Saos-2 osteosarcoma cell line<sup>35</sup> and in p53 null glioblastoma cells, to investigate the role of p53 in the angiogenic process.<sup>36</sup> More recently, tetracycline-inducible expression of p21<sup>WAF1</sup> and WT1 was achieved in human tumour cell lines.<sup>37,38</sup> Thus, the tetracycline system has satisfied both of the original requirements and it seems reasonable to conclude that it will make a significant contribution to murine models of human neoplasia.

### Site-specific recombinases

All inducible promoter-based strategies rely on the removal of endogenous control sequences and their replacement with inducible promoters via gene targeting. Although the presence of the inducible promoter allows control of gene expression, there are problems associated with the loss of the normal promoter. The targeted gene is no longer responsive to normal cell signals which would induce expression, and the levels of expression seen after addition of the inducer may not be an accurate representation of the standard physiological levels nor the time course of induction. Site-specific recombinase-based strategies circumvent this problem by manipulating sequences out with the promoter or coding regions of a gene to allow inducible control of gene expression.

Site-specific recombinases, such as Cre or FLP, bind to specific recognition sequences within the DNA (called loxP and FRT sites, respectively). When these recognition sites are directly repeated within a gene sequence, the intervening DNA is spliced out by recombinase, leaving one recognition site retained. Inversely repeated sites do not lead to the excision of the intervening DNA, but instead to the inversion of the flanked sequence.<sup>39</sup> It is the ability of the recombinase enzymes to catalyse excessive recombination which is being manipulated to achieve inducible gene targeting. Thus, recombinase-based strategies are being developed which allow either the inducible activation or inactivation of a target gene, depending on the site-specific deletion introduced via excessive recombination. Furthermore, by combining this approach with inducible expression systems and by driving Cre from a tissue-specific promoter, this genetic manipulation can be finely controlled both temporally and spatially.

Conditional inactivation of gene function can be achieved by inserting loxP sites around coding regions of the target gene. In the presence of active recombinase, the intervening DNA will be excised and gene function abolished. Alternatively, if a 'stop' codon surrounded by loxP recognition sites is inserted upstream of a coding region, transcription will be abolished. Activation of Cre will remove this impediment and thus allow activation of gene expression, a potential model for germline gene therapy. Preliminary studies have highlighted the potential of inducible targeting strategies based on conditional inactivation.<sup>40</sup>

Embryos which are homozygous null for DNAPol $\beta$ , an enzyme thought to be part of mammalian DNA



repair machinery, are non-viable<sup>41</sup> but an inducible targeting strategy allowed inactivation of the DNAPol $\beta$  gene only in tissues of the adult mouse.<sup>40</sup> LoxP sites were introduced into the DNAPol $\beta$  gene which did not affect gene expression in the absence of Cre. Induction of Cre expression in the adult mice caused excision of the LoxP flanked DNA, creating a conditional knockout. Control of gene inactivation was achieved as Cre recombinase expression was under the control of the *Mx1*-inducible promoter. Interestingly, differences in the efficiency of DNAPol $\beta$  inactivation were seen between tissues, with up to 100 per cent efficiency in the liver and spleen but only 20 per cent or below in the tail and brain.

Inducible control of gene expression is not the only way in which the Cre/lox system could further attempt to model human neoplasia. It may also provide an *in vivo* approach for chromosome manipulation both in cells and in the whole mouse. The introduction of loxP sites into non-homologous chromosomes via targeting, followed by Cre expression, can lead to chromosome translocation which mimic those seen in a variety of disease processes. For example, the chromosome translocation t(6;9) seen in a subtype of human acute myeloid leukaemia was created artificially in murine ES cells.<sup>42</sup>

### THE FUTURE OF INDUCIBLE, TISSUE-SPECIFIC GENE TARGETING

In the long term, inducible and tissue-specific control of gene expression will undoubtedly make an important contribution to the modelling of all human genetic diseases, particularly cancer. The ability to inactivate gene function within specific tissues of adult mice should provide an excellent model of the somatic mutational events characteristic of human neoplasia. The engineered mice may provide not only models of disease, but also models for possible gene therapy. Most human cancers have mutations in more than one oncogene or tumour suppressor gene, so there are many candidate genes which could be used in gene therapy for cancer. p53 is an obvious candidate and mice with inducible expression of this gene should provide information about the usefulness of a p53-based gene therapy protocol.

It is clear that the development of these technologies for precise identification of critical steps in cancer progression requires careful interpretation. For example, many tissue-specific promoters operate only in differentiated cells. Thus, one possible problem in future tumorigenesis studies is that the critical stem cell compartment is not targeted. Such questions remain to be answered and emphasize the importance of a histopathological and molecular genetic partnership as we seek to unravel the pathogenesis of cancer and design new strategies for treatment.

### ACKNOWLEDGEMENTS

EAL is supported by a studentship awarded by the Pathological Society of Great Britain and Ireland. ARC

is a Royal Society University Research Fellow. The authors are supported by CRC, MRC, and AICR.

### REFERENCES

1. Foulkes WD. A tale of four syndromes: familial adenomatous polyposis, Gardner syndrome, attenuated APC and Turcot syndrome. *Q J Med* 1993; **88**: 853–863.
2. Li FP, Thurber WA, Seddon J, Holmes GE. Hepatoblastoma in man with polyposis coli. *J Am Med Assoc* 1987; **257**: 2475–2477.
3. Bodmer WF, Bailey CJ, Bodmer J, et al. Localisation of the familial adenomatous polyposis on chromosome 5. *Nature* 1987; **326**: 614–616.
4. Malkin D, Li FP, Strong LC, et al. Germ line mutations in a syndrome of breast cancer, sarcomas and other neoplasms. *Science* 1990; **250**: 1233–1238.
5. Srivastava S, Zou Z, Pirolo K, Blattner W, Chang EH. Germ-line mutation of a mutated p53 gene in a cancer-prone family with Li-Fraumeni syndrome. *Nature* 1990; **348**: 747–749.
6. Knudson AG. Antioncogenes and human cancer. *Proc Natl Acad Sci USA* 1993; **90**: 10914–10921.
7. Longnecker DS. The azaserine-induced model of pancreatic carcinoma in rats. In: Scarpelli DG, Reddy JK, Longnecker DS, eds. *Experimental Pancreatic Carcinogenesis*. Boca Raton, FL: CRC Press, 1987; 11.
8. Shibata D, Capella G, Perucho M. Mutational activation of the c-Ha-ras gene in human pancreatic carcinoma. *Baillieres Clin Gastroenterol* 1990; **4**: 1–10.
9. Schaeffler BK, Zurlo J, Longnecker DS. Activation of c-Ki-ras detectable in adenomas or adenocarcinomas arising in the rat pancreas. *Carcinogen* 1990; **3**: 165–170.
10. Moser AR, Pitot HC, Dove WF. A dominant mutation that predisposes to multiple intestinal neoplasia in the mouse. *Science* 1990; **247**: 322–324.
11. Su L-K, Kinzler KW, Vogelstein B, et al. Multiple intestinal neoplasia caused by a mutation in the murine homologue of the APC gene. *Nature* 1992; **256**: 668–670.
12. Dietrich WF, Lander ES, Smith JS, et al. Genetic identification of a major modifier locus affecting Min-induced intestinal neoplasia in mice. *Cell* 1993; **75**: 631–639.
13. Berg P. Co-chairman's remarks: reverse genetics: directed modification of DNA for functional analysis. *Gene* 1993; **135**: 261–264.
14. Quail CE, Pinkert CA, Ornitz DM, Palmiter RD, Brinster RL. P-neoplasia induced by *ras* expression in acinar cells of transgenic mice. *Nature* 1987; **48**: 1023–1034.
15. Evans MJ, Kaufman MH. Establishment in culture of pluripotent mouse embryos. *Nature* 1981; **292**: 154–156.
16. Martin G. Isolation of a pluripotent cell line from early mouse embryos cultured in medium conditioned by teratocarcinoma stem cells. *Fertil Steril* 1981; **33**: 370–373.
17. [http://www.cco.caltech.edu/~mercer/htmls/rodent\\_genetics.html](http://www.cco.caltech.edu/~mercer/htmls/rodent_genetics.html)  
<http://www.informatics.jax.org/locus.html>  
<http://lena.jax.org/resources/documents/lmr/imir.html>
18. Harvey M, McArthur MJ, Montgomery CA, Butel JS, Brinster RL, Donehower LA. Spontaneous and carcinogen-induced tumorigenesis in p53-deficient mice. *Nature Genet* 1993; **5**: 225–229.
19. Purdie CA, Harrison DJ, Peter A, et al. Tumour incidence, spectrum and ploidy in mice with a large deletion in the p53 gene. *Oncogene* 1994; **9**: 603–609.
20. Jacks T, Remington L, Williams BO, et al. Tumour spectrum analysis in p53-deficient mice. *Curr Biol* 1994; **4**: 1–7.
21. Armstrong JF, Kaufman MH, Harrison DJ, Clarke AR. High frequency of developmental abnormalities in p53-deficient mice. *Curr Biol* 1994; **4**: 931–936.
22. Clarke AR, Maandag ER, van Roon M, et al. Requirement for a functional pRB gene in murine development. *Nature* 1992; **359**: 328–330.
23. Lee EY-HP, Chang C-Y, Hu N, et al. Mice deficient for RB are normal and show defects in neurogenesis and haematopoiesis. *Nature* 1993; **366**: 849–851.
24. Jacks T, Fazeli A, Schimdt E, Bronson R, Goodell M, Weinberg R. A mutation in the pRB gene in the mouse. *Nature* 1992; **359**: 295–300.
25. Morgenbesser SD, Williams BO, Jacks T, DePinho RA. p53-dependent apoptosis produced by Rb-deficiency in the developing mouse lens. *Nature* 1994; **371**: 72–74.
26. Windle JJ, Albert DM, O'Brien JM, et al. Retinoblastoma in transgenic mice. *Nature* 1990; **343**: 665–669.
27. Williams BO, Remington L, Albert DM, Mukai S, Bronson RT. Cooperative tumorigenic effects of germline mutations in Rb and p53. *Nature Genet* 1994; **7**: 480–484.
28. Umanoff H, Edelman W, Pellicer A, Kucherlapati R. The murine pRB gene is not essential for growth and development. *Proc Natl Acad Sci USA* 1995; **92**: 1709–1713.
29. Yarranton GT. Inducible vectors for expression in mammalian cells. *Opin Biotechnol* 1992; **3**: 506–511.
30. Hug H, Costas M, Staeheli P, Aebi M, Weissman C. Organisation of the murine *Mx* gene and characterisation of its interferon- and virus-inducible promoter. *Mol Cell Biol* 1988; **8**: 3065–3079.

- n M, Bonin AL, Bujard H. Control of gene activity in higher eukaryotic cells by prokaryotic regulatory elements. *Trends Biochem Sci* 1988; **13**: 471-475.
- n M, Bujard H. Tight control of gene expression in mammalian cells by tetracycline-responsive promoters. *Proc Natl Acad Sci USA* 1992; **89**: 5551-5555.
- n M, Freundlieb S, Bender G, Muller G, Hillen W, Bujard H. Transcriptional activation in mammalian cells. *Science* 1995; **268**: 1766-1768.
- ett P, Difilippantonio M, Hellman N, Schatz DG. A modified tetracycline-regulated system provides autoregulatory, inducible gene expression in cultured cells and transgenic mice. *Proc Natl Acad Sci USA* 1993; **90**: 6522-6526.
- inder L, Talbott R, Seeiziger BR, Kley N. Gene regulation by temperature sensitive p53 mutants: identification of p53 response genes. *Natl Acad Sci USA* 1994; **91**: 10640-10644.
- Meir EG, Polverini PJ, Chazin VR, Su Huang H-J, de Tribolet N, Lee WK. Release of an inhibitor of angiogenesis upon induction of wild type p53 expression in glioblastoma cells. *Nature Genet* 1994; **8**: 171-176.
37. Chen YQ, Cipriano SC, Arenkiel JM, Miller FR. Tumor suppression by p21<sup>WAF1</sup>. *Cancer Res* 1995; **55**: 4536-4539.
38. Englert C, Hou X, Maheswaran S, et al. WT1 suppresses synthesis of epidermal growth factor receptor and induces apoptosis. *EMBO J* 1995; **14**: 4662-4675.
39. Baringa M. Knockout mice: round two. *Science* 1994; **265**: 26-28.
40. Kuhn R, Schwenk F, Aguet M, Rajewsky K. Inducible gene targeting in mice. *Science* 1995; **269**: 1427-1429.
41. Gu H, Marth JD, Orban PC, Mossmann H, Rajewsky K. Deletion of a DNA polymerase  $\beta$  gene segment in T cells using cell type specific gene targeting. *Science* 1994; **265**: 103-106.
42. van Deursen J, Fornerod M, van Rees B, Grosveld G. Cre-mediated site-specific translocation between nonhomologous mouse chromosomes. *Proc Natl Acad Sci USA* 1995; **92**: 7376-7380.

**An intronic domain within the rat Preprotachykinin-A gene  
containing a CCCT repetitive motif acts as an enhancer in  
differentiating embryonic stem cells**

**C.E Fiskerstrand, E. Lovejoy<sup>1</sup>, L. Gerrard and J.P. Quinn\***

Department of Veterinary Pathology, Summerhall and Department of Pathology, Teviot  
Building<sup>1</sup>, University of Edinburgh EH9 1QH

\*Corresponding Author

Telephone 0131 650 7925

fax 0131 650 6511

email [j.quinn@ed.ac.uk](mailto:j.quinn@ed.ac.uk)

Keywords: PPT, substance P, gene expression, transcription, ES cells, enhancer, intron,  
nociception.

Previous attempts by several groups to clone fragments containing intron 2 of the rat preprotachykinin-A gene have generated deletions of various sizes. We have determined that these deletions occur within a specific region of the intron spanning a CCCT tandem repeat domain. We show that this intronic domain is able to support reporter gene expression in mouse embryonic stem (ES) cells that have been induced to differentiate but not in undifferentiated ES cells. No significant expression was observed in the HeLa clonal cell line. This demonstrates that this intron 2 domain is a highly restrictive enhancer and may be associated with differentiation.

The rat preprotachykinin-A gene (rPPT) encodes the neuropeptides substance P, neurokinin A, neuropeptide K and neuropeptide  $\gamma$ , which are derived by alternative splicing of primary RNA transcripts and post translational processing of the peptide precursors [6]. There is a plethora of *in vivo* observations on the expression of the preprotachykinin-A gene or modulation of tachykinin peptide content in a variety of physiological and pathological conditions [1, 4, 5, 19]. A molecular model for transcription of this gene will allow us to generate hypotheses concerning the mechanisms that result in these observations. The expression of PPT *in vivo* is restricted to specific tissues and under stimulus inducible regulation. Analysis of rPPT transcriptional control has focused on a proximal promoter region spanning -3500 to +500 relative to the transcriptional start [3, 8, 9, 12-16]. This region, or fragments derived from it, have been demonstrated to restrict promoter activity in reporter gene constructs to neurons rather than non neuronal cells in primary cultures of DRG or cell lines [8, 10, 16]. This restricted tissue specific expression is regulated by the combinatorial action of multiple positive and negative *cis*-acting regulatory domains. However this region of the promoter does not support any expression in a transgenic model of gene expression [10, 16].

Historically the region spanning -3500 to +500 was used because of the ease of manipulating various subfragments spanning the major transcriptional start site contained within a lambda clone. The initial region we cloned and analysed was a 5 Kb BamH1 fragment that extended the sequence at least 1kb 3' of +500 [15]. However this fragment was unstable when cloned in high copy number plasmids. Further analysis demonstrated that deletions were occurring in the region 3' of +500 (J. Quinn, personal observations). The original DNA sequence of the lambda clone identified was also

incomplete over this region [2]. Published DNA sequence was available to +871 followed by CCTCCCTCCCT then a gap of 0.58kb and resumed with CCCT suggesting that the gap may consist entirely of CCCT repeated units. As the 'continued' sequence began CCCT the assumption was that the entire 0.58kb might consist of CCCT repeated units. Although eukaryotic sequences that are difficult to clone in bacteria often contain endonuclease recognition sites, they can also contain structures that might have secondary structures such as palindromes and origins [17]. We therefore set out to clone, sequence and determine the function if any of this region.

The cloning of the region in intron 2 normally deleted in previous experiments was obtained by PCR of a 5.5Kb Bam HI restriction fragment spanning intron 2 using primers derived from the original sequence of Carter and Krause, 1990. These primers use the original numbering of Carter and Krause and are: the sense primer, termed hole1 5'TGTCCTGGGTTCA GTGTCT, 5' spanning bases +822 to 840, and the antisense primer, termed hole2, 5'GGCGATTCTCTGAAGAAGATGCTCAAAGGG spanning bases +1707to +1688 which is within exon 3. The PCR fragment generated was termed the HOLE. An equivalent PCR product was obtained from rat tail genomic DNA as template. This PCR product was cloned into PCR2.1 (InVitrogen) and sequenced. A ~920bp PCR product was obtained which consisted of 128 bases of CCCT repeats plus 511 bases of new sequence flanking the CCCT in addition to the known sequence, Fig. 1. An internal antisense primer, hole3, 5'TGCAACTCACTAAGATCCAG was derived from this new flanking sequence adjacent to the CCCT region. When used with hole primer 1 to obtain a PCR fragment containing the CCCT region with minimal flanking bases, the CCCT region was again deleted upon cloning. This highlights the instability



of the region. Intermediate sized clones using restriction fragments of the 'Hole' PCR2.1 clone have also proved to be unstable.

To test the ability of the HOLE region to act as a transcriptional enhancer we made reporter gene constructs in which luciferase expression is directed by this fragment. Reporter gene constructs used for transfection analyses consisted of the pGL3 promoter vector (pGL3p, Promega) with the HOLE sequence subcloned into the BamHI site. A chloramphenicol acetyl transferase (CAT) construct under the control of the RSV promoter was used to control for transfection efficiencies. There are no good cell line models for PPT gene expression or cells that support reporter gene expression directed by PPT promoter fragments. However PPT expression has been demonstrated in sub-populations of ES cells which are differentiated to a neuronal phenotype. We therefore used ES cells for testing reporter gene expression of our HOLE construct. HeLa were used as non-neuronal cell line.

ES cells, HM-1, were cultured as per Magin et al [7] in the presence of LIF (leukaemia inhibitory factor). Cells at 70-80% confluence in 24 well plates were used for transfections. 45min prior to transfection, cells were transferred to serum-free medium. Lipofectin (Life Technologies) was used as the transfection agent, following the manufacturer's directions. DNA and lipofectin were incubated separately in serum-free medium + or - LIF as required, for 45min then the two solutions combined for a further 45min. 250µl of the mix was added to each well and 3 separate wells transfected for each sample. Each transfection contained 1ug specific PPT intron plasmid construct plus 366ng RSV-CAT. Post transfection, cells were transferred to specific medium + / - LIF and + / - retinoic acid (RA). All trans retinoic acid, when required, was dissolved in

ethanol and used immediately. After a further 64h incubation cells were washed twice with PBS, 250ul Promega lysis buffer was added. After 15-30min at room temperature lysates were harvested, vortexed and microfuged for 15sec. Supernatants were stored at -70°C. HeLa cells were grown in Dulbecco's modified Eagle's media (DMEM) supplemented with 10% heat inactivated calf serum. HeLa cells were transfected by electroporation in 4mm cuvettes using the EquiBio Easyject at 250V and 1500uF (optimal settings). 20µg specific PPT intron 2 construct plus 2µg RSV-CAT was transfected per  $5 \times 10^6$  HeLa cells in 800µl medium + 0.5% serum. The cells were immediately resuspended in fresh medium in 6 well plates and incubated for 48h at 37°C then treated in the same way as the ES cells. For each sample, 20µl was assayed for luciferase activity using the Promega system and the Life Sciences Labsystems Luminoskan RT and 200µl was assayed for CAT activity using the Promega CAT ELISA system. Luciferase results were normalised to CAT values to control for transfection efficiency.

ES cells are pluripotent cells derived from the inner cell mass of blastocysts. The culturing of ES cells in the presence of LIF allows them to be maintained in an undifferentiated state for many passages in culture [18]. When such undifferentiated cells were transfected with the PPT-luciferase construct reporter gene expression over that of the vector alone was not increased. Reporter gene expression in general was higher when cells were transfected in the presence of LIF Fig2a. However, withdrawal of LIF permitted the PPT intronic domain to act as a strong enhancer of reporter gene expression, with a 150-fold increase in activity observed, Fig. 2a and b. There was no further enhancement with RA. Withdrawal of LIF is sufficient to induce the differentiation of ES cells into endoderm-like cells. Although differentiation of ES cells into

morphologically distinguishable cell populations normally occurs over a period of days, changes at the molecular level can be seen as early as 36hrs after LIF withdrawal or 12 hours after the addition of RA [11].

In conclusion, the withdrawal of LIF for 64 hours is insufficient to induce gross morphological changes in ES cell appearance. However, it is sufficient to induce molecular alterations within these cells that permit the enhancer activity of the novel PPT intronic domain. This domain contains a tandem CCCT repeat motif of 148bp that was previously uncharacterised within the rPPT promoter as this region is unstable when cloned into high copy number plasmids in bacteria. It will be of interest to determine precisely the enhancer domain within intron 2 and test it both individually and within the context of transgenic models of PPT gene expression that we are developing.

Acknowledgements. We would like to thank Ms S. Shaw for excellent technical support. This work was supported by the BBSRC.

## References:

- 1 Barakat-Walter, I., Affolter, H.U. and Droz, B., Expression of substance P and preprotachykinin mRNA by primary sensory neurons in culture: regulation by factors present in peripheral and central target tissues, *Molecular Brain Research*, 10 (1991) 107-114.
- 2 Carter, M.S. and Krause, J.E., Structure, expression, and some regulatory mechanisms of the rat preprotachykinin gene encoding substance P, neurokinin A, neuropeptide K, and neuropeptide  $\gamma$ , *Journal of Neuroscience*, 10 (1990) 2203-2214.
- 3 Fiskerstrand, C. and Quinn, J.P., The molecular biology of preprotachykinin-A gene expression, *Neuropeptides*, 30 (1996) 602-610.
- 4 Hart, R.P., Shadiack, A.M. and Jonakait, G.M., Substance P gene expression is regulated by interleukin-12 in cultured sympathetic ganglia, *Journal of Neuroscience Research*, 29 (1991) 282-291.
- 5 Holzer, P. and Holzer-Petsche, U., Tachykinins in the gut .1. Expression, release and motor function, *Pharmacology & Therapeutics*, 73 (1997) 173-217.
- 6 Maggio, J.E., Tachykinins, *Annual Review of Neuroscience*, 11 (1988) 13-28.
- 7 Magin, T.M., McWhir, J. and Melton, D.W., A new mouse embryonic stem cell line with good germ line contribution and gene targeting frequency, *Nucleic Acids Res*, 20 (1992) 3795-6.
- 8 Mendelson, S.C., Morrison, C.F., McAllister, J., Paterson, J.M., Dobson, S.P., Mulderry, P.K. and Quinn, J.P., Repression of preprotachykinin-A promoter activity is mediated by proximal promoter element, *Neuroscience* (1995) 837-847.

- 9 Mendelson, S.C. and Quinn, J.P., Characterisation of potential regulatory elements within the rat preprotachykinin-A promoter, *Neuroscience letters*, 184 (1995) 125-128.
- 10 Mulderry, P.K., Chapman, K.E., Lyons, V. and Harmar, A.J., 5'-flanking sequences from the rat preprotachykinin gene direct high-level expression of a reporter gene in adult rat sensory neurons transfected in culture by microinjection, *Molecular and Cellular Neurosciences*, 4 (1993) 164-172.
- 11 Nemetz, C. and Hocke, G.M., Transcription factor Stat5 is an early marker of differentiation of murine embryonic stem cells, *Differentiation*, 62 (1998) 213-20.
- 12 Paterson, J.M., Mendelson, S.C., McAllister, J., Morrison, C.F., Dobson, S., Grace, C. and Quinn, J.P., Three immediate early gene response elements in the proximal preprotachykinin-A promoter in two functionally distinct domains, *Neuroscience* (1995) 921-932.
- 13 Paterson, J.M., Morrison, C.F., Mendelson, S.C., McAllister, J. and Quinn, J.P., An upstream stimulatory factor (USF) binding motif is critical for rat preprotachykinin-A promoter activity in PC12 cells., *Biochemical Journal*, 310 (1995) 401-406.
- 14 Paterson, J.M., Morrison, J.F., Dobson, S.P., McAllister, J. and Quinn, J.P., Characterisation of a functional E box motif in the proximal rat preprotachykinin-A promoter, *Neuroscience Letters*, 191 (1995) 185-188.
- 15 Quinn, J.P., Multiple protein binding sites within the rat preprotachykinin promoter: Demonstration of a site with neuronal specificity that is 3' of the major transcriptional start, *Molecular and Cellular Neurosciences*, 3 (1992) 11-16.
- 16 Quinn, J.P., Neuronal-specific gene expression - The interaction of both

positive and negative transcriptional regulators, *Progress In Neurobiology*, 50 (1996) 363-379.

- 17 Quinn, J.P. and McGeoch, D.J., DNA sequence of the region in the genome of herpes simplex virus type 1 containing the genes for DNA polymerase and the major DNA binding protein, *Nucleic Acids Res*, 13 (1985) 8143-63.
- 18 Suda, Y., Suzuki, M., Ikawa, Y. and Aizawa, S., Mouse embryonic stem cells exhibit indefinite proliferative potential, *J Cell Physiol*, 133 (1987) 197-201.
- 19 Vedder, H., Affolter, H.U. and Otten, U., Nerve growth factor (NGF) regulates tachykinin gene expression and biosynthesis in rat sensory neurons during early postnatal development, *Neuropeptides*, 24 (1993) 351-357.



### Figure 1 PCR of rPPT Intron 2 'HOLE'

a) A ~900bp HOLE PCR product was obtained from both genomic DNA (lane 2) and a 5.5Kb BamHI restriction fragment derived from the >14Kb genomic  $\lambda$ 11.1 clone of Carter and Krause, 1990 (lane 3). PCR primers hole1, hole2 and hole3 were used at an annealing temperature of 55°C. b) Sequence of the HOLE PCR product showing the position of the CCCT repeat. PCR primers are underlined and previously unpublished sequence is shown in bold characters. The start and end of the sequence correspond to positions +822 and +1707 of Carter and Krause respectively.

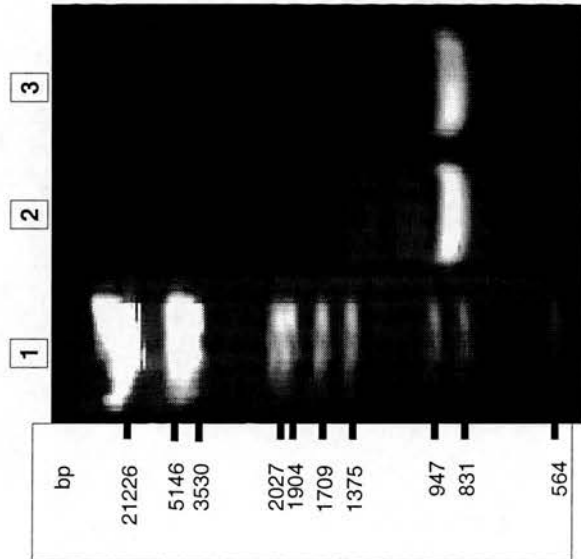


**Figure 1a** Fiskerstrand, Lovejoy, Gerrard and Quinn

hole 1 →

1 TGTCTTGGGTTCAGTGTCTCCCCAACAGAAAAGGAGTTCTTCTTTTCCTTCCT (CCCT)<sub>32</sub>  
182 CCTTCCTTCCCTCCCTCTCTCCTTCTCTCCTCTCCTGGTCCTGGTTTTAATCCCTACTTA  
242 TGTGATTGTAATCTCGGGGGCTTTGATCAAAC TGAGCTGCCAGACCATT TGGAGATGTTG  
302 GGAAGAGACGTGAATTGTCAATGGGGGCAAAGCTGGATCTTAGTGAGTTGCAAGGTCCT  
← hole 3

362 AAGTGGCTGGCGGCAATTAAC TCTATACTCAGTATTCGGTGCTCCAAGTTTCCCTTTAAA  
422 TGGCTCTTGAATTTTGGCTCCTAAGGAAGGGCGGCTTGGGCAACGGTGAAAGTTGTCGGT  
482 GGTGCTAGTTCGCTTTTAAAGTATCAGGCACCCCTTCTGCTTCCCAACCCTTGCATGTTTT  
542 TCAGTGAGGACAAATGAGCGGACTCCGAAGCGTCACTGAGAGCAAACAAAGGTGATAGCA  
602 AGACCTCGAGTGAGTCCCTCTGATGCGAATTGAGAGCAGAAAGCATACAGGACCCCAGAAC  
662 CGGAAGGCAGTTGGTGGGTGCGCAGAAGCGTCCCTGATAGACTTTGGGGGAGAAGGAAAT  
722 CTCAGGCGGGTCCGGGTGTTGGGGAAAGTGCTGCATAGATTCTAGTATGGCACGGTCTCATG  
782 CTAGCGGCTGCTTCTGTGGCTCTGAGGAAAGCTCAGGCACACCGTGAATGTGGACCTTGT  
842 TCACTTAATTTGTCTACTCGCTGGTTTGTCCCTCCAGGAGGCAATGCCGGAGCCCTTTGA  
902 GCATCTTCTGCAGAGAATCGCC  
← hole 2

Figure 1b Fiskerstrand, Lovejoy, Gerrard and Quinn

## **Figure 2 Enhancer Activity of rPPT Intron 2 CCCT Element in ES Cells**

a) Luciferase expression from cells transfected with either the pGL3p vector or CCCT-pGL3p construct. Luciferase units are normalised using RSVCAT expression in each sample to correct for transfection efficiencies. Results are shown for roughly equivalent numbers of cells in HeLa and ES + and - LIF with no added retinoic acid. b) The enhancer activity of the rPPT Intron 2 CCCT element is shown as the increase in luciferase units over the basal activity of the expression vector. Results are corrected for transfection efficiencies. Data is shown as + and - LIF at increasing retinoic acid concentrations from 0 – 500 $\mu$ M.

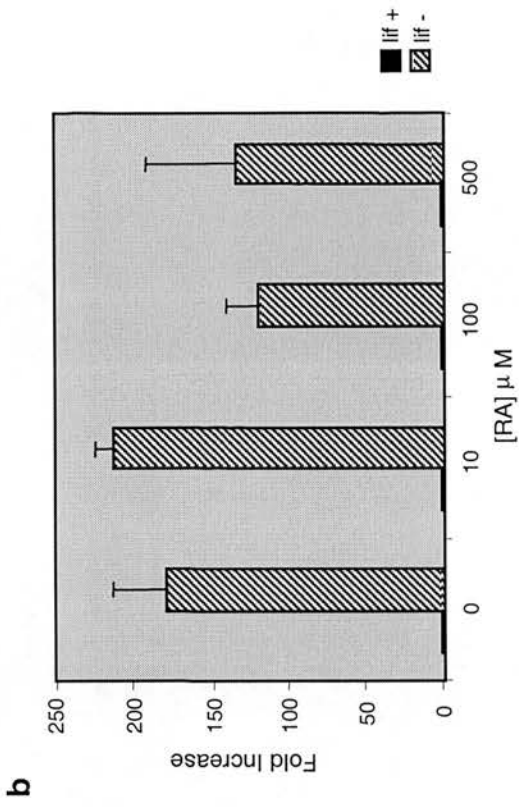
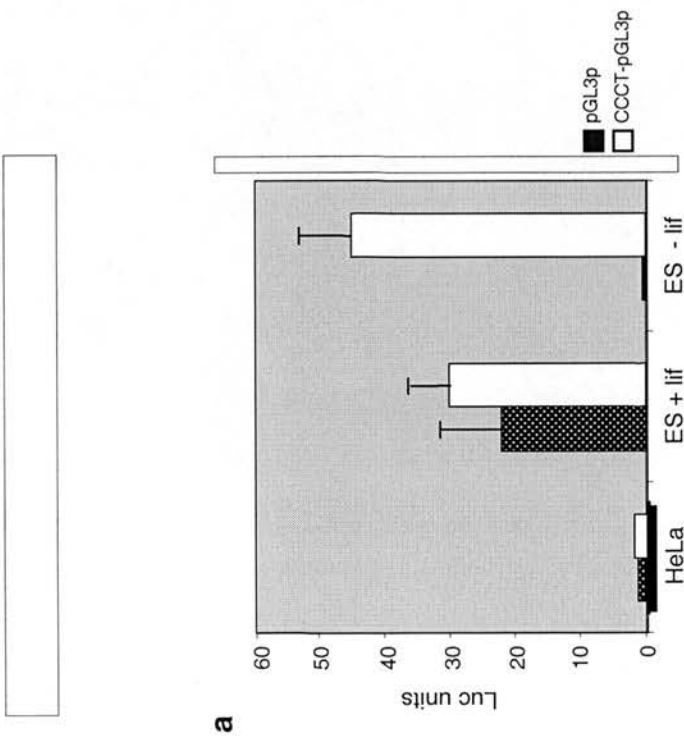


**Figure 2** Fiskerstrand, Lovejoy, Gerrard and Quinn